Queen Mary
University of London

Mechanical and biochemical guidance of hMSC developmental trajectories monitored by cytoskeletal morphometrics

Submitted in fulfilment of the
Degree of Doctor of Philosophy

Luís Rafael Pereira do Carmo Flores

School of Engineering and Materials Science

Queen Mary University of London

2015-2019

To my father

Statement of Originality

I, Luís Rafael Pereira do Carmo Flores, confirm that the research included within this thesis is my own work or that where it has been carried out in collaboration with, or supported by others, that this is duly acknowledged below and my contribution indicated. Previously published material is also acknowledged below.

I attest that I have exercised reasonable care to ensure that the work is original, and does not to the best of my knowledge break any UK law, infringe any third party's copyright or other Intellectual Property Right, or contain any confidential material.

I accept that the College has the right to use plagiarism detection software to check the electronic version of the thesis.

I confirm that this thesis has not been previously submitted for the award of a degree by this or any other university.

The copyright of this thesis rests with the author and no quotation from it or information derived from it may be published without the prior written consent of the author.

Details of collaboration and publications:

The cytoskeleton image analysis and single-cell trajectory algorithms used in this thesis were developed by Dr. Núria Gavara. Chapter 7 has been published in the scientific journal *Scientific Reports*, Nature Group. Michael Keeling provided his aid with some of the AFM measurements conducted in this chapter. Western blot experiments were performed with the assistance of Xiaoli Zhang and Su Fu. Dr. Kristina Sliogeryte contributed to discussions during production of the manuscript. The analytical approach was jointly developed by Dr. Núria Gavara and Luís Flores. Experiments on the remaining chapters of this thesis were performed exclusively by its author

Abstract

Morphology, cytoskeleton organisation and nuclear states are important biomarkers to characterise and modulate cell behaviours. Bilateral interactions between cells and their surroundings are critical aspects of biology, evidenced by the role of extracellular environment mechanical properties in directing human mesenchymal stem cell differentiation. Yet, mesenchymal stem cell differentiation studies have been mostly conducted on static linear-elastic hydrogels, neglecting important features of natural extracellular matrices.

This thesis describes the development and characterisation of 2D collagen-coated agarose substrates with non-linear mechanical properties. Single-cell morphometric descriptors, extracted from cytoskeletal and nuclear images, were used to assess the combined impact of the substrate mechanical stimuli and biochemical differentiation factors on human mesenchymal stem cell morphological, cytoskeletal and nuclear states. A methodology based on Supervised Machine Learning algorithms was further employed to extend discrete population-based morphometric trends to single-cell developmental trajectories.

Similar image quantification approaches were used to characterise the effects of Lifeact-GFP, a commonly used agent in fluorescent imaging of microfilaments, on cell F-actin organization, morphology and biophysical behaviour.

The results in this work suggest that mesenchymal stem cells undergo dynamic non-monotonic morphometric changes under mechanical and biochemical stimuli. Contrary to established reports in linear-elastic hydrogels, cells responded similarly to collagen-coated agarose substrates covering a range of stiffnesses (1 to 30 kPa). This was accredited to the effects of the collagen coating on top of the hydrogels. Inclusion of osteogenic and adipogenic supplements conditioned the cells into assuming distinct morphologies through well-defined developmental trajectories, overriding the influence of the cell culture substrates. Single-cell developmental trajectories

were akin to populational trends and helped reveal highly dynamic morphometric changes in greater detail.

It was also shown that Lifeact induces changes in the cytoskeleton architecture and nucleus in a dose-response manner, ultimately leading to altered F-actin dynamics, reduced cell migration and increased cellular stiffness.

Altogether, this work illustrates how morphometric analysis is uniquely poised to study morphological trends, such as characterising developmental trajectories or measuring the effects of mechanical and biochemical stimuli on cell behaviour.

Acknowledgments

I must start by thanking Dr. Núria Gavara for welcoming me as part of her research group and for her considerate supervision. Núria has never declined from providing guidance and her help has been instrumental in overcoming the hurdles I've encountered over the past four years. She has fostered a collaborative, friendly working environment in the research group, is endlessly passionate about her research, and is consistently engaged with her students in the development of their projects. Núria has instilled in me the importance of thinking beyond the conventional while making the most out of the treasure trove of data analysis. I am truly thankful to her. I hope that this document does justice to her outstanding performance as supervisor and group leader.

Secondly, I'd like to acknowledge my friends and colleagues in the group. Dr. Asad Dodhy, with whom I shared the privilege of being Núria's first PhD students, helped set-up the imaging analysis approach I employed in this project. Xiaoli Zhang and Michael Keeling, who joined the group shortly after, have helped me many times with their expertise in AFM and live-cell imaging. To them, as well as to Dr. Kristina Sliogeryte, Hongxu Meng, and Marta Ferreira, the newest members of the group, I must thank the kinship and fun, collaborative work environment. To all I wish the very best luck and success.

I would also like to thank all the friends I made at the School of Engineering and Materials Science. You have made the school more than a working place. I will not soon forget the movie sessions or the group luncheons, and meeting some of the brighter personalities in London (especially Will, Matt and Stefania!). A particular acknowledgment should be dedicated to Dr. Stephen Thorpe. As a senior post-doc, Steve has been a tireless source of help and advice for me and my colleagues. He is a brilliant researcher and I wish him the very best.

A quick word of appreciation must also go to all the teachers who have taught and inspired me, across ages and subject matters.

My achievements during the PhD I dedicate to my parents. They have motivated me to put utmost dedication in all endeavours and to never cease

learning. They are unwavering in their love and support, and I truly hope this work can make them proud.

Lastly, my girlfriend Raquel, deserves all the laurels I can possibly give. Her support and sage advice, optimism and forbearance, persistently came through in times of need. To her, I wish to relay my most enthusiastic appreciation and admiration.

I'd also like to acknowledge the Marie Sklodowska-Curie grant funding (CSKFingerprints) which supported my PhD studentship.

Table of Contents

List of Figures

List of Tables

Abbreviations

TE - Tissue Engineering

SCs - Stem Cells

MSCs - Mesenchymal Stem Cells

TCP - Tissue Culture Plastic

hMSCs - Human Mesenchymal Stem Cells

FBS - Feotal Bovine Serum

ECM - Extra Cellular Matrix

rtPCR - Reverse Transcription Polymerase Chain Reaction

PPAR - Peroxisome Proliferator Activated Receptor-γ

Runx2 - Runt-related Transcription Factor 2

AFM - Atomic Force Microscopy

PAA - Polyacrylamide

NMM II - Non-muscle Myosin II

PAA - Polyacrylamide

FA - Focal Adhesion

FAK - Focal Adhesion Kinase

RGD - Arginine-Glycine-Aspartate sequence

MTs - Microtubules

IFs - Intermediate Filaments

MFs - Microfilaments

YAP - Yes-associated Protein

TAZ - Transcriptional Co-activator with PDZ-binding Motif

LINC - Linker of Nucleoskeleton and Cytoskeleton

BMP - Bone Morphogenic Protein

2D - Two Dimensional

3D - Three Dimensional

E - Young's Modulus

σ - Stress

ε - Strain

PDMS - Polydimethylsiloxane

PEG - Polyethylene glycol

ML - Machine Learning

SVM - Support Vector Machine

Sulfo-Sanpah - Sulfosuccinimidyl-6-[4-azido-2-nitrophenylamino] Hexanoate

NHS - N-hydroxysuccinimide

COL I - Collagen Type I

DMEM - Dulbecco's Modified Eagle Medium

PIV - Particle Image Velocimetry

OOS - Out-of-sample

BC - Box Contraint

KS - Kernel Scale

Ep - Epsilon

MOI - Multiplicity of Infection

RoV - Ratio of Variances

DRC - Dose-response Curve

GAPDH - Glyceraldehyde 3-phosphate Dehydrogenase

LatA - Lantrunculin A

Introduction

Mesenchymal stem cells are an important cell source in Regenerative Medicine and Tissue Engineering. These cells are extremely sensitive to the mechanical attributes of the surrounding environment, constituting central models in the study of Mechanobiology

Currently, substantial amounts of research are dedicated to the interactions between cells and biomaterial substrates with a wide range of mechanical properties. While the mesenchymal stem cell response to linear-elastic substrates has been extensively characterised, it has become evident that non-linear properties, patent in many extracellular matrices, can have unexpected impacts on cell adaptation and behaviour.

Cell morphology, cytoskeleton organisation and nuclear properties encode valuable information about the cell state. The combination of microscopy and image analysis techniques are uniquely primed to assess this information and identify common trends among highly variable and dynamic cell phenotypes, in response to both mechanical and biochemical stimuli. Our research group has previously developed a morphometric image analysis pipeline which can extract 18 parameters linked to whole cell morphology, cytoskeleton fibre architecture and relative nuclear features. This approach provides the flexibility of evaluating average populational trends, as well as using single-cell metrics to resolve heterogeneous behaviours.

For the work described in this thesis, morphometric image analysis was combined with an experimental approach whereby cell samples, seeded in concert, are subsequently fixed in a sequence of discrete time points to monitor mesenchymal stem cell morphometric changes. Following this methodological rationale, the work described in this thesis can be divided into two overall goals:

1) The study of how the mechanical properties of collagen-coated 2D agarose substrates, together with biochemical differentiation induction supplements, impact stem cell developmental trajectories. Research linked to this objective is presented in Chapters 3 to 6.

2) Characterising the dose-dependent effects of the actin labelling agent, Lifeact-GFP, on the cytoskeleton, cell morphology and additional biological and biophysical properties. Research linked to this subject is presented on Chapter 7.

Thesis outline

- Chapter 1 – Review of the literature, contextualising mesenchymal stem cells in Mechanobiology
- Chapter 2 – Technical overview, providing supporting information to the techniques and methodological approaches used in this thesis.
- Chapter 3 – Relates how preliminary attempts to redesign an agarose construct to employ in active mechanical stimulation of cells lead to the optimization of novel collagen-coated 2D agarose substrates. Mechanical characterisation of substrate non-linear-elastic properties is also described.
- Chapter 4 – Details the morphometric trajectories undergone by mesenchymal stem cell populations in the collagen-coated agarose substrates in the absence of biochemical differentiation induction
- Chapter 5 – Describes the morphometric trajectories undergone by mesenchymal stem cell populations in the collagen-coated agarose substrates in the presence of osteogenic and adipogenic differentiation induction supplements
- Chapter 6 – Introduces a newly developed Machine Learning Supervised Regression approach to order single-cell morphometric data along a continuous developmental trajectory.
- Chapter 7 – Presents the results of an extensive evaluation of Lifeact-GFP as an actin labelling agent for live-cell microscopy. This chapter is currently under review (third revision) for publication.
- Chapter 8 – Final chapter summarising the results achieved during the project.

Chapter 1 – Literature Review

1.1 The potential of mesenchymal stem cells in Regenerative Medicine

1.1.1 Recent promises of Regenerative Medicine and Tissue Engineering

The astounding technological and societal advancements made in recent decades have greatly extended the life expectancy of human populations worldwide [1]. As a result, a new set of clinical demands must be tailored for these increasingly aged demographics. Numerous illnesses, such as autoimmune and degenerative diseases, cancer [2], or osteoporosis [3], are a limited subset of the most recent health challenges which must be addressed with urgency [4], [5].

Regenerative Medicine is a subject born from the past *circa* 25 years of concerted progress in Cell Biology and Biomedical Engineering [6]. One of the foremost topics in biomedical research, Regenerative Medicine is grounded on the principle of engineering viable substitutes for deficient cells, tissues or organs, to restore or sustain biological functions for therapeutic purposes. This discipline may thus provide an appropriate answer to many of the novel challenges in medical care [7].

One of the main branches of Regenerative Medicine, Tissue Engineering (TE), is mainly represented by a conventional approach combining Cell Therapy with the development of biomaterial scaffolds that mimic physical and biochemical features of the living cell niche [4]. These constructs are then implanted to serve as *de novo* tissues or organs. In the long term, these technologies may overcome the increasing demand and shortage for organ transplants [8]. Furthermore, the possibility of using autologous cells in the treatment of each patient is an exciting prospect in the evolving adaptation of modern medicine to individual needs [7]. This would not only increase treatment efficacy, but also decrease potential hazards by lowering the probability of immunity-mediated tissue rejection.

1.1.2 Mesenchymal stem cells

A great amount of the work conducted on the field of TE has been dedicated to the study and manipulation of stem cells (SCs) [6], [8]. The therapeutic potential of these cells arises from two specific properties. First, SCs are unspecialized cells capable of self-renewal for extended periods of time under standard culture conditions [9]. For this reason, SCs can be greatly expanded *in vitro* to originate tissues for therapy or modelling purposes. Secondly, they can be induced, under a variety of biochemical [10] and physical methods [11], to differentiate into mature cells of several lineages, depending on their inherent degree of cell plasticity, or potency. Totipotent cells can differentiate into all cell types in the human body, while pluripotent cells can form any tissue, except for the placenta. Finally, multipotent or progenitor cells can only generate a limited subset of closely related cell types [5].

Several SC sources in the body have been explored for translational research purposes [8]. For instance, embryonic SCs are pluripotent, but their research potential has been limited by ethical hurdles [12]. Adult SCs, on the other hand, can be found throughout the entire human body, but demonstrate restricted potency. Although termed adult SCs, these cells are originated during foetal development and are retained throughout life. Thus, it is accepted that these cells may act as reservoirs for maintenance of tissue growth, homeostasis and wound healing [13]. However, adult SCs generally exist in isolated niches which can be difficult to unequivocally identify and access [14]. More recently, researchers have been able to transform somatic cells into an undifferentiated pluripotent-like state termed induced pluripotent SCs [15]. Nonetheless, this process is still associated with low efficiency and potential health risks related to the use of viral vectors.

Mesenchymal stem cells (MSCs), one kind of adult SC, have merited close attention by the scientific community. MSCs were first isolated from bone marrow extracts in the 1970's [16] as a rare subset of non-heamatopoetic tissue culture plastic (TCP) adherent cells. Several authors have since established MSC multipotency [17] in originating cell lines of the mesenchyme, namely osteoblasts, chondrocytes and adipocytes (Fig. 1.1). Later on, MSCs

were reported to differentiate into myoblasts [18], as well as cells of endoderm and ectodermal origin [10], such as neuronal tissue [19], although the reliability of these later protocols is still a topic of scientific dispute.

Human mesenchymal stem cells (hMSCs) are advantageous in not only originating a great variety of clinically coveted tissues without severe ethical implications, but in demonstrating reduced propensity for teratoma formation and immune rejection [20], [21]. In fact, MSCs are held as viable candidates for immunomodulatory and regenerative cell therapy, with clinical evidence suggesting a beneficial paracrine effect to *in vivo* tissue regeneration [2], [21]. Additionally, there is a wide variety of putative MSC niches reported throughout the human body. These include the previously mentioned bone marrow, but also the periosteum, peripheral and cord blood or adipose tissue, among others [13], but the relative cell content reported for each niche varies considerably throughout the literature [21].

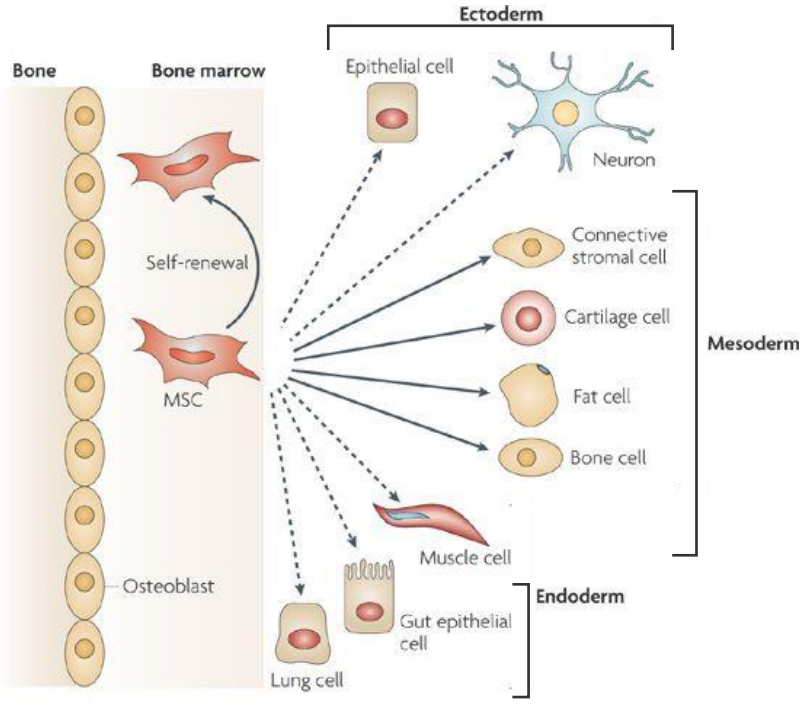

Figure 1-1 – Mesenchymal stem cell lineages – Schematics illustrating MSCs residing in the bone marrow niche. Mesodermal lineages (originating cartilage, fat and bone cells) have been well substantiated in the literature. Conversely, there is little consensus about the induction of other lineages (e.g. epithelial and neuronal cells) in MSCs. Adapted from [22].

The heterogeneity in hMSC populations, both within and between individuals, coupled to the want of an unambiguous classification system, still hinder interpretation of results in the use of these cells [2], [13], [21]. The current standard method for identifying hMSCs was systematized by the International Society for Cellular Therapy in 2006 [23], [24]. These reports suggest that MSCs must adhere to culture plasticware under standard conditions. The cells must furthermore be CD105, CD73 and CD90 positive, while lacking the expression of CD45, CD34, CD14 or CD11b, CD79a/CD19 or HLA-DR surface markers. A final criterion is to prove differentiation plasticity into osteo-, adipo- and chondrogenic lineages *in vitro*. Although extensive, these criteria are not exhaustive enough to unequivocally discriminate a single cell type. Hence, MSC non-clonal cultures are considered a collection of heterogeneous (uni-, bi-, tri- and multipotent) progenitors with potentially distinct and complex phenotypic, replicative and differentiation propensities [25], [26].

For this reason, there is an ongoing debate about the correct nomenclature with which to address these cells. The term MSC was popularized in the 1990's [27], but there is now contention that the term "multipotent mesenchymal stromal cells" more accurately describes the initial overall population isolated by plastic adhesion [23]. Among these, a putative smaller subset could then be considered "true" SCs and be designated as MSCs [28]. Unfortunately, there is no univocal marker to resolve this issue, and therefore the MSC nomenclature still prevails in the literature[*]. Such a marker would also allow more thorough characterisation of MSC niches *in vivo*, as it is yet unclear where, within SC niches, MSCs reside. There have, however, been reports of a close association between MSCs and pericytes [13], [14], cells which share many of the markers attributed to MSCs, and which exist throughout the body in close proximity to endothelial linings. A shared identity between the two cell types has been proposed but is not yet fully resolved [29].

Another issue is that *ex vivo* MSCs may be phenotypically distinct from those *in vivo* [14], as phenotypic shifts occur in these cells during *in vitro*

[*] For that reason, the classic MSC nomenclature will be adopted in this document.

cultures. For instance, abrupt changes in the morphology of MSCs become evident after the cells are kept in TCP for a few weeks, or for more than an average of six sub-cultures [30]. In general, adherent “p0” MSCs adopt a spindle-like shape, but the percentage of wider and more polygonal cells, with stronger anchorage points, increases during culture, along with the preponderance of quiescence [14]. These observations are related to the mechanical cues provided by rigid (stiffness ~GPa) TCP. Importantly, there is recent evidence to suggest that these cells preserve this mechanical bias when cultured beyond a temporal threshold of several days, even if they are subsequently transferred onto a soft substrate [31].

1.1.3 MSC isolation, expansion and differential potential

In addition to a variety of MSC reservoirs, there are multiple isolation and expansion procedures for collecting MSCs [14]. MSC isolation involves the collection of donors’ native tissue, followed by cycles of density centrifugation. The mononucleated cell fraction is culture plated, and adherent cells are assayed for fulfilment of putative-MSC requisites. These cells are then cultured and expanded using standard cell culture methods, i.e provision of growth medium supplemented with antibiotics, foetal bovine serum (FBS), and additional growth factors [32].

As previously mentioned, MSCs demonstrate multipotent differentiation potential into cell lineages from the primary germ layers [17]. However, the osteogenic, chondrogenic and adipogenic differentiations are currently the most well-established MSC lineages (Fig. 1.2). Classically, MSC differentiation has relied on supplying the cells with batches of defined biochemical factors [13]. Culturing the cells with ascorbic acid, β-glycerophosphate and dexamethasone is the standard method for generating osteoblasts. Adipocytes, on the other hand, can be obtained by a combination of dexamethasone, insulin, isobutylmethylxanthine and indomethacin. For chondrocytes [33] it is also necessary to plate cells as pellets (very high density and close cell-cell contact) while providing a defined media supplemented with dexamethasone, ascorbic acid, insulin, selenious acid, transferrin, sodium pyruvate, and transforming growth factor-β.

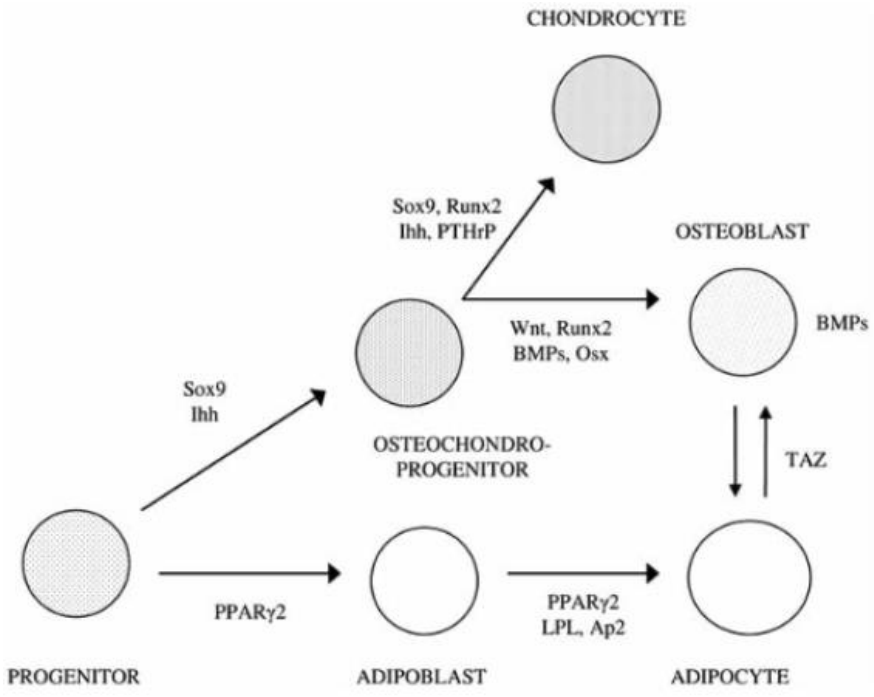

Figure 1-2 – Molecular markers of MSC differentiation – Simplified model identifying transcription regulators expressed during conventional MSC tri-differentiation and transdifferentiation. Adapted from [34].

Assessing the efficiency of each of these differentiation pathways can be achieved through a variety of techniques. For instance, since bone is highly mineralized, detecting increased levels of Alkaline Phosphatase activity can be used as a surrogate assessment of mineralization [35] to track osteoblastic differentiation [36]. Additional histological stains include Alizarin Red and Von Kossa stains, used to detect calcium phosphate deposits. In relation to the genesis of adipocytes, the accumulation of lipid vacuoles within the cytosol of the cells is commonly visualised with the aid of Oil Red O staining [37]. Finally, chondrogenic differentiation is correlated with the production of extracellular matrix (ECM) sulfated glycosaminoglycans which can be detected by the Toluidine or Alcian Blue dyes [33], [37].

Apart from histological analysis, expression of lineage-specific cell markers (Fig. 1.2) can be assessed by fluorescence activated cell sorting or reverse transcription polymerase chain reaction (rtPCR) [38]. As examples,

peroxisome proliferator activated receptor-γ (PPARγ) is assumed to be one of the major transcriptional factors involved in the regulation of adipogenesis, while Runt-related transcription factor 2 (Runx2) functions as its osteogenic analogue [39] (Fig 1.2). The upregulation of these transcriptional modulators is thus used to confirm the success of differentiation induction.

1.1.4 MSCs beyond the biochemical perspective

The main disadvantage of biochemical assays to assess differentiation is sample destruction. Therefore, it is not straightforward to establish the temporal evolution of differentiation processes using these methods. Despite the recognition that MSCs can differentiate into the three main mesenchymal lineages over a 21-day period, these processes are still only partly characterized. In fact, there is a dearth in the literature relative to the dynamics of differentiation [40]. The simple hypothetical differentiation models which have been described are based on the onset of average expression levels of genetic markers [41], [42] but in-depth morphological analyses of hMSC differentiation are missing [43]–[45].

A major difficulty of studying hMSC differentiation is the intrinsic variability in these cells. Moreover, heterogeneous SC populations are likely asynchronous [46], i.e. comprised of cells at different developmental stages. Consequently, standard “population-averaging” assays [45], [47] may not offer suitable levels of analysis and control over the differentiation process. State-of-the art microscopic imaging and quantification methods, on the other hand, can now be applied to further resolve the dynamics of differentiation and provide rigorous analysis of differentiation biomarkers [46]. Recent technological developments may further permit real-time monitoring and dynamic culturing environments to be devised in a near future.

Many of these developments have roots in the field of Mechanobiology, which has experienced notable traction in the scientific community during the past decade.

1.2. Mechanobiology – how mechanical stimuli direct cell behaviour

1.2.1 Onset of Mechanobiology in TE

Mechanobiology, the study of the mechanical impact of extracellular environments on cell behaviour, has recently come into focus as a key area of TE research interest. The capacity of the external milieu, in particular the ECM, to mechanically impact cell behaviours was first recognised, to lesser extent, when biomechanical studies demonstrated that mechanical stimulation was crucial in the growth, functioning and maintenance of several tissues at a macroscopic level [48], [49]. The development and homeostatic balance of the musculoskeletal, circulatory, respiratory, auditory and integumentary systems are dependent on the dynamic loading conditions that the body is subjected to [50]. This relationship is evident in medical disorders with mechanical aetiologies. For instance, bone mass is lost due to stress shielding caused by metallic hip implants [51] and disturbances in blood flow can give rise to hyperplasia or thrombosis [52]. Of note, atherosclerotic plaques form upon persistent inflammation of inner blood vessel lining [53], preferentially occurring in or regions with disturbed blood flow (e.g. bifurcations and curvatures). Interestingly, the mechanical properties of cancerous tissues are also altered relative to healthy tissues, which conditions tumour progression [54].

In recent years, it has become increasingly evident that many of these macroscopic events are rooted on parallel phenomena at the cellular level. This realization has come about, in part, due to growing multidisciplinary crosstalk. Intersections between Cellular and Molecular Biology and Biophysics have created new analytical instruments and quantitative methods for assessing the cell state, including biological image analysis, traction force microscopy and atomic force microscopy (AFM). The emergence of new biomaterials and microfabrication techniques have also majorly contributed to Mechanobiology. Versatile biomaterials allow researchers to model different aspects of cellular niches and provide simple platforms for probing the intricate relations between cells and their surrounding environment [49].

Growing interest in Mechanobiology derived from the realization that ECM mechanics act as fundamental mediators of cell behaviour. The convention that cells mostly respond to biochemical signals has changed, and it is now established that mechanical inputs can be equally important stimuli in the control of cellular responses [48]. The connections between ECM stiffness, recruitment of actomyosin contractile machinery and cell adhesion were cornerstones in Mechanobiology research [55]. During 2006, a seminal study [11] evidenced that MSCs can be committed into osteogenic, myogenic and neurogenic differentiation by matching the stiffness of collagen-coated polyacrylamide (PAA) scaffolds to the rigidities found in corresponding native tissues (i.e. bone stroma, muscle and brain). Thus, on the absence of additional biochemical stimuli, soft hydrogels (stiffness < 1 kPa) were associated with neurogenic commitment of MSCs, while increasing hydrogel substrate stiffness to 20 kPa and 40 kPa, respectively originated cells from the muscle and bone developmental lineages. The authors likewise correlated this process with focal adhesion formation and Non-Muscle Myosin (NMM) II induced contractility.

These results validated the study of cell-ECM interactions as a novel way of inducing and controlling SC differentiation. New possibilities in biological and translational research were unveiled, and the number of publications under the topic of Mechanobiology became more prevalent in the past decade [48]. Some of this excitement can perhaps be attributed to the intrinsic multidisciplinary of the subject which has benefited from the collaborative expertise of biologists, physicists, engineers and material scientists.

These increments in mechanobiological knowledge have resulted in refined approaches to TE [56], with classical approaches (based on biochemical differentiation factors) having been supplemented by the additional layers of precise control offered in the manipulation of extracellular mechanical environments [57], [58].

1.2.2 Molecular processes in mechanobiological pathways

Despite intensive research, the extensive network of molecular pathways that govern mechanobiology processes is still not completely understood. The mechanisms of mechanobiology coordinate substrate adhesion, mechanical probing of the extracellular environment, and subsequent growth, migration and cell division [59]. Yet, a cohesive view of sensing and response mechanisms to passive and active forces in the cell is still lacking.

Molecular Biology dictates that cells consist of intricate and dynamic networks of biochemical reactions mediated by enzymes, in the context of extracellular environments. In conventional signalling pathways, soluble biochemical factors interact with cell surface receptors, generating signals which are amplified by phosphorylation cascades. These cascades ultimately coalesce in the nucleus, regulating the activation and localisation of transcriptional factors that control gene expression.

In mechanotransduction, it is the biophysical features of the extracellular environment/ forces acting on the cell, which are converted (transduced) into biochemical signals and propagated by signalling cascades [12], [60]. The discovery of mechanotransduction pathways has helped complement the models of several biochemical pathways [61], comprised new ways to modulate cellular fate, and helped identify novel targets for pharmaceutical intervention [59], [61].

A lot of information on mechanotransduction has been accrued over the past two decades, allowing the development of models to broadly explain biophysical changes in cells [61], [62]. According to some of these models, the process of mechanotransduction can be divided into three interrelated stages: 1) sensing of mechanical signals, 2) transmission through the cytosol, and 3) activation of biological responses altering cell morphology and behaviour. Each of these stages is associated with a set of molecular machinery which will be briefly addressed in the following subsections.

1) Mechanosensing and integrins

Mechanosensing is attributed to complexes of macromolecules which change conformation and/or binding affinities when subjected to forces. In cells, the cytoskeleton is responsible for many of the forces generated and transmitted across individual cells [63]. Cellular contractility is influenced by external factors, such as fluid flow, or compression/tension stimuli [60]. NMM II-independent forces can also be responsible for mechanosensing by, for instance, regulating new adhesion assembly and controlling cell spreading [64]. Force sensing and transmission thus guide several processes, such as morphological changes, or the degree of tension sustained on ECMs. Biophysical behaviours such as these play an important role in cell adhesion, migration and division.

The most studied mechanosensors in mechanobiology are focal adhesions (FAs). FAs are protein complexes (Fig 1.3) organised around transmembrane receptors called integrins [62]. Integrins recognize and clutch to peptide sequences in the ECM, establishing spatially restricted linkages to auxiliary proteins in the cytosol. Some of these proteins, such as talin, vinculin or α-actinin, serve structural roles; whereas others, like focal adhesion kinases (FAKs) or the proto-oncogene tyrosine-protein kinase Src, phosphorylate protein partners, propagating signalling cascades [59]. Of note, Talin [65] and Vinculin [66] also serve important signalling roles.

The complexity of FAs is patent in the number of molecular combinations which can be formed out of hundreds of elements [62], [67]. Of these, around 20 are integrin homologs displaying diverse affinities for peptide sequences in ECM proteins, including collagen, fibronectin, laminin or vitronectin [68]. The arginine-glycine-aspartate (RGD) peptide sequence is the most studied adhesion ligand, marking the attachment site of nearly half of known integrins [69]. These peptides also promote cell attachment when functionalized onto a substrate, and are often used as anchoring moieties in TE scaffolds [70].

a)

b)

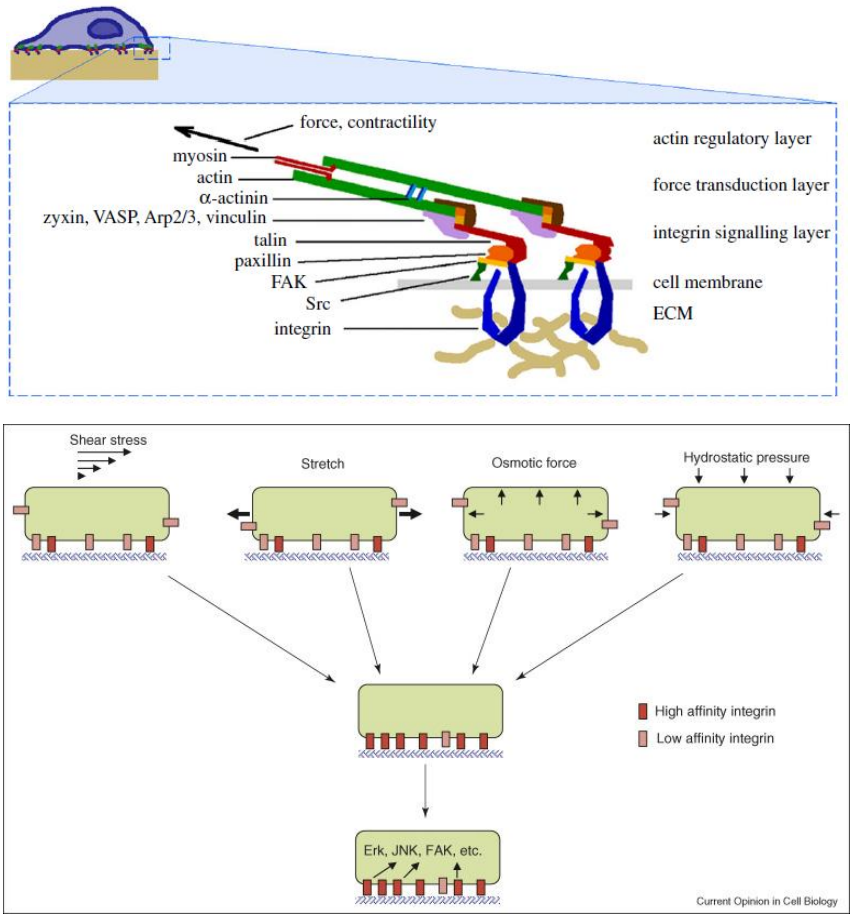

Figure 1-3 – Structure of a focal adhesion and mechanotransduction – a) Schematics illustrating structural levels in FAs. Integrins link the complexes to the ECM, and intracellularly recruit auxiliary proteins. These serve diverse functions, from structural reinforcement, to biochemical signal generation and propagation. The distal end is then connected to the actin cytoskeleton to allow for a bidirectional communication between cells and their environments. Adapted from [62]**; b) Illustration of focal adhesion maturation and activation of signalling pathways in response to forces acting on a cell. Adapted from** [71]**.**

FAs are dynamic molecular complexes [12], [61]. For instance, increases in cell tension, among other factors, may cause nascent adhesions, made up of few integrins, to be reinforced by positive feed-back loops, to mature into FAs [72]. FA maturation equally results in increased cell traction, so that mechanotransduction can be seen as a bidirectional process between

cells and their surroundings [73], [74]. Furthermore, even in apparently static FAs there is continued protein turnover.

It should be noted that there are further mechanosensory elements of relevance in the cells. Cell-cell junctions and force activated channels are two examples which may be as important as FAs in the context of mechanotransduction [75]. However, the mechanical role of these elements remains comparatively under-characterised.

2) Mechanotransmission and the cytoskeleton

For mechanosensing to produce downstream effects, mechanotransducers must be coupled to internal “circuitry” that can propagate and direct the signal to effector molecules (e.g. transcription factors), a role fulfilled by mechanotransmitters [61]. The principal structure in mechanotransmission is the cytoskeleton, a network of protein fibres which allow forces to be propagated from the point of application to distal structures inside a cell [12]. As the name implies the cytoskeleton works as a cellular skeleton analogue, conferring mechanical integrity, dictating cell morphology and mediating cell motility, as well as participating in cell division, cytosol organisation and transport processes [61]. The structures that make up the cytoskeleton are extremely dynamic, being subjected to constant remodelling as cells probe their surroundings.

The cytoskeleton is composed of three classes of filaments: microtubules (MTs) of tubulin, multiple types of intermediate filaments (IFs), and microfilaments (MFs) built out of actin monomers (Fig 1.4). These different fibres serve complementary functions and therefore present distinctive properties and behaviours.

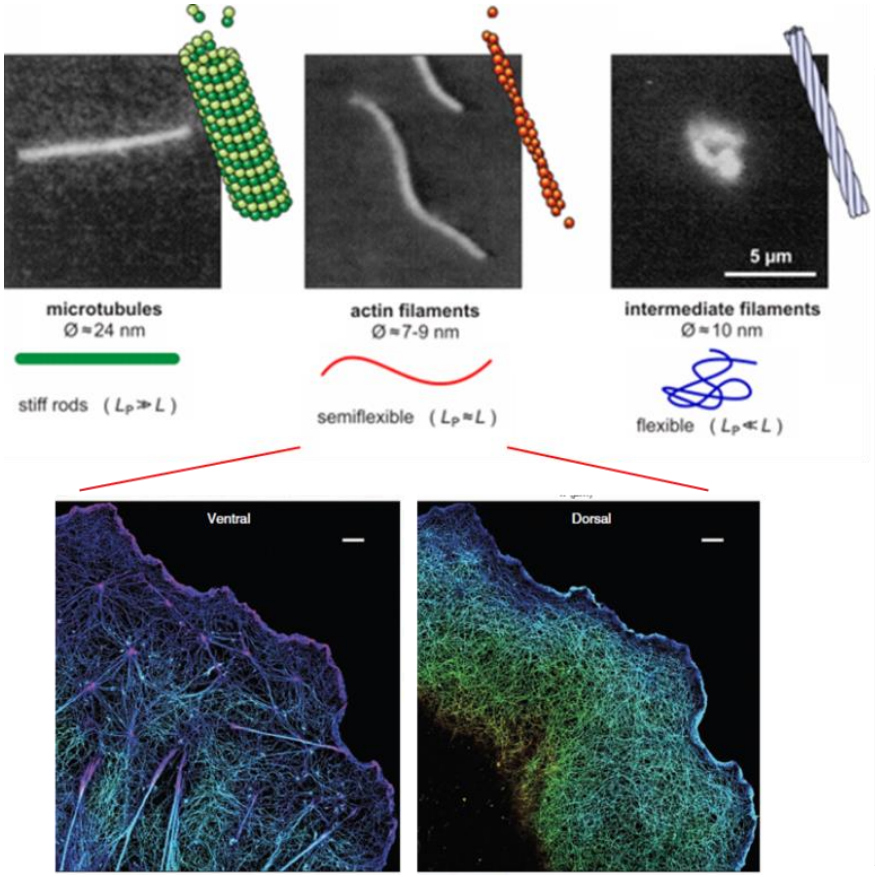

Figure 1-4 – Cytoskeleton elements and detailed structure – Microscopic images and schematic representations of cytoskeleton filaments (Upper panels); Super resolution microscopy image of actin networks in ventral and dorsal planes (Lower planes). Adapted from [76] **and** [77]**.**

MTs are hollow rods composed of globular tubulin dimers. The metabolic roles of MTs in organelle transport and support of cell polarity, mitosis and migration are well-established. These cytoskeleton elements also intervene in mechanobiology. For instance, MT networks have been shown to provide a significant role in the maintenance of cell shape and structure in 3D fibrous networks [78], [79], while seemingly assuming a secondary role in 2D substrates [78]. For this reason, and the relatively minor attention dedicated to these structures in mesenchymal stem cell differentiation [80], the work described on this thesis did not focus on MTs.

IFs are the second cytoskeleton element, serving important structural functions by reinforcing cells against mechanical exertion and intervening in the control of cell stiffness [61]. As with MTs, many IFs have not been exhaustively investigated in mechanotransmission. One exception is that of

lamins, a class of IFs encased in the nucleus, which exist in close association with other auxiliary proteins and the inner nuclear envelope membrane. The dense fibrillar structure formed by lamins and lamin-associated proteins is called the lamina. This structure is a crucial mechanotransmitter [81] linking mechanical stimuli to the nucleus and mediating molecular interactions with binding partners such as actin, emerin or heterochromatin DNA. Vertebrate somatic cells mainly express two lamin families: A-lamins and B-lamins, the relative expression of which confer distinct mechanical properties to the nucleus [82]. Interestingly, lamina composition was shown to scale with tissue stiffness [83]: B-type lamins being over-represented in the nuclei of soft-tissue cells, whereas nuclei in stiff/stressed tissues tend to be dominated by A-type lamins that confer shock-absorbing properties to the nucleus. Lamin expression has equally been found to influence matrix-directed SC differentiation [82].

MFs, the last class of cytoskeleton elements, are the most intensively studied in the context of Mechanobiology [62]. Actin fibres, jointly referred to as F-actin, are assembled from the non-covalent polymerization of globular actin monomers, or G-actin. Individual MFs consist of two actin strands twisted into a helix with asymmetrical ends, a barbed (+) end where net addition of monomers occurs, and a more inert pointed (-) end. The polymerization of actin, as well as the branching of filaments, are directed by nucleation factors, such as formins or the Arp 2/3 complex [84]. Moreover, a large array of actin-binding proteins, controlling elongation and disassembly, along with nucleation of MFs, mutually direct the architecture of actin into complex highly dynamic polymer networks. Precise regulation of these structures is essential to cell activity [85], e.g. coordinated polymerization of actin filaments at the cell edge is responsible for membrane protrusions during migration and morphogenesis, and for the formation of plasma membrane invaginations in intracellular transport phenomena [86].

MFs are associated with the motor protein NMM II. ATP-driven movement of NMM II domains along MFs result in the generation of forces that contract the actomyosin bundle. Consequently, actomyosin machinery is the driver of tension and cell contractility, two key points in mechanotransmission.

Cytoskeletal tension drives cell shape and serves a pivotal role in SC lineage commitment [38].

Some of the structures comprised by actin assembly include filopodia, lamellipodia, the cell cortex and stress fibres (Fig. 1.5).

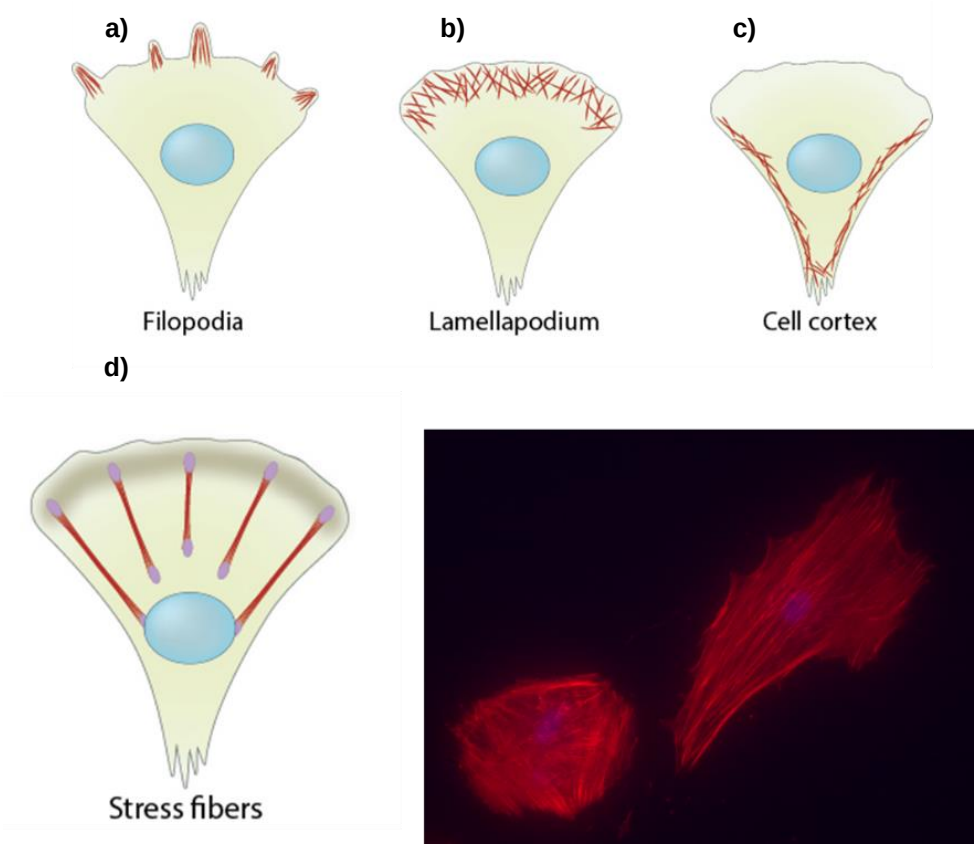

Figure 1-5 – Examples of prevalent actin structures– a) Filopodia; b) Lamellipodium; c) Cortical actin; d) Stress fibre schematics and fluorescent image illustrating phalloidin-TRITC labelled stress fibres in hMSCs. Adapted from [87]**.**

Filopodia are phalange-like projections, while lamellipodia are quasi-two-dimensional networks situated beneath the leading edge of migratory cells. Both structures are involved in environmental sensing and motility. In contrast, the cell cortex is a layer of contractile actin and Myosin underlying the inner surface of the plasma membrane. Apart from its structural role, the cortex is implicated in modulating membrane and cell surface receptor organization. Ezrin, radixin, and moesin, collectively known as the ERM protein family, are responsible for crosslinking MFs with apical transmembrane proteins.

Stress fibres are highly prominent contractile actin bundles found in substrate adherent cells, composed of 10-30 MFs in association with NNM II, tropomyosin, and crosslinkers such as α-actinin [62]. These structures are often anchored to FAs, thereby assuming a central role in cell adhesion [38], morphogenesis [72] and responses to mechanical loading [88]. As such, stress fibres are fundamental not only in the propagation of loads throughout the cell but also in eliciting mechanoresponses, described in the following section.

There are several drugs that disrupt MF dynamics, such as polymerisation inhibitors, including latrunculin A and cytochalasin. Conversely, jasplakinolide promotes polymerisation and stabilises F-actin. There are also molecules that indirectly act on MF assembly via changes to cell contractility, such as the ROCK inhibitor Y-27632.

3) Mechanoresponse and gene expression

Apart from sensors for transduction, and transmitters for conductance of mechanical signals, these stimuli need effectors to promote a response. FAs and cytoskeletal components can act as mechanoresponders when their properties are altered due to mechanical inputs being integrated into mechanotransduction feedback loops (Fig 1.6) [61]. For instance, FA maturation and reinforcement occurs in response to applied forces (Fig. 1.6 a), or to the intracellular tension generated in a stiff substrate. When stress fibres transmit an optimal level of mechanical force to FAs, conformation of mechanosensitive proteins, such as β-integrin [89] or talin [90] can be altered, revealing cryptic binding sites, and increasing their affinity for structural, signalling and adaptor proteins. The recruitment of these auxiliary proteins, in turn, further strengthens the FA complex and cytoskeleton linkages [60]. Conversely, inhibition of NMM II contractility leads to a decrease in FA size.

Mechanoresponses involve the convergence of mechanobiological and surface receptor pathways (Fig. 1.6 b). Many signalling cascades can be activated by mechanosensors and growth factor receptors alike, influencing actomyosin machinery and FA formation. For instance, contraction of stress fibres is regulated by a Ca2+-dependent calmodulin/myosin light chain kinase

pathways or by Ca^{2+}-independent Ras homology-kinase systems through the phosphorylation of Myosin light chain [62]. Mechanotransduction thus feeds into the complex network of molecular events that govern cell responses.

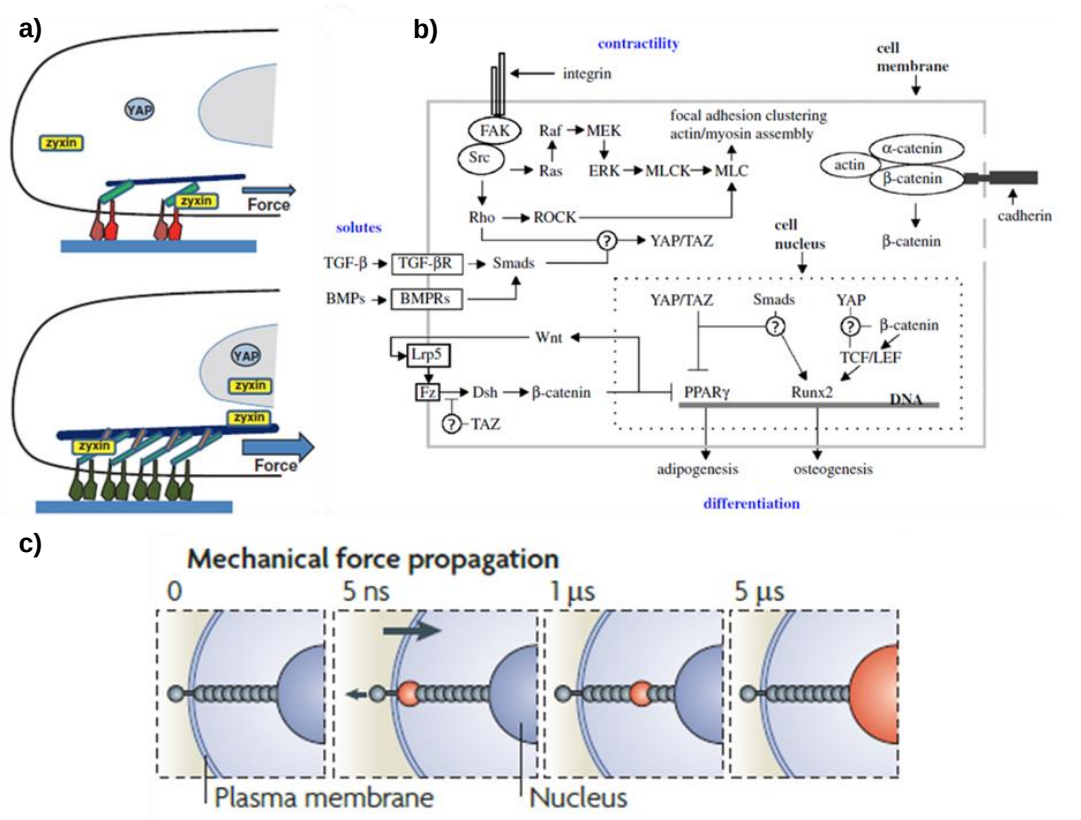

Figure 1-6 – Mechanoresponse pathways – Schematics of feedback mechanisms and mechanoresponses. a) Mechanical stimuli reinforce FAs by actin mediated contraction resulting in either: b) the generation of phosphorylation cascades and nuclear translocation of transcription factors like YAP/TAZ, or c) direct propagation of forces to the nucleus by the association of actin with LINC - forces applied to cytoskeleton-linked integrins propagate into the nucleus in <5 µs. The red dot indicates the transmitted mechanical signal reaching the nucleus. For comparison, biochemical signal propagating through receptor second-messenger systems take seconds to reach the nucleus. Adapted from [60], [62], [91].

Depending on the inputs of the cellular environment and the current cell state, the net effect of competing pathways will converge downstream at the nuclear level, where DNA transcription is controlled, resulting in the modulation of gene expression and changes in cell behaviour.

The propagation of biochemical and mechanical signals into the nucleus can be divided into two types.

The first of these is made up by signalling cascades, relying on protein kinase mediated phosphorylation and secondary messengers. These pathways generally culminate in nuclear translocation/activation of transcription factors and alterations to chromatin organisation, modifying gene expression.

The effectors of the Hippo pathway tumor suppressor yes-associated protein (YAP) and transcriptional co-activator with PDZ-binding motif (TAZ) are powerful regulators of cell proliferation and survival, playing important roles in the control of organ growth, stem cell self-renewal and cell differentiation [92], [93]. YAP and TAZ shuttling between cytoplasm and nucleus is regulated by multiple inputs and signalling pathways, including the Hippo kinase cascade, Wnt signalling and G-protein coupled receptors. Accumulation/ ubiquitin-dependent degradation of YAP and TAZ in the cytoplasm is controlled by phosphorylation via LATS1/2 kinases, but the precise mechanisms are still not understood in depth [94]. Importantly, YAP and TAZ have recently gained attention in Mechanobiology due to their strong connection to substrate mediated cell growth, proliferation and differentiation [92], [93]. More concretely, several studies have found that increased cell spread area and contractility on rigid/non-confined substrata promoted the nuclear internalisation of YAP/TAZ, with ensuing osteogenic differentiation. Nuclear depletion of the transcription factors, on the other hand, occurred in softer/cell area limiting scaffolds and preferentially lead to adipogenesis. Due to their roles in substrate stiffness regulated SC differentiation, YAP and TAZ are now important markers in the study of Mechanobiology [93]. However, the newly identified mechano-related YAP/TAZ pathways remain particularly obscure, requiring continued study.

In contrast, a second type of mechanoresponse is thought to be direct and instantaneous [91] (Fig 1.5 c). The direct force transmission model suggests that the cell surface is mechanically coupled to the nucleus through the actin cytoskeleton, and that external loads can directly distort nuclear shape and influence chromatin organisation [95]. The lamina plays an instrumental part in this mechanism, along with the actin cytoskeleton, intermediate filaments, and the linker of nucleoskeleton and cytoskeleton (LINC) complex [91]. Surprising new findings have further suggested that force

transmission to the nucleus might drive nuclear YAP internalization by stretch induced nuclear pore complex relaxation [96].

Fig 1.5b provides a simplified “global” view of how mechanotransduction and biochemical pathways might direct hMSC differentiation in a series of interrelated steps. This schematic shows two types of mechanosensors, namely FAs and cell-cell junctions, allowing cells to integrate mechanical stimuli through the cytoskeleton. Soluble growth factors are equally shown binding with transmembrane receptors on the cell surface. These signals initiate a range of biochemical pathways activated by phosphorylation cascades. For instance, build-up of tension on FAs leads to the phosphorylation of FAK/Src kinases, which propagate the signal into MLC, feeding into a forward loop that stimulates FA maturation and further increases cell tension. This loop results in YAP/TAZ nuclear internalisation, promoting Runx2 expression and osteogenic differentiation. Simultaneously, wingless pathway activation, and N-cadherin in cell junctions, regulate β-catenin nuclear translocation, which silences PPARγ and upregulates Runx2. Finally, transforming growth factor/bone morphogenic protein (BMP) receptors activate Smad, resulting in preferential expression of genes associated with osteogenesis and chondrogenesis. Conversely, exposure to adipogenic induction supplements, or lack of cell contractility, preferentially result in recruitment of transcription factors that upregulate PPARγ expression, and adipogenesis.

Although this is a simplified view of a limited subset of the pathways mediating cell behaviour, it nevertheless serves to illustrate how mechanical sensitivity arises from a diverse and complementary set of mechanical and biochemical phenomena. This extensive set of feedback loops and complementary/competing processes is integrated into complex gene expression patterns which ultimately dictate mechanobiological responses in cells.

1.3 hMSC differentiation is influenced by a complex interplay of mechanical factors

1.3.1 The influence of mechanical stimuli on MSC differentiation

Mechanobiology research has shown that mechanical, chemical and topological cues can direct cell shape and function. This research has been based on the development of a wide range of polymeric scaffolds to assay the relationship between biophysical environments and biological processes (Fig 1.7). Most of these studies have been conducted on two-dimensional (2D) cell culture substrates, which are artificial in relation to three-dimensional (3D) niches *in vivo*.

Nonetheless, 2D substrates have been instrumental in elucidating the impact of distinct biophysical features in directing SC differentiation. Examples of major research findings in 2D hydrogels are presented in subsections 1.3.2 to 1.3.6. A transition towards more realistic 3D systems is also currently taking place, as it becomes more evident that dimensionally is an important factor in the interactions between cells and their surroundings. The topic of substrate dimensionality is briefly addressed in section 1.3.7. Finally, emerging research on the effects of non-linear properties of the extracellular environment on differentiation are presented in section 1.3.8.

1.3.2 Bulk substrate stiffness

As the foremost SC differentiation factor in the seminal article by Engler *et al*. [11], substrate stiffness has been the focus of a wide number of follow-up studies.

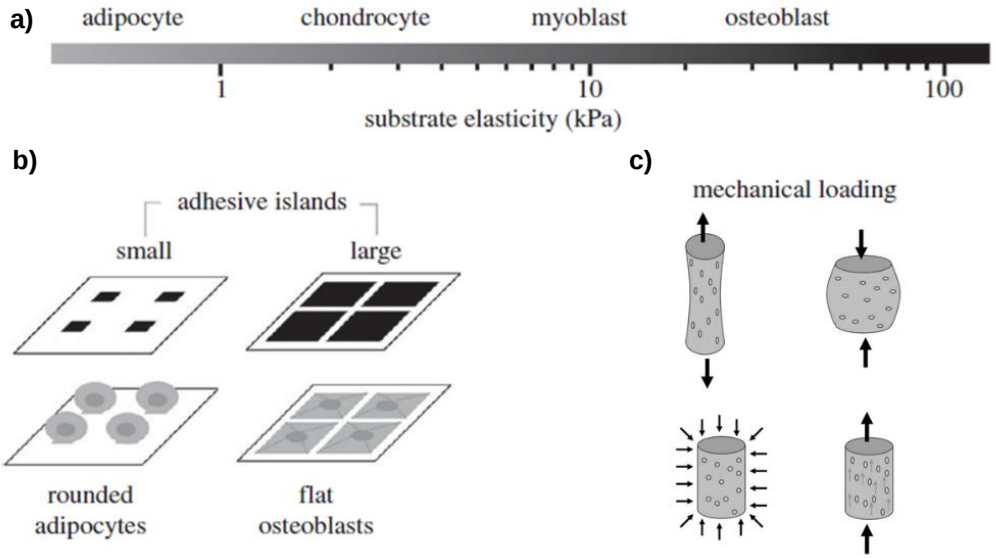

Figure 1-7 – Examples of biophysical properties influencing hMSC mechanobiology – a) Tissue stiffness range reproduced in multiple studies for control of MSC differentiation; b) 2D adhesive ligand islands used for regulation of cell shape and spread area; c) Several scaffold loading modalities (traction, compression, hydrostatic pressure and fluid flow) for studying the effect of applied forces on cells. Adapted from [62], [97]**.**

The stiffness of materials is a property describing resistance to deformation in response to applied forces. Young's modulus (**E**) is a commonly used size-independent measure of stiffness, communicated in the units of pressure, N/m^2 or Pa. In linear-elastic materials it is straightforward to estimate this value by subjecting a sample of the material to compression or tension in specialized mechanical loading rigs. **E** is then calculated as the ratio between stress ($\sigma = \frac{F}{A}$, acting force normalized by the area of application) and strain ($\epsilon = \frac{\Delta l}{lo}$, the resulting percent change along the axis of an initial dimension lo), or $\boldsymbol{E} = \frac{\sigma}{\epsilon}$. Idealised linear-elastic materials have constant **E**. In these materials, elastic deformations are completely reversed upon removal of actuating forces.

Biological materials rarely behave like purely linear-elastic solids, which creates difficulties in mechanical characterisation [48]. Furthermore, a range of different techniques has routinely been used to describe the mechanical properties of biomaterial substrates. Examples include AFM nanoindentation,

macroscopic rheology and compression tests. The lack of established measurement standards hinders comparison between studies and across techniques [98]–[100]. Nonetheless, despite potential discrepancies, past publications have withdrawn general conclusions about the impact of bulk substrate stiffness on differentiation.

Fu et al. [101] used elastomeric arrays of polydimethylsiloxane (PDMS) microposts to separate the effects of substrate rigidity from conflicting properties, such as ligand density and substrate porosity. These authors modulated stiffness by tailoring micropost height: long pillars were easily deformed by the cells, mimicking a soft environment; whereas shorter posts resisted bending, behaving as stiff materials. It was observed that increased rigidity promoted hMSC spread, stress fibre development and FA maturation. Conversely, soft micropillars produced round morphologies with reduced actin cytoskeleton and FA formation. The correlation between cell spread area, FA formation and traction force build-up evidenced that these properties are instrumental in rigidity sensing. Interestingly, this study contrasted with previous reports [11], as it found that substrate compliance was not sufficient to induce differentiation. Supplementation with bipotential differentiation media was necessary to allow cells to preferentially differentiate into osteoblasts in rigid microposts, or into adipocytes in softer microposts. Moreover, the authors detected a correlation between development of traction forces and differentiation fate. Traction forces at differing rigidities diverged from the onset of differentiation. Based on this observation, the authors proposed the existence of a window of early cytoskeletal responses and confirmed predictive power in the data using a simple Naive Bayes classifier.

Dynamic modulation of stiffness has also provided valuable insights into hMSC differentiation. One critical hypothesis emerging from these studies is that mechanical dosing can influence long-term cell fate [31]. In a pivotal report, it was shown that culture in even moderately stiff environments (10 kPa hydrogels) can mediate the transport of YAP/TAZ into hMSC nuclei and activate the preferential expression of Runx2/osteogenesis, downregulating PPARγ/adipogenesis. Moreover, by subsequently transferring cells from TCP into soft hydrogels, or by using photodegradable polyethylene glycol (PEG) to

soften substrates from 10 kPa down to 2 kPa, it was shown that persistent gene expression was a function of the duration of mechanical priming. Effects of short-term culture (less than a week) on stiff substrates were reversible within a few days. On the other hand, mechanical priming beyond 10 days caused irreversible YAP nuclear translocation and Runx2 upregulation. Thus, it was suggested that hMSCs possess a “mechanical memory” capable of retaining information from past environments and influencing cell fate decisions. This memory was suggested to be regulated by YAP/TAZ acting as mechanical rheostats through nuclear internalisation and persistence.

Burdick and Guvendiren [102] reported on short and long-term cell responses to stiffening substrates in the 3 to 30 kPa range. With the requirement of bipotential differentiation media, these authors found that adipogenic differentiation is favoured the longer cells are kept on softer substrates before light-triggered induction of hydrogel stiffening. In contrast, osteogenic differentiation was promoted by stiffening at earlier times. As expected, hydrogel stiffening at an intermediate time-point produced mixed populations of adipogenic and osteogenic cells. The authors related this observation to hMSC heterogeneity, with pre-committed cells being unresponsive to substrate change. Kilian et al. [103] produced a similar report, exploring a bidirectional change in hydrogel stiffness from soft (0.5 kPA) to stiff (40 kPa), and vice-versa. As expected, after 10 days of culture on stiff substrates, hMSCs displayed osteogenic traits while cells on very soft substrates exhibited neuronal like phenotype, supporting Engler *et al*.’s findings [11]. After this initial period, hMSCs were transferred to hydrogels of opposite compliance and cultured for an additional time. Neurogenic markers in cells from initially soft conditions decreased relative to osteogenesis markers. Osteogenic markers, in turn, reached levels comparable to those of persistent culture on stiffer hydrogels. In contrast, hMSCs first cultured on stiff substrates showed a modest decrease of osteogenic markers on softer substrates, in agreement with the “mechanical memory” theory set by Anseth et al. [31]. The authors further coupled geometrical confinement to substrate stiffness, to illustrate that controlling cell shape can further influence lineage outcome even upon microenvironmental switches.

As a final example, it can be mentioned that coupling biochemical supplements with substrate stiffness can enhance the modulation of cell behaviour. Durrieu *et al*. [104] separately grafted BMP 2 mimetic peptides and RGD peptides onto PAA/polyacrylic acid substrates. These authors again found that intermediate stiffness (~15 kPa) lead to myogenic differentiation, whereas higher stiffness (~45 kPa) promoted osteogenesis in the absence of BMP. However, when adhesion moieties were substituted by the growth factor mimic, osteoblasts replaced myoblasts in cultures of intermediate stiffness and differentiation was inhibited in very soft gels (~1 kPa). These results suggest that the effects of stiffness on MSC differentiation should be interpreted in the biochemical context of each environment.

1.3.3 Adhesive ligands and fibrillar configuration

In order to attach and apply traction forces to substrates, cells must develop anchorage points. As such, it is often necessary to crosslink substrates with attachment moieties or to coat them with ECM proteins. However, it has been difficult to decouple the effects of ligands from bulk substrate stiffness because both properties can indirectly influence each other.

Two articles have recently examined the interplay between ligand spacing and stiffness in controlling SC fates. The first publication, by Trappmann *et al*. [105], studied the impact of collagen coated PDMS and PAA stiffness on keratinocytes and hMSCs. It was found that cell area and differentiation were independent of stiffness in PDMS substrates, but not on PAA gels. The authors used these observations to rule out bulk stiffness as the principal differentiation stimulus in 2D substrates. The alternative model proposed by the authors was based on the inverse relationship between substrate stiffness and surface porosity, i.e. soft PAA hydrogels have larger pore sizes, whereas pore size decreases in stiffer PAA. According to the authors, alterations in surface porosity influence the spatial tethering of the overlaying collagen fibres. Long, easily deformable, fibre tethers are originated in soft PAA, while smaller tethers in stiffer hydrogels resist deformation. Thus, it was suggested that cell behaviour is mediated by mechanical properties of

differently crosslinked fibres on substrate surfaces, rather than by bulk substrate stiffness.

This model was contested in a subsequent reference by Adam Englers's group [100] showing that formulations of PAA varying in porosity but maintaining constant stiffness (of 4, 13 and 30 kPa), did not significantly change protein tethering, substrate deformation, or the osteogenic/adipogenic propensity of hMSCs. The authors further sought to rule out tethering effects by changing collagen/crosslinker densities, integrating RGD peptides directly into PAA and by re-assessing the mechanical constitution of PDMS substrates and their effects on hMSCs. The results in this publication substantiated the role of 2D bulk stiffness on differentiation induction, independently of tethering effects and porosity. The disparity between the two reports clearly underlines the difficulties in isolating the mechanical effects of interdependent substrate properties [106].

More straightforward investigations of ligand/biomaterial combinations have also been conducted. As an example, Rowlands *et al*. [107] investigated the effect of 16 hydrogel stiffness/ligand combinations in directing MSC osteogenic and myogenic differentiation. The authors crosslinked collagen types I and IV, as well as laminin and fibronectin into hydrogels of stiffness ranging between 1 to 80 kPa. Osteogenic differentiation occurred prominently on collagen I-coated gels with the highest **E**, while myogenic differentiation was detected to varying extents on all substrates surpassing 9 kPa, with peak myogenic marker expression occurring on 25 kPa fibronectin-coated hydrogels. The same group published a comprehensive analysis of integrin expression during hMSC differentiation [68] using block co-polymer surfaces and tailored substrates to present the cell with short peptides of known integrin specificity. In this report, hMSCs displayed distinct morphologies according to different adhesion motifs, and the highest rates of both osteo- and adipogenic induction happened in surfaces displaying the laminin-derived peptide IKVAV.

Ligand spacing has also been shown to be a determinant factor in controlling cell morphology. In a 2007 study [108], J.S Spatz's group investigated the effects of lateral clustering on integrin function. To do so, the authors produced nanoscale variations in the spacing between adhesive RGD ligands on a hard nanopatterned substrate, and studied their effects on cell

spreading, migration, and focal adhesion dynamics. Critically, the authors found that the formation of stable FAs and persistent cell spreading was sensitive to ligand density, while the converse was true for cell attachment. Cells plated on a 108-nm-spaced pattern exhibited delayed spreading and more erratic motility compared to cells on a 58-nm pattern. Such findings suggested that an RGD density threshold is essential for integrin adhesion maturation, FA formation and efficient cell spreading. These findings have been expanded upon by many other research groups. For instance, more refined techniques combining molecular-scale nanolithography with site-selective biochemistry have allowed the creation of biomimetic arrays. These arrays provide individual protein binding sites, arranged in heterogeneous geometrical patterns. Shalom Wind's group used these arrays to explore how the geometric organization of RGD ligands affects cells [109]. Systematic variation of spacing, density, and cluster size of individual integrin binding sites revealed a dramatic increase in cell spreading when at least four liganded sites were spaced up to 60 nm apart. This threshold showed no dependence on global ligand density. As such the authors hypothesised the existence of a defined minimal stoichiometric/spatial adhesion unit.

In the subject of MSC differentiation, Wang et al. [110] evaluated the effect of controlling RGD ligand nanospacing from 40 to 125 nm. These results confirmed that cell spread is severely reduced if ligands are moved beyond a 70 nm threshold apart. Surprisingly, an incremental trend was observed in both osteogenic and adipogenic differentiation with augmented spacing, when the cells were supplemented with single lineage induction media. When mixed media was used, osteogenesis was favoured over adipogenesis, even in larger nanospacings. These results opposed well-established correlations between cell spread area and MSC differentiation, but the authors could not identify the precise cause of the discrepancy. This again evidences the difficulty in interpreting the effect of interrelated substrate features. Similarly, J. Cooper-White's group showed [111] that cells seeded on block co-polymers functionalised with RGD peptides with lateral spacing around 40 nm acquire larger morphologies and thicker stress fibres, than cells placed on larger ligand spacings (> 50 nm apart). In the latter case, the cells were smaller, presenting fewer stress fibres and an abundance of membrane protrusions. hMSC

differentiation was equally influenced as a function of these morphological changes.

More recently, the fibrillar properties of cell microenvironments have started to be recognised as critical features in mechanosensing, particularly in softer materials. Recently, Baker et al. [112] employed electrospinning of a synthetic polymer to produce substrates with tuneable individual fibre mechanics. In softer individual fibres the cells were able to remodel the microenvironment, dynamically increasing ligand density at the cell surface, thereby fostering FA formation and cell spreading, whereas harder fibres prevented these effects. This relationship was lost when the cells were seeded on bulk hydrogels formulated from the same material. The authors concluded that fibre recruitment serves a critical role in the cellular response to fibrous interfaces.

A related study reported that controlling the fibrillar microarchitecture of collagen gels can elicit different cellular responses [113]. In this report, the authors tailored both bulk collagen hydrogel stiffness and individual fibre stiffness by controlling gelation temperature and polymerisation times. It was found that short fibres with higher local stiffness, limited the transfer of cellular tractions to neighbouring fibres, whereas on softer microenvironments, hMSCs were able to recruit local fibres and induce long-range deformations in the collagen network, increasing local collagen density. These rearrangements promoted cell spreading, proliferation and migration, and primed differentiation towards an osteoblastic fate.

Altogether, it is evident that the chemistry and fibrillar arrangement of ECM ligands are important factors in the study and modulation of SC Mechanobiology which should be carefully considered in the design of cell culture scaffolds.

1.3.4 Geometry and topography

Substrate geometry is dictated by parameters related to dimension and shape. A range of geometrical conditions have been exploited in past studies to condition hMSC behaviour.

McBeath *et al.* [38] reported that cell shape can preferentially drive hMSC differentiation into the adipogenic and osteogenic lineages. Single cells were seeded on fibronectin micropatterned PDMS and cultured in mixed induction media. Under these conditions, the authors observed that MSCs grown on restricted areas (~1000 μm^2) preferentially differentiated into adipocytes, while areas an order of magnitude larger promoted osteogenic fates (Fig 1.7). Furthermore, it was shown that these effects were dependent on the Rho A/ ROCK pathway, and therefore reliant on actin cytoskeleton tension.

The impact of shape on hMSC differentiation was also evidenced by Mrksich *et al*. [114] by culturing single cells in mixed media on fibronectin coated PDMS islands. These results again suggested that sharp perimeters eliciting contractility could promote the genesis of osteoblasts, while smooth shapes benefited adipogenesis and decreased NMM II contractility. Ding and coworkers further reiterated these findings with studies on the effects of shape [115] and aspect ratio [116] on MSCs, conducted on RGD islands imprinted on non-fouling PEG hydrogels. These authors again reported that circular shapes preferentially induce adipogenesis, while the anisotropy conferred by higher single-cell cell aspect ratios resulted in the promotion of osteogenesis, even in the absence of differentiation factors.

In addition to geometry, the topography of substrates is an important factor which can also be tailored to drive SC differentiation. One of the most relevant articles to state the importance of topographical features was published on 2007 by Dalby et al. [117]. By embossing five different patterns of nanopits into polymethylmethacrylate, the authors were able to alter hMSC morphology, observing a shift in differentiation dynamics in the absence of differentiation supplements. Highly ordered nanotopographies produced low cellular adhesion and poor osteogenic induction. Cells on random nanotopographies exhibited a more osteoblastic morphology after two weeks, but limited expression of late differentiation markers. Critically, topographies built from randomly displacing nanopits around an initially regular template, were able to enhance osteogenic behaviour in both MSCs and osteoprogenitor cells.

A number of studies have addressed the effect of ridges and grooves in MSC differentiation. Recently, Abgnale et al. [118] tested 25 combinations of micropatterns in polyimide and found that 15 μm ridges increased adipogenic differentiation, whereas 2 μm ridges enhanced osteogenic differentiation. The authors then studied the effects of cells in nanopatterns 600 μm in diameter with 200 nm deep grooves at a regular periodicity of 650 nm and found that both osteogenic and adipogenic lineages were induced by this topography, in comparison to unpatterned substrates. Additionally, it was found that the nanostructures did not affect YAP/TAZ states.

1.3.5 Seeding density

Cell density can influence a wide range of cellular processes. Cells can communicate via paracrine factors and cell-cell junctions, which has direct implications in SC differentiation. For instance, seeding cells as pellets is necessary for hMSC chondrogenic differentiation [33]. Similarly, adipogenic differentiation is substantially impacted by cell density, although the magnitude of effects varies between reports [38], [119].

Peng et al. [120] developed cell-adhesive micro-islands to control MSC seeding density and cell size. Sole induction and mixed media induction led to small cells favouring adipogenic pathways, while larger cells preferentially underwent osteogenic differentiation. However, effects of cell density were harder to interpret and dependent on differentiation induction media. Whereas in sole induction, osteogenic differentiation was generally insensitive to cell density, the adipogenic lineage benefited from increased cell-cell contact. In co-induction media, however, osteoblast yield was outcompeted by adipogenesis in higher cell density, perhaps due to the constraining effects of seeding density on individual cell spread area. In a later report, the same group was able to observe the regular substrate stiffness/cell spread area/differentiation relationships when cells were sparsely seeded on RGD nanopatterned hydrogels but reported that this relationship was disrupted by seeding cells in confluence. Unexpectedly, the joint effects of high cell density and adipogenic differentiation medium yielded an increase in adipogenic differentiation in the stiffest substrates.

More recently, Cosgrove et al. [121] included both RGD and N-cadherin adhesive peptide motifs into hyaluronic acid hydrogels. The authors' results suggested that cadherin binding (mimicking cell-cell contacts) hampers YAP/TAZ nuclear internalisation at intermediate substrate stiffnesses (circa 10 kPa) and lowers the contractility state of cells, thus attenuating MSC mechanosensing.

Jointly, these results underscore the relative impact of cell-cell contacts on the complex interplay between biophysical substrate features and cell behaviour.

1.3.6 Direct application of forces

In addition to the physical and chemical aspects of substrate design, it is also possible to manipulate MSC fate through direct mechanical loading. In fact, the sensitivity of SCs to mechanical stress is fundamental in processes ranging from development, to tissue regeneration [122]. Cells can be directly manipulated with instruments like the AFM or laser tweezers, as well as subjected to macroscopic loads in specialised rigs. There are multiple parameters which can be tailored in these systems, including orientation of strain (uniaxial vs. multiaxial) [123] or magnitude, frequency and duration of load. Moreover, cells can be subjected to compression, tension or fluid shear in 2D or 3D matrices and membranes. Due to the sheer variety of loading conditions, it is difficult to generalize which stimuli preferentially modulate each of the MSC differentiation lineages.

One of the most emulated *in vivo* mechanical niches is articular cartilage. Typically, to promote chondrogenesis, MSCs are encapsulated into agarose, collagen or other biomaterial, and subjected to uniaxial compressive stress. It has been found that compressive forces induce the production of typical chondrocytic ECM proteins like collagen type II, aggrecan as well as chondrogenic-specific transcription factors [124]–[127].

A comparatively smaller number of reports have been published on the effects of loading and hydrostatic compression on osteogenesis. In one example, low hydrostatic compression was observed to promote osteogenesis in MSCs [128]. In another system, under the absence of external chemical

cues, MSCs were directed toward osteogenic differentiation with 10% cyclic compressive strains. Strains of 15% upregulated both chondrogenic and osteogenic markers, indicating an osteochondrogenic differentiation pathway [129]. In a final example, MSC osteogenic differentiation was enhanced by intermittent loading consisting of 2 hours of mechanical stimuli interspersed by 5-day intervals [130].

In contrast to compression, higher magnitudes of tensile loading seemingly favour myogenesis [131], [132] and tenogenesis [133], while osteogenesis has been shown to benefit from relatively lower magnitudes of tensile stress [134]. However, static stretching, as well as long-term continuous loading, has equally proven detrimental to differentiation under certain conditions [135]. Stretching has also been shown to inhibit adipogenesis [136] and is not generally favourable for chondrogenesis.

Finally, many studies on fluid shear stress have focused on osteogenic differentiation of MSCs, due to the fact that both osteoblasts and osteocytes (terminally differentiated bone cells) are sensitive to flows *in vitro* and *in vivo* [3]. Osteocytes are thought to act as orchestrators of bone remodelling through the regulation of both osteoclasts and osteoblasts. This regulation is likely dependent on mechanical signals in lacunocanalicular flows by cell mechanosensors – potentially, dendritic processes or specialised cilia [137]. Fluid flow also potentially enhances osteogenesis [138].

1.3.7 Dimensionality

The previous sections presented some of the major findings on the biophysical factors affecting MSC differentiation, mainly gathered from studies conducted in 2D substrates. However, most *in vivo* niches are 3D. As such, the study of mechanobiology has started to progress towards the evaluation of more complex environments.

<u>2.5D – A compromise between dimensions</u>

The transition of research from 2D to 3D presents several hindrances. The biomaterials for 3D studies must be selected based on permitting cell

encapsulation, and the added dimension often increases the difficulty of performing microscopic imaging. For instance, 2D hMSCs can reach up to 200 µm in length, adopting prominent stress fibres and distinctive morphologies, while in 3D environments the cells tend to adopt much smaller (~ 50 nm diameter) and rounded morphologies. Additionally, culturing cells in depth disperses them through different focal planes [139]. Imaging is therefore constrained by limited microscope objective working distances, particularly in higher magnification objectives (e.g. x40, x63) which can only focus hundreds of µm into the samples. As a result, cells in thick hydrogels (> 250 µm) cannot be imaged beyond the periphery of the material.

To address these difficulties, several authors have attempted to construct 2.5D hydrogel systems [140]–[142]. These systems consist on seeding cells in between two overlaying substrates. A bottom layer provides the initial substrate for cells to attach to, and a second layer is then deposited on top of the cells.

Rehfeldt *et al*. [142] reported that hMSCs react differently to 2D, 2.5D and 3D environments of differing bulk stiffness. When directly encapsulated into hyaluronic acid hydrogels, hMSCs adopted a spherical shape (apparent radius 20 µm) with a cortical actin cytoskeleton and no discernible stress fibres. The intensity of cortical actin was found to scale with 3D hydrogel elasticity. On 2.5D substrates, however, the authors confirmed that MSCs interacted with both substrates and that the cells adopted projected areas comparable to 2D substrates. Moreover, it was observed that in 2.5D mechanical response was mainly dependent on the stiffer hydrogel layer, irrespective of its position relative to the cells.

Seeding cells in-between 2D and 3D facilitates imaging and analysis of cell behaviour and is thus a valuable compromise in bridging the gap between these two environments.

The shift to 3D

Although the lessons gathered from 2D systems are of undisputable value, the initial shifts to 3D have demonstrated that the patterns found in 2D are not necessarily universal.

This conclusion is well exemplified in a report by Huebsch et al. [143] in which the authors encapsulated MSCs into RGD-functionalized 3D alginate gels. In similar findings to Engler et al.'s [11], it was observed that an intermediate stiffness of 10-30 kPa was osteoinductive. However, in stark contrast to previous 2D studies, differentiation was uncorrelated with cell morphology, depending instead on integrin binding and cell traction-mediated reorganization of adhesion ligands.

More recently, it was shown that 3D geometrical and topographical cues can also influence MSC differentiation. For instance, Wilhelm T.S. Huck's group added a third dimension to geometrical micropatterns and reported [144] that the interplay between chamber volume and geometry played a significant role in FA and stress fibre formation, nuclear state and MSC lineage commitment. Viswanathan *et al*. [145] demonstrated that internal 3D biomaterial interconnectivity, architecture and surface topology are important in mediating MSC differentiation potential.

Collectively, these results illustrate that despite the intensive research in 2D, a wider range of study possibilities remains relative to 3D substrates.

1.3.8 Non-linear substrate properties

Contrary to many synthetic polymers, the mechanical behaviour of most biological materials presents non-linear attributes (Fig. 1.8). However, the impact of non-linearity on cell morphology has only recently began to be researched. The three dynamic, non-linear-elastic properties discussed in this section are 1) viscoelasticity, 2) strain-stiffening and 3) degradability.

1) Viscoelasticity

Biological tissues are composite materials, consisting of cells imbued within ECM elements. These elements regularly demonstrate viscoelastic features which play important roles in tissue function.

Elasticity theory describes reversible solid deformations, usually modelled through linear relationships between stress and strain. Viscosity, on the other hand, is a property describing a fluid's resistance to flow. Viscosity

constants, therefore, relay the proportionality between shear stress and the resulting velocity gradients along a fluid. As the name implies, viscoelasticity describes the behaviour of materials displaying both elasticity and viscosity related phenomena.

Viscoelastic responses are time and frequency dependent. Typically, biopolymer viscoelasticity is studied at the microscopic level via rheological measurements, or uniaxial strain tests, but micro-characterisation modalities have also been developed [146].

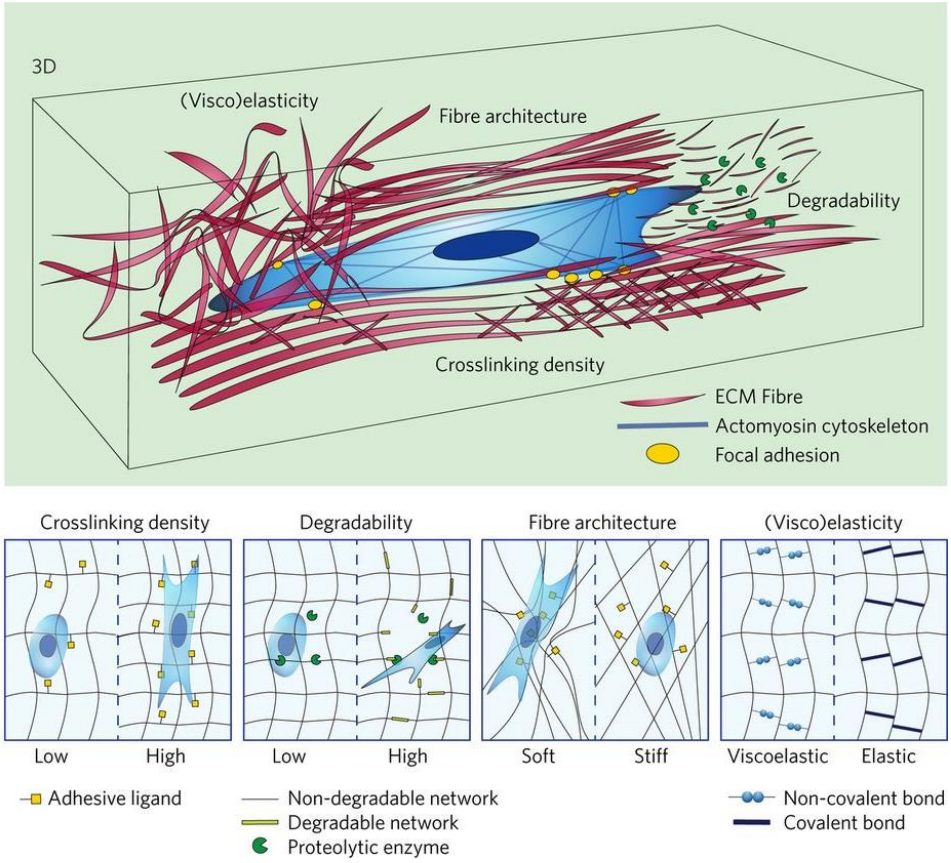

Figure 1-8 – Novel substrate properties in the study of hMSC differentiation – Illustration of dynamic biomaterials properties influencing differentiation: viscoelasticity, fibre architecture, crosslinking density and degradability may favour/hinder ECM rearrangements in 2D and 3D microenvironments. Adapted from [147]**.**

Uniaxial compression tests provide simple and swift examination of the mechanical properties of materials. To study viscoelastic properties under uniaxial loads, two time-dependent responses can be characterised – creep and stress relaxation. Fig. 1.9 a displays and example of creep, i.e. specimens

loaded with constant stress value σ0 experience subsequent increases in strain during application of static stress. Stress relaxation, schematised in Fig. 1.9 b, is analogous to creep. In this case, the material is subjected to a constant strain ε0, and decreases in specimen stress are tracked. These decreases correspond to stress relaxation in the material. In the absence of creep or stress relaxation, purely elastic materials retain constant amounts of both stress and strain throughout measurement.

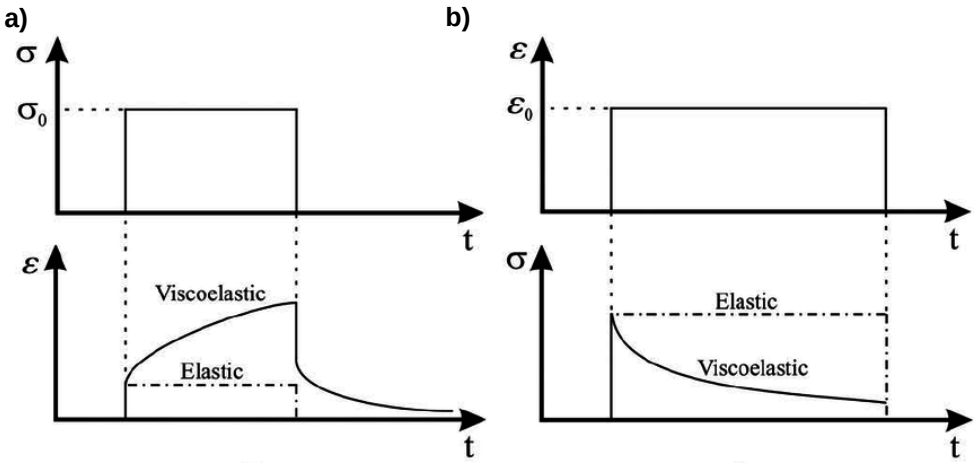

Figure 1-9 – Viscoelastic elastic behaviour under uniaxial loads – a) Creep results from increases in strain at constant stress; b) Stress relaxation results from the decrease in stress at constant strains. Adapted from [148]**.**

One of the earliest reports on viscoelasticity as an important parameter in SC biology was published in 2011. In this report, J. Cooper-White and colleagues employed PAA formulations with constant compressive moduli but variable loss moduli, to identify the impact of substrate creep in MSCs [149]. The authors found that substrate creep increased average cell area and altered the organisation of FAs, enhancing multi-lineage differentiation capacity in hMSCs.

In 2015, David Mooney's group started investigating the role of stress relaxation on cell behaviour [150]. Using computational molecular clutch model simulations, the authors predicted that cell spreading would be augmented in stress relaxing viscoelastic substrates, relative to purely elastic biomaterials of comparable stiffness. These predictions were confirmed by seeding hMSCs into 2D linear-elastic and viscoelastic alginate hydrogel

formulations. Importantly, the authors confirmed that cells on soft viscoelastic substrates were able to spread as much as cell on stiffer elastic substrates. These results were later extended onto 3D by a subsequent publication [151]. In this system, fibroblastic cells encapsulated inside RGD functionalised hydrogels with fast stress relaxation timescales displayed improved proliferation and spread out considerably through the formation of long cellular protrusions. Critically, in MSCs, differentiation was substantially impacted by substrate viscoelasticity, with osteogenesis being favoured by increased stiffness and stress relaxation, and adipogenesis experiencing the opposite trends. The authors hypothesised that internal ligand clustering was facilitated by substrate viscoelasticity. Interestingly, YAP internalisation was decoupled from MSC fate in this study, again illustrating the complexity of cellular responses in varying substrates.

Finally, a very recent publication by the same lead author has found that viscoelasticity potentiates regeneration *in vivo* [56]. Three months post implantation on a rat model of bone defects, animals that received fast-relaxing scaffolds showed more bone growth than those treated with elastic stiffness-matched controls. Strikingly, these results were observed even in acellular stress relaxing scaffolds, suggesting that viscoelasticity may be a critical parameter in tissue regeneration.

2) Strain-stiffening

Strain-stiffening is the property of non-linear-elastic materials that become stiffer with increasing strain. This biophysical feature is rare in synthetic materials, but common in filamentous biological polymers, including F-actin, fibrin and collagen [152]. Recent publications have highlighted the potential role of non-linear elasticity on guiding cellular environmental adaptations.

Winer *et al.* [153] reported that sparsely seeded fibroblasts and hMSCs could spread as much on soft (1 kPa) strain-stiffening fibrin networks, as on linear elastic hydrogels an order of magnitude stiffer (10 kPa). The authors employed AFM, rheology and live-cell microscopy to confirm that neighbouring cells communicated by applying local substrate deformations, which globally

stiffened the hydrogel, driving cellular elongation and patterning. It was concluded that cells are responsive to the nonlinear elasticity of fibrous substrates and can manipulate this property to orchestrate joint responses.

More recently, Alan Rowan's group reported [154] that differentiation of hMSCs can be influenced by stress stiffening in very soft (<0.5 kPa) 3D polyisocyanopeptide hydrogels. The authors showed that the expression of adipogenesis markers can be switched to osteogenic markers by changing the critical stress threshold in the materials, thus triggering earlier onset of stress stiffening, without altering hydrogel stiffness or ligand density. A caveat of this system, however, is that the cells are confined to circular morphologies.

These examples illustrate that non-linear elasticity may be an important attribute of ECMs, tightly coupled to the influence of fibrillar microenvironments (described in section 1.3.3 and depicted in Fig. 1.8). These features of the cell niche therefore require continued study.

3) Degradability

Native tissues are highly dynamic and constantly subjected to remodelling. Static biomaterials are unlikely to emulate critical aspects of these dynamics. Furthermore, 3D encapsulation often constricts cells into acquiring round morphologies, which do not accurately represent the highly specialised shapes that cells present *in vivo*. Controllable degradability has therefore been introduced as a study parameter in novel hydrogel systems.

In 2013, Khetan *et al*. [155] described that degradation-mediated cellular traction could direct the differentiation of hMSCs encapsulated in hyaluronic acid hydrogels, independently of morphology or matrix mechanics. By employing photo-crosslinkable materials which become resistant to degradation when irradiated with UV, the authors observed that cell spread, traction and osteogenic differentiation were dependent on cell-mediated matrix degradation. The converse was true for adipogenic differentiation, fostered by impeded degradation. Curiously, inactivating degradation after allowing cells to attain spread out morphologies, in partly degraded hydrogels for 7 days, shifted the differentiation fate of MSCs into the adipogenic lineage in bi-potent media, without alterations to cell morphology. The same behaviour was found

by downregulating contractility in spread cells, with the ROCK pathway inhibitor Y-27632. The same group further studied the interplay between substrate stiffness, dimensionality and degradability by culturing hMSCs in both 2D and 3D non-degradable environments [156]. The authors observed a positive correlation between spreading, YAP internalisation and substrate stiffness in 2D, which was reversed in 3D encapsulation. However, in 3D stiffness-matched degradable hydrogels, cells were able to acquire more spread out morphologies and preferentially internalise YAP relative to the static controls. The authors concluded that differentiation is dependent on stiffness and degradability, but that dimensionality conditions the overall influence of these factors.

Finally, Jiadong Ding's group recently studied the influence of 2D degradation rates in substrates of varying stiffness [157]. This report presented interesting conclusions, as both adipogenesis and osteogenesis were substantially bolstered in soft substrates (<1 kPa) with fast degradation rates.

Altogether, these publications illustrate that degradability is an important feature of cell environments.

To conclude this topic, it bears mentioning that viscoelasticity [158], non-linearity [159] and degradability in natural biopolymers may be instrumental to the ability of cells to impart plastic deformations into the surrounding environment. Plastic rearrangements of the cell niche have so far been ignored in biomaterial research [160], but the vision of these environments as elastic, essentially static, scaffolds is being called into question.

It may therefore be time to call for a paradigm shift in biomaterial design to better emulate the mechanical traits of native tissues and foster regenerative abilities of these materials.

Chapter 2 – Technical Overview

2.1 Single-cell morphometric analysis

2.1.1 Single cell analysis

Standard Molecular Biology techniques have traditionally relied on the detection of average traits in samples containing large numbers of cells, in the context of genomics, transcriptomics and proteomics [47]. While these techniques allowed researchers to establish the fundamentals of cell function, the emergence of single-cell technologies has started to evidence critical information that was otherwise obscured by average representation of heterogeneous samples (Fig. 2.1) [47], [161]. For instance, hMSC non-clonal cultures are comprised of several subpopulations, potentially varying in differentiation potential [26]. Temporal dynamics, such as morphological or developmental trajectories, are another aspect which is hard to characterise without robust single-cell methodologies. While recent advances in analytical techniques (e.g. single-cell transcriptomics) are extending the boundaries of the "-omics" fields, new capabilities in data processing have allowed the extraction of single-cell data from established techniques, such as fluorescence microscopy.

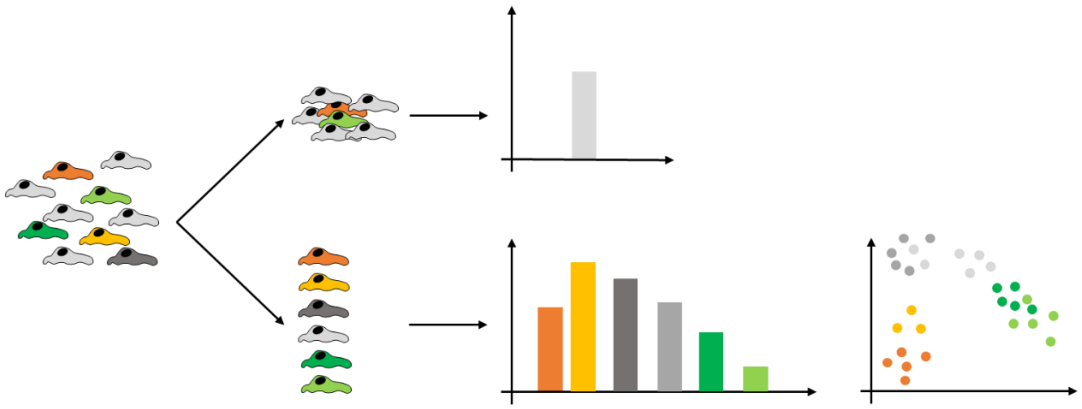

Figure 2-1 – Single-cell analysis reveals heterogeneity in cell populations – Schematics illustrating average populational traits masking heterogeneities between cells. Single-cell analysis can identify subpopulations and hidden dynamics within the data.

2.1.2 Morphometric image analysis

Optical microscopy is a fundamental and widespread technique in biological research, which is inherently compatible with the study of single-cells. However, to extract informative metrics from large collections of single-cell images, i.e. convert visual information into quantitative data in an automated and unbiased way, sophisticated computational image processing is necessary [162].

Image processing pipelines that can quantify cytoskeleton states are essential for elucidating the complex interplay between cells and biophysical environments. Characterising the morphological changes [163], structure and dynamics of actomyosin stress fibres [164], [165], as well as nuclear alterations [166] during hMSC differentiation, or cellular adaptations to distinct environments [167], may provide valuable insights to our understanding of these processes.

To this end, our research group has developed a specialised image processing pipeline for the analysis of single-cell cytoskeletal and nuclear images, as described in previous publications [165], [168], [169]. The output of this pipeline are 18 morphometric descriptors, divided into morphology metrics, cytoskeleton fibre metrics, and nuclear state metrics.

Briefly, the morphometric image processing and quantification pipeline implemented in MATLAB proceeds in the 6 following steps:

1) Manual cropping of single-cells from an imaging field

A user first manually crops single-cell images from larger composite imaging fields (collected with a x20 objective) by selecting a rectangular area delimiting the cell of interest. Fig. 2.2 a-c depicts examples of three channels extracted for a single cell.

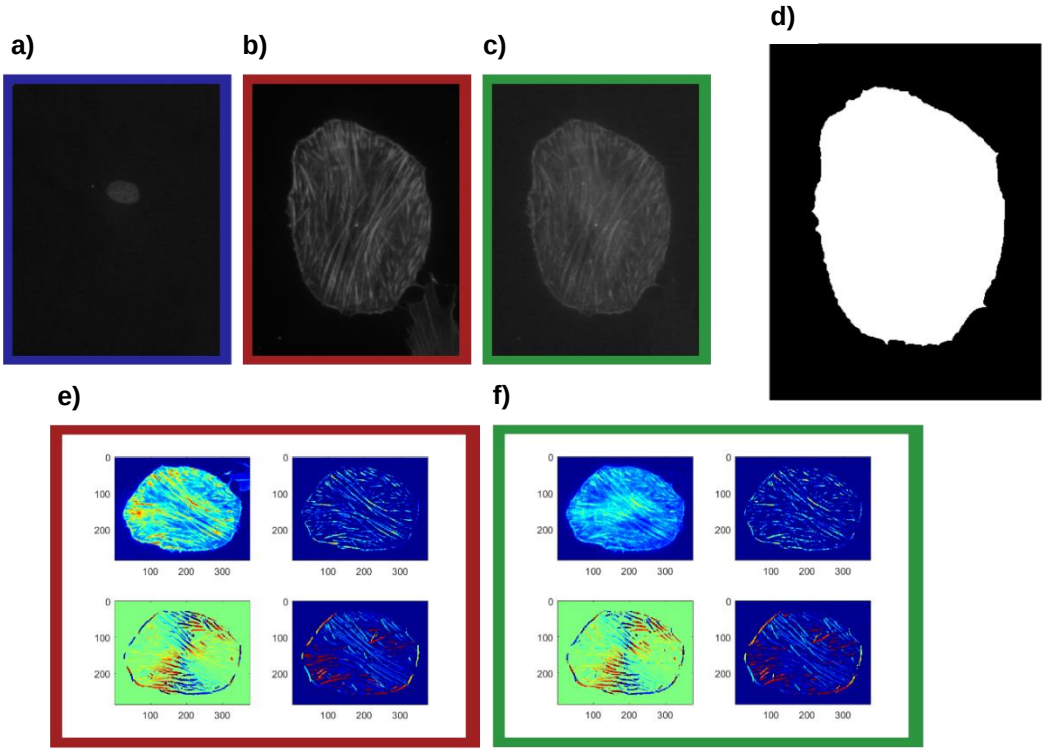

Figure 2-2 – Example inputs and outputs of our image analysis pipeline – a) DAPI nuclear images and b) phalloidin-TRITC c) Lifeact-GFP actin cytoskeleton images were provided as inputs to calculate nuclear properties and cytoskeleton morphometric parameters. d) An individual mask was generated from these images to identify the perimeter of a single cell. e,f) Comparative examples of cytoskeleton fibre sampling maps from e) the TRITC channel and f) GFP channel; in cells with intermediate to high Lifeact expression, as displayed, fibre sampling is similar between the two. Top quadrants represent maps of total intensity and identified fibres, bottom quadrants map angular orientation of fibres. More extensive information can be found in previous publications [165], [168], [169]**.**

2) Cell boundary identification

An initial step of image segmentation is based on the identification of cell boundaries (Fig. 2.2 c). Boundary detection is performed by thresholding greyscale images based on a contour dilation algorithm. To improve segmentation, an outward contour of the cell is provided to the algorithm by “manually” drawing a course outline around the cell perimeter with a digital cursor.

3) Cytoskeleton segmentation

Following morphological segmentation, cytoskeleton fibres are resolved by convolution of the cell image with elongated Laplace of Gaussian (eLoG) kernels, as described by Zemel et al. [170]. The 21x21 pixel window, consisting of the eLoG “fibre template” filter, is applied at each pixel location within the cell boundary. At each position, the filter is rotated 180º stepwise, in 30 increments of 6°, and putative fibres are recognised by the maximisation of image cross correlation signals. This approach generates a map of signal intensity across the cell which represents the initial fibre sampling. Angles maximising the cross-correlation signal in each position are equally registered to map fibre angular orientation.

4) Fibre refinement

Fibre refinement is carried out using a coherence-enhancing diffusion filter. The fibre map is refined by extension and interconnection of interrupted fibres. In the angular orientation map, the values of newly inserted pixels are compared to the average orientation of neighbouring pixels within the same fibre, inside a 9 × 9 pixel window. If the difference between window average and the new pixel value lies outside a per-defined threshold, the pixel is discarded. These fibre enhancement and trimming steps are iterated until convergence of the algorithm. Fibre refinement also corrects for artefacts, such as bright dots.

5) Background subtraction

Background fluorescence caused by unbound fluorophores/ auto-fluorescence, is also corrected by the algorithm. A background fluorescence map is generated by computing median signal intensity within a 21 x 21 window surrounding each non-fibre pixel near fibre edges. The result is a smoothed intensity map with fibre pixels replaced by the median of non-fibre pixels. This background map is then subtracted from the original image and the pixels in the fibre map that obtained negative values are removed. The process is again iterated until convergence. This process ensures that only

pixels with a high certainty of belonging to a fibre are included in the resultant fibre map.

Parameter calculations

18 morphometric features are calculated from several operations in the fibre (Fig. 2.2 e-f upper right quadrant) and angular orientation (Fig. 2.2 e-f lower quadrants) maps. Direct visual representation of the relationship between the numerical values of the different cytoskeletal morphometric descriptors and actual cell morphology can be found in **Appendix A**.

The morphometric descriptors are as follows:

Morphology metrics

- Cell spread area – sum of pixels within the mask of cell shape, converted into metric system (μm^2)
- Aspect ratio – Ratio between major and minor axis of cell shape
- Stellate factor – Measurement of the convexity of cell area; larger values generally indicate the presence of filopodia or more stellate shapes, whereas lower values indicate a more uniform shape.

Cytoskeleton fibre metric

- Cytoskeleton amount – Sum of pixel intensities for all pixels identified as belonging to a fibre
- Thickness – Average pixel intensity for all pixels identified as belonging to a fibre. Given that in our imaging conditions, pixel size is larger than the diffraction limit and thickness of an individual actin filament, pixel intensity constitutes a good surrogate measure to estimate the number of individual fluorophores bound to a filament and the number of filaments making up a stress fibre.
- Thickness variation – Variability in the distribution of pixel intensities for all pixels identified as belonging to a fibre.

- Alignment of fibres – Using the orientations for pixels identified as belonging to a fibre, alignment is defined as 1 - circular variance, computed using directional statistics of the distribution of angles. Values close to 1 indicate that most fibres are oriented in the same direction, whereas values close to 0 indicate random orientation of fibres.
- Curvature of fibres – Similar to alignment but computed as circular variance for all pixels *within a single fibre*. Values close to 1 indicate fibres that are very curvy, whereas values close to 0 indicate straight fibres.
- Location of fibres – Radial position where fibres are preferentially found in the cell. A value of 1 indicates the cell edge (closer to the cell periphery), whereas a value of 0 indicates the cell's centroid (closer to the centre of the cell)
- Fibre spread – Variance associated with location of fibres in the radial position. A larger value indicates that fibres are well spread through the cell diameter, whereas a smaller value indicates that fibres are preferentially localized in a single radial position.
- Length – Average length of the fibres in a cell (in µm).
- Length variability – Variance associated with the length of the fibres in a cell.
- Chirality – Once the centroid of the cell is identified, the fibre orientation map is converted to compute the relative orientation of each fibre with respect to the cell's centroid. A value close to 0° indicates that fibres are preferentially pointing in the radial direction (towards the centre of the cell) whereas a value close to 90° indicates that fibres are preferentially pointing in the circumferential direction (in parallel to the cell edge)
- Chirality variability – Variance associated with chirality measurements

Nuclear state metrics

- Chromatin condensation – A measure of the localised changes in nuclear DAPI fluorescence intensity. Increased number/fluorescence of nuclear speckles surrounded by regions of dimmer intensity reflects chromatin condensation.
- Relative nuclear volume – Scaled metric in which unit value is assigned (as a reference point) to the volume of a "fully relaxed" nucleus (theoretical isolated nucleus existing in the absence of applied forces). Relative nuclear volume is estimated by measuring lateral nuclear dimensions (a, b axis) and extrapolating a fluorescence intensity gradient in 2D nuclear images to approximate the nuclear height profile (c axis). Relative volumes are calculated through the equation of a 3D ellipse (defined by a, b and c axes).
- Poisson's ratio – Ratio determined with the boundary condition that the cell nuclei assume perfectly spherical shapes in the absence of external forces. For each nucleus, Poisson's ratio is described through the relationship between volumetric changes and length changes in stretched materials.
- Apparent Nuclear stiffness – an apparent measure of nuclear stiffness, as reflected by the amount of nuclear 3D deformation induced by the cell's intracellular tension. Based on a model pondering relative changes in nuclear radii, and relative forces imposed onto the nucleus, scaled according with cell spread area.

A more complete description of the rationale beyond the estimation of nuclear metrics can be found in a former reference [165]. More information

2.1.3 Morphometric features as biomarkers for lineage specification

There is mounting evidence that biophysical traits can be powerful biomarkers of the cell state [171], which can be used for classification and prediction of cellular fates [26].

For instance, the group led by Prabhas Moghe has used images of the actin cytoskeleton in hMSCs to extract a set of quantitative descriptors and identify cell subpopulations [172]. Critically, the authors demonstrated that hMSCs committed into the osteogenic lineage on fibronectin coated glass could be discriminated from adipogenic/non-committed cells after the initial 24 h. The authors further showed that on non-coated glass the adipogenic and osteogenic lineages could be fully discriminated by 72 hours post induction, and that the cytoskeletal morphometric descriptors could forecast SC fates across a series of synthetic substrates. The group later extended this methodology to include information about nuclear states [173], concluding that these parameters are sensitive biological markers for classifying differentiation and how cells interact with their environmental milieu. Similarly, the Kato group used morphological descriptors to predict hMSC multi-lineage differentiating potential across a range of conditions [174].

These reports illustrate that morphometric parameters such as cell morphology, cytoskeleton organisation and nuclear states encode valuable information in the characterisation of hMSC differentiation. Both groups have also employed Machine Learning principles to discriminate between different cell classes, evidencing that morphometric data can be employed in tasks involving the prediction of future cell behaviour.

2.1.4 Machine learning – new frontiers in lineage reconstruction

Machine Learning (ML) is a discipline comprised of algorithms that aim to recognise underlying patterns in data [175], and ultimately train mathematical models to perform classification and prediction tasks. ML algorithms can be divided into unsupervised (Fig. 2.3 a) and supervised (Fig. 2.3 b-c) learning [176].

Unsupervised learning algorithms organise the data based on proximity measures, without prior assignment of a class to the data points (e.g. clustering algorithms, Fig. 2.3 a). For this reason, a growing body of research has employed unsupervised ML approaches to identify and reconstruct development lineages using single-cell data from asynchronous samples (i.e. heterogeneous samples containing cells at different developmental stages)

[177]–[179]. The theoretical assumption for these methods is that single-cell data captures a range of transitional cell states in developmental processes [177]. These intermediate states can be chronologically re-organised (in the absence of any temporal information) to construct trajectories that model development (Fig. 2.4).

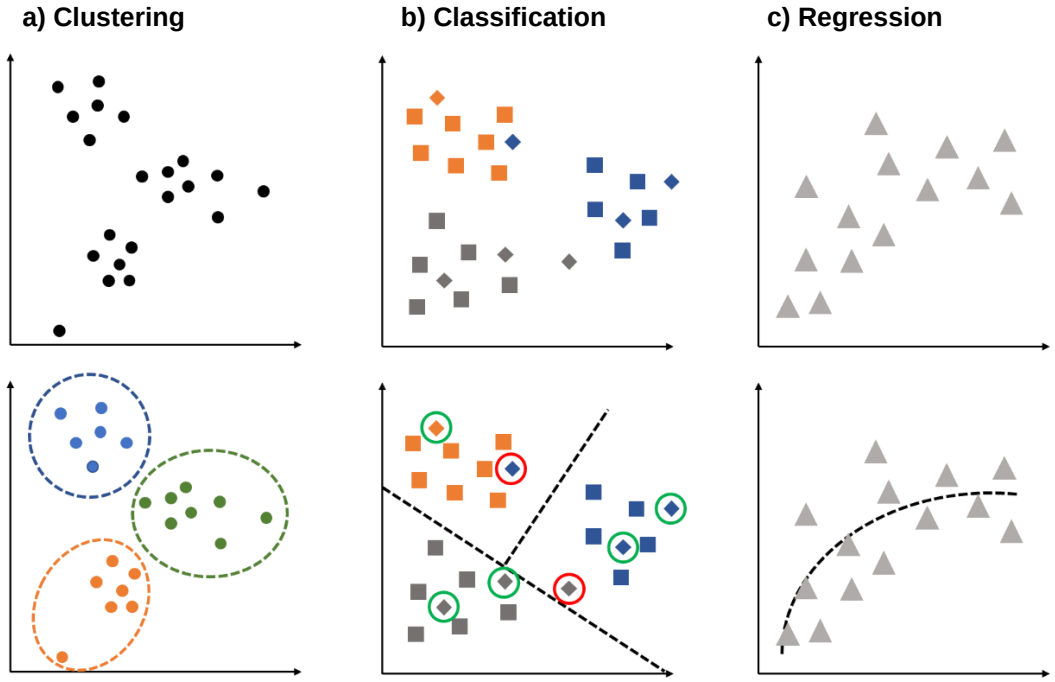

Figure 2-3 – Graphical depiction of unsupervised and supervised Machine Learning tasks – Unsupervised ML example: a) Clustering groups data points based on distance metrics without prior knowledge of classes in the data; Supervised ML learning examples: b) Classification uses training data (squares) to train a model (dotted lines) that can discriminate between *a priori* known classes (orange, blue and grey). Test data (losanges), not used during training stages, is classified *a posteriori* according to the thresholds set by the model. The example highlights two misclassifications (one blue losange is misclassified as orange, and one grey losange is classified as blue) and four correct classifications of test data. Consequently, a classification accuracy around 70% is expected with this model, c) Regression optimises the fit of a continuous curve to describe the quantitative relationships between input parameters and a predicted output.

Terminal cell types can thus be traced through intermediate stages back to the start of differentiation in asynchronous samples. Although innovative, these algorithms are still in their infancy and present important limitations. One of the main weaknesses of current single-cell lineage reconstruction approaches is the lack of temporal information, i.e. pseudo-

temporal lineage reconstruction represents a chronological ordering of events but cannot relate the real timespan of biological processes.

By contrast, supervised learning algorithms act on class annotated data sets (i.e. data points are labelled *a priori* as belonging to a particular class) inferring statistical relationships, or optimising mathematical thresholds, to distinguish between predefined categorical classes (classification, Fig. 2.3 b) or predict a continuous output (regression, Fig. 2.3 c).

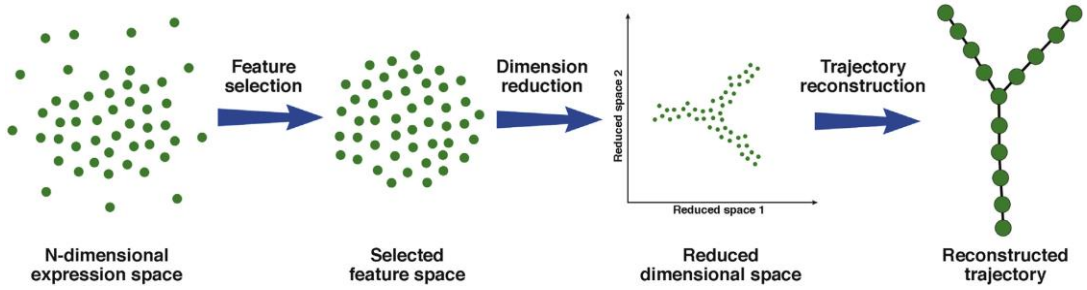

Figure 2-4 – General workflow of an unsupervised trajectory analysis algorithms – Current developmental lineage reconstruction approaches rely on single-cell transcriptional/cytometry multidimensional data sets. After pre-processing (feature selection and dimensionality reduction) developmental trajectories are reconstructed by specialised unsupervised ML algorithms developed by several groups (e.g. Wonderlust [178]**, Monocle** [180]**). The main disadvantage of these approaches is that the reconstructed trajectory is represented in pseudotime, a chronological ordering that does not convey the real timespan of events. Adapted from** [177]

The general workflow of a classification task is to provide the algorithm with a training set, i.e. a number of class-annotated data points, each described by a vector of descriptive features (quantitative variables). The algorithm then fits a mathematical model to the training data in order to optimise boundaries that discriminate between each class. After a model has been trained, its performance can be assessed on a test data set. Test sets must also be annotated (to provide terms of comparison for the results of classification) but should not have been used in training the algorithm (to prevent overfitting). The ML model assigns a predicted class to each point in the test set, which can then be compared to the real class the test point is known to belong to. If the predicted class matches the real class, the data point was correctly classified. Otherwise, a misclassification has occurred. The

number of matches and mismatches can then be quantified to assess the reliability of the model. Regression tasks are akin to classification, in that a model is fitted to a set of training data. However, while classification assigns a categorical output to input data (a “class”), the outputs of regression are continuous quantitative values. Therefore, regressions can map both discrete and continuous inputs into continuous outputs.

Support Vector Machines (SVM) are a supervised ML algorithm which can be used for both classification or regression (Fig. 2.5). Briefly, in classification tasks, SVMs find the multi-dimensional planes (hyperplanes) which maximise margins separating the outermost points (support vectors) belonging to different classes in the data. A similar rationale is used by SVMs in regressions tasks, to fit a continuous regression line to sets of discrete training data. The SVM regression model can then be used to classify new data points.

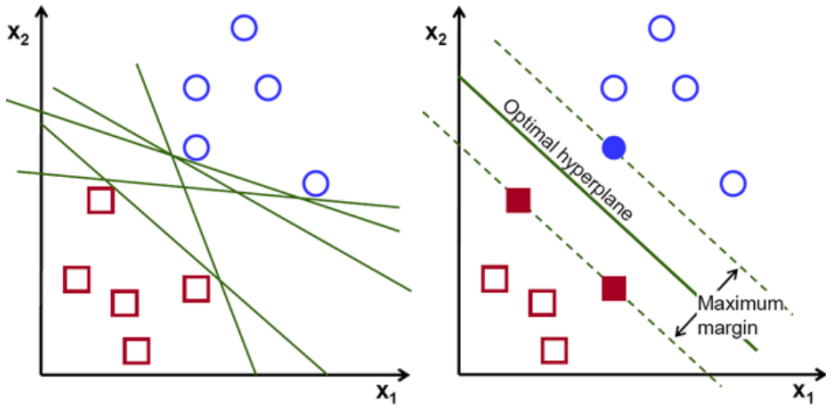

Figure 2-5 – Schematics of Support Vector Machine classifier optimization – SVMs identify the optimal hyperplane that maximizes the margin between outermost points (support vectors) in different classes in the training data. Adapted from [181]**.**

2.2 General methods

2.2.1 Supplementary information

This section conveys information about some of the materials routinely used during this project.

Actin staining agents and the Lifeact probe

Live-imaging techniques to explore behaviour and function from sub-cellular to whole organism scales are at the forefront of biology research. A critical aspect of these methods is the reliance on intracellular fluorescent probes to label specific proteins. Due to the multiple roles of the actin cytoskeleton in cell biology, several MF probes have been developed over the past decades (Fig. 2.6 represents the current gold standards in actin staining).

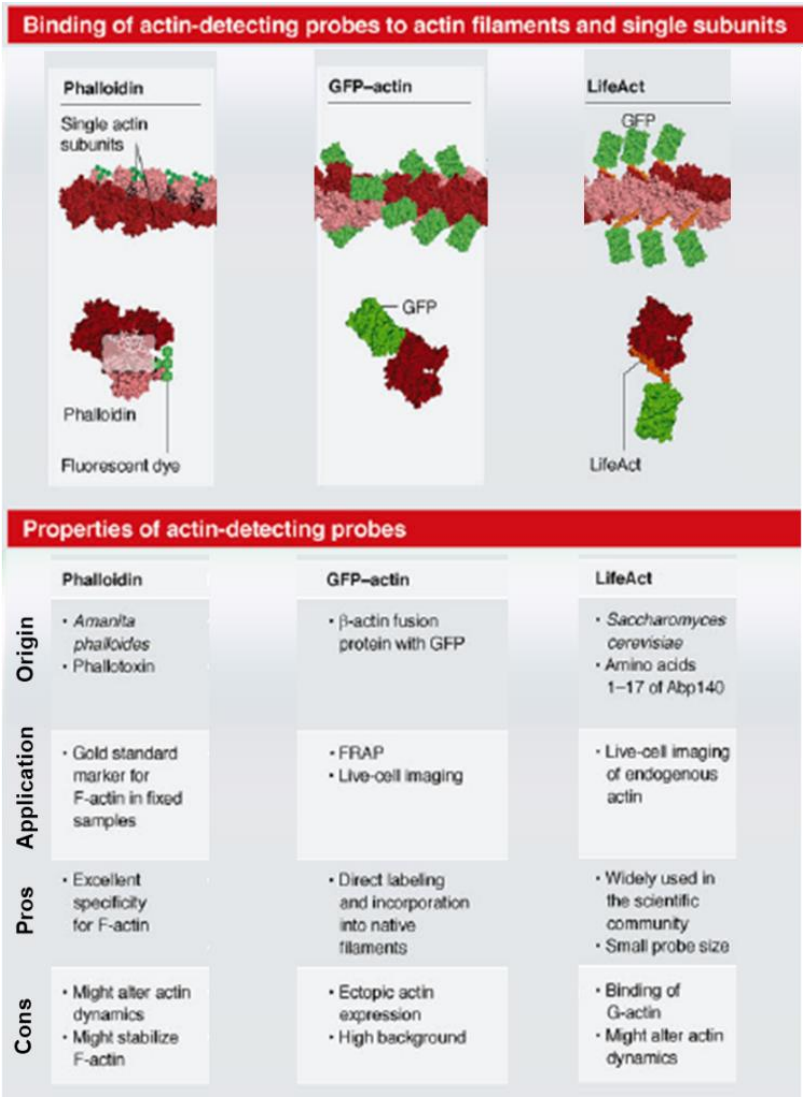

Figure 2-6 – Examples of prevalent actin binding probes and their properties – The upper panel depicts molecular models of the binding of the actin probes phalloidin, actin-GFP and the Lifeact peptide to actin filaments; the lower panels provide details about the origin, applications, advantages and disadvantages associated with each probe. Adapted from [182]**.**

Phalloidin, a phallotoxin from the Amanita *phalloides* fungi species, is the most prevalent actin probe for standard fixed sample imaging [88]. Fluorescently tagged phalloidin has the advantage of specifically staining F-actin stress fibres with minimal background signal. A considerable drawback of this probe, however, is the difficulty of use in live-cell imaging, requiring microinjection techniques to overcome the low permeability of the cell membrane [182]. Furthermore, phalloidin stabilizes the actin cytoskeleton by interfering with disassembly rates [183]. Consequently, live cell imaging of the actin cytoskeleton routinely demands transfection of cells with plasmids encoding ectopic actin tagged with GFP. This approach also presents limitations which include arduous optimization, low transfection yields in primary cells, and high background intensity. Critically, overexpression of tagged actin variants can be problematic, as even subtle changes in the amount of global actin can interfere with physiological dynamics, and trigger actin polymerization [182]. Nonetheless, actin-GFP is a well-established probe, with an extensive body of research already dedicated to its uses and pitfalls.

Recently, the Lifeact probe has become one of the main contenders for live-cell actin labelling. Lifeact is a small peptide with affinity for MFs, originating from the Saccharomyces *cerevisiae* actin binding protein 140 [184]. Lifeact-GFP has been commercialised for several years and has become widely employed in cytoskeleton imaging [182]. Conveniently, Lifeact-GFP adenoviral transduction formulations can be directly acquired from the supplier, facilitating the use of the probe with hard-to-transfect primary cells.

Yet, potential artefacts created by this probe remain under-characterised. Consequently, the conditions under which the probe can be employed risk-free have not been well reported, despite two recent publications raising concerns about Lifeact-associated artefacts at the molecular [185] and whole organism level [186]. More extensive characterisation of the impact of Lifeact in live cells is therefore necessary to understand the likelihood and magnitude of Lifeact-induced artefact occurrence. The particularities of our morphometric approach equipped our group with the opportunity of performing an in-depth characterisation of

Lifeact-GFP. This work, presented in Chapter 7, constituted a second goal in the project described by this thesis.

Ultra-low gelling temperature agarose

Agarose is a natural linear polysaccharide extracted from red seaweed, routinely employed to encapsulate cells in 3D environments [187] due to its excellent biocompatibility, optical transparency, and easily tuneable mechanical properties. There are several examples of agarose being used in the development of composite formulations to culture diverse cells types, such as neurons [188], osteoblasts [189] or smooth muscle cells [190], but the majority of publications directly employ agarose as a simple scaffold to research the impact of active mechanical strain in chondrocytes [191], [192].

Importantly, the molecular carbohydrate chains of unmodified agarose lack cell attachment groups. As such, cells directly encapsulated into agarose cannot adhere to the polymer or acquire spread out morphologies. The cells consequently retain a spherical shape, reminiscent of chondrocytes on native cartilage. It bears saying that most cells in the human body, including hMSCs, reside within ECMs which actively promote cell attachment, spread and remodelling in the orchestration of tissue formation, maintenance, growth and regeneration, restricting the potential of inert agarose as an ECM model.

However, the polymer is advantageous because of its thermally-driven gelation process. To prepare agarose hydrogels, dry powder is suspended in aqueous medium and melted at temperatures over 45ºC. Hydrogel structures then spontaneously form within minutes after the agarose is cooled below gelation temperature. The time needed for gelation is dependent on temperature, on the type of agarose, and on hydrogel concentration and volume. Through this thermal crosslinking mechanism, cells can be readily encapsulated by direct mixing with low gelling temperature agarose variants (at 37ºC), such as Seaprep agarose.

The properties of agarose also justify its use as a go-to material in the assembly of constructs for mechanical loading. Cell-seeded agarose suspensions can be easily cast within custom-made moulds, spontaneously forming hydrogel constructs with predefined shapes after brief periods of

cooling. Melted agarose also promptly invades porous endplates, allowing seeded constructs to be gripped without any cytotoxic effects [193].

Sulfo-Sanpah crosslinking

Sulfosuccinimidyl-6-[4-azido-2-nitrophenylamino] hexanoate (Sulfo-Sanpah) is an 18.2 angstrom hetero-bifunctional photocrosslinker comprised of a carbon chain terminating in two reactive groups (Fig. 2.7): an amine-reactive N-hydroxysuccinimide (NHS) ester and a photoactivatable nitrophenyl azide. NHS esters react with primary amines (-NH2) to form amide bonds. The prevalence of amines in amino acid side-chains allow Sulfo-Sanpah to form conjugates with a wide range of peptides and proteins. On the other hand, the exposure of nitrophenyl azides to UV light, promotes the formation of nitrene groups that can initiate addition reactions with double bonds, insertion into C-H and N-H sites, or subsequent reactions with nucleophiles such as primary amines [194]. Of note, Sulpho-Sanpah has a limited window of reactivity in aqueous solutions as the NHS esters tend to hydrolyse and become non-reactive within minutes.

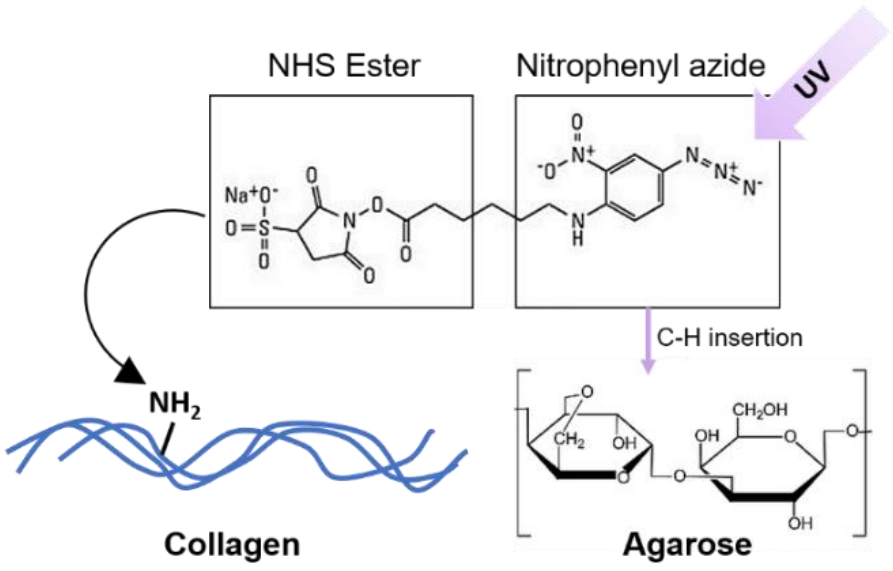

Figure 2-7 – Sulfo-Sanpah crosslinking chemistry – the NHS ester end of the crosslinker reacts with NH_2 groups in proteins and peptides but is unstable in aqueous solution; UV-activated nitrophenyl azide rings can be inserted into C-H atoms in hydrogel sidechains.

Collagen I

Collagen is routinely used as a coating agent to promote cell attachment in untreated cell culture surfaces. Collagen I (COL I) is known to promote hMSC osteogenic differentiation [195], [196], while its effects on adipogenic differentiation are less well documented. A qualitative assessment of the potential influence of COL I on osteogenic and adipogenic differentiation (which can be consulted on **Appendix B**) suggested that the ECM protein does not negatively influence the maturation of adipocytes in culture. Due to its ease of access, being a main component of natural ECMs, and compatibility with differentiation, COL I was considered an ideal component for hMSC differentiation studies conducted during this project.

Microscope Coupled loading rig

A uniaxial loading rig was developed by researchers in the School of Engineering and Materials Science [193] which can be mounted on top of microscope stages and coupled to imaging capabilities. This instrument was originally designed to apply strain to cell-seeded agarose constructs gripped by sintered glass endplates. The loading rig consists of three main components: stepper motors located on opposite sides of the rig that are connected to a linear actuator to translate rotation into linear motion; gripping elements to hold the specimen through the endplates, and a detachable central hydration chamber with a glass coverslip bottom. The stepper motors are controlled by a custom LabView GUI (National Instruments), based on displacement and loading rate inputs.

Rig set-up starts with assembling the hydration chamber. A large rectangular coverslip is placed into a metal bracket and sealed with silicone grease to prevent leakage. The chamber is then assembled into place and filled with cell culture media. Agarose constructs are gripped and held into place with the aid of a spacer (additional information can be found on reference [197]). Gripped constructs are then transferred onto the rig, with the specimen fully immersed in the hydration medium. The grip spacer is then removed rendering the specimen ready for testing. After setting the rig onto the stage

of a standard epifluorescence or confocal microscope, cells inside the agarose constructs can be imaged through the bottom of the central chamber during/after loading sessions.

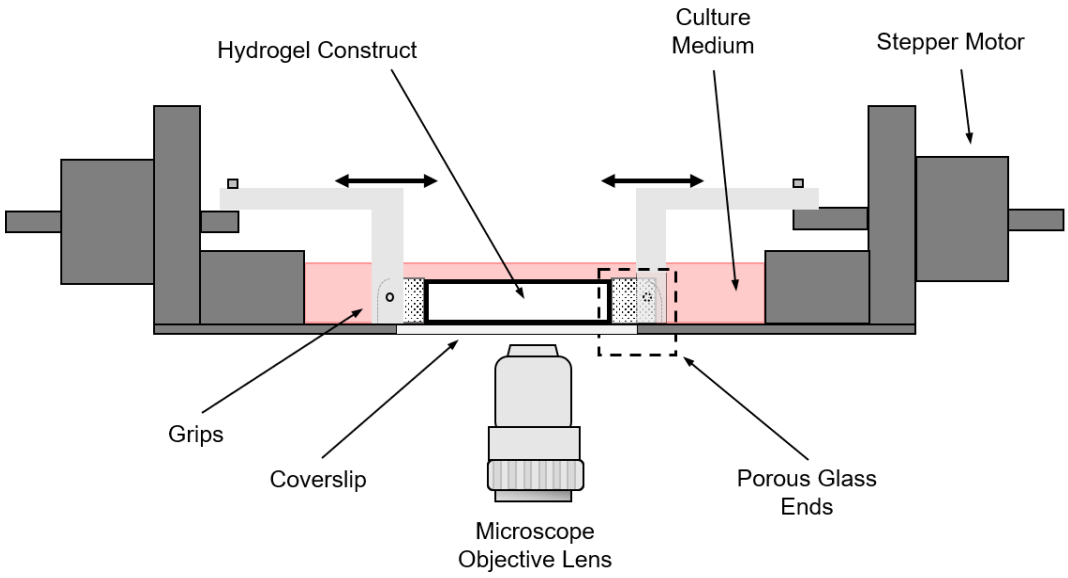

Figure 2-8 – Microscope coupled loading rig schematics – Depiction of the main components of a uniaxial loading rig which can be mounted on a microscope stage. Alignment of the central chamber with a microscope objective allows the observation of cells within agarose constructs through a glass coverslip bottom interface.

2.2.2 General methods

This subsection addresses some of the materials and methods which were consistently used throughout the project. More specific methods are described in each of the subsequent experimental chapters.

Standard Cell culture

All cell culture procedures were performed under sterile conditions in a laminar flow hood. Unless stated otherwise, chemical reagents used throughout this work were acquired from Sigma-Aldrich (USA).

Primary Bone Marrow hMSCs were purchased from STEMCELL (Canada) technologies. These cells were collected from a single patient and provided at passage “p1”. hMSCs were thawed and handled according to

manufacturer's recommendations and expanded into passage "p4". At this point, surplus volumes of cells were cryopreserved in liquid nitrogen for later use.

Nunc EasYFlasks were used to culture hMSCs in Dulbecco's Modified Eagle Medium (DMEM) from Thermo Scientific (USA). Growth medium was supplemented with 10% (v/v) FBS, 100 units/ml penicillin+100 µg/ml streptomycin and 10 ng/ml Fibroblast Growth Factor 2 (Peprotech, USA). Growth media was replaced at least twice per week. A humidified incubator with 5% CO2 atmospheric content at 37ºC was used for cell storage and growth.

To minimize senescence, cells were prevented from reaching confluency and sub-culturing was minimised whenever possible. hMSCs employed in experiments corresponded to passages 5 to 7. For sub-culturing/ to collect adherent cells, TCP vessels were covered in Accutase (Thermo Scientific) stock solution and incubated for 3 minutes at 37ºC. Gentle tapping was used to aid in cell detachment. The cells were collected in culture media and centrifuged for 5 minutes at 1200 RPM. After discarding the supernatant, the cell pellet was resuspended in supplemented media and cells were seeded back into new tissue culture vessels.

For direct cell imaging experiments, cells were transferred into sterile petri dishes containing glass coverslips (13 mm in diameter) and allowed to attach uniformly in the surface area of the vessel at sparse densities (between 800 and 2000 cells per cm^2) to achieve single-cell conditions. Experiments were performed after a minimum of three days post-seeding to minimise the effects of sub-culturing. In hydrogel substrates, cells were seeded at similar densities inside TCP vessels, directly over the surface of the substrates. In all experiments involving cell encapsulation, the temperature of solutions was kept at 37ºC to ensure the cell viability.

Differentiation media

To induce osteogenic and adipogenic differentiation, hMSCs were cultured for periods of at least 10 days. Osteogenic induction media was freshly prepared by supplementing DMEM with 10% (v/v) FBS, 100 units/ml

penicillin+100 µg/ml streptomycin, as well as 100 nM of Dexamethasone, 10 mM β-glycerophosphate and 50 µM L-ascorbic acid. For adipogenic differentiation, growth media was supplemented with 1 µM of Dexamethasone, 500 µM of 3-Isobutyl-1-methylxanthine, 100 µM Indomethacin, and 10 µg/ml human recombinant insulin.

Differentiation progression was qualitatively tracked by regular visual inspection of cell morphology, and by histological staining with Oil Red O and Alizarin Red (**Appendix B**). Quantitative methods to assess differentiation were not performed in this thesis due to time restraints. It is nonetheless acknowledged that this analysis is critical and should be performed in future studies.

Fluorescent staining and Epifluorescence imaging conditions

To prepare samples for imaging, cells were first fixed in 3.7% (v/v) paraformaldehyde for 10 minutes. Fixed samples were permeabilized with 0.25% (v/v) Triton-X100 for 5 minutes and incubated with 1 µg/ml phalloidin–tetramethylrhodamine B isothiocyanate for 2 hours at room temperature. After washing with PBS, nuclei were stained with 1 µg/ml DAPI for 15 minutes. Excess staining agents were further removed by washing thrice with PBS. For all steps, working volumes of 350 µl were applied per cm^2 of sample area. Cells seeded on coverslips were further mounted onto microscope glass slides with a droplet of ProLong Glass Antifade Mountant (Invitrogen, USA). Cells seeded on hydrogel substrates were not mounted and were preserved hydrated in PBS at 4ºC until imaging.

All fixed samples were imaged with a Leica DMI4000B Epifluorescence Microscope (Leica Microsystems, Germany) using a x20/0.50 NA objective lens and a CCD camera (Leica DFC300FX). The x20 objective was chosen as a compromise between capturing whole cell morphology and maximising the resolution of cytoskeleton and nuclear traits. Objective selection also streamlined data acquisition by allowing the collection of several single-cell images per imaging field. Gain and exposure settings were adjusted to optimise the quality of each collected image. These values were subsequently provided (in the form of metadata files) as inputs in the image processing

pipeline to normalise the fluorescence intensity signals before parameter quantification.

General experimental workflow

Our imaging methodology (Fig. 2.9) aims to describe temporal dynamics of cell behaviour through discrete single-cell imaging. The general workflow of most experiments in ensuing chapters starts by concurrently preparing a range of identical samples (t_0). Each of these samples, containing thousands of cells, is then fixed at subsequent time points of interest (t_{1-4}). After fluorescent staining, imaging fields are acquired in various sample regions, to extract between 100 to 400 individual cell images per sample. Single-cell images are then analysed with the image processing pipeline described in 2.1.2 and labelled according to experimental conditions and timestamp.

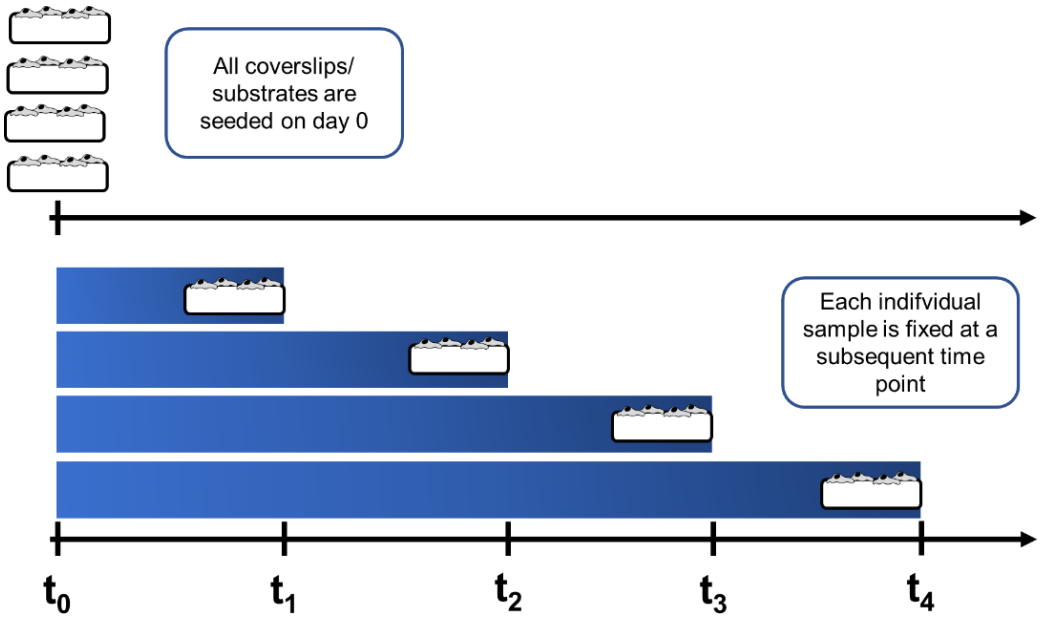

Figure 2-9 – Experimental workflow for characterising temporal dynamics – For most experiments individual samples were seeded at an initial time point t0 and then fixed at later time points t1-4.

Chapter 3 - Development of 2D collagen-coated agarose substrates for studying mechanical induction of hMSC differentiation

3.1 Introduction

In-depth characterisation and precise control of SC differentiation are key aspects of TE. Over the past few decades biochemical supplements have been optimised to stimulate differentiation, and still constitute the gold standard in the field. More recently, it became apparent that mechanical inputs can also mediate SC commitment towards multiple lineages [11], [31], [143], [151]. As a result, substantial research is currently dedicated to the study of innovative materials with distinct mechanical environments and their effects on cell behaviour. Over the past decades, the importance of applying active mechanical loading to biomaterials to influence cell responses has also been well-established [198]. The combination of these factors is expected to approximate the structure and function of native tissues to accurately model disease, or to provide new solutions for a range of medical conditions.

But to understand and control the dynamics of differentiation and tailor mechanical loading profiles, it is first necessary to closely monitor and characterise cell behaviours. To ideally achieve these objectives, a mechanical rig should be integrated into a bioreactor, along with a dedicated imaging system for real-time analysis. This combination of technologies could allow the anticipation of cellular needs at each stage of differentiation. Mechanical loading regimes could then be adjusted accordingly to optimise the engineered tissues. Thus far, however, long-term cell loading experiments have been conducted under mechanical loading regimes which do not dynamically adapt to the needs of the tissue [198], often in the absence of real-time analysis. But technological advancements, such as more compact cell imaging systems, the development of morphometric image analysis, or the coupling of ML to biological data, have brought the development of automated mechanical loading systems closer to reality.

It has recently been reported that the state of the cytoskeleton and overall cell shape can be useful biomarkers for differentiation, with predictive value towards terminal phenotypes as early as 24 hours post-induction [172]. Moreover, our group has used image analysis-based cytoskeletal morphometrics to show that the hMSC actin cytoskeleton changes significantly in the initial 24 hours after osteogenic and adipogenic differentiation induction (results currently published in dissertation form in reference [169]). Given these findings, mechanical loading regimes that efficiently induce the first stages of SC differentiation towards different lineages should be identified.

The work related in this chapter had the objective of developing an experimental set-up capable of integrating microscopic analysis, mechanical loading, and morphometric image processing to lay the foundations for the long-term development of a mechanical system capable of actively responding to cell changes. While initial studies in our group have successfully tracked the phenotypic changes that occur during standard biochemical SC differentiation [169], a further critical step would be to correlate these changes with specific regimes of mechanical stimuli. To do so, our pilot studies had to combine mechanical inputs with direct microscopic observation and morphometric characterisation of the SCs, as discussed in section 3.2. Implementing the proposed set-up presupposed the redesign of agarose constructs originally used with a mechanical loading rig, as discussed in section 3.3, in addition to the functionalisation of agarose with ECM proteins, the topic addressed in section 3.4. Given the influence of the biophysical properties of substrates on cell behaviour, a mechanical characterisation of agarose was also conducted, described in section 3.6. Lastly, a general discussion about the feasibility of the set-up is presented in section 3.7.

3.2 Experimental set-up for real-time imaging and analysis of mechanically-induced hMSC morphometric changes

As mentioned in section 3.1, optimal mechanical loading regimes might efficiently induce SC differentiation. As such, it is pertinent to identify sets of loading conditions that can produce SC phenotypes matching those committed through biochemical means. Fulfilling this objective, however,

required the development of a protocol for real-time imaging and morphometric analysis of mechanically-induced hMSC phenotypic changes:

1) First and foremost, a mechanical loading system had to be coupled to an epifluorescence microscope for immediate monitoring of cellular responses. A purpose-built mechanical loading rig for microscopic observation of loaded cells (section 2.2.1, Fig. 2.8), formerly developed by researchers at the School of Engineering and Materials Science, was chosen for this purpose.

2) The operation of the rig is dependent on embedding the cells into deformable hydrogel constructs. But this presents an important operational constraint, as it is not possible to directly clip a soft hydrogel using the stiff metallic grips in the device. As a result, cells must be seeded into agarose constructs integrated with porous glass endplates, which are required for the rig's gripping system. Seaprep ultra-low gelling temperature agarose was consequently selected as the biomaterial used in this project.

3) To extract useful features from the mechanically-primed cell culture an image processing pipeline was also required. The image analysis pipeline developed within our research group to quantify features linked to cell morphology, the cytoskeleton and the nucleus was described in Chapter 2. Due to the prevalent role of actin stress fibres and the nucleus in mediating mechanical processes, our parameters are ideally suited for monitoring cellular responses to stretch. This pipeline, however, presented an experimental "bottleneck" in that it was developed for the analysis of 2D adherent cell morphology. While 3D conditions are of unquestionable relevance in the context of biological studies, the addition of a third dimension is still a major technological hindrance on both the throughput of imaging, as well as of subsequent processing steps. Furthermore, there is an extensive body of literature addressing hMSC differentiation in 2D, but a dearth of information relative to the same processes in 3D. Considering these limitations, devising a 2D version of the hydrogel constructs used with the rig would provide a well-established means of analysis, supported by currently available research, and compatible with the pre-established image analysis pipelines.

Thus, implementing the intended experimental set-up entailed the development of 2D agarose constructs for use with the microscope-mounted

loading rig. This process included re-designing the simple 3D constructs used with the rig, as well as functionalising the agarose with anchorage groups to promote cell attachment; topics described in sections 3.3 and 3.4, respectively.

3.3 Redesign of agarose constructs for imaging hMSC responses to mechanical loading

The present section describes the redesign of the simple 3D agarose constructs that had formerly been employed with the mechanical loading rig. The original design of the constructs is schematised in Fig. 3.1 a, and described in more detail in [193].

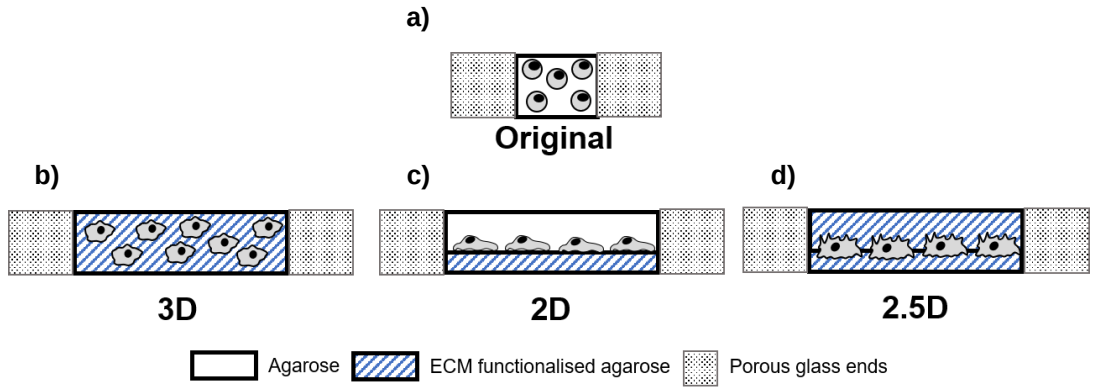

Figure 3-1 – Schematics illustrating the sideview of agarose construct designs – a) Original 3D construct, resulting from direct encapsulation of cells into inert agarose; b) proposed 3D redesign, similar to original constructs but employing ECM functionalised agarose to promote cell attachment and spreading post-encapsulation; c) proposed 2D redesign, based on the assembly of an initial layer of ECM surface coated/ functionalised agarose, seeded with cells and topped with a layer of inert agarose; d) proposed 2.5 redesign, similar to 2D but employing ECM functionalised agarose in the top layer to promote cell attachment in both ventral and dorsal regions.

In the original setup (Fig. 3.1 a), melted agarose/cell suspensions were poured into cubic moulds (0.5 x 0.5 x 0.5 cm^3) and bilaterally attached to porous glass endplates with the same dimensions. Cells in this design were encapsulated in 3D within inert agarose, thereby assuming spherical morphologies. However, these morphologies are of limited relevance beyond the modelling of cartilaginous tissues. To fulfil the objectives cited in section

3.2 it was therefore imperative to adapt the original construct to accommodate a wider range of cell morphologies and to comply with the constraints of the cytoskeleton image analysis pipeline.

As represented on Fig 3.1, three redesigns were conceptualised at the start of the project, namely: encapsulating cells within constructs in a 3D-environment while providing anchorage points in-bulk to promote cell spreading (Fig. 3.1 b); seeding the cells on a 2D plane on top of a strip of agarose coated/ functionalised in-bulk with ECM and topped with a layer of unmodified agarose for mechanical integrity (Fig. 3.1c); and finally a 2.5D intermediate design, seeding cells into a single plane but with access to ECM elements in both the top and bottom layers of the construct (Fig. 3.1d). The present section, along with Section 3.4, jointly present the optimisation of conditions required to fulfil these designs.

To accommodate a larger cell seeding area, the first modification to the original construct (Fig. 3.2 a) was an extension of hydrogel length from 0.5 cm to 1.5 cm. This would be particularly critical when considering sparsely seeded cells in 2D/2.5D, due to the increase in projected area relative to 3D.

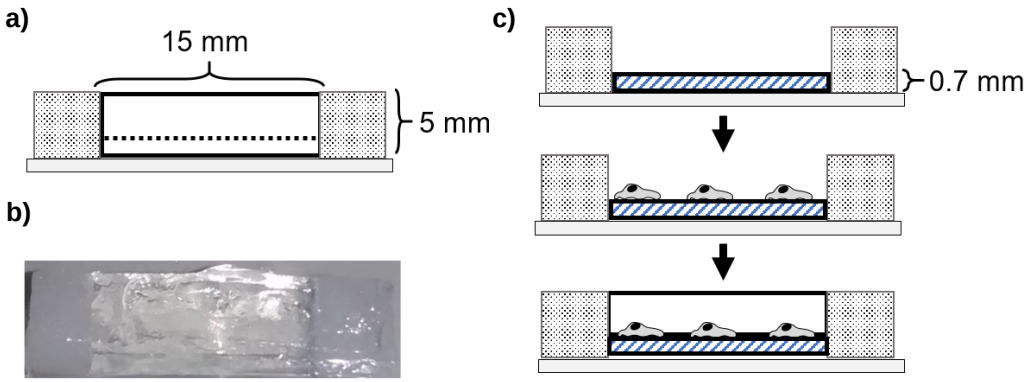

Figure 3-2 – Sideview schematics of layer-by-layer construct assembly methodology and example of a mock construct built from this approach – a) illustration of a mock construct specifying length and height; b) image of a mock construct; c) layer-by-layer assembly for 2D and 2.5 constructs consists on depositing a bottom layer of agarose, either coated or functionalised in-bulk with ECM. Cells are then seeded on top of the layer and allowed to attach and spread. The constructs are finalised with a top layer of either inert or functionalised agarose. Both the bottom and top layers are incorporated into the porous endplates while the agarose is still melted, via capillarity effects, in order to be integrated into a cohesive whole when gelation is concluded.

A subsequent modification, introduced to achieve non-3D conditions, was rethinking the approach to construct assembly. Instead of seeding and preparing the construct simultaneously when encapsulating cells, seeding cells in a single plane demanded a method of layer-by-layer assembly, schematised in Fig 3.2c.

To attain 2D cell morphologies following this approach, a bottom agarose substrate appropriately coated with ECM elements was required. Upon a few hours following cell seeding, attachment and spreading, the construct could then be topped off with a final enclosing layer of agarose. Critically, the height of the lower portion of the construct would have to be restricted to circa 0.7 mm (figure 3.2c) to comply with the focusing limits set by the microscope objective selected for imaging (HC PL FLUOTAR 20x/0.5 PH2, working distance ~1.15 mm). Achieving 2.5D cell morphologies would follow a similar approach but would require homogenous bulk functionalisation of the top agarose layer with ECM elements, such that both surfaces would permit cell anchorage. Given the needs of 2D and 2.5D constructs it was fundamental to incorporate cell adhesion elements into the agarose substrates, described in detail in section 3.4.

3.3.1 Proof-of-concept for construct assembly and instrument operation

Prior to incorporating cells into the constructs, the reliability of the layer-by-layer approach had to first be tested out. Mock constructs of unmodified agarose (Fig. 3.2 b), were assembled using custom-made moulds, to confirm that the assembly strategy was viable and that the constructs could be used with the mechanical loading rig.

Strain in the constructs is created by translation motion of the grips, which in turn is generated by lateral stepper motors controlled by a custom LabView program. Because of the redesign of the agarose constructs, it was necessary to calibrate the relationship between the displacement inputs in the Labview program and the actual strain imparted onto the hydrogel by the instrument, as described further ahead. These preliminary results served as a proof-of-concept for construct assembly and instrument operation with the new constructs.

Materials and methods

Assembly of agarose constructs

Seaprep agarose powder (Lonza, Switzerland) was weighted and suspended in PBS at a concentration of 3% (w/v) and subsequently melted at 121ºC in for 20 minutes in a benchtop autoclave, for sterility and ease of access. The solution was kept heated at 60ºC to prevent gelation. Fluorescent microparticles (Thermo Scientific 10 µm FluoSpheres) were mixed with a separate batch of melted agarose at 4µl/ml. Eight porous glass endplates were placed facing opposite positions in two rows across the base of a custom-made detachable mould, and a 0.7mm layer of microparticle containing agarose was deposited in-between them. After gelation, and incorporation of the endplates into the bottom agarose substrate, plain agarose was cooled down to 37ºC (simulating the conditions of cell seeding) and the remaining volume of the mould was filled to achieve the desired height (approximately 5 mm). The mould was then stored at 4ºC for 10 minutes. The top casing of the mould was removed, and individual constructs (Fig. 3.2 b) were separated out with a scalpel and isolated into separate petri dishes with the help of tweezers. Constructs were stored hydrated in PBS at 4ºC.

Calibration between displacement inputs and hydrogel strain

To calibrate the relationship between digital inputs and the actual strain in the construct, microparticles were incorporated into the hydrogel as previously described. For each experiment, a single agarose construct was gripped and transferred into the loading rig mounted onto the stage of a Leica DMI4000B microscope. The displacement and loading rate (0.3 mm/s) were digitally controlled in a laptop though the Labview GUI. An imaging field containing fluorescent microparticles dispersed in recognizable patterns was located on the constructs and focused on with the underlying x20 objective and a digital image of the unstrained field was collected. Following the initial image, the construct was incrementally compressed in steps of 2% “negative” strain relative to the starting dimensions. After each step a new digital image of the field was collected until a maximum strain of 16% was reached. These

calibration steps were repeated for the characterisation of tension by stretching the hydrogel in “positive” strain increments up to 12% strain.

Particle Tracker, a third-party ImageJ particle image velocimetry (PIV) plugin [199] was used to calculate the displacement fields in the strained hydrogel images. Each pair of two subsequent images within each experiment, i.e. unstrained vs 2%, 2% vs 4%, etc, were analysed with the plugin to generate displacement fields mapped to uniform pixel intervals. A Matlab (Mathworks, USA) code was developed to compute vertical, horizontal and shear components of deformation from each displacement field (Fig. 3.3). The values of five replicates were plotted as average and standard deviation for both compressive and tensional strains.

Results and discussion

The results presented in this section act as a proof-of-concept for the layer-by-layer approach to construct assembly, developed to accommodate 2D and 2.5D cell seeding within agarose constructs. Upon briefly assessing the assembly of constructs using this method, it was necessary to test out the operation of the microscope mountable loading rig with the new construct designs. To do so, unseeded mock constructs were gripped onto the instrument and strained via uniaxial compression and tension. An initial set of experiments verified that the constructs could maintain their integrity under dynamic loading for at least two hours under mild operating conditions (low maximum strains of 5% and slow rate of 0.3 mm/s). This was considered the minimum period of analysis to observe appreciable changes in cell morphology [200], [201]. It was therefore critical that the constructs were able to resist fatigue under these conditions.

Following these preliminary tests, it was necessary to characterize the operation of the rig with the modified constructs. Calibration curves were established to compensate for discrepancies between the digital inputs into the instrument and the actual strain imparted onto the hydrogels. To do so, fluorescent microparticles were incorporated into the constructs to act as visual references (Fig. 3.3 a) with which to compute displacement fields from epifluorescence images using PIV (Fig. 3.3 b).

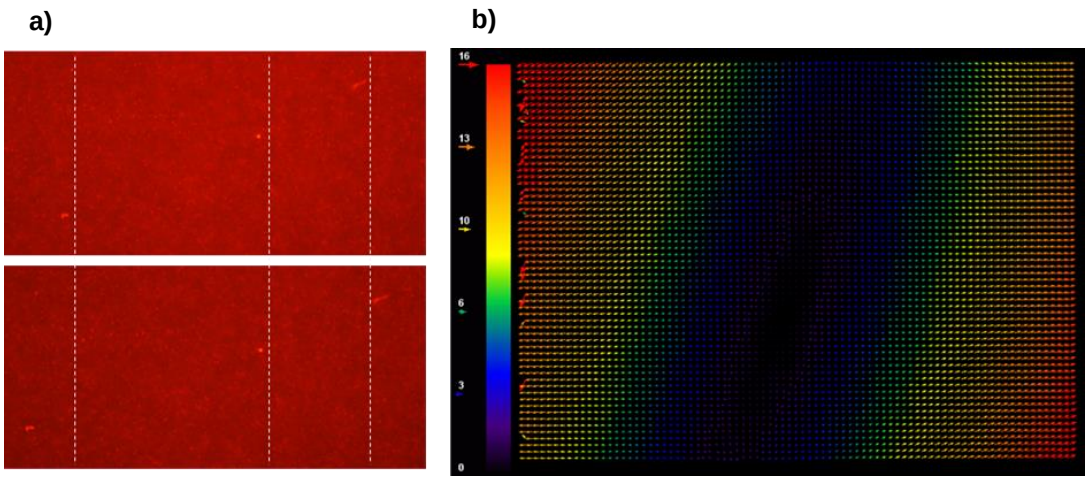

Figure 3-3 – Calculation of displacement fields in hydrogel constructs – a) example of initial and final imaging fields in a stretched construct, white dotted lines inserted to evidence the displacement of bead marks; b) displacement field obtained from PIV analysis of the images in the left panel

These displacement fields were used in the calculation of the average compressive and tensional strains acting on the constructs, decomposed into horizontal (component of strain field aligned with axis of loading), vertical (component of strain field perpendicular to axis of loading) and shear (shear component of strain field) contributions, displayed on Fig. 3.4.

Fig. 3.4 shows that the horizontal stain components (Fig. 3.4 a,b) measured on the hydrogels were substantially larger than either the vertical (Fig. 3.4 c,d) or shear components (Fig. 3.4 e,f) in both compression and tension. These results were expected due to the uniaxial configuration of the instrument. Nonetheless, the calibration curves showed considerable discrepancies between displacement inputs and the deformations measured on the constructs. More concretely, compressions imparted on the hydrogels were on average 1.2 times larger than the values programmed onto the rig. Conversely, tension measurements corresponded to just over half (0.6 times) the intended strain.

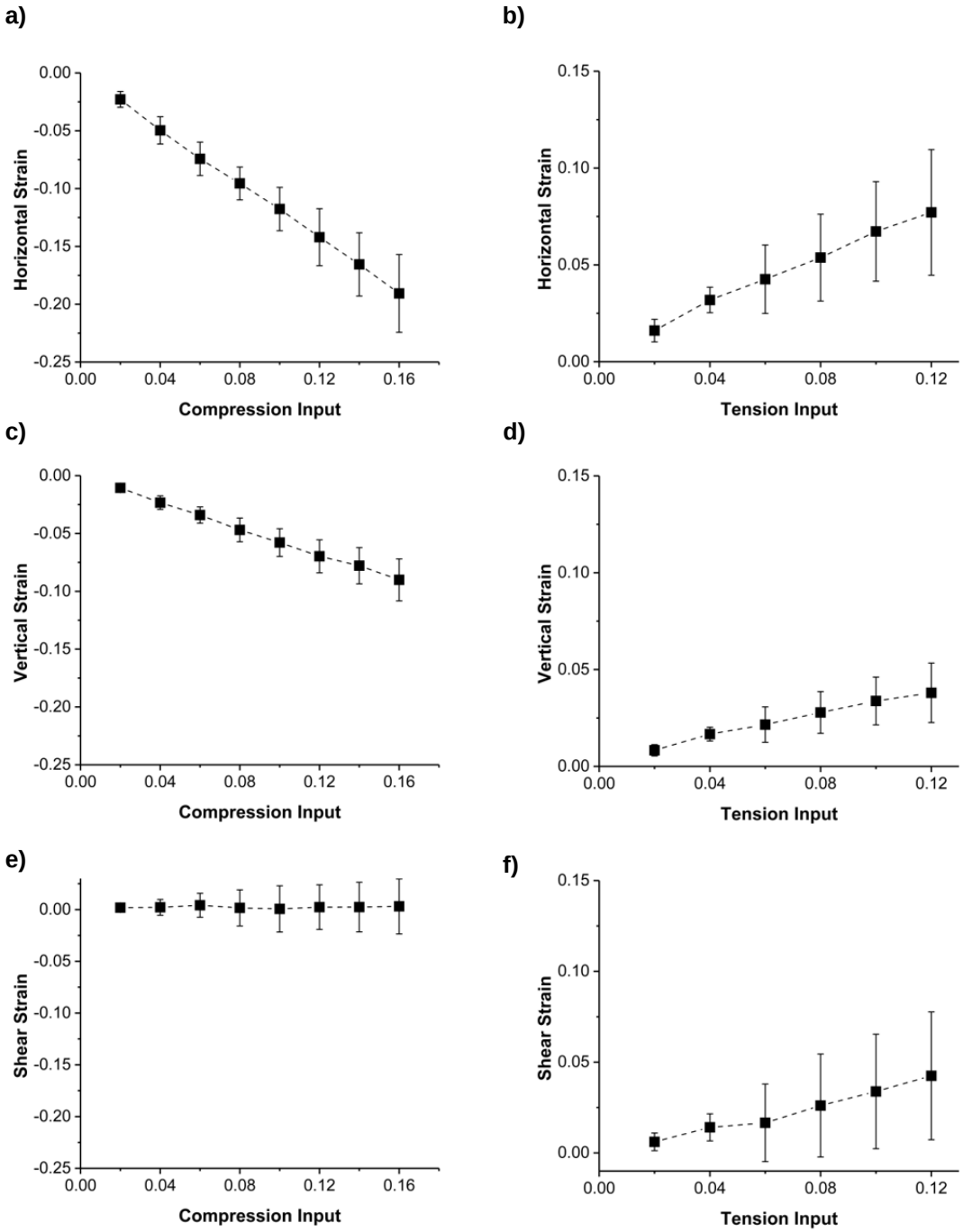

Figure 3-4 – Calibration between rig displacement inputs and deformations measured on the constructs – a, b) Horizontal deformations aligned with the axis of compression and tension; c, d) Vertical deformations perpendicular to the axis of compression and tension; e, f) Diagonal component indicating shear in the constructs in compression and tension

It is important to note that the calibration curves were linear. As such, the digital strain inputs can be adjusted by the appropriate factors when employing the mechanical loading rig. Compression inputs should therefore be adjusted to 80% of the intended deformation, and tension inputs should be increased 1.7 times.

Another observation relative to the calibration of the mechanical loading rig was the existence of considerable shear in uniaxial tension. The observed shearing of the constructs can be attributed to lateral deviations, relative to the horizontal axis, induced by mechanical vibration of the gripping system during rig operation. These effects could not be mitigated as they are inherent to the construction and operation of the system. However, being comparatively minor relative to the strains along the main axis of loading, the low shear values are unlikely to noticeably disrupt cell behaviour, and therefore should not invalidate utilisation of the rig.

Overall, the results in this section confirmed that the layer-by-layer approach provided the flexibility to devise 2D, 2.5D or 3D agarose constructs. Furthermore, preliminary trials proved that mock constructs could successfully be assembled into the rig and subjected to mild mechanical loading for a period of a few hours. Finally, calibration curves were constructed showing that maximum strains of 20% in compression, and 10% in tension, could be reached in the hydrogels using the proposed experimental set-up.

3.4 Optimisation of Sulfo-Sanpah functionalisation and collagen crosslinking to promote cell attachment in agarose constructs

Along with the preliminary validation of versatile constructs for imaging the mechanical loading of hMSCs, it was necessary to work on the parallel objective of functionalising the agarose with ECM elements. The approaches undertaken to accomplish these aims are described in the following sub-sections.

Although agarose is naturally devoid of properties facilitating cell adhesion, several approaches have been described in the literature through which the hydrogel can be chemically modified and subsequently coupled to

cell anchorage groups. A simple protocol was first described by Dodla and Bellamkonda [194], and later adapted by Connelly et al. [202], [203], employing Sulfo-Sanpah to bind agarose to ECM elements (Fig. 2.7). The initial step in both publications consists on a 4-hour incubation to conjugate the Sulfo-Sanpah NHS ester to laminin/RGD peptides. By initiating the protocol with NHS ester crosslinking, this in-bulk approach has the advantage of mitigating decays in crosslinker reactivity caused by the short lifetime of hydrated esters. This step is followed by mixing the conjugated proteins/peptides with a solution of melted agarose. The agarose/functionalised ECM suspension is exposed to an UV light source to couple the photoactivable end of the Sulfo-Sanpah molecules to the hydrogel. After ECM crosslinking, agarose working solutions can be stored, to be re-melted and seeded with cells upon later demand. In this work, the protocol was adapted to attempt the in-bulk crosslinking of agarose with collagen to produce the 3D or 2.5D constructs described in section 3.3 (Fig. 3.5 a).

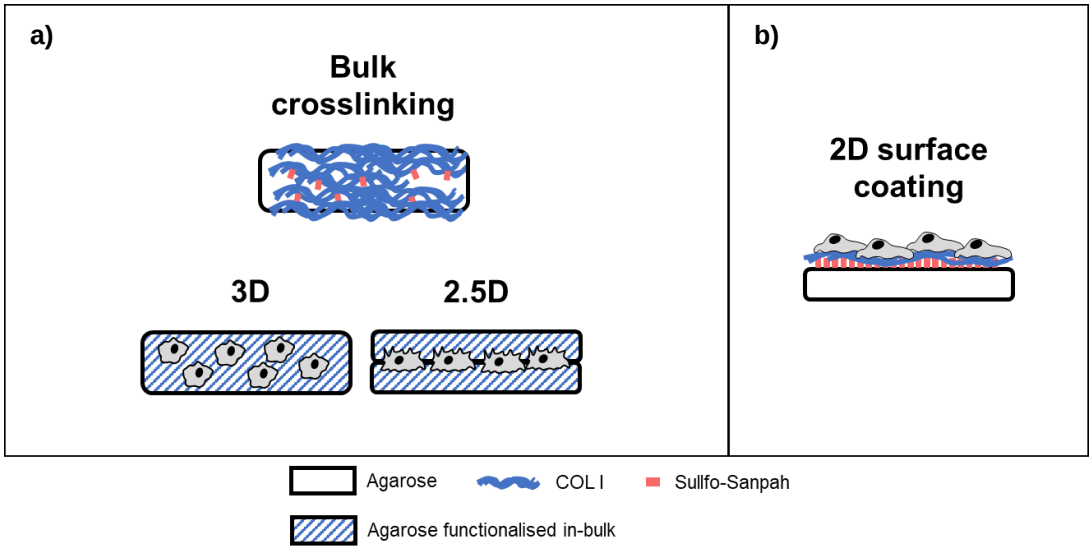

Figure 3-5 – Collagen crosslinking approaches – a) Crosslinking in-bulk consisted on attempting to homogenously functionalise agarose with collagen using Sulfo-Sanpah. If successful, this approach would allow cells to attain spread morphologies when encapsulated in 3D. Collagen availability at the surface of agarose crosslinked in-bulk was also required to overcome the constraints of integration into porous glass endplates in 2.5D constructs. b) 2D surface coating was an alternative approach to the Sulfo-Sanpah functionalisation of inert agarose. However, this approach was only compatible with pre-assembled bottom agarose layers in 2D constructs.

A second form of the crosslinking protocol is predominant in the literature (Fig. 3.5 b), mostly used to produce surface coatings in PAA hydrogels. This alternative consists in reversing the order of the crosslinking reactions, such that hydrogel surfaces are first functionalised with UV-light activated Sulfo-Sanpah, and only subsequently reacted with the ECM elements through the NHS ester.

Subsection 3.4.1 presents the optimisation of a protocol to crosslink collagen in-bulk, and subsection 3.4.2 presents the optimisation of collagen surface coatings on 2D agarose substrates.

3.4.1 Initial attempts to crosslink collagen to agarose in-bulk

Replicating a simple protocol to crosslink collagen into Seaprep agarose in-bulk was critical to consider further development of 3D or 2.5D constructs. In 3D, encapsulated cells would require ECM attachments to be freely available inside the hydrogel. In 2.5D, on the other hand, the objective was to allow both construct layer surfaces to be decorated with collagen and allow cells to attach and spread. In this case, the melted agarose to form top layers of the construct needed to be pre-crosslinked with ECM in order to both be compatible with the layer-by-layer methodology and be integrated into the porous glass ends, as presented in section 3.3. This subsection thus addresses the viability of crosslinking collagen to agarose in-bulk.

Materials and methods

Preparation of Sulfo-Sanpah and collagen stocks

50 mg of Sulfo-Sanpah (ThermoScientific) powder were diluted in 1 ml of dimethylsulfoxide as per supplier instructions, aliquoted into small volumes and stored at -80ºC for up to a few months. Collagen from calf skin type I was reconstituted at 1mg/ml in 0.1M acetic acid and stored at 4ºC.

Preparation of agarose hydrogels crosslinked in-bulk with collagen

Working solutions of COL I were prepared shortly before crosslinking by 1:2 dilution of stock solution in PBS to a concentration of 500 µg/ml. At the start of experiments, Sulfo-Sanpah aliquots were equilibrated at room temperature in the dark, added to collagen solutions at an estimated molar ratio of 100:1 and incubated in the dark at room temperature for 4 hours, under agitation.

Working solutions of 6% (w/v) Seaprep agarose in PBS were melted at 121ºC in a benchtop autoclave cycle and cooled down to 60ºC. All subsequent protocol steps were conducted under aseptic technique inside a laminar flow hood to prevent microbial infections before cell encapsulation. Equal volumes of agarose and functionalised collagen were mixed together to produce a hydrogel mixture at a final agarose concentration of 3% (w/v) and COL I concentration of 250 µg/ml, and immediately cast into optically transparent glass vials. The vials were placed under a portable UV lamp (4 mW/cm^2 of 365nm wavelength, about 35 cm from sample), irradiated for 15 minutes and subsequently allowed to solidify at room temperature. The collagen functionalised hydrogels were then washed and stored hydrated in PBS at 4ºC for two days, to remove unreacted Sulfo-Sanpah. Control samples consisted on non-crosslinked agarose, or agarose directly mixed with collagen without addition of Sulfo-Sanpah.

To test the suitability of agarose functionalised with collagen in-bulk as a substrate for either 3D or 2D cell culture, hMScs were, respectively, either directly encapsulated within the hydrogel, or seeded on the top surface of 2D hydrogel disks.

Cell culture and seeding

hMSCs were cultured as described in Chapter 2, collected in accutase, and re-suspended in culture media at the desired concentration, depending on seeding conditions:

To achieve 3D cell encapsulation, collagen functionalised agarose was re-heated at 80ºC, cooled down to 37ºC and promptly mixed with recently collected cell suspensions. Two-parts of hydrogel solution where mixed with

one-part cell suspension to achieve final concentrations of 2% agarose (w/v), up to 166 µg/ml COL I and $2x10^5$ cells/ml. Cell loaded hydrogels were cast on the central well of a glass bottom petri dish (Fig. 3.6 a) at 150 µl/cm^2. The hydrogels were quickly stored at 4ºC and allowed to solidify for a brief 5-minute period to minimise thermal shock. Encapsulated cells were then supplied with fresh culture media and stored back in an incubator. Identical protocols were repeated for control samples.

To seed hMSCs onto the surface of 2D hydrogel disks, collagen functionalised agarose working solutions were again heated at 80ºC and subsequently cast on the central well of glass bottom petri dishes. To ensure a flat surface on top of the disks, 150 µl volumes were stamped onto the 2 cm^2 of well area with the help of 1.3 cm diameter coverslips wrapped in a hydrophilic layer of parafilm (to facilitate subsequent detachment from the gel). These disk-shaped substrates were allowed to solidify at 4ºC for 2 hours before gentle removal of the coverslip stamps with the aid of tweezers. The substrates were covered in PBS and stored at 4ºC overnight. On the following day, the substrates were sterilised under a germicidal UV-lamp for 40 minutes before seeding. 300 µl of cell suspension containing 5000 cells were gently pipetted on top of each hydrogel disk (Fig. 3.6 b).

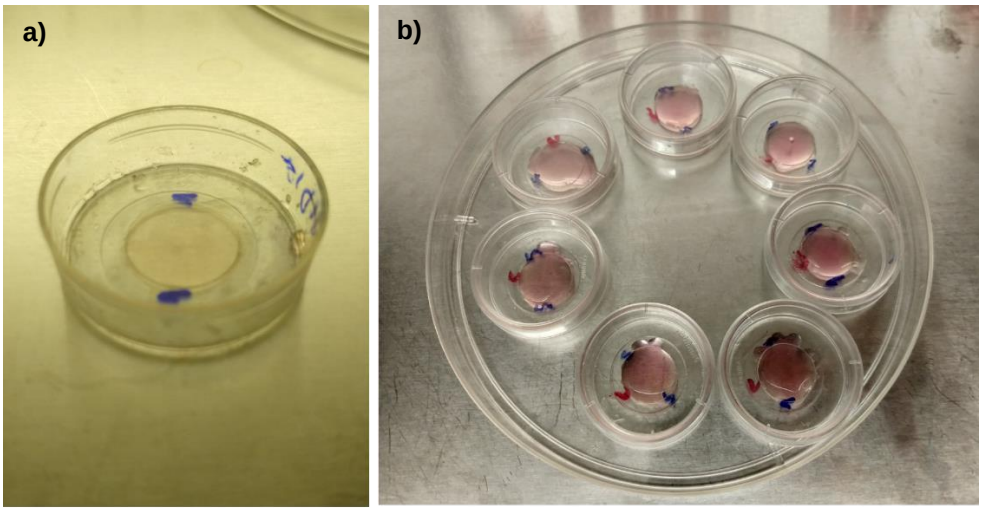

Figure 3-6 – Hydrogel substrate seeding – a) Example of a glass bottom petri dish, note the central well that retains the hydrogel samples during culture; b) Cell seeded agarose substrates

Petri dishes containing the samples were then transported into an incubator to allow overnight cell attachment and spreading. Control samples from unmodified agarose and agarose directly mixed with collagen were prepared and seeded as described.

Cell attachment following encapsulation or surface seeding was monitored for 3 days in culture via standard transmitted light microscopy observation of cell morphology, using x10 and x20 objectives.

Results and discussion

The aim of these experiments was to test the possibility of conjugating collagen to agarose in-bulk, as well as assess the suitability of the resulting substrates for development of 3D or 2.5D constructs. Although replicating the overall methodological approach of former authors, the choice to substitute laminin/RGD peptides for COL I constituted a decisive factor in protocol performance: it was verified that the cells retained the same spherical morphology across samples, both in crosslinked hydrogels and controls, after a period of a few days. As such, it was concluded that the protocol to crosslink agarose was not successful.

The reasons for the lack of success with this approach likely stemmed from the limitations of working with COL I. Being comprised of sets of fibrillar molecules, COL I must be kept at low concentrations (< 1mg/ml), and under acidic conditions, to prevent precipitation. These were major constraints when devising the conditions of the adapted crosslinking protocol. On the one hand, the concentration of collagen working solutions had to be kept as high as possible before Sulfo-Sanpah crosslinking, to ensure that subsequent dilutions did not overly minimise the protein amounts bound onto the hydrogel. On the other hand, failing to dilute the collagen stock equally hindered the success of the reaction in two ways: first, due to the tendency of Sulfo-Sanpah to precipitate collagen into macroscopic clumps, and secondly due to the non-amenable chemistry of NHS esters to the acidic conditions that solubilise the collagen, as the protonation state of amine groups is optimal at slightly basic ph.

As a compromise between these conflicting needs, collagen stock was first diluted in half in PBS buffer to keep the amount of COL I soluble while reducing the acidity of the medium. However, due to the subsequent dilutions entailed in the protocol, the concentration of collagen left in the hydrogel (a maximum of 166 µg/ml) was likely too sparse to allow sufficient density of accessible attachments to the cells, compounded by the fact that the yield of the bulk crosslinking reaction has been reported to be as low as 15 – 30% of the starting ECM amount [203]. This hypothesis is consistent with the fact that other reports in the literature report higher collagen concentrations, e.g. an agarose re-enforced collagen gel formed at a concentration of 500 µg/ml [204], or a 3D printable collagen/agarose blend with a collagen concentration of 2 mg/ml [190].

Another potential point of failure was the reactivity between Sulfo-Sanpah, agarose and collagen. Given that the chemical make-up of Seaprep agarose is devoid of double bonds and nitrogen atoms, the binding of Sulfo-Sanpah to agarose occurs through an unfavourable C-H insertion and is likely of low efficiency. Furthermore, the molecular ratio of 100:1 presented in the methods section was based on a coarse estimate of an average molecular weight of COL I (assumed to be around 150 kDa). Therefore, it was not clear if an adequate amount of Sulfo-Sanpah had been employed for the reaction.

It should be mentioned that it would have been possible to directly assess the degree of success of the crosslinking reaction by resorting to labelling methods (for instance, through fluorescently labelled antibodies against COL I or using histological stains such as Picrosirius red). However, resorting to these methods would not confirm the suitability of agarose functionalised with collagen in-bulk as a viable substrate for cell culture. Conversely, direct observation of cells seeded on the hydrogels allowed for direct confirmation of the degree of success in achieving cell attachment. Due to the limited number of optimisation strategies for bulk COL I agarose crosslinking, it was considered that a more extensive assessment of the protocol would not be opportune.

In addition to encapsulation into 3D, hMSCs were equally seeded on the surface of the agarose substrates crosslinked in-bulk. Under these conditions it was again observed that cells failed to attach to the hydrogel

surface. As before, it was likely that the concentration of collagen in the hydrogel was not enough to allow a substantial density of cell attachment groups in the surface of the substrates.

Considering all these results, it was decided that crosslinking agarose in bulk would not be achievable with the designated protocol.

3.4.2 Optimisation of the covalent attachment of a collagen surface coating onto 2D agarose scaffolds

Although the initial attempts at bulk crosslinking of COL I to agarose were not fruitful, the use of Sulfo-Sanpah in the covalent attachment of a 2D surface coating to hydrogel substrates was still a viable possibility. This protocol variation had not yet been described in coating of agarose substrates, presumably because agarose is a standard biomaterial in 3D non-adherent cell culture studies. The novelty of producing 2D agarose cell culture substrates further justified attempts at repurposing Sulfo-Sanpah for covalent binding of a collagen surface coating onto the agarose substrates.

It should be noted that there is a lack of consistency throughout the multiple protocols currently available in the literature describing Sulfo-Sanpah hydrogel surface functionalisation. Differences have been reported in the amounts of Sulfo-Sanpah relative to substrate area, in the exposure time to UV-light (ranging from 30 s to over 10 minutes), in the distance to the UV-lamp and wave-length of the light-source, as well as in the concentration and duration of incubation (2 hours to overnight, at both room temperature and 4ºC), and in the diversity of ECM elements selected for coating [105], [194], [202], [205]–[213]. Such a wide range of reports suggested that the functionalisation of agarose with Sulfo-Sanpah would be easily achieved without extensive experimental optimisation. This, however, was not the case, as early attempts to crosslink COL I to the surface of agarose proved remarkably inconsistent. This section therefore describes the heuristic approach undertaken to develop a protocol to reproducibly coat agarose substrates with COL I through Sulfo-Sanpah crosslinking chemistry.

Materials and methods

Preparation of 2D agarose substrates coated with COL I

Working solutions of 3%(w/v) Seaprep agarose in PBS were prepared as before. 2D disk-shaped substrates were cast onto the central well of glass bottom petri dishes. To ensure a flat surface on top of the disks, 150 µl volumes were stamped onto the 2 cm^2 well areas with the help of 1.3 cm diameter coverslips. These disk-shaped scaffolds were gelled at 4ºC for 2 hours before gentle removal of the coverslip stamps with the aid of tweezers. The scaffolds were covered in PBS and stored at 4ºC overnight.

To optimise the COL I surface coating protocol, several combinations of Sulfo-Sanpah dilutions, UV-activation time and collagen amounts and incubation time were tested. For every experimental condition four samples were prepared and tested. Due to the instability of Sulfo-Sanpah in aqueous environments, protocol steps preceding ECM incubation were executed rapidly. One day following agarose substrate preparation, Sulfo-Sanpah aliquots were equilibrated at room temperature in the dark and diluted in distilled H2O at different ratios (1:25, 1:50, 1:100, 1:200). A volume corresponding to 100 µl/cm2 of each dilution was added to the top surface of individual agarose disks. The disks were quickly placed under a portable UV lamp, and irradiated for varying amount of time (30s to 20 min). Unreacted crosslinker was aspirated and the hydrogels were washed three times in PBS.

Working solutions of COL I were prepared shortly before crosslinking by diluting collagen stock in PBS to varying final concentrations (10 – 60 µg COL I/ 200 µl PBS/ cm^2). These collagen solutions were added to the functionalised agarose surfaces and incubated at room temperature for several hours (1 h to overnight) under agitation. After incubation the excess ECM solution was aspirated from atop the gels and the scaffolds were washed in PBS and stored at 4ºC overnight.

In the following morning the scaffolds were covered with sterilised PBS and transferred into a laminar flow hood equipped with a germicidal UV-lamp. The substrates were sterilised under the lamp for 40 minutes before cell seeding.

Cell culture and seeding

Hydrogel samples were consistently prepared a single day in advance to hMSC surface seeding. hMSCs were collected from culture as previously described and volumes of 300 µl of cell suspension containing 2000 cells were gently pipetted on top of each hydrogel disk. The petri dishes containing seeded substrates were gently transported into an incubator to allow overnight cell attachment and spreading. Control samples were prepared in equal manner from unmodified agarose and agarose incubated with collagen without Sulfo-Sanpah crosslinking.

Cell attachment was again monitored by standard transmitted light microscopy observation of the morphology of cells after 1 day in culture.

Results and discussion

Despite the ubiquity of protocols detailing Sulfo-Sanpah surface functionalisation in PAA hydrogels, the use of the crosslinker with agarose resulted in a low yield of success for the combinations of reaction parameters tested. The development of a reproducible protocol to bind COL I surface coatings onto agarose therefore required extensive optimisation.

No live cells were observed on the surface of control samples suggesting that Sulfo-Sanpah was necessary to promote coating of the hydrogel surface with ECM. However, hMSC seeding into crosslinked samples consistently produced three concurrent scenarios: 1) no cell attachment (Fig. 3.7 a); 2) partly successful cell attachment (Fig. 3.7 b); 3) homogeneous surface coverage of spread out cells (Fig. 3.7 c).

Upon successive protocol replications, it became clear that most parameter configurations would produce an unpredictable combination of scenarios 1-3. As such, optimisation of the protocol required the identification of parameters that would maximise the yield of viable substrates. It was first noticed that incubating COL I with the functionalised substrates for longer than 3 hours would lead to the formation of macroscopic protein clumps atop the hydrogel surface. These clumps could washed-off at a later point, but this was associated with impaired cell attachment.

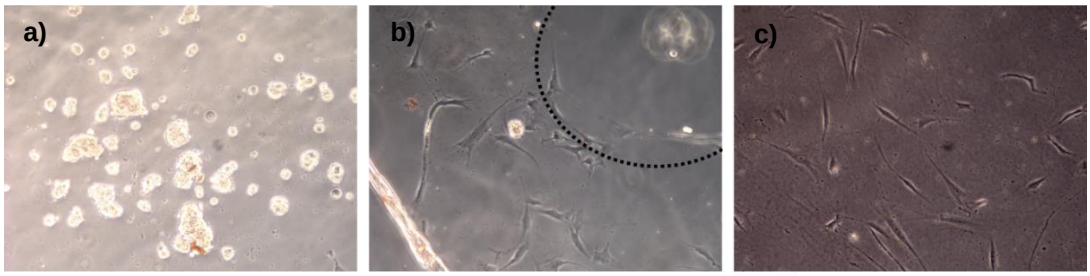

Figure 3-7 — Three concurrent results in 2D surface coating optimisation – a) Unsuccessful coating, no attached cells throughout hydrogel surface; b) Non-homogenous coating, resulting in variable surface portions (20-80%) of the substrate being successfully coated, with large patches of naked agarose in between (inside dotted line in the image); c) Homogeneous surface coating

On the other hand, any period of incubation under 2 hours was also quickly excluded due to generally poor results. The incubation time was therefore fixed at 2 hours to reduce the reaction parameter landscape. Similarly, COL I amounts bellow 20 µg/cm^2 lead to incomplete surface coatings, whereas collagen amounts over 50 µg/cm^2 would equally contribute to the formation of clumps during incubation. To mitigate adverse effects the amount of ECM was therefore set to 30 µg/cm^2.

Unlike with other parameters, varying the amounts of Sulfo-Sanpah and UV-light irradiation did not clearly influence methodological consistency. The volume of Sulfo-Sanpah was therefore set at 1 µl/ cm^2 of surface area (corresponding to a 1:100 stock dilution) and the UV exposure time brought down to 2 minutes. These choices reflected a minimum utilisation of crosslinker without substantially compromising reaction efficacy, and a reduction in sample preparation time. These were important compromises as the overall success rate of sample preparation (i.e. the number of substrates in each batch which were coated with a layer of collagen and thus viable for cell culture) remained at less than 50%, demanding the production of an excess of hydrogel substrates relative to the number intended for analysis, to compensate for unsuccessful crosslinking.

After this initial phase of optimisation, the protocol was still not reproducible enough to reliably produce agarose substrates. As such, one final alteration was introduced, namely the repetition of the Sulfo-Sanpah functionalisation step before COL I incubation. This modification increased the reproducibility of the protocol, leading to a proportion of viable samples of around 60%. The increase in number of viable substrates was considered sufficient to perform future experiments, and therefore further protocol optimisation was not attempted. Furthermore, it is likely that the main hurdle of this approach was an incompatibility between the chemistries of Sulfo-Sanpah and agarose, would not be to overcome without substantially altering the experimental approach. This is discussed in further detail in the following section.

3.4.3 Potential mechanisms of Sulfo-Sanpah/agarose crosslinking

PAA has been extensively functionalised with Sulfo-Sanpah in the literature [208], [210], [212], which is typically justified by an amenable reactivity between the crosslinker and the amines (NH2) in acrylamide monomers. Agarose, on the other hand, is made entirely of C, O and H atoms bound by single covalent bonds. Nonetheless, due to the non-specificity of arylazide reactions [214] , the concrete functionalisation pathway between Sulfo-Sanpah and either PAA or agarose remains unconfirmed, as it has so far not been validated by robust chemical analysis. Consequently, there is a possibility that the crosslinking chemistry of Sulfo-Sanpah is inherently unsuitable for use with agarose, and similar, hydrogels. However, reports on this issue are conflicting.

An important argument on the pitfalls of Sulfo-Sanpah crosslinking was presented by Adam Engler's group. Using force spectroscopy to assess the Sulfo-Sanpah mediated tethering of collagen fibres to PDMS, the authors demonstrated that the chemistry of the polymer is not amenable to functionalisation with Sulfo-Sanpah, which was attributed to the absence of NH_2 groups in PDMS monomers [100]. Like PDMS, the chemical make-up of agarose does not include amines, and therefore a similar conclusion could be drawn relative to the functionalisation of agarose. Yet, additional reports on

this issue provide contradictory evidence. For instance, several different groups have reported Sulfo-Sanpah was a necessary requirement to successfully conjugate ECM elements to polymers ranging from PDMS [211], [215], [216], to agarose [143], [194], [202], [217], and chitosan [218]. Interestingly, in the latter report [218], extensive characterisation of the Sulfo-Sanpah crosslinking onto chitosan was performed. In this reference, the authors provided evidence that the crosslinker does not primarily bind to the NH_2 groups in chitosan monomers, the mechanism assumed in Engler et al.'s publication, but rather, first binds to hydroxyl (OH) moieties. Although lacking amines, agarose does similarly exhibit hydroxyl groups in its structure. As such, while previous authors have speculated that Sulfo-Sanpah covalently binds agarose through a C-H insertion [194], it is possible that the preferred crosslinking reaction pathway proceeds similarly to the one described in chitosan [218], or perhaps through a ring expansion process. Alternatively, it possible that Sulfo-Sanpah, does not in fact covalently bind to the hydrogel, but rather promotes ECM coating through other types of interaction (e.g. electrostatic).

The particulars of the crosslinking reaction notwithstanding, the high rate of crosslinking failure attained in this work, suggests that the underlying affinity of the UV-activated arylazide nitrene for agarose is quite low. Consequently, to increase the overall yield of the protocol for future projects it may be worthwhile to explore different reaction chemistries. As an example, several authors have described agarose derivatives with amino, carboxylic acid and other side groups [219], [220] which are more amenable to a wider range of crosslinking chemistries. Nonetheless, these alternative chemistries are formulated through complex reactions, falling outside the scope of this thesis.

3.4.4 Detachment of collagen coatings over prolonged culture

The results described in this chapter support the hypothesis that Sulfo-Sanpah plays a role in binding collagen to the agarose surface. Although the efficiency of functionalisation remained low throughout experiments, all hydrogel controls (i.e. "naked" agarose substrates and substrates incubated

with collagen in the absence of crosslinker) persistently failed to produce viable cell attachment. In these cases, the cells retained spherical morphologies indicating that the surface of agarose was not appropriately functionalised, as shown in Fig. 3.8.

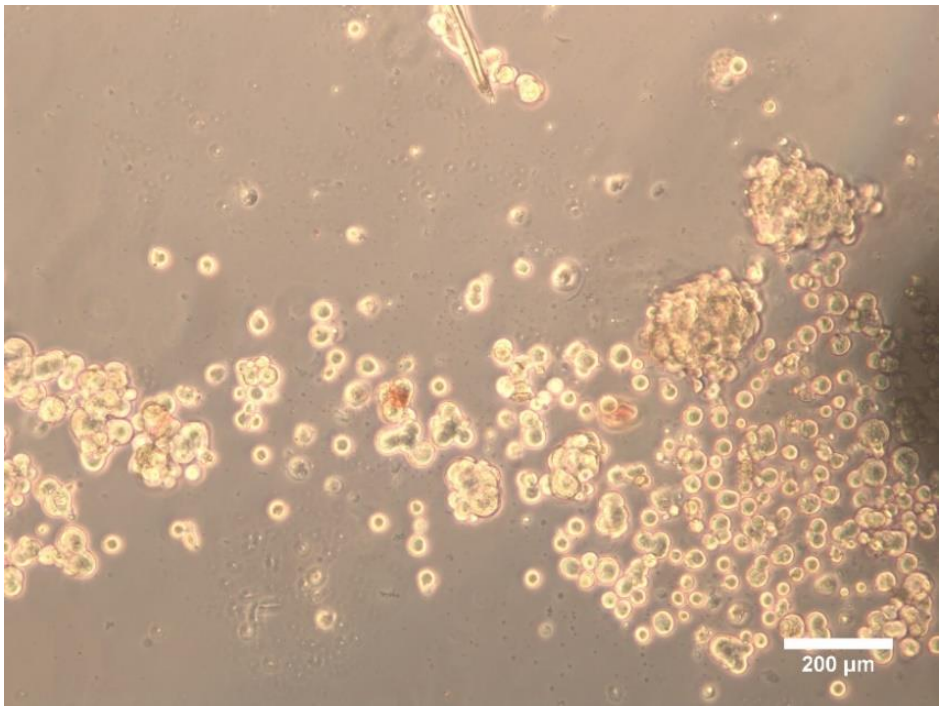

Figure 3-8 – Failed cell attachment in the absence of Sulfo-Sanpah crosslinking

On the other hand, Figure 3.9 illustrates example morphologies of hMSCs seeded into viable 2D collagen-coated 1% agarose substrates prepared according to the optimised protocol, 1 and 3 days after seeding. In these cases, the cells were able to attach and spread on the surface of the substrates. Moreover, as Fig. 3.10 illustrates, the cells maintained these spread-out morphologies for periods of culture exceeding one week.

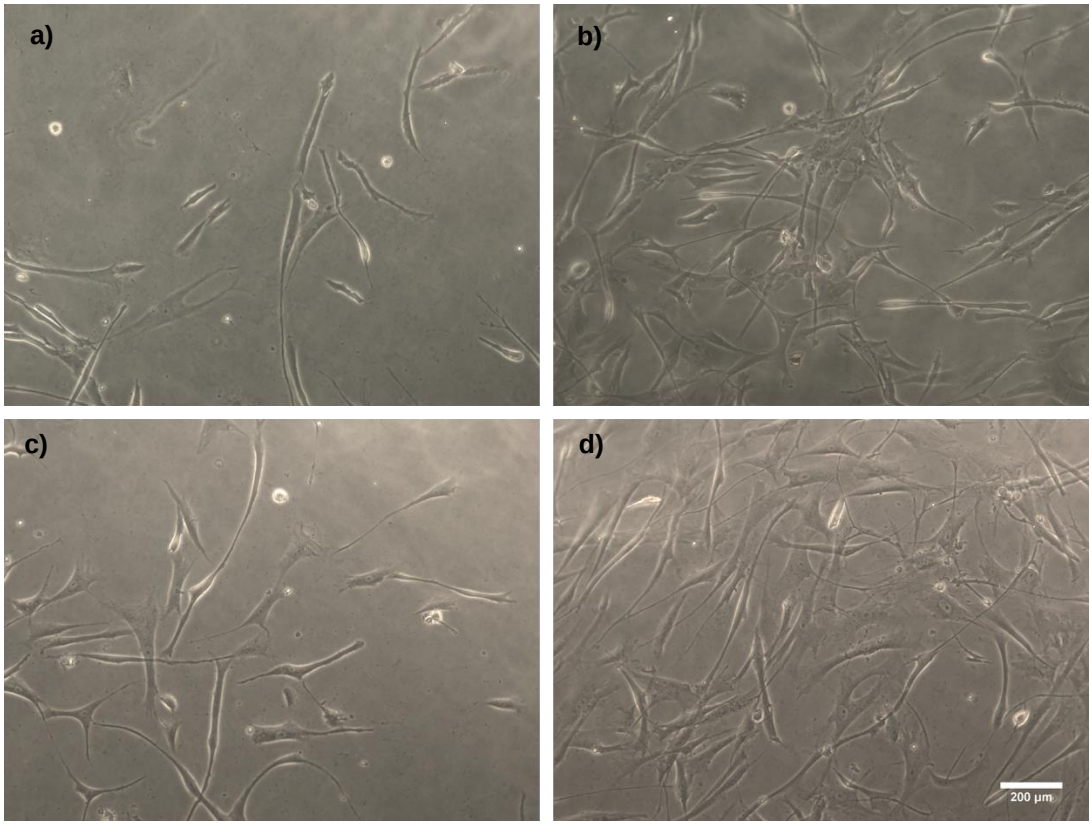

Figure 3-9 – Examples of hMSC morphology in optimised 2D collagen-coated 1% agarose substrates; a) Sparse cell morphology at day 1 after seeding; b) High seeding density cell morphology at day 1 after seeding; c) Sparse cell morphology at day 3 after seeding; d) High seeding density cell morphology at day 3 after seeding

Nonetheless, one major limitation of the collagen-coated substrates was that prolonged periods of culture (over 3 days) resulted in the partial detachment of the collagen coating in several of the samples (Fig. 3.10 c,f,i).

The reasons for the partial detachment of collagen surface layers can potentially be attributed to a combination of some, or all, of the following factors: cell remodelling and contraction of collagen fibres, thermal degradation of the ultra-low gelling temperature agarose, or again, due to weak/unstable crosslinking between Sulfo-Sanpah and the polymer chains.

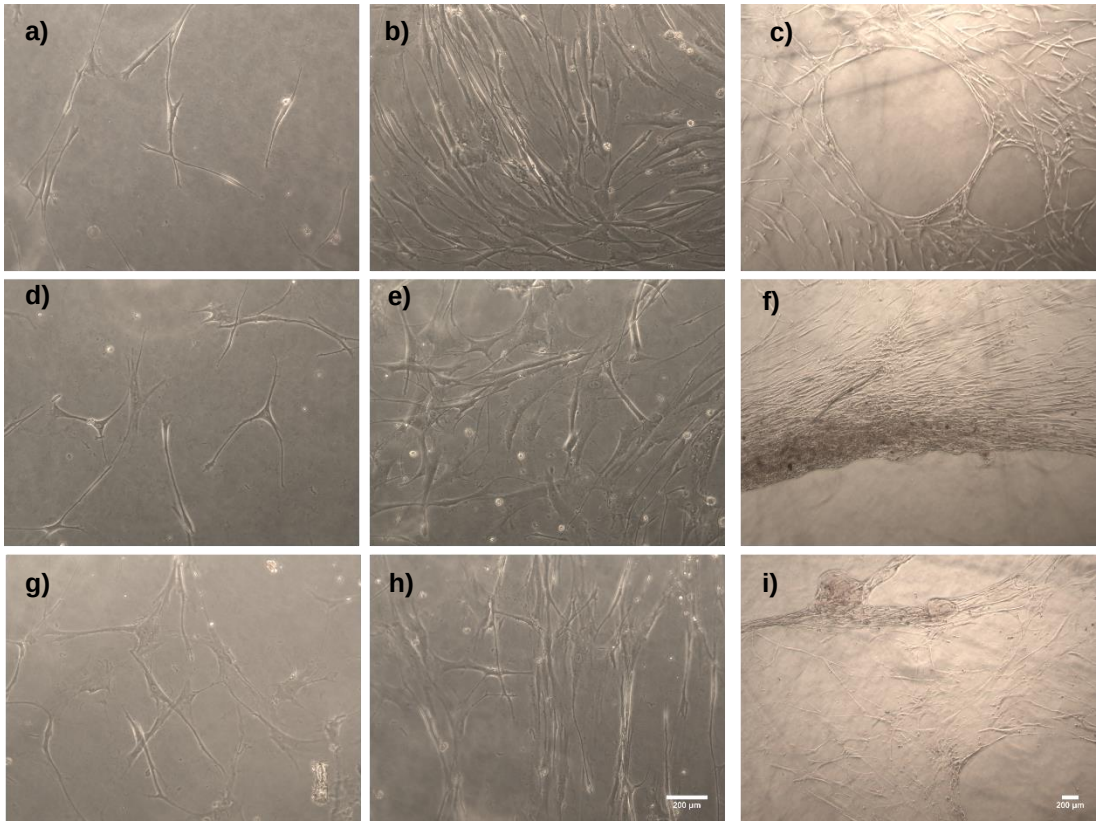

Figure 3.10 – Examples of hMSC morphology and collagen coating detachment after prolonged culture; a) Sparse cell morphology at day 5 after seeding (x10 magnification); b) High seeding density cell morphology at day 5 after seeding (x10 magnification); c) Partial detachment of collagen coating at day 5 after seeding (x4 magnification); d) Sparse cell morphology at day 7 after seeding (x10 magnification); e) High seeding density cell morphology at day 7 after seeding (x10 magnification); f) Partial detachment of collagen coating at day 7 after seeding (x4 magnification); g) Sparse cell morphology at day 10 after seeding (x10 magnification); h) High seeding density cell morphology at day 10 after seeding (x10 magnification); i) Partial detachment of collagen coating at day 10 after seeding (x4 magnification);

3.4.5 Reassessment of agarose construct dimensionality

Sections 3.4.1 and 3.4.2 described attempts made at devising two different approaches for crosslinking collagen to agarose. While in-bulk crosslinking of ECM proved unsuccessful, a protocol was sufficiently optimised for preparation of 2D collagen-coated agarose substrates. 2D agarose constructs therefore remained the only viable redesign option (schematised in Fig. 3.8) to fulfil the objectives proposed in 3.2.

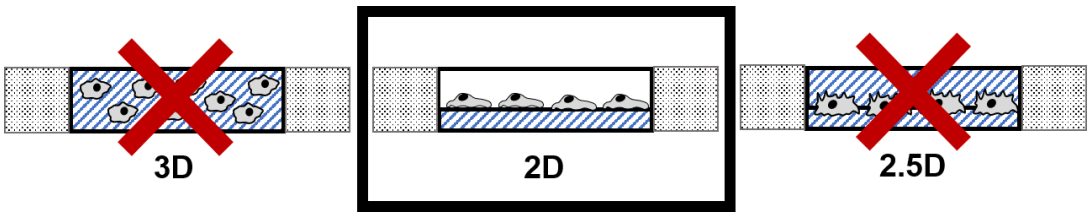

Figure 3-11 – Final selection of a favourable redesign for agarose constructs – After development of a layer-by-layer construct assembly methodology, and optimisation of collagen surface coatings onto agarose substrates, the 2D construct redesign was the only viable alternative of the three proposed in section 3.2.

3.5 Mechanical characterisation of agarose through AFM microindentation and unconfined compression testing

Having established a method to coat ultra-low gelling temperature agarose substrates with collagen, it became relevant to perform a mechanical characterisation of the hydrogel. AFM microindentation measurements were first conducted to characterise the effects of typical cell culture conditions on the agarose scaffolds. These experiments are relayed in section 3.5.1. Agarose samples were also subjected to unconfined mechanical compression tests and stress relaxation experiments as described in 3.5.2.

3.5.1 AFM microidentation to characterise long-term influences of cell culture environment on 2D agarose substrates

It has been documented that the mechanical properties of agarose can be influenced by the thermal history of the hydrogel specimens [221]. To determine if cell culture environment conditions sustained an effect on the 2D agarose substrates, bio-AFM microindentation was chosen to assess substrate mechanical properties. This instrument provided two main advantages: the integration of temperature control onto the measurements, and the determination of hydrogel sample stiffness at a scale more comparable to that of cellular activities. The methodology and results of this study are presented in the following sections.

Materials and methods

Preparation of 2D agarose substrates

Flat 2D hydrogel substrates were prepared from 1%, 3% and 5% (w/v) Seaprep agarose cast onto the central well of glass bottom petri dishes, as previously described. To simulate the conditions of long-term cell culture environments, hydrated samples were transferred to an incubator and maintained for periods of up to 8 days at the start of each experiment.

AFM microindentation measurements

All measurements were performed on a Nanowizard 4 (JPK, Germany), integrated with an Axio Observer Z.1 epifluorescence microscope with Plan-Apochromat lenses (x20) equipped with a cooled CMOS camera (Orca Flash 4). The samples were probed using MSNL-10 gold-coated rectangular cantilevers (0.1 N/m nominal spring constant) with pyramidal tips (2.5-8 μm high, supplied by Bruker, USA). Petri-dishes were mounted on a heating accessory to maintain temperature at 37º C. Prior to measurement, the cantilevers were thermally equilibrated submerged in PBS. Cantilever sensitivity was calibrated in contact mode on a bare plastic region in a reference petri-dish (i.e. not containing hydrogel samples) at the beginning of each session. The calibration was performed under these conditions to compensate for the lack of probe access to glass regions on the petri-dishes loaded with samples. The cantilever was subsequently pulled away from the plastic surface to calibrate the force constant through thermal fluctuations.

At the onset of experiments new samples were measured at room temperature. The same samples were then stored in an incubator and re-measured at 1h, 3h, and 1 to 8 days. AFM measurements were performed using JPK's proprietary QI mode, for rapid acquisition of force-curves and topography mapping. Regions of 100 by 100 μm^2 (comprising 255 force curves) were randomly selected and measured in each sample. These dimensions were selected to be representative of the area encompassing a single hMSC. Force curves were collected with z-length of 7.5 μm, extension speed of 100 μm/s and a setpoint of ~20 nN. Data analysis of the force-

displacement curves was carried out using Snedon's model for a conical indenter [222] using a pipeline written in Matlab [223]. Median **E** values were calculated from the 255 force-curves in each imaging field. Sample averages where plotted in time, with the error bars representing standard deviations. For each sample a minimum of three random fields were measured, and four samples were averaged per time point.

Results and discussion

2D agarose substrates were kept under cell culture environment for a period of 8 days and their stiffness was assessed from the analysis of AFM force-curves. The results of this procedure are represented in Fig. 3.8.

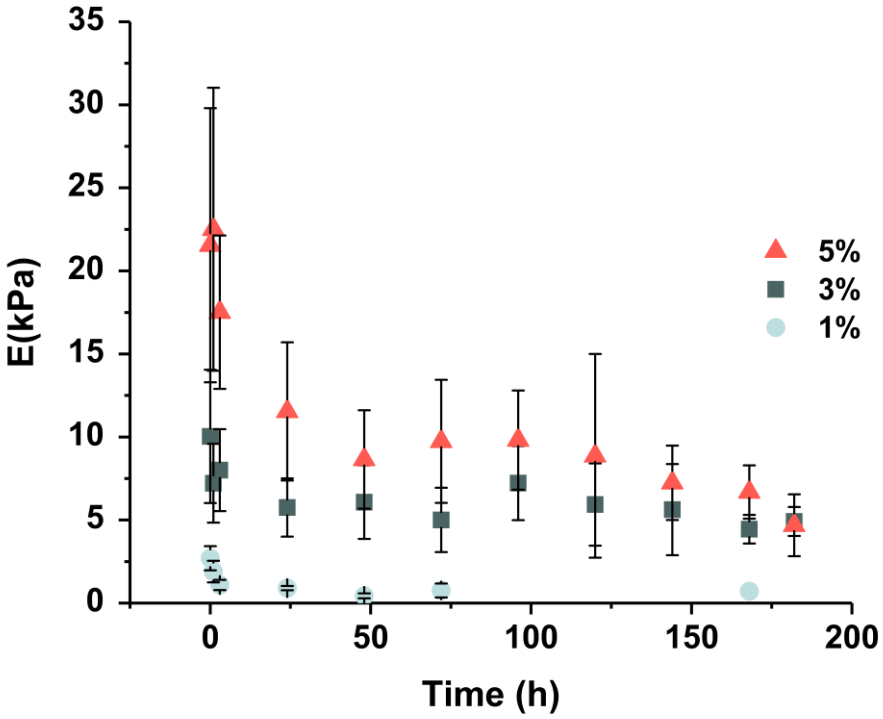

Figure 3-12 – Stiffness changes over time in agarose substrates kept under cell culture environment – This plot illustrates the decline in E in 1% (soft), 3% (intermediate) and 5% (stiff) 2D agarose substrates over a week. Data is plotted as average values of N = 4 replicates. Error bars indicate standard deviation.

As the plot shows, at t=0 (room temperature measurements) the expected relationship between agarose concentration and hydrogel stiffness was observed: hydrogels with highest agarose concentration (5% agarose) had the largest average stiffnesses (**E** over 20 KPa), whereas intermediate 3% gels displayed **E** around 10 kPa and 1% hydrogels being substantially softer with **E** of 2 kPa.

Importantly, Fig. 3.9 evidences steep decreases in hydrogel stiffness throughout the measurement period. Across conditions, **E** decreased to about half the initial values within the first 24 hours, after which point the decay rate decreased, plateauing at around 48 hours. It can also be observed that 5% and 3% agarose hydrogels developed similar **E,** around 5 kPa, as result of prolonged exposure to cell culture conditions. Conversely, 1% agarose hydrogels had a final stiffness of 700 Pa – an order of magnitude softer than the other samples. These results confirmed that the cell culture environment had a substantial effect on the mechanical properties of agarose. Critically, this effect must be accounted for when considering the application of the hydrogels in biological scenarios.

It is important to refer that two limitations were encountered when performing these measurements. Firstly, the range of horizontal motion of the AFM was limited by the edges of the petri dish containing the hydrogel samples, thereby obstructing probe positioning on top of an exposed glass or plastic surface. To overcome this limitation, calibrations were performed on an empty petri-dish at the beginning of each session.

Secondly, unlike with PAA hydrogels, there is no standard chemical reaction to covalently bind agarose to a glass substrate. Consequently, agarose sample movement was solely restricted by the central well in the petri-dishes were the hydrogels were cast (Fig. 3.6 a). Due to this, samples commonly lost contact from the bottom surface after a few days in incubation, as water infiltrated the interface between samples and the petri-dish. This occurrence often disrupted the acquisition of AFM measurements, resulting in force-distance curves with artefacts. This was likely due to a cushioning effect of the layer of water under the samples preventing the probe from indenting the material. To overcome this issue, the AFM was retracted, PBS was drained from the affected samples and the hydrogel disks were gently pressed down

with a glass coverslip and tweezers to regain contact with the petri-dish surface. The samples were then re-hydrated before subsequent measurements were performed. However, this correction was not successful in many of the 1% hydrogels due to sample fragility, accounting for the absent values in Fig. 3.9.

Despite these limitations, it was still possible to successfully establish a relationship between agarose concentration and scaffold stiffness and divide the substrates into three categories: stiff substrates – 5% hydrogels with expected initial **E** of about 20 kPa; intermediate substrates – 3% hydrogels with **E** circa 7 kPa; and soft substrates – 1% hydrogels of 2 kPa **E**. It was also possible to identify the gradual softening of the hydrogels, with the terminal **E** values falling just below half the corresponding stiffness at room temperature. This characterisation is relevant when employing agarose as a substrate for mechanobiology experiments, the topic described in Chapters 4 and 5.

It should be mentioned that, in the future, similar measurements may be improved by using a hydrogel-compatible adhesive to prevent samples from slipping in-between measurements, and decreasing sample dimensions to allow AFM probe access to a plastic substrate for calibration purposes.

3.5.2 Unconfined compression tests to study bulk properties of agarose scaffolds

Apart from standard determination of hydrogel stiffness, an objective of this work was to assess nonlinear-elastic behaviours in agarose. To do so, agarose samples were characterised through unconfined compression tests – first, to study the effects of increasing strain on specimen mechanical properties, and second, to characterise stress relaxation responses on the agarose hydrogels.

Materials and methods

Preparation of agarose specimens

1%, 3% and 5% (w/v) working solutions of Seaprep agarose were prepared as described in former sections. Melted agarose was cast on cylindrical moulds to form specimens of 1.2 cm in height and 1.3 cm in diameter. These specimens were set at 4ºC for several hours, removed from the moulds and hydrated in PBS before testing.

Unconfined bulk mechanical compression and stress relaxation

All experiments were conducted on an Instron (USA) 3342 mechanical testing apparatus providing displacement control of uniaxial compression platens. Measurements were performed with a 500 N load cell, at the rate of 1mm/min. Agarose specimens were placed on top of a strip of latex to prevent slippage and maintained submerged in PBS inside a plastic petri-dish positioned on the stage of the instrument. The top platens (75 mm in diameter) was lowered until full contact with the hydrogel surface was established. Bluehill v3 software was used to program the instrument and generate force-displacement curves by inputting 30% strain/sample breakdown as test endpoints. Data from the measurements was exported, and manually converted into stress (σ) and strain (ε) values. Matlab was used to remove noise and smoothen the curves through a moving average filter with window size of 20 points. Tangent moduli were approximated by calculating the slope of a linear fit in an equilateral window (15 points wide) centred on 5%, 10%, 15% and 20% strains.

To conduct stress-relaxation measurements, maximum strains of 10% (ε_0=0.1) were imposed on the specimens, and the deformation was maintained at a constant level, while tracking the forces acting on the load cell over a 10-minute period. Stress-relaxation curves were generated by plotting stress vs. time. Data precluding relaxation (before reaching ε_0) was excluded from analysis, stress decay curves were smoothed as before, and normalised by peak stress as σ/σ_0. Terminal stress values were used to calculate the ratio of relaxation for each specimen as σ_{10min}/σ_0.

Results and discussion

Fig. 3.10 contains an example of the data obtained from unconfined compression tests in a cylindrical 3% agarose specimen. Fig. 3.10 a) displays an example of unprocessed data. The substantial amounts of noise in the curve stemmed from the forces generated during compression (around 10^{-1} N) matching the lower sensitivity range of the 500 N load cell used in the measurements. After application of a moving average filter, the noise was successfully removed, as exemplified in Fig. 3.10 b).

As expected from a biopolymer curve, and more specifically non-covalently crosslinked hydrogels [224], an approximate linear region at small deformations (**ε** < 0.1) was observed, along with a non-linear dependence between stress and strain when applying large strains (**ε** > 0.1).

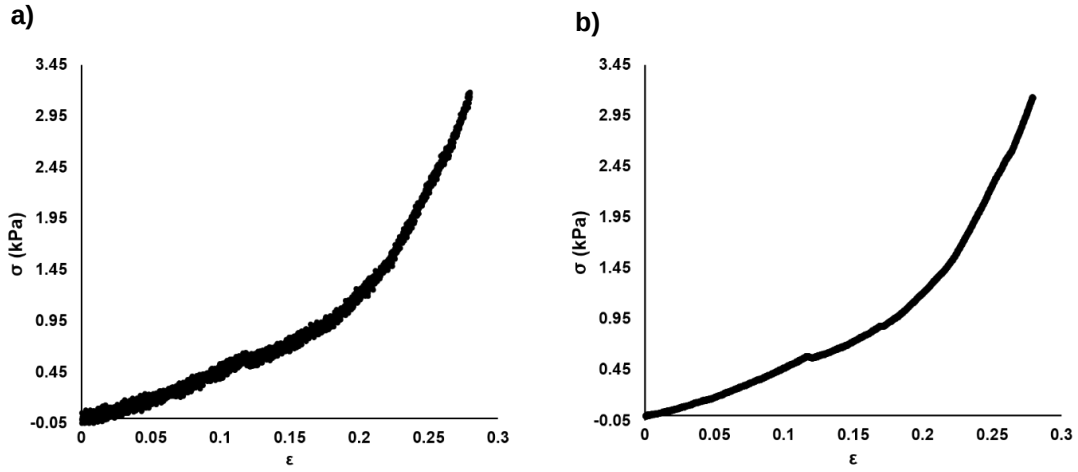

Figure 3-13 – Representative stress-strain curve from unconfined compression tests in a 3% agarose specimen – a) acquired data, b) data smoothed by application of a moving average filter.

This trend was observed among all samples independently of hydrogel composition. It should be stated that there is no trivial procedure to quantify stiffness in non-linear stress-strain curves, such as the ones in Fig. 3.10. As such, a simple method was devised to estimate **E** values at strains of 0.05, 0.1, 0.15 and 0.2, relayed by tangent moduli. This method consisted on fitting a linear equation to the near vicinity (7 points in either direction) of the point of interest and using the slope as an approximation of the tangent modulus at

that strain. This methodology is analogous to the standard calculation of **E** in the linear elastic regime of standard materials but generalised to any point of a non-linear curve. Stiffness values obtained for each hydrogel concentration are plotted in Fig. 3.11.

This figure demonstrates that Seaprep agarose specimens at concentrations ranging from 1% (soft) to 5% (stiff) display non-linear stain-stiffening behaviours, i.e. the stiffness (resistance to deformation) of the material increases with the amount of compression it is subjected to. Differences in the magnitude of **E** between soft and stiff hydrogels, however, make it difficult to visually compare the degree of strain-stiffening between different conditions. Fig. 3.12 therefore represents a normalisation of the data by the moduli at 0.05 ($\mathbf{E_{0.05}}$) for each of the experimental conditions tested.

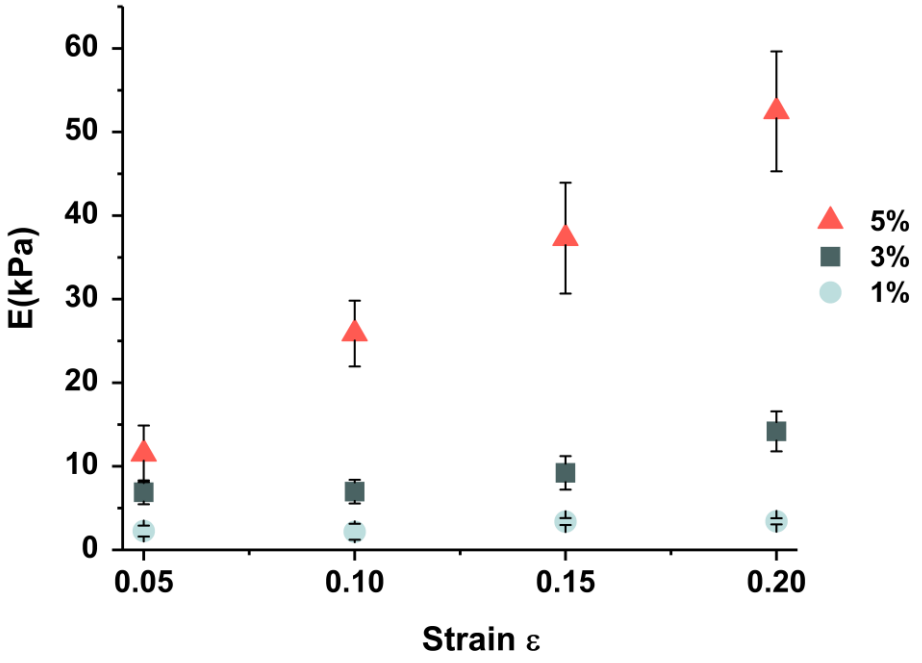

Figure 3-14 – Strain-stiffening in agarose hydrogels – Tangent moduli were calculated as the slope of lines fitted to the vicinity of the points of interest. Data is plotted as average of N = 3 replicates. Error bars represent standard deviations.

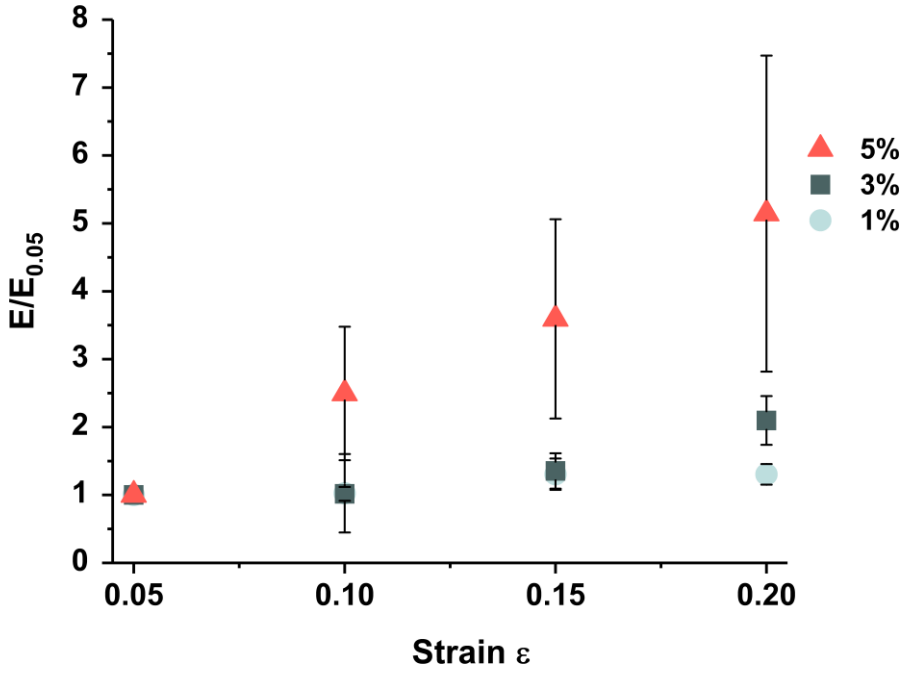

Figure 3-15 – Normalised strain-stiffening in agarose hydrogels – Relative amount of strain stiffening relative to 5% strains. Data is plotted as average of N = 3 replicates. Error bars represent standard deviations.

Upon normalisation, the strain stiffening behaviour of 5% specimens is still more pronounced comparatively to the other hydrogels. Conversely, the data suggests that 1% and 3% hydrogels behave in nearly identical way until large strains ($\boldsymbol{\varepsilon} \geq 0.15$) are reached, after which point the intermediate stiffness samples present a higher strain-stiffening ratio.

Although the precise molecular mechanisms through which hydrogels display this type of behaviour are still not well known, the properties reported in this work are typical of many biopolymers [158], [159], [224]. A conceivable hypothesis to explain these results is that in stiffer agarose hydrogels - with higher densities of polymer chains - compressive loads encounter higher resistance in the reorganisation of the internal structure of the specimen at earlier strains. In other words, in stiffer and denser hydrogels the free volume available for chain rearrangement might be reduced relative to softer samples, and the resistance to compression could therefore be a product of repulsive interactions between a higher number of adjacent biopolymer networks. The validity of this hypothesis, however, would have to be scrutinised by molecular

simulations and further experimental work falling beyond the scope of this thesis.

It is interesting to note that there is good agreement between the data obtained from AFM microindentation experiments (Fig. 3.9), and those in Fig. 3.11. In section 3.5.1 it was reported that, at room temperature, stiff substrates presented average **E** from 10 to 30 KPa, 3% substartes had values of **E** circa 5-12 kPa and softer 1% substrates exhibited **E** near 2 kPa. These values closely match those contained in the initial region of the stress-strain curves from macroscopic compression tests (**ε** ~ 0.05 – 0.1). The correlation between the AFM microindentation and mechanical testing results (**ε** = 0.1) are shown in Fig. 3.13.

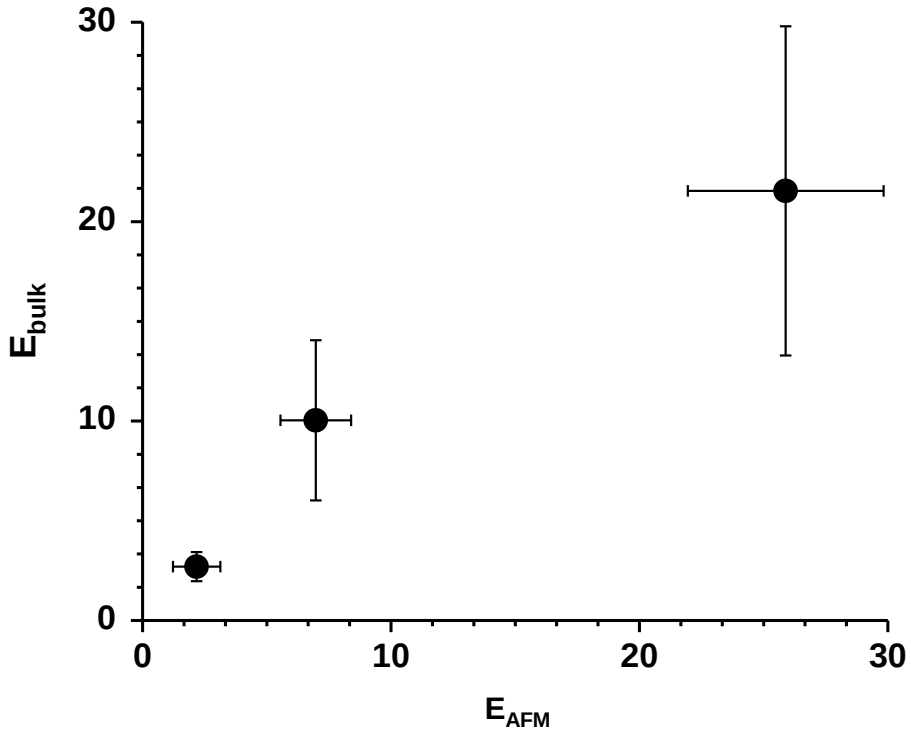

Figure 3-16 – Comparison between AFM microindentation and macroscopic compression tests – Room temperature stiffness values for 1%, 3% and 5% agarose hydrogels are presented left to right.

Interestingly, this observation raises the question of which segments of a stress-strain curve from macroscopic analysis are relevant for the activity of cells seeded on the material. If cells do indeed probe their surrounding environment in a scale comparable to the local raster of an AFM probe, rather than the bulk compression of an anvil, the relevance of bulk strain-stiffening in influencing cell behaviour might be called into question. The results presented in this section, however, cannot provide definitive answers as to this question. Information from advanced computational simulations might be necessary to estimate the microscale profile of loads and displacements in hydrogel materials locally subjected to cell tractions [225], [226]. Likewise, state-of-the art experimental tools, such as traction force microscopy and super-resolution microscopy might be particularly useful in building appropriate models with which to estimate these mechanical profiles in a near future [227], [228].

One major point of interest in current mechanobiology research is the influence of viscoelasticity in mediating cell responses. The behaviour of viscoelastic materials results from the combination of elastic and viscous properties. Thus, the mechanical responses of these materials are time dependent and can manifest as stress relaxation.

An unconfined compression study was performed to preliminarily assess the stress relaxation response of soft, intermediate and stiff agarose specimens. Fig. 3.14 a) shows the results of a representative stress relaxation experiment in a 5% agarose specimen.

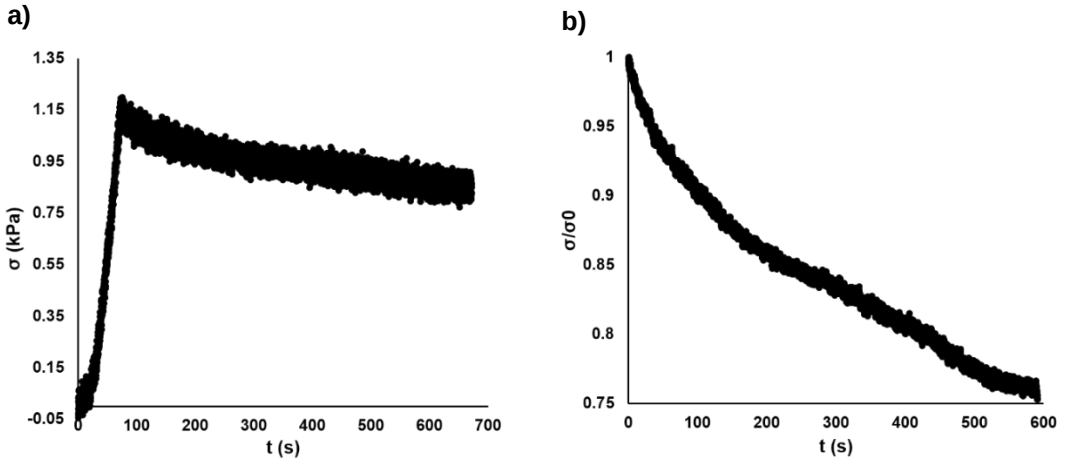

Figure 3-17 – Representative example of stress-relaxation in 5% agarose specimens – a) acquired data, b) normalised stress relaxation

To conduct the measurements, stress was first built-up in the samples during compression, until peak strain $\varepsilon_0 = 0.1$ was achieved. The strain was maintained for a 10-minute period, during which changes in stress in the specimen were monitored. A moving average filter was applied to the data and stress-relation portion of the curve was normalised by σ_0, as exemplified in Fig. 3.14 b).

Despite considerable amount of noise being present in the measurements, the analysis provided by on 3% and 5% hydrogel stress-relaxation curves was amenable to analysis. This was not the case in 1% hydrogels. As evidenced by Fig. 3.15 a), the scale of the stresses involved in 1% agarose specimens fell below the lower limit of detection of the load cell used in this work. As such, mechanical trends were superseded by measurement noise, leading to artefacts in the stress-relaxation behaviour (Fig. 3.15 b). This data was therefore excluded from further analysis.

In viable samples the terminal stress values (at t=600 s) were recorded to calculate the ratio of relaxation for each specimen. These results are shown in Fig 3.16. Fig. 3.16 shows that there is a positive correlation between the total amount of relaxation and agarose hydrogel concentration. The stiffest hydrogels display the largest amount of relaxation, just over 75% of σ_0. Intermediate stiffness hydrogels, on the other hand, relaxed to around 85% of the maximum stress.

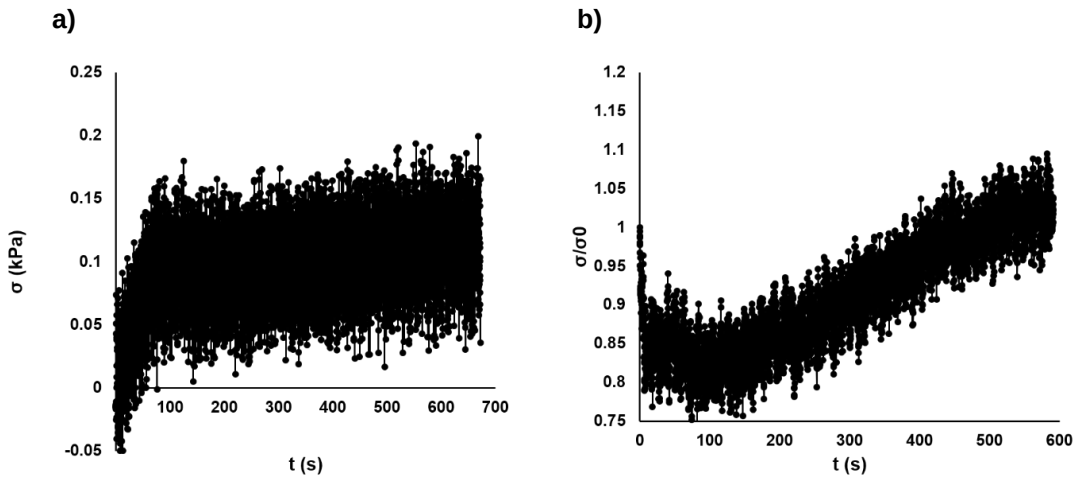

Figure 3-18 – **Representative example of stress-relaxation in 1% agarose specimens – a) acquired data, b) normalised stress relaxation**

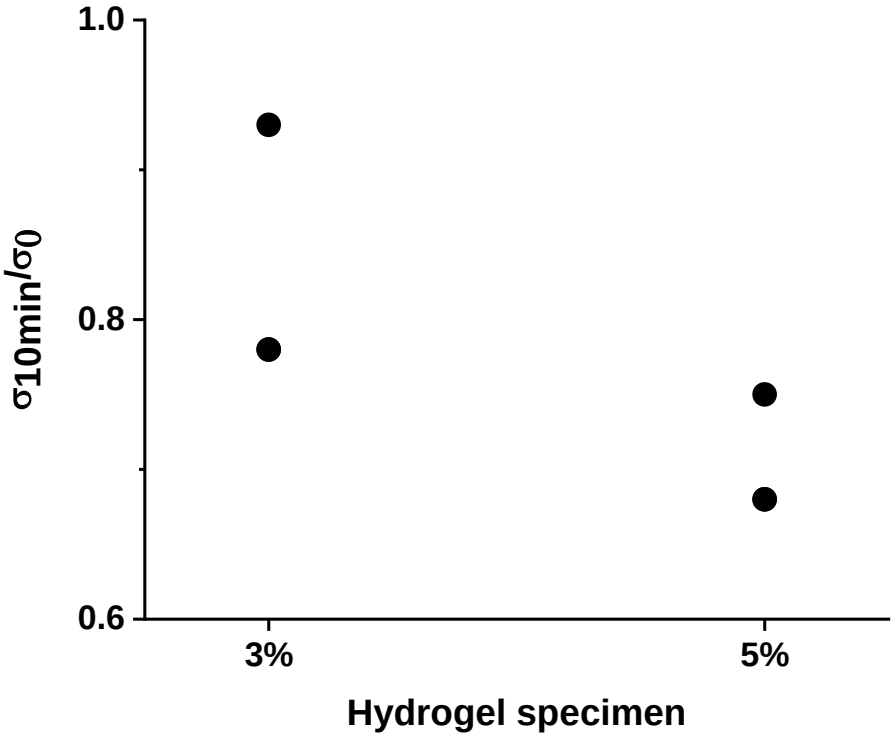

Figure 3-19 – Percentage of stress relaxation in agarose specimens – Relative decay in stress due to stress relaxation during a 10-minute period in 3% and 5% agarose hydrogels. Data of N = 2 replicates was plotted directly.

Although preliminary, this data clearly illustrates that Seaprep agarose specimens present viscoelastic properties under compression, which are dependent on the concentration of the hydrogel.

However, it is also important to recognise the limitations of this study. Firstly, the use of a 500 N load cell in these measurements resulted in the acquisition of noisy data and prevented the characterisation of the softest samples. Consequently, future measurements should be performed with a 10N load cell. The protocol should also be adjusted to accommodate different strain rates and peak strain values, which were kept to a minimum in this work to preserve sample integrity. Ideally, the hydrogels should be probed with parameters that mimic the characteristics of deformations imparted by cells, although this might not be achievable in uniaxial compression. A larger sample size should also be used to improve measurement accuracy. A wider measurement window can also be contemplated in future measurements to

allow the specimens to achieve maximum relaxation. Finally, these measurements can be complemented through alternative methods, such as bulk rheological analysis or AFM nanorheology.

To conclude, Seaprep agarose presents non-linear mechanical properties, such as strain stiffening and stress-relaxation, which are dependent on hydrogel concentration. These properties are of interest in the study of mechanobiology, therefore raising the interest of employing the substrates in the culture of hMSCs.

3.6 Limitations of the experimental set-up and 2D agarose constructs

Having produced and mechanically characterised 2D agarose cell culture substrates, it was possible to test out the assembly of the redesigned constructs schematised in Fig. 3.8. To do so, preliminary experiments were conducted which were successful in incorporating cells into the 2D constructs. These initial results confirmed that collagen crosslinking could be integrated into the layer-by-layer methodology.

Despite this early success, however, several limitations of the protocol quickly became apparent. First, construct assembly was work intensive, requiring several steps and producing a low sample throughput of six samples per mould. Another point was that subjecting these hydrogels to large strains greatly increased the probability of a brittle fracture. During uniaxial compression tests, it was observed that Seaprep agarose specimens at intermediate concentration (3%) were able to withstand compressions of 25-30%, but softer samples often fractured at 10% strains, while stiffer samples tended to fracture shortly after achieving strain of 20%. As such, the range of strains that could be applied to cell constructs would have to be restricted, especially after factoring in the build-up of fatigue in the material during long term experiments.

More critically, construct failures repeatedly occurred at several stages of the assembly process. For instance, the relatively low yield of collagen crosslinking compromised several attempts at establishing the experimental set-up. Moreover, adding cell culture to the assembly steps lead to increased

rates of construct fracture. This was due to prolonged exposure to cell culture conditions substantially altering the mechanical properties of agarose (as described in Fig. 3.9).

Two points of fracture were mainly responsible for construct destruction during these experiments. The first one was the 0.7 mm layer supporting cell growth. Due to its dimensions this layer tended to be fragile when manipulated during gripping and would display brittle fractures. Consequently, the reinforcement conferred by the thicker agarose layer topping the constructs proved insufficient to guarantee construct integrity thereby invalidating the proposed construct redesign. In instances when successful gripping was achieved, a second fracture point became apparent in the interfaces between the agarose and the porous glass endplates. Theoretically, porous glass is an ideal endplate, as it allows the agarose to fuse into its pores, creating a uniform attachment. In practice, however, the viscosity and brittleness of the material creates a weak attachment interface. Other authors have reported an aluminium griping system [197] developed to mitigate this issue. Yet, the aluminium grips are only compatible with 3D constructs, excluding their use with the redesigned 2D constructs.

Due to the prevalence and severity of these issues it was not possible to successfully apply mechanical loads to cells using the experimental set-up proposed in section 3.2.

3.7 Conclusions and future work

This chapter described the redesign of agarose constructs to implement an experimental set-up for morphometric analysis of mechanically-induced hMSC phenotypic changes. To fulfil these objectives, a layer-by-layer construct assembly approach was devised and first tested with the production of mock constructs. Subsequently, a protocol was optimised to crosslink collagen coatings into 2D agarose substrates, which was successfully used to promote cell attachment onto the hydrogel surface. Finally, it was established that agarose substrates present non-linear mechanical properties, and that cell culture conditions bear substantial impacts on the integrity of ultra-low gelling temperature agarose.

Despite working as a proof-of-concept, the results gathered during construct redesign were associated with severe limitations, compromising the mechanical integrity of the construct. Ultimately, these limitations greatly superseded the practicality of the experimental set-up, as the constructs proved too fragile to fulfil the objectives proposed in section 3.2. As such, substantial work must be dedicated in subsequent stages of this project to devise an experimental set-up that is simple, yet robust.

For the continuation of this project, future work will be dedicated to fundamentally redesigning the mechanical loading system, to overcome the limitations associated with gripping of the hydrogels. This system will likely be based on acoustic stimulation of the cells, allowing for increased flexibility in substrate choice and dimensionality. The agarose substrates devised in this work can potentially be employed with the acoustic rig, but new biomaterials (e.g. gelatin hydrogels) will also be developed to extend the range of mechanical environments assayed.

Overall, the limitations discussed in this work allowed the identification of critical experimental “bottlenecks” restricting the applicability of the original concepts for the project. In turn, new research opportunities were achieved by the development of novel 2D agarose cell culture substrates. Chapters 4 and 5 describe the continuation of this work by characterising long-term morphometric changes in hMSCs under the influence of substrate mechanical properties and differentiation induction media.

Chapter 4 – Population-based hMSC morphometric trajectories guided by the mechanical properties of 2D agarose substrates

4.1 Introduction

Cell morphology, cytoskeleton organisation and nuclear states have been recognised as useful biomarkers to characterise, predict and modulate cell behaviours [163], [172], [229].

The mechanical properties of cell culture environments are decisive factors in the morphology and behaviour of hMSCs. A great number of studies have provided fundamental insights into the bilateral interactions between cells and their surroundings, highlighting the critical impact of mechanobiological processes on SC differentiation. Nonetheless, these studies have been mostly conducted on static linear-elastic PAA hydrogels, neglecting critical features of natural ECMs [230]. Examples of previously disregarded factors include viscoelasticity and non-linear stiffness of the substrates, as well as their impacts on cellular morphology [147].

Non-linear-elastic 2D collagen-coated agarose substrates were employed in this chapter as culture systems to study long-term influences (> 10 days) of the biophysical traits of the extracellular environment on the morphometric profile of hMSC populations.

4.2 Methodology

This section briefly describes the methodology employed to perform long-term morphometric characterisation of cells seeded on 2D collagen-coated agarose substrates.

Materials and methods

Preparation of 2D agarose substrates coated with COL I

Working solutions of 1%, 3% and 5% (w/v) Seaprep agarose in PBS were prepared as before. 2D disk-shaped substrates were cast onto the central well of glass bottom petri dishes by stamping 150 µl volumes of melted agarose onto the 2 cm^2 well areas and solidified at 4ºC for 2 hours. These substrates were covered in PBS and stored at 4ºC overnight.

The chemical crosslinking protocol described in section 3.4.2 was used to produce COL I surface coatings on the agarose substrates. Briefly, Sulfo-Sanpah aliquots were equilibrated at room temperature in the dark and diluted in distilled H2O at 1:100. A volume corresponding to 100 µl/cm2 of the dilution was added to the top surface of individual agarose disks. The disks were quickly placed under a portable UV lamp, and irradiated for 2 minutes. Unreacted crosslinker was aspirated and the process was repeated a second time. The hydrogels were then washed three times in PBS.

Working solutions of COL I were prepared shortly before crosslinking by diluting collagen stock in PBS to 30 µg COL I/ 200 µl PBS/ cm^2 of available substrate area). The collagen solution was added to the Sulfo-Sanpah functionalised surfaces and incubated at room temperature for 2 hours under orbital agitation. After incubation the excess ECM solution was aspirated from atop the gels and the scaffolds were washed in PBS and stored at 4ºC overnight.

In the following morning the scaffolds were covered with sterilised PBS and transferred into a laminar flow hood equipped with a germicidal UV-lamp. The substrates were sterilised under the lamp for 40 minutes before cell seeding.

These substrates were then seeded with sparse hMSCs (passage 7), at a density of 1000 cells/cm^2. The cells were cultured as described in Chapter 2 in standard growth media. Cells seeded onto the hydrogels were fixed in 3.7% PFA after 1, 3, 5, 7, 10 or 15 days, stained with DAPI and Phalloidin-TRITC. To prevent dehydration the samples were maintained in PBS at 4ºC for short periods of time until imaging. An inverted Leica epifluorescence

microscope was used to collects cell images through the transparent hydrogel. Single-cell images were processed using the morphometric analysis pipeline described in Chapter 2.

The time-course of the experiments (10 days) was selected to cover a span comparative to differentiation studies. Sampling intervals were designed to reflect early, intermediate and later end-points in the characterisation of cell morphology, cytoskeletal and nuclear architecture under the effect of the mechanical environment provided by collagen-coated 2D agarose substrates.

Statistical Analysis

Shapiro-Wilk normality tests, coupled to visual inspection of histogram distributions of the morphometric descriptors, were used on a subset of data to confirm that the morphometric descriptors were not normally distributed (Appendix C). To assess the sensitivity of parametric tests to data skewness, sample data was jointly analysed through non-parametric Kruskal-Wallis ANOVA on ranks and parametric one-way ANOVA. As excellent agreement was found between parametric and non-parametric tests, it was considered that the data was compatible with parametric analysis (Appendix C). Two-way ANOVA (N= 3 experimental replicates, n> 100 single-cells in each time-point and per repeat, as detailed in Table 1) was employed to test the statistical significance (at $\alpha = 0.05$) of mean differences on the data driven by two dependent variables: time and type of substrate. Multiple comparison post-hoc tests were performed using a Bonferroni correction to adjust the error rate. To adequately illustrate skews in the data, morphometric descriptors were plotted as median values, with error bars corresponding to the 1^{st} and 3^{rd} quartiles. Statistical analysis was conducted in Origin Lab and GraphPad Prism.

Table 1 – Number of single-cell images analysed per time point and type of substrate across experimental replicates

	1	3	5	7	10	(days)
1%	328	326	132	183	96	
3%	377	288	320	398	181	
5%	348	251	208	302	157	

4.3 Results and Discussion

A large majority of mechanobiology studies have been conducted on linear-elastic scaffolds, such as standard PAA [230]. More recently, researchers have become aware that dynamic mechanical properties including viscoelasticity, non-linear stiffness and degradability are fundamental aspects of native ECMs [147] influencing how cells adapt to the surrounding environment.

As described in Chapter 3, 2D agarose substrates display a unique combination of biophysical attributes – including viscoelasticity, stain-stiffening and thermosensitivity. Hence, our hypothesis was that cells cultured on the substrates would exhibit behaviours more akin to those reported in novel hydrogels presenting non-linear-elastic properties. Accordingly, this section describes the morphometric effects of long-term hMSC culture on a range of 2D collagen-coated agarose substrates.

Fig. 4.1 shows some examples of the diverse phenotypes obtained in different substrates and experimental time-points.

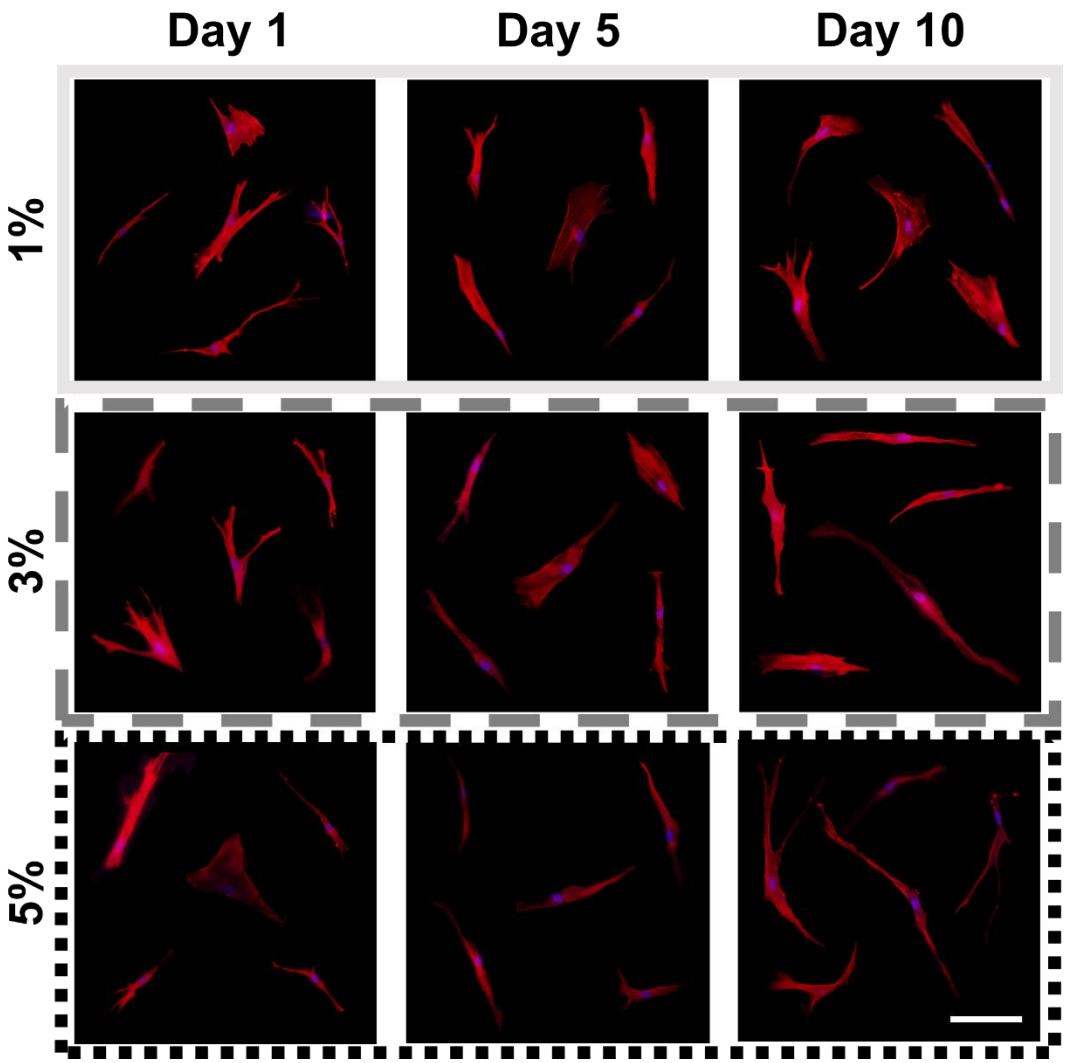

Figure 4-1 – hMSC phenotypic diversity in 2D agarose substrates – single-cell images of hMSCs in different agarose substrates (1%, 3% and 5%) and time points (days 1, 5 and 10). The images were digitally manipulated to enhance contrast and brightness for visualisation purposes. Scale bar indicates 100 μm.

4.3.1 Effects of non-linear-elastic substrate mechanical properties on hMSC morphology

Fig. 4.2 illustrates the time-course of the three morphological descriptors, namely area (Fig. 4.2 a), aspect ratio (Fig. 4.2 b) and stellate factor (Fig. 4.2 c), in cells seeded onto collagen-coated surfaces in agarose hydrogels of different formulations. Cell samples were successfully collected over a 15-day period in soft (1%) and intermediate (3%) stiffnesses, but the stiffer (5%) hydrogels could only be tracked for up to 10-days. Statistically

significant mean differences were found across factors, i.e. time and hydrogel type, in all parameters in Fig. 4.2 (Tables 15-27 in **Appendix C**).

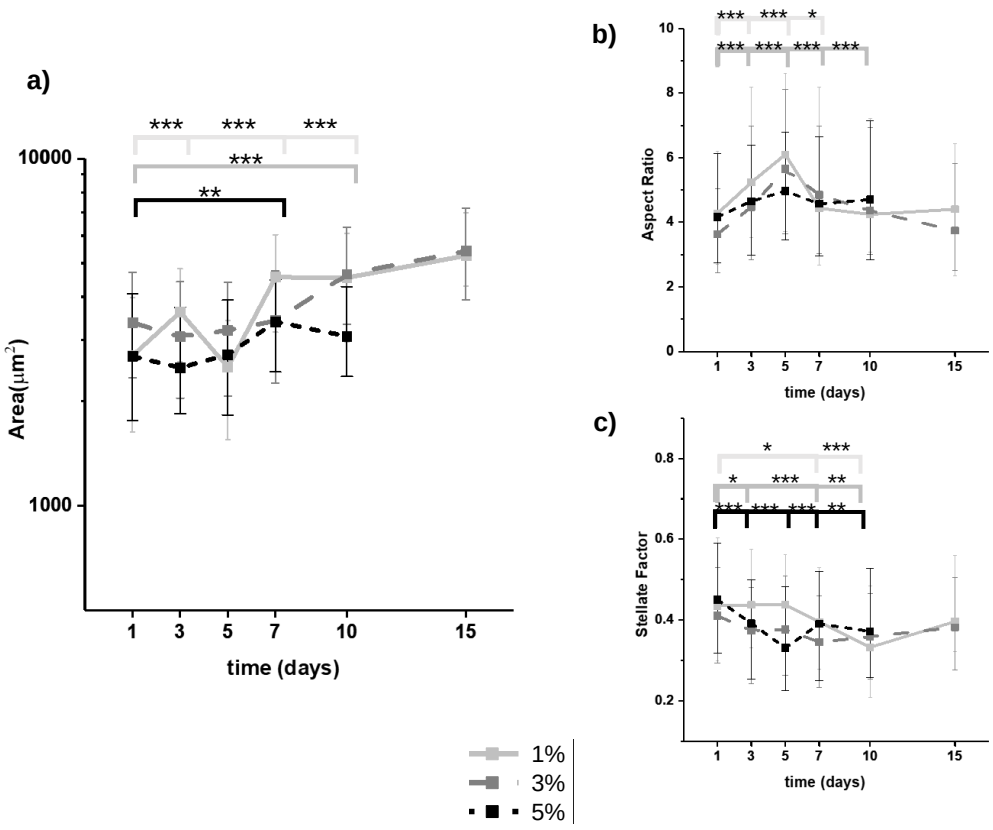

Figure 4-2 – Population-based hMSC morphologic trajectories guided by mechanical stimuli – a) cell area; b) aspect ratio; c) stellate factor; Continuous light grey line indicates 1% substrates, dashed dark grey line indicates 3% substrates, dotted black line indicates 5% substrates. Data is plotted as median values of N = 3 experimental replicates per substrate and timepoint. Error bars correspond to 1st and 3rd quartiles. The number of cells analysed per condition can be found in Table 1. More exhaustive statistical analysis can be consulted in Appendix C, tables 19, 20 and 25. * indicates p < 0.05, * indicates p < 0.001. D1 was used as reference in the statistical tests.**

The results in Fig. 4.2a show that, despite clear differences in the mechanical properties of the three agarose formulations used in this work (Chapter 3, section 3.5), morphological parameters displayed identical trends on the different hydrogels. In 1% and 3% agarose substrates, cell area underwent pronounced increases over time, which were less noticeable in 5% hydrogels. This was due to lower stability of the stiffest samples during the period of analysis, causing substantial portions of the top layer of collagen to

detach before the later time points, and excluding the possibility of acquiring data up to day 15. Sample stability is discussed in more detail in section 3.4.4. Aspect ratio, on the other hand, displayed non-monotonic trends, peaking at day 5 and subsequently decreasing back to the starting values. Shifts in aspect ratio can potentially be attributed to cytoskeletal rearrangements leading to more isotropic cell spreading. These results suggest that the cells initially responded to the hydrogels by becoming on average more elongated, whereas in later time points the cells become wider as they increased in area. In contrast, trends in stellate factor were less marked relative to the other parameters, with statistically significant decreases nonetheless indicative of changes in cell periphery over time.

Despite sporadic morphological differences between hydrogel environments achieving statistical significance in several time points, the close resemblance between the trends observed in the three mechanical environments suggests that, in the 2D collagen-coated agarose substrates, cell populations essentially experienced the same changes in shape throughout the culture period. These results are striking, as they are not in accordance with the well-established positive correlation between substrate stiffness and cell spread area in linear-elastic hydrogels. This is clear in the observation that median cell areas on the very soft agarose substrates were persistently close to those in stiffer hydrogels, reaching 2000 – 4000 μm^2 upon the initial 24 hours of culture. Moreover, the overall magnitude of long-term cell area increase over time was also comparable between environments, plateauing at over 6000 μm^2 after 10 days. In contrast, the literature suggests that cells in soft PAA hydrogels (<2 kPa, comparable to the initial stiffness of 1% agarose) tend to display small morphologies (~ 1000-1500 μm^2), while cells in stiffer hydrogels (> 5 kPa, comparable to the initial stiffness of 3% and 5% agarose) develop increasingly more spread-out areas of adhesion (~ 2000 – 4000 μm^2) in the initial 24 hours of culture (reference cell area values found in [11], [102], [105], [107], [231]).

The contradiction in results between Fig. 4.2 a) and the literature strongly suggests that linear elastic hydrogel stiffness was not the determinant factor for cell morphology in the agarose substrates. This conclusion is compounded by the fact that agarose hydrogels were shown, in the previous

chapter, to become softer upon exposure to the humidity and temperature inside incubator chambers. Concretely, AFM mechanical characterisation of the hydrogels (Fig 3.9) revealed that mean agarose substrate stiffness decays to half the starting value within a few days of culture. The results in Fig. 4.2 a) are, again, in opposition to previously reported trends in dynamic cell environments. For instance, in dynamic “stiff-to-soft” cell-culture substrates [232], [233], spread-out cells revert to smaller areas upon the onset of hydrogel softening. But, in stark contrast to these reports, the results in Fig. 4.2 a) showed marked increases in median cell area concurrent to the thermal softening of the substrates. These results were particularly noteworthy in the softest (1%) hydrogels, expected to acquire very low stiffnesses (hundreds of Pa) after a few days in culture, whereas in PAA hydrogels stiffnesses under 1 kPa have been associated with the absence of cell spreading [107]. The justification for the discrepancies between cell behaviour on PAA and agarose is unclear but possible explanations are addressed in section 4.3.4.

Collectively, the data in Fig. 4.2 indicates that in 2D collagen-coated agarose substrates developed in this work, in the absence of further differentiation factors, whole-cell morphology was altered as the cells adapt to their environment, but that these changes cannot be attributed to the effect of the underlying agarose substrates’ bulk stiffness.

4.3.2 Effects of substrate mechanical properties on F-actin architecture

Morphometric features pertaining to F-actin stress fibres were divided into two categories: features describing fibre amount and shape are presented in Fig. 4.3. Features describing the relative positioning of stress fibres within cells are shown in Fig. 4.4. Two-way ANOVA indicated multi-factorial statistically significant differences across parameters, with the exception of overall agarose concentration differences on fibre length (Fig. 4.3 b), chirality (Fig. 4.4 e) and chirality variability (Fig 4.4 f).

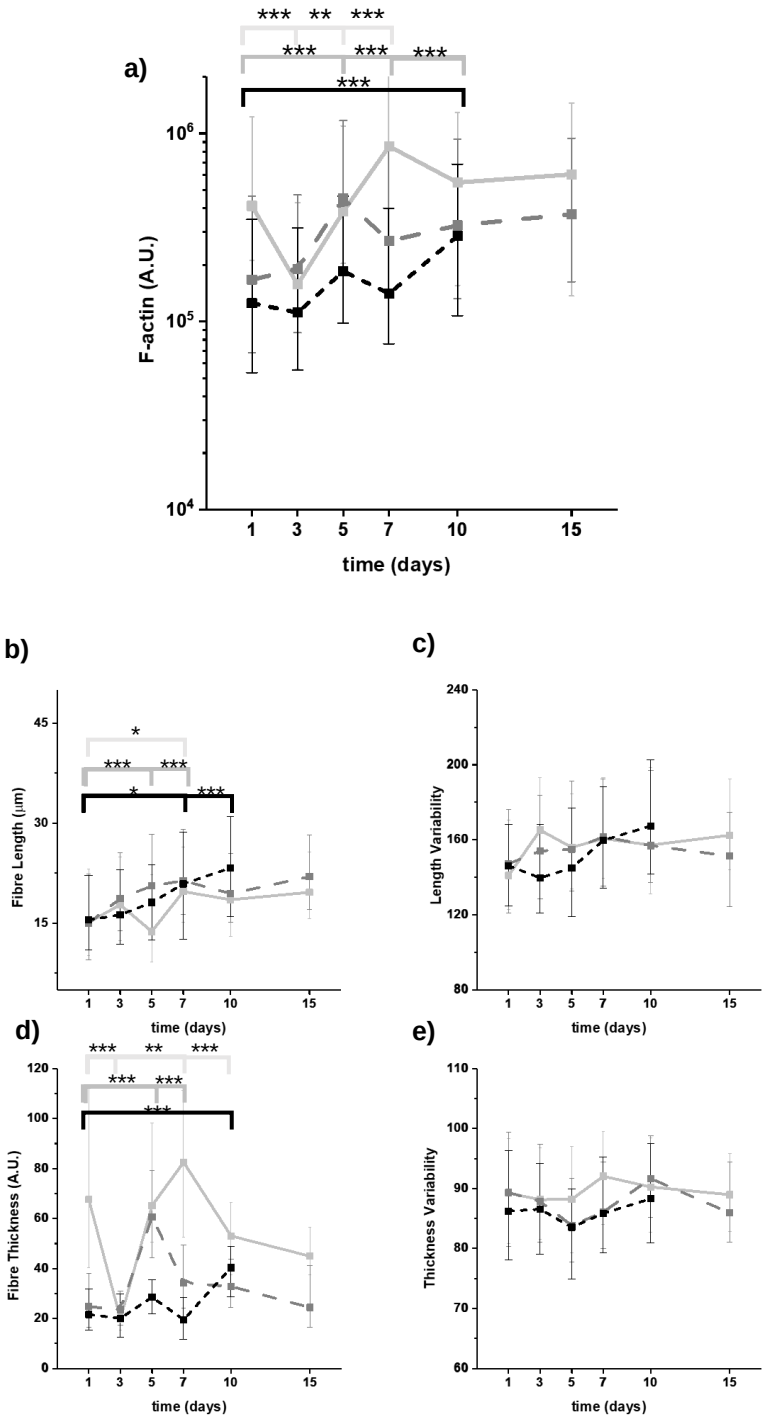

Figure 4-3 – Population-based F-actin shape descriptor trajectories guided by mechanical stimuli – a) F-actin amount; b) Fibre length; c) Length variability; d) Fibre thickness; e) Thickness variability; Data is plotted as median values of N = 3 experimental replicates per substrate and timepoint. Error bars correspond to 1st and 3rd quartiles. The number of cells analysed per condition can be found in Table 1. More exhaustive statistical analysis can be consulted in Appendix C, tables 21-22 and 26. * indicates $p < 0.05$, * indicates $p < 0.001$. D1 was used as reference in the statistical tests.**

Fig 4.3 a) shows that the amount of F-actin increased over time, to a plateau after day 7, across mechanical environments. Again, contrary to established reports, cells on the agarose substrates displayed close F-actin values among the different substrates. These trends were reminiscent of those observed in cell area, which is unsurprising given the well-established correlation between the two parameters [165], [168]. Concurrently to these changes, stress fibres became on average longer (Fig. 4.3 b), and less homogeneous (Fig. 4.3 c) over time. The thickness of the actin bundles, on the other hand, displayed non-monotonic trends (Fig. 4.3 d), with cells cultured on soft agarose displaying the thickest fibres. These trends in fibre thickness closely correlated with those in F-actin levels, potentially indicating that fibre reinforcement might have been the main contributor to the accumulation of F-actin in the cells. Finally, the variability of fibre thickness remained approximately constant in relation to temporal and mechanical factors (Fig. 4.3 e).

The next set of features, presented on Fig. 4.4, describe changes in the orientation of stress fibres within the cells. The values of peak location (Fig. 4.4 a) of radial fibre distributions did not show appreciable trends, whereas radial spread (Fig. 4.4b) displayed a downward trend in 1% and 3% agarose substrates, in contrast to a spurious increment at day 10 in the stiffest substrate. Conversely, fibre alignment steadily increased across conditions, plateauing after day 5 (Fig. 4.4c), while curvature displayed non-monotonic trends across substrates, resulting in statistically significant net increments relative to day 1 (Fig. 4.4d). Finally, in terms of radial angular orientation, chirality measurements remained consistently close to values of 90º (Fig. 4.4 e), showing that fibres are, on average, preferentially oriented parallel to the cell edge, which is to be expected in highly elongated cells [234]. Chirality variability (Fig. 4.4 f), on the other hand, seemed to display non-monotonic trends, but the evidence was poorly substantiated by statistical analysis.

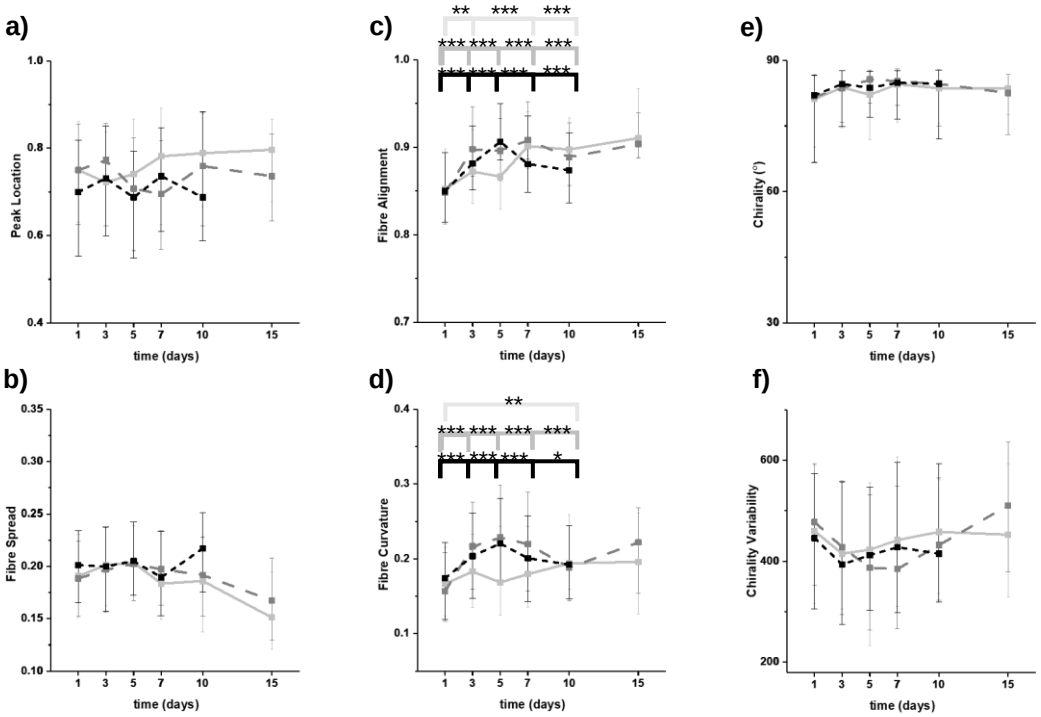

Figure 4-4 – Population-based F-actin positioning descriptor trajectories guided by mechanical stimuli – a) Radial peak fibre location; b) Radial fibre spread; c) Fibre alignment; d) Fibre curvature; e) Fibre chirality; f) Chirality variability; Data is plotted as median values of N = 3 experimental replicates per substrate and timepoint. Error bars correspond to 1st and 3rd quartiles. The number of cells analysed per condition can be found in Table 1. More exhaustive statistical analysis can be consulted in Appendix C, tables 23 and 24. * indicates p < 0.05, * indicates p < 0.001. D1 was used as reference in the statistical tests.**

The results from Fig. 4.3 and Fig. 4.4 suggest that the configuration of the actin cytoskeleton changes as hMSCs integrate the biophysical and biochemical signals of their surroundings, before acquiring stable phenotypes. The wide variety and complexity of hMSC morphologies (Fig. 4.1), however, make it difficult to resolve ambiguities and distinguish clear patterns in some of the morphometric descriptors. Continued development of high-throughput imaging methods and image-processing strategies is therefore critical in countering the inherent variability in biological samples and maximizing information from cell images.

4.3.3 Effects of non-linear elastic substrate mechanical properties on nuclear state

Like the cytoskeleton, the nucleus is a highly dynamic structure which can provide valuable information about the cellular state. The nuclear descriptors originated by our image processing pipeline, displayed in Fig. 4.5, are relative nuclear volume, chromatin condensation, apparent nuclear stiffness and nucleus compressibility/Poisson's Ratio. Again, multi-factorial statistically significant mean differences were found across parameters, except for chromatin condensation levels among agarose substrates (Fig. 4.5 c).

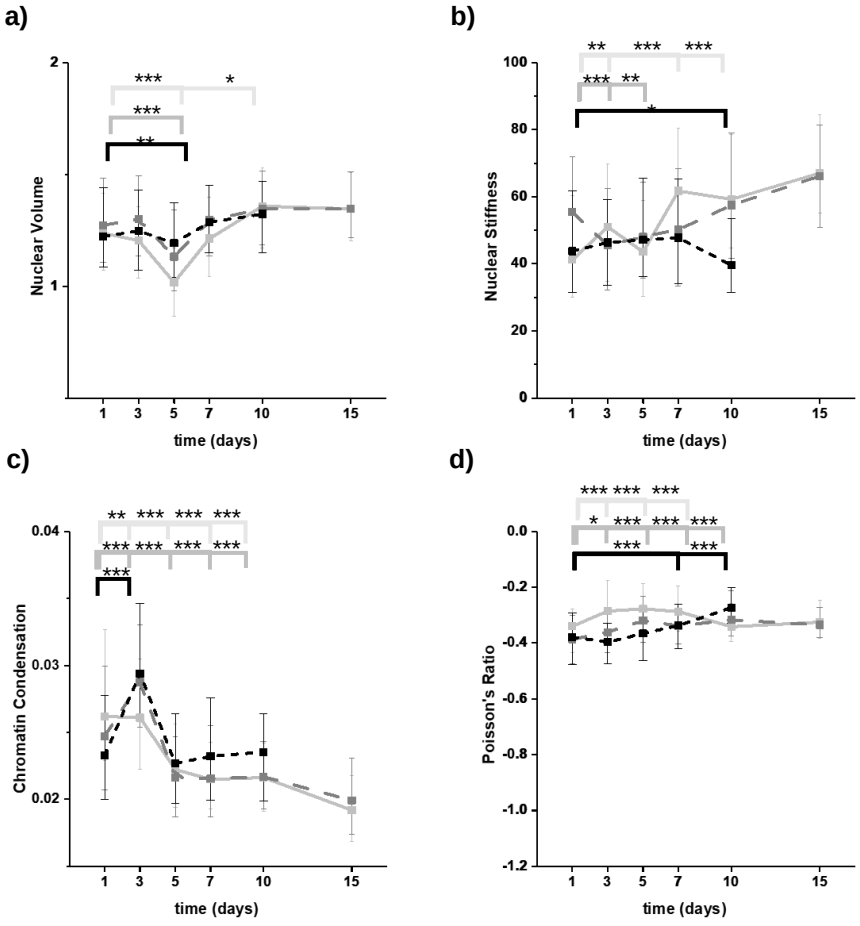

Figure 4-5 – Population-based nuclear state descriptor trajectories guided by mechanical stimuli – a) Nuclear Volume; b) Nuclear Stiffness; c) Chromatin Condensation; d) Poisson's Ratio; Data is plotted as median values of N = 3 experimental replicates per substrate and timepoint. Error bars correspond to 1st and 3rd quartiles. The number of cells analysed per condition can be found in Table 1. More exhaustive statistical analysis can be consulted in Appendix C, tables 27-30. * indicates p < 0.05, * indicates p < 0.001. D1 was used as reference in the statistical tests.**

Relative nuclear volume, shown in Fig. 4.5 a), behaved in a non-monotonic way across conditions. At day 5, statistically significant decreases relative to day 1 were registered in all agarose samples. By day 7 relative nuclear volumes had reverted to those found in the first day, subsequently stabilizing in all substrates.

These results were quite surprising given the expected dependency between nuclear volume, cell spread area and intracellular F-actin amount. Previous work [234] has reported that augmented cellular spread increases the strain imposed on the nucleus by the perinuclear actin cap. This action results in vertical nuclear compression, accompanied by stretches in the horizontal "cell-plane" directions. The net effect of these opposing forces, registered by our group in a former publication [165], are upsurges in nuclear volume in hMSCs freely cultured in TCP. Contrary to these results, nuclear volume trends in Fig. 4.5 a) did not correlate with cell spread area (Fig. 4.2 a) or F-actin states (Fig. 4.3 a). However, negative correlations between nuclear volumes and cell aspect ratio (Fig. 4.2 b) were apparent, with peaks in median cell aspect ratio at day 5 coinciding with depressions in nuclear volume. These results are in agreement with Gabriele et al.'s findings [234] which attribute changes in nuclear volume to a concomitant elongation of the nuclei and cell shapes. It should be noted that in the latter reference cell shapes were confined and modulated by micropatterned substrates resulting in artificially elongated cell morphologies. The morphology of hMSCs seeded onto agarose substrates is similarly distinct from those freely spread on glass or TCP surfaces, being generally more elongated. This is likely the reason for the discrepancies between Fig. 4.5 a) and our group's report.

Other authors, studying the effects of stiffness gradients in a PAA hydrogel [235], described a positive correlation between cell aspect ratio and substrate stiffness, but no concomitant changes on nuclear aspect ratio were detected. Taken together, the observations presented in this section suggest that substrate choice might bear unexpected influences in the relationships between cytoskeleton structures and the nucleus. This research question merits further enquiry.

A second nuclear feature, chromatin condensation (Fig. 4.5 c), was also non-monotonic in time. Peak condensation was observed across samples on

day 3, followed by a steep relaxation maintained from day 5 onwards. After 15 days, the density of chromatin in cells cultured on soft hydrogels was substantially lower comparative to day 1. Contrary to nuclear volume, no correlation was found between aspect ratio and chromatin condensation, which is in contrast with Gabriele et al.'s [234] assessment. Our manuscript [165], on the other hand, reports that chromatin condensation can display complex behaviours due to competing influences of the actin and vimentin cytoskeletons on the nucleus. F-actin enrichment was found to compact the chromatin, whereas vimentin was negatively correlated with chromatin condensation. Based on this evidence, it is possible that the behaviours registered in early chromatin condensation in Fig. 4.5 c) were mainly determined by the reinforcement of actin stress fibres (Fig. 4.3 a), with the vimentin network contributing more influence at later time points. This hypothesis could be confirmed by adapting the methodology described in this chapter, swapping phalloidin-TRITC staining for a vimentin specific antibody. It would also be of interest to ask if the fluctuations in chromatin condensation are associated with detectable modifications in gene expression patterns, by monitoring a range of genes through DNA microarray technology, or by selecting a few target mRNA candidates for rtPCR amplification.

The two final nuclear parameters in Fig. 4.5 are related to the mechanical properties of the nucleus. Apparent nuclear stiffness steadily increased over time, apart from a sudden depression in the final time point on 5% agarose. Finally, statistically significant differences over time and across substrates were registered for Poisson's ratio, but the magnitude of effect was negligible. In agreement with previous reports [165], the nuclei were found to behave as auxetic materials, i.e. displaying negative Poisson's ratio values.

4.3.4 Bulk stiffness of 2D collagen-coated agarose substrates failed to modulate hMSC differentiation

As discussed in the previous sections, the morphometric behaviour of hMSCs was very similar among the 2D collagen-coated agarose substrates of varying bulk stiffness. This suggests that factors beyond linear elasticity played a role in directing cell behaviour. This section discusses three hypotheses that

might explain these results: 1) collagen-coated agarose providing an unsuitable environment for cell culture, 2) non-linear-elastic properties of agarose influencing cell morphometric adaptations, or 3) the unintended formation of a fibrillar film of collagen during coating shielding the cells from responding to the stiffness of underlying substrates.

1) One hypothesis to explain the discrepancies between the results reported in this chapter, and the relationships between substrate stiffness and cell morphology typically found in the literature, is that the collagen-coated agarose substrates did not provide a suitable environment for cell growth. This hypothesis stems from the low efficiency of the Sulfo-Sanpah/agarose cross-linking reactions in concert with the progressive detachment of collagen coatings, as described in Chapter 3. But, despite the substrates' limitations, this hypothesis is not consistent with the results presented in Chapters 3 and 4. Figures 3.9, 3.10 and 4.1 display representative examples of the morphology of cells cultured for over a week on the 2D substrates. These images illustrate that, dependant on successful retention of a collagen coating, the cells remained attached to the substrate and were observed to spread, proliferate, and acquire long filopodial protrusions throughout the culture period. Additionally, even in substrates with partly detached coating, substantial portions of surface area still contained live spread-out cells which could be fixed, stained and imaged. Similarly, morphometric quantification showed that the cell phenotype changed through the culture period, with cells increasing in area (Fig. 4.2 a) and retaining large spread areas (> 6000 μm^2) over time.

On this topic, it should be mentioned that 5% agarose substrates where persistently harder to functionalise and were less stable than the softer hydrogels across all experiments conducted in this thesis (Chapters 4 and 5), leading to an overall higher rate of sample failure. This observation explains why less pronounced trends were observed in 5% substrates in this chapter, and why less time points could be collected for these substrates. It can be speculated that the increased polymer concentration generates surface properties which are less favourable to the crosslinking reaction, but it is

unclear if this was related to topological alterations, changes in hydrophilicity or other factors.

In general, it is unlikely that hypothesis 1) has played a significant role in the results obtained in 1% and 3% collagen-coated agarose substrates.

2) As presented in Chapter 3, agarose hydrogels display non-linear-elastic mechanical properties which might have influenced cell behaviour. These include viscoelasticity, strain stiffening and thermal degradation. Relative to the first property, a recent publication [236] has integrated viscoelasticity theory into the ECM element of a FA motor clutch model. This allowed the researchers to infer and experimentally validate that in soft viscoelastic hydrogels (< 3 kPa) cell spread area is maximised when substrate stress relaxation and cellular clutch binding time-scales are matched. Conversely, cell area was shown to slightly decrease in stiffer (9 kPa) viscoelastic hydrogels, suggesting that viscoelasticity may offset the effects of stiff environments in some conditions. The viscosity of the agarose substrates might therefore partly explain why cells on collagen-coated agarose spread considerably even in the softest substrates. On the other hand, the same authors experimentally verified that viscoelasticity only influenced the cells when the material's stress relaxation spectrum appropriately matched the characteristic time of cellular clutch binding. Given this information, it would be interesting to perform an in-depth characterisation of the agarose substrates to verify if their relaxation profiles do match the timescale of hMSC FA molecular probes. It is equally important to note that the authors still observed the stiffest viscoelastic substrates to cause the highest increase in cell area. This was not the case in the substrates employed in this work, which suggests that viscoelasticity alone cannot explain the results presented in Chapter 4.

Local strain-stiffening, induced by cellular traction forces on the substrates, might also have played a role in cell responses. This hypothesis was, however, not substantiated by the results in Fig. 3.12, describing normalised strain-stiffening in agarose specimens under compression. According to the mechanical characterisation, 5% agarose hydrogels presented the highest rate of strain-stiffening, whereas strain-stiffening on 1% and 3% agarose specimens was smaller, and undistinguishable below very

high (> 10%) compressive strains. As such, bulk strain-stiffening did not appear to have played a role in the adaptation of hMSCs to the substrates. Nevertheless, it was not possible to exclude potential strain-stiffening effects occurring on the collagen layers at the cell-material interface [153]. A more detailed mechanical characterisation of the substrates should therefore be extended to evaluating the properties of this interface.

Relative to thermal degradation, while degradability is an important feature for 3D cell culture, allowing cells embedded in confined porous hydrogel networks to spread out and increase in volume [155]–[157], in 2D substrates degradation/softening has been reported to dramatically decrease cell area [232], [233], which is in stark contrast to the observations reported herein.

It is therefore unlikely that the non-linear-elastic properties of the agarose substrates can provide an adequate explanation for the cell behaviours reported in this work.

3) The final hypotheses proposed here, are related to the characteristics of the collagen surface coating on the substrates. The results reported in Chapter 4 are akin to those described in PDMS in Trappmann et al.'s seminal work [105] ascribing SC mechanotransduction to the tethering of fibres on the surface of 2D substrates. By employing Sulfo-Sanpah to crosslink collagen to PDMS and PAA hydrogels, the authors showed that hMSCs would spread equally well in a range of PDMS stiffnesses (ranging from very soft 0.1 kPa to stiff 800 kPa substrates), while in PAA hydrogels cell area expectedly scaled with elastic modulus.

Like PAA, agarose is a highly porous hydrogel, and an inverse correlation between pore size and hydrogel concentration has been well established in this material [237], [238]. Yet, despite the structural similarity between agarose and PAA, the results in Fig. 4.2 a) were more akin to those described by the authors on PDMS. Consequently, the results obtained in Fig. 4.2 a) cannot be attributed to porosity-driven collagen tethering effects.

As previously mentioned, Engler et al. responded to this report by providing evidence that Sulfo-Sanpah does not covalently bind to PDMS [100]. If this is the case, a similar phenomenon leading to non-covalent/unstable

binding of the collagen coating to the underlying agarose substrates could have prevented the cells from responding to the underlying substrate stiffness, explaining the results obtained in Chapter 4.

Alternatively, studies have shown that factors such as the length and stiffness of individual fibres in natural [113], as well as synthetic [112] ECMs, locally affect the response of cells in 2D substrates, and have the potential to overrule bulk material properties. A hypothesis which could reasonably explain the results obtained in this thesis is therefore the unintended formation of a film of fibrillar collagen during coating that shielded the cells from responding to the underlying agarose substrates. Relative to this hypothesis, the literature again provides conflicting reports, as presented in the following paragraphs.

The most convincing evidence to support this premise is that the morphologies of hMSC observed in the collagen-coated agarose substrates presented close similarities to those described in MSCs, fibroblasts and other cell types, in a range of fibrillar collagen environments [112], [113], [163], [227], [239], [240]. Shared morphological traits include more elongated or stellate morphologies, relative to cells in homogeneous hydrogels ([112], [163]), which develop long, often bifurcated cell protrusions (Fig. 3.9, 3.10, 4.1). Moreover, it has been reported that, as a result of local fibre architecture or the mechanical properties of individual fibres, cells can spread considerably in environments with bulk stiffnesses as low as hundreds of Pa [112], [113], [153], [241], which is the range typically reported for collagen matrices. As such, it seems possible that an excessive accumulation of collagen/unsuccessful crosslinking onto agarose during substrate preparation could have resulted in a decoupling of the cell response from the underlying bulk agarose stiffness. The fibrillar configuration of this collagen network might, nonetheless, have provided the necessary mechanical stimuli for the cells to spread and grow, as reported in Chapters 3 and 4.

On the other hand, there are additional considerations which raise questions about the former hypothesis. First, the experimental parameters of the collagen coatings attempted in this work, i.e. the use of a type I collagen solution at a concentration of 0.2 mg/ml, are similar to those previously reported by authors employing Sulfo-Sapah in the functionalisation of PAA (e.g. [210], [242], [243]). Secondly, a collagen concentration of 0.2 mg/ml is

below the lower threshold of 1mg/ml typically reported in the formation of collagen hydrogels for cell culture [244]. Moreover, incubations with collagen were performed for a relatively short time interval of 3h and at R.T.. The conditions in which collagen was incubated were therefore relatively mild, and not expected to result in excessive sedimentation of the collagen fibres [113]. While it is possible that the collagen deposited on top of the agarose substrates acquired a configuration in-between a fully formed hydrogel and a single monolayer of ECM, comparable results in the literature provide conflicting evidence as to the verisimilitude of this hypothesis. For example, in thin collagen films formed at concentrations of 0.3-0.4 mg/ml, comparable to the one used in this work , vascular smooth muscle cells [245], [246] and NHI 3T3 fibroblasts [247] have been shown to spread poorly. In these studies, the cells were only capable of attaining spread areas upon further stiffening of the collagen films driven by dehydration, denaturation or crosslinking reagents. In a separate report [248], hMSCs were able to acquire large areas (> 4000 μm^2), develop prominent stress fibres, and acquire stellate morphologies similar to the ones observed in Chapters 3 and 4, in a 130 µm thick layer of collagen, whereas in a thick collagen hydrogel (1400 µm) hMSCs were not able to fully spread, nor form tick stress fibres. Interestingly, in this latter report, the authors claim that the morphological response of the cells on the thin collagen layer might result in part from the influence of an underlying stiff glass substrate, suggesting that in thin fibrous layers cells might still be influenced by stiffer underlying substrates. Other authors made similar claims that cells can spread by sensing their surrounding environment in soft fibrous environments, and that this ability extends to within a range of hundreds of microns away from the cell body [153]. In the latter report, the authors attributed cell spread to the non-linear properties, mainly local fibre strain stiffening, in natural hydrogels such as fibrin and collagen.

As a final note, it should be mentioned that recent work [249] has demonstrated that adherent cells can be seeded in liquid-liquid interfaces, suggesting that favourable nanoscale properties of the substrate allow cells to spread without the need for bulk solid stiffness.

In the context of the reports described throughout the former paragraphs, the results described in this chapter underscore the fundamental

differences between fibrous environments and synthetic hydrogels. While the morphologies of the cells described in this thesis strongly suggests that collagen was a determinant factor in hMSC mechanobiological response to the substrates, the possibility of interactions with the underlying agarose substrates could not be fully excluded.

Confirming any of these hypotheses would require continued study. For instance, live cell imaging coupled to fluorescent labelling of collagen could provide more evidence on the potential role of the COL I interface overlayed on agarose in influencing cell behaviour. Functionalised AFM probes could also be employed to study the properties of the ECM protein on the vicinity of seeded cells [100]. Finally, traction force microscopy could be used to establish what deformations were imparted on the agarose substrates [163] and study if plasticity was retained on the agarose after cell removal [158], perhaps driven by hydrogel thermosensitivity.

4.3.5 Additional Study Limitations

The studies discussed in this section present some further imitations. Firstly, data on linear-elastic hydrogels could not be directly collected during this project. This data would serve as a reference for comparison with non-linear-elastic agarose substrates. Despite well-substantiated reports in the literature about linear-elastic substrates, it would be a compelling effort to apply the methodology developed in this chapter to probe the long-term effects of hMSC cultured in linear-elastic PAA, as well as viscoelastic PDMS substrates. An important study would be to assess hMSC morphometrics in fibrous 2D-collagen hydrogels. These would serve as a reference for the isolated effects of the ECM relative to its coupling to synthetic materials, and would confirm if a soft collagenous environment is sufficient to elicit cell spread.

Another limitation of this work is that the primary hMSCs were acquired from a single donor. Donor variability bears a substantial impact on hMSC behaviour [250], [251]. As such, cells from different donors should be used in future studies to provide a more general evaluation of hMSC morphometric dynamics. Finally, the results of this study should be extended by more

detailed analysis of the cell-seeded substrates. Techniques such as live-cell and traction force microscopy could help identify key factors mediating hMSC responses to 2D collagen-coated agarose substrates.

4.4 General Conclusions

Despite limitations in the methodological approach, the results in this section substantiate recent findings [147] on the importance of considering previously overlooked properties of the ECM as fundamental cues capable of guiding cell morphology and provide new evidence on the unexpected effects of non-linear-elastic collagen-coated agarose substrates on cell morphology, F-actin architecture and nuclear state.

Unlike reports in standard linear-elastic hydrogels, no positive correlation was observed between substrate stiffness and parameters such as cell spread area or F-actin amount. Moreover, cell behaviour was not static through time, with cell morphology and the actin cytoskeleton changing over a two-week period. All together the results described in this section call to attention the importance of studying cell behaviours in a range of different biomaterial systems and over extended periods of time.

Chapter 5 – Population-based hMSC morphometric trajectories guided by simultaneous biochemical and mechanical differentiation stimuli

5.1 Introduction

Morphometric data has the potential to identify opportunities for the control of SC lineage commitment and cytoskeletal maturation. Yet, the body of work describing the phenotypic changes undergone by hMSCs during differentiation remains limited.

In this chapter, 2D collagen-coated agarose substrates like those described in Chapters 3 and 4, are employed as culture systems to study the joint influence of long-term biophysical and biochemical stimuli on the morphometrics of hMSC differentiation into the osteogenic and adipogenic lineages.

5.2 Methodology

Materials and methods

Preparation of 2D agarose substrates coated with COL I

2D collagen-coated substrates were prepared as before and again seeded with sparse hMSCs (at passage 5). For the first set of experiments the cells were cultured in osteogenic induction media, as described in Chapter 2. For the second set of experiments adipogenic induction media was supplied to the cells. Cells seeded onto the hydrogels were fixed in 3.7% PFA after 1, 3, 5, 7, 10, 15 or 21 days, and stained with DAPI / Phalloidin-TRITC. To prevent dehydration the samples were maintained in PBS at 4ºC for short periods of time until imaging. Imaging and analysis were conducted as previously described.

The time-course of the experiments (> 15 days) was selected to cover the typical span of hMSC differentiation studies. Sampling intervals were

designed to reflect early, intermediate and later end-points of differentiation under the combined effect of 2D collagen-coated agarose substrates and biochemical differentiation supplements.

Statistical Analysis

The sensitivity of parametric tests to the data was assessed as before. Excellent agreement was found between parametric and non-parametric tests (Appendix C), so that two-way ANOVA (N= 3 osteogenic experimental replicates / N = 2 adipogenic experimental replicates, n > 100 single-cells in each time-point per experimental condition and per repeat, as detailed in Tables 2 and 3) was employed to test the statistical significance (at $\alpha = 0.05$) of mean differences on the data driven by time and type of substrate. Multiple comparison post-hoc tests were performed using a Bonferroni correction. To adequately illustrate skews in the data, morphometric descriptors were plotted as median values, with error bars corresponding to the 1st and 3rd quartiles.

Table 2 – Number of single-cell images analysed per time point and type of substrate across experimental replicates in osteogenic experiments

	1	3	5	7	10	15	(days)
1%	428	543	538	336	517	401	
3%	202	747	629	459	369	318	
5%	343	697	446	290	105	156	

Table 3 – Number of single-cell images analysed per time point and type of substrate across experimental replicates in adipogenic experiments

	1	3	5	7	10	15	(days)
1%	192	218	195	342	379	257	
3%	215	400	549	428	384	291	
5%	259	123	439	392	178	106	

5.3 Results and Discussion

SC differentiation can be induced by both mechanical and biochemical means. Providing novel evidence relative to the complex interplay between these factors is of interest in SC research. This chapter addresses the morphological changes in hMSCs resulting from the combination of

biochemical differentiation stimuli (differentiation induction supplements), and the biophysical attributes of collagen-coated agarose substrates. This study was conducted by adapting the methodology of chapter 4, substituting standard culture media by osteogenic or adipogenic induction media. The experimental period was also extended to include the full time-span of differentiation. As in the previous section, it was possible to track cells on softer hydrogels for a period of 21 days, while samples in 5% hydrogels could only be analysed up to day 15. Two-way ANOVA tests identified statistically significant mean differences in all parameters, with exception of the effects of hydrogel type on chromatin condensation in adipogenic differentiation (Tables 28-51 in **Appendix C**).

5.3.1 Combined effects of osteogenic differentiation media and substrate mechanical properties on cell morphology

Fig. 5.1 represents the morphological changes undergone by hMSCs under the influence of mechanical environment and biochemical osteogenic induction media.

Morphometric analysis revealed that the inclusion of biochemical cues caused the morphological trends in Fig. 5.2 to be consistently more identical between substrates relative to those in the absence of differentiation supplements (Fig. 4.2), again suggesting that the bulk stiffness of the substrates failed to modulate hMSC differentiation.

Fig. 5.2 shows that cell morphology changed drastically during the experimental period. Firstly, there were clear linear increases of an order of magnitude in cell area (Fig. 5.2 a) over the time course of analysis. In contrast to the results in Chapter 4, there was an initial positive correlation between substrate stiffness and cell spread area at 24h from the induction of differentiation. Yet, this relationship subsequently disappeared after the initial time point.

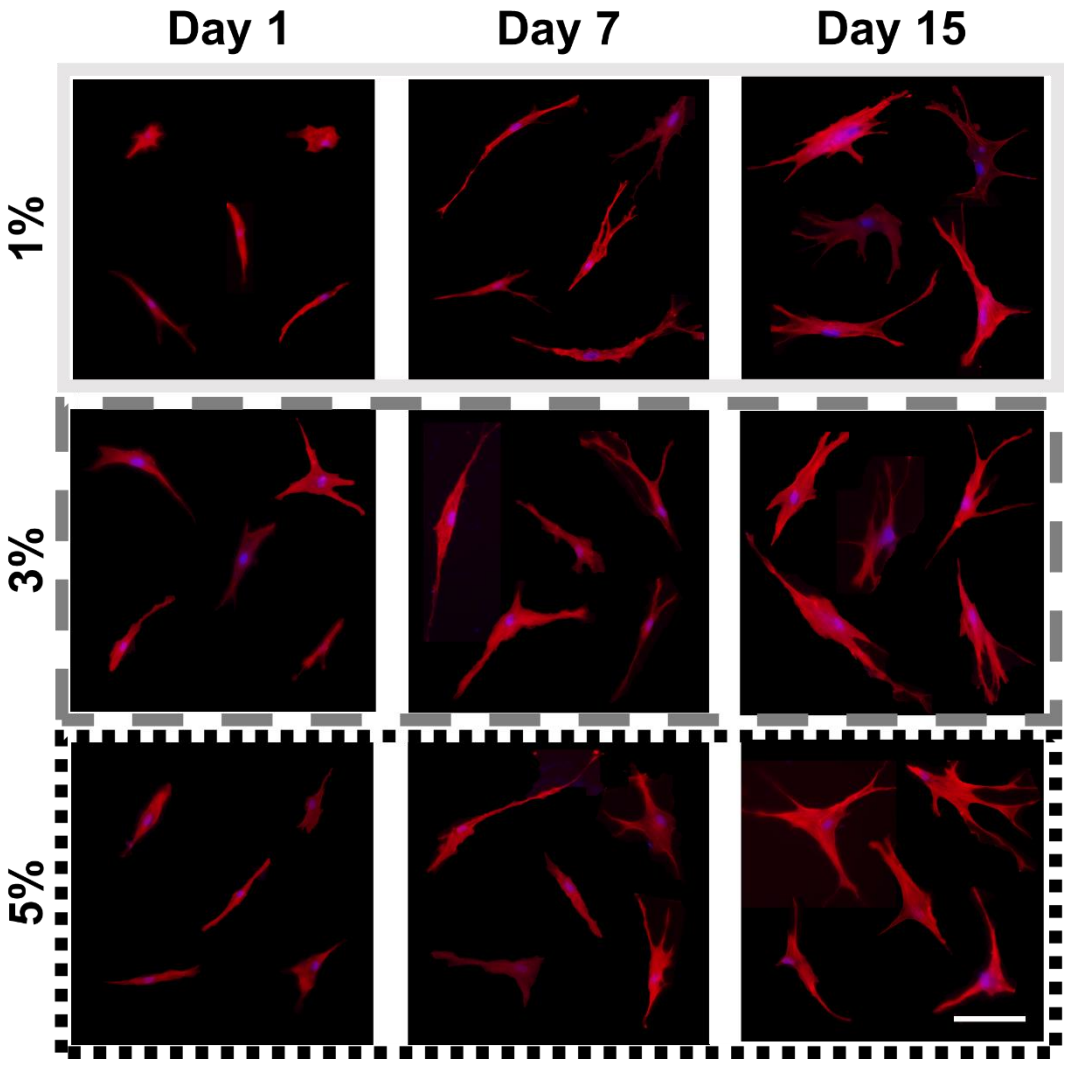

Figure 5-1 – hMSC phenotypic diversity under the combined effects of osteogenic induction supplements and substrate mechanical properties – single-cell images of hMSC osteogenic differentiation in different agarose substrates (1%, 3% and 5%) and time points (days 1, 7 and 15). The images were digitally manipulated to enhance contrast and brightness for visualisation purposes. Scale bar indicates 100 µm.

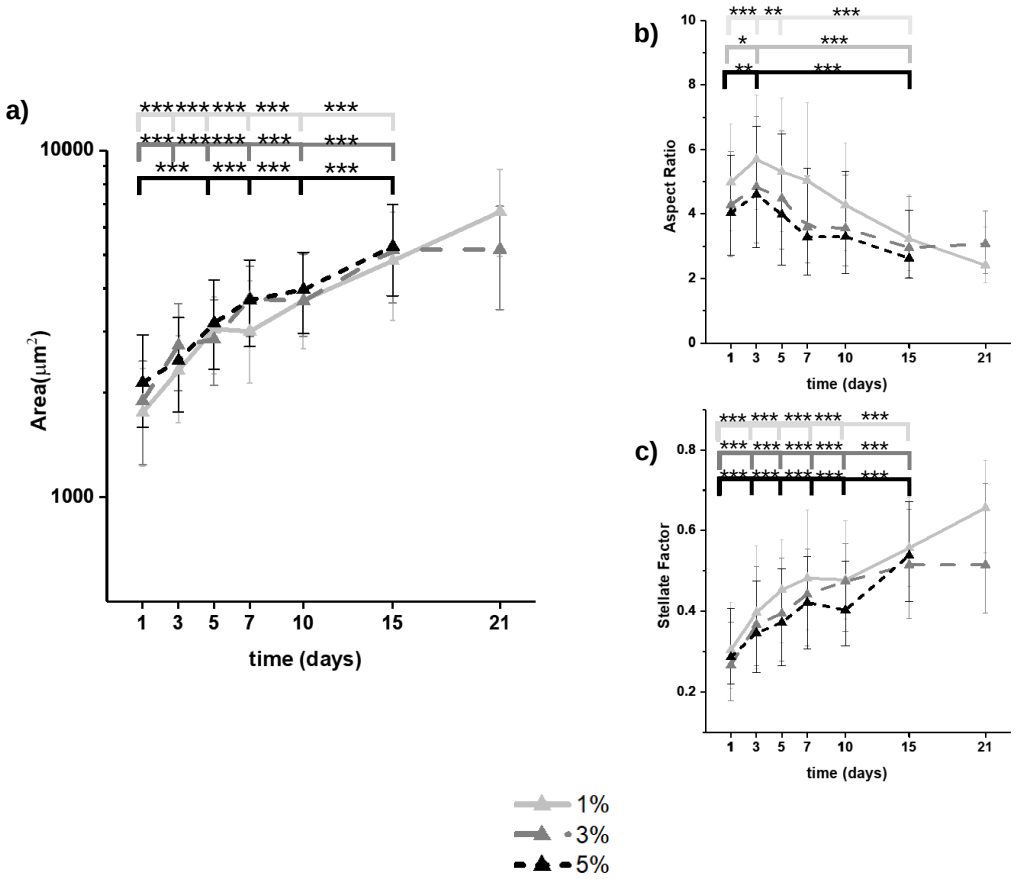

Figure 5-2 – Population-based hMSC morphologic trajectories guided by osteogenic media and mechanical stimuli – a) cell area; b) aspect ratio; c) stellate factor; Continuous light grey line indicates 1% substrates, dashed dark grey line indicates 3% substrates, dotted black line indicates 5% substrates. Data is plotted as median values of N = 3 experimental replicates per substrate and timepoint. Error bars correspond to 1st and 3rd quartiles. The number of cells analysed per condition can be found in Table 2. More exhaustive statistical analysis can be consulted in Appendix C, tables 31-32 and 37. * indicates p < 0.05, * indicates p < 0.001. D1 was used as reference in the statistical tests.**

On the other hand, cellular aspect ratio (Fig. 5.2 b) was noticeably larger in 1% substrates during the scope of 10 days, whereas the aspect ratio of cells in 3% and 5% hydrogels remained identical up until day 15. Curiously, aspect ratio peaked at day 3 in all mechanical conditions, followed by a slow return to below the initial values. The close agreement between independent group trends indicates that changes in cell conformation during the earlier days were not an artefact, but instead driven by the inclusion of biochemical differentiation factors.

Additionally, dramatic linear increases were observed in cell stellate factor (Fig. 5.2 c) achieving an increment of 2-3 times within two weeks. This

observation probably reflects the appearance of numerous long “dendritic” processes in the cells (rightmost panels in Fig. 5.1). Interestingly, osteocytes, the terminal phenotype of the osteoblastic lineage, form extensive networks of dendritic-like processes *in vivo*. Thus, the formation of long extensions in a collagenous environment [252]–[254], observed under the effect of osteogenic supplements, may reflect a natural tendency of osteoblastic differentiation progression.

Altogether these results show that the combination of mechanical and biochemical stimuli resulted in pronounced effects on cell shape, that were primarily dependent on biochemical differentiation signals, as opposed to the biophysical characteristics of the underlying substrates.

5.3.2 Combined effects of osteogenic differentiation media and substrate mechanical properties on F-actin architecture

Relative to the state of F-actin, there were linear increases close to an order of magnitude across samples during the span of differentiation, as shown in Fig 5.3 a). Equal trends were observed between the two hydrogels with the highest stiffness moduli, whereas cells on the softest hydrogels consistently displayed the largest F-actin amounts. These results are reminiscent to those shown in Fig. 4.3 a), i.e. the highest increases in F-actin occurring in cells cultured on the softest substrates, in standard growth media. Given that actin assembly is hampered in soft linear-elastic substrates, the similarity between findings further suggests that mechanical factors apart from bulk substrate stiffness directed cytoskeleton architecture.

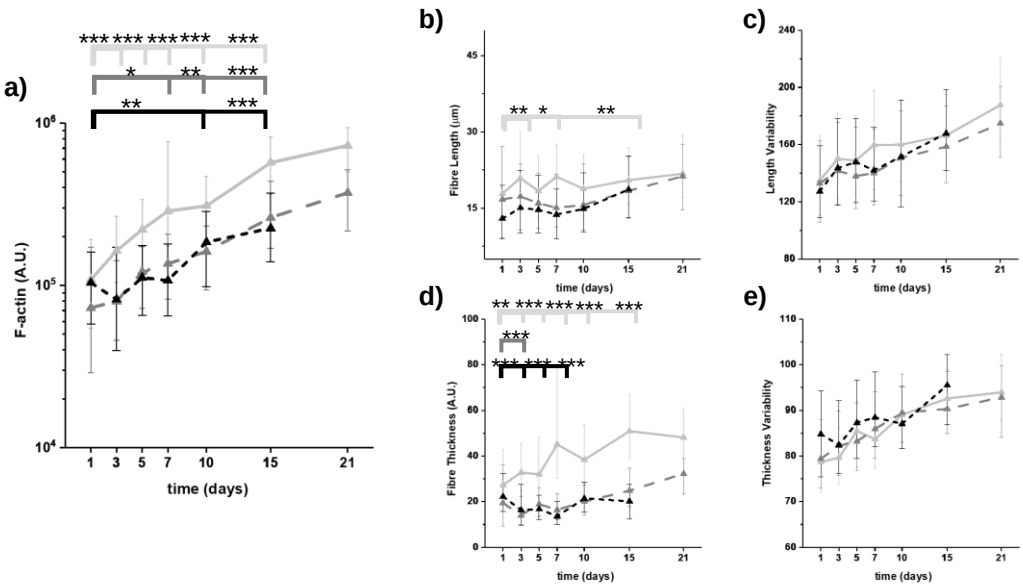

Figure 5-3 – Population-based F-actin shape descriptor trajectories guided by osteogenic media and mechanical stimuli – a) F-actin amount; b) Fibre length; c) Length variability; d) Fibre thickness; e) Thickness variability; Data is plotted as median values of N = 3 experimental replicates per substrate and timepoint. Error bars correspond to 1st and 3rd quartiles. The number of cells analysed per condition can be found in Table 2. More exhaustive statistical analysis can be consulted in Appendix C, tables 33-34 and 38. * indicates p < 0.05, * indicates p < 0.001. D1 was used as reference in the statistical tests.**

While the reinforcement of the actin cytoskeleton was not accompanied by manifest changes in the average length of the stress fibres (Fig. 5.3 b), the differentiation stimuli did increase the variability of fibre length (Fig. 5.3 c) across mechanical environments. Concurrently to these changes, stress fibres became thicker in 1% agarose hydrogels, but displayed only moderate non-monotonic trends in 3% hydrogels and 5% hydrogels (Fig. 5.2 d). In comparison, the variability of fibre thickness (Fig. 5.3 e) behaved identically to the variability in length, suggesting that stress fibre make-up becomes more diverse with the progression of differentiation, irrespective of agarose substrate.

Fig 5.4 shows that, like with other parameters, trends in fibre orientation were easier to discern when differentiation supplements were added to the mechanical effects of the extracellular environment, relative to culture in standard growth media (Fig. 4.4).

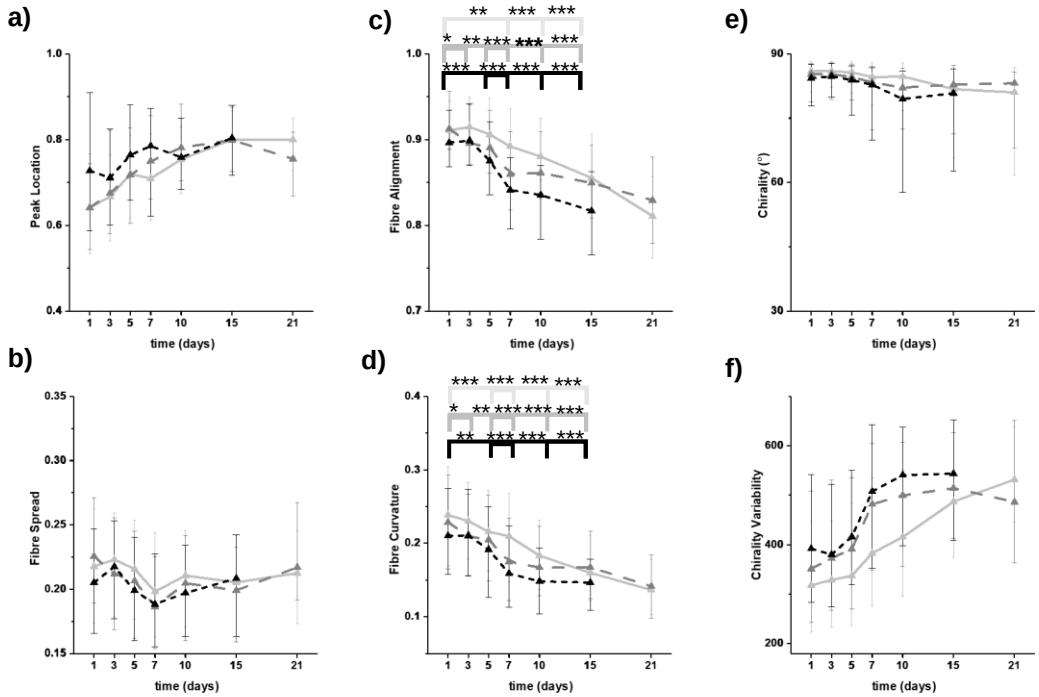

Figure 5-4 – Population-based F-actin positioning descriptor trajectories guided by osteogenic media and mechanical stimuli – a) Radial peak fibre location; b) Radial fibre spread; c) Fibre alignment; d) Fibre curvature; e) Fibre chirality; f) Chirality variability; Data is plotted as median values of N = 3 experimental replicates per substrate and timepoint. Error bars correspond to 1st and 3rd quartiles. The number of cells analysed per condition can be found in Table 2. More exhaustive statistical analysis can be consulted in Appendix C, tables 35 and 36. * indicates p < 0.05, * indicates p < 0.001. D1 was used as reference in the statistical tests.**

For example, the radial location of fibre peak (Fig. 5.4 a) showed a noticeable tendency for phalloidin-TRITC intensity to concentrate nearer the cell edge. On the contrary, although associated with the former parameter, radial fibre intensity spread (Fig. 5.4 b) displayed non-monotonic trends which, despite statistical significance, were relatively negligible. Very clear downward trends were registered in both fibre alignment (Fig. 5.4 c) and curvature (Fig. 5.4 d). In both cases, the stress fibres became straighter but less parallel among cells on different substrates. Finally, in terms of angular orientation, distributions of average cell chirality values (Fig. 5.4 e) did not show appreciable trends, yet chirality variability distributions (Fig. 5.4 f) exhibited sharp increments across conditions.

Overall, the results in Fig. 5.3 and Fig. 5.4 suggest that stress fibre morphometrics in osteoblast precursors (> day 10) were quite distinct from those of recently committed SCs. Mature cell phenotypes developed a more complex network of fibres, probably linked to the marked alterations in cell size and shape.

Many reports in the literature have called into the attention connections between cell spread, cytoskeletal tension and the YAP/TAZ signalling pathway in osteogenesis. Like in these reports, hMSCs subjected to osteogenic differentiation stimuli in 2D collagen-coated agarose substrates displayed increasingly larger cell areas and F-actin amounts. It is therefore likely that cell tension increased during the differentiation period, promoting nuclear recruitment of YAP/TAZ. Future experiments are needed to confirm if this was the case. It would also be worthwhile to investigate if the nuclear sequestration of the transcriptional regulators is maintained throughout the full span of 21 days, and if this can be correlated with fluctuations in the expression of lineage specific genes (RUNX2, Osterix, Alkaline Phosphatase, OCN, etc).

5.3.3 Combined effects of osteogenic differentiation media and substrate mechanical properties on nuclear state

In addition to the changes in cell morphology and actin fibres, Fig. 5.5 shows that hMSC nuclei also displayed identical trends across agarose substrates. Fig. 5.5 show that, in every substrate, nuclei became larger (Fig. 5.5 a) and stiffer (Fig. 5.5 b), achieving volume saturation approximately two weeks from the induction of differentiation. Unlike in Chapter 4, fluctuations in nuclear volume did not correlate with cell aspect ratio. Thus, potential relationships between the nucleus and cell morphology might be altered under the action of biochemical differentiation cues.

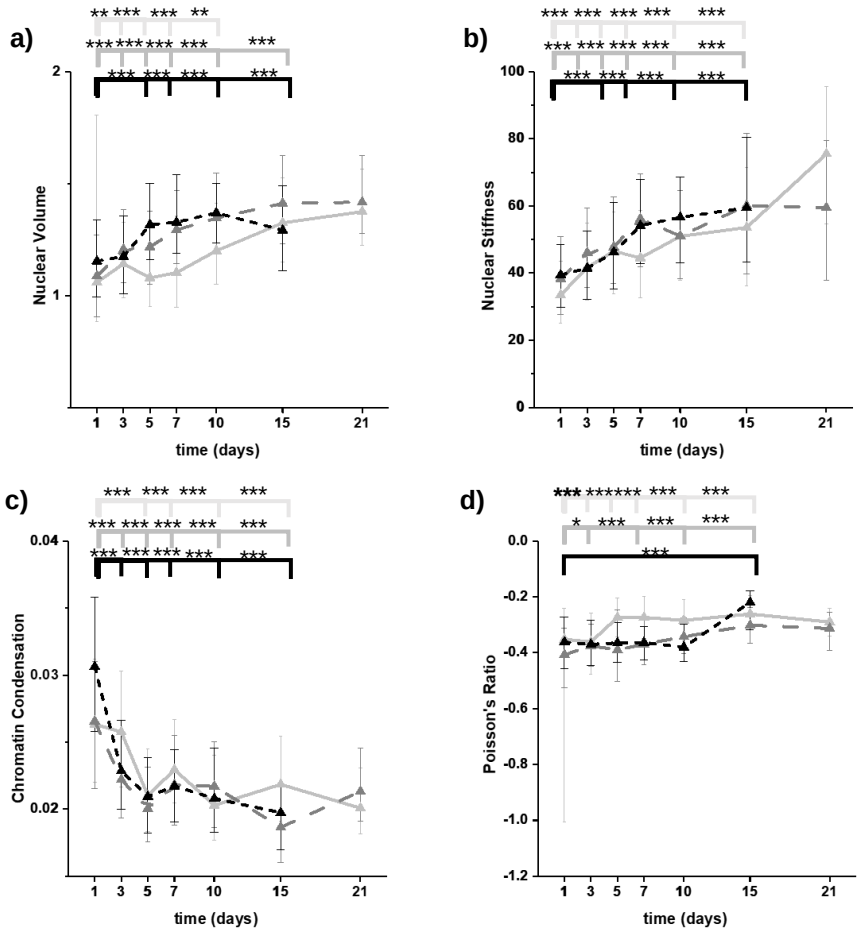

Figure 5-5 – Population-based nuclear state descriptor trajectories guided by osteogenic media and mechanical stimuli – a) Nuclear Volume; b) Nuclear Stiffness; c) Chromatin Condensation; d) Poisson's Ratio; Data is plotted as median values of N = 3 experimental replicates per substrate and timepoint. Error bars correspond to 1st and 3rd quartiles. The number of cells analysed per condition can be found in Table 2. More exhaustive statistical analysis can be consulted in Appendix C, tables 39-42. * indicates p < 0.05, * indicates p < 0.001. D1 was used as reference in the statistical tests.**

Levels of chromatin condensation (Fig. 5.5 c) were also identical between substrates. Overall, the density of chromatin steadily relaxed over the first five days of the experiment and was maintained at a lower level over the following weeks. This result was unanticipated, as differentiation has been linked with gene silencing driven by chromatin condensation, thought to result in preferential expression of lineage-specific genes [255]. Accordingly, it is broadly accepted that euchromatin regions are more prevalent in the SC nucleus, but this contention was not supported by the results in Fig. 5.5 c).

Conversely, it is equally recognised that chromatin states result from the integration of complex relationships between multiple environmental factors [256]. These include extracellular conditions (e.g. substrate mechanical properties and topography), presence of differentiation stimuli (e.g. biochemical factors, active mechanical loads), overall cell morphology and the organisation and tension of cytoskeleton networks, as well as the composition of nuclear lamina, and the resulting interplay between cytoplasmic and nuclear rheological properties [81]. This scenario is further complicated by the hypothesis that SCs retain a "memory" of previous culture environments, which can condition subsequent behaviours [31]. Conflicting evidence on these subjects muddles the identification of universal relationships between chromatin condensation, gene expression, and differentiation [163]. It would therefore be worthwhile to extend morphometric analyses to a range of culture systems and evaluate similarities/differences in chromatin state across environments, as well as their impact on cellular fate. Furthermore, these studies should be complemented with robust characterisation of gene expression during differentiation.

The final nuclear descriptor, nuclear Poisson's Ratio (Fig. 5.5 d), increased across time. In both Poisson's Ratio and Nuclear Volume, an unexpected level of variability was observed in cells seeded on 1% agarose hydrogels on day 1. This was possibly due to the presence of outliers which skewed he distribution of the two parameters.

As a final note, it can be mentioned that nuclear parameters are also influenced by the state of the nucleoskeleton. Future studies should therefore monitor critical components in nuclear mechanosensitivity, such as lamin A/C or elements in the LINC complex.

5.3.4 Combined effects of adipogenic differentiation media and substrate mechanical properties on cell morphology

The previous sections highlighted populational morphometric changes resulting from the combined effects of osteogenic differentiation media and the mechanical stimuli of 2D collagen-coated agarose hydrogels. Section 5.3.4

extends these results by addressing the effects of adipogenic differentiation factors on cells cultured in the same substrates.

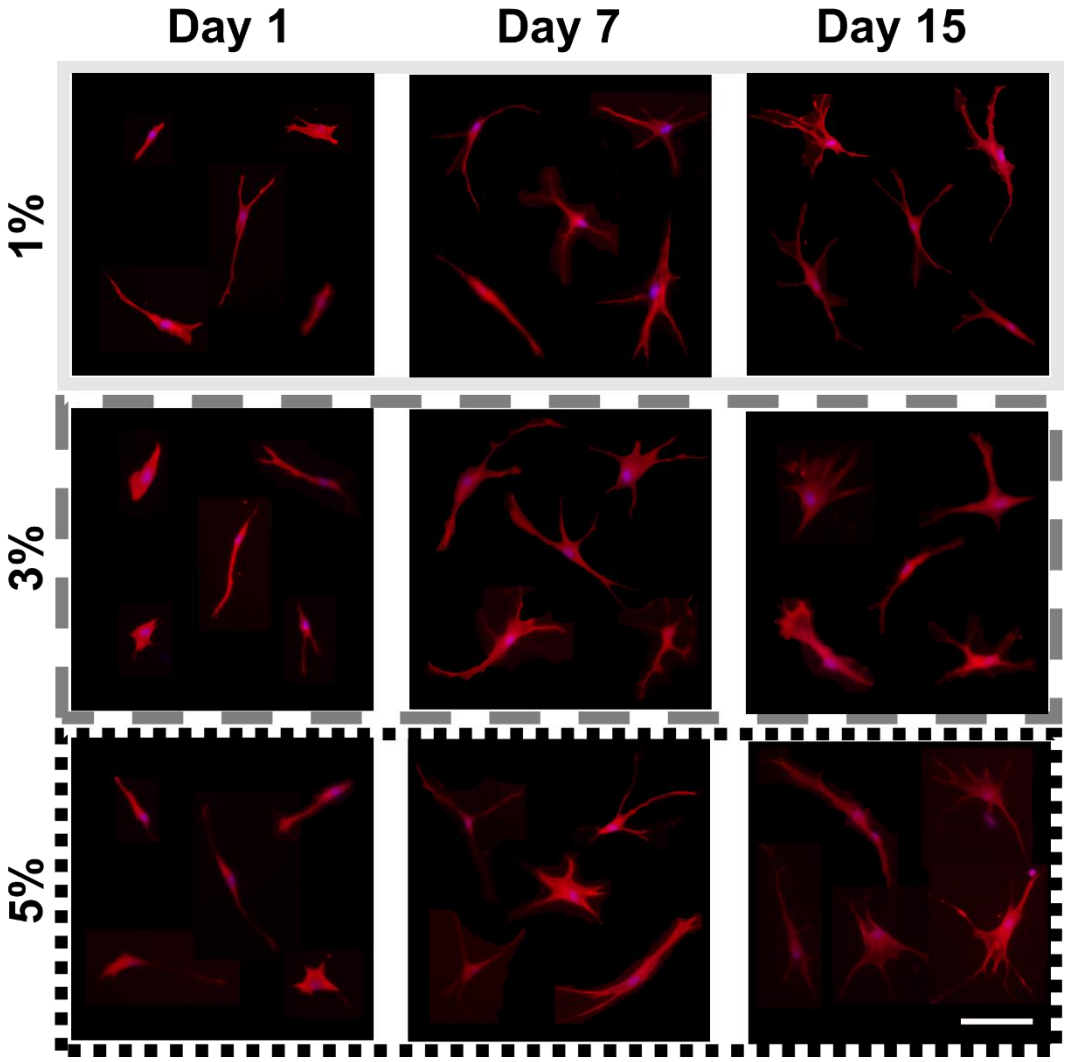

Figure 5-6 – hMSC phenotypic diversity under the combined effects of adipogenic induction supplements and substrate mechanical properties – single-cell images of hMSC adipogenic differentiation in different agarose substrates (1%, 3% and 5%) and time points (days 1, 7 and 15). The images were digitally manipulated to enhance contrast and brightness for visualisation purposes. Scale bar indicates 100 μm.

As before, the first set of results (Fig. 5.6) present morphological alterations in cells seeded in different substrates over a period of at least two weeks.

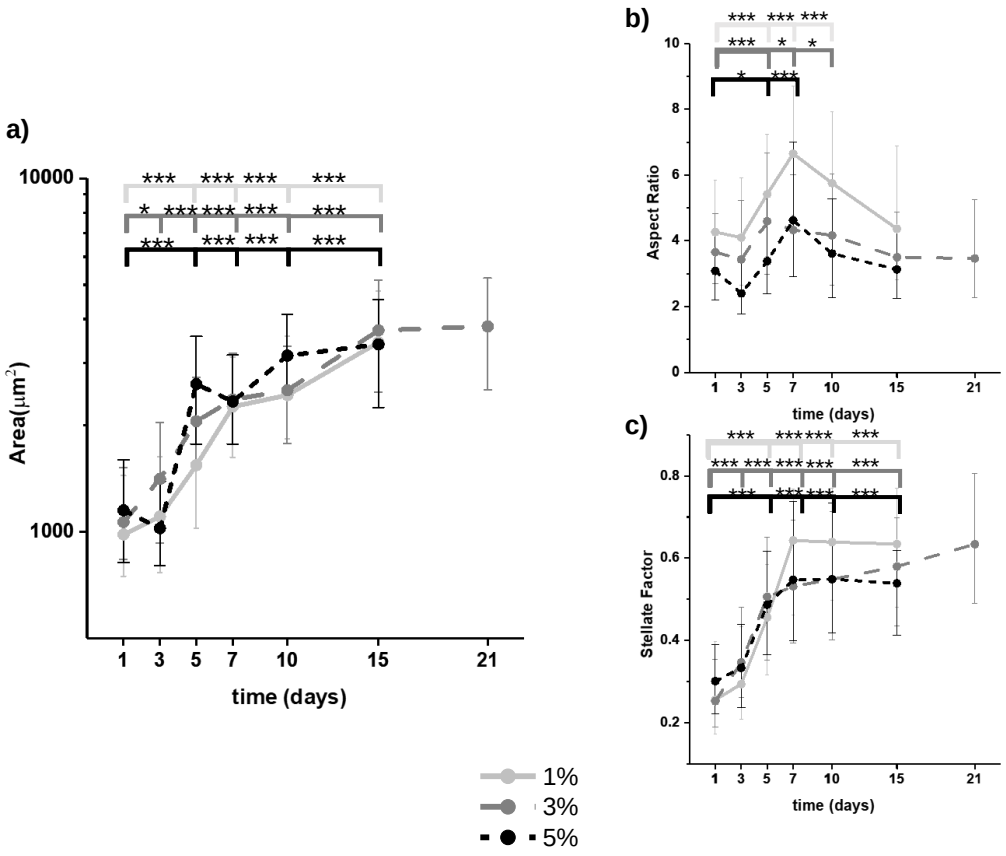

Figure 5-7 – Population-based hMSC morphologic trajectories guided by adipogenic media and mechanical stimuli – a) cell area; b) aspect ratio; c) stellate factor; Continuous light grey line indicates 1% substrates, dashed dark grey line indicates 3% substrates, dotted black line indicates 5% substrates. Data is plotted as median values of N = 2 experimental replicates per substrate and timepoint. Error bars correspond to 1st and 3rd quartiles. The number of cells analysed per condition can be found in Table 3. More exhaustive statistical analysis can be consulted in Appendix C, tables 43-44 and 49. * indicates p < 0.05, * indicates p < 0.001. D1 was used as reference in the statistical tests.**

During the experiments, cells grew considerably larger (Fig. 5.7 a) attaining maximum median spread areas circa 5000 μm^2 after day 10. As in previous experiments, no distinctions could be observed between cells seeded in distinct mechanical environments. Aspect ratio, on the other hand, behaved in a non-monotonic manner (Fig. 5.7 b). Despite noticeably larger aspect ratio values having, once again, been associated with cells in the softest hydrogels, the overall trends in the parameter were still consistent between mechanical environments. Concretely, an initial decrease in aspect ratio between the two earliest time points, was followed by a pronounced elongation of the cells culminating a week from the induction of differentiation. Following this

threshold, cell aspect ratio slowly reverted to values close to those displayed at day 1. In addition to aspect ratio, the shape of cell periphery also displayed interesting trends with three regimes being evident in Fig. 5.7 c). These were, namely, early minute changes in stellate factor between days 1 and 3, followed by an accelerated increase until days 5 to 7, and a final plateau in later time-points, when the “star-like” quality of cell perimeters was either maintained or slightly increased.

Overall, the results in Fig. 5.7 suggest that the inclusion of adipogenic factors induced dynamic changes in cell morphology. In general, differentiation proceeded with minor changes between days 1 and 3, followed by stark increases in the intermediate days, and slower morphological shifts in later stages. As with osteogenic differentiation, morphological trends were remarkably consistent across parameters independently of the substrate factor, which reflects an independence between differentiation processes and substrate choice in 2D collagen-coated agarose.

It has been published that hMSC confinement on micropatterned islands of different sizes, geometrical shapes and aspect ratios can modulate osteogenic and adipogenic fates [115], [116]. In these reports, adipogenesis is regularly associated with cells constrained by small areas, with rounder, less elongated shapes. However, the results presented in this section demonstrate that unconstrained cells, supplemented with biochemical differentiation factors, do not necessarily behave in accordance with these norms. Moreover, this data suggests that cell adaptation to mechanical and biochemical stimuli is not a static process, but rather highly dynamic.

As presented on Appendix B, pilot studies were conducted in collagen coated TCP to confirm that the hMSCs used in this work preserved the capacity to differentiate into osteoblasts and adipocytes. In these studies, cell seeding density was confirmed as a critical factor in achieving terminal cell fates. In the adipogenic lineage, in particular, fully-differentiated adipocytes were exclusively identified within clusters of neighbouring cells. Furthermore, adipocytes surrounded by closely-compacted cell clusters tended to develop large and immediately evident lipid vacuoles, while cells in sparser neighbourhoods would accumulate numerous smaller lipid reserves, more readily identified by Oil Red O staining.

Due to the clear dependency between terminal adipocytes and cell density, a subset of collagen-coated 1% agarose hydrogels was seeded at higher density (10x larger), and again cultured in adipogenic media. Under these conditions it was visually confirmed that only a subset of cells could reach a recognisable terminal state of adipogenesis shortly after a week of biochemical differentiation, as shown in Fig. 5.8.

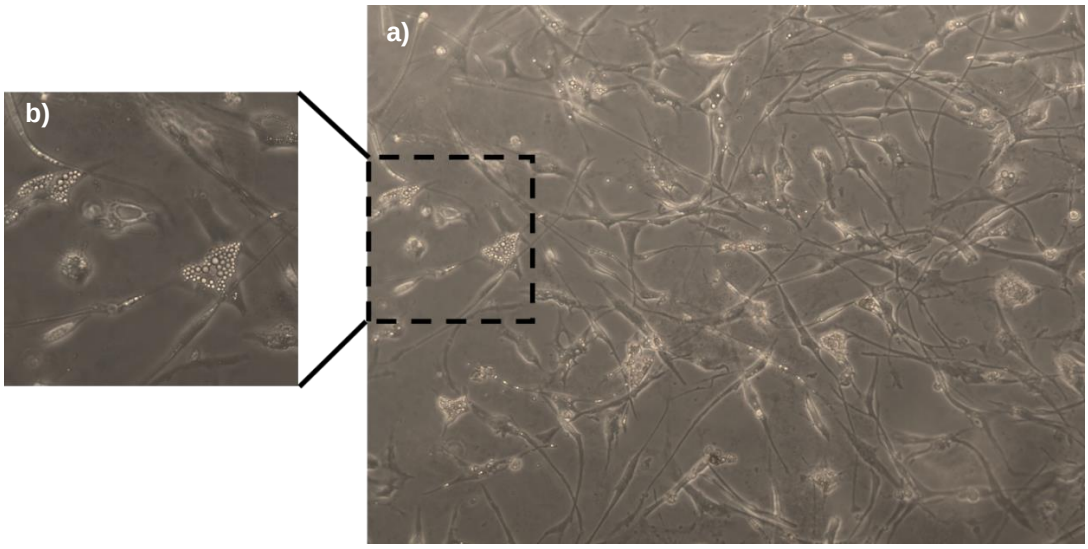

Figure 5-8 – High confluency was required to achieve terminal adipogenesis in the substrates – In a subset of qualitative experiments, hMSCs were seeded at a density 10 times larger than in the experiments for morphometric characterisation. a) Terminal adipocytes were observed following a week of culture in the presence of differentiation supplements. The occurrence of terminal phenotypes coincided with regions of high cell density in the hydrogel surface. The image was collected using a x10 objective. b) Magnified detail of terminal adipocytes collected using a x20 objective.

Interestingly, as evidenced by Fig. 5.8, it was observed that the accumulation of lipid vacuoles, i.e. terminal adipogenesis, was limited to cells constrained to smaller, round phenotypes. This observation corroborated standard results in micropatterns and PAA hydrogels. Thus, it is not clear if the populational trajectories reported in this work reflect adipocyte precursor stages that will ultimately coalesce into fully mature cells, or an alternative differentiation pathway resulting in a currently unidentified cell fates.

5.3.5 Combined effects of adipogenic differentiation media and substrate mechanical properties on F-actin architecture

The joint influence of biochemical adipogenic differentiation induction and substrate mechanical properties on hMSC F-actin states was equally addressed. These results are shown in Fig. 5.9 and Fig. 5.10. As in osteogenic differentiation, parameters behaved nearly identically irrespective of the hydrogel factor.

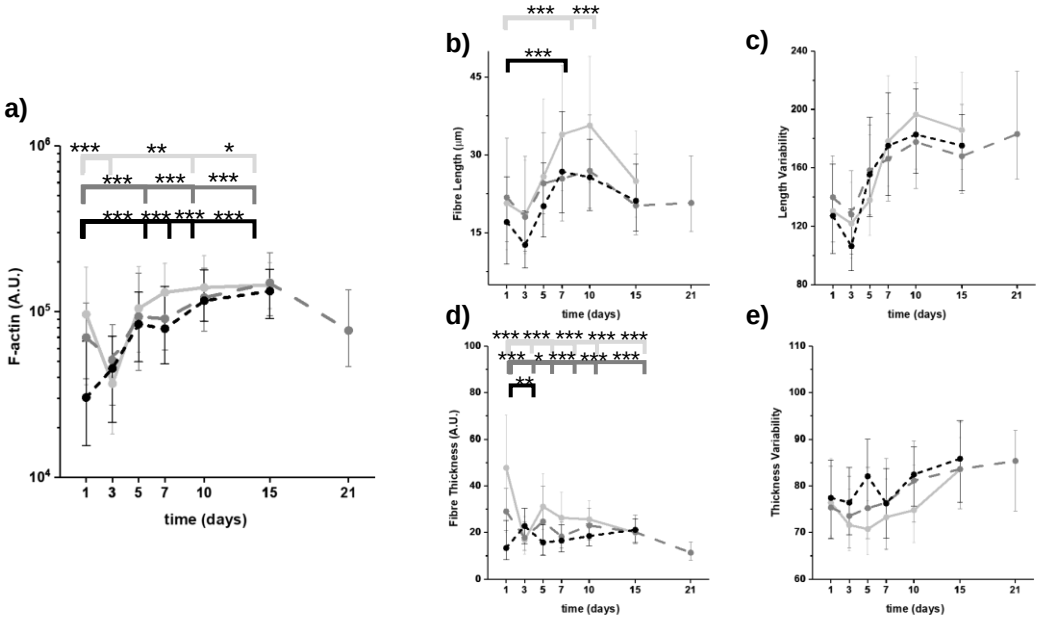

Figure 5-9 – Population-based F-actin shape descriptor trajectories guided by adipogenic media and mechanical stimuli – a) F-actin amount; b) Fibre length; c) Length variability; d) Fibre thickness; e) Thickness variability; Data is plotted as median values of N = 2 experimental replicates per substrate and timepoint. Error bars correspond to 1st and 3rd quartiles. The number of cells analysed per condition can be found in Table 3. More exhaustive statistical analysis can be consulted in Appendix C, tables 45-46 and 50. * indicates p < 0.05, * indicates p < 0.001. D1 was used as reference in the statistical tests.**

Under the effect of adipogenic conditioning, the initial amounts of F-actin in the cells displayed high variability (Fig. 5.9 a). There were minor discrepancies between cells seeded on different hydrogels: cells on 1% and 3% hydrogels had initially larger F-actin contents and experienced a decrease in F-actin levels at day 3, which did not happen on cells on 5% hydrogels. Across samples F-actin values continually increased after day 1 during the span of two weeks. The incremental trend was inverted at day 21 in 3% agarose, but since no other hydrogel samples could be collected at 21 days,

the hypothesis that this was an artefact due to biased sampling cannot be excluded.

The behaviour of fibre length (Fig. 5.9 b), on the other hand, closely followed that of cell aspect ratio, suggesting a possible connection between the two parameters. Concomitantly, an increase in the variability of fibre length took place from day 3 onwards (Fig. 5.9 c), stabilising after 10 days. Alterations in median fibre thickness were less pronounced (Fig. 5.9 d), resulting in an overall decrease relative to day 1. It is noteworthy that a positive relationship between F-actin amount and fibre thickness was not evident under adipogenic factors, as it had in osteogenic differentiation. Conversely, variability in thickness (Fig. 5.9 e) scaled with time, as in osteogenic differentiation. Thus, the actin cytoskeleton network became substantially more complex under the influence of adipogenic supplements and biophysical cues.

Changes in the orientation of the actin cytoskeleton were also observed, as represented in Fig. 5.10.

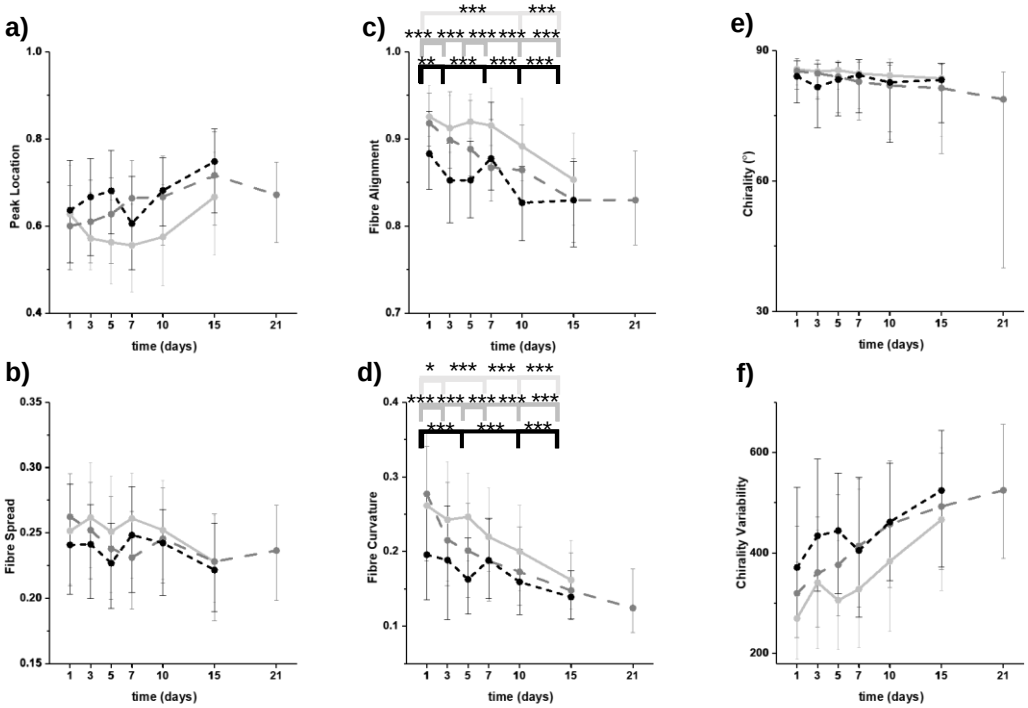

Figure 5-10 – Population-based F-actin positioning descriptor trajectories guided by adipogenic media and mechanical stimuli – a) Radial peak fibre location; b) Radial fibre spread; c) Fibre alignment; d) Fibre curvature; e) Fibre chirality; f) Chirality variability; Data is plotted as median values of N = 2 experimental replicates per substrate and timepoint. Error bars correspond to 1st and 3rd quartiles. The number of cells analysed per condition can be found in Table 3. More exhaustive statistical analysis can be consulted in Appendix C, tables 47 and 48. * indicates p < 0.05, * indicates p < 0.001. D1 was used as reference in the statistical tests.**

The addition of adipogenic media caused fibre positioning within the cytoplasm to change, with peak location increasing over time (Fig. 5.10 a), and fibre spread displaying the inverse trend (Fig. 5.10 b). Alongside these alterations, actin fibre bundles became straighter (Fig. 5.10 c) but grew less aligned (Fig. 5.10 d), while the distribution of median fibre chirality (Fig. 5.10 e) remained fundamentally unchanged. Cells seeded in 3% agarose hydrogels for 21 days presented an unexpectedly wide range of median chirality values, likely due to an experimental artefact. Finally, intracellular fibre chirality variability also increased over this period among all substrates (Fig. 5.10 f).

The results from Fig. 5.9 and Fig. 5.10 confirm that the combination of adipogenic differentiation factors and biophysical inputs from the selected substrates imparted highly dynamic changes onto the hMSC F-actin cytoskeleton, which were markedly distinct from those observed during osteogenic differentiation.

5.3.6 Combined effects of adipogenic differentiation media and substrate mechanical properties on nuclear state

In addition to cytoskeletal features, nuclear traits were also studied in hMSCs seeded on 2D collagen-coated agarose substrates and cultured with adipogenic differentiation supplements. The first image on the panel (Fig. 5.11 a) shows that nuclear volume underwent subtle fluctuations, which were nonetheless very consistent among cells in the different substrates. This might indicate that nucleus volume is tightly regulated during adipogenic differentiation and might thus constitute an important biomarker for this lineage. Further studies should be conducted to investigate this hypothesis in more detail. Surprisingly, although the nuclei did not experience large volume changes, considerable nuclear stiffening was still measured over time (Fig. 5.11 b). The independence between nuclear volume and stiffness, in this case, suggests that stiffening resulted from increases in cell area and the associated nuclear strains exerted by nematic cytoskeletons.

It would be interesting to assess this effect from the perspective of changes in lamina constitution during differentiation. Adipogenic differentiation has been mostly studied in soft PAA substrates or in confined micropatterns,

which artificially limit cell spread area and the assembly of prominent actin stress fibres. In these systems, increased adipogenic differentiation yield has been associated with downregulation of lamin A, resulting in decreased nuclear stiffness [83], which is in direct opposition to the results presented in Fig. 5.11 b). Again, these results suggest that standard substrates might fail to capture important dynamic aspects of freely spread cells. A more complete understating of differentiation processes therefore requires the integration of studies in a range of distinct cellular environments.

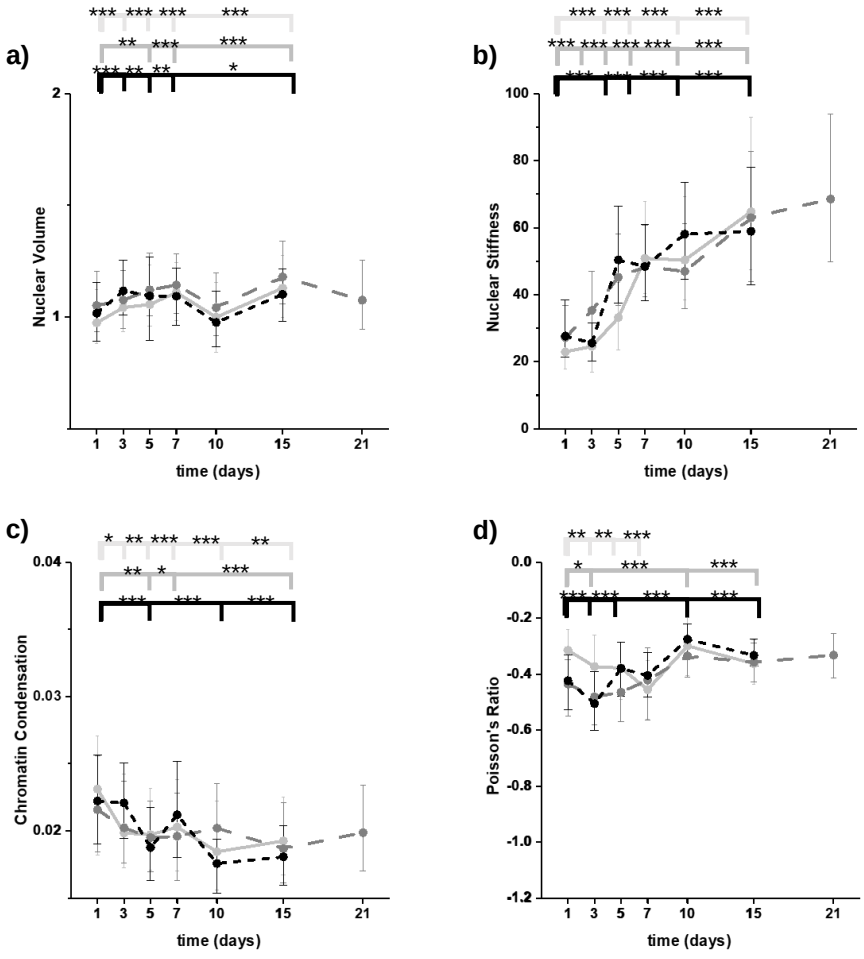

Figure 5-11 – Population-based nuclear state descriptor trajectories guided by adipogenic media and mechanical stimuli – a) Nuclear Volume; b) Nuclear Stiffness; c) Chromatin Condensation; d) Poisson's Ratio; Data is plotted as median values of N = 2 experimental replicates per substrate and timepoint. Error bars correspond to 1st and 3rd quartiles. The number of cells analysed per condition can be found in Table 3. More exhaustive statistical analysis can be consulted in Appendix C, tables 51-54. * indicates p < 0.05, * indicates p < 0.001. D1 was used as reference in the statistical tests.**

Finally, trends in chromatin condensation (Fig. 5.11 c) and nuclear Poisson's ratio (Fig. 5.11 d) were equally moderate. In the former case, later days displayed marginal relaxation in the state of chromatin, whereas the absolute values of nuclear Poisson's ratio were decreased in time across substrates.

5.3.7 Comparison of the effects of osteogenic and adipogenic induction media on hMSCs cultured on 2D collagen-coated agarose substrates

Having characterised the effects of osteogenic and adipogenic supplements on hMSCs cultured on 2D collagen-coated agarose substrates, it is of interest to establish a general comparison between these conditions.

First, it is noteworthy that there were negligible differences in morphological, cytoskeletal and nuclear trends observed in soft, intermediate or stiff substrates, in either of the differentiation media. Similarities like these had also been observed amid cells seeded in standard growth medium (Chapter 4), but these trends became clearer when the cells were exposed to biochemical differentiation supplements. This observation strongly suggests that biochemical stimuli were more impactful in guiding hMSC differentiation than the biophysical properties of the surrounding environments.

In PAA hydrogels [11], osteogenic differentiation is favoured by culturing hMSCs on relatively stiff substrates (in the order of tens of kPa) which permit spread-out morphologies. Adipogenesis, on the other hand, is promoted by round-up morphologies, and the subsequent disruption of actin assembly. Similarly, micropatterns which permit large spreading areas, with straight and sharper edges, promote cytoskeleton assembly and contractility, thereby promoting osteogenic fates; whereas small patterns with rounded shapes tend to upregulate the expression of adipogenic genes [115], [116].

Yet, the results gathered in this chapter were in direct contradiction to the expected dichotomy in osteogenic and adipogenic lineages in hMSC mechanobiology, since both types of differentiation resulted in parallel and highly dynamic behaviours in cell morphology, cytoskeleton architecture and nuclear state. For instance, the populational trajectories of cell morphology shared traits between the two differentiation pathways. Firstly, there were pronounced increases in median cell area in both cases, reaching an order of

magnitude within two weeks of culture. In osteogenic differentiation (Fig. 5.2) these increases behaved linearly, while a sigmoidal-like relationship was found in adipogenesis (Fig. 5.7). In second place, aspect ratio displayed non-monotonic trends in both conditions, with peak elongation achieved at an intermediate day (day 3 in osteogenic media, and day 7 in adipogenic media), followed by subsequent decrease in the ratio between cell axes. Finally, in both types of culture, mature cells tended to acquire “star-like” morphologies, developing long processes and a convex perimeter. The morphologies herein described, and displayed on Fig. 5.1 and 5.6, are reminiscent of those typically found in fibrillar environments [112], [113], [227]. Morphological results were therefore likely guided by the collagen layer coating the substrates in which the cells were seeded [207], [209].

Coupled to cell area increase, F-actin build-up was likewise observed in both lineages, but to a larger degree in osteogenic differentiation (Fig. 5.3) relative to adipogenic differentiation (Fig. 5.9). Curiously, in osteogenic differentiation, fibre bundle reinforcement was more closely associated with fibre thickness, whereas, under adipogenic stimuli, F-actin states were mainly associated with median stress fibre length. Moreover, the complexity of the actin networks increased in both osteogenic (Fig. 5.4) and adipogenic (Fig. 5.10) media, as reflected by changes in the variability of fibre length, thickness and angular orientation, and downward trends in stress fibre alignment and curvature were comparable in both types of differentiation.

Although identical trends could be observed for nuclear stiffness, chromatin condensation and Poisson’s ratio, nuclear volume behaved quite differently between the osteogenic (Fig. 5.5) and adipogenic (Fig. 5.11) lineages. Thus, a potential role for nuclear volume as an important biomarker of differentiation can be postulated, although it must be subjected to further scrutiny.

Interestingly, dynamic non-monotonic trends, akin to those described in this section, were equally described regarding the mechanical properties (stiffness and viscosity) of hMSCs after long-term culture on PDMS substrates of varying bulk-stiffness [257]. Based on these findings, Zhang et al. divided parameter trends into three zones: days 1 through 5 corresponded to an initial adaptation, where cell moduli decreased as a response to the change in

culture environment upon cell seeding; a growth zone, culminating on day 11, resulting in cell stiffness increase; and a convergent zone, where cell properties were closely matched irrespectively of substrate stiffness. This classification is in general agreement with the morphometric trends reported in this chapter. Altogether, these results highlight the importance of conducting long-term analysis of the behaviour and biophysical properties of cells under varied conditions.

5.3.8 Study limitations

This study presents a morphometric characterisation of SC differentiation in non-conventional hydrogel substrates. As such, extending the analysis to include standard hydrogel substrates, such as PAA or PDMS, would allow the identification of shared trends, as well as establishing which cell adaptations are restricted to each culture system. As in Chapter 4, data was acquired from primary hMSCs from a single-donor. It would be worthwhile to reproduce this study using a more diverse batch of cells, to better establish the level of agreement between developmental trends reported among different donors.

The most important limitation of this work, however, is the fact that terminal differentiation could not be carefully assessed due to time restrictions. Although the morphometric trends herein reported can be ascribed to the action of biochemical differentiation supplements, no evidence could be provided as to the phenotypic maturity of the cells obtained after long-term culture on the hydrogel substrates. Future studies should therefore address this limitation by histological staining protocols, complemented with gene expression analysis, to confirm the presence of terminal osteoblasts and adipocytes.

5.6 General Conclusions

Methodological limitations notwithstanding, the results shown in this chapter demonstrated that biochemical differentiation supplements where able to override the biophysical inputs of the collagen-based extracellular

environment and promote dynamic morphometric behaviours over a long span of time. It was also observed that hMSC populations follow distinct morphometric trajectories during osteogenic and adipogenic differentiation, which nonetheless presented noticeable similarities, in part due to the fibrillar nature of cell-substrate interfaces.

Overall it can be concluded that populational morphometric traits present informative value in the discrimination between cell fates. The context provided by the combination of biochemical and mechanical factors should always be considered during differentiation and morphological studies.

Chapter 6 – Single-cell morphometric developmental trajectories

6.1 Introduction

Studies based on SC populations, such as those discussed in Chapter 5, are hindered by high heterogeneity and asynchronicity. During differentiation cells within the same population will be at distinct developmental stages at any moment in time [46]; some cells will have quickly integrated differentiation signals present in the environment, while others will lag behind, or not respond to the stimuli, remaining closer to a stem-like state. In order to reconstruct more accurate developmental trajectories and overcome the limitations of populational analysis, these processes must be understood at the single-cell level.

State-of-the-art research in single-cell lineage reconstruction has so far relied on distance-based clustering methods to parse high-throughput genetic marker profiles in unlabelled samples [178]–[180]. A critical oversight of these approaches is their outputs do not currently accommodate temporal information. Instead, an artificial ordering of cells based upon an inferred trajectory, interpreted as chronological, is represented through a pseudo-time axis [258]. Pseudo-time trajectories, therefore, are not mapped onto real time (Fig. 2.4). Moreover, no such studies have yet been conducted on hMSCs, or solely from the perspective of morphological changes. Given these opportunities, populational data collected in Chapter 5 was used to test a new approach for the assembly of developmental trajectories, based on the single-cell capabilities of our experimental methodology. This big data approach is based on ML techniques, and more specifically, on supervised regression algorithms (Fig. 2.3).

With these objectives in mind, section 6.2 covers the novel methodology to reconstruct continuous single-cell morphometric trajectories from discrete populational time-courses.

6.2 A new methodology to construct single-cell developmental trajectories

The algorithm to predict trajectory day based on multidimensional single-cell data (consisting of thousands of data points characterised by 18 morphometric descriptors) is based on SVM regression.

The first step in the algorithm standardises the morphometric descriptors, consigning their values to intervals of comparable magnitude (to prevent descriptors with larger values, such as cell area and F-actin amount, from overtaking the fitting of the model). Standardisation is performed by computing z-scores of all morphometric descriptors ($X_{standardised}=\frac{(X-\mu)}{\sigma}$; X is a descriptor value, μ is the mean value of the descriptor and σ is the descriptor standard deviation).

Each global iteration of the algorithm first randomly splits the data into two groups. 80% of the data points are used to train/test an SVM regression, and each point in the remaining 20% of the data (the out of sample (OOS) group) is assigned a predicted trajectory day as a final output of the trained regression model.

The following steps are carried out by the algorithm with the 80% of cells selected as training/test data to fit and evaluate the ML model. To use the SVM regression implemented in the MATLAB ML toolbox, three main hyperparameters need to be optimized: Box Constraint (BC), Kernel Scale (KS) and Epsilon (Ep).

Computation of the parameters is conducted by an optimiser developed by Dr. Núria Gavara. This optimiser identifies values of BC, KS and Ep hyperparameters based on minimising an error estimate, which reflects the difference between the predicted (trajectory day) values and the known (experimental day) values for a set of test data (Fig. 6.1). The custom optimiser is based on an error metric specifically devised for the task. Briefly, a linear regression is fitted to the predicted class versus real class values and the slope and offset of the regression are calculated. The error value for the trained models is computed as the product between the values of |1 – slope| and the

absolute offset. Combinations of hyperparameters that lead to the smallest errors are carried forward for subsequent iterations.

In order to find the optimal set of hyperparameters to build a model, iterations are run based on further dividing the 80% modelling data into 50% train and 50% test (40/40 of the total data available at start). Values for BC, KS and Ep are randomly initiated, and the algorithm is trained with the train dataset. Test data is classified by the recently fitted SVM regression model. The predicted trajectory day outputs are compared to the real experimental days using the previously described error metrics. This assessment if conducted 8 times with different cells randomly allocated to the train or test populations (to account for sampling bias).

These steps are repeated for 12 random hyperparameter combinations. The combination with lowest error is selected for that iteration. Subsequent iterations repeat this process, constricting the selection of the 12 combinations to a window around the optimal BC, KS, Ep values in the previous iteration. Optimal hyperparameter values are thus focused on over the course of 20 iterations. This pipeline has been optimized for performance of the algorithm in terms of accuracy and computation time.

Finally, the OOS data is classified using the best trained model. The data is then resampled, and the process is reinitiated. The classification is conducted 50 times to ensure each cell has, on average, been assigned 10 prediction outputs (days in the trajectory). The final predicted days used to reconstruct the single-cell morphometric trajectories resulted from averaging the range of predictions in each data-point.

The predicted data is further processed with a custom-made averaging filter and linked together with a spline operation.

6.3 Results and discussion

The populational trajectories described in Chapter 5 are hindered by the variability and asynchronocity of hMSCs. As such, this data set was favourably poised for testing of a new methodology developed by our group which aims to construct single-cell morphometric developmental trajectories. This methodology is advantageous because it incorporates the discrete

temporal information associated with the experimental approach described in Chapter 5, allowing the reordering of discrete populational data along a continuous single-cell trajectory, which is optimised on the multidimensional morphometric space. As such, the algorithm identifies cells which fall earlier, or later, on in the developmental pathway, relative to the experimental day of differentiation. Altogether, the integration of this information into a ML regression model is expected to provide a representation of the most likely developmental trajectories undergone by single-cells during differentiation in specific mechanical and biochemical environments.

As this chapter represents work-in-progress within our research group, only a subset of data from Chapter 5 was selected for analysis. This data corresponded to the morphometric descriptors characterising osteogenic and adipogenic differentiation in 2D collagen-coated 3% agarose hydrogels.

6.3.1 Single-cell morphometric developmental trajectories in osteogenic and adipogenic differentiation guided by biochemical and mechanical stimuli

Fig. 6.1 provides a visual comparison of the discrepancies between the predicted trajectory day assigned by the SVM regression to each data point (Y-axis) and the experimental time (corresponding to the real day of differentiation, X-axis).

In both osteogenic (Fig. 6.1 a) and adipogenic (Fig. 6.1 b) differentiation hMSCs have been classified to belong to time points earlier to, concurrent with and following the day of differentiation. These points correspond to those falling respectively below, along or above the line illustrated by black markers (with slope 1 and offset 0) which relates exact matches between predicted and experimental time. The presence of a data-points assigned to a “negative day” (experimental days 3 and 5 in Fig. 6.1 b) were artefacts of the regression algorithm and excluded from further analysis.

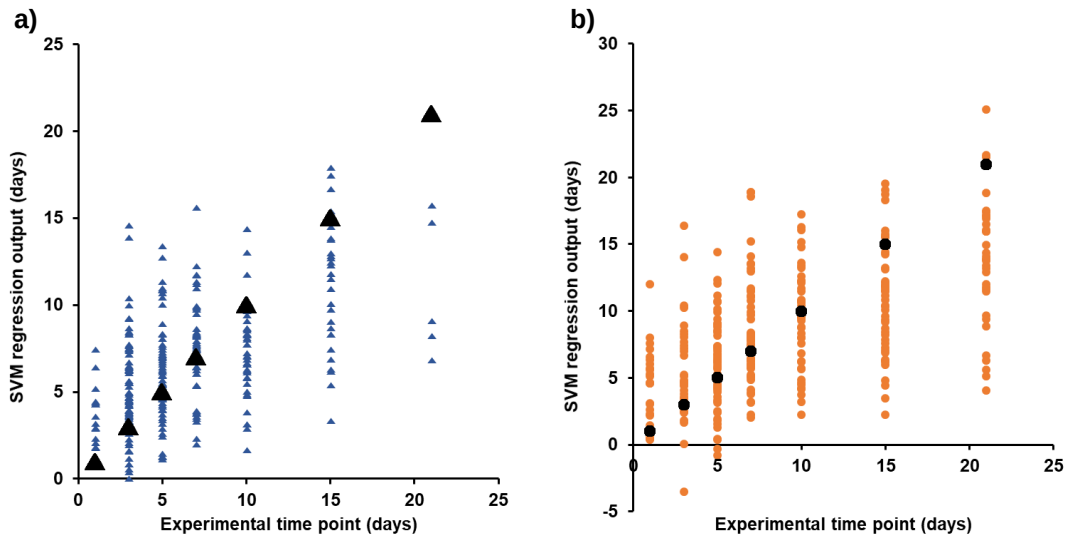

Figure 6-1 – Visual comparison of SVM predictions versus real experimental time points – a) Osteogenic differentiation, b) Adipogenic differentiation; Black markers were introduced to aid the identification of perfect matches between predicted and experimental classes. Data points falling on top of these markers represent hMSCs classified as belonging to a later time point. Data points below the markers represent hMSCs which have been assigned to earlier points in the trajectory relative to experimental time.

In general, there was substantial overlap between the spread of predicted days in each experimental time point, with the notable exception of day 21 in the osteogenic differentiation. In this condition, most cells remained assigned to their experimental day, suggesting that the terminal phenotypes in osteogenic differentiation were substantially distinct from the remaining cell states along the trajectory. The converse was observed in adipogenic differentiation, where predictions remained consistently spread out, even in the last experimental time point.

Using the information contained in the Y-axis of Fig. 6.1, single-cell morphometric osteogenic and adipogenic developmental trajectories were constructed. Trajectories based on morphological descriptors, namely cell area, aspect ratio and stellate factor, are presented in Fig. 6.2

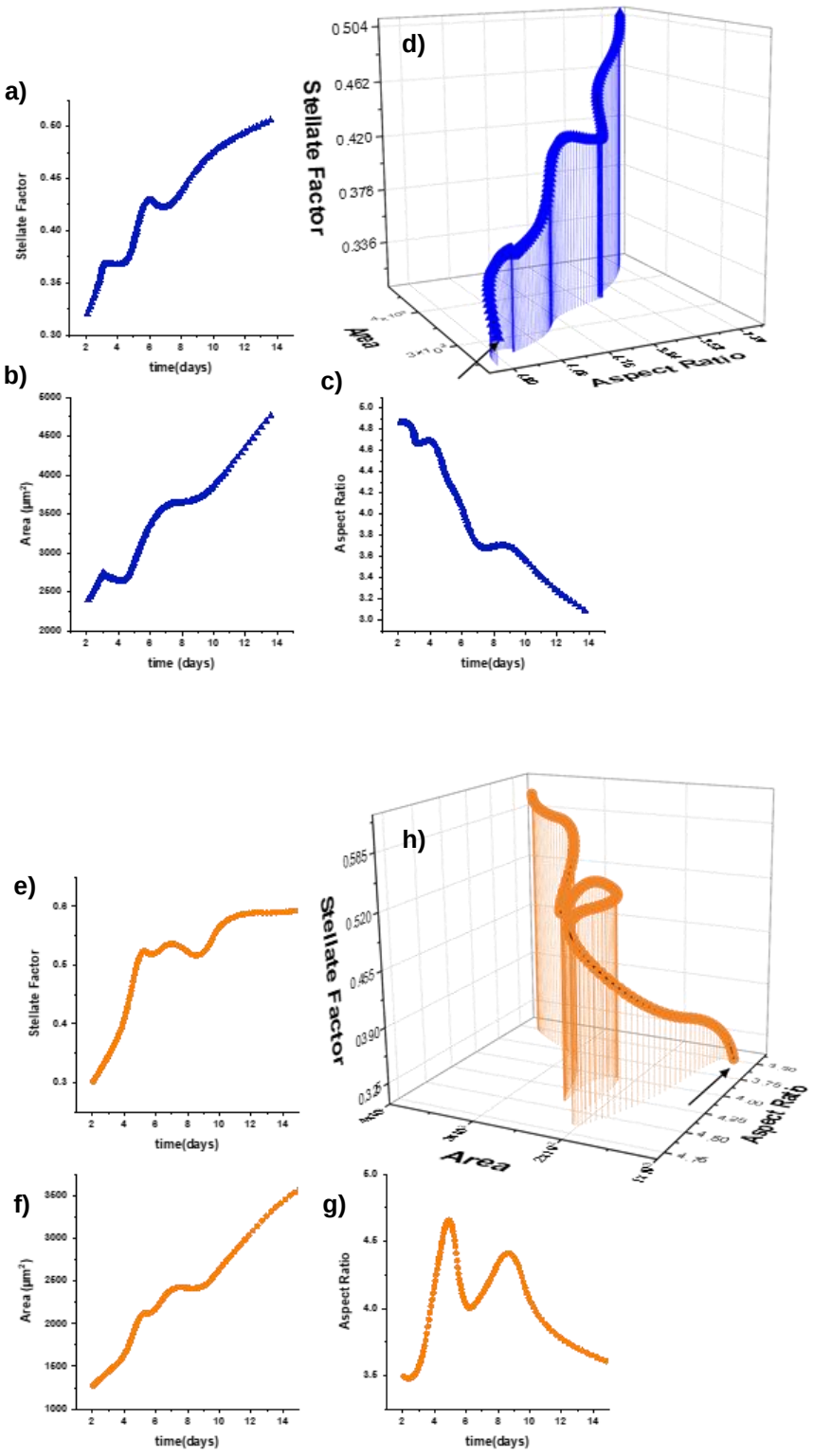

Figure 6-2 – Single-cell morphological developmental trajectories – a - c) Osteogenic morphological (Stellate Factor, Area and Aspect Ratio) trajectories predicted by the SVM regression model; d) 3D multiparametric Osteogenic developmental trajectory reconstructed from parameters a – c); e - g) Adipogenic morphological (Stellate Factor, Area and Aspect Ratio) trajectories predicted by the SVM regression model; h) 3D multiparametric Adipogenic developmental trajectory reconstructed from parameters e – g). The black arrow in the 3D plots indicates the start of the trajectory.

. In osteogenic differentiation (Fig. 6.2 a - c) these trajectories are essentially monotonic, with cell area and stellate factor increasing in time, and aspect ratio decaying during differentiation. On adipogenic differentiation (Fig. 6.2 e - f), on the other hand, the morphological trends were more dynamic. While cell area increased nearly linearly, stellate factor reached a plateau after a week of differentiation, and aspect ratio displayed a highly non-monotonic trajectory. For osteogenic differentiation the single-cell trajectories were fairly similar to the population-based trends described in Chapter 5 (Fig. 5.2). The exception in this case was that an initial increment in aspect ratio between days 1 and 3 which had been present in populational trends was lost in the new trajectory. Similarly, adipogenic area and stellate factor single-cell trajectories were akin to their populational morphological counterparts (Fig. 5.7). Aspect ratio was again the descriptor with more notable differences between approaches. A more dynamic behaviour was found in the single-cell aspect ratio trajectory, which still bore considerable semblance to the respective populational trend (i.e. an initial increase in aspect ratio followed by a peak around a week of differentiation and subsequent decrease until the end of the experiment).

Combining the morphological information encoded by the three descriptors into 3D multiparametric trajectories (Fig. 6.2 d, h) evidences the complex set of phenotypic changes undergone by hMSCs during differentiation. Furthermore, it is clear from these two plots that the morphological trajectory of the osteogenic lineage is quite distinct from the adipogenic trajectory. Fig. 6.3 further emphasises this point, by displaying trajectories undergone by the actin stress fibres (represented by F-actin amount, fibre thickness and length in Fig. 6.3 a and b) and nuclear properties (represented by relative nuclear volume, stiffness and Poisson’s ratio in Fig. 6.3 c and d).

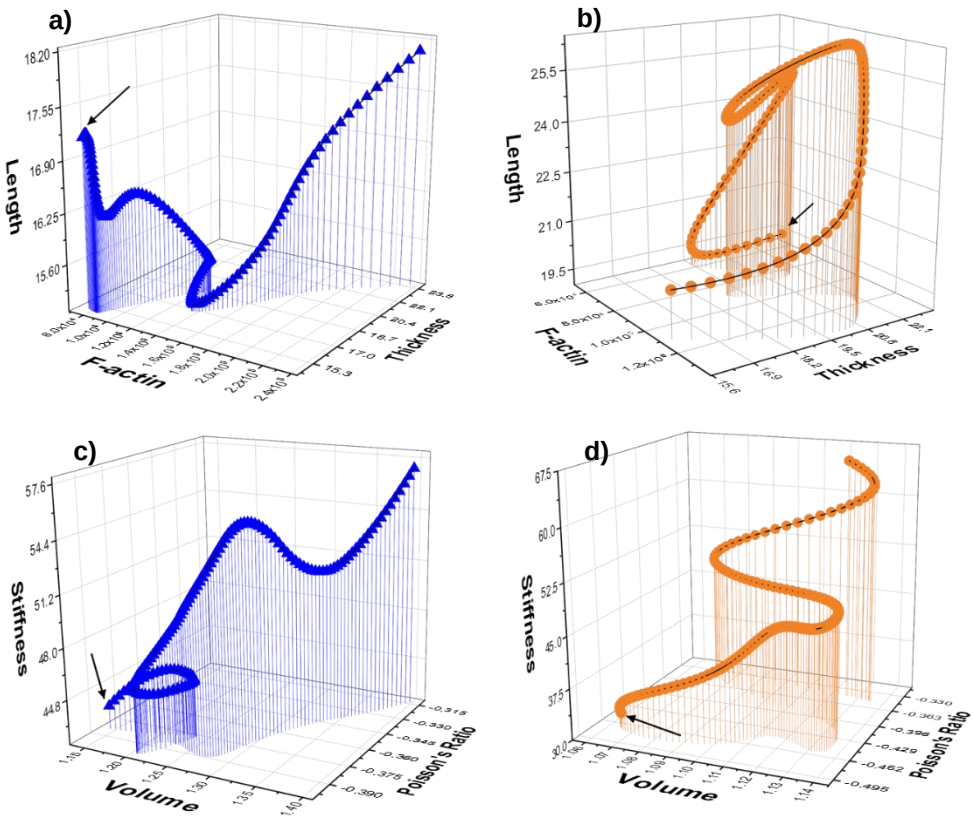

Figure 6-3 – Single-cell stress fibre and nuclear developmental trajectories – a) 3D multiparametric Osteogenic stress developmental trajectory reconstructed from F-actin amount, fibre length and fibre thickness; b) 3D multiparametric Adipogenic stress fibre developmental trajectory reconstructed from F-actin amount, fibre length and fibre thickness; c) 3D multiparametric Osteogenic nuclear developmental trajectory reconstructed from relative nuclear volume, stiffness and Poisson's ratio; d) 3D multiparametric Adipogenic nuclear developmental trajectory reconstructed from relative nuclear volume, stiffness and Poisson's ratio. The black arrow in the 3D plots indicates the start of the trajectory.

As a final example, Fig. 6.4 depicts the trajectories of chromatin condensation in osteogenic and adipogenic differentiation. In the first case, the behaviour of the descriptor was identical in the populational (Fig. 5.5 c) and single-cell trajectories (Fig. 6.4 a). In the second case, similarities were also present in both adipogenic chromatin condensation trends, but the single-cell trajectory (Fig. 6.4 b) nevertheless displayed a more dynamic version relative to the population-based variant (Fig. 5.11 c).

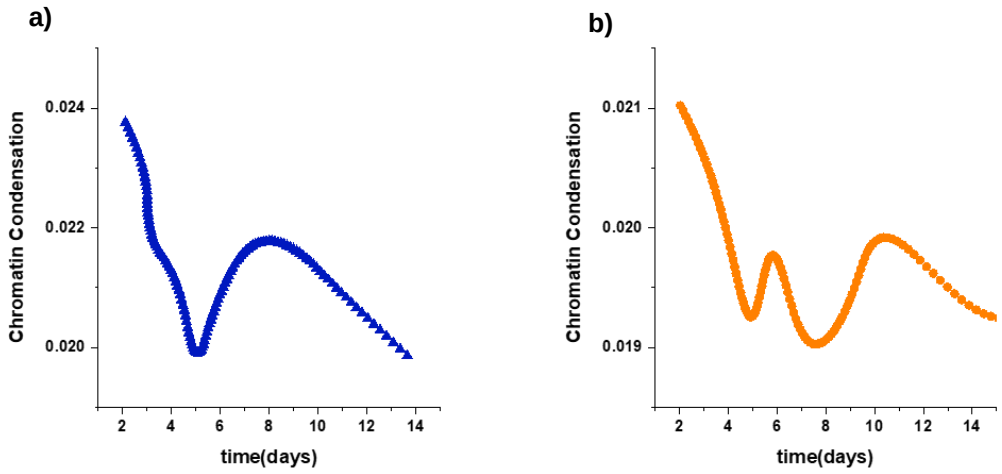

Figure 6-4 – Single-cell chromatin condensation trajectory – a) Osteogenic chromatin condensation trajectory predicted by the SVM regression model; b) Adipogenic chromatin condensation trajectory predicted by the SVM regression model

6.3.2 Study limitations

This section describes preliminary results for the methodology that has been recently developed in our research group to produce single-cell morphometric developmental trajectories. However, this project is still part of a work in progress, and therefore this chapter must be integrated in the context of broader research. The methodology will therefore be tested in different datasets in a near future and continually refined.

It should be pointed that the methodological approach pursued by our group is fundamentally distinct from most similar publications currently in the literature [178]–[180]. More concretely, we have chosen to employ supervised ML algorithms to maximise the information collected from our experimental approaches. As such, the regression-based strategy described in this chapter is reliant on class annotated datasets. For this reason, our methodology is not currently equipped to simultaneously operate on multiple lineages or find branching points on the data.

6.4 General Conclusions

The results acquired in this work suggested that there are close similarities between discrete population-based and continuous single-cell morphometric developmental trajectories, in both the osteogenic and adipogenic lineages. Single-cell trajectories helped clarify the trends obtained in the highly heterogeneous hMSCs samples and revealed that the dynamics of some of the morphometric descriptors (e.g. aspect ratio and chromatin condensation) might not be reconstructed with full-accuracy with sparse temporal sampling (i.e. experimental intervals several days apart) using standard analytical techniques. As such, these results suggest that, by resolving the information encoded at single-cell level in any given asynchronous populational sample, the reconstruction of continuous developmental trajectories might be feasible without resorting to continuous imaging modalities, which can be prohibitively resource intensive.

By using time as a target variable during computation of the regression model, the day to which experimental points belong to is directly used to optimise the fit of a regression function. This new method therefore assimilates real-time information (i.e. days in differentiation experiments) into analysis of biological trajectories for the first time. Furthermore, the regression is based on multiparametric function fitting, which means that information across all parameters is pooled together during analysis. As such, the information separately encoded by 18 populational descriptors is integrated together into a single-cell trajectory. Finally, the ML aspect of the approach means that the temporal positioning of each single-cell is re-evaluated, so that cells are assigned a value along the trajectory according to similarities with the closest surrounding cells. Each cell can thus remain essentially static in time, meaning that it was representative of its experimental time point, or be assigned to a later/earlier time point, depending on how its characteristics related to the expected morphometric profiles along the trajectory (e.g. an hMSC collected at experimental day 10 sorted into day 5 by the regression model, potentially signifying that it differentiated at a slower rate than other cells in the sample).

This methodology is the first to integrate real temporal information into the estimation of development trajectories, as well as extending this approach to morphometric traits (as opposed to protein/genetic markers) and to the study of hMSCs.

In general, this chapter confirms that the novel methodology to produce single-cell morphometric developmental trajectories can be successfully applied to datasets generated with the experimental approaches employed in our research group. Discrete temporal population-based morphometric information can therefore be used to postulate continuous single-cell developmental trajectories.

Chapter 7 – Lifeact-GFP alters F-actin organization, cellular morphology and biophysical behaviour

Please note, a version of this chapter is published in Scientific Reports, Nature group, as reference [259] *. Contributions to the work are stated in detail in the Statement of Originality.*

7.1 Introduction

Live-cell actin visualization is routinely performed and presented in a large percentage of cell biology research, including studies where actin or the cytoskeleton may only be secondary players on the reported observations. Lifeact, a small peptide with affinity for actin microfilaments[182], [184], [260], has become one of the gold standards in live cell imaging of actin structures in particular, and overall cell morphology in general.

A number of reports have assessed the suitability of Lifeact as a cytoskeletal marker, focusing primarily on qualitative observations of which structures are preferentially labelled by Lifeact relative to other probes such as phalloidin, utrophin or actin-GFP [261], [262]. It has been recently reported that Lifeact alters actin filament arrangement and dynamics in fission yeast cells [185]. Similarly, strong *in vivo* Lifeact expression causes sterility in fruit flies [186], associated with severe actin defects and multiple nuclei in follicle cells. In addition, the detrimental effects of strong Lifeact expression in cells appear to be linked to the specific promoter and fluorescent protein tag used [263], [264].

The aforementioned studies have focused on highlighting the abnormal morphologies, dynamics and overall behaviour of cells associated with strong Lifeact expression. Nevertheless, it remains to be discerned whether low to mid-level expression of Lifeact results in unaltered actin dynamics, or conversely if Lifeact induces broad dose-dependent effects on the actin cytoskeleton. Such an understanding is still missing to better define the experimental conditions under which Lifeact is to be considered a suitable probe to image actin structures.

7.2 Methodology

Materials and Methods

Cell culture, Lifeact-GFP transduction and immunostaining

The majority of measurements were performed in hMSCs, while additional measurements were performed in NIH/3T3 and COS-7 cells. Cells were maintained in culture medium consisting of low glucose DMEM supplemented with 10% FBS, and 100U/ml Penicillin- 100µg/ml Streptomycin. Cells were kept in tissue culture flasks and cultured at 37°C and 5% CO2.

Lifeact-GFP transductions were performed using commercial rAV-CMV-LifeAct-TagGFP2 Adenoviral Vectors (Ibidi, Germany) according to supplier's instructions, by addition of viral transduction reagent volumes required to achieve the desired multiplicity of infection (MOI) on each sample (i.e. 100, 300, 600 or 1000). After the initial 18 hours of incubation for vector uptake, media containing viral particles was exchanged. Cell samples were allowed to express Lifeact-GFP for a total of 1, 3, 5 or 7 days prior to fixation.

The pCMV-EGFP plasmid was a kind gift from Dr Julien Gautrot. Plasmid transfection was performed with Avalanche-Omni Transfection Reagent from EZ Biosystems (USA), following supplier's instructions.

For experiments using recombinant Lifeact-GFP protein, Lifeact-TagGFP2 peptides and proprietary Fuse-it-P intracellular protein delivery kits were acquired from Ibidi and prepared according to instructions. Briefly, hMSCs were seeded into coverslips inside 6-well TCP vessels, three days before experiments. Lyophilised peptides were reconstituted in sterile water, and further diluted in 20mM HEPES buffer to a concentration of 0.1 mg/ml. Fuse-it-P was loaded with peptides by following supplier's instructions. Cells were washed in PBS, and 1ml of 1:50 fusogenic mixture was dispensed to each well. After incubation for 5 minutes at 37ºC, fusogenic mixture was replaced with cell culture medium and returned to an incubator. Cell samples were fixed after 6 hours, to mitigate toxicity effects, stained and imaged as in other experiments.

All live cell experiments (migration, AFM and Latrunculin-A treatment) were conducted on cells transduced at MOI 1000, at 5 days post transduction. The same conditions were used for NIH3/3 and COS-7 cells. At least 3 independent transductions were performed for each set of experiments. For live cell imaging experiments, cells were directly plated onto 6-well plates and cultured in FBS and antibiotic supplemented Flurobrite-DMEM imaging specific media (Thermofisher). For AFM measurements, cells were plated in petri dishes and imaging media were supplemented with 50 mM HEPES.

For immunostaining experiments, cells were sparsely seeded onto serum coated coverslips inside sterile petri dishes at least 1 day prior to transductions. In brief, cells were fixed by treatment with 3.7% paraformaldehyde in PBS for 15 min and permeabilised for 5 min in 0.25% Triton X-100. To simultaneously visualize F-actin via Lifeact and Phalloidin, cells were stained with phalloidin-TRITC at 2 µg/ml in PBS for 2 hours. For additional immunostaining experiments to visualize other cytoskeletons and proteins, permeabilized cells were treated overnight with primary antibodies against vimentin (1:400 dilution; RV202), α-tubulin (1:50 dilution; TU-02), YAP (1:200, 63.7) and cofilin (1:200; E-8) diluted in goat serum blocking buffer at 4 °C (all antibodies mouse monoclonal from Santa Cruz Biotechnologies, USA). The next morning, the samples were washed with PBS and treated with a TRITC-tagged secondary antibody (1:400 dilution, goat anti-mouse IgG-TRITC, sc-3796) for 1 hour at room temperature. Nuclei staining was performed with 1 µg/ml DAPI for 15 minutes. All coverslips were mounted onto glass slides using antifade mountant. Control samples were cultured and stained in parallel to transduced cell cultures, but without having been subjected to the transduction protocol.

Quantification of cell morphology, cytoskeletal structures and nuclear state from fluorescence images

All fixed samples were imaged using the conditions described in Chapter 2. Cells were sequentially imaged on the DAPI (nuclei), TRITC (phalloidin/antibody staining), and FITC (Lifeact-GFP) channels and analysed with the MATLAB (Mathworks) algorithm for single-cell quantification of

cytoskeleton structures and nuclear properties[165], [168]. In this chapter, the term ‘fibre amount’ is used to signify the amount of protein organized in fibres, that is, identified by the pipeline as part of the segmented cytoskeleton in the raw image.

Critically, the total intensity from GFP images belonging to individual cells was used as a metric for intracellular Lifeact amount, to produce graphs correlating cellular morphometrics with peptide expression. Total GFP intensity was measured by adding up the fluorescence intensity measured for all pixels within the outline of a cell, once background intensity was subtracted. To statistically identify the three regimes in the dose-response curves, namely a no effect regime, a dose-response regime, and a saturation plateau, threshold points were calculated across all parameters by adapting a method previously developed by us and based on the ratio of variances (RoV) [223] around each point of a Dose Response Curve (DRC). Briefly, a test parameter RoV is defined as $RoV\mathrm{i} = \frac{var(di+1:\mathrm{d}i+N)}{var(d\mathrm{i}-N:d\mathrm{i}-1)}$, i.e. the ratio of the variances computed in two N-sized small windows to each side of every point *i* in each DRC. Peaks in RoV displaying regions of high variability in the data, signifying a transition between regimes, were identified in each DRC curve. Two global GFP intensity values corresponding to the transitions point to dose-response and saturation regimes were obtained by averaging out all threshold GFP intensities in hMSC DRCs. The values for the two global GFP intensity thresholds are included in Fig. 7.1 and were used to sort individual cells into the 3 regimes depicted in Fig. 7.12.

Quantification of Nuclear/Cytosolic ratio of YAP

Nuclear/Cytosolic ratio of YAP was assessed as previously described by others [96]. Briefly, we measured the average fluorescence intensities of YAP staining in the nucleus and in an annular region with equal size in the cytosol immediately adjacent to the nuclear region and computed their ratio.

Western Blotting

Cells were washed with chilled PBS and lysed in RIPA buffer for 15 min on ice. The total protein concentration was determined by the BCA assay. Cell lysates were mixed with Laemmeli buffer and denatured by heating at 100°C for 5 min. Proteins were separated by SDS–PAGE and transferred onto a nitrocellulose membrane. Membranes were blocked in 5% dry milk for 1 h, followed by incubation with primary antibodies for cofilin (1:125, E-8, Santa Cruz), p-cofilin (1:250, E-5 Santa Cruz) and control glyceraldehyde 3-phosphate dehydrogenase (GAPDH) (1:500, 0411, Santa Cruz) over night at 4 ℃. Excess of antibody was removed by washing with PBST three times and the secondary antibody donkey anti-mouse (IRDye® 680RD Donkey anti-Mouse IgG (H + L), [P/N 926-68072]; 1:10000) was added for 1h at room temperature in dark. The proteins recognized by the antibody were visualized by chemiluminescence. ImageJ was used to quantify the intensity of cofilin, p-cofilin and GAPDH protein bands from each blot.

Migration and cytoskeleton disassembly experiments

For migration and Latrunculin-A treatment experiments, live-cell imaging was performed under temperature and CO_2 controlled environment, using an incubator-encased epifluorescence imaging system (Lumascope 720, Etaluma, USA) at x20 magnification. Transduced cells were cultured inside 6-well plates until the time of imaging. Individual cells were continuously tracked for 18 hours at 10-minute intervals and imaged in the FITC channel. To produce videos of long-term behaviour in Lifeact-GFP expressing cells, imaging was conducted under similar conditions using x10 magnification for a period of 4 days, sampled at 1-hour intervals. Control cells remained untransduced for the duration of the experiment. Other conditions consisted of cells transduced at MOIs of 250 or 500.

To characterize migration patterns, every frame on the 18 hours time-lapse video pertaining to the Lifeact-GFP channel was analysed using the formerly described image processing algorithms. The positions of cell centroids were tracked from masks of instantaneous cell shape and used to

quantify total distance migrated. Migration directionality was defined as the ratio between net cell displacement (the euclidian distance between starting and ending centroid positions) and the overall distance travelled by the cell, as $MD = \frac{d(P_{t=0},P_{t=T})}{\sum_{i=0}^{T} d(P_{t=i},P_{t=i+1})}$. F-actin interframe change was calculated comparing values of F-actin between successive frames, as $IFC_i = 100 \cdot \frac{FA_{i+1}-FA_i}{FA_i}$. For cytoskeleton disassembly studies, cells were imaged for 30 minutes at 2-minute intervals immediately upon addition of Latrunculin A (0.075µg/ml) to the culture medium. F-actin disassembly was quantified as $100 \cdot \frac{FA_{t=0min}-FA_{t=30min}}{FA_{t=0min}}$

Determination of cellular stiffness and viscosity with atomic force microscopy

All measurements of cell mechanics were performed on a Nanowizard 4 (JPK), integrated with an Axio Observer Z.1 epifluorescence microscope with Plan-Apochromat lenses (x20) equipped with a cooled CMOS camera (Orca Flash 4). Cells were probed using gold-coated rectangular cantilevers (0.03 N/m nominal spring constant) with pyramidal tips (12 µm high with 35° half cone angle, supplied by BudgetSensors, Bulgaria). Experiments were conducted on petri dishes mounted on a heating accessory to maintain cells at 37º C. AFM experiments were conducted for a maximum of 1hr per petri dish. Prior to measurement, the cantilevers were allowed to thermally equilibrate fully submerged in cell media. The cantilever sensitivity was calibrated in contact mode on a bare region of the container, following which the cantilever was moved a minimum of 500 µm from the surface to calibrate the force constant using thermal fluctuations. Individual adherent cells exhibiting varied levels of GFP expression were identified and a fluorescence image of the GFP channel at x20 magnification was recorded, before measuring cell mechanics. Imaging parameters (exposure time and gain) were kept constant for these experiments. AFM measurements were performed using JPK's QI mode, which rapidly acquires force-curves generating a detailed image of the topography and mechanical properties of the sample. For each measurement we selected a region of 100 by 100 µm (32x32 force curves) ranging from lamellar and cytosolic to nuclear regions of the cell. Force

curves had a z-length of ~10 μm, extension speed of 125 μm/s and a setpoint of 3-5 nN.

Data analysis of the force-displacement curves was carried out using the BECC model for thin adherent cells on a stiff substrate using a pipeline written in MATLAB as previously described [223]. Cellular viscosity was computed using the same force-displacement curves following the method outlined by Rebelo *et al* [265].

Statistical Analysis

Statistical tests were produced with the OriginLab analysis software. Population results were plotted as box charts presenting median values and first and third quartiles, with error bars indicating the 1^{st} and 99^{th} quartiles. Single cell results were expressed either as means or geometric means with error bars representing interquartile range. Two-way ANOVA tests were used to establish the significance of concentration and time effects on the levels of Lifeact expression and of morphological alterations of cell populations. Dunnett's post-hoc tests where used to determine significant differences between the control group (no transduction) and groups treated with increasing MOIs for each day measured.

7.3 Results and discussion

7.3.1 Cell cultures transduced with Lifeact-GFP display altered morphologies

In our experiments, we first performed an overnight transduction of hMSCs with increasing concentrations (presented as Multiplicity of Infection - MOI) of commercial adenoviral vectors delivering rAVCMV-LifeAct-TagGFP2 plasmid. We transduced cells with MOI ranging from low levels (MOI 100) up to the highest dose recommended by the supplier (MOI 1000). Samples were fixed 1-7 days post transduction, co-stained with TRITC-phalloidin and DAPI, and subsequently imaged via standard epifluorescence microscopy at x20 magnification (Fig. 2.2 contains an example of the stress

fibre sampling in a cell transduced with Lifeact-GFP and co-stained with phalloidin and DAPI). When pooling together data at the population level, we found a statistically significant increase in GFP intensity for experiments using higher MOIs (Fig. 7.1).

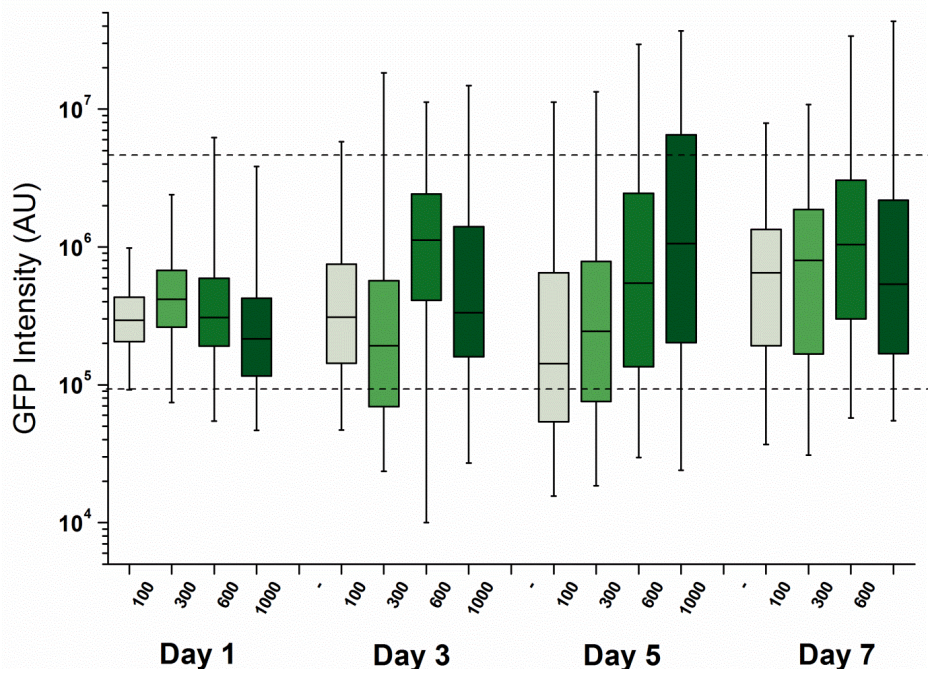

Figure 7-1 – GFP intensity increases in cell populations transfected at higher MOIs and with longer expression time – Box plots represent median values, and first and third quartiles, while error bars represent the 1st and 99th percentiles. N > 2500 cells. Two-way ANOVA test showed significant differences for MOI (p<0.001) and expression time (P<0.001). Dashed lines indicate the thresholds separating the 'no effect', dose-response and saturation regimes.

Likewise, we found that GFP levels significantly changed with increasing expression time, with the peak of expression occurring 5 days post transduction. Surprisingly, we found comparable trends when we measured simple parameters that describe cellular morphology and actin assembly, such as cell area and F-actin amount (Fig. 7.2). These analogous temporal and concentration-dependent trends observed at the population level suggested that intracellular Lifeact may result in altered cellular and cytoskeletal morphology.

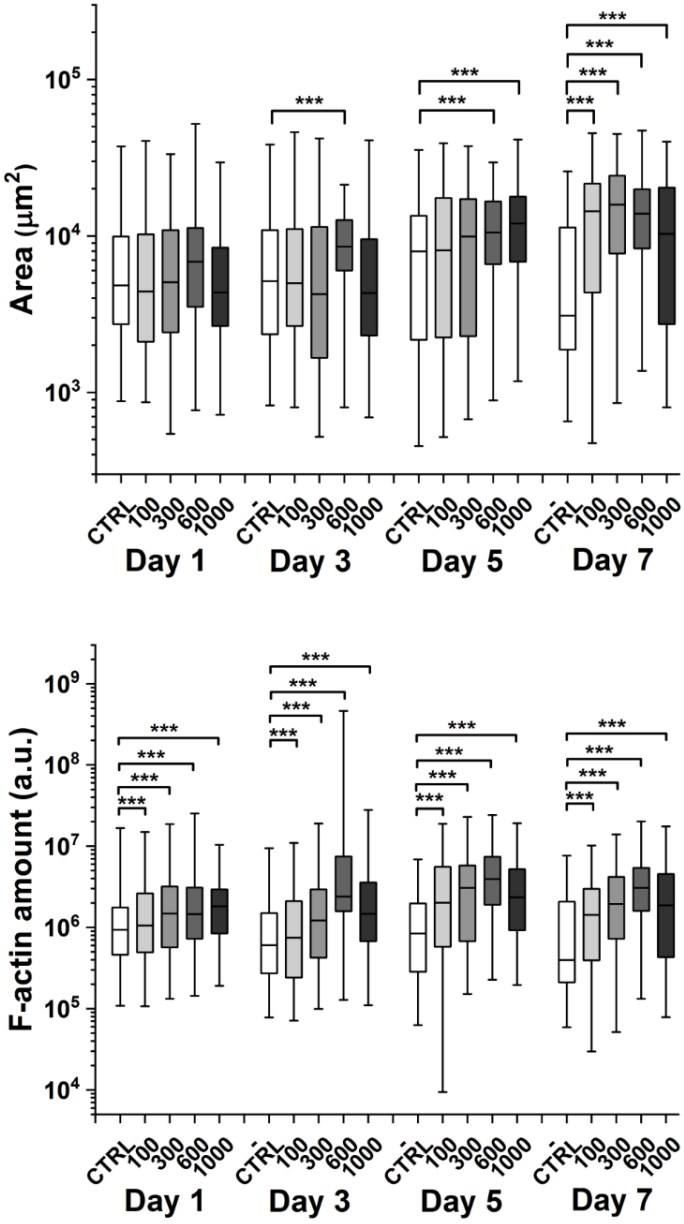

Figure 7-2 – Cell area and stress fibres amount increase in cell populations transfected at higher MOIs and with longer expression time – Box plots represent median values, and first and third quartiles, while error bars represent the 1st and 99th percentiles. N > 2500 cells. Two-way ANOVA tests showed significant differences for MOI (p<0.001) and expression time (P<0.001) for both cell area and stress fibre amount. * indicates p<0.001 as obtained from Dunnett's post hoc test against control for each day.**

7.3.2 Lifeact-GFP alters actin organization in a dose-response manner

Traditional methods based on population averages may mask the fact that a great variation exists in the uptake of plasmid or vector copy number for

each cell within a transduced cell culture [266], [267]. Thus, to accurately assess the dose-response effects of Lifeact expression at the cellular level, we devised an alternative approach based on pooling together single-cell data according to their measured Lifeact expression, irrespective of initial MOI or time post-transduction. Two critical aspects of our methodological approach need to be emphasised here. First, the quantification of parameters related to cytoskeleton organization and cell morphology was performed using images obtained through TRITC-phalloidin staining, i.e. independently of Lifeact-GFP driven fluorescence. By doing so the cytoskeleton of cells with low Lifeact-GFP expression (displaying low GFP fluorescence intensities, Fig. 7.3 b) could be resolved with similar accuracy to those expressing larger Lifeact-GFP levels (Fig. 7.3 d).

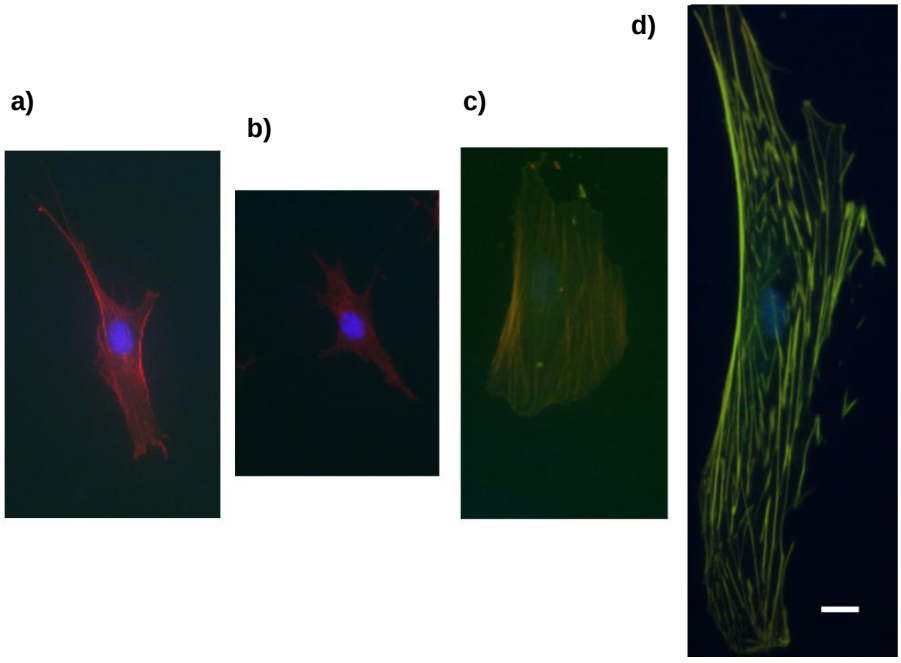

Figure 7-3 – Characteristic phenotypes of cells expressing increasing amounts of Lifeact-GFP and co-stained with phalloidin-TRITC and DAPI – a) hMSC cultured on a coverslip dish that was not transduced, b) hMSC sorted as 'no-effect regime', c) hMSC sorted as 'dose-response-regime', d) hMSC sorted as 'saturation plateau'. Scale bar corresponds to 15 µm and is the same for all cells pictured.

Second, we took advantage of the 1:1 stoichiometry between the Lifeact peptide and the GFP tag and measured, for each cell, its total GFP fluorescence as a surrogate indicator of Lifeact expression [268]. Furthermore,

we used our previously-developed image quantification pipelines [165], [168] to describe in a multiplex fashion the organization of the cytoskeleton and nucleus of individual cells. We constructed dose-response curves (DRC) to depict morphometric parameters as a function of intracellular GFP intensity and observed clear morphological trends linking increased Lifeact expression with altered cellular phenotypes (Fig. 7.4 and Appendix D Fig. 12.1).

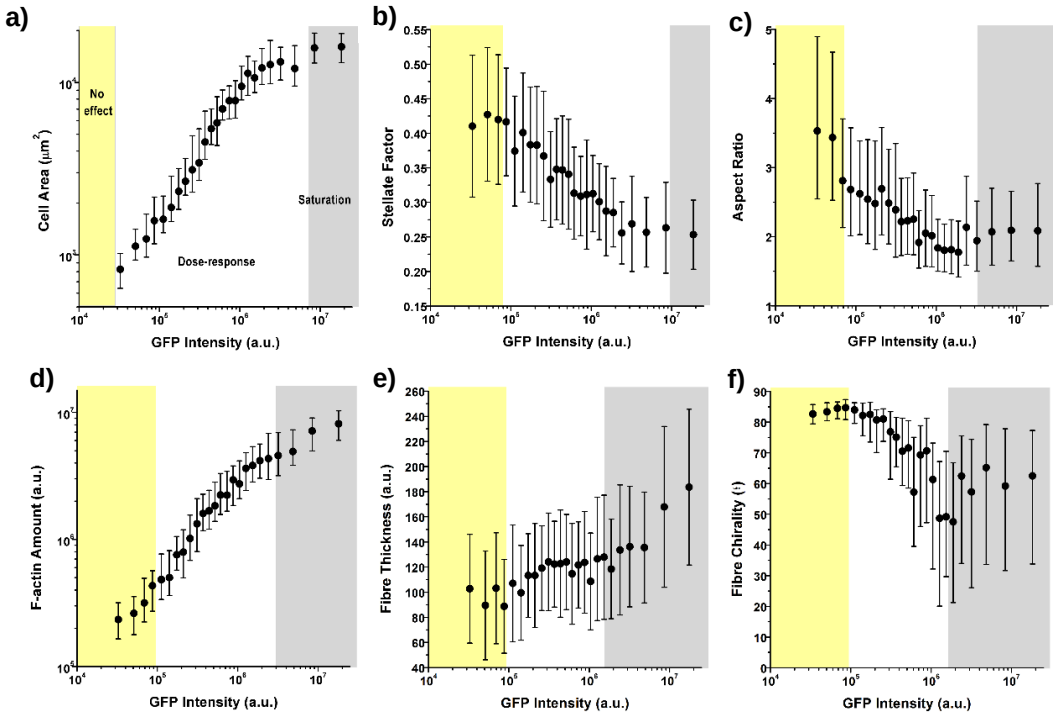

Figure 7-4 – Dose-response curves quantifying the effect of Lifeact expression – a) in cell spread area, b) cell perimeter stellate factor, c) aspect ratio, d) F-actin amount, e) fibre thickness and f) chirality of fibres. Values for >100 cells were pooled together to compute each individual data point. Data is presented as geometric mean (a and d), mean (b and e) or median (c and f); error bars indicate geometric standard deviation, standard deviation or Q1-Q3, accordingly. Background colours indicate the regimes where cells display no Lifeact-induced effect (yellow background), a dose-response trend (white background) and a saturation plateau (gray background), as identified from analyses of peak changes in variability in the neighbourhood of each point for each parameter plotted.

In particular, cells displaying the highest Lifeact expression had 10-fold larger spread areas, smaller aspect ratios and a less stellate morphology (Fig. 7.4). Concurrently, when assessing actin organization, Lifeact expression caused a 50-fold increase in F-actin assembly (Fig. 7.4 d), leading to stress

fibres that were longer (Appendix D Fig. 12.1 b), thicker (Fig. 7.4 e) and with an increasing radial orientation (Fig. 12.1 f).

To verify that the effects observed were associated with Lifeact rather than its fluorescent tag, we generated similar DRC with cells transduced with the same promoter and a GFP tag only (Fig. 7.5). While the DRCs obtained were not so broad in terms of expression levels reached, we verified that the dose-response behaviour was lost when only GFP was transduced.

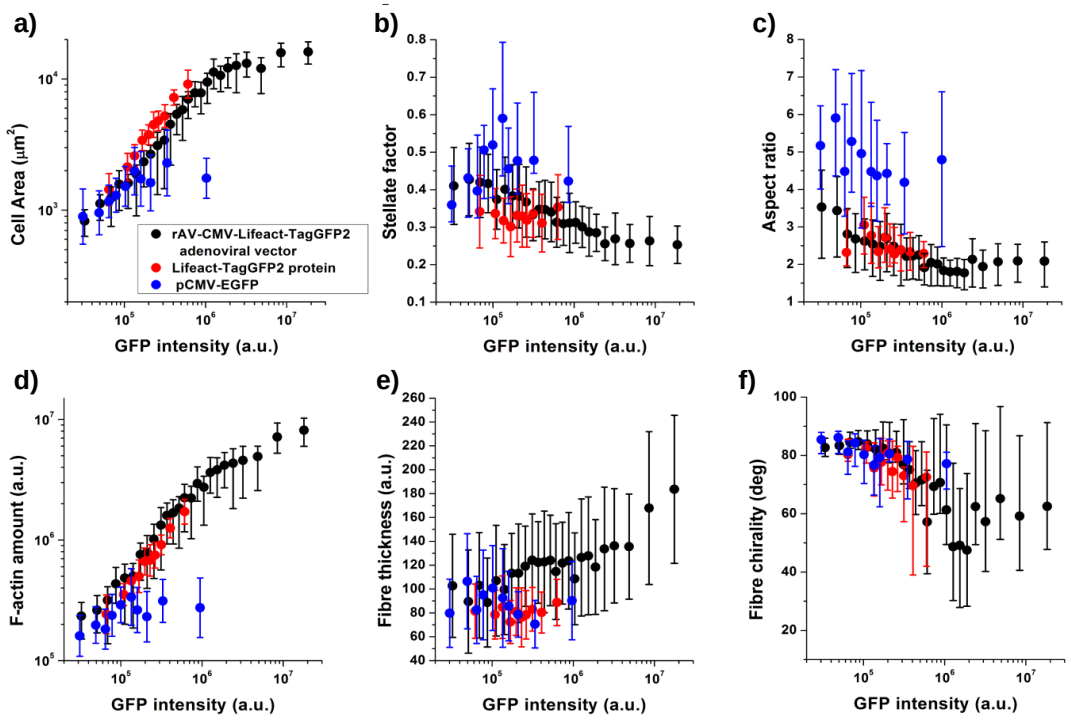

Figure 7-5 – Similar Lifeact-induced effects are observed irrespective of Lifeact intracellular delivery – Dose-response curves quantifying the effect of Lifeact expression when cells are transduced with a rAV-CMV-Lifeact-TAG2 plasmid (black), recombinant Lifeact-TAG2 protein (red) and pCMV-EGFP (blue). Plotted is a) cell spread area, b) cell perimeter stellate factor, c) aspect ratio, d) F-actin amount, e) fibre thickness and f) chirality of fibres. Values for >10 cells were pooled together to compute each individual data point. Data is presented as geometric mean (a and d), mean (b and e) or median (c and f) error bars indicate geometric standard deviation, standard deviation or Q1-Q3, accordingly.

Additional experiments using Lifeact-GFP recombinant protein delivered into the cellular cytoplasm using a membrane fusion reagent resulted again in a dose-response behaviour that displayed marked overlap with the results obtained using adenoviral transduction of Lifeact-GFP (Fig. 7.5).

Of note, DRCs generated for all cytoskeletal parameters had at least two marked regimes (Fig. 7.4 and Appendix D Fig. 12.1), namely a dose-response behaviour for low to mid expression levels of Lifeact-GFP (*white background area in panels*) followed by a saturation plateau at very high expression levels (*gray background area in panels*). In addition, for some cytoskeletal parameters measured we could also identify a range of low Lifeact-GFP expression levels for which no dose-response effect was observed (*yellow background area in panels*). Similar dose-response trends were also obtained when NIH/3T3 or COS-7 cells were transduced with Lifeact-GFP vector, even though overall values for parameters such as cell area or F-actin amount were different, as expected for different cell types (Fig. 7.6).

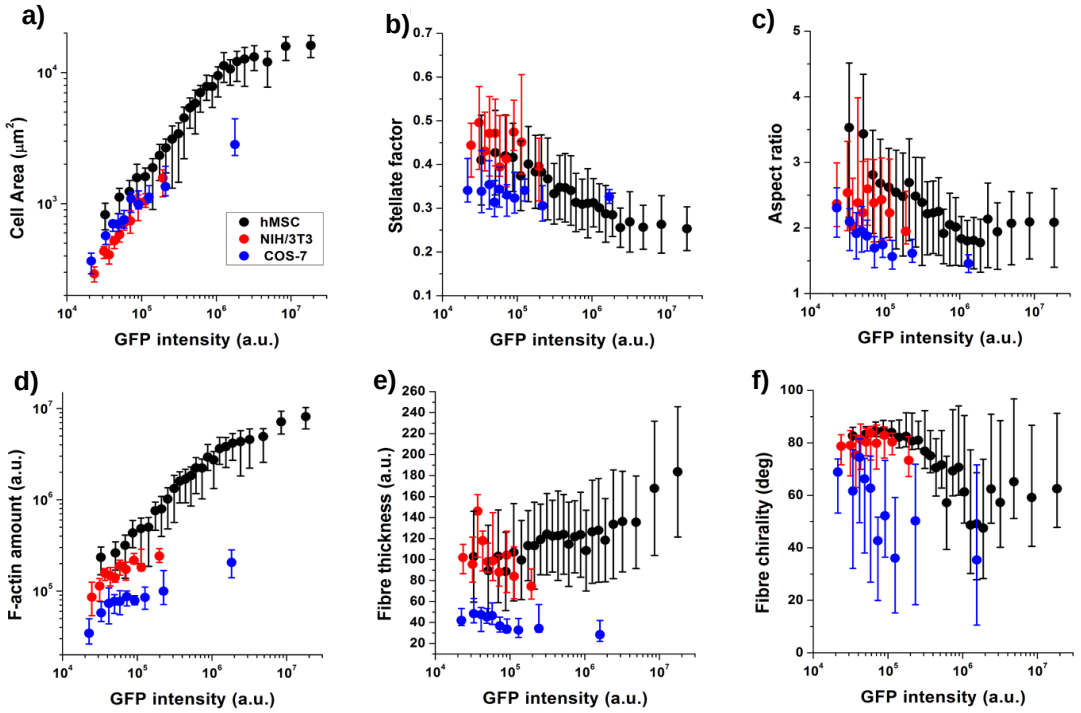

Figure 7-6 – Similar Lifeact-induced effects are observed in several cell types – Dose-response curves quantifying the effect of Lifeact expression in human SCs (black), NIH/3T3 (red) and COS-7 (blue). Plotted is a) cell spread area, b) cell perimeter stellate factor, c) aspect ratio, d) F-actin amount, e) fibre thickness and f) chirality of fibres. Values for >10 cells were pooled together to compute each individual data point. Data is presented as geometric mean (a and d), mean (b and e) or median (c and f) error bars indicate geometric standard deviation, standard deviation or Q1-Q3, accordingly.

Altogether, these data evidences that Lifeact-GFP can have a pronounced effect on cellular morphology and actin cytoskeleton organization. While at the population level these effects are largely dependent on transduction conditions (MOI and duration of expression), at the single cell level Lifeact-induced side effects display large heterogeneity, being predominantly dependent on the amount of peptide expressed by each cell.

7.3.3 Lifeact-induced effects extend to other cytoskeletal networks and the nucleus

Having confirmed the marked effects on whole cell morphology and stress fibre architecture induced by Lifeact expression, we chose to focus on Lifeact-GFP adenoviral transduction on hMSC and we next investigated cellular components with a strong link to the actin cytoskeleton, such as MTs and IFs. We limited our protocol to MOI 1000 and 5 days post transduction -to maximise the range of Lifeact expression levels- and replaced TRITC-phalloidin staining with antibodies against tubulin and vimentin. Surprisingly, we found that increased levels of Lifeact expression were associated with a build-up in the MT and IF networks (Fig. 7.7). Given the close interconnectedness between the three cytoskeletal networks [165], we hypothesise that alterations in tubulin and vimentin assembly are a secondary result from the effects of Lifeact on cell spread area, rather than a direct interaction between Lifeact peptides and tubulin or vimentin monomers.

We additionally investigated if Lifeact could also influence the nucleus, since nuclear structure is coupled to cytoskeletal organization and cellular morphology. Based on DAPI images from our previous transduction experiments, we quantified changes in three-dimensional nuclear shape, mechanical attributes and chromatin condensation state [165]. As before, we observed that Lifeact expression altered nuclear state, giving rise to nuclei that were up to 1.5 times larger in volume and less auxetic (Fig. 7.8), while chromatin condensation remained unaffected (not shown). Again, we hypothesize that the effects of Lifeact on the nucleus are a secondary result of alterations in cellular morphology and cytoskeletal architecture [165]. Together, our results uncover for the first time that Lifeact-induced artefacts

on the actin cytoskeleton may have knock-on effects that extend into other critical cellular structures.

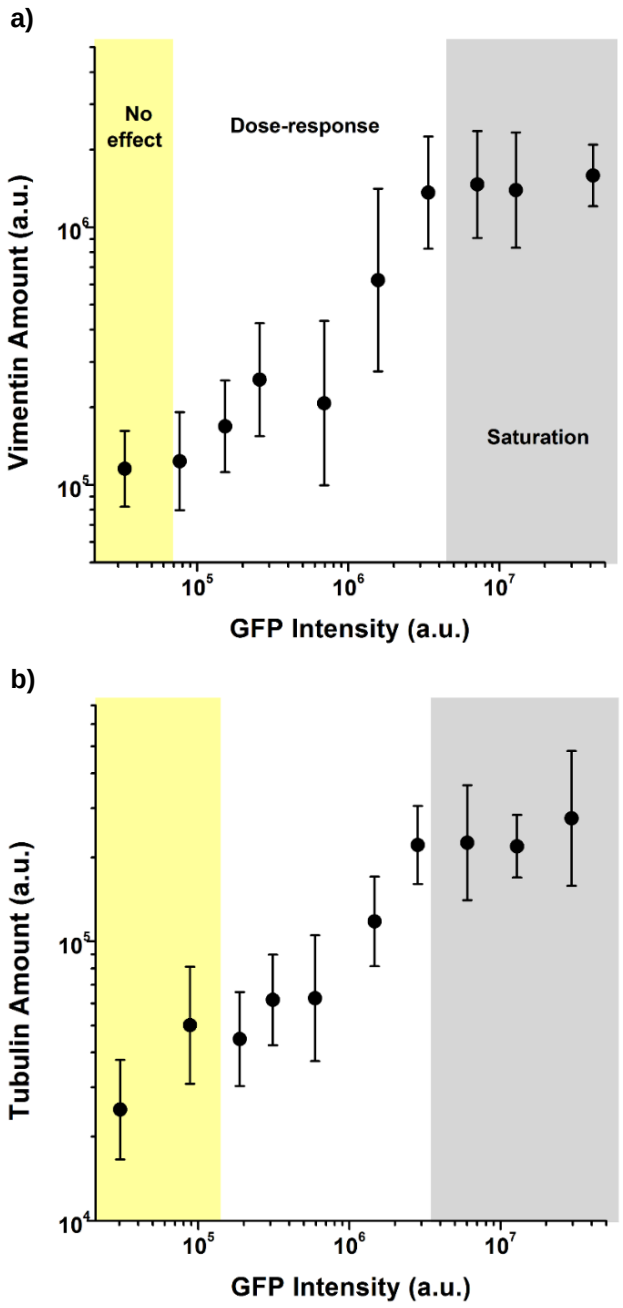

Figure 7-7 – Lifeact-driven effects extend to non-actin-based cytoskeletal networks – Quantification of Lifeact effects on a) intermediate filaments assembly and b) microtubule assembly. Values for >40 cells were pooled together to compute each individual data point. Data is presented as geometric mean, error bars indicate geometric standard deviation. Background colours indicate the regimes where cells display no Lifeact-induced effect (yellow background), a dose-response trend (white background) and a saturation plateau (gray background), as identified from analyses of peak changes in variability in the neighbourhood of each point for each parameter plotted.

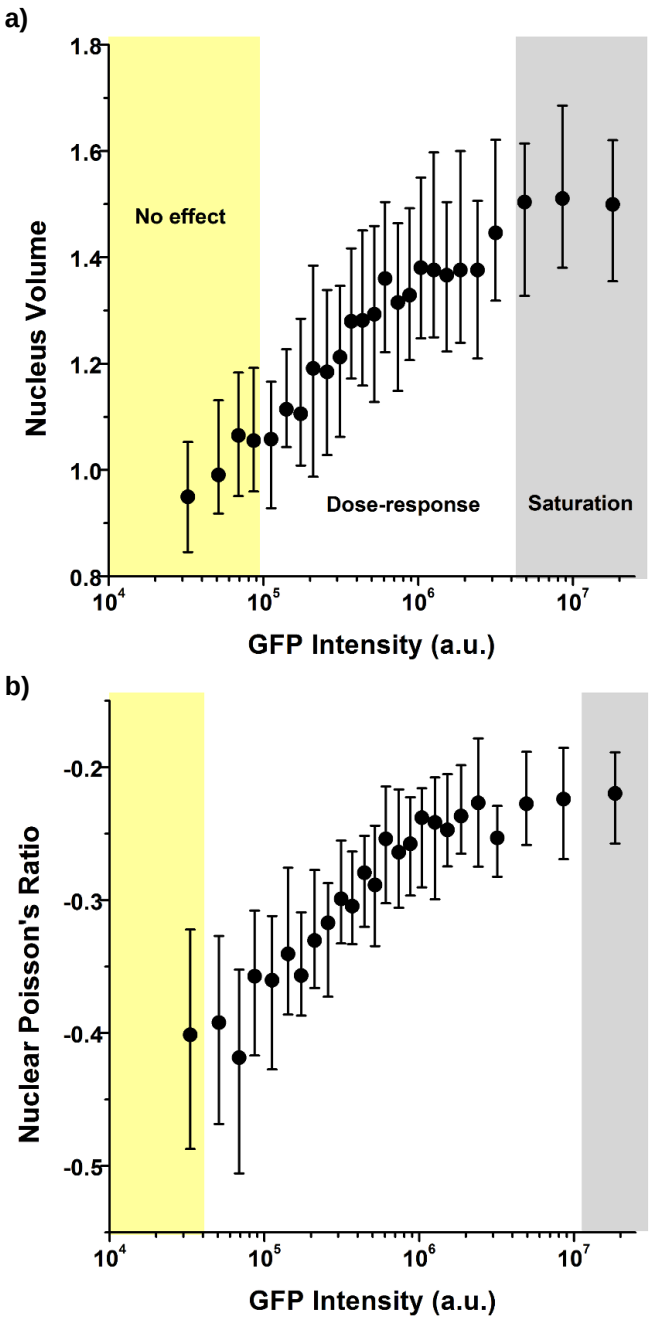

Figure 7-8 – Lifeact-driven effects modulate nuclear state – Quantification of Lifeact effects on a) nuclear volume and b) nuclear Poisson's Ratio. Values for >40 cells were pooled together to compute each individual data point. Data is presented as mean, error bars indicate standard deviation. Background colours indicate the regimes where cells display no Lifeact-induced effect (yellow background), a dose-response trend (white background) and a saturation plateau (gray background), as identified from analyses of peak changes in variability in the neighbourhood of each point for each parameter plotted.

7.3.4 Lifeact-induced effects on the cytoskeleton lead to altered cell biophysical behaviour

Having established the multiple effects of Lifeact on cellular structures, we moved to examine their impact on cell biophysical behaviour. First, we used AFM to probe the nanomechanical properties of Lifeact-transduced cells. Our results showed a mild decrease in cellular stiffness at very large peptide concentrations together with a steady dose-response increase in cellular viscosity (Fig. 7.9). These results were initially surprising, as we have previously shown a strong correlation between F-actin assembly and cellular stiffness [168]. Nevertheless, it's worth stressing that cells with very large levels of Lifeact expression displayed thick fibres disjointed from each other (cell #2 in Fig. 7.10), sometimes leaving between them large cell areas devoid of any actin-rich structure. This scenario is thus very different from the previously described nematic phase of actin organization [167] (cell #1 in Fig. 7.10) and may rather resemble the liquid-like behaviour of actin structures recently observed *in vitro* after coalescence and shortening of actin bundles[269].

Increasing evidence points towards the YAP/TAZ pathway as a crucial regulator of cellular mechanosensing in SCs [270]. In particular, the translocation of YAP into the cell nucleus constitutes a hallmark of increased intra or extracellular forces that are transmitted through the cytoskeleton and to the nucleus [96]. Accordingly, we set to quantify whether YAP intracellular localization would be affected by Lifeact transduction, as a second evidence of altered cell biophysical properties. To this end, we quantified the ratio of nuclear to cytosolic YAP and explored whether it was affected by cell spread area, as found by others [271]. In control cells (not transduced) we found a constant value of nuclear to cytosolic YAP ratio that was not modulated by cell area (Fig. 7.11 a). Conversely, for cells transduced with Lifeact, nuclear to cytosolic YAP ratios were overall larger, and they tended to decrease with increasing cell area.

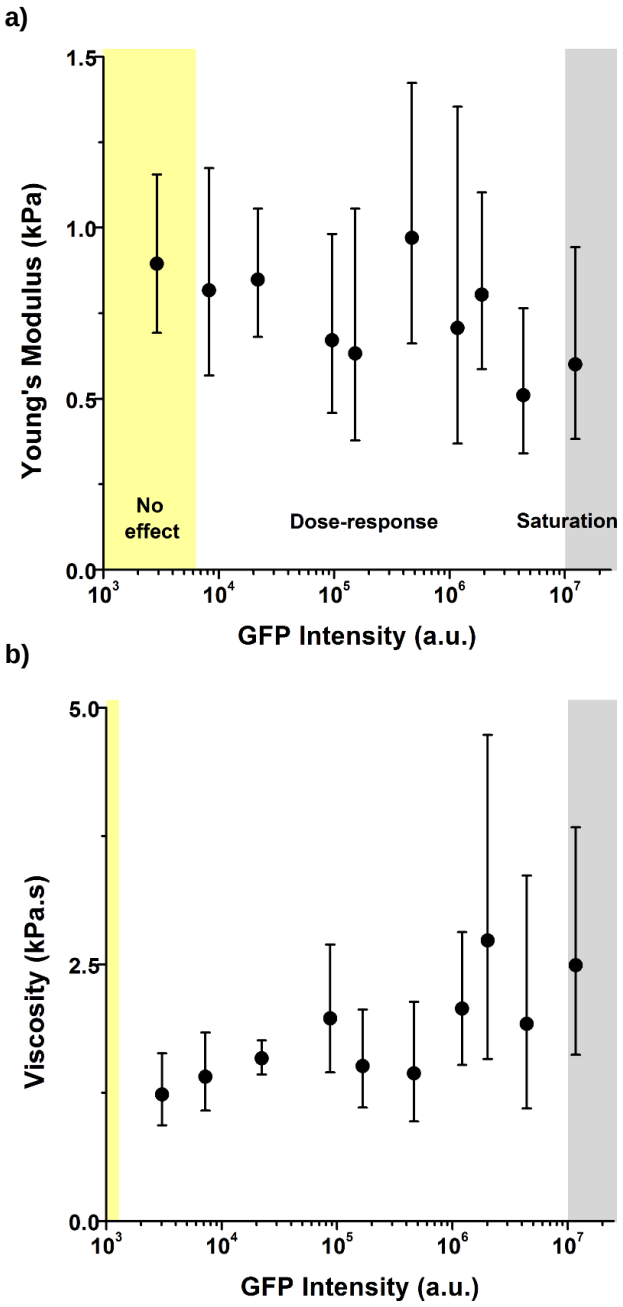

Figure 7-9 – Lifeact expression alters cellular mechanical properties – Lifeact dose dependent effects on a) cell stiffness and b) viscosity. Values for >10 cells were pooled to compute each individual data point. Data is presented as geometric mean, error bars indicate geometric standard deviation. Background colours indicate the regimes where cells display no Lifeact-induced effect (yellow background), a dose-response trend (white background) and a saturation plateau (gray background), as identified from analyses of peak changes in variability in the neighbourhood of each point for each parameter plotted.

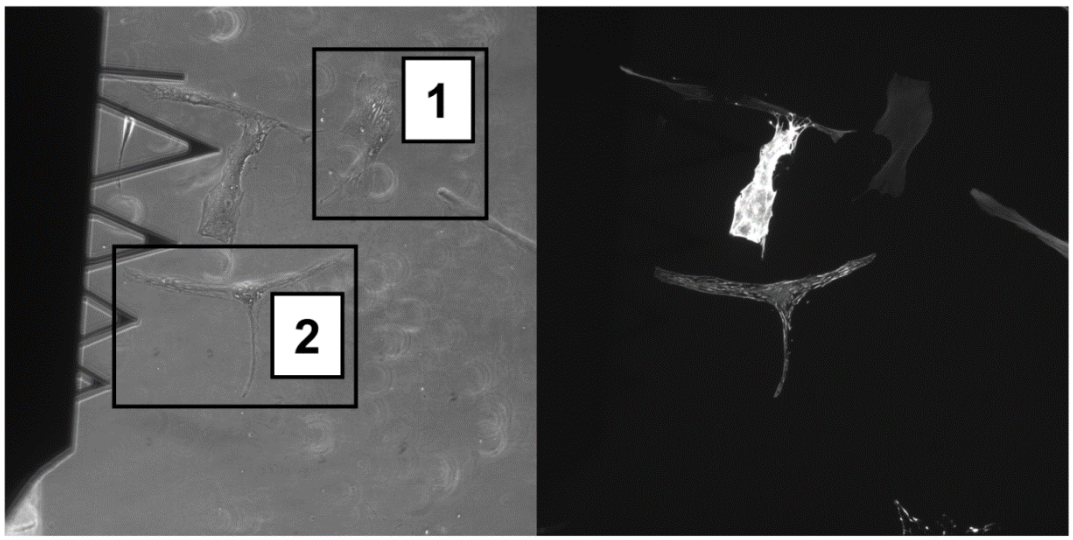

Cell #	Cell E (kPa)	E CoV (%)	Viscosity (kPa.s)	GFP Intensity (a.u.)
1	1.14	47	2.15	1.43×10^6
2	0.24	82	2.32	4.06×10^6

Figure 7-10 – Example of cells probed using AFM and displaying dissimilar actin organization – Cell #1 displays a nematic-like actin organization and exhibits larger stiffness with reduced CoV, whereas cell #2 displays liquid-like actin bundles and exhibits reduced stiffness with larger CoV. Left panel shows the phase contrast image (including the cantilever chip used for cell probing) and right panel shows the fluorescence image used to quantify GFP expression. Force-indentation experiments were carried out shortly after these two images were obtained. The whole process of taking the optical images and AFM probing for the two cells lasted < 15 min.

This behaviour is reminiscent of that observed in Fig. 7.9 a) for cellular stiffness and may reflect a mild decrease is intracellular tension with increasing Lifeact expression that then results in decreased nuclear translocation of YAP. Of note, immunostaining images of YAP used for this analysis showed a striking unexpected feature, that is, Lifeact-dense stress fibres appeared to be decorated with YAP (Fig. 7.11 b) while the preferred nuclear localization of YAP was still preserved. Furthermore, we verified that this observation was not due to bleed-through between the GFP and TRITC fluorescence signals, or unspecificity of the TRITC-tagged secondary antibody used throughout this study (Appendix D Fig. 12.2). Conversely, our analysis shows that YAP colocalization with F-actin fibres increases with increasing Lifeact expression levels (Figure 7.11 c).

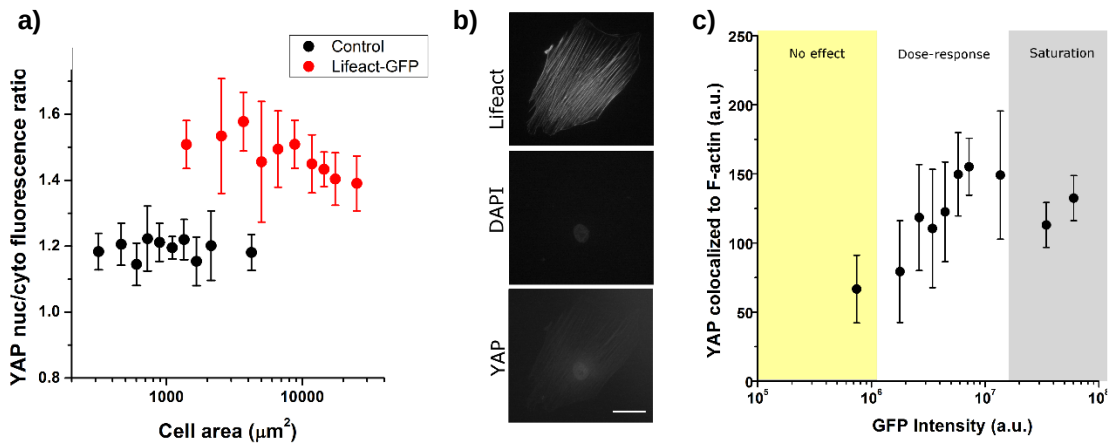

Figure 7-11 – Lifeact expression alters intracellular localization of YAP – a) Ratio of nuclear to cytoplasmic YAP localization according to cell area for control (black) or Lifeact-treated cells (red). b) Example cell displaying localization of YAP staining to Lifeact-containing stress fibres, the cell has been transduced with Lifeact (top) subsequently stained with DAPI (middle) and against YAP (bottom). Scale bar is 20 μm. c) Average pixel intentisty of YAP fluorescence colocalized to Lifeact-containing stress fibres is dependent on the total amount of Lifeact expressed in the cell. Data is presented as mean, error bars indicate standard deviation. For c), background colours indicate the regimes where cells display no Lifeact-induced effect (yellow background), a dose-response trend (white background) and a saturation plateau (gray background), as identified from analyses of peak changes in variability in the neighbourhood of each point for each parameter plotted.

As a third biophysical behaviour, we evaluated whether Lifeact expression would affect cell motility by performing long-term live cell imaging 5 days post-transduction. Individual cells were tracked by acquiring fluorescence images of the GFP channel every 10 minutes over a period of 18 hours and the resulting videos were later analysed using the same image analysis pipeline as before. In addition to the parameters describing cytoskeletal organization presented above, we also computed the total distance migrated by each cell along with the directionality of migration (Fig. 7.12). We found that cells displaying low Lifeact expression migrated for longer distances in a less directed fashion. Conversely, cells with intermediate Lifeact expression tended to exhibit shorter but directionally-persistent trails, consistent with our previous finding that these cells tend to display more aligned stress fibers (Appendix D Fig. 12.1 d). Finally, cells with very high levels of Lifeact expression exhibited severely impaired migration, remaining quasi-static and erratic in their displacements.

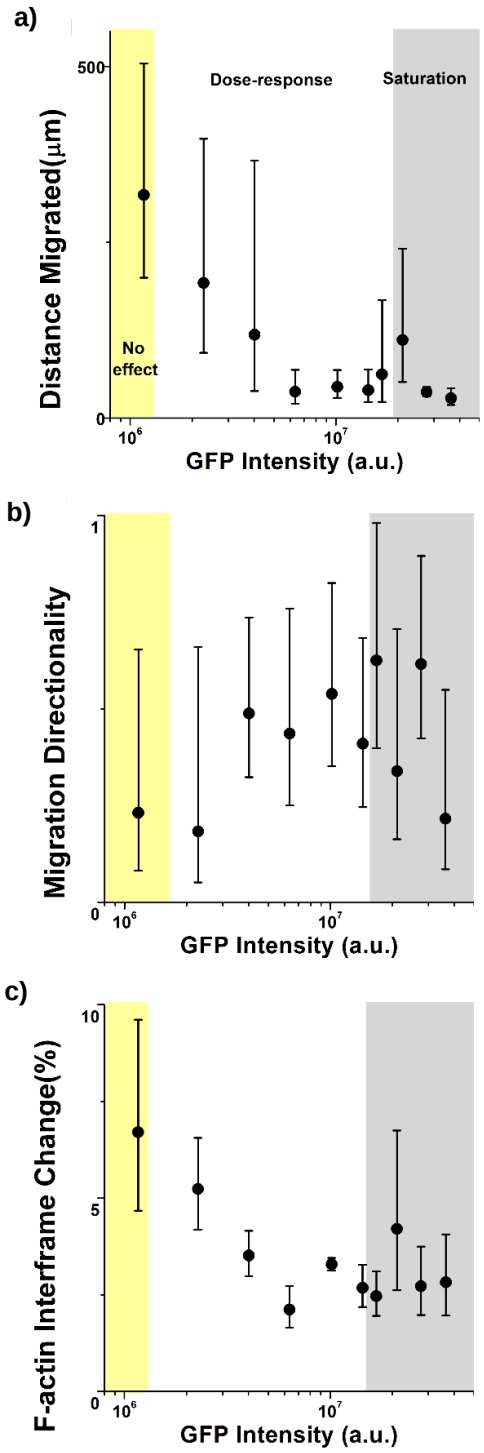

Figure 7-12 – Lifeact expression alters cell migration and F-actin dynamics – Lifeact dose dependent effects on a) distance migrated, b) directionality of migration and c) F-actin inter-frame changes. Values for >5 cells were pooled to compute each individual data point. Data is presented as geometric mean, error bars indicate geometric standard deviation. Background colours indicate the regimes where cells display no Lifeact-induced effect (yellow background), a dose-response trend (white background) and a saturation plateau (gray background), as identified from analyses of peak changes in variability in the neighbourhood of each point for each parameter plotted.

Of note, cells that had lower Lifeact expression did reorganize their cytoskeleton to a larger extend in the timeframe of minutes, as shown by the frame-to-frame changes in F-actin assembly (Fig. 7.12 c). Accordingly, we hypothesize that the impaired migration displayed by cells expressing high levels of Lifeact expression is due to reduced F-actin dynamics when reorganizing their cytoskeleton.

7.3.5 Impaired cofilin binding to F-actin as an underlying mechanism for the Lifeact-induced aberrations in actin organization and dynamics

Finally, we set out to pinpoint the potential mechanism by which Lifeact alters F-actin organization and dynamics. Cofilin was identified as a plausible key player, since Lifeact has been suggested by others to impair actin filament severing by cofilin both *in vitro* and in yeast cells [185]. We thus carried out several experiments to assess if and how Lifeact expression led to reduced cofilin activity. On the one hand, we followed the procedure devised by Hotulainen *et al.,* which elegantly show that the G-actin sequestering drug Latrunculin A (LatA) fails to depolymerize the actin cytoskeleton when cofilin activity is impaired [272]. We incubated Lifeact-transduced cells with LatA and simultaneously conducted live-cell fluorescence imaging for 30 minutes at 2-minute intervals. By measuring the relative drop in F-actin amount during treatment, we verified that Lifeact reduced LatA-induced cytoskeletal depolymerisation in an expression-dependent manner (Fig. 7.13 a). While this experiment suggested that Lifeact inhibits cofilin activity, it did not identify whether the underlying mechanism is associated with chemical inactivation of cofilin (via phosphorylation at serine residue 3 [273]) or conformational changes of the f-actin filament upon Lifeact binding that prevent cofilin binding [185], [260]. Accordingly, we performed western blot measurements of cofilin and p-cofilin expression levels for cell populations transduced with Lifeact or controls (Fig. 7.13 b, Appendix D Fig. 12.3). Cells transduced with Lifeact displayed 81% increase in overall cofilin expression, while the expression levels of p-cofilin increased only by 51%.

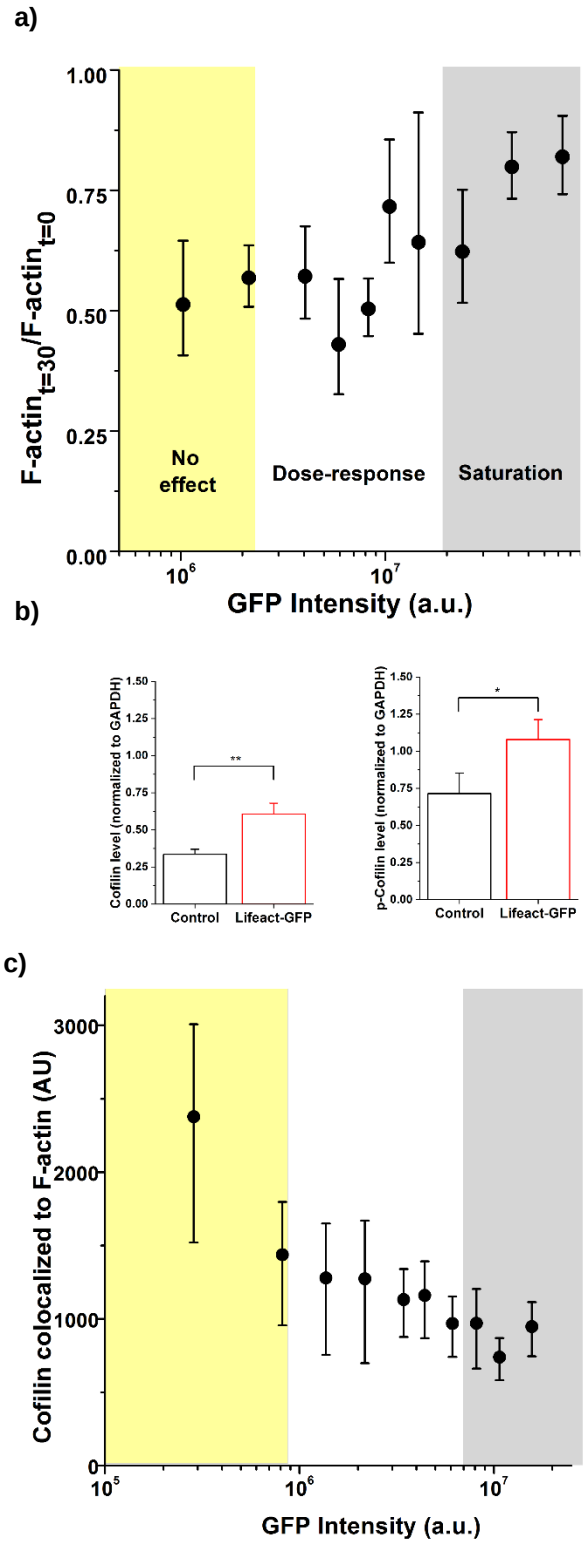

Figure 7-13 – Lifeact expression alters cofilin activity – a) Lifeact dose dependent effects on F-actin disassembly after 30 min of Latrunculin A (0.075µg/ml) treatment. b) Western blot results for cofilin and p-cofilin expression levels relative to GAPDH. c) Lifeact dose dependent effects on fluorescence intensities of cofilin colocalized to F-actin fibres. For a) and c), data is presented as median, error bars indicate Q1-Q3, N>100 cells; for b) data is presented as mean, error bars indicate standard deviation, N=3 experimental replicates.

Together, these results suggest that Lifeact-transduced cells have higher total amounts of cofilin, and that a lower percentage of said cofilin is in the inactive phosphorylated state. Finally, we performed immunostaining against cofilin to assess whether the drop in cofilin activity was associated with changes in cofilin binding to F-actin. Following the approach devised by Hayakawa et al [274] using fluorescence image quantification, we measured fluorescence intensity levels of cofilin in pixels previously identified as corresponding to an F-actin fibre, thus obtaining a measure of cofilin colocalization to F-actin. When we produced dose-response curves, we found that cells with higher expression of Lifeact had lower amount of cofilin colocalization (Fig. 7.13 c). Collectively, our results reinforce the hypothesis proposed by Courtemanche et, where Lifeact binding to F-actin induces a conformational change in actin filament structure which is then incompatible with subsequent cofilin binding [185]. This hypothesis should be contextualized with recent findings on the dual activity of cofilin, involving both severing and depolymerisation of actin filaments [275]. Of note, saturation of actin filaments with cofilin dramatically changes their dynamics towards a depolymerisation-prone state from both barbed and pointed ends [275]. Based on our findings, prior binding of Lifeact to actin filaments would prevent cofilin saturation of said filaments, thus inhibiting cofilin-induced actin depolymerisation and reducing overall actin filament dynamics.

7.3.6 Optimisation of Lifeact dosage requires careful consideration

Given that the effects of Lifeact in cytoskeletal organization exhibit a dose-response behaviour with a saturation plateau, our results bring new light to the difficult compromise during transduction optimization, that is, maximising the number of transduced cells while reducing the number of cells which are either dead or with aberrant morphologies. Contrary to expected, for all transduction protocols tested, the number of cells that are transduced but not aberrant is constant and much lower than anticipated (<20%) (Fig. 7.14). Rather, our data suggests that the presence of few clearly obvious aberrant cells (gray bars in Fig. 7.14) should be used as a tell-tale sign that a large

percentage of cells are within the dose-response regime (white bars in Fig. 7.14) and that few cells will be truly non-artefactual.

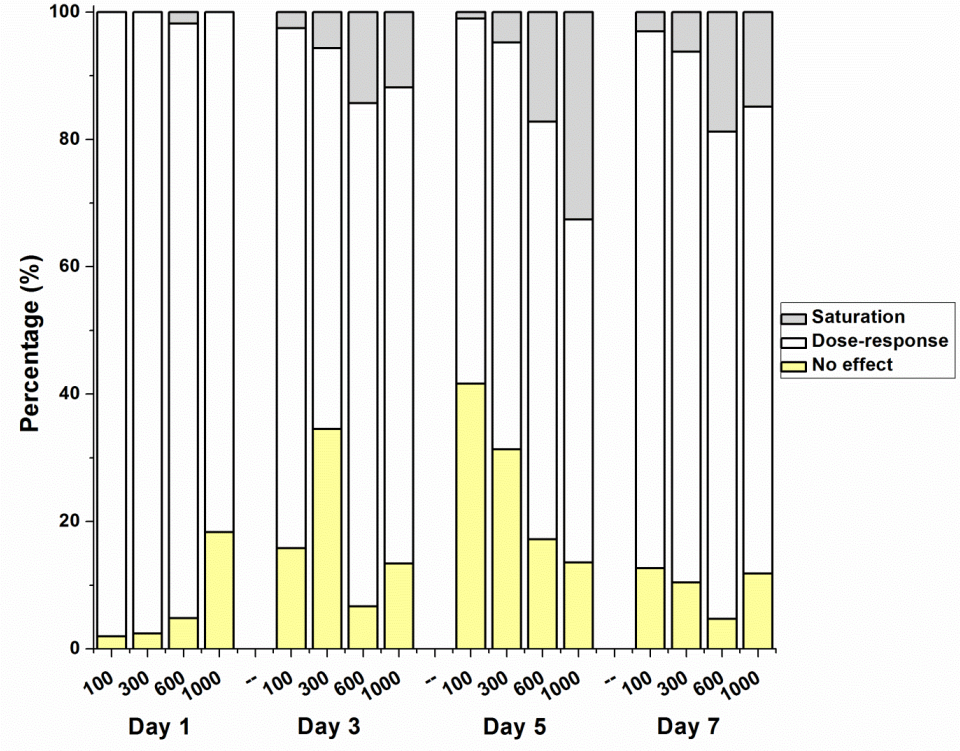

Figure 7-14 – Distribution of different cell phenotypes in Lifeact-GFP transduced samples according to MOI and time of expression – Transduced cells were categorized into three regimes ('no effect', dose response and saturation), using the previously identified threshold value for GFP expression levels. N>2500 cells.

7.4 General Conclusions

In summary, our results suggest that Lifeact-GFP induces dose-response alterations in the actin cytoskeleton, likely stemming from altered cofilin activity and reduced filament dynamics. The effects extend beyond the actin cytoskeleton, also affecting other cytoskeletal structures and impairing the overall biophysical behaviour of cells.

Our findings are more strongly marked in undifferentiated human SCs, which may be due to a higher capacity to uptake the adenovirally-delivered Lifeact plasmid. Nevertheless, we obtain similar dose-response trends in immortalized cell lines (NIH/3T3 and COS-7), thus expanding the range of cells types were Lifeact has been shown to induce aberrant morphologies

[263], [264], [276]. The Lifeact plasmid we used included a CMV promoter, which has been shown by others to induce milder aberrations than pBABE and CAG [263]. Of note, our results using a recombinant Lifeact-GFP protein show that the effect of Lifeact is similar regardless of the way in which the DNA (or protein) is delivered and expressed into the cell. Similarly, the GFP tag used (TagGFP2) is a next-generation monomeric fluorescent protein, again being linked to milder aberrations than other dimerization-prone GFP tags [263]. Our results are thus obtained in conditions identified by others as conductive to fewest aberrant morphologies in terms of choice of promoter and fluorescence protein tag used. In spite of that, we find a clear dose-response effect at all MOI and conditions used, thus raising strong concerns on the use of Lifeact as a cytoskeletal marker.

We note here that transduced cells that display minor aberrations are likely to go unnoticed to the naked eye during the course of an experiment. Selection of these cells in a study will lead to experimental bias or lack of reproducibility with results obtained using other live cell actin probes. Prior to performing experiments, it is important researchers establish a reliable protocol to identify and select only suitable cells within the whole population of heterogeneously transduced cells. Similarly, it would be advisable to report the percentages of not-affected, aberrant and grossly-aberrant cells within the cell population for any given transduction protocol used in a study. Preliminary tests based on co-staining with an actin marker such as phalloidin and image quantification at the single cell level can provide this type of information in a swift manner. With this study, we hope to start an active discussion on what are the limits of suitability of our current live-cell cytoskeletal reporters. This is a timely and much-needed debate, especially with the advent of other actin reporters, such as SiR-actin, Utrophin or F-tractin, which may display similar associated issues.

Chapter 8 – Summary

A common throughline of this thesis was the use of morphometric image processing to identify trends in highly variable phenotypic data. The single-cell capabilities of these approaches provided further flexibility to the characterisation of dynamic cell features, providing the extension from populational to individual behaviours.

Two main topics of research were tackled in this work. The first, covering Chapters 3 to 6, was the study of how hMSCs respond to the non-linear properties of 2D collagen-coated agarose substrates. Chapter 3 described how preliminary attempts to redesign a cell culture construct for active mechanical loading resulted in the development of 2D agarose substrates, while evidencing the atypical mechanical attributes of the hydrogel. Chapter 4 presented the characterisation of the populational trends observed during prolonged hMSC culture on the collagen-coated substrates in the absence of differentiation supplements. On the other hand, Chapter 5 described the populational trends resulting from joint mechanical and biochemical induction of osteogenic and adipogenic differentiation. Finally, Chapter 6 presented a new avenue of research in our group, with the objective of employing ML algorithms to extrapolate continuous single-cell trends from discrete temporal sampling of biological processes. While this work is currently on-going, the results presented in this document have shown that the methodology is feasible and represents a promising opportunity.

The second major research topic of the thesis was covered in Chapter 7. This chapter dealt with the dose-dependent effects of the Lifeact peptide on the actin cytoskeleton, which were shown to influence a wide range of cell properties. Although seemingly underrepresented in the extension of the thesis, the work contained in Chapter 7 was developed in parallel with that in the remaining chapters. It should also be noted that this chapter covered a wider scope of techniques (e.g. biological AFM, live-cell microscopy, genetic transfection, work in multiple cell lines) and has been published in the Journal *Scientific Reports* as of March 2019.

A summary of the main findings, limitations and research opportunities resulting from each of the former chapters is presented below.

8.1 Development of constructs for active mechanical loading and real-time imaging of hMSC differentiation induction

The results presented in this Chapter 3 acted as a proof-of-concept for a redesign of agarose constructs. Upon briefly testing the operation of the microscope mountable loading rig with mock constructs, a calibration between digital instrument inputs and actual strain on the hydrogels was successfully performed. It was found that both compression and tension inputs would need to be adjusted in future measurements to compensate for discrepancies on the translation of movement in the instrument.

The proposed redesigns of the agarose constructs were dependent on the in-bulk crosslinking or surface coating of an ECM element to the agarose. Sulfo-Sanpah was selected as a crosslinking agent, as a starting point in adapting formerly described methodologies [194], [202]. However, it was found that the choice of COL I as the cell anchorage component prevented the optimisation of in-bulk crosslinking, likely due to the fibrillar nature of the biomolecule and the acidity of its solvent having prevented the use of larger ECM amounts necessary to promote cell attachment.

Although the attempts at bulk crosslinking of COL I to agarose were not fruitful, the use of Sulfo-Sanpah in the covalent attachment of a 2D surface coating to hydrogel substrates was explored as a viable alternative. After extensive optimisation the final yield of collagen-coated substrates in the protocol was improved to around 60%. Although low, this yield allowed facile production of enough samples to conduct further experiments.

Of note, the 2D collagen-coated agarose disks described in this work represented a novel cell culture substrate for Mechanobiology studies. Furthermore, characterisation of the mechanical properties of the agarose hydrogel revealed that the substrates presented atypical mechanical attributes. Concretely, AFM microindentation showed a propensity of the agarose substrates to substantially soften following brief periods of culture time (> 24 hours). Moreover, compression tests showed that the substrates display strain stiffening and viscoelastic properties, which are now recognised as important attributes of natural ECMs.

Having produced and mechanically characterised 2D agarose cell culture substrates, the assembly and use of the redesigned constructs was tested in cell culture conditions. Although initial tests were successful in incorporating cells into the 2D constructs, severe limitations of the system, including work intensive assembly, and a propensity for fracture under manipulation or after prolonged exposure to cell culture conditions, prevented further use of the redesigned scaffolds.

Despite this setback, the development of novel 2D collagen-coated agarose substrates was a favourable result, which opened up the possibility of conducting the work described in Chapters 4 and 5.

Future work

The results from Chapter 3 showed that the application of conventional loading rigs is limited by cumbersome gripping mechanisms which are needed to couple soft hydrogels into the instruments. As such, to fulfil the objectives described in section 3.2, it would be worthwhile to develop *de novo* a microscope-mountable system, supporting both 2D and 3D substrates, and dispensing with gripping mechanisms. The assembly of the system could potentially be based on membranes/pliable moulds, or on acoustic/magnetic loading processes.

Several of the limitations encountered throughout Chapter 3 could also be tackled in future studies. For instance, agarose variants containing reactive side-groups (e.g. amine or carboxylic acids) could be employed with more robust crosslinking reagents (e.g. EDC carbodiimide / NHS) to improve crosslinking yields.

Mechanical characterisation of the substrates should also be extended. The AFM calibration and sample drift issues could be resolved by changing the conformation of the TCP vessels used in previous measurements. A more sensitive 10N load cell should also be used when assessing hydrogel specimen properties in macroscopic compression, and a longer period of time should be allocated for stress relaxation studies. Extensive characterisation of the collagen coating should also be conducted,

to confirm if coupling of the ECM to the substrates was successful and assess the thickness of the collagen layer.

8.2 – Mechanical and biochemical guidance of hMSC developmental trajectories monitored by cytoskeletal morphometrics

While a great number of studies provide fundamental insights into the interactions between cells and their surroundings, these studies have been mostly conducted on static linear-elastic hydrogels, neglecting critical features of natural ECMs, like viscoelasticity, non-linear stiffness and degradability.

In Chapters 4 and 5, 2D collagen-coated agarose substrates were employed as culture systems to study long-term influences of atypical substrate mechanical properties on the morphometric profile of hMSC populations.

The results obtained in these chapters were unexpected relative to the effects of non-linear biophysical properties on cell morphology, F-actin architecture and nuclear state. The most critical observation was that, unlike in standard elastic hydrogels, parameters such as cell spread area or F-actin amount did not scale according to substrate stiffness, suggesting that bulk substrate properties were not able to influence cell behaviour. Nonetheless, cell behaviour was not static through time, with cell morphology, the actin cytoskeleton and the nucleus changing over a two-week period.

In the absence of further differentiation factors, whole-cell morphology was altered during environmental adaptations, as the hMSCs integrated the biophysical and biochemical signals of their surroundings. Mature cell phenotypes generally developed complex F-actin networks, probably linked to the marked alterations in cell size and shape.

Of note, throughout Chapters 4 and 5, morphometric parameters identical trends on the different substrates, despite clear differences in the mechanical properties of the agarose formulations used in this work. Overall, nuclear features displayed less inter-substrate variability, than morphological and cytoskeletal morphometric descriptors, indicating that nuclear architecture may be tightly regulated in response to passive mechanical stimuli.

Addition of biochemical differentiation supplements resulted in pronounced effects on cell morphometrics that were primarily dependent on the biochemical signals, as opposed to the biophysical characteristics of the underlying substrates. Both types of differentiation produced distinctive osteogenic and adipogenic developmental trajectories, with parallel and highly dynamic behaviours in cell morphology, cytoskeleton architecture and nuclear state. In both types of culture mature cells tended to acquire “star-like” morphologies, developing long processes and a convex perimeter, larger cell areas and a build-up of F-actin.

Overall it can be concluded that populational morphometric traits present informative value in the discrimination between cell fates and that the specific context provided by biochemical and mechanical factors should always be considered during differentiation and morphological studies.

Future work

A critical aspect of Chapters 4 and 5 was that the observed cell morphologies were reminiscent of those typically found in fibrillar environments. As such, the biophysical properties of the fibrillar layer of collagen crosslinked to the substrate surface should be investigated in greater detail. Traction force microscopy, live-cell imaging, and AFM should be used to conduct an in-depth analysis of the interactions between the cells and the underlying substrate. Moreover, the methodology followed in Chapters 4 and 5 should be repeated on linear-elastic, PDMS and fibrillar hydrogels to further elucidate and compare the long-term impact of the different culture environments on cell morphometrics.

Another important limitation of this work was the fact that terminal differentiation could not be assessed due to time restrictions. To provide conclusive evidence as to the phenotypic maturity of the cells obtained after long-term culture on the hydrogel substrates, future studies should include histological staining (Oil Red O, Alizarin Red or Alkaline Phosphatase), complemented with gene expression analysis, to confirm the presence of terminal osteoblasts and adipocytes. Cells from different donors should

equally be used in future studies. Finally, the number of passages during hMSC expansion in this type of work should be minimized and controlled, to ensure that the results between experiments (e.g. in Chapters 4 and 5) are comparable. In this work, the cells used in Chapter 4 corresponded to passage 7 and tended to display initially larger phenotypes, whereas all passage 5 cells used throughout Chapter 5 still displayed the spindle-like shape of early SCs. As such, care should be taken in future experiments to standardise the experimental conditions for accurate comparison.

8.3 – From populational to single-cell trajectories

In order to reconstruct more accurate developmental trajectories and overcome the limitations of populational analysis, these processes must be understood at the single-cell level. Chapter 6 describes how populational data collected in Chapter 5 was used to test the assembly of single-cell developmental trajectories, based on supervised regression ML algorithms. This new method assimilates real-time information (i.e. days in differentiation experiments) into the analysis of biological trajectories for the first time. Additionally, it is the first single-cell trajectory study conducted in hMSCs, or solely from the perspective of morphological changes.

The results acquired in Chapter 6 suggested that there are close similarities between discrete population-based and continuous single-cell morphometric developmental trajectories, in both the osteogenic and adipogenic lineages. However, single-cell trajectories helped clarify the trends obtained in the highly heterogeneous hMSCs samples and revealed the dynamics of some of the morphometric descriptors in higher detail.

Chapter 6 confirmed that the novel methodology can be successfully applied to datasets generated in our research group, consisting of discrete temporal population-based morphometric information, and used to postulate continuous single-cell developmental trajectories.

Ultimately, the integration of this information into a ML model is expected to provide a representation of the most likely developmental trajectories undergone by single-cells during biological processes within specific mechanical and biochemical environments.

Future Work

The results described in this section have served as a trial for the methodology under development in our research group to produce single-cell morphometric developmental trajectories. As part of a work in progress the results presented in this chapter must be analysed in the context of broader research. The methodology will therefore be tested in different datasets in a near future and continually refined.

8.4 – Morphometric and biophysical analysis show that Lifeact-GFP causes detrimental dose-dependent effects on cells

Chapter 7 showed that Lifeact-GFP induces dose-response alterations in the actin cytoskeleton, likely stemming from altered cofilin activity and reduced cytoskeletal dynamics. These effects extend to several cytoskeletal structures, nuclear properties and the overall biophysical behaviour of cells.

Dose-response trends were observed in two cell lines, as well as in primary hMSCs, demonstrating that the negative impacts of Lifeact are common to several cell types. Clear dose-response effects at all MOI and conditions raise concerns on the use of Lifeact as a cytoskeletal marker.

Furthermore, our results suggest that the identification of aberrant cells is not trivial and may require image analysis-based methods to fully resolve. Researchers should therefore take care in attempting to optimise Lifeact-GFP use and establish reliable protocols to identify suitable cells within heterogeneously transduced populations.

Future Work

The methodology described in Chapter 7 can be repurposed to provide more extensive characterisation of additional actin reporters, such as SiR-actin, Utrophin or F-tractin, which may display similar issues to Lifeact-GFP.

8.5 – Concluding remarks

The wide variety and complexity of hMSC morphologies create ambiguities and difficult the identification of trends in the morphometric characterisation of cells. Continued development of high-throughput imaging methods and image-processing strategies is therefore critical in countering these hindrances and maximizing information from biological data.

Altogether, this thesis illustrates how morphometric analysis is uniquely poised to tackle these issues and study morphological trends, such as characterising developmental trajectories or measuring the effects of mechanical and biochemical factors on cell behaviour.

Appendix A – Examples of cell phenotypes and associated morphometric descriptor values

a)

Cell spread area (μm^2)

0-∞

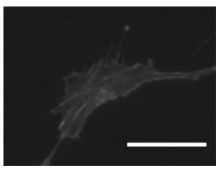

686 μm^2

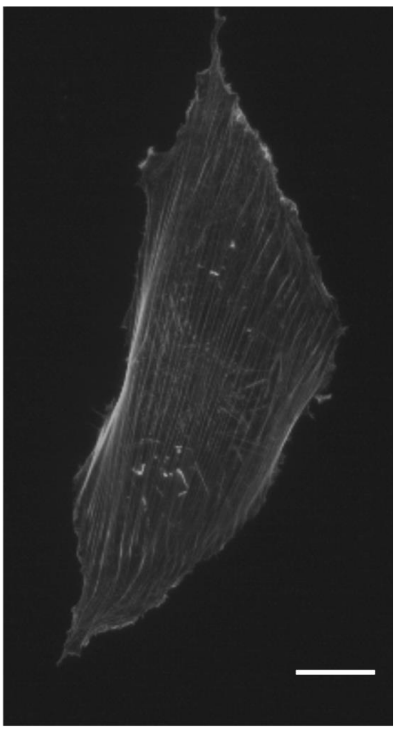

12292 μm^2

b)

Aspect ratio

1-∞

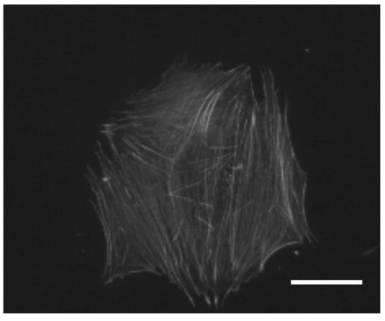

1.13

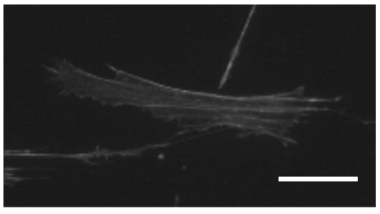

5.89

c)

Stellate factor

0-∞

(typically 0.1-0.8)

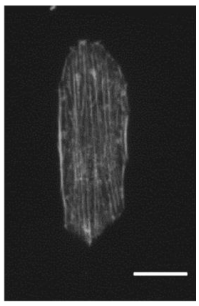

0.11

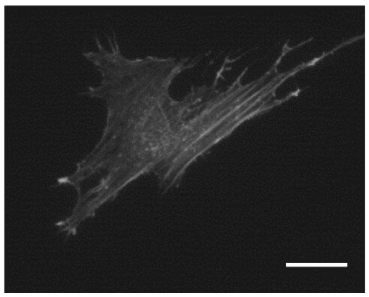

0.62

d)

F-actin amount (AU)

1-∞

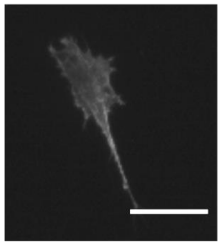

$3.1 \cdot 10^5$

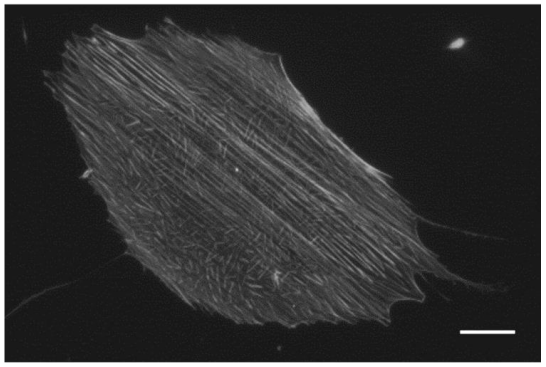

$1.3 \cdot 10^7$

e)

Fibre thickness

(AU)

1-∞

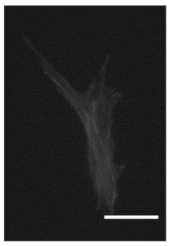

65

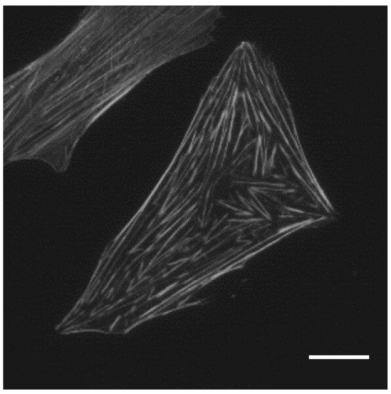

425

f)

Fibre thickness

CoV (%)

0-∞

(typically 50-200%)

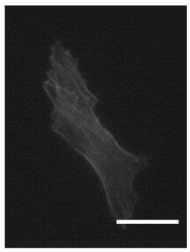

81%

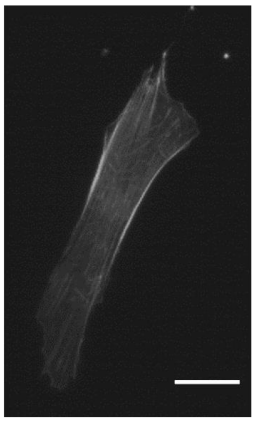

149%

g)

Fibre alignment

0-1

(typically 0.6-1)

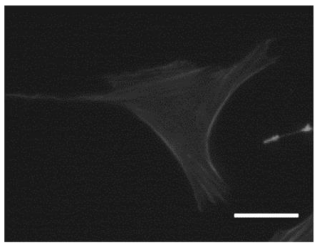

0.74

0.96

h)

Fibre curvature

0-1

(typically 0-0.6)

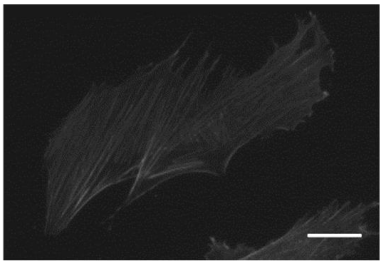

0.074

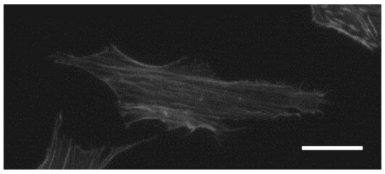

0.418

i)

Fibre spread

0-1

(typically 0.1-0.3)

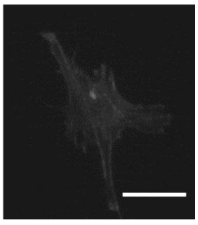

0.10267

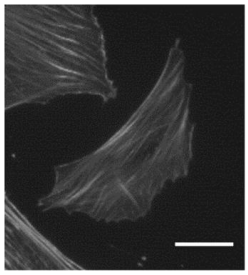

0.27147

j)

Location of fibres

0-1

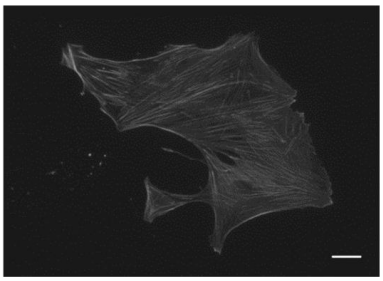

0.336

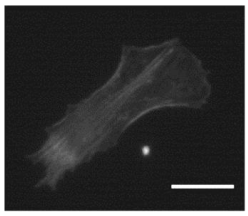

0.898

k)

Fibre length (µm)

0-∞

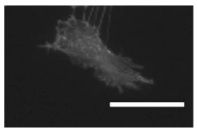

7.4 µm

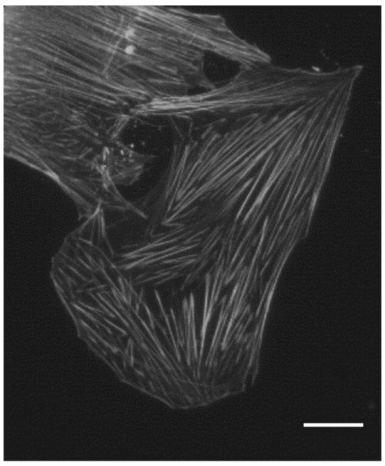

39.4 µm

l)

Fibre length CoV (%)

0-∞

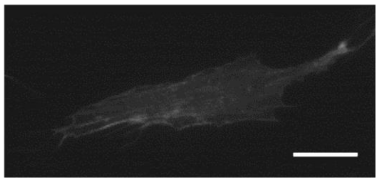

71.3 %

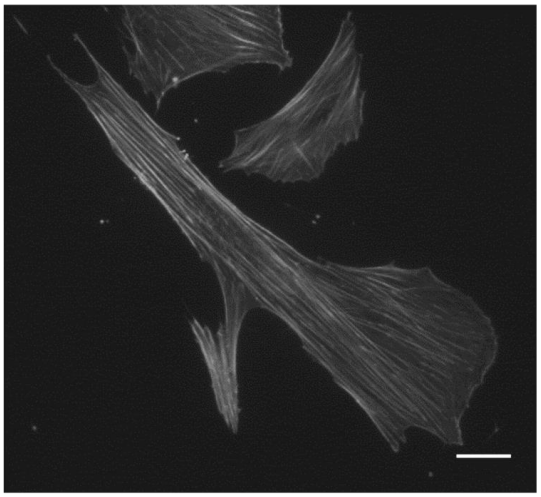

247.7 %

m)

Chirality (deg)

0-90

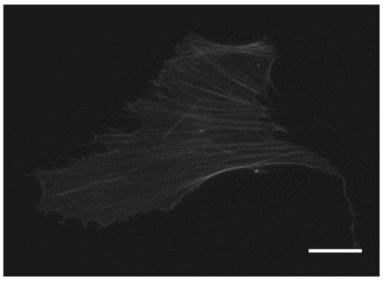

35.2 deg

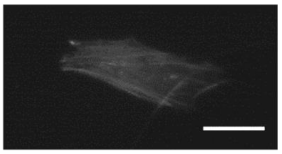

89.6 deg

n)

Chirality variance (deg^2)

0-8100

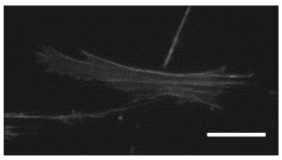

239.8 deg^2

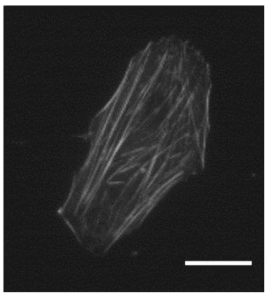

772.5 deg^2

Figure 9-1 – Representative cytoskeleton morphometric values – a) area, b) aspect ratio, c) stellate factor, d) F-actin, e) fibre thickness, f) thickness variability, g) fibre alignment, h) fibre curvature, i) radial fibre spread, j) radial fibre peak, k) fibre length, l) length variability, m) fibre chirality, n) chirality variability. Scale bar represents 30 µm.

Appendix B – Qualitative assessment of the influence of COL I and seeding density on adipogenic and osteogenic differentiation

TCP vessels were coated with a density of 30 µg/cm^2 of COL I. hMSCs (passage 5) were seeded into the vessels at a low density (2000 cells/cm^2) and high density (8000 cells/cm^2) and cultured in either osteogenic or adipogenic differentiation media for the span of 25 days. To validate the propensity of the hMSCs towards the differentiation lineages, cells cultured in adipogenic media were stained with Oil Red O, while cells cultured in osteogenic media were stained with Alizarin Red.

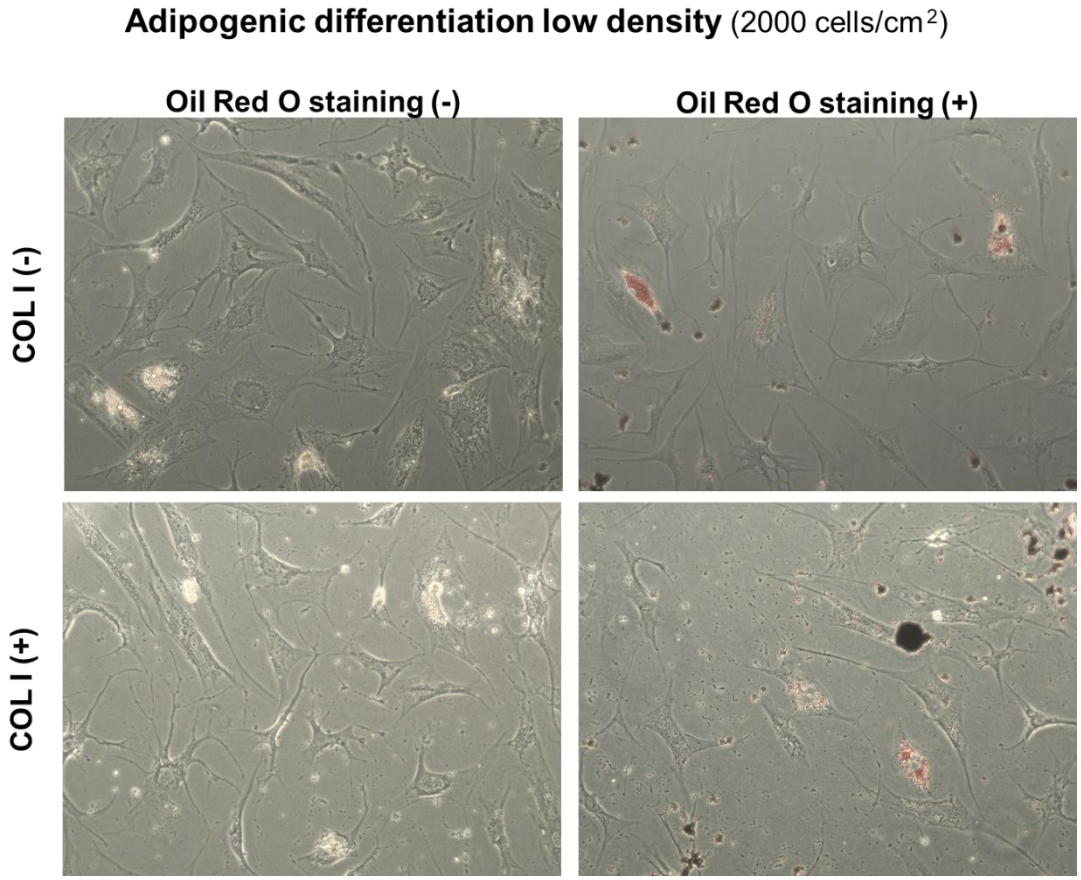

Figure 10-1 – Representative examples of adipogenic differentiation at low initial cell density in the absence (top panels) and presence (bottom panels) of COL I. Cells on the right panels were stained with Oil Red O.

Although qualitative, the preliminary study presented in this appendix allowed the validation of adipogenic and osteogenic differentiation with the hMSC batch employed throughout this work.

In general, it was observed that initial seeding density was highly determinant in the adipogenic lineage. Across conditions terminal adipocytes at day 25 were almost exclusively found surrounded by dense clusters of neighbouring cells (Fig. 10.1 and Fig. 10.2). Oil Red O staining aided in the identification of adipocytes displaying an abundance of lipid vesicles of reduced size, whereas cells with larger lipid deposits were easily identifiable through standard microscopic inspection. A positive effect of COL I in adipogenic differentiation was not sufficiently clear to withdraw determinant conclusions, but potential negative effects to adipogenic differentiation of the coating were ruled-out. As such, it was concluded that COL I does not hinder adipogenesis and can be used in coating substrates for differentiation studies.

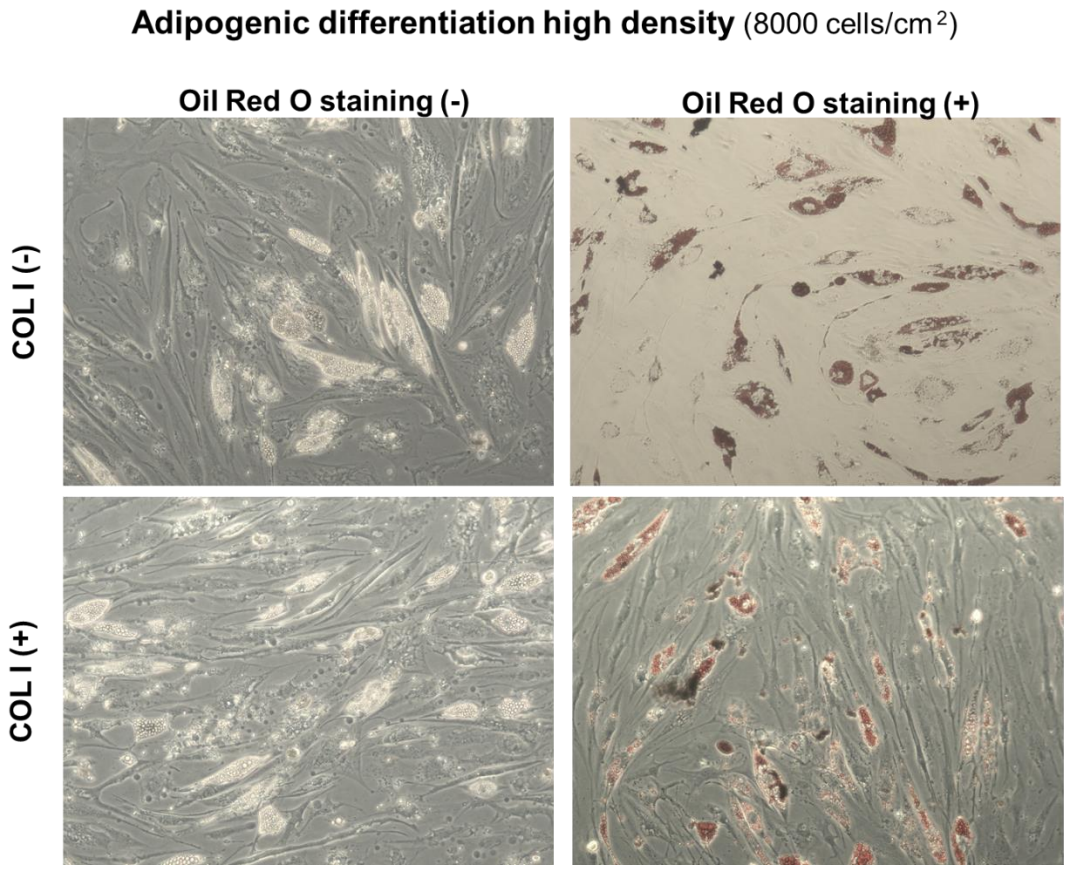

Figure 10-2 – Representative examples of adipogenic differentiation at high initial cell density in the absence (top panels) and presence (bottom panels) of COL I. Cells on the right panels were stained with Oil Red O.

Conversely, osteogenic differentiation was positively impacted by COL I (Fig. 10.3 and Fig. 10.4).

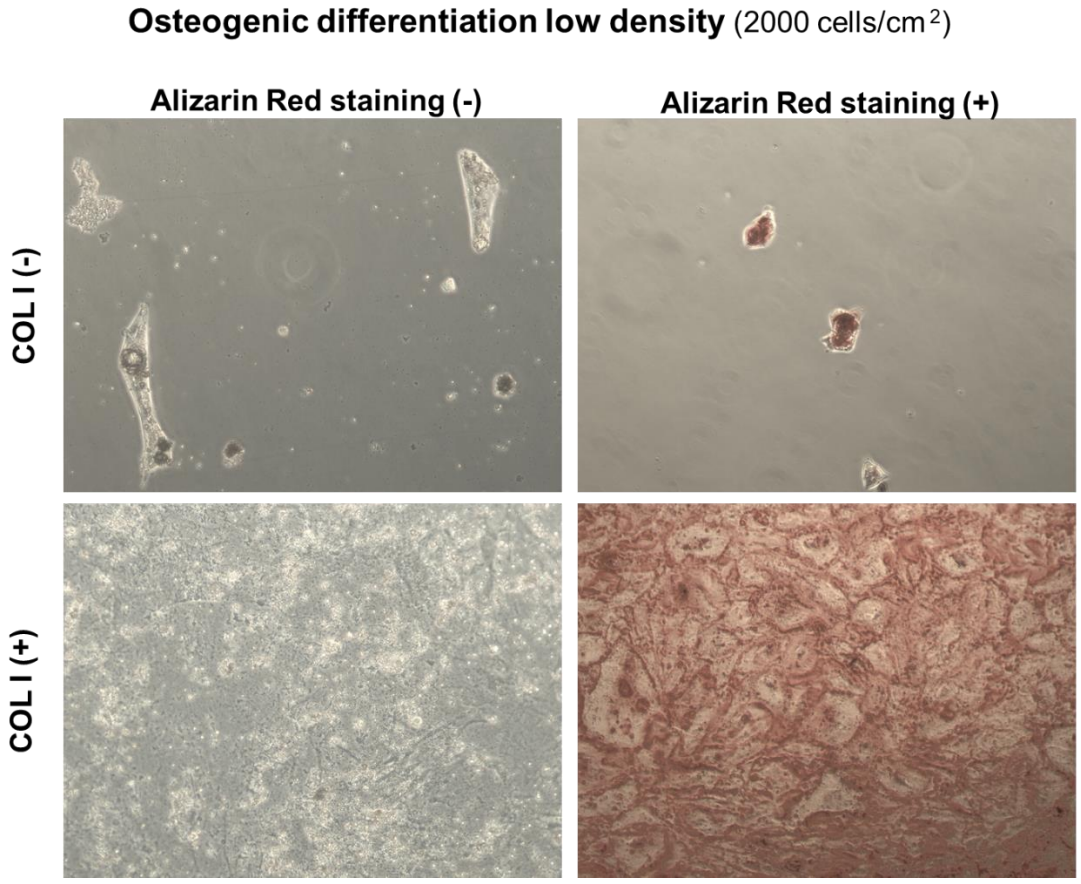

Figure 10-3 – Representative examples of osteogenic differentiation at low initial cell density in the absence (top panels) and presence (bottom panels) of COL I. Cells on the right panels were stained with Alizarin Red.

A persistent issue with the hMSC batch used in this work was a propensity of the cells to rapidly divide under the effect of osteogenic supplements. These cells would then form aggregated monolayers after a week of culture, which would detach from the surface of the TCP vessel (top left panels in Fig. 10.3 and 10.4). COL I coating prevented this issue in both low and high cell densities (lower panels). Furthermore, the cells produced high amounts of deposits which can be seen in the lower left panels of Fig. 10.3 and Fig 10.4. Alizarin Red staining (rightward panels) confirmed the mineral origin of the deposits, confirming the activity of the osteogenic

differentiation supplements. It was not possible to conclude about the importance of cell density to osteogenesis as the cells quickly proliferated across conditions to form fully confluent monolayers.

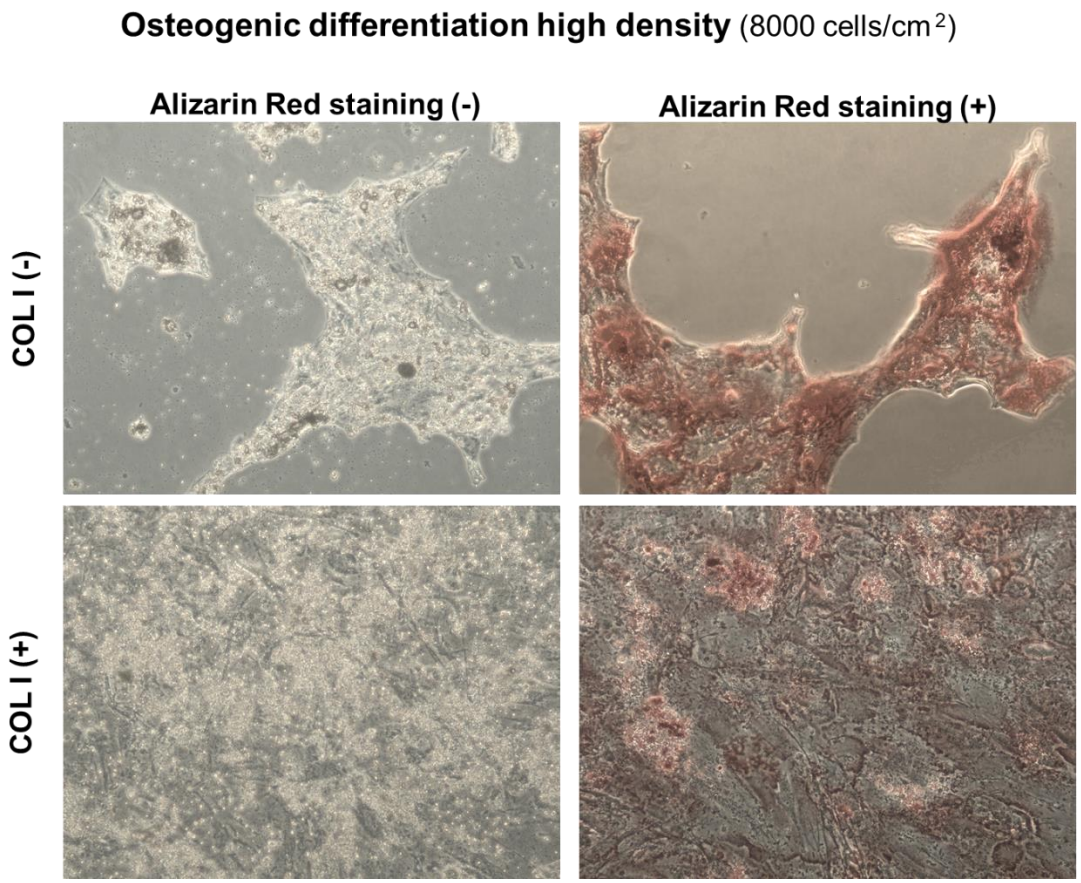

Figure 10-4 – Representative examples of osteogenic differentiation at high initial cell density in the absence (top panels) and presence (bottom panels) of COL I. Cells on the right panels were stained with Alizarin Red.

Appendix C – Statistical analysis for Chapter 4 and Chapter 5

Please note that the data contained in this Appendix are representative examples of an extensive analyses

Table 4 – Example of Shapiro-Wilk normality tests used in Chapter 4 with morphometrics data from day 1 from cells in 1% agarose hydrogels

1%

CTRL

	DF	Statistic	p-value	Decision at level(5%)
Area	328	0.88603	6.49E-15	Reject normality
AR	328	0.91134	5.63E-13	Reject normality
F-actin	328	0.79567	0	Reject normality
Thickness	328	0.88804	8.99E-15	Reject normality
Thickness VAR	328	0.9727	7.22E-06	Reject normality
Alignment	328	0.97802	6.50E-05	Reject normality
Curvature	328	0.97412	1.27E-05	Reject normality
Peak	328	0.94588	1.34E-09	Reject normality
Spread	328	0.99503	0.37456	Can't reject normality
Convexity	328	0.96612	6.28E-07	Reject normality
Length	328	0.83345	0	Reject normality
Length VAR	328	0.95222	7.72E-09	Reject normality
Chirality	328	0.7263	0	Reject normality
Chirality VAR	328	0.97747	5.12E-05	Reject normality
Nuc Brightness	328	0.95363	1.16E-08	Reject normality
Chromatin	328	0.91023	4.55E-13	Reject normality
Poisson Ratio	328	0.90822	3.11E-13	Reject normality
Nuc Volume	328	0.99008	0.02551	Reject normality
Nuc Stiffness	328	0.86732	3.89E-16	Reject normality

Table 5 – Example of Shapiro-Wilk normality tests used in Chapter 4 with morphometrics data from day 1 from cells in 3% agarose hydrogels

3%

CTRL

Area	377	0.91969	2.58E-13	Reject normality
AR	377	0.88579	3.89E-16	Reject normality
F-actin	377	0.80371	0	Reject normality
Thickness	377	0.91534	1.02E-13	Reject normality
Thickness VAR	377	0.90913	2.86E-14	Reject normality
Alignment	377	0.98787	0.00311	Reject normality
Curvature	377	0.9786	2.22E-05	Reject normality
Peak	377	0.94672	2.09E-10	Reject normality
Spread	377	0.99566	0.38321	Can't reject normality
Convexity	377	0.9696	4.43E-07	Reject normality
Length	377	0.7952	0	Reject normality
Length VAR	377	0.94444	1.10E-10	Reject normality
Chirality	377	0.74471	0	Reject normality
Chirality VAR	377	0.98444	4.39E-04	Reject normality
Nuc Brightness	377	0.96942	4.11E-07	Reject normality
Chromatin	377	0.69462	0	Reject normality
Poisson Ratio	377	0.85439	0	Reject normality
Nuc Volume	377	0.96983	4.85E-07	Reject normality
Nuc Stiffness	377	0.89836	3.61E-15	Reject normality

Table 6 – Example of Shapiro-Wilk normality tests used in Chapter 4 with morphometrics data from day 1 from cells in 5% agarose hydrogels

5%				
	CTRL			
Area	348	0.87344	2.78E-16	Reject normality
AR	348	0.92814	6.80E-12	Reject normality
F-actin	348	0.83977	0	Reject normality
Thickness	348	0.90932	1.32E-13	Reject normality
Thickness VAR	348	0.8831	1.28E-15	Reject normality
Alignment	348	0.97954	7.48E-05	Reject normality
Curvature	348	0.95642	1.20E-08	Reject normality
Peak	348	0.96327	1.14E-07	Reject normality
Spread	348	0.99593	0.51087	Can't reject normality
Convexity	348	0.97491	9.58E-06	Reject normality
Length	348	0.78864	0	Reject normality
Length VAR	348	0.94166	1.81E-10	Reject normality
Chirality	348	0.7302	0	Reject normality
Chirality VAR	348	0.97655	1.94E-05	Reject normality
Nuc Brightness	348	0.96374	1.34E-07	Reject normality
Chromatin	348	0.97671	2.08E-05	Reject normality
Poisson Ratio	348	0.79387	0	Reject normality
Nuc Volume	348	0.97468	8.69E-06	Reject normality
Nuc Stiffness	348	0.7858	0	Reject normality

Table 7 – Example of Shapiro-Wilk normality tests used in Chapter 4 with morphometrics data from day 10 from cells in 1% agarose hydrogels

1%				
	CTRL			
	DF	Statistic	p-value	Decision at level(5%)
Area	96	0.95135	1.34E-03	Reject normality
AR	96	0.91538	1.18E-05	Reject normality
F-actin	96	0.91371	9.74E-06	Reject normality
Thickness	96	0.94375	4.44E-04	Reject normality
Thickness VAR	96	0.97683	8.69E-02	Can't reject normality
Alignment	96	0.92623	4.36E-05	Reject normality
Curvature	96	0.99263	8.80E-01	Can't reject normality
Peak	96	0.94296	3.97E-04	Reject normality
Spread	96	0.98851	0.57639	Can't reject normality
Convexity	96	0.94477	5.13E-04	Reject normality
Length	96	0.73251	6.22E-12	Reject normality
Length VAR	96	0.95331	1.80E-03	Reject normality
Chirality	96	0.6199	2.13E-14	Reject normality
Chirality VAR	96	0.98785	5.27E-01	Can't reject normality
Nuc Brightness	96	0.95563	2.57E-03	Reject normality
Chromatin	96	0.52314	3.89E-16	Reject normality
Poisson Ratio	96	0.97671	8.50E-02	Can't reject normality
Nuc Volume	96	0.98727	0.48575	Can't reject normality
Nuc Stiffness	96	0.92678	4.67E-05	Reject normality

Table 8 – Example of Shapiro-Wilk normality tests used in Chapter 4 with morphometrics data from day 10 from cells in 3% agarose hydrogels

3%				
	CTRL			
Area	181	0.9489	4.27E-06	Reject normality
AR	181	0.90689	2.86E-09	Reject normality
F-actin	181	0.89576	5.88E-10	Reject normality
Thickness	181	0.97285	1.33E-03	Reject normality
Thickness VAR	181	0.9458	2.26E-06	Reject normality
Alignment	181	0.93413	2.42E-07	Reject normality
Curvature	181	0.98284	2.54E-02	Reject normality
Peak	181	0.93787	4.82E-07	Reject normality
Spread	181	0.99229	0.45194	Can't reject normality
Convexity	181	0.96191	7.87E-05	Reject normality
Length	181	0.91841	1.67E-08	Reject normality
Length VAR	181	0.88039	7.85E-11	Reject normality
Chirality	181	0.63342	0	Reject normality
Chirality VAR	181	0.98336	2.99E-02	Reject normality
Nuc Brightness	181	0.94528	2.03E-06	Reject normality
Chromatin	181	0.98281	0.02513	Reject normality
Poisson Ratio	181	0.98956	0.20725	Can't reject normality
Nuc Volume	181	0.9847	4.54E-02	Reject normality
Nuc Stiffness	181	0.95055	6.04E-06	Reject normality

Table 9 – Example of Shapiro-Wilk normality tests used in Chapter 4 with morphometrics data from day 10 from cells in 5% agarose hydrogels

5%				
	CTRL			
Area	157	0.91905	1.08E-07	Reject normality
AR	157	0.92665	3.50E-07	Reject normality
F-actin	157	0.89416	3.42E-09	Reject normality
Thickness	157	0.93721	2.03E-06	Reject normality
Thickness VAR	157	0.98937	2.83E-01	Can't reject normality
Alignment	157	0.9656	5.96E-04	Reject normality
Curvature	157	0.97025	1.80E-03	Reject normality
Peak	157	0.91884	1.04E-07	Reject normality
Spread	157	0.99008	3.39E-01	Can't reject normality
Convexity	157	0.96854	0.00119	Reject normality
Length	157	0.27069	0.00E+00	Reject normality
Length VAR	157	0.97947	0.01934	Reject normality
Chirality	157	0.66309	0.00E+00	Reject normality
Chirality VAR	157	0.974	4.60E-03	Reject normality
Nuc Brightness	157	0.96696	8.19E-04	Reject normality
Chromatin	157	0.97648	0.00874	Reject normality
Poisson Ratio	157	0.98454	7.74E-02	Can't reject normality
Nuc Volume	157	0.99393	0.75813	Can't reject normality
Nuc Stiffness	157	0.95433	5.12E-05	Reject normality

Table 10 – Example of Shapiro-Wilk normality tests used in Chapter 5 with morphometrics data from day 1 from cells in 3% agarose hydrogels and osteogenic media

	Osteo			
Area	202	0.9372	1.17E-07	Reject normality
AR	202	0.92412	1.04E-08	Reject normality
F-actin	202	0.87065	4.14E-12	Reject normality
Thickness	202	0.92102	6.06E-09	Reject normality
Thickness	202	0.96286	3.73E-05	Reject normality
Alignmen	202	0.87781	1.02E-11	Reject normality
Curvature	202	0.99201	0.33605	Can't reject normality
Peak	202	0.96518	6.86E-05	Reject normality
Spread	202	0.99268	0.41134	Can't reject normality
Convexity	202	0.93547	8.35E-08	Reject normality
Length	202	0.88709	3.50E-11	Reject normality
Length VA	202	0.91502	2.22E-09	Reject normality
Chirality	202	0.58214	0	Reject normality
Chirality V	202	0.95765	1.01E-05	Reject normality
Nuc Bright	202	0.95041	1.86E-06	Reject normality
Chromatir	202	0.95385	4.07E-06	Reject normality
Poisson Ra	202	0.97773	0.00268	Reject normality
Nuc Volur	202	0.97897	0.004	Reject normality
Nuc Stiffn	202	0.93744	1.22E-07	Reject normality

Table 11 – Example of Shapiro-Wilk normality tests used in Chapter 5 with morphometrics data from day 1 from cells in 3% agarose hydrogels and adipogenic media

	Adipo			
Area	215	0.75819	0	Reject normality
AR	215	0.90178	1.11E-10	Reject normality
F-actin	215	0.85797	3.08E-13	Reject normality
Thickness	215	0.92093	2.54E-09	Reject normality
Thickness '	215	0.97315	4.04E-04	Reject normality
Alignment	215	0.89158	2.46E-11	Reject normality
Curvature	215	0.97967	0.00339	Reject normality
Peak	215	0.96565	4.45E-05	Reject normality
Spread	215	0.9691	1.19E-04	Reject normality
Convexity	215	0.93734	5.56E-08	Reject normality
Length	215	0.68052	0	Reject normality
Length VA	215	0.95345	1.91E-06	Reject normality
Chirality	215	0.55815	0	Reject normality
Chirality V	215	0.95596	3.51E-06	Reject normality
Nuc Bright	215	0.96921	1.23E-04	Reject normality
Chromatin	215	0.97353	4.54E-04	Reject normality
Poisson Ra	215	0.87842	4.02E-12	Reject normality
Nuc Volur	215	0.95879	7.14E-06	Reject normality
Nuc Stiffne	215	0.9647	3.42E-05	Reject normality

Table 12 – Example of Shapiro-Wilk normality tests used in Chapter 5 with morphometrics data from day 10 from cells in 3% agarose hydrogels and osteogenic media

	Osteo			
Area	369	0.92477	1.16E-12	Reject normality
AR	369	0.89017	1.28E-15	Reject normality
F-actin	369	0.93943	4.03E-11	Reject normality
Thickness	369	0.93585	1.62E-11	Reject normality
Thickness	369	0.90116	9.27E-15	Reject normality
Alignmen	369	0.97341	2.71E-06	Reject normality
Curvature	369	0.95964	1.54E-08	Reject normality
Peak	369	0.93219	6.57E-12	Reject normality
Spread	369	0.99617	0.51716	Can't reject normality
Convexity	369	0.97983	4.96E-05	Reject normality
Length	369	0.89938	6.66E-15	Reject normality
Length VA	369	0.94147	6.90E-11	Reject normality
Chirality	369	0.70461	0	Reject normality
Chirality V	369	0.97733	1.53E-05	Reject normality
Nuc Bright	369	0.9636	6.04E-08	Reject normality
Chromatir	369	0.95349	2.14E-09	Reject normality
Poisson Ra	369	0.94414	1.42E-10	Reject normality
Nuc Volun	369	0.98639	0.00154	Reject normality
Nuc Stiffn	369	0.97504	5.48E-06	Reject normality

Table 13 – Example of Shapiro-Wilk normality tests used in Chapter 5 with morphometrics data from day 10 from cells in 3% agarose hydrogels and adiopgenic media

	Adipo			
Area	384	0.92817	1.27E-12	Reject normality
AR	384	0.9027	5.72E-15	Reject normality
F-actin	384	0.78497	0.00E+00	Reject normality
Thickness	384	0.79426	0.00E+00	Reject normality
Thickness	384	0.99438	1.71E-01	Can't reject normality
Alignmen	384	0.96854	2.32E-07	Reject normality
Curvature	384	0.93919	1.98E-11	Reject normality
Peak	384	0.97774	1.23E-05	Reject normality
Spread	384	0.9889	5.15E-03	Reject normality
Convexity	384	0.98045	4.62E-05	Reject normality
Length	384	0.46448	0	Reject normality
Length VA	384	0.9754	4.18E-06	Reject normality
Chirality	384	0.70125	0	Reject normality
Chirality V	384	0.9843	3.50E-04	Reject normality
Nuc Bright	384	0.97293	1.41E-06	Reject normality
Chromatir	384	0.97503	3.53E-06	Reject normality
Poisson Ra	384	0.97624	6.11E-06	Reject normality
Nuc Volun	384	0.99432	1.65E-01	Can't reject normality
Nuc Stiffn	384	0.9538	1.32E-09	Reject normality

Normality tests for osteogenic and adipogenic differentiation were also conducted for 1% and 5% hydrogels at days 1 and 10 (not shown).

Table 14 – Example showing near exact matching between Kruskal-Wallis non-parametric test and parametric ANOVA results for Chapter 4 cell area data in 1% hydrogels

KW

Table Anal	Data 1					
Kruskal-Wallis test						
P value	<0.0001					
Exact or a	Approximate					
P value sui	****					
Do the me	Yes					
Number of	6					
Kruskal-W	223.6					
Data summary						
Number of	6					
Number of	1155					

Number of	1					
Number of	5					
Alpha	0.05					
Dunn's mu	Mean rank	Significant	Summary	Adjusted P	A-?	
Column A	-167.6	Yes	****	<0.0001	B	Column B
Column A	46.41	No	ns	0.8854	C	Column C
Column A	-294.4	Yes	****	<0.0001	D	Column D
Column A	-278.3	Yes	****	<0.0001	E	Column E
Column A	-427.7	Yes	****	<0.0001	F	Column F

Test detail	Mean rank	Mean rank	Mean rank	n1	n2
Column A	432.9	600.5	-167.6	328	326
Column A	432.9	386.5	46.41	328	132
Column A	432.9	727.3	-294.4	328	183
Column A	432.9	711.1	-278.3	328	96
Column A	432.9	860.6	-427.7	328	90

ANOVA

Table Anal	Data 1					
Data sets i	A : Data S	B : Data S	C : Data S	D : Data S	E : Data Set-E	
ANOVA summary						
F	48.26					
P value	<0.0001					
P value sui	****					
Significant	Yes					
R square	0.1736					
Brown-Forsythe test						
F (DFn, DF	4.077 (5, 1149)					
P value	0.0011					
P value sui	**					
Are SDs si	Yes					
Bartlett's test						
Bartlett's s	19.92					
P value	0.0013					
P value sui	**					
Are SDs si	Yes					

ANOVA ta	SS	DF	MS	F (DFn, DF	P value
Treatment	8.3E+10	5	1.66E+10	F (5, 1149)	P<0.0001
Residual (v	3.95E+11	1149	3.44E+08		
Total	4.78E+11	1154			

Data summary	
Number of	6
Number of	1155

Number of	1					
Number of	5					
Alpha	0.05					
Dunnett's r	Mean Diff.	95.00% CI	Significant	Summary	Adjusted P	A-?
Column A	-8048	-11697 to -	Yes	****	0.0001	B Column B
Column A	3341	-1468 to 81	No	ns	0.277	C Column C
Column A	-16747	-21052 to -	Yes	****	0.0001	D Column D
Column A	-15368	-20782 to -	Yes	****	0.0001	E Column E
Column A	-24967	-30519 to -	Yes	****	0.0001	F Column F

Test detail	Mean 1	Mean 2	Mean Diff.	SE of diff.	n1	n2	q	DF
Column A	29848	37897	-8048	1451	328	326	5.548	1149
Column A	29848	26507	3341	1912	328	132	1.747	1149
Column A	29848	46595	-16747	1712	328	183	9.785	1149
Column A	29848	45216	-15368	2153	328	96	7.139	1149
Column A	29848	54816	-24967	2207	328	90	11.31	1149

Table 15 – Example showing near exact matching between Kruskal-Wallis non-parametric test and parametric ANOVA results for Chapter 4 F-actin data in 1% hydrogels

KW

		Number of	1					
Table Anal	Data 1	Number of	5					
		Alpha	0.05					
Kruskal-Wallis test								
P value	<0.0001	Dunn's mu	Mean rank	Significant	Summary	Adjusted P	A-	?
Exact or a	Approximate							
P value su	****	Column A	259.6	Yes	****	<0.0001	B	Column B
Do the me	Yes	Column A	42.05	No	ns	>0.9999	C	Column C
Number of	6	Column A	-273.7	Yes	****	<0.0001	D	Column D
Kruskal-W	352.7	Column A	-96.93	No	ns	0.0614	E	Column E
		Column A	-170.9	Yes	****	<0.0001	F	Column F
Data summary								
Number of	6							
Number of	1155	Test detail	Mean rank	Mean rank	Mean rank	n1	n2	
		Column A	591.3	331.7	259.6	328	326	
		Column A	591.3	549.3	42.05	328	132	
		Column A	591.3	865.1	-273.7	328	183	
		Column A	591.3	688.3	-96.93	328	96	
		Column A	591.3	762.3	-170.9	328	90	

ANOVA

Table Anal	Data 1	Number of	1					
Data sets i	A : Data S B : Data S C : Data S D : Data S E : Data Set-E	Number of	5					
		Alpha	0.05					
ANOVA summary								
F	58.37	Dunnett's r	Mean Diff.	95.00% CI	Significant	Summary	Adjusted P	A- ?
P value	<0.0001							
P value sui	****	Column A	329118	239081 to	Yes	****	0.0001	B Column B
Significant	Yes	Column A	117468	-1199 to 2	No	ns	0.0534	C Column C
R square	0.2026	Column A	-367112	-473337 to	Yes	****	0.0001	D Column D
		Column A	-12732	-146326 to	No	ns	0.9996	E Column E
Brown-Forsythe test		Column A	-108417	-245413 to	No	ns	0.1723	F Column F
F (DFn, DF	16.15 (5, 1149)							
P value	<0.0001							
P value sui	****	Test detail	Mean 1	Mean 2	Mean Diff.	SE of diff.	n1	n2	q	DF
Are SDs si	Yes	Column A	598877	269759	329118	35797	328	326	9.194	1149
		Column A	598877	481409	117468	47180	328	132	2.49	1149
Bartlett's test		Column A	598877	965989	-367112	42233	328	183	8.693	1149
Bartlett's s	159.6	Column A	598877	611608	-12732	53114	328	96	0.2397	1149
P value	<0.0001	Column A	598877	707294	-108417	54467	328	90	1.991	1149
P value sui	****							
Are SDs si	Yes							

ANOVA ta	SS	DF	MS	F (DFn, DF	P value
Treatment	6.11E+13	5	1.22E+13	F (5, 1149)	P<0.0001
Residual (v	2.41E+14	1149	2.1E+11		
Total	3.02E+14	1154			

Data summary	
Number of	6
Number of	1155

Table 16 – Example showing near exact matching between Kruskal-Wallis non-parametric test and parametric ANOVA results for Chapter 4 nuclear volume data in 1% hydrogels

Table Anal	Data 1
Kruskal-Wallis test	
P value	<0.0001
Exact or a	Approximate
P value sui	****
Do the me	Yes
Number of	6
Kruskal-W	133.9
Data summary	
Number of	6
Number of	1155

Number of	1
Number of	5
Alpha	0.05

Dunn's mu	Mean rank	Significant	Summary	Adjusted P	A-?	
Column A	50.18	No	ns	0.2721	B	Column B
Column A	281.3	Yes	****	<0.0001	C	Column C
Column A	19.95	No	ns	>0.9999	D	Column D
Column A	-135.9	Yes	**	0.0022	E	Column E
Column A	-167.3	Yes	***	0.0001	F	Column F

Test detail	Mean rank	Mean rank	Mean rank	n1	n2
Column A	603.1	553	50.18	328	326
Column A	603.1	321.8	281.3	328	132
Column A	603.1	583.2	19.95	328	183
Column A	603.1	739	-135.9	328	96
Column A	603.1	770.5	-167.3	328	90

Table Anal	Data 1
Data sets i	A : Data S B : Data S C : Data S D : Data S E : Data Set-E
ANOVA summary	
F	26.43
P value	<0.0001
P value sui	****
Significant	Yes
R square	0.1031
Brown-Forsythe test	
F (DFn, DF	2.371 (5, 1149)
P value	0.0375
P value sui	*
Are SDs si	Yes
Bartlett's test	
Bartlett's s	33.22
P value	<0.0001
P value sui	****
Are SDs si	Yes

ANOVA ta	SS	DF	MS	F (DFn, DF	P value
Treatment	9.855	5	1.971	F (5, 1149)	P<0.0001
Residual (v	85.7	1149	0.07458		
Total	95.55	1154			

Data summary	
Number of	6
Number of	1155

Number of	1
Number of	5
Alpha	0.05

Dunnett's r	Mean Diff.	95.00% CI	Significant	Summary	Adjusted P	A-?	
Column A	0.05137	-0.002347 t	No	ns	0.0664	B	Column B
Column A	0.2309	0.1601 to (	Yes	****	0.0001	C	Column C
Column A	0.03	-0.03338 t	No	ns	0.6391	D	Column D
Column A	-0.1053	-0.185 to -(	Yes	**	0.0043	E	Column E
Column A	-0.1312	-0.213 to -(	Yes	***	0.0003	F	Column F

Test detail	Mean 1	Mean 2	Mean Diff.	SE of diff.	n1	n2	q	DF
Column A	1.268	1.217	0.05137	0.02136	328	326	2.405	1149
Column A	1.268	1.037	0.2309	0.02815	328	132	8.202	1149
Column A	1.268	1.238	0.03	0.0252	328	183	1.19	1149
Column A	1.268	1.374	-0.1053	0.03169	328	96	3.323	1149
Column A	1.268	1.4	-0.1312	0.0325	328	90	4.039	1149

Table 17 – Example showing near exact matching between Kruskal-Wallis non-parametric test and parametric ANOVA results for Chapter 4 cell area data in 3% hydrogels

Table Anal	Data 1
Kruskal-Wallis test	
P value	<0.0001
Exact or a	Approximate
P value sui	****
Do the me	Yes
Number of	6
Kruskal-W	127.3
Data summary	
Number of	6
Number of	1643

Number of	1
Number of	5
Alpha	0.05

Dunn's mu	Mean rank	Significant	Summary	Adjusted P	A	-?
Column A	69.83	No	ns	0.3	B	Column B
Column A	75.1	No	ns	0.1865	C	Column C
Column A	-13.63	No	ns	>0.9999	D	Column D
Column A	-295.6	Yes	****	<0.0001	E	Column E
Column A	-368.5	Yes	****	<0.0001	F	Column F

Test detail	Mean rank	Mean rank	Mean rank	n1	n2
Column A	795.3	725.5	69.83	377	288
Column A	795.3	720.2	75.1	377	320
Column A	795.3	808.9	-13.63	377	398
Column A	795.3	1091	-295.6	377	181
Column A	795.3	1164	-368.5	377	79

Table Anal	Data 1
Data sets i	A : Data S B : Data S C : Data S D : Data S E : Data Set-E
ANOVA summary	
F	28.17
P value	<0.0001
P value sui	****
Significant	Yes
R square	0.07923
Brown-Forsythe test	
F (DFn, DF	2.814 (5, 1637)
P value	0.0155
P value sui	*
Are SDs si	Yes
Bartlett's test	
Bartlett's s	15.45
P value	0.0086
P value sui	**
Are SDs si	Yes

ANOVA ta	SS	DF	MS	F (DFn, DF	P value
Treatment	5.14E+10	5	1.03E+10	F (5, 1637)	P<0.0001
Residual (\	5.97E+11	1637	3.65E+08		
Total	6.49E+11	1642			

Data summary	
Number of	6
Number of	1643

Number of	1
Number of	5
Alpha	0.05

Dunnett's r	Mean Diff.	95.00% CI	Significant	Summary	Adjusted P	A	-?
Column A	2895	-863.5 to 6	No	ns	0.1922	B	Column B
Column A	3245	-405.9 to 6	No	ns	0.1002	C	Column C
Column A	-862.5	-4314 to 2	No	ns	0.9563	D	Column D
Column A	-12270	-16614 to -	Yes	****	0.0001	E	Column E
Column A	-16079	-22022 to -	Yes	****	0.0001	F	Column F

Test detail	Mean 1	Mean 2	Mean Diff.	SE of diff.	n1	n2	q	DF
Column A	36394	33499	2895	1495	377	288	1.937	1637
Column A	36394	33149	3245	1452	377	320	2.235	1637
Column A	36394	37257	-862.5	1373	377	398	0.6282	1637
Column A	36394	48664	-12270	1728	377	181	7.103	1637
Column A	36394	52473	-16079	2364	377	79	6.802	1637

Table 18 – Example showing near exact matching between Kruskal-Wallis non-parametric test and parametric ANOVA results for Chapter 4 cell area data in 5% hydrogels

Table Anal	Data 1			Number of	1		
				Number of	4		
Kruskal-Wallis test				Alpha	0.05		
P value	<0.0001						
Exact or a	Approximate			Dunn's mu	Mean rank	Significant	Summary	Adjusted P	A-?	
P value su	****									
Do the me	Yes			Column A	39	No	ns	0.791	B	Column B
Number of	5			Column A	-23.82	No	ns	>0.9999	C	Column C
Kruskal-W	54.39			Column A	-154.5	Yes	****	<0.0001	D	Column D
				Column A	-128.7	Yes	**	0.001	E	Column E
Data summary										
Number of	5									
Number of	1266			Test detail	Mean rank	Mean rank	Mean rank	n1	n2	
				Column A	584.5	545.5	39	348	251	
				Column A	584.5	608.3	-23.82	348	208	
				Column A	584.5	739	-154.5	348	302	
				Column A	584.5	713.2	-128.7	348	157	

Table Anal	Data 1									
Data sets i	A : Data S	B : Data S	C : Data S	D : Data S	E : Data Set-E					
ANOVA summary										
F	8.942									
P value	<0.0001									
P value su	****									
Significant	Yes									
R square	0.02758									
Brown-Forsythe test										
F (DFn, DF	2.246 (4, 1261)									
P value	0.0621									
P value su	ns									
Are SDs si	No									
Bartlett's test										
Bartlett's s	18.65									
P value	0.0009									
P value su	***									
Are SDs si	Yes									
ANOVA ta	SS	DF	MS	F (DFn, DF	P value					
Treatment	9.48E+09	4	2.37E+09	F (4, 1261)	P<0.0001					
Residual (v	3.34E+11	1261	2.65E+08							
Total	3.44E+11	1265								
Data summary										
Number of	5									
Number of	1266									

Number of	1									
Number of	4									
Alpha	0.05									
Dunnett's r	Mean Diff.	95.00% CI	Significant	Summary	Adjusted P	A-?				
Column A	2395	-901 to 565	No	ns	0.2259	B	Column B			
Column A	-300.5	-3788 to 3	No	ns	0.9986	C	Column C			
Column A	-4892	-8021 to -1	Yes	***	0.0006	D	Column D			
Column A	-4242	-8068 to -4	Yes	*	0.0242	E	Column E			
Test detail	Mean 1	Mean 2	Mean Diff.	SE of diff.	n1	n2	q	DF		
Column A	30109	27714	2395	1348	348	251	1.777	1261		
Column A	30109	30409	-300.5	1427	348	208	0.2106	1261		
Column A	30109	35001	-4892	1280	348	302	3.822	1261		
Column A	30109	34351	-4242	1565	348	157	2.711	1261		

Comparisons between parametric and non-parametric statistical analysis showed very good agreement for Chapter 4 data relative to all 18 parameters in 1%, 3% and 5% hydrogels, as well as for Chapter 5 - 1% adipogenic and 1% osteogenic data.

Table 19 – One-way ANOVA for the effects of time and hydrogel stiffness on Chapter 4 data – AREA

†

Table Analyze Data 1

Two-way ANO Ordinary
Alpha 0.05

Source of Var	% of total \	P value	P value sui	Significant?
Interaction	2.66	<0.0001	****	Yes
Time	5.527	<0.0001	****	Yes
Agarose	1.895	<0.0001	****	Yes

ANOVA table	SS	DF	MS	F (DFn, Df	P value
Interaction	3.71E+10	8	4.64E+09	F (8, 3880)	P<0.0001
Time	7.72E+10	4	1.93E+10	F (4, 3880)	P<0.0001
Agarose	2.64E+10	2	1.32E+10	F (2, 3880)	P<0.0001
Residual	1.26E+12	3880	3.23E+08		

Number of mis 2075

Within each column, compare rows (simple effects within columns)

Number of fam 3
Number of cor 10
Alpha 0.05

Bonferroni's m	Mean Diff.	95.00% CI	Significant?	Summary	Adjusted P Value
1%					
1 vs. 3	-8048	-11999 to -	Yes	****	<0.0001
1 vs. 5	3341	-1866 to 8	No	ns	0.7159
1 vs. 7	-16747	-21408 to -	Yes	****	<0.0001
1 vs. 10	-15368	-21230 to -	Yes	****	<0.0001
3 vs. 5	11390	6178 to 16	Yes	****	<0.0001
3 vs. 7	-8698	-13365 to -	Yes	****	<0.0001
3 vs. 10	-7319	-13185 to -	Yes	**	0.0046
5 vs. 7	-20088	-25857 to -	Yes	****	<0.0001
5 vs. 10	-18709	-25485 to -	Yes	****	<0.0001
7 vs. 10	1379	-4987 to 7	No	ns	>0.9999
3%					
1 vs. 3	2895	-1058 to 6	No	ns	0.3975
1 vs. 5	3245	-594.8 to 7	No	ns	0.1767
1 vs. 7	-862.5	-4493 to 2	No	ns	>0.9999
1 vs. 10	-12270	-16839 to -	Yes	****	<0.0001
3 vs. 5	349.5	-3754 to 4	No	ns	>0.9999
3 vs. 7	-3758	-7666 to 1	No	ns	0.0695
3 vs. 10	-15166	-19957 to -	Yes	****	<0.0001
5 vs. 7	-4107	-7900 to -3	Yes	*	0.0237
5 vs. 10	-15515	-20214 to -	Yes	****	<0.0001
7 vs. 10	-11408	-15937 to -	Yes	****	<0.0001
5%					
1 vs. 3	2395	-1789 to 6	No	ns	>0.9999
1 vs. 5	-300.5	-4728 to 4	No	ns	>0.9999
1 vs. 7	-4892	-8865 to -9	Yes	**	0.0055
1 vs. 10	-4242	-9099 to 6	No	ns	0.1421
3 vs. 5	-2695	-7432 to 2	No	ns	>0.9999
3 vs. 7	-7286	-11601 to -	Yes	****	<0.0001
3 vs. 10	-6636	-11777 to -	Yes	**	0.0029
5 vs. 7	-4591	-9143 to -3	Yes	*	0.0463
5 vs. 10	-3941	-9282 to 1	No	ns	0.3826
7 vs. 10	649.8	-4320 to 5	No	ns	>0.9999

Test details	Mean 1	Mean 2	Mean Diff.	SE of diff.	N1	N2	t	DF
1%								
1 vs. 3	29848	37897	-8048	1407	328	326	5.722	3880
1 vs. 5	29848	26507	3341	1854	328	132	1.802	3880
1 vs. 7	29848	46595	-16747	1660	328	183	10.09	3880
1 vs. 10	29848	45216	-15368	2087	328	96	7.363	3880
3 vs. 5	37897	26507	11390	1856	326	132	6.138	3880
3 vs. 7	37897	46595	-8698	1661	326	183	5.236	3880
3 vs. 10	37897	45216	-7319	2089	326	96	3.504	3880
5 vs. 7	26507	46595	-20088	2054	132	183	9.781	3880
5 vs. 10	26507	45216	-18709	2413	132	96	7.755	3880
7 vs. 10	46595	45216	1379	2267	183	96	0.6085	3880
3%								
1 vs. 3	36394	33499	2895	1408	377	288	2.057	3880
1 vs. 5	36394	33149	3245	1367	377	320	2.374	3880
1 vs. 7	36394	37257	-862.5	1293	377	398	0.6673	3880
1 vs. 10	36394	48664	-12270	1626	377	181	7.544	3880
3 vs. 5	33499	33149	349.5	1461	288	320	0.2392	3880
3 vs. 7	33499	37257	-3758	1391	288	398	2.701	3880
3 vs. 10	33499	48664	-15166	1706	288	181	8.89	3880
5 vs. 7	33149	37257	-4107	1350	320	398	3.042	3880
5 vs. 10	33149	48664	-15515	1673	320	181	9.275	3880
7 vs. 10	37257	48664	-11408	1612	398	181	7.075	3880
5%								
1 vs. 3	30109	27714	2395	1489	348	251	1.608	3880
1 vs. 5	30109	30409	-300.5	1576	348	208	0.1906	3880
1 vs. 7	30109	35001	-4892	1414	348	302	3.458	3880
1 vs. 10	30109	34351	-4242	1729	348	157	2.453	3880
3 vs. 5	27714	30409	-2695	1686	251	208	1.598	3880
3 vs. 7	27714	35001	-7286	1536	251	302	4.743	3880
3 vs. 10	27714	34351	-6636	1830	251	157	3.626	3880
5 vs. 7	30409	35001	-4591	1621	208	302	2.833	3880
5 vs. 10	30409	34351	-3941	1902	208	157	2.073	3880
7 vs. 10	35001	34351	649.8	1770	302	157	0.3672	3880

Within each row, compare columns (simple effects within rows)

Number of fam 5
Number of con 3
Alpha 0.05

Bonferroni's m	Mean Diff.	95.00% CI	Significant?	Summary	Adjusted P Value
1					
1% vs. 3%	-6546	-9798 to -3	Yes	****	<0.0001
1% vs. 5%	-260.9	-3576 to 3	No	ns	>0.9999
3% vs. 5%	6285	3083 to 94	Yes	****	<0.0001
3					
1% vs. 3%	4398	914.4 to 7	Yes	**	0.0075
1% vs. 5%	10182	6565 to 13	Yes	****	<0.0001
3% vs. 5%	5784	2064 to 95	Yes	***	0.0006
5					
1% vs. 3%	-6642	-11098 to -	Yes	**	0.0011
1% vs. 5%	-3903	-8696 to 8	No	ns	0.1538
3% vs. 5%	2740	-1097 to 6	No	ns	0.2619
7					
1% vs. 3%	9338	5491 to 13	Yes	****	<0.0001
1% vs. 5%	11594	7559 to 15	Yes	****	<0.0001
3% vs. 5%	2256	-1032 to 5	No	ns	0.3011
10					
1% vs. 3%	-3449	-8887 to 1	No	ns	0.3868
1% vs. 5%	10865	5284 to 16	Yes	****	<0.0001
3% vs. 5%	14314	9616 to 19	Yes	****	<0.0001

Test details	Mean 1	Mean 2	Mean Diff.	SE of diff.	N1	N2	t	DF
1								
1% vs. 3%	29848	36394	-6546	1358	328	377	4.82	3880
1% vs. 5%	29848	30109	-260.9	1384	328	348	0.1885	3880
3% vs. 5%	36394	30109	6285	1337	377	348	4.701	3880
3								
1% vs. 3%	37897	33499	4398	1454	326	288	3.024	3880
1% vs. 5%	37897	27714	10182	1510	326	251	6.742	3880
3% vs. 5%	33499	27714	5784	1553	288	251	3.724	3880
5								
1% vs. 3%	26507	33149	-6642	1861	132	320	3.57	3880
1% vs. 5%	26507	30409	-3903	2001	132	208	1.95	3880
3% vs. 5%	33149	30409	2740	1602	320	208	1.71	3880
7								
1% vs. 3%	46595	37257	9338	1606	183	398	5.813	3880
1% vs. 5%	46595	35001	11594	1685	183	302	6.881	3880
3% vs. 5%	37257	35001	2256	1373	398	302	1.643	3880
10								
1% vs. 3%	45216	48664	-3449	2271	96	181	1.519	3880
1% vs. 5%	45216	34351	10865	2330	96	157	4.663	3880
3% vs. 5%	48664	34351	14314	1962	181	157	7.297	3880

† Please note that the statistical data of secondary radial and variance based morphometric descriptors has not been included in the Appendix

Table 20 –One-way ANOVA for the effects of time and hydrogel stiffness on Chapter 4 data – ASPECT RATIO

Table Analyze Data 1

Two-way ANC Ordinary
Alpha 0.05

Source of Var	% of total \	P value	P value sui	Significant?
Interaction	0.5905	0.0026	**	Yes
Time	2.275	<0.0001	****	Yes
Agarose	0.4715	<0.0001	****	Yes

ANOVA table	SS	DF	MS	F (DFn, DF	P value
Interaction	216.7	8	27.09	F (8, 3880)	P=0.0026
Time	834.9	4	208.7	F (4, 3880)	P<0.0001
Agarose	173	2	86.52	F (2, 3880)	P<0.0001
Residual	35472	3880	9.142		

Number of mis 2075

Within each column, compare rows (simple effects within columns)

Number of fan 3
Number of cor 10
Alpha 0.05

Bonferroni's m	Mean Diff.	95.00% CI	Significant	Summary	Adjusted P Value
1%					
1 vs. 3	-1.396	-2.06 to -0.	Yes	****	<0.0001
1 vs. 5	-1.688	-2.563 to -(	Yes	****	<0.0001
1 vs. 7	-0.7866	-1.57 to -0.	Yes	*	0.0483
1 vs. 10	-0.4306	-1.416 to 0	No	ns	>0.9999
3 vs. 5	-0.2915	-1.168 to 0	No	ns	>0.9999
3 vs. 7	0.6096	-0.1749 to	No	ns	0.2913
3 vs. 10	0.9655	-0.02059 to	No	ns	0.0599
5 vs. 7	0.9011	-0.06866 to	No	ns	0.0909
5 vs. 10	1.257	0.118 to 2.	Yes	*	0.0195
7 vs. 10	0.356	-0.7142 to	No	ns	>0.9999
3%					
1 vs. 3	-1.439	-2.104 to -(	Yes	****	<0.0001
1 vs. 5	-2.249	-2.894 to -:	Yes	****	<0.0001
1 vs. 7	-1.329	-1.939 to -(	Yes	****	<0.0001
1 vs. 10	-1.159	-1.927 to -(	Yes	***	0.0002
3 vs. 5	-0.81	-1.5 to -0.1	Yes	**	0.0098
3 vs. 7	0.1103	-0.5467 to	No	ns	>0.9999
3 vs. 10	0.2795	-0.526 to 1	No	ns	>0.9999
5 vs. 7	0.9202	0.2826 to 1	Yes	***	0.0005
5 vs. 10	1.089	0.2996 to 1	Yes	**	0.0011
7 vs. 10	0.1692	-0.5921 to	No	ns	>0.9999
5%					
1 vs. 3	-0.4331	-1.136 to 0	No	ns	0.8379
1 vs. 5	-0.672	-1.416 to 0	No	ns	0.1125
1 vs. 7	-0.3731	-1.041 to 0	No	ns	>0.9999
1 vs. 10	-0.5887	-1.405 to 0	No	ns	0.4291
3 vs. 5	-0.239	-1.035 to 0	No	ns	>0.9999
3 vs. 7	0.05997	-0.6654 to	No	ns	>0.9999
3 vs. 10	-0.1557	-1.02 to 0.	No	ns	>0.9999
5 vs. 7	0.2989	-0.4663 to	No	ns	>0.9999
5 vs. 10	0.08329	-0.8145 to	No	ns	>0.9999
7 vs. 10	-0.2156	-1.051 to 0	No	ns	>0.9999

Test details	Mean 1	Mean 2	Mean Diff.	SE of diff.	N1	N2	t	DF
1%								
1 vs. 3	4.773	6.169	-1.396	0.2365	328	326	5.904	3880
1 vs. 5	4.773	6.461	-1.688	0.3117	328	132	5.415	3880
1 vs. 7	4.773	5.56	-0.7866	0.279	328	183	2.82	3880
1 vs. 10	4.773	5.204	-0.4306	0.3509	328	96	1.227	3880
3 vs. 5	6.169	6.461	-0.2915	0.3119	326	132	0.9346	3880
3 vs. 7	6.169	5.56	0.6096	0.2793	326	183	2.183	3880
3 vs. 10	6.169	5.204	0.9655	0.3511	326	96	2.75	3880
5 vs. 7	6.461	5.56	0.9011	0.3453	132	183	2.61	3880
5 vs. 10	6.461	5.204	1.257	0.4056	132	96	3.1	3880
7 vs. 10	5.56	5.204	0.356	0.381	183	96	0.9342	3880
3%								
1 vs. 3	4.06	5.499	-1.439	0.2366	377	288	6.081	3880
1 vs. 5	4.06	6.309	-2.249	0.2298	377	320	9.785	3880
1 vs. 7	4.06	5.389	-1.329	0.2173	377	398	6.114	3880
1 vs. 10	4.06	5.22	-1.159	0.2734	377	181	4.241	3880
3 vs. 5	5.499	6.309	-0.81	0.2456	288	320	3.298	3880
3 vs. 7	5.499	5.389	0.1103	0.2339	288	398	0.4715	3880
3 vs. 10	5.499	5.22	0.2795	0.2868	288	181	0.9746	3880
5 vs. 7	6.309	5.389	0.9202	0.227	320	398	4.054	3880
5 vs. 10	6.309	5.22	1.089	0.2812	320	181	3.874	3880
7 vs. 10	5.389	5.22	0.1692	0.2711	398	181	0.6242	3880
5%								
1 vs. 3	4.663	5.096	-0.4331	0.2504	348	251	1.73	3880
1 vs. 5	4.663	5.335	-0.672	0.265	348	208	2.536	3880
1 vs. 7	4.663	5.036	-0.3731	0.2378	348	302	1.569	3880
1 vs. 10	4.663	5.252	-0.5887	0.2907	348	157	2.025	3880
3 vs. 5	5.096	5.335	-0.239	0.2835	251	208	0.8429	3880
3 vs. 7	5.096	5.036	0.05997	0.2583	251	302	0.2322	3880
3 vs. 10	5.096	5.252	-0.1557	0.3077	251	157	0.506	3880
5 vs. 7	5.335	5.036	0.2989	0.2724	208	302	1.097	3880
5 vs. 10	5.335	5.252	0.08329	0.3197	208	157	0.2606	3880
7 vs. 10	5.036	5.252	-0.2156	0.2975	302	157	0.7249	3880

Within each row, compare columns (simple effects within rows)

Number of fam 5
Number of cor 3
Alpha 0.05

Bonferroni's m	Mean Diff.	95.00% CI	Significant	Summary	Adjusted P Value
1					
1% vs. 3%	0.713	0.1662 to :	Yes	**	0.0054
1% vs. 5%	0.1099	-0.4474 to	No	ns	>0.9999
3% vs. 5%	-0.6031	-1.141 to -(	Yes	*	0.022
3					
1% vs. 3%	0.6702	0.08459 to	Yes	*	0.0185
1% vs. 5%	1.073	0.4649 to :	Yes	****	<0.0001
3% vs. 5%	0.4028	-0.2225 to	No	ns	0.3688
5					
1% vs. 3%	0.1518	-0.5973 to	No	ns	>0.9999
1% vs. 5%	1.126	0.3198 to :	Yes	**	0.0025
3% vs. 5%	0.9738	0.3288 to :	Yes	***	0.0009
7					
1% vs. 3%	0.1709	-0.4758 to	No	ns	>0.9999
1% vs. 5%	0.5234	-0.1549 to	No	ns	0.194
3% vs. 5%	0.3525	-0.2001 to	No	ns	0.38
10					
1% vs. 3%	-0.01583	-0.9301 to	No	ns	>0.9999
1% vs. 5%	-0.04818	-0.9864 to	No	ns	>0.9999
3% vs. 5%	-0.03235	-0.8221 to	No	ns	>0.9999

Test details	Mean 1	Mean 2	Mean Diff.	SE of diff.	N1	N2	t	DF
1								
1% vs. 3%	4.773	4.06	0.713	0.2283	328	377	3.123	3880
1% vs. 5%	4.773	4.663	0.1099	0.2327	328	348	0.4724	3880
3% vs. 5%	4.06	4.663	-0.6031	0.2248	377	348	2.683	3880
3								
1% vs. 3%	6.169	5.499	0.6702	0.2445	326	288	2.741	3880
1% vs. 5%	6.169	5.096	1.073	0.2539	326	251	4.226	3880
3% vs. 5%	5.499	5.096	0.4028	0.2611	288	251	1.543	3880
5								
1% vs. 3%	6.461	6.309	0.1518	0.3128	132	320	0.4853	3880
1% vs. 5%	6.461	5.335	1.126	0.3365	132	208	3.345	3880
3% vs. 5%	6.309	5.335	0.9738	0.2693	320	208	3.616	3880
7								
1% vs. 3%	5.56	5.389	0.1709	0.2701	183	398	0.633	3880
1% vs. 5%	5.56	5.036	0.5234	0.2832	183	302	1.848	3880
3% vs. 5%	5.389	5.036	0.3525	0.2307	398	302	1.528	3880
10								
1% vs. 3%	5.204	5.22	-0.01583	0.3818	96	181	0.04146	3880
1% vs. 5%	5.204	5.252	-0.04818	0.3917	96	157	0.123	3880
3% vs. 5%	5.22	5.252	-0.03235	0.3298	181	157	0.09811	3880

Table 21 – One-way ANOVA for the effects of time and hydrogel stiffness on Chapter 4 data – F-ACTIN

Table Analyze Data 1

Two-way ANC Ordinary
Alpha 0.05

Source of Var	% of total \	P value	P value sui	Significant?
Interaction	7.102	<0.0001	****	Yes
Time	6.308	<0.0001	****	Yes
Agarose	14.04	<0.0001	****	Yes

ANOVA table	SS	DF	MS	F (DFn, DF	P value
Interaction	4E+13	8	5E+12	F (8, 3880)	P<0.0001
Time	3.55E+13	4	8.88E+12	F (4, 3880)	P<0.0001
Agarose	7.91E+13	2	3.96E+13	F (2, 3880)	P<0.0001
Residual	4.09E+14	3880	1.05E+11		

Number of mis 2075

Within each column, compare rows (simple effects within columns)

Number of fan 3
Number of cor 10
Alpha 0.05

Bonferroni's m	Mean Diff.	95.00% CI	Significant	Summary	Adjusted P Value
1%					
1 vs. 3	329118	257830 to	Yes	****	<0.0001
1 vs. 5	117468	23511 to 2	Yes	**	0.0045
1 vs. 7	-367112	-451217 to	Yes	****	<0.0001
1 vs. 10	-12732	-118506 to	No	ns	>0.9999
3 vs. 5	-211650	-305689 to	Yes	****	<0.0001
3 vs. 7	-696230	-780427 to	Yes	****	<0.0001
3 vs. 10	-341850	-447698 to	Yes	****	<0.0001
5 vs. 7	-484580	-588672 to	Yes	****	<0.0001
5 vs. 10	-130200	-252469 to	Yes	*	0.028
7 vs. 10	354381	239509 to	Yes	****	<0.0001
3%					
1 vs. 3	4573	-66764 to 7	No	ns	>0.9999
1 vs. 5	-295334	-364620 to	Yes	****	<0.0001
1 vs. 7	-182831	-248341 to	Yes	****	<0.0001
1 vs. 10	-199308	-281736 to	Yes	****	<0.0001
3 vs. 5	-299907	-373945 to	Yes	****	<0.0001
3 vs. 7	-187403	-257921 to	Yes	****	<0.0001
3 vs. 10	-203880	-290342 to	Yes	****	<0.0001
5 vs. 7	112504	44062 to 1	Yes	****	<0.0001
5 vs. 10	96027	11250 to 1	Yes	*	0.0148
7 vs. 10	-16477	-98197 to 6	No	ns	>0.9999
5%					
1 vs. 3	18782	-56703 to 9	No	ns	>0.9999
1 vs. 5	-45185	-125074 to	No	ns	>0.9999
1 vs. 7	-1975	-73661 to 6	No	ns	>0.9999
1 vs. 10	-145483	-233118 to	Yes	****	<0.0001
3 vs. 5	-63966	-149436 to	No	ns	0.3562
3 vs. 7	-20757	-98613 to 5	No	ns	>0.9999
3 vs. 10	-164265	-257015 to	Yes	****	<0.0001
5 vs. 7	43209	-38924 to 1	No	ns	>0.9999
5 vs. 10	-100298	-196667 to	Yes	*	0.0348
7 vs. 10	-143508	-233194 to	Yes	****	<0.0001

Test details	Mean 1	Mean 2	Mean Diff.	SE of diff.	N1	N2	t	DF
1%								
1 vs. 3	598877	269759	329118	25382	328	326	12.97	3880
1 vs. 5	598877	481409	117468	33453	328	132	3.511	3880
1 vs. 7	598877	965989	-367112	29945	328	183	12.26	3880
1 vs. 10	598877	611608	-12732	37661	328	96	0.3381	3880
3 vs. 5	269759	481409	-211650	33482	326	132	6.321	3880
3 vs. 7	269759	965989	-696230	29978	326	183	23.22	3880
3 vs. 10	269759	611608	-341850	37687	326	96	9.071	3880
5 vs. 7	481409	965989	-484580	37061	132	183	13.08	3880
5 vs. 10	481409	611608	-130200	43533	132	96	2.991	3880
7 vs. 10	965989	611608	354381	40899	183	96	8.665	3880
3%								
1 vs. 3	229688	225115	4573	25399	377	288	0.18	3880
1 vs. 5	229688	525022	-295334	24669	377	320	11.97	3880
1 vs. 7	229688	412519	-182831	23325	377	398	7.839	3880
1 vs. 10	229688	428996	-199308	29348	377	181	6.791	3880
3 vs. 5	225115	525022	-299907	26361	288	320	11.38	3880
3 vs. 7	225115	412519	-187403	25107	288	398	7.464	3880
3 vs. 10	225115	428996	-203880	30784	288	181	6.623	3880
5 vs. 7	525022	412519	112504	24368	320	398	4.617	3880
5 vs. 10	525022	428996	96027	30184	320	181	3.181	3880
7 vs. 10	412519	428996	-16477	29096	398	181	0.5663	3880
5%								
1 vs. 3	173284	154502	18782	26876	348	251	0.6988	3880
1 vs. 5	173284	218468	-45185	28444	348	208	1.589	3880
1 vs. 7	173284	175259	-1975	25523	348	302	0.07738	3880
1 vs. 10	173284	318767	-145483	31202	348	157	4.663	3880
3 vs. 5	154502	218468	-63966	30431	251	208	2.102	3880
3 vs. 7	154502	175259	-20757	27720	251	302	0.7488	3880
3 vs. 10	154502	318767	-164265	33023	251	157	4.974	3880
5 vs. 7	218468	175259	43209	29243	208	302	1.478	3880
5 vs. 10	218468	318767	-100298	34312	208	157	2.923	3880
7 vs. 10	175259	318767	-143508	31932	302	157	4.494	3880

Within each row, compare columns (simple effects within rows)

Number of fam 5
Number of cor 3
Alpha 0.05

Bonferroni's m	Mean Diff.	95.00% CI	Significant	Summary	Adjusted P Value
1					
1% vs. 3%	369189	310498 to	Yes	****	<0.0001
1% vs. 5%	425593	365775 to	Yes	****	<0.0001
3% vs. 5%	56404	-1378 to 1	No	ns	0.0583
3					
1% vs. 3%	44643	-18215 to 1	No	ns	0.2671
1% vs. 5%	115257	49985 to 1	Yes	****	<0.0001
3% vs. 5%	70613	3494 to 13	Yes	*	0.0354
5					
1% vs. 3%	-43614	-124020 to	No	ns	0.582
1% vs. 5%	262940	176443 to	Yes	****	<0.0001
3% vs. 5%	306554	237324 to	Yes	****	<0.0001
7					
1% vs. 3%	553470	484047 to	Yes	****	<0.0001
1% vs. 5%	790730	717914 to	Yes	****	<0.0001
3% vs. 5%	237260	177942 to	Yes	****	<0.0001
10					
1% vs. 3%	182613	84472 to 2	Yes	****	<0.0001
1% vs. 5%	292842	192135 to	Yes	****	<0.0001
3% vs. 5%	110229	25457 to 1	Yes	**	0.0056

Test details	Mean 1	Mean 2	Mean Diff.	SE of diff.	N1	N2	t	DF
1								
1% vs. 3%	598877	229688	369189	24505	328	377	15.07	3880
1% vs. 5%	598877	173284	425593	24976	328	348	17.04	3880
3% vs. 5%	229688	173284	56404	24126	377	348	2.338	3880
3								
1% vs. 3%	269759	225115	44643	26246	326	288	1.701	3880
1% vs. 5%	269759	154502	115257	27253	326	251	4.229	3880
3% vs. 5%	225115	154502	70613	28024	288	251	2.52	3880
5								
1% vs. 3%	481409	525022	-43614	33572	132	320	1.299	3880
1% vs. 5%	481409	218468	262940	36116	132	208	7.28	3880
3% vs. 5%	525022	218468	306554	28906	320	208	10.61	3880
7								
1% vs. 3%	965989	412519	553470	28987	183	398	19.09	3880
1% vs. 5%	965989	175259	790730	30403	183	302	26.01	3880
3% vs. 5%	412519	175259	237260	24767	398	302	9.58	3880
10								
1% vs. 3%	611608	428996	182613	40977	96	181	4.456	3880
1% vs. 5%	611608	318767	292842	42049	96	157	6.964	3880
3% vs. 5%	428996	318767	110229	35395	181	157	3.114	3880

Table 22 – One-way ANOVA for the effects of time and hydrogel stiffness on Chapter 4 data – THICKNESS

Table Analyze Data 1

Two-way ANC Ordinary
Alpha 0.05

Source of Var	% of total \	P value	P value su	Significant?
Interaction	10.14	<0.0001	****	Yes
Time	7.678	<0.0001	****	Yes
Agarose	19.79	<0.0001	****	Yes

ANOVA table	SS	DF	MS	F (DFn, DF	P value
Interaction	473966	8	59246	F (8, 3880)	P<0.0001
Time	358834	4	89708	F (4, 3880)	P<0.0001
Agarose	925021	2	462510	F (2, 3880)	P<0.0001
Residual	2915710	3880	751.5		

Number of mis 2075

Within each column, compare rows (simple effects within columns)

Number of fan 3
Number of cor 10
Alpha 0.05

Bonferroni's m	Mean Diff.	95.00% CI	Significant?	Summary	Adjusted P Value
1%					
1 vs. 3	53.99	47.96 to 6(	Yes	****	<0.0001
1 vs. 5	6.573	-1.363 to 1	No	ns	0.2006
1 vs. 7	-8.425	-15.53 to -:	Yes	**	0.0087
1 vs. 10	28.45	19.51 to 3)	Yes	****	<0.0001
3 vs. 5	-47.41	-55.36 to -:	Yes	****	<0.0001
3 vs. 7	-62.41	-69.52 to -!	Yes	****	<0.0001
3 vs. 10	-25.54	-34.48 to -:	Yes	****	<0.0001
5 vs. 7	-15	-23.79 to -(	Yes	****	<0.0001
5 vs. 10	21.88	11.55 to 3:	Yes	****	<0.0001
7 vs. 10	36.87	27.17 to 4(	Yes	****	<0.0001
3%					
1 vs. 3	3.774	-2.251 to 9	No	ns	0.7861
1 vs. 5	-35.71	-41.56 to -:	Yes	****	<0.0001
1 vs. 7	-9.32	-14.85 to -:	Yes	****	<0.0001
1 vs. 10	-5.204	-12.17 to 1	No	ns	0.3587
3 vs. 5	-39.48	-45.74 to -:	Yes	****	<0.0001
3 vs. 7	-13.09	-19.05 to -:	Yes	****	<0.0001
3 vs. 10	-8.978	-16.28 to -:	Yes	**	0.0056
5 vs. 7	26.39	20.61 to 3:	Yes	****	<0.0001
5 vs. 10	30.5	23.34 to 3)	Yes	****	<0.0001
7 vs. 10	4.116	-2.786 to 1	No	ns	0.9404
5%					
1 vs. 3	1.977	-4.399 to 8	No	ns	>0.9999
1 vs. 5	-5.066	-11.81 to 1	No	ns	0.3503
1 vs. 7	4.238	-1.817 to 1	No	ns	0.494
1 vs. 10	-16.62	-24.03 to -!	Yes	****	<0.0001
3 vs. 5	-7.044	-14.26 to 0	No	ns	0.0617
3 vs. 7	2.261	-4.316 to 8	No	ns	>0.9999
3 vs. 10	-18.6	-26.43 to -:	Yes	****	<0.0001
5 vs. 7	9.304	2.367 to 1(	Yes	**	0.0017
5 vs. 10	-11.56	-19.7 to -3.	Yes	***	0.0007
7 vs. 10	-20.86	-28.44 to -:	Yes	****	<0.0001

Test details	Mean 1	Mean 2	Mean Diff.	SE of diff.	N1	N2	t	DF
1%								
1 vs. 3	83.92	29.94	53.99	2.144	328	326	25.18	3880
1 vs. 5	83.92	77.35	6.573	2.826	328	132	2.326	3880
1 vs. 7	83.92	92.35	-8.425	2.529	328	183	3.331	3880
1 vs. 10	83.92	55.47	28.45	3.181	328	96	8.943	3880
3 vs. 5	29.94	77.35	-47.41	2.828	326	132	16.76	3880
3 vs. 7	29.94	92.35	-62.41	2.532	326	183	24.65	3880
3 vs. 10	29.94	55.47	-25.54	3.183	326	96	8.022	3880
5 vs. 7	77.35	92.35	-15	3.13	132	183	4.791	3880
5 vs. 10	77.35	55.47	21.88	3.677	132	96	5.949	3880
7 vs. 10	92.35	55.47	36.87	3.455	183	96	10.67	3880
3%								
1 vs. 3	29.27	25.5	3.774	2.145	377	288	1.759	3880
1 vs. 5	29.27	64.98	-35.71	2.084	377	320	17.14	3880
1 vs. 7	29.27	38.59	-9.32	1.97	377	398	4.731	3880
1 vs. 10	29.27	34.48	-5.204	2.479	377	181	2.099	3880
3 vs. 5	25.5	64.98	-39.48	2.227	288	320	17.73	3880
3 vs. 7	25.5	38.59	-13.09	2.121	288	398	6.174	3880
3 vs. 10	25.5	34.48	-8.978	2.6	288	181	3.453	3880
5 vs. 7	64.98	38.59	26.39	2.058	320	398	12.82	3880
5 vs. 10	64.98	34.48	30.5	2.55	320	181	11.96	3880
7 vs. 10	38.59	34.48	4.116	2.458	398	181	1.675	3880
5%								
1 vs. 3	25.18	23.2	1.977	2.27	348	251	0.8709	3880
1 vs. 5	25.18	30.24	-5.066	2.403	348	208	2.109	3880
1 vs. 7	25.18	20.94	4.238	2.156	348	302	1.966	3880
1 vs. 10	25.18	41.8	-16.62	2.635	348	157	6.308	3880
3 vs. 5	23.2	30.24	-7.044	2.57	251	208	2.74	3880
3 vs. 7	23.2	20.94	2.261	2.341	251	302	0.9655	3880
3 vs. 10	23.2	41.8	-18.6	2.789	251	157	6.669	3880
5 vs. 7	30.24	20.94	9.304	2.47	208	302	3.767	3880
5 vs. 10	30.24	41.8	-11.56	2.898	208	157	3.988	3880
7 vs. 10	20.94	41.8	-20.86	2.697	302	157	7.735	3880

Within each row, compare columns (simple effects within rows)

Number of fam 5
Number of con 3
Alpha 0.05

Bonferroni's m	Mean Diff.	95.00% CI	Significant?	Summary	Adjusted P Value
1					
1% vs. 3%	54.65	49.69 to 5(	Yes	****	<0.0001
1% vs. 5%	58.74	53.69 to 6:	Yes	****	<0.0001
3% vs. 5%	4.096	-0.7846 to	No	ns	0.1335
3					
1% vs. 3%	4.436	-0.8731 to	No	ns	0.1363
1% vs. 5%	6.735	1.222 to 1:	Yes	*	0.0104
3% vs. 5%	2.299	-3.37 to 7.!	No	ns	0.9946
5					
1% vs. 3%	12.37	5.576 to 1!	Yes	****	<0.0001
1% vs. 5%	47.1	39.8 to 54.	Yes	****	<0.0001
3% vs. 5%	34.74	28.89 to 4(	Yes	****	<0.0001
7					
1% vs. 3%	53.75	47.89 to 5!	Yes	****	<0.0001
1% vs. 5%	71.41	65.26 to 7!	Yes	****	<0.0001
3% vs. 5%	17.65	12.64 to 2:	Yes	****	<0.0001
10					
1% vs. 3%	21	12.71 to 2!	Yes	****	<0.0001
1% vs. 5%	13.67	5.165 to 2:	Yes	***	0.0004
3% vs. 5%	-7.324	-14.48 to -(	Yes	*	0.043

Test details	Mean 1	Mean 2	Mean Diff.	SE of diff.	N1	N2	t	DF
1								
1% vs. 3%	83.92	29.27	54.65	2.07	328	377	26.4	3880
1% vs. 5%	83.92	25.18	58.74	2.11	328	348	27.85	3880
3% vs. 5%	29.27	25.18	4.096	2.038	377	348	2.01	3880
3								
1% vs. 3%	29.94	25.5	4.436	2.217	326	288	2.001	3880
1% vs. 5%	29.94	23.2	6.735	2.302	326	251	2.926	3880
3% vs. 5%	25.5	23.2	2.299	2.367	288	251	0.9712	3880
5								
1% vs. 3%	77.35	64.98	12.37	2.836	132	320	4.361	3880
1% vs. 5%	77.35	30.24	47.1	3.051	132	208	15.44	3880
3% vs. 5%	64.98	30.24	34.74	2.442	320	208	14.23	3880
7								
1% vs. 3%	92.35	38.59	53.75	2.448	183	398	21.95	3880
1% vs. 5%	92.35	20.94	71.41	2.568	183	302	27.81	3880
3% vs. 5%	38.59	20.94	17.65	2.092	398	302	8.439	3880
10								
1% vs. 3%	55.47	34.48	21	3.461	96	181	6.066	3880
1% vs. 5%	55.47	41.8	13.67	3.552	96	157	3.849	3880
3% vs. 5%	34.48	41.8	-7.324	2.99	181	157	2.45	3880

Table 23 – One-way ANOVA for the effects of time and hydrogel stiffness on Chapter 4 data – ALIGNMENT

Table Analyze Data 1

Two-way ANC Ordinary
Alpha 0.05

Source of Var	% of total \	P value	P value sui	Significant?
Interaction	1.798	<0.0001	****	Yes
Time	5.06	<0.0001	****	Yes
Agarose	0.4896	<0.0001	****	Yes

ANOVA table	SS	DF	MS	F (DFn, DF	P value
Interaction	0.2192	8	0.02739	F (8, 3880)	P<0.0001
Time	0.6167	4	0.1542	F (4, 3880)	P<0.0001
Agarose	0.05968	2	0.02984	F (2, 3880)	P<0.0001
Residual	11.29	3880	0.002911		

Number of mis 2075

Within each column, compare rows (simple effects within columns)

Number of fan 3
Number of cor 10
Alpha 0.05

Bonferroni's m	Mean Diff.	95.00% CI	Significant	Summary	Adjusted P Value
1%					
1 vs. 3	0.01461	0.002761 t	Yes	**	0.0054
1 vs. 5	0.01384	-0.001783	No	ns	0.1289
1 vs. 7	0.03581	0.02183 to	Yes	****	<0.0001
1 vs. 10	0.03902	0.02143 to	Yes	****	<0.0001
3 vs. 5	-0.00078	-0.01641 to	No	ns	>0.9999
3 vs. 7	0.0212	0.007206 t	Yes	***	0.0002
3 vs. 10	0.02441	0.006812 t	Yes	***	0.001
5 vs. 7	0.02198	0.004675 t	Yes	**	0.0036
5 vs. 10	0.02518	0.004858 t	Yes	**	0.0051
7 vs. 10	0.003205	-0.01589 to	No	ns	>0.9999
3%					
1 vs. 3	0.03984	0.02798 to	Yes	****	<0.0001
1 vs. 5	0.04407	0.03255 to	Yes	****	<0.0001
1 vs. 7	0.05022	0.03933 to	Yes	****	<0.0001
1 vs. 10	0.03381	0.02011 to	Yes	****	<0.0001
3 vs. 5	0.00423	-0.008077	No	ns	>0.9999
3 vs. 7	0.01039	-0.001335	No	ns	0.1286
3 vs. 10	-0.00602	-0.0204 to	No	ns	>0.9999
5 vs. 7	0.006157	-0.00522 to	No	ns	>0.9999
5 vs. 10	-0.01025	-0.02435 to	No	ns	0.4108
7 vs. 10	-0.01641	-0.02999 to	Yes	**	0.007
5%					
1 vs. 3	0.0283	0.01575 to	Yes	****	<0.0001
1 vs. 5	0.04813	0.03485 to	Yes	****	<0.0001
1 vs. 7	0.02544	0.01352 to	Yes	****	<0.0001
1 vs. 10	0.02552	0.01096 to	Yes	****	<0.0001
3 vs. 5	0.01983	0.005623 t	Yes	***	0.0009
3 vs. 7	-0.00286	-0.0158 to	No	ns	>0.9999
3 vs. 10	-0.00278	-0.0182 to	No	ns	>0.9999
5 vs. 7	-0.02269	-0.03635 to	Yes	****	<0.0001
5 vs. 10	-0.02261	-0.03863 to	Yes	***	0.0008
7 vs. 10	0.000083	-0.01483 to	No	ns	>0.9999

Test details	Mean 1	Mean 2	Mean Diff.	SE of diff.	N1	N2	t	DF
1%								
1 vs. 3	0.1525	0.1379	0.01461	0.004219	328	326	3.463	3880
1 vs. 5	0.1525	0.1387	0.01384	0.005561	328	132	2.488	3880
1 vs. 7	0.1525	0.1167	0.03581	0.004978	328	183	7.195	3880
1 vs. 10	0.1525	0.1135	0.03902	0.00626	328	96	6.233	3880
3 vs. 5	0.1379	0.1387	-0.00078	0.005566	326	132	0.1394	3880
3 vs. 7	0.1379	0.1167	0.0212	0.004983	326	183	4.255	3880
3 vs. 10	0.1379	0.1135	0.02441	0.006265	326	96	3.896	3880
5 vs. 7	0.1387	0.1167	0.02198	0.006161	132	183	3.567	3880
5 vs. 10	0.1387	0.1135	0.02518	0.007237	132	96	3.48	3880
7 vs. 10	0.1167	0.1135	0.003205	0.006799	183	96	0.4714	3880
3%								
1 vs. 3	0.1562	0.1164	0.03984	0.004222	377	288	9.435	3880
1 vs. 5	0.1562	0.1121	0.04407	0.004101	377	320	10.75	3880
1 vs. 7	0.1562	0.106	0.05022	0.003877	377	398	12.95	3880
1 vs. 10	0.1562	0.1224	0.03381	0.004879	377	181	6.931	3880
3 vs. 5	0.1164	0.1121	0.00423	0.004382	288	320	0.9653	3880
3 vs. 7	0.1164	0.106	0.01039	0.004174	288	398	2.489	3880
3 vs. 10	0.1164	0.1224	-0.00602	0.005117	288	181	1.177	3880
5 vs. 7	0.1121	0.106	0.006157	0.004051	320	398	1.52	3880
5 vs. 10	0.1121	0.1224	-0.01025	0.005018	320	181	2.043	3880
7 vs. 10	0.106	0.1224	-0.01641	0.004837	398	181	3.393	3880
5%								
1 vs. 3	0.1569	0.1285	0.0283	0.004468	348	251	6.335	3880
1 vs. 5	0.1569	0.1087	0.04813	0.004728	348	208	10.18	3880
1 vs. 7	0.1569	0.1314	0.02544	0.004243	348	302	5.996	3880
1 vs. 10	0.1569	0.1313	0.02552	0.005187	348	157	4.921	3880
3 vs. 5	0.1285	0.1087	0.01983	0.005059	251	208	3.92	3880
3 vs. 7	0.1285	0.1314	-0.00286	0.004608	251	302	0.6209	3880
3 vs. 10	0.1285	0.1313	-0.00278	0.005489	251	157	0.5061	3880
5 vs. 7	0.1087	0.1314	-0.02269	0.004861	208	302	4.668	3880
5 vs. 10	0.1087	0.1313	-0.02261	0.005704	208	157	3.964	3880
7 vs. 10	0.1314	0.1313	0.000083	0.005308	302	157	0.01564	3880

Within each row, compare columns (simple effects within rows)

Number of fam 5
Number of con 3
Alpha 0.05

Bonferroni's m	Mean Diff.	95.00% CI	Significant	Summary	Adjusted P Value
1					
1% vs. 3%	-0.00367	-0.01342 to	No	ns	>0.9999
1% vs. 5%	-0.00432	-0.01426 to	No	ns	0.8948
3% vs. 5%	-0.00065	-0.01026 to	No	ns	>0.9999
3					
1% vs. 3%	0.02156	0.01111 to	Yes	****	<0.0001
1% vs. 5%	0.009371	-0.001479	No	ns	0.116
3% vs. 5%	-0.01219	-0.02334 to	Yes	*	0.0268
5					
1% vs. 3%	0.02656	0.0132 to (	Yes	****	<0.0001
1% vs. 5%	0.02998	0.0156 to (	Yes	****	<0.0001
3% vs. 5%	0.003415	-0.008093	No	ns	>0.9999
7					
1% vs. 3%	0.01074	-0.000798	No	ns	0.0775
1% vs. 5%	-0.01469	-0.0268 to	Yes	*	0.011
3% vs. 5%	-0.02543	-0.03529 to	Yes	****	<0.0001
10					
1% vs. 3%	-0.00887	-0.02519 to	No	ns	0.5783
1% vs. 5%	-0.01781	-0.03455 to	Yes	*	0.0326
3% vs. 5%	-0.00894	-0.02303 to	No	ns	0.3861

Test details	Mean 1	Mean 2	Mean Diff.	SE of diff.	N1	N2	t	DF
1								
1% vs. 3%	0.1525	0.1562	-0.00367	0.004074	328	377	0.9002	3880
1% vs. 5%	0.1525	0.1569	-0.00432	0.004152	328	348	1.04	3880
3% vs. 5%	0.1562	0.1569	-0.00065	0.00401	377	348	0.1626	3880
3								
1% vs. 3%	0.1379	0.1164	0.02156	0.004363	326	288	4.941	3880
1% vs. 5%	0.1379	0.1285	0.009371	0.00453	326	251	2.069	3880
3% vs. 5%	0.1164	0.1285	-0.01219	0.004659	288	251	2.616	3880
5								
1% vs. 3%	0.1387	0.1121	0.02656	0.005581	132	320	4.76	3880
1% vs. 5%	0.1387	0.1087	0.02998	0.006004	132	208	4.993	3880
3% vs. 5%	0.1121	0.1087	0.003415	0.004805	320	208	0.7107	3880
7								
1% vs. 3%	0.1167	0.106	0.01074	0.004818	183	398	2.229	3880
1% vs. 5%	0.1167	0.1314	-0.01469	0.005054	183	302	2.907	3880
3% vs. 5%	0.106	0.1314	-0.02543	0.004117	398	302	6.178	3880
10								
1% vs. 3%	0.1135	0.1224	-0.00887	0.006812	96	181	1.303	3880
1% vs. 5%	0.1135	0.1313	-0.01781	0.00699	96	157	2.549	3880
3% vs. 5%	0.1224	0.1313	-0.00894	0.005884	181	157	1.52	3880

Table 24 – One-way ANOVA for the effects of time and hydrogel stiffness on Chapter 4 data – CURVATURE

Table Analyze Data 1

Two-way ANC Ordinary
Alpha 0.05

Source of Var	% of total \	P value	P value sur	Significant?
Interaction	1.368	<0.0001	****	Yes
Time	2.617	<0.0001	****	Yes
Agarose	0.8774	<0.0001	****	Yes

ANOVA table	SS	DF	MS	F (DFn, DF	P value
Interaction	0.3751	8	0.04688	F (8, 3880)	P<0.0001
Time	0.7175	4	0.1794	F (4, 3880)	P<0.0001
Agarose	0.2406	2	0.1203	F (2, 3880)	P<0.0001
Residual	26.08	3880	0.006722		

Number of mis 2075

Within each column, compare rows (simple effects within columns)

Number of fan 3
Number of co 10
Alpha 0.05

Bonferroni's m	Mean Diff.	95.00% CI	Significant?	Summary	Adjusted P Value
1%					
1 vs. 3	-0.014	-0.03201 to	No	ns	0.2905
1 vs. 5	-0.01083	-0.03457 to	No	ns	>0.9999
1 vs. 7	-0.01803	-0.03928 to	No	ns	0.1719
1 vs. 10	-0.03651	-0.06323 to	Yes	**	0.0013
3 vs. 5	0.003171	-0.02059 to	No	ns	>0.9999
3 vs. 7	-0.00403	-0.0253 to	No	ns	>0.9999
3 vs. 10	-0.02251	-0.04925 to	No	ns	0.1811
5 vs. 7	-0.0072	-0.0335 to	No	ns	>0.9999
5 vs. 10	-0.02568	-0.05657 to	No	ns	0.1959
7 vs. 10	-0.01848	-0.0475 to	No	ns	0.7376
3%					
1 vs. 3	-0.05539	-0.07341 to	Yes	****	<0.0001
1 vs. 5	-0.06886	-0.08636 to	Yes	****	<0.0001
1 vs. 7	-0.05803	-0.07458 to	Yes	****	<0.0001
1 vs. 10	-0.03175	-0.05257 to	Yes	***	0.0002
3 vs. 5	-0.01347	-0.03217 to	No	ns	0.432
3 vs. 7	-0.00264	-0.02045 to	No	ns	>0.9999
3 vs. 10	0.02364	0.001797 to	Yes	*	0.0238
5 vs. 7	0.01083	-0.006459	No	ns	0.7859
5 vs. 10	0.03711	0.01569 to	Yes	****	<0.0001
7 vs. 10	0.02628	0.005632 to	Yes	**	0.0035
5%					
1 vs. 3	-0.03128	-0.05035 to	Yes	****	<0.0001
1 vs. 5	-0.04876	-0.06894 to	Yes	****	<0.0001
1 vs. 7	-0.02849	-0.0466 to	Yes	***	0.0001
1 vs. 10	-0.02359	-0.04572 to	Yes	*	0.0279
3 vs. 5	-0.01748	-0.03907 to	No	ns	0.2302
3 vs. 7	0.002793	-0.01688 to	No	ns	>0.9999
3 vs. 10	0.007694	-0.01574 to	No	ns	>0.9999
5 vs. 7	0.02028	-0.000474	No	ns	0.0609
5 vs. 10	0.02518	0.0008305	Yes	*	0.037
7 vs. 10	0.004901	-0.01776 to	No	ns	>0.9999

Test details	Mean 1	Mean 2	Mean Diff.	SE of diff.	N1	N2	t	DF
1%								
1 vs. 3	0.1722	0.1862	-0.014	0.006412	328	326	2.184	3880
1 vs. 5	0.1722	0.1831	-0.01083	0.008451	328	132	1.282	3880
1 vs. 7	0.1722	0.1903	-0.01803	0.007565	328	183	2.384	3880
1 vs. 10	0.1722	0.2087	-0.03651	0.009514	328	96	3.838	3880
3 vs. 5	0.1862	0.1831	0.003171	0.008459	326	132	0.3749	3880
3 vs. 7	0.1862	0.1903	-0.00403	0.007573	326	183	0.5321	3880
3 vs. 10	0.1862	0.2087	-0.02251	0.009521	326	96	2.364	3880
5 vs. 7	0.1831	0.1903	-0.0072	0.009363	132	183	0.7691	3880
5 vs. 10	0.1831	0.2087	-0.02568	0.011	132	96	2.335	3880
7 vs. 10	0.1903	0.2087	-0.01848	0.01033	183	96	1.789	3880
3%								
1 vs. 3	0.1656	0.2209	-0.05539	0.006417	377	288	8.633	3880
1 vs. 5	0.1656	0.2344	-0.06886	0.006232	377	320	11.05	3880
1 vs. 7	0.1656	0.2236	-0.05803	0.005892	377	398	9.848	3880
1 vs. 10	0.1656	0.1973	-0.03175	0.007414	377	181	4.282	3880
3 vs. 5	0.2209	0.2344	-0.01347	0.006659	288	320	2.022	3880
3 vs. 7	0.2209	0.2236	-0.00264	0.006343	288	398	0.4157	3880
3 vs. 10	0.2209	0.1973	0.02364	0.007777	288	181	3.04	3880
5 vs. 7	0.2344	0.2236	0.01083	0.006156	320	398	1.759	3880
5 vs. 10	0.2344	0.1973	0.03711	0.007625	320	181	4.866	3880
7 vs. 10	0.2236	0.1973	0.02628	0.00735	398	181	3.575	3880
5%								
1 vs. 3	0.1763	0.2076	-0.03128	0.00679	348	251	4.607	3880
1 vs. 5	0.1763	0.225	-0.04876	0.007186	348	208	6.786	3880
1 vs. 7	0.1763	0.2048	-0.02849	0.006448	348	302	4.418	3880
1 vs. 10	0.1763	0.1999	-0.02359	0.007883	348	157	2.992	3880
3 vs. 5	0.2076	0.225	-0.01748	0.007688	251	208	2.274	3880
3 vs. 7	0.2076	0.2048	0.002793	0.007003	251	302	0.3988	3880
3 vs. 10	0.2076	0.1999	0.007694	0.008343	251	157	0.9223	3880
5 vs. 7	0.225	0.2048	0.02028	0.007388	208	302	2.744	3880
5 vs. 10	0.225	0.1999	0.02518	0.008668	208	157	2.904	3880
7 vs. 10	0.2048	0.1999	0.004901	0.008067	302	157	0.6075	3880

Within each row, compare columns (simple effects within rows)

Number of fam 5
Number of con 3
Alpha 0.05

Bonferroni's m	Mean Diff.	95.00% CI	Significant?	Summary	Adjusted P Value
1					
1% vs. 3%	0.006661	-0.008166	No	ns	0.846
1% vs. 5%	-0.00406	-0.01917 to	No	ns	>0.9999
3% vs. 5%	-0.01072	-0.02532 to	No	ns	0.2359
3					
1% vs. 3%	-0.03473	-0.05061 to	Yes	****	<0.0001
1% vs. 5%	-0.02134	-0.03783 to	Yes	**	0.0059
3% vs. 5%	0.01339	-0.003566	No	ns	0.176
5					
1% vs. 3%	-0.05137	-0.07168 to	Yes	****	<0.0001
1% vs. 5%	-0.04199	-0.06384 to	Yes	****	<0.0001
3% vs. 5%	0.009376	-0.008113	No	ns	0.5977
7					
1% vs. 3%	-0.03334	-0.05087 to	Yes	****	<0.0001
1% vs. 5%	-0.01452	-0.03291 to	No	ns	0.1766
3% vs. 5%	0.01882	0.003835 to	Yes	**	0.0079
10					
1% vs. 3%	0.01142	-0.01337 to	No	ns	0.8098
1% vs. 5%	0.008866	-0.01658 to	No	ns	>0.9999
3% vs. 5%	-0.00256	-0.02397 to	No	ns	>0.9999

Test details	Mean 1	Mean 2	Mean Diff.	SE of diff.	N1	N2	t	DF
1								
1% vs. 3%	0.1722	0.1656	0.006661	0.006191	328	377	1.076	3880
1% vs. 5%	0.1722	0.1763	-0.00406	0.00631	328	348	0.6436	3880
3% vs. 5%	0.1656	0.1763	-0.01072	0.006095	377	348	1.759	3880
3								
1% vs. 3%	0.1862	0.2209	-0.03473	0.00663	326	288	5.238	3880
1% vs. 5%	0.1862	0.2076	-0.02134	0.006885	326	251	3.099	3880
3% vs. 5%	0.2209	0.2076	0.01339	0.00708	288	251	1.891	3880
5								
1% vs. 3%	0.1831	0.2344	-0.05137	0.008481	132	320	6.056	3880
1% vs. 5%	0.1831	0.225	-0.04199	0.009124	132	208	4.602	3880
3% vs. 5%	0.2344	0.225	0.009376	0.007302	320	208	1.284	3880
7								
1% vs. 3%	0.1903	0.2236	-0.03334	0.007323	183	398	4.552	3880
1% vs. 5%	0.1903	0.2048	-0.01452	0.007681	183	302	1.89	3880
3% vs. 5%	0.2236	0.2048	0.01882	0.006257	398	302	3.008	3880
10								
1% vs. 3%	0.2087	0.1973	0.01142	0.01035	96	181	1.103	3880
1% vs. 5%	0.2087	0.1999	0.008866	0.01062	96	157	0.8346	3880
3% vs. 5%	0.1973	0.1999	-0.00256	0.008942	181	157	0.2858	3880

Table 25 – – One-way ANOVA for the effects of time and hydrogel stiffness on Chapter 4 data – STELLATE FACTOR

Table Analyze Data 1

Two-way ANC Ordinary
Alpha 0.05

Source of Var	% of total \	P value	P value su	Significant?
Interaction	1.106	<0.0001	****	Yes
Time	1.614	<0.0001	****	Yes
Agarose	0.696	<0.0001	****	Yes

ANOVA table	SS	DF	MS	F (DFn, DF	P value
Interaction	1.519	8	0.1899	F (8, 3880)	P<0.0001
Time	2.217	4	0.5542	F (4, 3880)	P<0.0001
Agarose	0.9559	2	0.4779	F (2, 3880)	P<0.0001
Residual	132.7	3880	0.03419		

Number of mis 2075

Within each column, compare rows (simple effects within columns)

Number of fan 3
Number of cor 10
Alpha 0.05

Bonferroni's m	Mean Diff.	95.00% CI	Significant?	Summary	Adjusted P Value
1%					
1 vs. 3	0.00866	-0.03195 to	No	ns	>0.9999
1 vs. 5	0.005279	-0.04825 to	No	ns	>0.9999
1 vs. 7	0.04837	0.0004525	Yes	*	0.046
1 vs. 10	0.1079	0.04765 to	Yes	****	<0.0001
3 vs. 5	-0.00338	-0.05696 to	No	ns	>0.9999
3 vs. 7	0.03971	-0.00826 to	No	ns	0.2012
3 vs. 10	0.09925	0.03894 to	Yes	****	<0.0001
5 vs. 7	0.04309	-0.01621 to	No	ns	0.4134
5 vs. 10	0.1026	0.03297 to	Yes	***	0.0004
7 vs. 10	0.05954	-0.005906	No	ns	0.1065
3%					
1 vs. 3	0.04169	0.001046 t	Yes	*	0.0399
1 vs. 5	0.02691	-0.01257 to	No	ns	0.5564
1 vs. 7	0.0717	0.03438 to	Yes	****	<0.0001
1 vs. 10	0.05517	0.008207 t	Yes	**	0.0098
3 vs. 5	-0.01478	-0.05696 to	No	ns	>0.9999
3 vs. 7	0.03001	-0.01017 to	No	ns	0.3598
3 vs. 10	0.01348	-0.03578 to	No	ns	>0.9999
5 vs. 7	0.04479	0.005799 t	Yes	*	0.0126
5 vs. 10	0.02826	-0.02004 to	No	ns	>0.9999
7 vs. 10	-0.01653	-0.06309 to	No	ns	>0.9999
5%					
1 vs. 3	0.06934	0.02634 to	Yes	****	<0.0001
1 vs. 5	0.1026	0.05709 to	Yes	****	<0.0001
1 vs. 7	0.07397	0.03313 to	Yes	****	<0.0001
1 vs. 10	0.063	0.01307 to	Yes	**	0.004
3 vs. 5	0.03326	-0.01543 to	No	ns	0.5512
3 vs. 7	0.004628	-0.03973 to	No	ns	>0.9999
3 vs. 10	-0.00634	-0.05919 to	No	ns	>0.9999
5 vs. 7	-0.02863	-0.07543 to	No	ns	0.8575
5 vs. 10	-0.03961	-0.09451 to	No	ns	0.4283
7 vs. 10	-0.01097	-0.06207 to	No	ns	>0.9999

Test details	Mean 1	Mean 2	Mean Diff.	SE of diff.	N1	N2	t	DF
1%								
1 vs. 3	0.4633	0.4546	0.00866	0.01446	328	326	0.5989	3880
1 vs. 5	0.4633	0.458	0.005279	0.01906	328	132	0.277	3880
1 vs. 7	0.4633	0.4149	0.04837	0.01706	328	183	2.835	3880
1 vs. 10	0.4633	0.3554	0.1079	0.02146	328	96	5.029	3880
3 vs. 5	0.4546	0.458	-0.00338	0.01908	326	132	0.1772	3880
3 vs. 7	0.4546	0.4149	0.03971	0.01708	326	183	2.325	3880
3 vs. 10	0.4546	0.3554	0.09925	0.02147	326	96	4.622	3880
5 vs. 7	0.458	0.4149	0.04309	0.02111	132	183	2.041	3880
5 vs. 10	0.458	0.3554	0.1026	0.0248	132	96	4.138	3880
7 vs. 10	0.4149	0.3554	0.05954	0.0233	183	96	2.555	3880
3%								
1 vs. 3	0.4267	0.385	0.04169	0.01447	377	288	2.881	3880
1 vs. 5	0.4267	0.3998	0.02691	0.01405	377	320	1.914	3880
1 vs. 7	0.4267	0.355	0.0717	0.01329	377	398	5.395	3880
1 vs. 10	0.4267	0.3715	0.05517	0.01672	377	181	3.299	3880
3 vs. 5	0.385	0.3998	-0.01478	0.01502	288	320	0.9843	3880
3 vs. 7	0.385	0.355	0.03001	0.0143	288	398	2.098	3880
3 vs. 10	0.385	0.3715	0.01348	0.01754	288	181	0.7686	3880
5 vs. 7	0.3998	0.355	0.04479	0.01388	320	398	3.226	3880
5 vs. 10	0.3998	0.3715	0.02826	0.0172	320	181	1.644	3880
7 vs. 10	0.355	0.3715	-0.01653	0.01658	398	181	0.9971	3880
5%								
1 vs. 3	0.4693	0.4	0.06934	0.01531	348	251	4.529	3880
1 vs. 5	0.4693	0.3667	0.1026	0.01621	348	208	6.331	3880
1 vs. 7	0.4693	0.3954	0.07397	0.01454	348	302	5.087	3880
1 vs. 10	0.4693	0.4063	0.063	0.01778	348	157	3.544	3880
3 vs. 5	0.4	0.3667	0.03326	0.01734	251	208	1.919	3880
3 vs. 7	0.4	0.3954	0.004628	0.01579	251	302	0.293	3880
3 vs. 10	0.4	0.4063	-0.00634	0.01881	251	157	0.3371	3880
5 vs. 7	0.3667	0.3954	-0.02863	0.01666	208	302	1.719	3880
5 vs. 10	0.3667	0.4063	-0.03961	0.01955	208	157	2.026	3880
7 vs. 10	0.3954	0.4063	-0.01097	0.01819	302	157	0.603	3880

Within each row, compare columns (simple effects within rows)

Number of fam 5
Number of con 3
Alpha 0.05

Bonferroni's m	Mean Diff.	95.00% CI	Significant	Summary	Adjusted P Value
1					
1% vs. 3%	0.03664	0.003197 t	Yes	*	0.0262
1% vs. 5%	-0.00604	-0.04012 to	No	ns	>0.9999
3% vs. 5%	-0.04268	-0.0756 to	Yes	**	0.0058
3					
1% vs. 3%	0.06966	0.03385 to	Yes	****	<0.0001
1% vs. 5%	0.05464	0.01745 to	Yes	**	0.0013
3% vs. 5%	-0.01503	-0.05326 to	No	ns	>0.9999
5					
1% vs. 3%	0.05826	0.01245 to	Yes	**	0.007
1% vs. 5%	0.09128	0.042 to 0.	Yes	****	<0.0001
3% vs. 5%	0.03302	-0.006422	No	ns	0.1351
7					
1% vs. 3%	0.05996	0.02041 to	Yes	***	0.0009
1% vs. 5%	0.01956	-0.02193 to	No	ns	0.7767
3% vs. 5%	-0.04041	-0.0742 to	Yes	*	0.0126
10					
1% vs. 3%	-0.0161	-0.07202 to	No	ns	>0.9999
1% vs. 5%	-0.05095	-0.1083 to	No	ns	0.1005
3% vs. 5%	-0.03485	-0.08314 to	No	ns	0.2522

Test details	Mean 1	Mean 2	Mean Diff.	SE of diff.	N1	N2	t	DF
1								
1% vs. 3%	0.4633	0.4267	0.03664	0.01396	328	377	2.624	3880
1% vs. 5%	0.4633	0.4693	-0.00604	0.01423	328	348	0.4246	3880
3% vs. 5%	0.4267	0.4693	-0.04268	0.01375	377	348	3.105	3880
3								
1% vs. 3%	0.4546	0.385	0.06966	0.01495	326	288	4.659	3880
1% vs. 5%	0.4546	0.4	0.05464	0.01553	326	251	3.519	3880
3% vs. 5%	0.385	0.4	-0.01503	0.01597	288	251	0.941	3880
5								
1% vs. 3%	0.458	0.3998	0.05826	0.01913	132	320	3.046	3880
1% vs. 5%	0.458	0.3667	0.09128	0.02058	132	208	4.436	3880
3% vs. 5%	0.3998	0.3667	0.03302	0.01647	320	208	2.005	3880
7								
1% vs. 3%	0.4149	0.355	0.05996	0.01651	183	398	3.631	3880
1% vs. 5%	0.4149	0.3954	0.01956	0.01732	183	302	1.129	3880
3% vs. 5%	0.355	0.3954	-0.04041	0.01411	398	302	2.864	3880
10								
1% vs. 3%	0.3554	0.3715	-0.0161	0.02335	96	181	0.6898	3880
1% vs. 5%	0.3554	0.4063	-0.05095	0.02396	96	157	2.127	3880
3% vs. 5%	0.3715	0.4063	-0.03485	0.02017	181	157	1.728	3880

Table 26 – – One-way ANOVA for the effects of time and hydrogel stiffness on Chapter 4 data – LENGTH

Table Analyze Data 1

Two-way ANC Ordinary
Alpha 0.05

Source of Var	% of total \	P value	P value su	Significant?
Interaction	0.7612	0.0002	***	Yes
Time	1.09	<0.0001	****	Yes
Agarose	0.07368	0.233	ns	No

ANOVA table	SS	DF	MS	F (DFn, DF	P value
Interaction	97393	8	12174	F (8, 3880)	P=0.0002
Time	139417	4	34854	F (4, 3880)	P<0.0001
Agarose	9427	2	4713	F (2, 3880)	P=0.2330
Residual	12548003	3880	3234		

Number of mi: 2075

Within each column, compare rows (simple effects within columns)

Number of fan 3
Number of coı 10
Alpha 0.05

Bonferroni's m	Mean Diff.	95.00% CI	Significant?	Summary	Adjusted P Value
1%					
1 vs. 3	-3.496	-15.99 to 8	No	ns	>0.9999
1 vs. 5	-3.323	-19.79 to 1	No	ns	>0.9999
1 vs. 7	-17.17	-31.91 to -2	Yes	*	0.0107
1 vs. 10	-7.243	-25.78 to 1	No	ns	>0.9999
3 vs. 5	0.173	-16.31 to 1	No	ns	>0.9999
3 vs. 7	-13.68	-28.43 to 1	No	ns	0.0926
3 vs. 10	-3.748	-22.29 to 1	No	ns	>0.9999
5 vs. 7	-13.85	-32.09 to 4	No	ns	0.3302
5 vs. 10	-3.921	-25.35 to 1	No	ns	>0.9999
7 vs. 10	9.929	-10.2 to 30	No	ns	>0.9999
3%					
1 vs. 3	-11.92	-24.42 to 0	No	ns	0.0742
1 vs. 5	-17.72	-29.86 to -5	Yes	***	0.0004
1 vs. 7	-21.15	-32.63 to -9	Yes	****	<0.0001
1 vs. 10	-9.992	-24.44 to 4	No	ns	0.5208
3 vs. 5	-5.794	-18.77 to 7	No	ns	>0.9999
3 vs. 7	-9.232	-21.59 to 3	No	ns	0.3593
3 vs. 10	1.93	-13.22 to 1	No	ns	>0.9999
5 vs. 7	-3.438	-15.43 to 8	No	ns	>0.9999
5 vs. 10	7.725	-7.13 to 22	No	ns	>0.9999
7 vs. 10	11.16	-3.157 to 2	No	ns	0.2862
5%					
1 vs. 3	-3.567	-16.79 to 9	No	ns	>0.9999
1 vs. 5	-7.448	-21.45 to 6	No	ns	>0.9999
1 vs. 7	-14.27	-26.84 to -1	Yes	*	0.0143
1 vs. 10	-31.94	-47.29 to -1	Yes	****	<0.0001
3 vs. 5	-3.881	-18.86 to 1	No	ns	>0.9999
3 vs. 7	-10.71	-24.35 to 2	No	ns	0.2756
3 vs. 10	-28.37	-44.62 to -1	Yes	****	<0.0001
5 vs. 7	-6.826	-21.22 to 7	No	ns	>0.9999
5 vs. 10	-24.49	-41.37 to -7	Yes	***	0.0005
7 vs. 10	-17.66	-33.38 to -1	Yes	*	0.0161

Test details	Mean 1	Mean 2	Mean Diff.	SE of diff.	N1	N2	t	DF
1%								
1 vs. 3	57.94	61.44	-3.496	4.447	328	326	0.786	3880
1 vs. 5	57.94	61.26	-3.323	5.862	328	132	0.5668	3880
1 vs. 7	57.94	75.11	-17.17	5.247	328	183	3.273	3880
1 vs. 10	57.94	65.18	-7.243	6.599	328	96	1.098	3880
3 vs. 5	61.44	61.26	0.173	5.867	326	132	0.02949	3880
3 vs. 7	61.44	75.11	-13.68	5.253	326	183	2.604	3880
3 vs. 10	61.44	65.18	-3.748	6.604	326	96	0.5675	3880
5 vs. 7	61.26	75.11	-13.85	6.494	132	183	2.133	3880
5 vs. 10	61.26	65.18	-3.921	7.628	132	96	0.514	3880
7 vs. 10	75.11	65.18	9.929	7.167	183	96	1.385	3880
3%								
1 vs. 3	56.09	68.01	-11.92	4.451	377	288	2.679	3880
1 vs. 5	56.09	73.81	-17.72	4.323	377	320	4.099	3880
1 vs. 7	56.09	77.24	-21.15	4.087	377	398	5.176	3880
1 vs. 10	56.09	66.08	-9.992	5.143	377	181	1.943	3880
3 vs. 5	68.01	73.81	-5.794	4.619	288	320	1.254	3880
3 vs. 7	68.01	77.24	-9.232	4.399	288	398	2.098	3880
3 vs. 10	68.01	66.08	1.93	5.394	288	181	0.3579	3880
5 vs. 7	73.81	77.24	-3.438	4.27	320	398	0.8051	3880
5 vs. 10	73.81	66.08	7.725	5.289	320	181	1.461	3880
7 vs. 10	77.24	66.08	11.16	5.098	398	181	2.189	3880
5%								
1 vs. 3	55.47	59.04	-3.567	4.709	348	251	0.7575	3880
1 vs. 5	55.47	62.92	-7.448	4.984	348	208	1.494	3880
1 vs. 7	55.47	69.75	-14.27	4.472	348	302	3.192	3880
1 vs. 10	55.47	87.41	-31.94	5.467	348	157	5.841	3880
3 vs. 5	59.04	62.92	-3.881	5.332	251	208	0.7278	3880
3 vs. 7	59.04	69.75	-10.71	4.857	251	302	2.204	3880
3 vs. 10	59.04	87.41	-28.37	5.786	251	157	4.903	3880
5 vs. 7	62.92	69.75	-6.826	5.124	208	302	1.332	3880
5 vs. 10	62.92	87.41	-24.49	6.012	208	157	4.073	3880
7 vs. 10	69.75	87.41	-17.66	5.595	302	157	3.156	3880

Table 27 — One-way ANOVA for the effects of time and hydrogel stiffness on Chapter 4 data – CHROMATIN CONDENSATION

Table Analyze Data 1

Two-way ANC Ordinary
Alpha 0.05

Source of Var	% of total v	P value	P value su	Significant?
Interaction	2.133	<0.0001	****	Yes
Time	8.723	<0.0001	****	Yes
Agarose	0.09622	0.1231	ns	No

ANOVA table	SS	DF	MS	F (DFn, DF	P value
Interaction	0.00483	8	0.000604	F (8, 3880)	P<0.0001
Time	0.01975	4	0.004937	F (4, 3880)	P<0.0001
Agarose	0.000218	2	0.000109	F (2, 3880)	P=0.1231
Residual	0.2016	3880	5.2E-05		

Number of mis 2075

Within each column, compare rows (simple effects within columns)

Number of fan 3
Number of cor 10
Alpha 0.05

Bonferroni's m	Mean Diff.	95.00% CI	Significant?	Summary	Adjusted P Value
1%					
1 vs. 3	0.002112	0.0005286	Yes	**	0.0018
1 vs. 5	0.005768	0.003681 t	Yes	****	<0.0001
1 vs. 7	0.006428	0.00456 to	Yes	****	<0.0001
1 vs. 10	0.005436	0.003087 t	Yes	****	<0.0001
3 vs. 5	0.003656	0.001567 t	Yes	****	<0.0001
3 vs. 7	0.004316	0.002446 t	Yes	****	<0.0001
3 vs. 10	0.003324	0.000973 t	Yes	***	0.0007
5 vs. 7	0.00066	-0.001652	No	ns	>0.9999
5 vs. 10	-0.00033	-0.003048	No	ns	>0.9999
7 vs. 10	-0.00099	-0.003543	No	ns	>0.9999
3%					
1 vs. 3	-0.00328	-0.004859	Yes	****	<0.0001
1 vs. 5	0.004319	0.00278 to	Yes	****	<0.0001
1 vs. 7	0.003403	0.001948 t	Yes	****	<0.0001
1 vs. 10	0.004324	0.002493 t	Yes	****	<0.0001
3 vs. 5	0.007594	0.00595 to	Yes	****	<0.0001
3 vs. 7	0.006678	0.005112 t	Yes	****	<0.0001
3 vs. 10	0.007599	0.005679 t	Yes	****	<0.0001
5 vs. 7	-0.00092	-0.002436	No	ns	0.9065
5 vs. 10	0.000005	-0.001878	No	ns	>0.9999
7 vs. 10	0.000921	-0.0008941	No	ns	>0.9999
5%					
1 vs. 3	-0.0063	-0.007976	Yes	****	<0.0001
1 vs. 5	0.001206	-0.0005684	No	ns	0.5635
1 vs. 7	-2.6E-05	-0.001618	No	ns	>0.9999
1 vs. 10	0.000407	-0.001539	No	ns	>0.9999
3 vs. 5	0.007505	0.005607 t	Yes	****	<0.0001
3 vs. 7	0.006273	0.004544 t	Yes	****	<0.0001
3 vs. 10	0.006706	0.004646 t	Yes	****	<0.0001
5 vs. 7	-0.00123	-0.003056	No	ns	0.5793
5 vs. 10	-0.0008	-0.002939	No	ns	>0.9999
7 vs. 10	0.000433	-0.001559	No	ns	>0.9999

Test details	Mean 1	Mean 2	Mean Diff.	SE of diff.	N1	N2	t	DF
1%								
1 vs. 3	0.02867	0.02656	0.002112	0.000564	328	326	3.746	3880
1 vs. 5	0.02867	0.0229	0.005768	0.000743	328	132	7.763	3880
1 vs. 7	0.02867	0.02224	0.006428	0.000665	328	183	9.665	3880
1 vs. 10	0.02867	0.02323	0.005436	0.000837	328	96	6.499	3880
3 vs. 5	0.02656	0.0229	0.003656	0.000744	326	132	4.916	3880
3 vs. 7	0.02656	0.02224	0.004316	0.000666	326	183	6.482	3880
3 vs. 10	0.02656	0.02323	0.003324	0.000837	326	96	3.971	3880
5 vs. 7	0.0229	0.02224	0.00066	0.000823	132	183	0.8018	3880
5 vs. 10	0.0229	0.02323	-0.00033	0.000967	132	96	0.3434	3880
7 vs. 10	0.02224	0.02323	-0.00099	0.000908	183	96	1.092	3880
3%								
1 vs. 3	0.02622	0.0295	-0.00328	0.000564	377	288	5.805	3880
1 vs. 5	0.02622	0.0219	0.004319	0.000548	377	320	7.883	3880
1 vs. 7	0.02622	0.02282	0.003403	0.000518	377	398	6.569	3880
1 vs. 10	0.02622	0.0219	0.004324	0.000652	377	181	6.633	3880
3 vs. 5	0.0295	0.0219	0.007594	0.000586	288	320	12.97	3880
3 vs. 7	0.0295	0.02282	0.006678	0.000558	288	398	11.98	3880
3 vs. 10	0.0295	0.0219	0.007599	0.000684	288	181	11.11	3880
5 vs. 7	0.0219	0.02282	-0.00092	0.000541	320	398	1.692	3880
5 vs. 10	0.0219	0.0219	0.000005	0.00067	320	181	0.007458	3880
7 vs. 10	0.02282	0.0219	0.000921	0.000646	398	181	1.425	3880
5%								
1 vs. 3	0.02415	0.03045	-0.0063	0.000597	348	251	10.55	3880
1 vs. 5	0.02415	0.02294	0.001206	0.000632	348	208	1.909	3880
1 vs. 7	0.02415	0.02418	-2.6E-05	0.000567	348	302	0.04586	3880
1 vs. 10	0.02415	0.02374	0.000407	0.000693	348	157	0.5873	3880
3 vs. 5	0.03045	0.02294	0.007505	0.000676	251	208	11.1	3880
3 vs. 7	0.03045	0.02418	0.006273	0.000616	251	302	10.19	3880
3 vs. 10	0.03045	0.02374	0.006706	0.000734	251	157	9.143	3880
5 vs. 7	0.02294	0.02418	-0.00123	0.00065	208	302	1.897	3880
5 vs. 10	0.02294	0.02374	-0.0008	0.000762	208	157	1.048	3880
7 vs. 10	0.02418	0.02374	0.000433	0.000709	302	157	0.6105	3880

Table 28 – – One-way ANOVA for the effects of time and hydrogel stiffness on Chapter 4 data – NUCLEUS VOLUME

Table Analyze Data 1

Two-way ANC Ordinary
Alpha 0.05

Source of Var	% of total \	P value	P value su	Significant?
Interaction	0.9968	<0.0001	****	Yes
Time	4.481	<0.0001	****	Yes
Agarose	1.004	<0.0001	****	Yes

ANOVA table	SS	DF	MS	F (DFn, DF	P value
Interaction	3.512	8	0.439	F (8, 3880)	P<0.0001
Time	15.79	4	3.947	F (4, 3880)	P<0.0001
Agarose	3.539	2	1.77	F (2, 3880)	P<0.0001
Residual	329.5	3880	0.08492		

Number of mis 2075

Within each column, compare rows (simple effects within columns)

Number of fan 3
Number of cor 10
Alpha 0.05

Bonferroni's m	Mean Diff.	95.00% CI	Significant	Summary	Adjusted P Value
1%					
1 vs. 3	0.05137	-0.01264 t	No	ns	0.2424
1 vs. 5	0.2309	0.1465 to (	Yes	****	<0.0001
1 vs. 7	0.03	-0.04552 t	No	ns	>0.9999
1 vs. 10	-0.1053	-0.2003 to	Yes	*	0.0186
3 vs. 5	0.1795	0.09507 to	Yes	****	<0.0001
3 vs. 7	-0.02138	-0.09698 t	No	ns	>0.9999
3 vs. 10	-0.1567	-0.2517 to	Yes	****	<0.0001
5 vs. 7	-0.2009	-0.2944 to	Yes	****	<0.0001
5 vs. 10	-0.3362	-0.446 to -(	Yes	****	<0.0001
7 vs. 10	-0.1353	-0.2384 to	Yes	**	0.0023
3%					
1 vs. 3	-0.01722	-0.08127 t	No	ns	>0.9999
1 vs. 5	0.1409	0.07865 to	Yes	****	<0.0001
1 vs. 7	0.004384	-0.05444 t	No	ns	>0.9999
1 vs. 10	-0.03836	-0.1124 to	No	ns	>0.9999
3 vs. 5	0.1581	0.0916 to (	Yes	****	<0.0001
3 vs. 7	0.0216	-0.04171 t	No	ns	>0.9999
3 vs. 10	-0.02114	-0.09878 t	No	ns	>0.9999
5 vs. 7	-0.1365	-0.1979 to	Yes	****	<0.0001
5 vs. 10	-0.1792	-0.2553 to	Yes	****	<0.0001
7 vs. 10	-0.04274	-0.1161 to	No	ns	>0.9999
5%					
1 vs. 3	0.04469	-0.02308 t	No	ns	0.6409
1 vs. 5	0.09246	0.02072 to	Yes	**	0.003
1 vs. 7	-0.0054	-0.06977 t	No	ns	>0.9999
1 vs. 10	-0.01882	-0.09751 t	No	ns	>0.9999
3 vs. 5	0.04776	-0.02898 t	No	ns	0.8054
3 vs. 7	-0.0501	-0.12 to 0.(	No	ns	0.4422
3 vs. 10	-0.06351	-0.1468 to	No	ns	0.3226
5 vs. 7	-0.09786	-0.1716 to	Yes	**	0.002
5 vs. 10	-0.1113	-0.1978 to	Yes	**	0.0031
7 vs. 10	-0.01342	-0.09395 t	No	ns	>0.9999

Test details	Mean 1	Mean 2	Mean Diff.	SE of diff.	N1	N2	t	DF
1%								
1 vs. 3	1.268	1.217	0.05137	0.02279	328	326	2.254	3880
1 vs. 5	1.268	1.037	0.2309	0.03004	328	132	7.687	3880
1 vs. 7	1.268	1.238	0.03	0.02689	328	183	1.116	3880
1 vs. 10	1.268	1.374	-0.1053	0.03382	328	96	3.114	3880
3 vs. 5	1.217	1.037	0.1795	0.03006	326	132	5.971	3880
3 vs. 7	1.217	1.238	-0.02138	0.02692	326	183	0.7942	3880
3 vs. 10	1.217	1.374	-0.1567	0.03384	326	96	4.63	3880
5 vs. 7	1.037	1.238	-0.2009	0.03328	132	183	6.037	3880
5 vs. 10	1.037	1.374	-0.3362	0.03909	132	96	8.6	3880
7 vs. 10	1.238	1.374	-0.1353	0.03672	183	96	3.684	3880
3%								
1 vs. 3	1.322	1.339	-0.01722	0.02281	377	288	0.7551	3880
1 vs. 5	1.322	1.181	0.1409	0.02215	377	320	6.359	3880
1 vs. 7	1.322	1.317	0.004384	0.02094	377	398	0.2093	3880
1 vs. 10	1.322	1.36	-0.03836	0.02635	377	181	1.456	3880
3 vs. 5	1.339	1.181	0.1581	0.02367	288	320	6.679	3880
3 vs. 7	1.339	1.317	0.0216	0.02254	288	398	0.9583	3880
3 vs. 10	1.339	1.36	-0.02114	0.02764	288	181	0.7648	3880
5 vs. 7	1.181	1.317	-0.1365	0.02188	320	398	6.237	3880
5 vs. 10	1.181	1.36	-0.1792	0.0271	320	181	6.613	3880
7 vs. 10	1.317	1.36	-0.04274	0.02613	398	181	1.636	3880
5%								
1 vs. 3	1.308	1.263	0.04469	0.02413	348	251	1.852	3880
1 vs. 5	1.308	1.215	0.09246	0.02554	348	208	3.62	3880
1 vs. 7	1.308	1.313	-0.0054	0.02292	348	302	0.2357	3880
1 vs. 10	1.308	1.327	-0.01882	0.02802	348	157	0.6717	3880
3 vs. 5	1.263	1.215	0.04776	0.02732	251	208	1.748	3880
3 vs. 7	1.263	1.313	-0.0501	0.02489	251	302	2.013	3880
3 vs. 10	1.263	1.327	-0.06351	0.02965	251	157	2.142	3880
5 vs. 7	1.215	1.313	-0.09786	0.02626	208	302	3.727	3880
5 vs. 10	1.215	1.327	-0.1113	0.03081	208	157	3.612	3880
7 vs. 10	1.313	1.327	-0.01342	0.02867	302	157	0.468	3880

Within each row, compare columns (simple effects within rows)

Number of fam 5
Number of con 3
Alpha 0.05

Bonferroni's m	Mean Diff.	95.00% CI	Significant	Summary	Adjusted P Value
1					
1% vs. 3%	-0.05337	-0.1061 to	Yes	*	0.046
1% vs. 5%	-0.03963	-0.09334 t	No	ns	0.2319
3% vs. 5%	0.01374	-0.03814 t	No	ns	>0.9999
3					
1% vs. 3%	-0.122	-0.1784 to	Yes	****	<0.0001
1% vs. 5%	-0.04631	-0.1049 to	No	ns	0.1755
3% vs. 5%	0.07565	0.01539 to	Yes	**	0.008
5					
1% vs. 3%	-0.1434	-0.2156 to	Yes	****	<0.0001
1% vs. 5%	-0.1781	-0.2557 to	Yes	****	<0.0001
3% vs. 5%	-0.03466	-0.09682 t	No	ns	0.5454
7					
1% vs. 3%	-0.07898	-0.1413 to	Yes	**	0.0073
1% vs. 5%	-0.07503	-0.1404 to	Yes	*	0.0181
3% vs. 5%	0.003955	-0.04931 t	No	ns	>0.9999
10					
1% vs. 3%	0.01356	-0.07456 t	No	ns	>0.9999
1% vs. 5%	0.04685	-0.04358 t	No	ns	0.6443
3% vs. 5%	0.03328	-0.04284 t	No	ns	0.8852

Test details	Mean 1	Mean 2	Mean Diff.	SE of diff.	N1	N2	t	DF
1								
1% vs. 3%	1.268	1.322	-0.05337	0.022	328	377	2.426	3880
1% vs. 5%	1.268	1.308	-0.03963	0.02243	328	348	1.767	3880
3% vs. 5%	1.322	1.308	0.01374	0.02166	377	348	0.6343	3880
3								
1% vs. 3%	1.217	1.339	-0.122	0.02357	326	288	5.175	3880
1% vs. 5%	1.217	1.263	-0.04631	0.02447	326	251	1.892	3880
3% vs. 5%	1.339	1.263	0.07565	0.02516	288	251	3.007	3880
5								
1% vs. 3%	1.037	1.181	-0.1434	0.03014	132	320	4.757	3880
1% vs. 5%	1.037	1.215	-0.1781	0.03243	132	208	5.491	3880
3% vs. 5%	1.181	1.215	-0.03466	0.02595	320	208	1.335	3880
7								
1% vs. 3%	1.238	1.317	-0.07898	0.02603	183	398	3.035	3880
1% vs. 5%	1.238	1.313	-0.07503	0.0273	183	302	2.748	3880
3% vs. 5%	1.317	1.313	0.003955	0.02224	398	302	0.1778	3880
10								
1% vs. 3%	1.374	1.36	0.01356	0.03679	96	181	0.3687	3880
1% vs. 5%	1.374	1.327	0.04685	0.03776	96	157	1.241	3880
3% vs. 5%	1.36	1.327	0.03328	0.03178	181	157	1.047	3880

Table 29 – One-way ANOVA for the effects of time and hydrogel stiffness on Chapter 4 data – POISSON'S RATIO

Table Analyze Data 1

Two-way ANC Ordinary
Alpha 0.05

Source of Var	% of total \	P value	P value su	Significant?
Interaction	3.013	<0.0001	****	Yes
Time	3.295	<0.0001	****	Yes
Agarose	1.985	<0.0001	****	Yes

ANOVA table	SS	DF	MS	F (DFn, DF	P value
Interaction	2.255	8	0.2819	F (8, 3880)	P<0.0001
Time	2.466	4	0.6165	F (4, 3880)	P<0.0001
Agarose	1.486	2	0.743	F (2, 3880)	P<0.0001
Residual	68.64	3880	0.01769		

Number of mis 2075

Within each column, compare rows (simple effects within columns)

Number of fan 3
Number of cor 10
Alpha 0.05

Bonferroni's m	Mean Diff.	95.00% CI	Significant?	Summary	Adjusted P Value
1%					
1 vs. 3	-0.07054	-0.09976 to	Yes	****	<0.0001
1 vs. 5	-0.0773	-0.1158 to	Yes	****	<0.0001
1 vs. 7	-0.07874	-0.1132 to	Yes	****	<0.0001
1 vs. 10	-0.02495	-0.0683 to	No	ns	>0.9999
3 vs. 5	-0.00676	-0.0453 to	No	ns	>0.9999
3 vs. 7	-0.0082	-0.04271 to	No	ns	>0.9999
3 vs. 10	0.04559	0.002211 to	Yes	*	0.0318
5 vs. 7	-0.00144	-0.0441 to	No	ns	>0.9999
5 vs. 10	0.05235	0.002241 to	Yes	*	0.0336
7 vs. 10	0.05379	0.006713 to	Yes	*	0.0134
3%					
1 vs. 3	-0.03048	-0.05972 to	Yes	*	0.0343
1 vs. 5	-0.08171	-0.1101 to	Yes	****	<0.0001
1 vs. 7	-0.05684	-0.08369 to	Yes	****	<0.0001
1 vs. 10	-0.08892	-0.1227 to	Yes	****	<0.0001
3 vs. 5	-0.05123	-0.08157 to	Yes	****	<0.0001
3 vs. 7	-0.02636	-0.05526 to	No	ns	0.1045
3 vs. 10	-0.05844	-0.09387 to	Yes	****	<0.0001
5 vs. 7	0.02487	-0.003179	No	ns	0.128
5 vs. 10	-0.00721	-0.04195 to	No	ns	>0.9999
7 vs. 10	-0.03208	-0.06557 to	No	ns	0.0717
5%					
1 vs. 3	0.00747	-0.02347 to	No	ns	>0.9999
1 vs. 5	-0.01419	-0.04693 to	No	ns	>0.9999
1 vs. 7	-0.04887	-0.07825 to	Yes	****	<0.0001
1 vs. 10	-0.1202	-0.1561 to	Yes	****	<0.0001
3 vs. 5	-0.02166	-0.05669 to	No	ns	0.825
3 vs. 7	-0.05634	-0.08825 to	Yes	****	<0.0001
3 vs. 10	-0.1277	-0.1657 to	Yes	****	<0.0001
5 vs. 7	-0.03468	-0.06834 to	Yes	*	0.0383
5 vs. 10	-0.106	-0.1455 to	Yes	****	<0.0001
7 vs. 10	-0.07133	-0.1081 to	Yes	****	<0.0001

Test details	Mean 1	Mean 2	Mean Diff.	SE of diff.	N1	N2	t	DF
1%								
1 vs. 3	-0.3571	-0.2866	-0.07054	0.0104	328	326	6.781	3880
1 vs. 5	-0.3571	-0.2798	-0.0773	0.01371	328	132	5.638	3880
1 vs. 7	-0.3571	-0.2784	-0.07874	0.01227	328	183	6.416	3880
1 vs. 10	-0.3571	-0.3322	-0.02495	0.01543	328	96	1.617	3880
3 vs. 5	-0.2866	-0.2798	-0.00676	0.01372	326	132	0.4926	3880
3 vs. 7	-0.2866	-0.2784	-0.0082	0.01229	326	183	0.6674	3880
3 vs. 10	-0.2866	-0.3322	0.04559	0.01544	326	96	2.952	3880
5 vs. 7	-0.2798	-0.2784	-0.00144	0.01519	132	183	0.09481	3880
5 vs. 10	-0.2798	-0.3322	0.05235	0.01784	132	96	2.934	3880
7 vs. 10	-0.2784	-0.3322	0.05379	0.01676	183	96	3.209	3880
3%								
1 vs. 3	-0.3929	-0.3625	-0.03048	0.01041	377	288	2.928	3880
1 vs. 5	-0.3929	-0.3112	-0.08171	0.01011	377	320	8.082	3880
1 vs. 7	-0.3929	-0.3361	-0.05684	0.009559	377	398	5.946	3880
1 vs. 10	-0.3929	-0.304	-0.08892	0.01203	377	181	7.393	3880
3 vs. 5	-0.3625	-0.3112	-0.05123	0.0108	288	320	4.742	3880
3 vs. 7	-0.3625	-0.3361	-0.02636	0.01029	288	398	2.562	3880
3 vs. 10	-0.3625	-0.304	-0.05844	0.01262	288	181	4.632	3880
5 vs. 7	-0.3112	-0.3361	0.02487	0.009987	320	398	2.49	3880
5 vs. 10	-0.3112	-0.304	-0.00721	0.01237	320	181	0.5829	3880
7 vs. 10	-0.3361	-0.304	-0.03208	0.01192	398	181	2.69	3880
5%								
1 vs. 3	-0.3929	-0.4004	0.00747	0.01101	348	251	0.6782	3880
1 vs. 5	-0.3929	-0.3787	-0.01419	0.01166	348	208	1.217	3880
1 vs. 7	-0.3929	-0.344	-0.04887	0.01046	348	302	4.672	3880
1 vs. 10	-0.3929	-0.2727	-0.1202	0.01279	348	157	9.4	3880
3 vs. 5	-0.4004	-0.3787	-0.02166	0.01247	251	208	1.737	3880
3 vs. 7	-0.4004	-0.344	-0.05634	0.01136	251	302	4.959	3880
3 vs. 10	-0.4004	-0.2727	-0.1277	0.01353	251	157	9.433	3880
5 vs. 7	-0.3787	-0.344	-0.03468	0.01198	208	302	2.894	3880
5 vs. 10	-0.3787	-0.2727	-0.106	0.01406	208	157	7.539	3880
7 vs. 10	-0.344	-0.2727	-0.07133	0.01309	302	157	5.451	3880

Within each row, compare columns (simple effects within rows)

Number of fam 5
Number of con 3
Alpha 0.05

Bonferroni's m	Mean Diff.	95.00% CI	Significant?	Summary	Adjusted P Value
1					
1% vs. 3%	0.0358	0.01175 to	Yes	**	0.0011
1% vs. 5%	0.03578	0.01127 to	Yes	**	0.0014
3% vs. 5%	-0.00002	-0.0237 to	No	ns	>0.9999
3					
1% vs. 3%	0.07586	0.0501 to (	Yes	****	<0.0001
1% vs. 5%	0.1138	0.08704 to	Yes	****	<0.0001
3% vs. 5%	0.03793	0.01042 to	Yes	**	0.0029
5					
1% vs. 3%	0.03139	-0.001563	No	ns	0.0677
1% vs. 5%	0.09889	0.06344 to	Yes	****	<0.0001
3% vs. 5%	0.0675	0.03913 to	Yes	****	<0.0001
7					
1% vs. 3%	0.0577	0.02925 to	Yes	****	<0.0001
1% vs. 5%	0.06565	0.03581 to	Yes	****	<0.0001
3% vs. 5%	0.00795	-0.01636 to	No	ns	>0.9999
10					
1% vs. 3%	-0.02817	-0.06839 to	No	ns	0.2806
1% vs. 5%	-0.05947	-0.1007 to	Yes	**	0.0017
3% vs. 5%	-0.0313	-0.06604 to	No	ns	0.093

Test details	Mean 1	Mean 2	Mean Diff.	SE of diff.	N1	N2	t	DF
1								
1% vs. 3%	-0.3571	-0.3929	0.0358	0.01004	328	377	3.565	3880
1% vs. 5%	-0.3571	-0.3929	0.03578	0.01024	328	348	3.496	3880
3% vs. 5%	-0.3929	-0.3929	-0.00002	0.009887	377	348	0.002023	3880
3								
1% vs. 3%	-0.2866	-0.3625	0.07586	0.01076	326	288	7.053	3880
1% vs. 5%	-0.2866	-0.4004	0.1138	0.01117	326	251	10.19	3880
3% vs. 5%	-0.3625	-0.4004	0.03793	0.01149	288	251	3.303	3880
5								
1% vs. 3%	-0.2798	-0.3112	0.03139	0.01376	132	320	2.281	3880
1% vs. 5%	-0.2798	-0.3787	0.09889	0.0148	132	208	6.681	3880
3% vs. 5%	-0.3112	-0.3787	0.0675	0.01185	320	208	5.698	3880
7								
1% vs. 3%	-0.2784	-0.3361	0.0577	0.01188	183	398	4.857	3880
1% vs. 5%	-0.2784	-0.344	0.06565	0.01246	183	302	5.269	3880
3% vs. 5%	-0.3361	-0.344	0.00795	0.01015	398	302	0.7832	3880
10								
1% vs. 3%	-0.3322	-0.304	-0.02817	0.01679	96	181	1.677	3880
1% vs. 5%	-0.3322	-0.2727	-0.05947	0.01723	96	157	3.451	3880
3% vs. 5%	-0.304	-0.2727	-0.0313	0.01451	181	157	2.158	3880

Table 30 – – One-way ANOVA for the effects of time and hydrogel stiffness on Chapter 4 data – NUCLEUS STIFFNESS

Table Analyze Data 1

Two-way ANC Ordinary
Alpha 0.05

Source of Var	% of total \	P value	P value su	Significant?
Interaction	2.852	<0.0001	****	Yes
Time	0.7574	<0.0001	****	Yes
Agarose	0.8333	<0.0001	****	Yes

ANOVA table	SS	DF	MS	F (DFn, DF	P value
Interaction	83155	8	10394	F (8, 3880)	P<0.0001
Time	22084	4	5521	F (4, 3880)	P<0.0001
Agarose	24298	2	12149	F (2, 3880)	P<0.0001
Residual	2786246	3880	718.1		

Number of mis 2075

Within each column, compare rows (simple effects within columns)

Number of fan 3
Number of cor 10
Alpha 0.05

Bonferroni's m	Mean Diff.	95.00% CI	Significant?	Summary	Adjusted P Value
1%					
1 vs. 3	-7.009	-12.89 to -:	Yes	**	0.0083
1 vs. 5	1.489	-6.269 to 9	No	ns	>0.9999
1 vs. 7	-16.82	-23.76 to -1	Yes	****	<0.0001
1 vs. 10	-16.18	-24.91 to -:	Yes	****	<0.0001
3 vs. 5	8.498	0.7329 to 1	Yes	*	0.0213
3 vs. 7	-9.811	-16.76 to -:	Yes	***	0.0008
3 vs. 10	-9.167	-17.91 to -1	Yes	*	0.0324
5 vs. 7	-18.31	-26.9 to -9.	Yes	****	<0.0001
5 vs. 10	-17.67	-27.76 to -:	Yes	****	<0.0001
7 vs. 10	0.6431	-8.842 to 1	No	ns	>0.9999
3%					
1 vs. 3	9.7	3.81 to 15.	Yes	****	<0.0001
1 vs. 5	7.529	1.808 to 1:	Yes	**	0.0022
1 vs. 7	5.2	-0.2088 to	No	ns	0.0696
1 vs. 10	-3.142	-9.948 to 3	No	ns	>0.9999
3 vs. 5	-2.172	-8.285 to 3	No	ns	>0.9999
3 vs. 7	-4.5	-10.32 to 1	No	ns	0.3001
3 vs. 10	-12.84	-19.98 to -1	Yes	****	<0.0001
5 vs. 7	-2.328	-7.98 to 3.:	No	ns	>0.9999
5 vs. 10	-10.67	-17.67 to -:	Yes	***	0.0002
7 vs. 10	-8.343	-15.09 to -:	Yes	**	0.0052
5%					
1 vs. 3	2.595	-3.638 to 8	No	ns	>0.9999
1 vs. 5	-2.381	-8.977 to 4	No	ns	>0.9999
1 vs. 7	0.2265	-5.693 to 6	No	ns	>0.9999
1 vs. 10	8.297	1.061 to 1:	Yes	*	0.0129
3 vs. 5	-4.976	-12.03 to 2	No	ns	0.4775
3 vs. 7	-2.368	-8.797 to 4	No	ns	>0.9999
3 vs. 10	5.702	-1.956 to 1	No	ns	0.3658
5 vs. 7	2.607	-4.174 to 9	No	ns	>0.9999
5 vs. 10	10.68	2.72 to 18.	Yes	**	0.0017
7 vs. 10	8.07	0.665 to 1:	Yes	*	0.0222

Test details	Mean 1	Mean 2	Mean Diff.	SE of diff.	N1	N2	t	DF
1%								
1 vs. 3	47.95	54.96	-7.009	2.096	328	326	3.344	3880
1 vs. 5	47.95	46.46	1.489	2.762	328	132	0.539	3880
1 vs. 7	47.95	64.77	-16.82	2.473	328	183	6.802	3880
1 vs. 10	47.95	64.13	-16.18	3.11	328	96	5.202	3880
3 vs. 5	54.96	46.46	8.498	2.765	326	132	3.074	3880
3 vs. 7	54.96	64.77	-9.811	2.475	326	183	3.963	3880
3 vs. 10	54.96	64.13	-9.167	3.112	326	96	2.946	3880
5 vs. 7	46.46	64.77	-18.31	3.06	132	183	5.983	3880
5 vs. 10	46.46	64.13	-17.67	3.595	132	96	4.914	3880
7 vs. 10	64.77	64.13	0.6431	3.377	183	96	0.1904	3880
3%								
1 vs. 3	59.14	49.44	9.7	2.097	377	288	4.625	3880
1 vs. 5	59.14	51.61	7.529	2.037	377	320	3.696	3880
1 vs. 7	59.14	53.94	5.2	1.926	377	398	2.7	3880
1 vs. 10	59.14	62.28	-3.142	2.423	377	181	1.297	3880
3 vs. 5	49.44	51.61	-2.172	2.177	288	320	0.9978	3880
3 vs. 7	49.44	53.94	-4.5	2.073	288	398	2.171	3880
3 vs. 10	49.44	62.28	-12.84	2.542	288	181	5.053	3880
5 vs. 7	51.61	53.94	-2.328	2.012	320	398	1.157	3880
5 vs. 10	51.61	62.28	-10.67	2.492	320	181	4.282	3880
7 vs. 10	53.94	62.28	-8.343	2.402	398	181	3.473	3880
5%								
1 vs. 3	51.47	48.87	2.595	2.219	348	251	1.169	3880
1 vs. 5	51.47	53.85	-2.381	2.349	348	208	1.014	3880
1 vs. 7	51.47	51.24	0.2265	2.107	348	302	0.1075	3880
1 vs. 10	51.47	43.17	8.297	2.576	348	157	3.22	3880
3 vs. 5	48.87	53.85	-4.976	2.513	251	208	1.98	3880
3 vs. 7	48.87	51.24	-2.368	2.289	251	302	1.035	3880
3 vs. 10	48.87	43.17	5.702	2.727	251	157	2.091	3880
5 vs. 7	53.85	51.24	2.607	2.415	208	302	1.08	3880
5 vs. 10	53.85	43.17	10.68	2.833	208	157	3.769	3880
7 vs. 10	51.24	43.17	8.07	2.637	302	157	3.061	3880

Within each row, compare columns (simple effects within rows)

Number of fam 5
Number of con 3
Alpha 0.05

Bonferroni's m	Mean Diff.	95.00% CI	Significant?	Summary	Adjusted P Value
1					
1% vs. 3%	-11.19	-16.04 to -4	Yes	****	<0.0001
1% vs. 5%	-3.517	-8.457 to 1	No	ns	0.2645
3% vs. 5%	7.673	2.902 to 12	Yes	***	0.0004
3					
1% vs. 3%	5.518	0.3282 to :	Yes	*	0.0328
1% vs. 5%	6.086	0.6967 to :	Yes	*	0.0206
3% vs. 5%	0.5678	-4.974 to 6	No	ns	>0.9999
5					
1% vs. 3%	-5.151	-11.79 to 1	No	ns	0.1896
1% vs. 5%	-7.387	-14.53 to -(	Yes	*	0.0399
3% vs. 5%	-2.236	-7.952 to 3	No	ns	>0.9999
7					
1% vs. 3%	10.83	5.097 to 1(	Yes	****	<0.0001
1% vs. 5%	13.53	7.516 to 1!	Yes	****	<0.0001
3% vs. 5%	2.7	-2.198 to 7	No	ns	0.5606
10					
1% vs. 3%	1.843	-6.26 to 9.!	No	ns	>0.9999
1% vs. 5%	20.96	12.64 to 2!	Yes	****	<0.0001
3% vs. 5%	19.11	12.11 to 2(	Yes	****	<0.0001

Test details	Mean 1	Mean 2	Mean Diff.	SE of diff.	N1	N2	t	DF
1								
1% vs. 3%	47.95	59.14	-11.19	2.023	328	377	5.531	3880
1% vs. 5%	47.95	51.47	-3.517	2.062	328	348	1.706	3880
3% vs. 5%	59.14	51.47	7.673	1.992	377	348	3.852	3880
3								
1% vs. 3%	54.96	49.44	5.518	2.167	326	288	2.546	3880
1% vs. 5%	54.96	48.87	6.086	2.25	326	251	2.705	3880
3% vs. 5%	49.44	48.87	0.5678	2.314	288	251	0.2454	3880
5								
1% vs. 3%	46.46	51.61	-5.151	2.772	132	320	1.858	3880
1% vs. 5%	46.46	53.85	-7.387	2.982	132	208	2.477	3880
3% vs. 5%	51.61	53.85	-2.236	2.387	320	208	0.9369	3880
7								
1% vs. 3%	64.77	53.94	10.83	2.393	183	398	4.524	3880
1% vs. 5%	64.77	51.24	13.53	2.51	183	302	5.389	3880
3% vs. 5%	53.94	51.24	2.7	2.045	398	302	1.32	3880
10								
1% vs. 3%	64.13	62.28	1.843	3.383	96	181	0.5447	3880
1% vs. 5%	64.13	43.17	20.96	3.472	96	157	6.036	3880
3% vs. 5%	62.28	43.17	19.11	2.923	181	157	6.54	3880

Table 31 – One-way ANOVA for the effects of time and hydrogel stiffness on Chapter 5 osteogenic data – AREA

Table Analyze Data 1

Two-way ANC Ordinary
Alpha 0.05

Source of Var	% of total v	P value	P value sur	Significant?
Interaction	0.4188	<0.0001	****	Yes
Time	26.61	<0.0001	****	Yes
Agarose	0.6109	<0.0001	****	Yes

ANOVA table	SS	DF	MS	F (DFn, DF	P value
Interaction	1.01E+10	10	1.01E+09	F (10, 750	P<0.0001
Time	6.43E+11	5	1.29E+11	F (5, 7506)	P<0.0001
Agarose	1.48E+10	2	7.38E+09	F (2, 7506)	P<0.0001
Residual	1.75E+12	7506	2.33E+08		

Number of mis 5922

Within each column, compare rows (simple effects within columns)

Number of fan 3
Number of cor 15
Alpha 0.05

Bonferroni's m	Mean Diff.	95.00% CI	Significant?	Summary	Adjusted P Value
1%					
1 vs. 3	-5195	-8091 to -2	Yes	****	<0.0001
1 vs. 5	-12102	-15004 to -	Yes	****	<0.0001
1 vs. 7	-14498	-17764 to -	Yes	****	<0.0001
1 vs. 10	-20707	-23635 to -	Yes	****	<0.0001
1 vs. 15	-30642	-33756 to -	Yes	****	<0.0001
3 vs. 5	-6907	-9633 to -4	Yes	****	<0.0001
3 vs. 7	-9303	-12413 to -	Yes	****	<0.0001
3 vs. 10	-15512	-18265 to -	Yes	****	<0.0001
3 vs. 15	-25447	-28397 to -	Yes	****	<0.0001
5 vs. 7	-2396	-5511 to 71	No	ns	0.3594
5 vs. 10	-8605	-11364 to -	Yes	****	<0.0001
5 vs. 15	-18540	-21495 to -	Yes	****	<0.0001
7 vs. 10	-6209	-9349 to -3	Yes	****	<0.0001
7 vs. 15	-16144	-19457 to -	Yes	****	<0.0001
10 vs. 15	-9935	-12916 to -	Yes	****	<0.0001
3%					
1 vs. 3	-9159	-12712 to -	Yes	****	<0.0001
1 vs. 5	-10291	-13914 to -	Yes	****	<0.0001
1 vs. 7	-19004	-22787 to -	Yes	****	<0.0001
1 vs. 10	-20582	-24504 to -	Yes	****	<0.0001
1 vs. 15	-34332	-38363 to -	Yes	****	<0.0001
3 vs. 5	-1132	-3556 to 12	No	ns	>0.9999
3 vs. 7	-9845	-12502 to -	Yes	****	<0.0001
3 vs. 10	-11423	-14274 to -	Yes	****	<0.0001
3 vs. 15	-25172	-28172 to -	Yes	****	<0.0001
5 vs. 7	-8713	-11464 to -	Yes	****	<0.0001
5 vs. 10	-10291	-13229 to -	Yes	****	<0.0001
5 vs. 15	-24041	-27123 to -	Yes	****	<0.0001
7 vs. 10	-1578	-4710 to 15	No	ns	>0.9999
7 vs. 15	-15327	-18596 to -	Yes	****	<0.0001
10 vs. 15	-13749	-17177 to -	Yes	****	<0.0001
5%					
1 vs. 3	-2813	-5768 to 14	No	ns	0.0781
1 vs. 5	-10093	-13310 to -	Yes	****	<0.0001
1 vs. 7	-17005	-20579 to -	Yes	****	<0.0001
1 vs. 10	-17355	-22352 to -	Yes	****	<0.0001
1 vs. 15	-32779	-37106 to -	Yes	****	<0.0001
3 vs. 5	-7280	-9997 to -4	Yes	****	<0.0001
3 vs. 7	-14192	-17323 to -	Yes	****	<0.0001
3 vs. 10	-14542	-19232 to -	Yes	****	<0.0001
3 vs. 15	-29966	-33935 to -	Yes	****	<0.0001
5 vs. 7	-6912	-10292 to -	Yes	****	<0.0001
5 vs. 10	-7262	-12122 to -	Yes	***	0.0002
5 vs. 15	-22686	-26854 to -	Yes	****	<0.0001
7 vs. 10	-349.9	-5453 to 47	No	ns	>0.9999
7 vs. 15	-15774	-20223 to -	Yes	****	<0.0001
10 vs. 15	-15424	-21080 to -	Yes	****	<0.0001

Test details	Mean 1	Mean 2	Mean Diff.	SE of diff.	N1	N2	t	DF
1%								
1 vs. 3	18473	23668	-5195	986.3	428	543	5.267	7506
1 vs. 5	18473	30576	-12102	988.3	428	538	12.25	7506
1 vs. 7	18473	32972	-14498	1112	428	336	13.04	7506
1 vs. 10	18473	39181	-20707	997.2	428	517	20.77	7506
1 vs. 15	18473	49115	-30642	1060	428	401	28.9	7506
3 vs. 5	23668	30576	-6907	928.2	543	538	7.442	7506
3 vs. 7	23668	32972	-9303	1059	543	336	8.784	7506
3 vs. 10	23668	39181	-15512	937.6	543	517	16.54	7506
3 vs. 15	23668	49115	-25447	1005	543	401	25.33	7506
5 vs. 7	30576	32972	-2396	1061	538	336	2.258	7506
5 vs. 10	30576	39181	-8605	939.7	538	517	9.157	7506
5 vs. 15	30576	49115	-18540	1007	538	401	18.42	7506
7 vs. 10	32972	39181	-6209	1069	336	517	5.807	7506
7 vs. 15	32972	49115	-16144	1129	336	401	14.31	7506
10 vs. 15	39181	49115	-9935	1015	517	401	9.785	7506
3%								
1 vs. 3	19381	28540	-9159	1210	202	747	7.569	7506
1 vs. 5	19381	29672	-10291	1234	202	629	8.34	7506
1 vs. 7	19381	38386	-19004	1288	202	459	14.75	7506
1 vs. 10	19381	39964	-20582	1335	202	369	15.41	7506
1 vs. 15	19381	53713	-34332	1373	202	318	25.01	7506
3 vs. 5	28540	29672	-1132	825.7	747	629	1.371	7506
3 vs. 7	28540	38386	-9845	904.9	747	459	10.88	7506
3 vs. 10	28540	39964	-11423	970.9	747	369	11.77	7506
3 vs. 15	28540	53713	-25172	1022	747	318	24.64	7506
5 vs. 7	29672	38386	-8713	936.7	629	459	9.302	7506
5 vs. 10	29672	39964	-10291	1001	629	369	10.29	7506
5 vs. 15	29672	53713	-24041	1050	629	318	22.9	7506
7 vs. 10	38386	39964	-1578	1067	459	369	1.479	7506
7 vs. 15	38386	53713	-15327	1113	459	318	13.77	7506
10 vs. 15	39964	53713	-13749	1168	369	318	11.78	7506
5%								
1 vs. 3	22790	25603	-2813	1006	343	697	2.795	7506
1 vs. 5	22790	32883	-10093	1096	343	446	9.21	7506
1 vs. 7	22790	39795	-17005	1217	343	290	13.97	7506
1 vs. 10	22790	40145	-17355	1702	343	105	10.2	7506
1 vs. 15	22790	55569	-32779	1474	343	156	22.25	7506
3 vs. 5	25603	32883	-7280	925.2	697	446	7.868	7506
3 vs. 7	25603	39795	-14192	1066	697	290	13.31	7506
3 vs. 10	25603	40145	-14542	1597	697	105	9.104	7506
3 vs. 15	25603	55569	-29966	1351	697	156	22.17	7506
5 vs. 7	32883	39795	-6912	1151	446	290	6.005	7506
5 vs. 10	32883	40145	-7262	1655	446	105	4.388	7506
5 vs. 15	32883	55569	-22686	1419	446	156	15.98	7506
7 vs. 10	39795	40145	-349.9	1738	290	105	0.2013	7506
7 vs. 15	39795	55569	-15774	1515	290	156	10.41	7506
10 vs. 15	40145	55569	-15424	1926	105	156	8.008	7506

Within each row, compare columns (simple effects within rows)

Number of fam 6
Number of con 3
Alpha 0.05

Bonferroni's m	Mean Diff.	95.00% CI	Significant?	Summary	Adjusted P Value
1					
1% vs. 3%	-907.9	-4027 to 2	No	ns	>0.9999
1% vs. 5%	-4317	-6965 to -1	Yes	***	0.0003
3% vs. 5%	-3409	-6649 to -1	Yes	*	0.0354
3					
1% vs. 3%	-4872	-6933 to -2	Yes	****	<0.0001
1% vs. 5%	-1935	-4026 to 15	No	ns	0.0803
3% vs. 5%	2937	1013 to 48	Yes	***	0.0008
5					
1% vs. 3%	903.4	-1242 to 30	No	ns	0.9402
1% vs. 5%	-2308	-4647 to 32	No	ns	0.0547
3% vs. 5%	-3211	-5473 to -9	Yes	**	0.002
7					
1% vs. 3%	-5414	-8037 to -2	Yes	****	<0.0001
1% vs. 5%	-6824	-9752 to -3	Yes	****	<0.0001
3% vs. 5%	-1410	-4150 to 13	No	ns	0.6546
10					
1% vs. 3%	-783	-3273 to 17	No	ns	>0.9999
1% vs. 5%	-964.4	-4875 to 29	No	ns	>0.9999
3% vs. 5%	-181.4	-4223 to 38	No	ns	>0.9999
15					
1% vs. 3%	-4597	-7341 to -1	Yes	***	0.0002
1% vs. 5%	-6454	-9902 to -3	Yes	****	<0.0001
3% vs. 5%	-1857	-5428 to 17	No	ns	0.6398

Test details	Mean 1	Mean 2	Mean Diff.	SE of diff.	N1	N2	t	DF
1								
1% vs. 3%	18473	19381	-907.9	1303	428	202	0.697	7506
1% vs. 5%	18473	22790	-4317	1106	428	343	3.904	7506
3% vs. 5%	19381	22790	-3409	1353	202	343	2.519	7506
3								
1% vs. 3%	23668	28540	-4872	860.5	543	747	5.662	7506
1% vs. 5%	23668	25603	-1935	873.4	543	697	2.215	7506
3% vs. 5%	28540	25603	2937	803.6	747	697	3.655	7506
5								
1% vs. 3%	30576	29672	903.4	896	538	629	1.008	7506
1% vs. 5%	30576	32883	-2308	977.1	538	446	2.362	7506
3% vs. 5%	29672	32883	-3211	944.5	629	446	3.399	7506
7								
1% vs. 3%	32972	38386	-5414	1096	336	459	4.942	7506
1% vs. 5%	32972	39795	-6824	1223	336	290	5.579	7506
3% vs. 5%	38386	39795	-1410	1145	459	290	1.231	7506
10								
1% vs. 3%	39181	39964	-783	1040	517	369	0.753	7506
1% vs. 5%	39181	40145	-964.4	1633	517	105	0.5905	7506
3% vs. 5%	39964	40145	-181.4	1688	369	105	0.1075	7506
15								
1% vs. 3%	49115	53713	-4597	1146	401	318	4.013	7506
1% vs. 5%	49115	55569	-6454	1440	401	156	4.483	7506
3% vs. 5%	53713	55569	-1857	1492	318	156	1.245	7506

Table 32 – One-way ANOVA for the effects of time and hydrogel stiffness on Chapter 5 osteogenic data – ASPECT RATIO

Table Analyze Data 1

Two-way ANOVA Ordinary
Alpha 0.05

Source of Vari	% of total V	P value	P value sur	Significant?
Interaction	0.3898	0.0005	***	Yes
Time	4.365	<0.0001	****	Yes
Agarose	1.81	<0.0001	****	Yes

ANOVA table	SS	DF	MS	F (DFn, DF	P value
Interaction	212.4	10	21.24	F (10, 750	P=0.0005
Time	2378	5	475.6	F (5, 7506)	P<0.0001
Agarose	986.1	2	493	F (2, 7506)	P<0.0001
Residual	50909	7506	6.782		

Number of mis 5922

Within each column, compare rows (simple effects within columns)

Number of fam 3
Number of cor 15
Alpha 0.05

Bonferroni's m	Mean Diff.	95.00% CI	Significant?	Summary	Adjusted P Value
1%					
1 vs. 3	-0.9289	-1.423 to -(	Yes	****	<0.0001
1 vs. 5	-0.5744	-1.07 to -0.	Yes	**	0.01
1 vs. 7	-0.3867	-0.944 to 0	No	ns	0.625
1 vs. 10	0.4458	-0.05394 to	No	ns	0.1325
1 vs. 15	1.526	0.9948 to 2	Yes	****	<0.0001
3 vs. 5	0.3545	-0.1106 to	No	ns	0.379
3 vs. 7	0.5422	0.01145 to	Yes	*	0.0407
3 vs. 10	1.375	0.9048 to 1	Yes	****	<0.0001
3 vs. 15	2.455	1.952 to 2.	Yes	****	<0.0001
5 vs. 7	0.1877	-0.344 to 0	No	ns	>0.9999
5 vs. 10	1.02	0.5492 to 1	Yes	****	<0.0001
5 vs. 15	2.101	1.596 to 2.	Yes	****	<0.0001
7 vs. 10	0.8325	0.2966 to 1	Yes	****	<0.0001
7 vs. 15	1.913	1.347 to 2.	Yes	****	<0.0001
10 vs. 15	1.08	0.5716 to 1	Yes	****	<0.0001
3%					
1 vs. 3	-0.6102	-1.217 to -(	Yes	*	0.0471
1 vs. 5	-0.43	-1.048 to 0	No	ns	0.6187
1 vs. 7	0.4433	-0.2023 to	No	ns	0.6576
1 vs. 10	0.517	-0.1523 to	No	ns	0.3504
1 vs. 15	1.154	0.4656 to 1	Yes	****	<0.0001
3 vs. 5	0.1803	-0.2335 to	No	ns	>0.9999
3 vs. 7	1.054	0.6 to 1.50	Yes	****	<0.0001
3 vs. 10	1.127	0.6406 to 1	Yes	****	<0.0001
3 vs. 15	1.764	1.252 to 2.	Yes	****	<0.0001
5 vs. 7	0.8732	0.4038 to 1	Yes	****	<0.0001
5 vs. 10	0.9469	0.4455 to 1	Yes	****	<0.0001
5 vs. 15	1.584	1.057 to 2.	Yes	****	<0.0001
7 vs. 10	0.07367	-0.461 to 0	No	ns	>0.9999
7 vs. 15	0.7103	0.1524 to 1	Yes	**	0.0028
10 vs. 15	0.6366	0.05151 to	Yes	*	0.0211
5%					
1 vs. 3	-0.6086	-1.113 to -(	Yes	**	0.006
1 vs. 5	-0.1683	-0.7174 to	No	ns	>0.9999
1 vs. 7	0.6031	-0.006939	No	ns	0.0556
1 vs. 10	0.4826	-0.3702 to	No	ns	>0.9999
1 vs. 15	1.134	0.3952 to 1	Yes	****	<0.0001
3 vs. 5	0.4403	-0.02335 to	No	ns	0.0797
3 vs. 7	1.212	0.6773 to 1	Yes	****	<0.0001
3 vs. 10	1.091	0.2907 to 1	Yes	***	0.0009
3 vs. 15	1.742	1.065 to 2.	Yes	****	<0.0001
5 vs. 7	0.7713	0.1945 to 1	Yes	**	0.0013
5 vs. 10	0.6509	-0.1785 to	No	ns	0.3187
5 vs. 15	1.302	0.5906 to 2	Yes	****	<0.0001
7 vs. 10	-0.1204	-0.9913 to	No	ns	>0.9999
7 vs. 15	0.5306	-0.2287 to	No	ns	0.6033
10 vs. 15	0.651	-0.3142 to	No	ns	0.7156

Test details	Mean 1	Mean 2	Mean Diff.	SE of diff.	N1	N2	t	DF
1%								
1 vs. 3	5.264	6.193	-0.9289	0.1683	428	543	5.518	7506
1 vs. 5	5.264	5.838	-0.5744	0.1687	428	538	3.405	7506
1 vs. 7	5.264	5.65	-0.3867	0.1898	428	336	2.037	7506
1 vs. 10	5.264	4.818	0.4458	0.1702	428	517	2.619	7506
1 vs. 15	5.264	3.738	1.526	0.181	428	401	8.432	7506
3 vs. 5	6.193	5.838	0.3545	0.1584	543	538	2.238	7506
3 vs. 7	6.193	5.65	0.5422	0.1808	543	336	2.999	7506
3 vs. 10	6.193	4.818	1.375	0.16	543	517	8.59	7506
3 vs. 15	6.193	3.738	2.455	0.1715	543	401	14.32	7506
5 vs. 7	5.838	5.65	0.1877	0.1811	538	336	1.037	7506
5 vs. 10	5.838	4.818	1.02	0.1604	538	517	6.361	7506
5 vs. 15	5.838	3.738	2.101	0.1718	538	401	12.23	7506
7 vs. 10	5.65	4.818	0.8325	0.1825	336	517	4.562	7506
7 vs. 15	5.65	3.738	1.913	0.1926	336	401	9.931	7506
10 vs. 15	4.818	3.738	1.08	0.1733	517	401	6.235	7506
3%								
1 vs. 3	4.64	5.25	-0.6102	0.2065	202	747	2.955	7506
1 vs. 5	4.64	5.07	-0.43	0.2106	202	629	2.041	7506
1 vs. 7	4.64	4.196	0.4433	0.2199	202	459	2.016	7506
1 vs. 10	4.64	4.123	0.517	0.2279	202	369	2.268	7506
1 vs. 15	4.64	3.486	1.154	0.2343	202	318	4.923	7506
3 vs. 5	5.25	5.07	0.1803	0.1409	747	629	1.279	7506
3 vs. 7	5.25	4.196	1.054	0.1545	747	459	6.821	7506
3 vs. 10	5.25	4.123	1.127	0.1657	747	369	6.802	7506
3 vs. 15	5.25	3.486	1.764	0.1744	747	318	10.11	7506
5 vs. 7	5.07	4.196	0.8732	0.1599	629	459	5.462	7506
5 vs. 10	5.07	4.123	0.9469	0.1708	629	369	5.545	7506
5 vs. 15	5.07	3.486	1.584	0.1792	629	318	8.837	7506
7 vs. 10	4.196	4.123	0.07367	0.1821	459	369	0.4046	7506
7 vs. 15	4.196	3.486	0.7103	0.19	459	318	3.738	7506
10 vs. 15	4.123	3.486	0.6366	0.1993	369	318	3.195	7506
5%								
1 vs. 3	4.557	5.166	-0.6086	0.1718	343	697	3.543	7506
1 vs. 5	4.557	4.725	-0.1683	0.187	343	446	0.8997	7506
1 vs. 7	4.557	3.954	0.6031	0.2078	343	290	2.903	7506
1 vs. 10	4.557	4.074	0.4826	0.2905	343	105	1.662	7506
1 vs. 15	4.557	3.423	1.134	0.2515	343	156	4.507	7506
3 vs. 5	5.166	4.725	0.4403	0.1579	697	446	2.788	7506
3 vs. 7	5.166	3.954	1.212	0.182	697	290	6.658	7506
3 vs. 10	5.166	4.074	1.091	0.2726	697	105	4.003	7506
3 vs. 15	5.166	3.423	1.742	0.2307	697	156	7.553	7506
5 vs. 7	4.725	3.954	0.7713	0.1965	446	290	3.926	7506
5 vs. 10	4.725	4.074	0.6509	0.2825	446	105	2.304	7506
5 vs. 15	4.725	3.423	1.302	0.2422	446	156	5.374	7506
7 vs. 10	3.954	4.074	-0.1204	0.2966	290	105	0.406	7506
7 vs. 15	3.954	3.423	0.5306	0.2586	290	156	2.052	7506
10 vs. 15	4.074	3.423	0.651	0.3287	105	156	1.98	7506

Within each row, compare columns (simple effects within rows)

Number of fam 6
Number of con 3
Alpha 0.05

Bonferroni's m	Mean Diff.	95.00% CI	Significant?	Summary	Adjusted P Value
1					
1% vs. 3%	0.6242	0.09186 to	Yes	*	0.015
1% vs. 5%	0.7068	0.2548 to 1	Yes	***	0.0005
3% vs. 5%	0.08258	-0.4705 to	No	ns	>0.9999
3					
1% vs. 3%	0.9429	0.5912 to 1	Yes	****	<0.0001
1% vs. 5%	1.027	0.6701 to 1	Yes	****	<0.0001
3% vs. 5%	0.0842	-0.2442 to	No	ns	>0.9999
5					
1% vs. 3%	0.7686	0.4024 to 1	Yes	****	<0.0001
1% vs. 5%	1.113	0.7136 to 1	Yes	****	<0.0001
3% vs. 5%	0.3443	-0.04177 to	No	ns	0.0983
7					
1% vs. 3%	1.454	1.006 to 1.	Yes	****	<0.0001
1% vs. 5%	1.697	1.197 to 2.	Yes	****	<0.0001
3% vs. 5%	0.2423	-0.2254 to	No	ns	0.6444
10					
1% vs. 3%	0.6954	0.2704 to 1	Yes	***	0.0003
1% vs. 5%	0.7436	0.0761 to 1	Yes	*	0.023
3% vs. 5%	0.04824	-0.6415 to	No	ns	>0.9999
15					
1% vs. 3%	0.2515	-0.2167 to	No	ns	0.5951
1% vs. 5%	0.3142	-0.2743 to	No	ns	0.6033
3% vs. 5%	0.06264	-0.5469 to	No	ns	>0.9999

Test details	Mean 1	Mean 2	Mean Diff.	SE of diff.	N1	N2	t	DF
1								
1% vs. 3%	5.264	4.64	0.6242	0.2223	428	202	2.808	7506
1% vs. 5%	5.264	4.557	0.7068	0.1887	428	343	3.745	7506
3% vs. 5%	4.64	4.557	0.08258	0.231	202	343	0.3575	7506
3								
1% vs. 3%	6.193	5.25	0.9429	0.1469	543	747	6.42	7506
1% vs. 5%	6.193	5.166	1.027	0.1491	543	697	6.89	7506
3% vs. 5%	5.25	5.166	0.0842	0.1372	747	697	0.614	7506
5								
1% vs. 3%	5.838	5.07	0.7686	0.1529	538	629	5.026	7506
1% vs. 5%	5.838	4.725	1.113	0.1668	538	446	6.673	7506
3% vs. 5%	5.07	4.725	0.3443	0.1612	629	446	2.135	7506
7								
1% vs. 3%	5.65	4.196	1.454	0.187	336	459	7.777	7506
1% vs. 5%	5.65	3.954	1.697	0.2087	336	290	8.127	7506
3% vs. 5%	4.196	3.954	0.2423	0.1954	459	290	1.241	7506
10								
1% vs. 3%	4.818	4.123	0.6954	0.1775	517	369	3.918	7506
1% vs. 5%	4.818	4.074	0.7436	0.2788	517	105	2.667	7506
3% vs. 5%	4.123	4.074	0.04824	0.2881	369	105	0.1675	7506
15								
1% vs. 3%	3.738	3.486	0.2515	0.1956	401	318	1.286	7506
1% vs. 5%	3.738	3.423	0.3142	0.2457	401	156	1.279	7506
3% vs. 5%	3.486	3.423	0.06264	0.2546	318	156	0.2461	7506

Table 33 – One-way ANOVA for the effects of time and hydrogel stiffness on Chapter 5 osteogenic data – F-ACTIN

Table Analyze Data 1

Two-way ANO Ordinary
Alpha 0.05

Source of Vari	% of total v	P value	P value su	Significant?
Interaction	5.241	<0.0001	****	Yes
Time	13.72	<0.0001	****	Yes
Agarose	10.64	<0.0001	****	Yes

ANOVA table	SS	DF	MS	F (DFn, DF	P value
Interaction	2.26E+13	10	2.26E+12	F (10, 750	P<0.0001
Time	5.91E+13	5	1.18E+13	F (5, 7506)	P<0.0001
Agarose	4.59E+13	2	2.29E+13	F (2, 7506)	P<0.0001
Residual	3.04E+14	7506	4.04E+10		

Number of mis 5922

Within each column, compare rows (simple effects within columns)

Number of fam 3
Number of cor 15
Alpha 0.05

Bonferroni's m	Mean Diff.	95.00% CI	Significant	Summary	Adjusted P Value
1%					
1 vs. 3	-68742	-106905 to	Yes	****	<0.0001
1 vs. 5	-134167	-172409 to	Yes	****	<0.0001
1 vs. 7	-394946	-437980 to	Yes	****	<0.0001
1 vs. 10	-221941	-260525 to	Yes	****	<0.0001
1 vs. 15	-508143	-549177 to	Yes	****	<0.0001
3 vs. 5	-65425	-101341 to	Yes	****	<0.0001
3 vs. 7	-326204	-367185 to	Yes	****	<0.0001
3 vs. 10	-153199	-189479 to	Yes	****	<0.0001
3 vs. 15	-439401	-478277 to	Yes	****	<0.0001
5 vs. 7	-260779	-301833 to	Yes	****	<0.0001
5 vs. 10	-87774	-124136 to	Yes	****	<0.0001
5 vs. 15	-373976	-412928 to	Yes	****	<0.0001
7 vs. 10	173005	131631 to	Yes	****	<0.0001
7 vs. 15	-113197	-156864 to	Yes	****	<0.0001
10 vs. 15	-286202	-325491 to	Yes	****	<0.0001
3%					
1 vs. 3	6231	-40592 to 5	No	ns	>0.9999
1 vs. 5	-20908	-68657 to 2	No	ns	>0.9999
1 vs. 7	-56386	-106238 to	Yes	*	0.0135
1 vs. 10	-64981	-116657 to	Yes	**	0.0034
1 vs. 15	-236904	-290026 to	Yes	****	<0.0001
3 vs. 5	-27140	-59091 to 4	No	ns	0.1898
3 vs. 7	-62618	-97634 to -	Yes	****	<0.0001
3 vs. 10	-71213	-108781 to	Yes	****	<0.0001
3 vs. 15	-243136	-282669 to	Yes	****	<0.0001
5 vs. 7	-35478	-71723 to 7	No	ns	0.061
5 vs. 10	-44073	-82789 to -	Yes	*	0.0125
5 vs. 15	-215996	-256622 to	Yes	****	<0.0001
7 vs. 10	-8595	-49877 to 3	No	ns	>0.9999
7 vs. 15	-180518	-223596 to	Yes	****	<0.0001
10 vs. 15	-171923	-217100 to	Yes	****	<0.0001
5%					
1 vs. 3	5825	-33117 to 4	No	ns	>0.9999
1 vs. 5	-9342	-51743 to 3	No	ns	>0.9999
1 vs. 7	-12989	-60089 to 3	No	ns	>0.9999
1 vs. 10	-78063	-143913 to	Yes	**	0.0075
1 vs. 15	-146525	-203542 to	Yes	****	<0.0001
3 vs. 5	-15166	-50968 to 2	No	ns	>0.9999
3 vs. 7	-18814	-60072 to 2	No	ns	>0.9999
3 vs. 10	-83887	-145694 to	Yes	**	0.001
3 vs. 15	-152350	-204644 to	Yes	****	<0.0001
5 vs. 7	-3648	-48186 to 4	No	ns	>0.9999
5 vs. 10	-68721	-132765 to	Yes	*	0.0245
5 vs. 15	-137184	-192103 to	Yes	****	<0.0001
7 vs. 10	-65073	-132319 to	No	ns	0.0676
7 vs. 15	-133536	-192159 to	Yes	****	<0.0001
10 vs. 15	-68462	-142991 to	No	ns	0.1051

Test details	Mean 1	Mean 2	Mean Diff.	SE of diff.	N1	N2	t	DF
1%								
1 vs. 3	135329	204070	-68742	12998	428	543	5.289	7506
1 vs. 5	135329	269496	-134167	13024	428	538	10.3	7506
1 vs. 7	135329	530274	-394946	14657	428	336	26.95	7506
1 vs. 10	135329	357270	-221941	13141	428	517	16.89	7506
1 vs. 15	135329	643472	-508143	13976	428	401	36.36	7506
3 vs. 5	204070	269496	-65425	12232	543	538	5.349	7506
3 vs. 7	204070	530274	-326204	13958	543	336	23.37	7506
3 vs. 10	204070	357270	-153199	12356	543	517	12.4	7506
3 vs. 15	204070	643472	-439401	13240	543	401	33.19	7506
5 vs. 7	269496	530274	-260779	13982	538	336	18.65	7506
5 vs. 10	269496	357270	-87774	12384	538	517	7.087	7506
5 vs. 15	269496	643472	-373976	13266	538	401	28.19	7506
7 vs. 10	530274	357270	173005	14091	336	517	12.28	7506
7 vs. 15	530274	643472	-113197	14872	336	401	7.611	7506
10 vs. 15	357270	643472	-286202	13381	517	401	21.39	7506
3%								
1 vs. 3	111733	105502	6231	15947	202	747	0.3907	7506
1 vs. 5	111733	132641	-20908	16262	202	629	1.286	7506
1 vs. 7	111733	168119	-56386	16979	202	459	3.321	7506
1 vs. 10	111733	176714	-64981	17600	202	369	3.692	7506
1 vs. 15	111733	348637	-236904	18092	202	318	13.09	7506
3 vs. 5	105502	132641	-27140	10882	747	629	2.494	7506
3 vs. 7	105502	168119	-62618	11926	747	459	5.251	7506
3 vs. 10	105502	176714	-71213	12795	747	369	5.566	7506
3 vs. 15	105502	348637	-243136	13464	747	318	18.06	7506
5 vs. 7	132641	168119	-35478	12344	629	459	2.874	7506
5 vs. 10	132641	176714	-44073	13186	629	369	3.342	7506
5 vs. 15	132641	348637	-215996	13836	629	318	15.61	7506
7 vs. 10	168119	176714	-8595	14060	459	369	0.6113	7506
7 vs. 15	168119	348637	-180518	14672	459	318	12.3	7506
10 vs. 15	176714	348637	-171923	15386	369	318	11.17	7506
5%								
1 vs. 3	124056	118232	5825	13263	343	697	0.4392	7506
1 vs. 5	124056	133398	-9342	14441	343	446	0.6469	7506
1 vs. 7	124056	137046	-12989	16041	343	290	0.8097	7506
1 vs. 10	124056	202119	-78063	22428	343	105	3.481	7506
1 vs. 15	124056	270582	-146525	19419	343	156	7.545	7506
3 vs. 5	118232	133398	-15166	12193	697	446	1.244	7506
3 vs. 7	118232	137046	-18814	14052	697	290	1.339	7506
3 vs. 10	118232	202119	-83887	21050	697	105	3.985	7506
3 vs. 15	118232	270582	-152350	17811	697	156	8.554	7506
5 vs. 7	133398	137046	-3648	15169	446	290	0.2405	7506
5 vs. 10	133398	202119	-68721	21812	446	105	3.151	7506
5 vs. 15	133398	270582	-137184	18705	446	156	7.334	7506
7 vs. 10	137046	202119	-65073	22903	290	105	2.841	7506
7 vs. 15	137046	270582	-133536	19966	290	156	6.688	7506
10 vs. 15	202119	270582	-68462	25383	105	156	2.697	7506

Within each row, compare columns (simple effects within rows)

Number of fam 6
Number of con 3
Alpha 0.05

Bonferroni's mu	Mean Diff.	95.00% CI	Significant	Summary	Adjusted P Value
1					
1% vs. 3%	23596	-17507 to 6	No	ns	0.5079
1% vs. 5%	11272	-23623 to 4	No	ns	>0.9999
3% vs. 5%	-12324	-55028 to 3	No	ns	>0.9999
3					
1% vs. 3%	98569	71414 to 1	Yes	****	<0.0001
1% vs. 5%	85838	58277 to 1	Yes	****	<0.0001
3% vs. 5%	-12730	-38088 to 1	No	ns	0.6881
5					
1% vs. 3%	136854	108578 to	Yes	****	<0.0001
1% vs. 5%	136098	105263 to	Yes	****	<0.0001
3% vs. 5%	-756.9	-30564 to 2	No	ns	>0.9999
7					
1% vs. 3%	362155	327584 to	Yes	****	<0.0001
1% vs. 5%	393228	354634 to	Yes	****	<0.0001
3% vs. 5%	31073	-5046 to 6	No	ns	0.1183
10					
1% vs. 3%	180555	147741 to	Yes	****	<0.0001
1% vs. 5%	155150	103609 to	Yes	****	<0.0001
3% vs. 5%	-25405	-78663 to 2	No	ns	0.7602
15					
1% vs. 3%	294834	258678 to	Yes	****	<0.0001
1% vs. 5%	372890	327455 to	Yes	****	<0.0001
3% vs. 5%	78056	30989 to 1	Yes	***	0.0002

Test details	Mean 1	Mean 2	Mean Diff.	SE of diff.	N1	N2	t	DF
1								
1% vs. 3%	135329	111733	23596	17166	428	202	1.375	7506
1% vs. 5%	135329	124056	11272	14573	428	343	0.7735	7506
3% vs. 5%	111733	124056	-12324	17834	202	343	0.691	7506
3								
1% vs. 3%	204070	105502	98569	11340	543	747	8.692	7506
1% vs. 5%	204070	118232	85838	11510	543	697	7.458	7506
3% vs. 5%	105502	118232	-12730	10590	747	697	1.202	7506
5								
1% vs. 3%	269496	132641	136854	11809	538	629	11.59	7506
1% vs. 5%	269496	133398	136098	12877	538	446	10.57	7506
3% vs. 5%	132641	133398	-756.9	12448	629	446	0.06081	7506
7								
1% vs. 3%	530274	168119	362155	14437	336	459	25.08	7506
1% vs. 5%	530274	137046	393228	16118	336	290	24.4	7506
3% vs. 5%	168119	137046	31073	15084	459	290	2.06	7506
10								
1% vs. 3%	357270	176714	180555	13704	517	369	13.18	7506
1% vs. 5%	357270	202119	155150	21525	517	105	7.208	7506
3% vs. 5%	176714	202119	-25405	22242	369	105	1.142	7506
15								
1% vs. 3%	643472	348637	294834	15100	401	318	19.53	7506
1% vs. 5%	643472	270582	372890	18975	401	156	19.65	7506
3% vs. 5%	348637	270582	78056	19656	318	156	3.971	7506

Table 34 – One-way ANOVA for the effects of time and hydrogel stiffness on Chapter 5 osteogenic data – THICKNESS

Table Analyze Data 1

Two-way ANO Ordinary
Alpha 0.05

Source of Vari	% of total v	P value	P value su	Significant?
Interaction	5.025	<0.0001	****	Yes
Time	1.991	<0.0001	****	Yes
Agarose	19.39	<0.0001	****	Yes

ANOVA table	SS	DF	MS	F (DFn, DF	P value
Interaction	192653	10	19265	F (10, 750	P<0.0001
Time	76322	5	15264	F (5, 7506)	P<0.0001
Agarose	743352	2	371676	F (2, 7506)	P<0.0001
Residual	2821325	7506	375.9		

Number of mis 5922

Within each column, compare rows (simple effects within columns)

Number of fam 3
Number of cor 15
Alpha 0.05

Bonferroni's m	Mean Diff.	95.00% CI	Significant	Summary	Adjusted P Value
1%					
1 vs. 3	-4.692	-8.371 to -1	Yes	**	0.0027
1 vs. 5	-9.714	-13.4 to -6.	Yes	****	<0.0001
1 vs. 7	-30.73	-34.88 to -2	Yes	****	<0.0001
1 vs. 10	-10.41	-14.13 to -6	Yes	****	<0.0001
1 vs. 15	-23.85	-27.8 to -19	Yes	****	<0.0001
3 vs. 5	-5.022	-8.485 to -1	Yes	***	0.0003
3 vs. 7	-26.04	-29.99 to -2	Yes	****	<0.0001
3 vs. 10	-5.721	-9.219 to -2	Yes	****	<0.0001
3 vs. 15	-19.16	-22.9 to -15	Yes	****	<0.0001
5 vs. 7	-21.02	-24.98 to -1	Yes	****	<0.0001
5 vs. 10	-0.6989	-4.205 to 2	No	ns	>0.9999
5 vs. 15	-14.13	-17.89 to -1	Yes	****	<0.0001
7 vs. 10	20.32	16.33 to 24	Yes	****	<0.0001
7 vs. 15	6.883	2.673 to 11	Yes	****	<0.0001
10 vs. 15	-13.44	-17.22 to -9	Yes	****	<0.0001
3%					
1 vs. 3	7.164	2.65 to 11.	Yes	****	<0.0001
1 vs. 5	3.17	-1.434 to 7	No	ns	0.6486
1 vs. 7	4.591	-0.2155 to	No	ns	0.0758
1 vs. 10	2.611	-2.371 to 7	No	ns	>0.9999
1 vs. 15	-4.054	-9.176 to 1	No	ns	0.3021
3 vs. 5	-3.995	-7.075 to -1	Yes	**	0.0021
3 vs. 7	-2.573	-5.949 to 0	No	ns	0.3786
3 vs. 10	-4.553	-8.175 to -1	Yes	**	0.0034
3 vs. 15	-11.22	-15.03 to -7	Yes	****	<0.0001
5 vs. 7	1.421	-2.073 to 4	No	ns	>0.9999
5 vs. 10	-0.5585	-4.291 to 3	No	ns	>0.9999
5 vs. 15	-7.224	-11.14 to -3	Yes	****	<0.0001
7 vs. 10	-1.98	-5.96 to 2.(	No	ns	>0.9999
7 vs. 15	-8.645	-12.8 to -4.	Yes	****	<0.0001
10 vs. 15	-6.666	-11.02 to -2	Yes	***	0.0001
5%					
1 vs. 3	5.897	2.142 to 9.	Yes	****	<0.0001
1 vs. 5	7.272	3.184 to 11	Yes	****	<0.0001
1 vs. 7	10.07	5.533 to 14	Yes	****	<0.0001
1 vs. 10	2.416	-3.933 to 8	No	ns	>0.9999
1 vs. 15	4.173	-1.324 to 9	No	ns	0.3879
3 vs. 5	1.375	-2.076 to 4	No	ns	>0.9999
3 vs. 7	4.178	0.1997 to 8	Yes	*	0.0308
3 vs. 10	-3.48	-9.439 to 2	No	ns	>0.9999
3 vs. 15	-1.724	-6.766 to 3	No	ns	>0.9999
5 vs. 7	2.802	-1.492 to 7	No	ns	0.8309
5 vs. 10	-4.856	-11.03 to 1	No	ns	0.3146
5 vs. 15	-3.099	-8.394 to 2	No	ns	>0.9999
7 vs. 10	-7.658	-14.14 to -1	Yes	**	0.0079
7 vs. 15	-5.901	-11.55 to -(	Yes	*	0.0327
10 vs. 15	1.757	-5.429 to 8	No	ns	>0.9999

Test details	Mean 1	Mean 2	Mean Diff.	SE of diff.	N1	N2	t	DF
1%								
1 vs. 3	32.17	36.87	-4.692	1.253	428	543	3.744	7506
1 vs. 5	32.17	41.89	-9.714	1.256	428	538	7.736	7506
1 vs. 7	32.17	62.91	-30.73	1.413	428	336	21.75	7506
1 vs. 10	32.17	42.59	-10.41	1.267	428	517	8.219	7506
1 vs. 15	32.17	56.02	-23.85	1.347	428	401	17.7	7506
3 vs. 5	36.87	41.89	-5.022	1.179	543	538	4.259	7506
3 vs. 7	36.87	62.91	-26.04	1.346	543	336	19.35	7506
3 vs. 10	36.87	42.59	-5.721	1.191	543	517	4.803	7506
3 vs. 15	36.87	56.02	-19.16	1.277	543	401	15.01	7506
5 vs. 7	41.89	62.91	-21.02	1.348	538	336	15.59	7506
5 vs. 10	41.89	42.59	-0.6989	1.194	538	517	0.5853	7506
5 vs. 15	41.89	56.02	-14.13	1.279	538	401	11.05	7506
7 vs. 10	62.91	42.59	20.32	1.359	336	517	14.96	7506
7 vs. 15	62.91	56.02	6.883	1.434	336	401	4.801	7506
10 vs. 15	42.59	56.02	-13.44	1.29	517	401	10.41	7506
3%								
1 vs. 3	24.17	17.01	7.164	1.538	202	747	4.66	7506
1 vs. 5	24.17	21	3.17	1.568	202	629	2.022	7506
1 vs. 7	24.17	19.58	4.591	1.637	202	459	2.805	7506
1 vs. 10	24.17	21.56	2.611	1.697	202	369	1.539	7506
1 vs. 15	24.17	28.23	-4.054	1.744	202	318	2.324	7506
3 vs. 5	17.01	21	-3.995	1.049	747	629	3.807	7506
3 vs. 7	17.01	19.58	-2.573	1.15	747	459	2.238	7506
3 vs. 10	17.01	21.56	-4.553	1.234	747	369	3.691	7506
3 vs. 15	17.01	28.23	-11.22	1.298	747	318	8.642	7506
5 vs. 7	21	19.58	1.421	1.19	629	459	1.194	7506
5 vs. 10	21	21.56	-0.5585	1.271	629	369	0.4393	7506
5 vs. 15	21	28.23	-7.224	1.334	629	318	5.415	7506
7 vs. 10	19.58	21.56	-1.98	1.356	459	369	1.46	7506
7 vs. 15	19.58	28.23	-8.645	1.415	459	318	6.112	7506
10 vs. 15	21.56	28.23	-6.666	1.483	369	318	4.493	7506
5%								
1 vs. 3	26.08	20.18	5.897	1.279	343	697	4.611	7506
1 vs. 5	26.08	18.81	7.272	1.392	343	446	5.223	7506
1 vs. 7	26.08	16.01	10.07	1.547	343	290	6.514	7506
1 vs. 10	26.08	23.66	2.416	2.162	343	105	1.117	7506
1 vs. 15	26.08	21.91	4.173	1.872	343	156	2.229	7506
3 vs. 5	20.18	18.81	1.375	1.176	697	446	1.17	7506
3 vs. 7	20.18	16.01	4.178	1.355	697	290	3.084	7506
3 vs. 10	20.18	23.66	-3.48	2.03	697	105	1.715	7506
3 vs. 15	20.18	21.91	-1.724	1.717	697	156	1.004	7506
5 vs. 7	18.81	16.01	2.802	1.462	446	290	1.916	7506
5 vs. 10	18.81	23.66	-4.856	2.103	446	105	2.309	7506
5 vs. 15	18.81	21.91	-3.099	1.803	446	156	1.718	7506
7 vs. 10	16.01	23.66	-7.658	2.208	290	105	3.468	7506
7 vs. 15	16.01	21.91	-5.901	1.925	290	156	3.066	7506
10 vs. 15	23.66	21.91	1.757	2.447	105	156	0.7178	7506

Within each row, compare columns (simple effects within rows)

Number of fam 6
Number of con 3
Alpha 0.05

Bonferroni's mu	Mean Diff.	95.00% CI	Significant	Summary	Adjusted P Value
1					
1% vs. 3%	8.001	4.038 to 1	Yes	****	<0.0001
1% vs. 5%	6.094	2.729 to 9.	Yes	****	<0.0001
3% vs. 5%	-1.907	-6.024 to 2	No	ns	0.8025
3					
1% vs. 3%	19.86	17.24 to 2	Yes	****	<0.0001
1% vs. 5%	16.68	14.02 to 1	Yes	****	<0.0001
3% vs. 5%	-3.175	-5.619 to -(	Yes	**	0.0056
5					
1% vs. 3%	20.88	18.16 to 2	Yes	****	<0.0001
1% vs. 5%	23.08	20.11 to 2	Yes	****	<0.0001
3% vs. 5%	2.195	-0.6786 to	No	ns	0.2023
7					
1% vs. 3%	43.32	39.99 to 4	Yes	****	<0.0001
1% vs. 5%	46.9	43.18 to 5	Yes	****	<0.0001
3% vs. 5%	3.576	0.094 to 7.	Yes	*	0.0418
10					
1% vs. 3%	21.02	17.86 to 2	Yes	****	<0.0001
1% vs. 5%	18.92	13.95 to 2	Yes	****	<0.0001
3% vs. 5%	-2.102	-7.237 to 3	No	ns	0.9811
15					
1% vs. 3%	27.79	24.31 to 3	Yes	****	<0.0001
1% vs. 5%	34.11	29.73 to 3	Yes	****	<0.0001
3% vs. 5%	6.32	1.783 to 1	Yes	**	0.0026

Test details	Mean 1	Mean 2	Mean Diff.	SE of diff.	N1	N2	t	DF
1								
1% vs. 3%	32.17	24.17	8.001	1.655	428	202	4.834	7506
1% vs. 5%	32.17	26.08	6.094	1.405	428	343	4.337	7506
3% vs. 5%	24.17	26.08	-1.907	1.719	202	343	1.109	7506
3								
1% vs. 3%	36.87	17.01	19.86	1.093	543	747	18.16	7506
1% vs. 5%	36.87	20.18	16.68	1.11	543	697	15.03	7506
3% vs. 5%	17.01	20.18	-3.175	1.021	747	697	3.109	7506
5								
1% vs. 3%	41.89	21	20.88	1.139	538	629	18.34	7506
1% vs. 5%	41.89	18.81	23.08	1.242	538	446	18.59	7506
3% vs. 5%	21	18.81	2.195	1.2	629	446	1.829	7506
7								
1% vs. 3%	62.91	19.58	43.32	1.392	336	459	31.12	7506
1% vs. 5%	62.91	16.01	46.9	1.554	336	290	30.18	7506
3% vs. 5%	19.58	16.01	3.576	1.454	459	290	2.459	7506
10								
1% vs. 3%	42.59	21.56	21.02	1.321	517	369	15.91	7506
1% vs. 5%	42.59	23.66	18.92	2.075	517	105	9.118	7506
3% vs. 5%	21.56	23.66	-2.102	2.144	369	105	0.9802	7506
15								
1% vs. 3%	56.02	28.23	27.79	1.456	401	318	19.09	7506
1% vs. 5%	56.02	21.91	34.11	1.829	401	156	18.65	7506
3% vs. 5%	28.23	21.91	6.32	1.895	318	156	3.335	7506

Table 35 – One-way ANOVA for the effects of time and hydrogel stiffness on Chapter 5 osteogenic data – ALIGNMENT

Table Analyze Data 1

Two-way ANOVA Ordinary
Alpha 0.05

Source of Vari	% of total v	P value	P value su	Significant?
Interaction	0.5727	<0.0001	****	Yes
Time	9.511	<0.0001	****	Yes
Agarose	2.269	<0.0001	****	Yes

ANOVA table	SS	DF	MS	F (DFn, DF	P value
Interaction	0.1415	10	0.01415	F (10, 750	P<0.0001
Time	2.349	5	0.4698	F (5, 7506)	P<0.0001
Agarose	0.5604	2	0.2802	F (2, 7506)	P<0.0001
Residual	21.65	7506	0.002884		

Number of mis 5922

Within each column, compare rows (simple effects within columns)

Number of fam 3
Number of cor 15
Alpha 0.05

Bonferroni's m	Mean Diff.	95.00% CI	Significant	Summary	Adjusted P Value
1%					
1 vs. 3	0.003661	-0.006532 t	No	ns	>0.9999
1 vs. 5	-0.00622	-0.01643 t	No	ns	>0.9999
1 vs. 7	-0.0175	-0.02899 t	Yes	***	0.0001
1 vs. 10	-0.03015	-0.04046 t	Yes	****	<0.0001
1 vs. 15	-0.05019	-0.06115 t	Yes	****	<0.0001
3 vs. 5	-0.00988	-0.01947 t	Yes	*	0.0377
3 vs. 7	-0.02116	-0.03211 t	Yes	****	<0.0001
3 vs. 10	-0.03382	-0.0435 to	Yes	****	<0.0001
3 vs. 15	-0.05385	-0.06423 t	Yes	****	<0.0001
5 vs. 7	-0.01128	-0.02225 t	Yes	*	0.0378
5 vs. 10	-0.02394	-0.03365 t	Yes	****	<0.0001
5 vs. 15	-0.04398	-0.05438 t	Yes	****	<0.0001
7 vs. 10	-0.01266	-0.0237 to	Yes	*	0.0116
7 vs. 15	-0.03269	-0.04435 t	Yes	****	<0.0001
10 vs. 15	-0.02004	-0.03053 t	Yes	****	<0.0001
3%					
1 vs. 3	-0.01441	-0.02692 t	Yes	*	0.0108
1 vs. 5	-0.01716	-0.02991 t	Yes	**	0.0012
1 vs. 7	-0.04257	-0.05588 t	Yes	****	<0.0001
1 vs. 10	-0.04442	-0.05822 t	Yes	****	<0.0001
1 vs. 15	-0.05056	-0.06475 t	Yes	****	<0.0001
3 vs. 5	-0.00274	-0.01128 t	No	ns	>0.9999
3 vs. 7	-0.02816	-0.03751 t	Yes	****	<0.0001
3 vs. 10	-0.03001	-0.04004 t	Yes	****	<0.0001
3 vs. 15	-0.03615	-0.04671 t	Yes	****	<0.0001
5 vs. 7	-0.02541	-0.03509 t	Yes	****	<0.0001
5 vs. 10	-0.02726	-0.0376 to	Yes	****	<0.0001
5 vs. 15	-0.0334	-0.04425 t	Yes	****	<0.0001
7 vs. 10	-0.00185	-0.01288 t	No	ns	>0.9999
7 vs. 15	-0.00799	-0.0195 to	No	ns	0.621
10 vs. 15	-0.00614	-0.01821 t	No	ns	>0.9999
5%					
1 vs. 3	0.000347	-0.01005 t	No	ns	>0.9999
1 vs. 5	-0.01844	-0.02977 t	Yes	****	<0.0001
1 vs. 7	-0.04351	-0.05609 t	Yes	****	<0.0001
1 vs. 10	-0.04523	-0.06282 t	Yes	****	<0.0001
1 vs. 15	-0.06345	-0.07868 t	Yes	****	<0.0001
3 vs. 5	-0.01879	-0.02835 t	Yes	****	<0.0001
3 vs. 7	-0.04386	-0.05487 t	Yes	****	<0.0001
3 vs. 10	-0.04558	-0.06209 t	Yes	****	<0.0001
3 vs. 15	-0.0638	-0.07776 t	Yes	****	<0.0001
5 vs. 7	-0.02507	-0.03696 t	Yes	****	<0.0001
5 vs. 10	-0.02679	-0.0439 to	Yes	****	<0.0001
5 vs. 15	-0.04501	-0.05968 t	Yes	****	<0.0001
7 vs. 10	-0.00172	-0.01968 t	No	ns	>0.9999
7 vs. 15	-0.01994	-0.0356 to	Yes	**	0.0028
10 vs. 15	-0.01822	-0.03812 t	No	ns	0.1083

Test details	Mean 1	Mean 2	Mean Diff.	SE of diff.	N1	N2	t	DF
1%								
1 vs. 3	0.102	0.09836	0.003661	0.003471	428	543	1.055	7506
1 vs. 5	0.102	0.1082	-0.00622	0.003479	428	538	1.787	7506
1 vs. 7	0.102	0.1195	-0.0175	0.003914	428	336	4.47	7506
1 vs. 10	0.102	0.1322	-0.03015	0.00351	428	517	8.592	7506
1 vs. 15	0.102	0.1522	-0.05019	0.003733	428	401	13.45	7506
3 vs. 5	0.09836	0.1082	-0.00988	0.003267	543	538	3.023	7506
3 vs. 7	0.09836	0.1195	-0.02116	0.003728	543	336	5.676	7506
3 vs. 10	0.09836	0.1322	-0.03382	0.0033	543	517	10.25	7506
3 vs. 15	0.09836	0.1522	-0.05385	0.003536	543	401	15.23	7506
5 vs. 7	0.1082	0.1195	-0.01128	0.003734	538	336	3.022	7506
5 vs. 10	0.1082	0.1322	-0.02394	0.003308	538	517	7.238	7506
5 vs. 15	0.1082	0.1522	-0.04398	0.003543	538	401	12.41	7506
7 vs. 10	0.1195	0.1322	-0.01266	0.003763	336	517	3.363	7506
7 vs. 15	0.1195	0.1522	-0.03269	0.003972	336	401	8.231	7506
10 vs. 15	0.1322	0.1522	-0.02004	0.003574	517	401	5.607	7506
3%								
1 vs. 3	0.1044	0.1189	-0.01441	0.004259	202	747	3.384	7506
1 vs. 5	0.1044	0.1216	-0.01716	0.004343	202	629	3.95	7506
1 vs. 7	0.1044	0.147	-0.04257	0.004535	202	459	9.388	7506
1 vs. 10	0.1044	0.1489	-0.04442	0.004701	202	369	9.45	7506
1 vs. 15	0.1044	0.155	-0.05056	0.004832	202	318	10.46	7506
3 vs. 5	0.1189	0.1216	-0.00274	0.002906	747	629	0.9441	7506
3 vs. 7	0.1189	0.147	-0.02816	0.003185	747	459	8.84	7506
3 vs. 10	0.1189	0.1489	-0.03001	0.003417	747	369	8.781	7506
3 vs. 15	0.1189	0.155	-0.03615	0.003596	747	318	10.05	7506
5 vs. 7	0.1216	0.147	-0.02541	0.003297	629	459	7.708	7506
5 vs. 10	0.1216	0.1489	-0.02726	0.003522	629	369	7.741	7506
5 vs. 15	0.1216	0.155	-0.0334	0.003695	629	318	9.039	7506
7 vs. 10	0.147	0.1489	-0.00185	0.003755	459	369	0.4929	7506
7 vs. 15	0.147	0.155	-0.00799	0.003918	459	318	2.04	7506
10 vs. 15	0.1489	0.155	-0.00614	0.004109	369	318	1.495	7506
5%								
1 vs. 3	0.1142	0.1139	0.000347	0.003542	343	697	0.09796	7506
1 vs. 5	0.1142	0.1327	-0.01844	0.003857	343	446	4.781	7506
1 vs. 7	0.1142	0.1577	-0.04351	0.004284	343	290	10.16	7506
1 vs. 10	0.1142	0.1595	-0.04523	0.00599	343	105	7.551	7506
1 vs. 15	0.1142	0.1777	-0.06345	0.005186	343	156	12.23	7506
3 vs. 5	0.1139	0.1327	-0.01879	0.003257	697	446	5.769	7506
3 vs. 7	0.1139	0.1577	-0.04386	0.003753	697	290	11.69	7506
3 vs. 10	0.1139	0.1595	-0.04558	0.005622	697	105	8.107	7506
3 vs. 15	0.1139	0.1777	-0.0638	0.004757	697	156	13.41	7506
5 vs. 7	0.1327	0.1577	-0.02507	0.004051	446	290	6.188	7506
5 vs. 10	0.1327	0.1595	-0.02679	0.005826	446	105	4.599	7506
5 vs. 15	0.1327	0.1777	-0.04501	0.004996	446	156	9.01	7506
7 vs. 10	0.1577	0.1595	-0.00172	0.006117	290	105	0.2817	7506
7 vs. 15	0.1577	0.1777	-0.01994	0.005332	290	156	3.74	7506
10 vs. 15	0.1595	0.1777	-0.01822	0.006779	105	156	2.687	7506

Within each row, compare columns (simple effects within rows)

Number of fam 6
Number of con 3
Alpha 0.05

Bonferroni's mu	Mean Diff.	95.00% CI	Significant	Summary	Adjusted P Value
1					
1% vs. 3%	-0.00242	-0.0134 to	No	ns	>0.9999
1% vs. 5%	-0.01221	-0.02153 t	Yes	**	0.0051
3% vs. 5%	-0.00979	-0.02119 t	No	ns	0.1199
3					
1% vs. 3%	-0.0205	-0.02775 t	Yes	****	<0.0001
1% vs. 5%	-0.01552	-0.02288 t	Yes	****	<0.0001
3% vs. 5%	0.004975	-0.001797	No	ns	0.2359
5					
1% vs. 3%	-0.01337	-0.02092 t	Yes	****	<0.0001
1% vs. 5%	-0.02443	-0.03267 t	Yes	****	<0.0001
3% vs. 5%	-0.01107	-0.01903 t	Yes	**	0.0026
7					
1% vs. 3%	-0.02749	-0.03673 t	Yes	****	<0.0001
1% vs. 5%	-0.03822	-0.04853 t	Yes	****	<0.0001
3% vs. 5%	-0.01073	-0.02037 t	Yes	*	0.0233
10					
1% vs. 3%	-0.01669	-0.02545 t	Yes	****	<0.0001
1% vs. 5%	-0.02729	-0.04105 t	Yes	****	<0.0001
3% vs. 5%	-0.0106	-0.02482 t	No	ns	0.2233
15					
1% vs. 3%	-0.00279	-0.01245 t	No	ns	>0.9999
1% vs. 5%	-0.02547	-0.0376 to	Yes	****	<0.0001
3% vs. 5%	-0.02267	-0.03524 t	Yes	****	<0.0001

Test details	Mean 1	Mean 2	Mean Diff.	SE of diff.	N1	N2	t	DF
1								
1% vs. 3%	0.102	0.1044	-0.00242	0.004585	428	202	0.5283	7506
1% vs. 5%	0.102	0.1142	-0.01221	0.003892	428	343	3.137	7506
3% vs. 5%	0.1044	0.1142	-0.00979	0.004763	202	343	2.055	7506
3								
1% vs. 3%	0.09836	0.1189	-0.0205	0.003029	543	747	6.768	7506
1% vs. 5%	0.09836	0.1139	-0.01552	0.003074	543	697	5.049	7506
3% vs. 5%	0.1189	0.1139	0.004975	0.002828	747	697	1.759	7506
5								
1% vs. 3%	0.1082	0.1216	-0.01337	0.003154	538	629	4.238	7506
1% vs. 5%	0.1082	0.1327	-0.02443	0.003439	538	446	7.105	7506
3% vs. 5%	0.1216	0.1327	-0.01107	0.003325	629	446	3.329	7506
7								
1% vs. 3%	0.1195	0.147	-0.02749	0.003856	336	459	7.13	7506
1% vs. 5%	0.1195	0.1577	-0.03822	0.004305	336	290	8.878	7506
3% vs. 5%	0.147	0.1577	-0.01073	0.004029	459	290	2.662	7506
10								
1% vs. 3%	0.1322	0.1489	-0.01669	0.00366	517	369	4.56	7506
1% vs. 5%	0.1322	0.1595	-0.02729	0.005749	517	105	4.746	7506
3% vs. 5%	0.1489	0.1595	-0.0106	0.00594	369	105	1.784	7506
15								
1% vs. 3%	0.1522	0.155	-0.00279	0.004033	401	318	0.6926	7506
1% vs. 5%	0.1522	0.1777	-0.02547	0.005068	401	156	5.025	7506
3% vs. 5%	0.155	0.1777	-0.02267	0.00525	318	156	4.319	7506

Table 36 – One-way ANOVA for the effects of time and hydrogel stiffness on Chapter 5 osteogenic data – CURVATURE

Table Analyze Data 1

Two-way ANO Ordinary
Alpha 0.05

Source of Vari	% of total v	P value	P value su	Significant?
Interaction	0.3866	0.0005	***	Yes
Time	6.642	<0.0001	****	Yes
Agarose	1.464	<0.0001	****	Yes

ANOVA table	SS	DF	MS	F (DFn, DF	P value
Interaction	0.1995	10	0.01995	F (10, 750	P=0.0005
Time	3.427	5	0.6855	F (5, 7506)	P<0.0001
Agarose	0.7553	2	0.3777	F (2, 7506)	P<0.0001
Residual	47.22	7506	0.006291		

Number of mis 5922

Within each column, compare rows (simple effects within columns)

Number of fam 3
Number of cor 15
Alpha 0.05

Bonferroni's m	Mean Diff.	95.00% CI	Significant	Summary	Adjusted P Value
1%					
1 vs. 3	0.006252	-0.008802 t	No	ns	>0.9999
1 vs. 5	0.02304	0.007951 t	Yes	***	0.0001
1 vs. 7	0.03029	0.01331 to	Yes	****	<0.0001
1 vs. 10	0.05329	0.03807 to	Yes	****	<0.0001
1 vs. 15	0.07232	0.05614 to	Yes	****	<0.0001
3 vs. 5	0.01678	0.002616 t	Yes	**	0.0076
3 vs. 7	0.02403	0.007869 t	Yes	***	0.0002
3 vs. 10	0.04704	0.03273 to	Yes	****	<0.0001
3 vs. 15	0.06607	0.05074 to	Yes	****	<0.0001
5 vs. 7	0.007251	-0.008943 t	No	ns	>0.9999
5 vs. 10	0.03026	0.01592 to	Yes	****	<0.0001
5 vs. 15	0.04929	0.03392 to	Yes	****	<0.0001
7 vs. 10	0.02301	0.006688 t	Yes	***	0.0005
7 vs. 15	0.04204	0.02481 to	Yes	****	<0.0001
10 vs. 15	0.01903	0.003531 t	Yes	**	0.0047
3%					
1 vs. 3	0.01849	1.582e-005	Yes	*	0.0496
1 vs. 5	0.02205	0.003218 t	Yes	**	0.0088
1 vs. 7	0.04804	0.02838 to	Yes	****	<0.0001
1 vs. 10	0.05049	0.03011 to	Yes	****	<0.0001
1 vs. 15	0.05589	0.03494 to	Yes	****	<0.0001
3 vs. 5	0.003567	-0.009036 t	No	ns	>0.9999
3 vs. 7	0.02955	0.01574 to	Yes	****	<0.0001
3 vs. 10	0.032	0.01719 to	Yes	****	<0.0001
3 vs. 15	0.03741	0.02181 to	Yes	****	<0.0001
5 vs. 7	0.02599	0.01169 to	Yes	****	<0.0001
5 vs. 10	0.02844	0.01317 to	Yes	****	<0.0001
5 vs. 15	0.03384	0.01782 to	Yes	****	<0.0001
7 vs. 10	0.00245	-0.01383 t	No	ns	>0.9999
7 vs. 15	0.007853	-0.009139 t	No	ns	>0.9999
10 vs. 15	0.005403	-0.01242 t	No	ns	>0.9999
5%					
1 vs. 3	-0.00167	-0.01703 t	No	ns	>0.9999
1 vs. 5	0.02126	0.004537 t	Yes	**	0.0029
1 vs. 7	0.04607	0.02749 to	Yes	****	<0.0001
1 vs. 10	0.06174	0.03577 to	Yes	****	<0.0001
1 vs. 15	0.07051	0.04802 to	Yes	****	<0.0001
3 vs. 5	0.02293	0.008805 t	Yes	****	<0.0001
3 vs. 7	0.04774	0.03146 to	Yes	****	<0.0001
3 vs. 10	0.06341	0.03903 to	Yes	****	<0.0001
3 vs. 15	0.07218	0.05155 to	Yes	****	<0.0001
5 vs. 7	0.02481	0.007243 t	Yes	***	0.0005
5 vs. 10	0.04048	0.01522 to	Yes	****	<0.0001
5 vs. 15	0.04925	0.02759 to	Yes	****	<0.0001
7 vs. 10	0.01567	-0.01085 t	No	ns	>0.9999
7 vs. 15	0.02444	0.001315 t	Yes	*	0.0288
10 vs. 15	0.008768	-0.02063 t	No	ns	>0.9999

Test details	Mean 1	Mean 2	Mean Diff.	SE of diff.	N1	N2	t	DF
1%								
1 vs. 3	0.2421	0.2358	0.006252	0.005127	428	543	1.219	7506
1 vs. 5	0.2421	0.2191	0.02304	0.005137	428	538	4.484	7506
1 vs. 7	0.2421	0.2118	0.03029	0.005781	428	336	5.239	7506
1 vs. 10	0.2421	0.1888	0.05329	0.005183	428	517	10.28	7506
1 vs. 15	0.2421	0.1698	0.07232	0.005513	428	401	13.12	7506
3 vs. 5	0.2358	0.2191	0.01678	0.004825	543	538	3.478	7506
3 vs. 7	0.2358	0.2118	0.02403	0.005506	543	336	4.365	7506
3 vs. 10	0.2358	0.1888	0.04704	0.004874	543	517	9.652	7506
3 vs. 15	0.2358	0.1698	0.06607	0.005223	543	401	12.65	7506
5 vs. 7	0.2191	0.2118	0.007251	0.005515	538	336	1.315	7506
5 vs. 10	0.2191	0.1888	0.03026	0.004885	538	517	6.194	7506
5 vs. 15	0.2191	0.1698	0.04929	0.005233	538	401	9.419	7506
7 vs. 10	0.2118	0.1888	0.02301	0.005558	336	517	4.139	7506
7 vs. 15	0.2118	0.1698	0.04204	0.005866	336	401	7.166	7506
10 vs. 15	0.1888	0.1698	0.01903	0.005278	517	401	3.605	7506
3%								
1 vs. 3	0.2298	0.2113	0.01849	0.00629	202	747	2.939	7506
1 vs. 5	0.2298	0.2077	0.02205	0.006415	202	629	3.438	7506
1 vs. 7	0.2298	0.1817	0.04804	0.006697	202	459	7.173	7506
1 vs. 10	0.2298	0.1793	0.05049	0.006942	202	369	7.273	7506
1 vs. 15	0.2298	0.1739	0.05589	0.007137	202	318	7.832	7506
3 vs. 5	0.2113	0.2077	0.003567	0.004292	747	629	0.831	7506
3 vs. 7	0.2113	0.1817	0.02955	0.004704	747	459	6.283	7506
3 vs. 10	0.2113	0.1793	0.032	0.005047	747	369	6.341	7506
3 vs. 15	0.2113	0.1739	0.03741	0.005311	747	318	7.043	7506
5 vs. 7	0.2077	0.1817	0.02599	0.004869	629	459	5.337	7506
5 vs. 10	0.2077	0.1793	0.02844	0.005201	629	369	5.467	7506
5 vs. 15	0.2077	0.1739	0.03384	0.005458	629	318	6.2	7506
7 vs. 10	0.1817	0.1793	0.00245	0.005546	459	369	0.4418	7506
7 vs. 15	0.1817	0.1739	0.007853	0.005787	459	318	1.357	7506
10 vs. 15	0.1793	0.1739	0.005403	0.006069	369	318	0.8902	7506
5%								
1 vs. 3	0.2164	0.2181	-0.00167	0.005232	343	697	0.3183	7506
1 vs. 5	0.2164	0.1951	0.02126	0.005696	343	446	3.733	7506
1 vs. 7	0.2164	0.1703	0.04607	0.006327	343	290	7.281	7506
1 vs. 10	0.2164	0.1546	0.06174	0.008846	343	105	6.979	7506
1 vs. 15	0.2164	0.1459	0.07051	0.00766	343	156	9.206	7506
3 vs. 5	0.2181	0.1951	0.02293	0.00481	697	446	4.767	7506
3 vs. 7	0.2181	0.1703	0.04774	0.005543	697	290	8.613	7506
3 vs. 10	0.2181	0.1546	0.06341	0.008303	697	105	7.637	7506
3 vs. 15	0.2181	0.1459	0.07218	0.007025	697	156	10.27	7506
5 vs. 7	0.1951	0.1703	0.02481	0.005983	446	290	4.147	7506
5 vs. 10	0.1951	0.1546	0.04048	0.008604	446	105	4.705	7506
5 vs. 15	0.1951	0.1459	0.04925	0.007378	446	156	6.675	7506
7 vs. 10	0.1703	0.1546	0.01567	0.009034	290	105	1.735	7506
7 vs. 15	0.1703	0.1459	0.02444	0.007876	290	156	3.103	7506
10 vs. 15	0.1546	0.1459	0.008768	0.01001	105	156	0.8757	7506

Within each row, compare columns (simple effects within rows)

Number of fam 6
Number of con 3
Alpha 0.05

Bonferroni's mu	Mean Diff.	95.00% CI	Significant	Summary	Adjusted P Value
1					
1% vs. 3%	0.01231	-0.003902	No	ns	0.2072
1% vs. 5%	0.0257	0.01193 to	Yes	****	<0.0001
3% vs. 5%	0.01339	-0.00346 t	No	ns	0.1714
3					
1% vs. 3%	0.02454	0.01383 to	Yes	****	<0.0001
1% vs. 5%	0.01778	0.008908 t	Yes	***	0.0003
3% vs. 5%	-0.00677	-0.01677 t	No	ns	0.3161
5					
1% vs. 3%	0.01133	0.0001745	Yes	*	0.0451
1% vs. 5%	0.02392	0.01176 to	Yes	****	<0.0001
3% vs. 5%	0.0126	0.0008378	Yes	*	0.031
7					
1% vs. 3%	0.03006	0.01643 to	Yes	****	<0.0001
1% vs. 5%	0.04148	0.02626 to	Yes	****	<0.0001
3% vs. 5%	0.01142	-0.002828	No	ns	0.165
10					
1% vs. 3%	0.009506	-0.003437	No	ns	0.2361
1% vs. 5%	0.03415	0.01382 to	Yes	***	0.0002
3% vs. 5%	0.02464	0.003633 t	Yes	*	0.015
15					
1% vs. 3%	-0.00412	-0.01838 t	No	ns	>0.9999
1% vs. 5%	0.02389	0.005964 t	Yes	**	0.0043
3% vs. 5%	0.02801	0.00944 to	Yes	***	0.0009

Test details	Mean 1	Mean 2	Mean Diff.	SE of diff.	N1	N2	t	DF
1								
1% vs. 3%	0.2421	0.2298	0.01231	0.006771	428	202	1.818	7506
1% vs. 5%	0.2421	0.2164	0.0257	0.005748	428	343	4.47	7506
3% vs. 5%	0.2298	0.2164	0.01339	0.007035	202	343	1.903	7506
3								
1% vs. 3%	0.2358	0.2113	0.02454	0.004473	543	747	5.487	7506
1% vs. 5%	0.2358	0.2181	0.01778	0.00454	543	697	3.916	7506
3% vs. 5%	0.2113	0.2181	-0.00677	0.004177	747	697	1.62	7506
5								
1% vs. 3%	0.2191	0.2077	0.01133	0.004658	538	629	2.432	7506
1% vs. 5%	0.2191	0.1951	0.02392	0.005079	538	446	4.71	7506
3% vs. 5%	0.2077	0.1951	0.0126	0.00491	629	446	2.565	7506
7								
1% vs. 3%	0.2118	0.1817	0.03006	0.005695	336	459	5.279	7506
1% vs. 5%	0.2118	0.1703	0.04148	0.006358	336	290	6.525	7506
3% vs. 5%	0.1817	0.1703	0.01142	0.00595	459	290	1.919	7506
10								
1% vs. 3%	0.1888	0.1793	0.009506	0.005405	517	369	1.759	7506
1% vs. 5%	0.1888	0.1546	0.03415	0.00849	517	105	4.022	7506
3% vs. 5%	0.1793	0.1546	0.02464	0.008773	369	105	2.809	7506
15								
1% vs. 3%	0.1698	0.1739	-0.00412	0.005956	401	318	0.6916	7506
1% vs. 5%	0.1698	0.1459	0.02389	0.007485	401	156	3.191	7506
3% vs. 5%	0.1739	0.1459	0.02801	0.007753	318	156	3.612	7506

Table 37 – One-way ANOVA for the effects of time and hydrogel stiffness on Chapter 5 osteogenic data – STELLATE FACTOR

Table Analyze Data 1

Two-way ANOVA Ordinary
Alpha 0.05

Source of Vari	% of total v	P value	P value su	Significant?
Interaction	0.3143	0.0026	**	Yes
Time	11.41	<0.0001	****	Yes
Agarose	1.072	<0.0001	****	Yes

ANOVA table	SS	DF	MS	F (DFn, DF	P value
Interaction	0.8296	10	0.08296	F (10, 750	P=0.0026
Time	30.12	5	6.024	F (5, 7506)	P<0.0001
Agarose	2.829	2	1.415	F (2, 7506)	P<0.0001
Residual	230.1	7506	0.03066		

Number of mis 5922

Within each column, compare rows (simple effects within columns)

Number of fam 3
Number of cor 15
Alpha 0.05

Bonferroni's m	Mean Diff.	95.00% CI	Significant	Summary	Adjusted P Value
1%					
1 vs. 3	-0.08317	-0.1164 to	Yes	****	<0.0001
1 vs. 5	-0.1226	-0.1559 to	Yes	****	<0.0001
1 vs. 7	-0.1763	-0.2138 to	Yes	****	<0.0001
1 vs. 10	-0.1653	-0.1989 to	Yes	****	<0.0001
1 vs. 15	-0.2434	-0.2792 to	Yes	****	<0.0001
3 vs. 5	-0.03939	-0.07066 tc	Yes	**	0.0033
3 vs. 7	-0.09312	-0.1288 to	Yes	****	<0.0001
3 vs. 10	-0.0821	-0.1137 to	Yes	****	<0.0001
3 vs. 15	-0.1603	-0.1941 to	Yes	****	<0.0001
5 vs. 7	-0.05374	-0.08949 tc	Yes	***	0.0002
5 vs. 10	-0.04271	-0.07437 tc	Yes	**	0.0011
5 vs. 15	-0.1209	-0.1548 to	Yes	****	<0.0001
7 vs. 10	0.01103	-0.025 to 0	No	ns	>0.9999
7 vs. 15	-0.06713	-0.1052 to	Yes	****	<0.0001
10 vs. 15	-0.07816	-0.1124 to	Yes	****	<0.0001
3%					
1 vs. 3	-0.09417	-0.1349 to	Yes	****	<0.0001
1 vs. 5	-0.1098	-0.1513 to	Yes	****	<0.0001
1 vs. 7	-0.1439	-0.1873 to	Yes	****	<0.0001
1 vs. 10	-0.1736	-0.2186 to	Yes	****	<0.0001
1 vs. 15	-0.2234	-0.2696 to	Yes	****	<0.0001
3 vs. 5	-0.0156	-0.04342 tc	No	ns	>0.9999
3 vs. 7	-0.04969	-0.08018 tc	Yes	****	<0.0001
3 vs. 10	-0.07948	-0.1122 to	Yes	****	<0.0001
3 vs. 15	-0.1292	-0.1636 to	Yes	****	<0.0001
5 vs. 7	-0.03409	-0.06565 tc	Yes	*	0.0229
5 vs. 10	-0.06388	-0.0976 to	Yes	****	<0.0001
5 vs. 15	-0.1136	-0.149 to -(	Yes	****	<0.0001
7 vs. 10	-0.02979	-0.06574 tc	No	ns	0.2247
7 vs. 15	-0.07951	-0.117 to -(	Yes	****	<0.0001
10 vs. 15	-0.04972	-0.08905 tc	Yes	**	0.0031
5%					
1 vs. 3	-0.05679	-0.0907 to	Yes	****	<0.0001
1 vs. 5	-0.0805	-0.1174 to	Yes	****	<0.0001
1 vs. 7	-0.1111	-0.1521 to	Yes	****	<0.0001
1 vs. 10	-0.1165	-0.1738 to	Yes	****	<0.0001
1 vs. 15	-0.2338	-0.2835 to	Yes	****	<0.0001
3 vs. 5	-0.02372	-0.05489 tc	No	ns	0.3832
3 vs. 7	-0.05433	-0.09025 tc	Yes	***	0.0001
3 vs. 10	-0.05966	-0.1135 to	Yes	*	0.0171
3 vs. 15	-0.1771	-0.2226 to	Yes	****	<0.0001
5 vs. 7	-0.03061	-0.06939 tc	No	ns	0.3076
5 vs. 10	-0.03595	-0.09172 tc	No	ns	0.8766
5 vs. 15	-0.1533	-0.2012 to	Yes	****	<0.0001
7 vs. 10	-0.00534	-0.0639 to	No	ns	>0.9999
7 vs. 15	-0.1227	-0.1738 to	Yes	****	<0.0001
10 vs. 15	-0.1174	-0.1823 to	Yes	****	<0.0001

Test details	Mean 1	Mean 2	Mean Diff.	SE of diff.	N1	N2	t	DF
1%								
1 vs. 3	0.3325	0.4156	-0.08317	0.01132	428	543	7.349	7506
1 vs. 5	0.3325	0.455	-0.1226	0.01134	428	538	10.81	7506
1 vs. 7	0.3325	0.5088	-0.1763	0.01276	428	336	13.81	7506
1 vs. 10	0.3325	0.4977	-0.1653	0.01144	428	517	14.44	7506
1 vs. 15	0.3325	0.5759	-0.2434	0.01217	428	401	20	7506
3 vs. 5	0.4156	0.455	-0.03939	0.01065	543	538	3.698	7506
3 vs. 7	0.4156	0.5088	-0.09312	0.01215	543	336	7.662	7506
3 vs. 10	0.4156	0.4977	-0.0821	0.01076	543	517	7.63	7506
3 vs. 15	0.4156	0.5759	-0.1603	0.01153	543	401	13.9	7506
5 vs. 7	0.455	0.5088	-0.05374	0.01218	538	336	4.414	7506
5 vs. 10	0.455	0.4977	-0.04271	0.01078	538	517	3.96	7506
5 vs. 15	0.455	0.5759	-0.1209	0.01155	538	401	10.46	7506
7 vs. 10	0.5088	0.4977	0.01103	0.01227	336	517	0.8988	7506
7 vs. 15	0.5088	0.5759	-0.06713	0.01295	336	401	5.183	7506
10 vs. 15	0.4977	0.5759	-0.07816	0.01165	517	401	6.708	7506
3%								
1 vs. 3	0.2992	0.3934	-0.09417	0.01389	202	747	6.781	7506
1 vs. 5	0.2992	0.409	-0.1098	0.01416	202	629	7.751	7506
1 vs. 7	0.2992	0.4431	-0.1439	0.01478	202	459	9.73	7506
1 vs. 10	0.2992	0.4729	-0.1736	0.01533	202	369	11.33	7506
1 vs. 15	0.2992	0.5226	-0.2234	0.01575	202	318	14.18	7506
3 vs. 5	0.3934	0.409	-0.0156	0.009476	747	629	1.646	7506
3 vs. 7	0.3934	0.4431	-0.04969	0.01038	747	459	4.785	7506
3 vs. 10	0.3934	0.4729	-0.07948	0.01114	747	369	7.134	7506
3 vs. 15	0.3934	0.5226	-0.1292	0.01172	747	318	11.02	7506
5 vs. 7	0.409	0.4431	-0.03409	0.01075	629	459	3.171	7506
5 vs. 10	0.409	0.4729	-0.06388	0.01148	629	369	5.564	7506
5 vs. 15	0.409	0.5226	-0.1136	0.01205	629	318	9.428	7506
7 vs. 10	0.4431	0.4729	-0.02979	0.01224	459	369	2.433	7506
7 vs. 15	0.4431	0.5226	-0.07951	0.01278	459	318	6.223	7506
10 vs. 15	0.4729	0.5226	-0.04972	0.0134	369	318	3.711	7506
5%								
1 vs. 3	0.3137	0.3705	-0.05679	0.01155	343	697	4.917	7506
1 vs. 5	0.3137	0.3942	-0.0805	0.01258	343	446	6.402	7506
1 vs. 7	0.3137	0.4248	-0.1111	0.01397	343	290	7.955	7506
1 vs. 10	0.3137	0.4301	-0.1165	0.01953	343	105	5.963	7506
1 vs. 15	0.3137	0.5475	-0.2338	0.01691	343	156	13.83	7506
3 vs. 5	0.3705	0.3942	-0.02372	0.01062	697	446	2.233	7506
3 vs. 7	0.3705	0.4248	-0.05433	0.01224	697	290	4.44	7506
3 vs. 10	0.3705	0.4301	-0.05966	0.01833	697	105	3.255	7506
3 vs. 15	0.3705	0.5475	-0.1771	0.01551	697	156	11.42	7506
5 vs. 7	0.3942	0.4248	-0.03061	0.01321	446	290	2.317	7506
5 vs. 10	0.3942	0.4301	-0.03595	0.01899	446	105	1.893	7506
5 vs. 15	0.3942	0.5475	-0.1533	0.01629	446	156	9.414	7506
7 vs. 10	0.4248	0.4301	-0.00534	0.01994	290	105	0.2677	7506
7 vs. 15	0.4248	0.5475	-0.1227	0.01739	290	156	7.059	7506
10 vs. 15	0.4301	0.5475	-0.1174	0.0221	105	156	5.311	7506

Within each row, compare columns (simple effects within rows)

Number of fam 6
Number of con 3
Alpha 0.05

Bonferroni's mu	Mean Diff.	95.00% CI	Significant	Summary	Adjusted P Value
1					
1% vs. 3%	0.03325	-0.002542	No	ns	0.0784
1% vs. 5%	0.01877	-0.01162 tc	No	ns	0.4178
3% vs. 5%	-0.01449	-0.05167 tc	No	ns	>0.9999
3					
1% vs. 3%	0.02226	-0.001387	No	ns	0.0727
1% vs. 5%	0.04515	0.02115 to	Yes	****	<0.0001
3% vs. 5%	0.02289	0.0008098	Yes	*	0.0392
5					
1% vs. 3%	0.04605	0.02142 to	Yes	****	<0.0001
1% vs. 5%	0.06082	0.03397 to	Yes	****	<0.0001
3% vs. 5%	0.01478	-0.01118 tc	No	ns	0.5187
7					
1% vs. 3%	0.06569	0.03559 to	Yes	****	<0.0001
1% vs. 5%	0.08395	0.05034 to	Yes	****	<0.0001
3% vs. 5%	0.01825	-0.0132 to	No	ns	0.494
10					
1% vs. 3%	0.02487	-0.003702	No	ns	0.1115
1% vs. 5%	0.06758	0.0227 to	Yes	***	0.0009
3% vs. 5%	0.04271	-0.003667	No	ns	0.0824
15					
1% vs. 3%	0.05331	0.02183 to	Yes	***	0.0002
1% vs. 5%	0.02835	-0.01122 tc	No	ns	0.2588
3% vs. 5%	-0.02497	-0.06595 tc	No	ns	0.4341

Test details	Mean 1	Mean 2	Mean Diff.	SE of diff.	N1	N2	t	DF
1								
1% vs. 3%	0.3325	0.2992	0.03325	0.01495	428	202	2.224	7506
1% vs. 5%	0.3325	0.3137	0.01877	0.01269	428	343	1.479	7506
3% vs. 5%	0.2992	0.3137	-0.01449	0.01553	202	343	0.9327	7506
3								
1% vs. 3%	0.4156	0.3934	0.02226	0.009875	543	747	2.254	7506
1% vs. 5%	0.4156	0.3705	0.04515	0.01002	543	697	4.505	7506
3% vs. 5%	0.3934	0.3705	0.02289	0.009222	747	697	2.482	7506
5								
1% vs. 3%	0.455	0.409	0.04605	0.01028	538	629	4.478	7506
1% vs. 5%	0.455	0.3942	0.06082	0.01121	538	446	5.424	7506
3% vs. 5%	0.409	0.3942	0.01478	0.01084	629	446	1.363	7506
7								
1% vs. 3%	0.5088	0.4431	0.06569	0.01257	336	459	5.225	7506
1% vs. 5%	0.5088	0.4248	0.08395	0.01404	336	290	5.981	7506
3% vs. 5%	0.4431	0.4248	0.01825	0.01314	459	290	1.39	7506
10								
1% vs. 3%	0.4977	0.4729	0.02487	0.01193	517	369	2.084	7506
1% vs. 5%	0.4977	0.4301	0.06758	0.01874	517	105	3.606	7506
3% vs. 5%	0.4729	0.4301	0.04271	0.01937	369	105	2.205	7506
15								
1% vs. 3%	0.5759	0.5226	0.05331	0.01315	401	318	4.055	7506
1% vs. 5%	0.5759	0.5475	0.02835	0.01652	401	156	1.716	7506
3% vs. 5%	0.5226	0.5475	-0.02497	0.01712	318	156	1.459	7506

Table 38 – One-way ANOVA for the effects of time and hydrogel stiffness on Chapter 5 osteogenic data – LENGTH

Table Analyze Data 1

Two-way ANOVA Ordinary
Alpha 0.05

Source of Vari	% of total v	P value	P value su	Significant?
Interaction	0.2868	0.015	*	Yes
Time	0.2939	0.0004	***	Yes
Agarose	1.776	<0.0001	****	Yes

ANOVA table	SS	DF	MS	F (DFn, DF	P value
Interaction	41436	10	4144	F (10, 750	P=0.0150
Time	42460	5	8492	F (5, 7506)	P=0.0004
Agarose	256595	2	128297	F (2, 7506)	P<0.0001
Residual	14108871	7506	1880		

Number of mis 5922

Within each column, compare rows (simple effects within columns)

Number of fam 3
Number of cor 15
Alpha 0.05

Bonferroni's m	Mean Diff.	95.00% CI	Significant	Summary	Adjusted P Value
1%					
1 vs. 3	-9.765	-17.99 to -1	Yes	**	0.0074
1 vs. 5	-0.4016	-8.647 to 7	No	ns	>0.9999
1 vs. 7	-9.402	-18.68 to -(	Yes	*	0.0441
1 vs. 10	-3.408	-11.73 to 4	No	ns	>0.9999
1 vs. 15	-7.054	-15.9 to 1.	No	ns	0.2888
3 vs. 5	9.363	1.62 to 17.	Yes	**	0.0058
3 vs. 7	0.3633	-8.473 to 9	No	ns	>0.9999
3 vs. 10	6.357	-1.465 to 1	No	ns	0.2558
3 vs. 15	2.711	-5.671 to 1	No	ns	>0.9999
5 vs. 7	-9	-17.85 to -(	Yes	*	0.0426
5 vs. 10	-3.006	-10.85 to 4	No	ns	>0.9999
5 vs. 15	-6.653	-15.05 to 1	No	ns	0.3008
7 vs. 10	5.994	-2.927 to 1	No	ns	0.7283
7 vs. 15	2.347	-7.067 to 1	No	ns	>0.9999
10 vs. 15	-3.646	-12.12 to 4	No	ns	>0.9999
3%					
1 vs. 3	-0.6029	-10.7 to 9.4	No	ns	>0.9999
1 vs. 5	2.856	-7.439 to 1	No	ns	>0.9999
1 vs. 7	4.112	-6.636 to 1	No	ns	>0.9999
1 vs. 10	3.111	-8.031 to 1	No	ns	>0.9999
1 vs. 15	-4.055	-15.51 to 7	No	ns	>0.9999
3 vs. 5	3.459	-3.43 to 10	No	ns	>0.9999
3 vs. 7	4.715	-2.835 to 1	No	ns	>0.9999
3 vs. 10	3.714	-4.386 to 1	No	ns	>0.9999
3 vs. 15	-3.452	-11.98 to 5	No	ns	>0.9999
5 vs. 7	1.256	-6.559 to 9	No	ns	>0.9999
5 vs. 10	0.2548	-8.092 to 8	No	ns	>0.9999
5 vs. 15	-6.911	-15.67 to 1	No	ns	0.3081
7 vs. 10	-1.001	-9.901 to 7	No	ns	>0.9999
7 vs. 15	-8.167	-17.45 to 1	No	ns	0.1477
10 vs. 15	-7.166	-16.91 to 2	No	ns	0.4618
5%					
1 vs. 3	-5.969	-14.36 to 2	No	ns	0.5535
1 vs. 5	-7.96	-17.1 to 1.	No	ns	0.1589
1 vs. 7	0.5141	-9.641 to 1	No	ns	>0.9999
1 vs. 10	-3.424	-17.62 to 1	No	ns	>0.9999
1 vs. 15	-11.99	-24.28 to 0	No	ns	0.0629
3 vs. 5	-1.991	-9.71 to 5.	No	ns	>0.9999
3 vs. 7	6.483	-2.413 to 1	No	ns	0.486
3 vs. 10	2.545	-10.78 to 1	No	ns	>0.9999
3 vs. 15	-6.023	-17.3 to 5.	No	ns	>0.9999
5 vs. 7	8.474	-1.128 to 1	No	ns	0.1438
5 vs. 10	4.536	-9.272 to 1	No	ns	>0.9999
5 vs. 15	-4.032	-15.87 to 7	No	ns	>0.9999
7 vs. 10	-3.938	-18.44 to 1	No	ns	>0.9999
7 vs. 15	-12.51	-25.15 to 0	No	ns	0.0552
10 vs. 15	-8.568	-24.64 to 7	No	ns	>0.9999

Test details	Mean 1	Mean 2	Mean Diff.	SE of diff.	N1	N2	t	DF
1%								
1 vs. 3	64.79	74.55	-9.765	2.802	428	543	3.484	7506
1 vs. 5	64.79	65.19	-0.4016	2.808	428	538	0.143	7506
1 vs. 7	64.79	74.19	-9.402	3.16	428	336	2.975	7506
1 vs. 10	64.79	68.19	-3.408	2.833	428	517	1.203	7506
1 vs. 15	64.79	71.84	-7.054	3.013	428	401	2.341	7506
3 vs. 5	74.55	65.19	9.363	2.637	543	538	3.55	7506
3 vs. 7	74.55	74.19	0.3633	3.009	543	336	0.1207	7506
3 vs. 10	74.55	68.19	6.357	2.664	543	517	2.386	7506
3 vs. 15	74.55	71.84	2.711	2.855	543	401	0.9495	7506
5 vs. 7	65.19	74.19	-9	3.015	538	336	2.985	7506
5 vs. 10	65.19	68.19	-3.006	2.67	538	517	1.126	7506
5 vs. 15	65.19	71.84	-6.653	2.86	538	401	2.326	7506
7 vs. 10	74.19	68.19	5.994	3.038	336	517	1.973	7506
7 vs. 15	74.19	71.84	2.347	3.207	336	401	0.7321	7506
10 vs. 15	68.19	71.84	-3.646	2.885	517	401	1.264	7506
3%								
1 vs. 3	59.93	60.53	-0.6029	3.438	202	747	0.1754	7506
1 vs. 5	59.93	57.07	2.856	3.506	202	629	0.8146	7506
1 vs. 7	59.93	55.82	4.112	3.661	202	459	1.123	7506
1 vs. 10	59.93	56.82	3.111	3.795	202	369	0.8199	7506
1 vs. 15	59.93	63.99	-4.055	3.901	202	318	1.04	7506
3 vs. 5	60.53	57.07	3.459	2.346	747	629	1.474	7506
3 vs. 7	60.53	55.82	4.715	2.571	747	459	1.834	7506
3 vs. 10	60.53	56.82	3.714	2.759	747	369	1.346	7506
3 vs. 15	60.53	63.99	-3.452	2.903	747	318	1.189	7506
5 vs. 7	57.07	55.82	1.256	2.661	629	459	0.4718	7506
5 vs. 10	57.07	56.82	0.2548	2.843	629	369	0.08963	7506
5 vs. 15	57.07	63.99	-6.911	2.983	629	318	2.317	7506
7 vs. 10	55.82	56.82	-1.001	3.031	459	369	0.3302	7506
7 vs. 15	55.82	63.99	-8.167	3.163	459	318	2.582	7506
10 vs. 15	56.82	63.99	-7.166	3.317	369	318	2.16	7506
5%								
1 vs. 3	49.1	55.07	-5.969	2.86	343	697	2.087	7506
1 vs. 5	49.1	57.06	-7.96	3.114	343	446	2.557	7506
1 vs. 7	49.1	48.59	0.5141	3.459	343	290	0.1487	7506
1 vs. 10	49.1	52.53	-3.424	4.835	343	105	0.7081	7506
1 vs. 15	49.1	61.09	-11.99	4.187	343	156	2.864	7506
3 vs. 5	55.07	57.06	-1.991	2.629	697	446	0.7575	7506
3 vs. 7	55.07	48.59	6.483	3.03	697	290	2.14	7506
3 vs. 10	55.07	52.53	2.545	4.539	697	105	0.5607	7506
3 vs. 15	55.07	61.09	-6.023	3.84	697	156	1.568	7506
5 vs. 7	57.06	48.59	8.474	3.271	446	290	2.591	7506
5 vs. 10	57.06	52.53	4.536	4.703	446	105	0.9645	7506
5 vs. 15	57.06	61.09	-4.032	4.033	446	156	0.9997	7506
7 vs. 10	48.59	52.53	-3.938	4.938	290	105	0.7975	7506
7 vs. 15	48.59	61.09	-12.51	4.305	290	156	2.905	7506
10 vs. 15	52.53	61.09	-8.568	5.473	105	156	1.565	7506

Within each row, compare columns (simple effects within rows)

Number of fam 6
Number of con 3
Alpha 0.05

Bonferroni's mu	Mean Diff.	95.00% CI	Significant	Summary	Adjusted P Value
1					
1% vs. 3%	4.854	-4.008 to 1	No	ns	0.5692
1% vs. 5%	15.68	8.16 to 23.	Yes	****	<0.0001
3% vs. 5%	10.83	1.623 to 2(	Yes	*	0.0146
3					
1% vs. 3%	14.02	8.161 to 1(	Yes	****	<0.0001
1% vs. 5%	19.48	13.54 to 2!	Yes	****	<0.0001
3% vs. 5%	5.464	-0.002941	No	ns	0.0502
5					
1% vs. 3%	8.112	2.015 to 1.	Yes	**	0.0043
1% vs. 5%	8.125	1.477 to 1.	Yes	*	0.0103
3% vs. 5%	0.01369	-6.413 to 6	No	ns	>0.9999
7					
1% vs. 3%	18.37	10.91 to 2!	Yes	****	<0.0001
1% vs. 5%	25.6	17.28 to 3(	Yes	****	<0.0001
3% vs. 5%	7.232	-0.5553 to	No	ns	0.0786
10					
1% vs. 3%	11.37	4.298 to 1(	Yes	***	0.0004
1% vs. 5%	15.67	4.555 to 2!	Yes	**	0.0022
3% vs. 5%	4.295	-7.188 to 1	No	ns	>0.9999
15					
1% vs. 3%	7.853	0.05747 to	Yes	*	0.0476
1% vs. 5%	10.75	0.9504 to 2	Yes	*	0.0259
3% vs. 5%	2.894	-7.254 to 1	No	ns	>0.9999

Test details	Mean 1	Mean 2	Mean Diff.	SE of diff.	N1	N2	t	DF
1								
1% vs. 3%	64.79	59.93	4.854	3.701	428	202	1.312	7506
1% vs. 5%	64.79	49.1	15.68	3.142	428	343	4.992	7506
3% vs. 5%	59.93	49.1	10.83	3.845	202	343	2.816	7506
3								
1% vs. 3%	74.55	60.53	14.02	2.445	543	747	5.732	7506
1% vs. 5%	74.55	55.07	19.48	2.482	543	697	7.85	7506
3% vs. 5%	60.53	55.07	5.464	2.283	747	697	2.393	7506
5								
1% vs. 3%	65.19	57.07	8.112	2.546	538	629	3.186	7506
1% vs. 5%	65.19	57.06	8.125	2.776	538	446	2.927	7506
3% vs. 5%	57.07	57.06	0.01369	2.684	629	446	0.005101	7506
7								
1% vs. 3%	74.19	55.82	18.37	3.113	336	459	5.901	7506
1% vs. 5%	74.19	48.59	25.6	3.475	336	290	7.367	7506
3% vs. 5%	55.82	48.59	7.232	3.252	459	290	2.224	7506
10								
1% vs. 3%	68.19	56.82	11.37	2.955	517	369	3.849	7506
1% vs. 5%	68.19	52.53	15.67	4.641	517	105	3.376	7506
3% vs. 5%	56.82	52.53	4.295	4.795	369	105	0.8956	7506
15								
1% vs. 3%	71.84	63.99	7.853	3.256	401	318	2.412	7506
1% vs. 5%	71.84	61.09	10.75	4.091	401	156	2.627	7506
3% vs. 5%	63.99	61.09	2.894	4.238	318	156	0.6828	7506

Table 39 – One-way ANOVA for the effects of time and hydrogel stiffness on Chapter 5 osteogenic data – CHROMATIN CONDENSATION

Table Analyze Data 1

Two-way ANC Ordinary
Alpha 0.05

Source of Var	% of total \	P value	P value sui	Significant?
Interaction	2.071	<0.0001	****	Yes
Time	9.408	<0.0001	****	Yes
Agarose	0.6438	<0.0001	****	Yes

ANOVA table	SS	DF	MS	F (DFn, DF	P value
Interaction	0.008009	10	0.000801	F (10, 750	P<0.0001
Time	0.03638	5	0.007277	F (5, 7505)	P<0.0001
Agarose	0.00249	2	0.001245	F (2, 7505)	P<0.0001
Residual	0.3398	7505	4.53E-05		

Number of mi 5923

Within each column, compare rows (simple effects within columns)

Number of fan 3
Number of coi 15
Alpha 0.05

Bonferroni's m	Mean Diff.	95.00% CI	Significant	Summary	Adjusted P Value
1%					
1 vs. 3	0.000553	-0.0007241	No	ns	>0.9999
1 vs. 5	0.005191	0.003911 t	Yes	****	<0.0001
1 vs. 7	0.002793	0.001353 t	Yes	****	<0.0001
1 vs. 10	0.005735	0.004444 t	Yes	****	<0.0001
1 vs. 15	0.003545	0.002171 t	Yes	****	<0.0001
3 vs. 5	0.004638	0.003436 t	Yes	****	<0.0001
3 vs. 7	0.00224	0.0008686	Yes	****	<0.0001
3 vs. 10	0.005182	0.003968 t	Yes	****	<0.0001
3 vs. 15	0.002992	0.00169 to	Yes	****	<0.0001
5 vs. 7	-0.0024	-0.003772 t	Yes	****	<0.0001
5 vs. 10	0.000544	-0.0006728	No	ns	>0.9999
5 vs. 15	-0.00165	-0.00295 tc	Yes	**	0.0032
7 vs. 10	0.002942	0.001557 t	Yes	****	<0.0001
7 vs. 15	0.000752	-0.0007101	No	ns	>0.9999
10 vs. 15	-0.00219	-0.003506 t	Yes	****	<0.0001
3%					
1 vs. 3	0.004034	0.002467 t	Yes	****	<0.0001
1 vs. 5	0.005885	0.004287 t	Yes	****	<0.0001
1 vs. 7	0.004163	0.002495 t	Yes	****	<0.0001
1 vs. 10	0.004366	0.002637 t	Yes	****	<0.0001
1 vs. 15	0.00752	0.005742 t	Yes	****	<0.0001
3 vs. 5	0.001851	0.0007818	Yes	****	<0.0001
3 vs. 7	0.000129	-0.001043	No	ns	>0.9999
3 vs. 10	0.000332	-0.0009252	No	ns	>0.9999
3 vs. 15	0.003486	0.002163 t	Yes	****	<0.0001
5 vs. 7	-0.00172	-0.002935 t	Yes	***	0.0005
5 vs. 10	-0.00152	-0.002815 t	Yes	**	0.0087
5 vs. 15	0.001635	0.0002755	Yes	**	0.0062
7 vs. 10	0.000203	-0.001178	No	ns	>0.9999
7 vs. 15	0.003357	0.001915 t	Yes	****	<0.0001
10 vs. 15	0.003154	0.001642 t	Yes	****	<0.0001
5%					
1 vs. 3	0.007489	0.006186 t	Yes	****	<0.0001
1 vs. 5	0.009655	0.008236 t	Yes	****	<0.0001
1 vs. 7	0.008562	0.006986 t	Yes	****	<0.0001
1 vs. 10	0.009064	0.00686 to	Yes	****	<0.0001
1 vs. 15	0.01112	0.009207 t	Yes	****	<0.0001
3 vs. 5	0.002166	0.0009679	Yes	****	<0.0001
3 vs. 7	0.001073	-0.0003077	No	ns	0.3379
3 vs. 10	0.001575	-0.0004933	No	ns	0.3809
3 vs. 15	0.003626	0.001876 t	Yes	****	<0.0001
5 vs. 7	-0.00109	-0.002583	No	ns	0.47
5 vs. 10	-0.00059	-0.002734	No	ns	>0.9999
5 vs. 15	0.00146	-0.0003778	No	ns	0.2955
7 vs. 10	0.000502	-0.001748	No	ns	>0.9999
7 vs. 15	0.002553	0.0005912	Yes	**	0.002
10 vs. 15	0.002051	-0.000443	No	ns	0.2367

Test details	Mean 1	Mean 2	Mean Diff.	SE of diff.	N1	N2	t	DF
1%								
1 vs. 3	0.02679	0.02624	0.000553	0.000435	428	543	1.271	7505
1 vs. 5	0.02679	0.0216	0.005191	0.000436	428	538	11.91	7505
1 vs. 7	0.02679	0.024	0.002793	0.000491	428	336	5.694	7505
1 vs. 10	0.02679	0.02106	0.005735	0.00044	428	517	13.04	7505
1 vs. 15	0.02679	0.02325	0.003545	0.000468	428	400	7.575	7505
3 vs. 5	0.02624	0.0216	0.004638	0.000409	543	538	11.33	7505
3 vs. 7	0.02624	0.024	0.00224	0.000467	543	336	4.796	7505
3 vs. 10	0.02624	0.02106	0.005182	0.000414	543	517	12.53	7505
3 vs. 15	0.02624	0.02325	0.002992	0.000443	543	400	6.748	7505
5 vs. 7	0.0216	0.024	-0.0024	0.000468	538	336	5.125	7505
5 vs. 10	0.0216	0.02106	0.000544	0.000414	538	517	1.313	7505
5 vs. 15	0.0216	0.02325	-0.00165	0.000444	538	400	3.705	7505
7 vs. 10	0.024	0.02106	0.002942	0.000472	336	517	6.239	7505
7 vs. 15	0.024	0.02325	0.000752	0.000498	336	400	1.51	7505
10 vs. 15	0.02106	0.02325	-0.00219	0.000448	517	400	4.887	7505
3%								
1 vs. 3	0.02657	0.02254	0.004034	0.000534	202	747	7.559	7505
1 vs. 5	0.02657	0.02069	0.005885	0.000544	202	629	10.81	7505
1 vs. 7	0.02657	0.02241	0.004163	0.000568	202	459	7.327	7505
1 vs. 10	0.02657	0.02221	0.004366	0.000589	202	369	7.413	7505
1 vs. 15	0.02657	0.01905	0.00752	0.000605	202	318	12.42	7505
3 vs. 5	0.02254	0.02069	0.001851	0.000364	747	629	5.083	7505
3 vs. 7	0.02254	0.02241	0.000129	0.000399	747	459	0.3232	7505
3 vs. 10	0.02254	0.02221	0.000332	0.000428	747	369	0.7754	7505
3 vs. 15	0.02254	0.01905	0.003486	0.000451	747	318	7.737	7505
5 vs. 7	0.02069	0.02241	-0.00172	0.000413	629	459	4.169	7505
5 vs. 10	0.02069	0.02221	-0.00152	0.000441	629	369	3.442	7505
5 vs. 15	0.02069	0.01905	0.001635	0.000463	629	318	3.531	7505
7 vs. 10	0.02241	0.02221	0.000203	0.000471	459	369	0.4315	7505
7 vs. 15	0.02241	0.01905	0.003357	0.000491	459	318	6.837	7505
10 vs. 15	0.02221	0.01905	0.003154	0.000515	369	318	6.126	7505
5%								
1 vs. 3	0.0309	0.02341	0.007489	0.000444	343	697	16.87	7505
1 vs. 5	0.0309	0.02125	0.009655	0.000483	343	446	19.98	7505
1 vs. 7	0.0309	0.02234	0.008562	0.000537	343	290	15.95	7505
1 vs. 10	0.0309	0.02184	0.009064	0.000751	343	105	12.08	7505
1 vs. 15	0.0309	0.01979	0.01112	0.00065	343	156	17.1	7505
3 vs. 5	0.02341	0.02125	0.002166	0.000408	697	446	5.308	7505
3 vs. 7	0.02341	0.02234	0.001073	0.00047	697	290	2.282	7505
3 vs. 10	0.02341	0.02184	0.001575	0.000704	697	105	2.236	7505
3 vs. 15	0.02341	0.01979	0.003626	0.000596	697	156	6.084	7505
5 vs. 7	0.02125	0.02234	-0.00109	0.000508	446	290	2.153	7505
5 vs. 10	0.02125	0.02184	-0.00059	0.00073	446	105	0.8097	7505
5 vs. 15	0.02125	0.01979	0.00146	0.000626	446	156	2.332	7505
7 vs. 10	0.02234	0.02184	0.000502	0.000766	290	105	0.655	7505
7 vs. 15	0.02234	0.01979	0.002553	0.000668	290	156	3.821	7505
10 vs. 15	0.02184	0.01979	0.002051	0.000849	105	156	2.415	7505

Within each row, compare columns (simple effects within rows)

Number of fam 6
Number of con 3
Alpha 0.05

Bonferroni's m	Mean Diff.	95.00% CI	Significant	Summary	Adjusted P Value
1					
1% vs. 3%	0.000218	-0.001157 t	No	ns	>0.9999
1% vs. 5%	-0.00411	-0.00528 t	Yes	****	<0.0001
3% vs. 5%	-0.00433	-0.005759 t	Yes	****	<0.0001
3					
1% vs. 3%	0.003699	0.00279 to	Yes	****	<0.0001
1% vs. 5%	0.002824	0.001902 t	Yes	****	<0.0001
3% vs. 5%	-0.00088	-0.001724 t	Yes	*	0.0407
5					
1% vs. 3%	0.000912	-3.424e-00	No	ns	0.0631
1% vs. 5%	0.000352	-0.0006795	No	ns	>0.9999
3% vs. 5%	-0.00056	-0.001557 t	No	ns	0.5366
7					
1% vs. 3%	0.001588	0.0004311	Yes	**	0.0031
1% vs. 5%	0.001657	0.0003655	Yes	**	0.0064
3% vs. 5%	0.000069	-0.00114 tc	No	ns	>0.9999
10					
1% vs. 3%	-0.00115	-0.002249 t	Yes	*	0.0363
1% vs. 5%	-0.00078	-0.002508 t	No	ns	0.8312
3% vs. 5%	0.000368	-0.001414 t	No	ns	>0.9999
15					
1% vs. 3%	0.004193	0.002982 t	Yes	****	<0.0001
1% vs. 5%	0.003458	0.001937 t	Yes	****	<0.0001
3% vs. 5%	-0.00074	-0.00231 tc	No	ns	0.7916

Test details	Mean 1	Mean 2	Mean Diff.	SE of diff.	N1	N2	t	DF
1								
1% vs. 3%	0.02679	0.02657	0.000218	0.000574	428	202	0.3795	7505
1% vs. 5%	0.02679	0.0309	-0.00411	0.000488	428	343	8.432	7505
3% vs. 5%	0.02657	0.0309	-0.00433	0.000597	202	343	7.255	7505
3								
1% vs. 3%	0.02624	0.02254	0.003699	0.00038	543	747	9.747	7505
1% vs. 5%	0.02624	0.02341	0.002824	0.000385	543	697	7.332	7505
3% vs. 5%	0.02254	0.02341	-0.00088	0.000354	747	697	2.469	7505
5								
1% vs. 3%	0.0216	0.02069	0.000912	0.000395	538	629	2.308	7505
1% vs. 5%	0.0216	0.02125	0.000352	0.000431	538	446	0.8168	7505
3% vs. 5%	0.02069	0.02125	-0.00056	0.000417	629	446	1.344	7505
7								
1% vs. 3%	0.024	0.02241	0.001588	0.000483	336	459	3.287	7505
1% vs. 5%	0.024	0.02234	0.001657	0.000539	336	290	3.072	7505
3% vs. 5%	0.02241	0.02234	0.000069	0.000505	459	290	0.1367	7505
10								
1% vs. 3%	0.02106	0.02221	-0.00115	0.000459	517	369	2.51	7505
1% vs. 5%	0.02106	0.02184	-0.00078	0.00072	517	105	1.087	7505
3% vs. 5%	0.02221	0.02184	0.000368	0.000744	369	105	0.4944	7505
15								
1% vs. 3%	0.02325	0.01905	0.004193	0.000506	400	318	8.294	7505
1% vs. 5%	0.02325	0.01979	0.003458	0.000635	400	156	5.444	7505
3% vs. 5%	0.01905	0.01979	-0.00074	0.000658	318	156	1.117	7505

Table 40 – One-way ANOVA for the effects of time and hydrogel stiffness on Chapter 5 osteogenic data – NUCLEUS VOLUME

Table Analyze Data 1

Two-way ANC Ordinary
Alpha 0.05

Source of Vari	% of total v	P value	P value su	Significant?
Interaction	3.772	<0.0001	****	Yes
Time	3.688	<0.0001	****	Yes
Agarose	0.7241	<0.0001	****	Yes

ANOVA table	SS	DF	MS	F (DFn, DF	P value
Interaction	29.44	10	2.944	F (10, 750	P<0.0001
Time	28.78	5	5.755	F (5, 7506)	P<0.0001
Agarose	5.651	2	2.825	F (2, 7506)	P<0.0001
Residual	716.5	7506	0.09546		

Number of mis 5922

Within each column, compare rows (simple effects within columns)

Number of fam 3
Number of con 15
Alpha 0.05

Bonferroni's m	Mean Diff.	95.00% CI	Significant?	Summary	Adjusted P Value
1%					
1 vs. 3	0.1511	0.0925 to 0	Yes	****	<0.0001
1 vs. 5	0.2238	0.165 to 0.	Yes	****	<0.0001
1 vs. 7	0.1571	0.09096 to	Yes	****	<0.0001
1 vs. 10	0.07515	0.01587 to	Yes	**	0.003
1 vs. 15	-0.04804	-0.1111 to	No	ns	0.3795
3 vs. 5	0.07264	0.01746 to	Yes	**	0.0017
3 vs. 7	0.005946	-0.05702 to	No	ns	>0.9999
3 vs. 10	-0.07598	-0.1317 to	Yes	***	0.001
3 vs. 15	-0.1992	-0.2589 to	Yes	****	<0.0001
5 vs. 7	-0.06669	-0.1298 to	Yes	*	0.0287
5 vs. 10	-0.1486	-0.2045 to	Yes	****	<0.0001
5 vs. 15	-0.2718	-0.3317 to	Yes	****	<0.0001
7 vs. 10	-0.08193	-0.1455 to	Yes	**	0.0023
7 vs. 15	-0.2051	-0.2722 to	Yes	****	<0.0001
10 vs. 15	-0.1232	-0.1836 to	Yes	****	<0.0001
3%					
1 vs. 3	-0.1391	-0.211 to -(	Yes	****	<0.0001
1 vs. 5	-0.1316	-0.205 to -(	Yes	****	<0.0001
1 vs. 7	-0.2174	-0.294 to -(	Yes	****	<0.0001
1 vs. 10	-0.2939	-0.3733 to	Yes	****	<0.0001
1 vs. 15	-0.3434	-0.425 to -(	Yes	****	<0.0001
3 vs. 5	0.007463	-0.04163 to	No	ns	>0.9999
3 vs. 7	-0.07838	-0.1322 to	Yes	***	0.0003
3 vs. 10	-0.1548	-0.2126 to	Yes	****	<0.0001
3 vs. 15	-0.2043	-0.2651 to	Yes	****	<0.0001
5 vs. 7	-0.08585	-0.1415 to	Yes	****	<0.0001
5 vs. 10	-0.1623	-0.2218 to	Yes	****	<0.0001
5 vs. 15	-0.2118	-0.2742 to	Yes	****	<0.0001
7 vs. 10	-0.07645	-0.1399 to	Yes	**	0.0061
7 vs. 15	-0.1259	-0.1921 to	Yes	****	<0.0001
10 vs. 15	-0.04948	-0.1189 to	No	ns	0.5458
5%					
1 vs. 3	-0.03737	-0.0972 to	No	ns	>0.9999
1 vs. 5	-0.1817	-0.2469 to	Yes	****	<0.0001
1 vs. 7	-0.2149	-0.2872 to	Yes	****	<0.0001
1 vs. 10	-0.2443	-0.3455 to	Yes	****	<0.0001
1 vs. 15	-0.146	-0.2336 to	Yes	****	<0.0001
3 vs. 5	-0.1444	-0.1994 to	Yes	****	<0.0001
3 vs. 7	-0.1775	-0.2409 to	Yes	****	<0.0001
3 vs. 10	-0.2069	-0.3019 to	Yes	****	<0.0001
3 vs. 15	-0.1086	-0.189 to -(	Yes	**	0.0011
5 vs. 7	-0.03313	-0.1016 to	No	ns	>0.9999
5 vs. 10	-0.06258	-0.161 to 0	No	ns	0.9283
5 vs. 15	0.03573	-0.04865 to	No	ns	>0.9999
7 vs. 10	-0.02945	-0.1328 to	No	ns	>0.9999
7 vs. 15	0.06886	-0.02121 to	No	ns	0.3722
10 vs. 15	0.09831	-0.01619 to	No	ns	0.1759

Test details	Mean 1	Mean 2	Mean Diff.	SE of diff.	N1	N2	t	DF
1%								
1 vs. 3	1.33	1.178	0.1511	0.01997	428	543	7.568	7506
1 vs. 5	1.33	1.106	0.2238	0.02001	428	538	11.18	7506
1 vs. 7	1.33	1.172	0.1571	0.02252	428	336	6.975	7506
1 vs. 10	1.33	1.254	0.07515	0.02019	428	517	3.722	7506
1 vs. 15	1.33	1.378	-0.04804	0.02147	428	401	2.237	7506
3 vs. 5	1.178	1.106	0.07264	0.01879	543	538	3.865	7506
3 vs. 7	1.178	1.172	0.005946	0.02144	543	336	0.2773	7506
3 vs. 10	1.178	1.254	-0.07598	0.01898	543	517	4.002	7506
3 vs. 15	1.178	1.378	-0.1992	0.02034	543	401	9.791	7506
5 vs. 7	1.106	1.172	-0.06669	0.02148	538	336	3.105	7506
5 vs. 10	1.106	1.254	-0.1486	0.01903	538	517	7.811	7506
5 vs. 15	1.106	1.378	-0.2718	0.02038	538	401	13.34	7506
7 vs. 10	1.172	1.254	-0.08193	0.02165	336	517	3.784	7506
7 vs. 15	1.172	1.378	-0.2051	0.02285	336	401	8.977	7506
10 vs. 15	1.254	1.378	-0.1232	0.02056	517	401	5.992	7506
3%								
1 vs. 3	1.1	1.239	-0.1391	0.0245	202	747	5.675	7506
1 vs. 5	1.1	1.231	-0.1316	0.02499	202	629	5.267	7506
1 vs. 7	1.1	1.317	-0.2174	0.02609	202	459	8.335	7506
1 vs. 10	1.1	1.394	-0.2939	0.02704	202	369	10.87	7506
1 vs. 15	1.1	1.443	-0.3434	0.0278	202	318	12.35	7506
3 vs. 5	1.239	1.231	0.007463	0.01672	747	629	0.4464	7506
3 vs. 7	1.239	1.317	-0.07838	0.01832	747	459	4.278	7506
3 vs. 10	1.239	1.394	-0.1548	0.01966	747	369	7.876	7506
3 vs. 15	1.239	1.443	-0.2043	0.02069	747	318	9.876	7506
5 vs. 7	1.231	1.317	-0.08585	0.01897	629	459	4.526	7506
5 vs. 10	1.231	1.394	-0.1623	0.02026	629	369	8.011	7506
5 vs. 15	1.231	1.443	-0.2118	0.02126	629	318	9.962	7506
7 vs. 10	1.317	1.394	-0.07645	0.0216	459	369	3.539	7506
7 vs. 15	1.317	1.443	-0.1259	0.02254	459	318	5.586	7506
10 vs. 15	1.394	1.443	-0.04948	0.02364	369	318	2.093	7506
5%								
1 vs. 3	1.173	1.211	-0.03737	0.02038	343	697	1.834	7506
1 vs. 5	1.173	1.355	-0.1817	0.02219	343	446	8.19	7506
1 vs. 7	1.173	1.388	-0.2149	0.02465	343	290	8.717	7506
1 vs. 10	1.173	1.418	-0.2443	0.03446	343	105	7.09	7506
1 vs. 15	1.173	1.319	-0.146	0.02984	343	156	4.893	7506
3 vs. 5	1.211	1.355	-0.1444	0.01873	697	446	7.705	7506
3 vs. 7	1.211	1.388	-0.1775	0.02159	697	290	8.221	7506
3 vs. 10	1.211	1.418	-0.2069	0.03234	697	105	6.398	7506
3 vs. 15	1.211	1.319	-0.1086	0.02737	697	156	3.969	7506
5 vs. 7	1.355	1.388	-0.03313	0.02331	446	290	1.421	7506
5 vs. 10	1.355	1.418	-0.06258	0.03351	446	105	1.867	7506
5 vs. 15	1.355	1.319	0.03573	0.02874	446	156	1.243	7506
7 vs. 10	1.388	1.418	-0.02945	0.03519	290	105	0.837	7506
7 vs. 15	1.388	1.319	0.06886	0.03068	290	156	2.245	7506
10 vs. 15	1.418	1.319	0.09831	0.039	105	156	2.521	7506

Within each row, compare columns (simple effects within rows)

Number of fam 6
Number of con 3
Alpha 0.05

Bonferroni's m	Mean Diff.	95.00% CI	Significant?	Summary	Adjusted P Value
1					
1% vs. 3%	0.2297	0.1666 to (	Yes	****	<0.0001
1% vs. 5%	0.1562	0.1025 to (	Yes	****	<0.0001
3% vs. 5%	-0.07355	-0.1392 to	Yes	*	0.0219
3					
1% vs. 3%	-0.06048	-0.1022 to	Yes	**	0.0016
1% vs. 5%	-0.03234	-0.07469 to	No	ns	0.2024
3% vs. 5%	0.02814	-0.01082 to	No	ns	0.2514
5					
1% vs. 3%	-0.1257	-0.1691 to	Yes	****	<0.0001
1% vs. 5%	-0.2493	-0.2967 to	Yes	****	<0.0001
3% vs. 5%	-0.1237	-0.1695 to	Yes	****	<0.0001
7					
1% vs. 3%	-0.1448	-0.1979 to	Yes	****	<0.0001
1% vs. 5%	-0.2158	-0.2751 to	Yes	****	<0.0001
3% vs. 5%	-0.07096	-0.1265 to	Yes	**	0.0066
10					
1% vs. 3%	-0.1393	-0.1897 to	Yes	****	<0.0001
1% vs. 5%	-0.1633	-0.2425 to	Yes	****	<0.0001
3% vs. 5%	-0.02396	-0.1058 to	No	ns	>0.9999
15					
1% vs. 3%	-0.06562	-0.1212 to	Yes	*	0.0141
1% vs. 5%	0.05821	-0.0116 to	No	ns	0.1377
3% vs. 5%	0.1238	0.05151 to	Yes	***	0.0001

Test details	Mean 1	Mean 2	Mean Diff.	SE of diff.	N1	N2	t	DF
1								
1% vs. 3%	1.33	1.1	0.2297	0.02637	428	202	8.71	7506
1% vs. 5%	1.33	1.173	0.1562	0.02239	428	343	6.975	7506
3% vs. 5%	1.1	1.173	-0.07355	0.0274	202	343	2.684	7506
3								
1% vs. 3%	1.178	1.239	-0.06048	0.01742	543	747	3.471	7506
1% vs. 5%	1.178	1.211	-0.03234	0.01768	543	697	1.829	7506
3% vs. 5%	1.239	1.211	0.02814	0.01627	747	697	1.729	7506
5								
1% vs. 3%	1.106	1.231	-0.1257	0.01814	538	629	6.926	7506
1% vs. 5%	1.106	1.355	-0.2493	0.01979	538	446	12.6	7506
3% vs. 5%	1.231	1.355	-0.1237	0.01913	629	446	6.467	7506
7								
1% vs. 3%	1.172	1.317	-0.1448	0.02218	336	459	6.528	7506
1% vs. 5%	1.172	1.388	-0.2158	0.02476	336	290	8.713	7506
3% vs. 5%	1.317	1.388	-0.07096	0.02318	459	290	3.062	7506
10								
1% vs. 3%	1.254	1.394	-0.1393	0.02106	517	369	6.617	7506
1% vs. 5%	1.254	1.418	-0.1633	0.03307	517	105	4.938	7506
3% vs. 5%	1.394	1.418	-0.02396	0.03417	369	105	0.7012	7506
15								
1% vs. 3%	1.378	1.443	-0.06562	0.0232	401	318	2.828	7506
1% vs. 5%	1.378	1.319	0.05821	0.02915	401	156	1.997	7506
3% vs. 5%	1.443	1.319	0.1238	0.0302	318	156	4.1	7506

Table 41 – One-way ANOVA for the effects of time and hydrogel stiffness on Chapter 5 osteogenic data – POISSON'S RATIO

Table Analyze Data 1

Two-way ANC Ordinary
Alpha 0.05

Source of Var	% of total v	P value	P value sui	Significant?
Interaction	5.275	<0.0001	****	Yes
Time	7.708	<0.0001	****	Yes
Agarose	0.1872	0.0003	***	Yes

ANOVA table	SS	DF	MS	F (DFn, DF	P value
Interaction	13.11	10	1.311	F (10, 750	P<0.0001
Time	19.15	5	3.831	F (5, 7506)	P<0.0001
Agarose	0.4653	2	0.2326	F (2, 7506)	P=0.0003
Residual	215.8	7506	0.02875		

Number of mis 5922

Within each column, compare rows (simple effects within columns)

Number of fan 3
Number of coi 15
Alpha 0.05

Bonferroni's m	Mean Diff.	95.00% CI	Significant	Summary	Adjusted P Value
1%					
1 vs. 3	-0.1957	-0.2279 to	Yes	****	<0.0001
1 vs. 5	-0.3073	-0.3396 to	Yes	****	<0.0001
1 vs. 7	-0.306	-0.3422 to	Yes	****	<0.0001
1 vs. 10	-0.29	-0.3226 to	Yes	****	<0.0001
1 vs. 15	-0.3212	-0.3558 to	Yes	****	<0.0001
3 vs. 5	-0.1116	-0.1419 to	Yes	****	<0.0001
3 vs. 7	-0.1103	-0.1448 to	Yes	****	<0.0001
3 vs. 10	-0.09432	-0.1249 to	Yes	****	<0.0001
3 vs. 15	-0.1255	-0.1583 to	Yes	****	<0.0001
5 vs. 7	0.00135	-0.03327 to	No	ns	>0.9999
5 vs. 10	0.01728	-0.01338 to	No	ns	>0.9999
5 vs. 15	-0.01393	-0.04677 to	No	ns	>0.9999
7 vs. 10	0.01593	-0.01896 to	No	ns	>0.9999
7 vs. 15	-0.01528	-0.0521 to	No	ns	>0.9999
10 vs. 15	-0.03121	-0.06434 to	No	ns	0.0853
3%					
1 vs. 3	-0.04522	-0.0847 to	Yes	*	0.0116
1 vs. 5	-0.03861	-0.07887 to	No	ns	0.0732
1 vs. 7	-0.05923	-0.1013 to	Yes	***	0.0005
1 vs. 10	-0.08539	-0.129 to -	Yes	****	<0.0001
1 vs. 15	-0.1217	-0.1665 to	Yes	****	<0.0001
3 vs. 5	0.00661	-0.02033 to	No	ns	>0.9999
3 vs. 7	-0.01401	-0.04354 to	No	ns	>0.9999
3 vs. 10	-0.04017	-0.07185 to	Yes	**	0.003
3 vs. 15	-0.07644	-0.1098 to	Yes	****	<0.0001
5 vs. 7	-0.02062	-0.05118 to	No	ns	0.7143
5 vs. 10	-0.04678	-0.07942 to	Yes	***	0.0004
5 vs. 15	-0.08305	-0.1173 to	Yes	****	<0.0001
7 vs. 10	-0.02616	-0.06097 to	No	ns	0.4105
7 vs. 15	-0.06243	-0.09875 to	Yes	****	<0.0001
10 vs. 15	-0.03627	-0.07436 to	No	ns	0.0779
5%					
1 vs. 3	-0.00289	-0.03573 to	No	ns	>0.9999
1 vs. 5	-0.00436	-0.04011 to	No	ns	>0.9999
1 vs. 7	0.00256	-0.03715 to	No	ns	>0.9999
1 vs. 10	-0.00427	-0.05979 to	No	ns	>0.9999
1 vs. 15	-0.1264	-0.1745 to	Yes	****	<0.0001
3 vs. 5	-0.00147	-0.03166 to	No	ns	>0.9999
3 vs. 7	0.00545	-0.02934 to	No	ns	>0.9999
3 vs. 10	-0.00138	-0.05349 to	No	ns	>0.9999
3 vs. 15	-0.1235	-0.1676 to	Yes	****	<0.0001
5 vs. 7	0.00692	-0.03063 to	No	ns	>0.9999
5 vs. 10	0.00009	-0.05391 to	No	ns	>0.9999
5 vs. 15	-0.1221	-0.1684 to	Yes	****	<0.0001
7 vs. 10	-0.00683	-0.06353 to	No	ns	>0.9999
7 vs. 15	-0.129	-0.1784 to	Yes	****	<0.0001
10 vs. 15	-0.1222	-0.185 to -	Yes	****	<0.0001

Test details	Mean 1	Mean 2	Mean Diff.	SE of diff.	N1	N2	t	DF
1%								
1 vs. 3	-0.5818	-0.386	-0.1957	0.01096	428	543	17.86	7506
1 vs. 5	-0.5818	-0.2744	-0.3073	0.01098	428	538	27.98	7506
1 vs. 7	-0.5818	-0.2758	-0.306	0.01236	428	336	24.76	7506
1 vs. 10	-0.5818	-0.2917	-0.29	0.01108	428	517	26.17	7506
1 vs. 15	-0.5818	-0.2605	-0.3212	0.01178	428	401	27.26	7506
3 vs. 5	-0.386	-0.2744	-0.1116	0.01031	543	538	10.82	7506
3 vs. 7	-0.386	-0.2758	-0.1103	0.01177	543	336	9.368	7506
3 vs. 10	-0.386	-0.2917	-0.09432	0.01042	543	517	9.053	7506
3 vs. 15	-0.386	-0.2605	-0.1255	0.01116	543	401	11.24	7506
5 vs. 7	-0.2744	-0.2758	0.00135	0.01179	538	336	0.1145	7506
5 vs. 10	-0.2744	-0.2917	0.01728	0.01044	538	517	1.655	7506
5 vs. 15	-0.2744	-0.2605	-0.01393	0.01119	538	401	1.245	7506
7 vs. 10	-0.2758	-0.2917	0.01593	0.01188	336	517	1.341	7506
7 vs. 15	-0.2758	-0.2605	-0.01528	0.01254	336	401	1.218	7506
10 vs. 15	-0.2917	-0.2605	-0.03121	0.01128	517	401	2.766	7506
3%								
1 vs. 3	-0.4236	-0.3784	-0.04522	0.01345	202	747	3.363	7506
1 vs. 5	-0.4236	-0.385	-0.03861	0.01371	202	629	2.816	7506
1 vs. 7	-0.4236	-0.3644	-0.05923	0.01432	202	459	4.137	7506
1 vs. 10	-0.4236	-0.3382	-0.08539	0.01484	202	369	5.754	7506
1 vs. 15	-0.4236	-0.302	-0.1217	0.01526	202	318	7.975	7506
3 vs. 5	-0.3784	-0.385	0.00661	0.009176	747	629	0.7204	7506
3 vs. 7	-0.3784	-0.3644	-0.01401	0.01006	747	459	1.393	7506
3 vs. 10	-0.3784	-0.3382	-0.04017	0.01079	747	369	3.723	7506
3 vs. 15	-0.3784	-0.302	-0.07644	0.01135	747	318	6.733	7506
5 vs. 7	-0.385	-0.3644	-0.02062	0.01041	629	459	1.981	7506
5 vs. 10	-0.385	-0.3382	-0.04678	0.01112	629	369	4.208	7506
5 vs. 15	-0.385	-0.302	-0.08305	0.01167	629	318	7.119	7506
7 vs. 10	-0.3644	-0.3382	-0.02616	0.01186	459	369	2.207	7506
7 vs. 15	-0.3644	-0.302	-0.06243	0.01237	459	318	5.047	7506
10 vs. 15	-0.3382	-0.302	-0.03627	0.01297	369	318	2.796	7506
5%								
1 vs. 3	-0.3706	-0.3677	-0.00289	0.01118	343	697	0.2584	7506
1 vs. 5	-0.3706	-0.3662	-0.00436	0.01218	343	446	0.3581	7506
1 vs. 7	-0.3706	-0.3732	0.00256	0.01353	343	290	0.1893	7506
1 vs. 10	-0.3706	-0.3663	-0.00427	0.01891	343	105	0.2258	7506
1 vs. 15	-0.3706	-0.2442	-0.1264	0.01637	343	156	7.721	7506
3 vs. 5	-0.3677	-0.3662	-0.00147	0.01028	697	446	0.143	7506
3 vs. 7	-0.3677	-0.3732	0.00545	0.01185	697	290	0.46	7506
3 vs. 10	-0.3677	-0.3663	-0.00138	0.01775	697	105	0.07775	7506
3 vs. 15	-0.3677	-0.2442	-0.1235	0.01502	697	156	8.226	7506
5 vs. 7	-0.3662	-0.3732	0.00692	0.01279	446	290	0.541	7506
5 vs. 10	-0.3662	-0.3663	0.00009	0.01839	446	105	0.004894	7506
5 vs. 15	-0.3662	-0.2442	-0.1221	0.01577	446	156	7.74	7506
7 vs. 10	-0.3732	-0.3663	-0.00683	0.01931	290	105	0.3537	7506
7 vs. 15	-0.3732	-0.2442	-0.129	0.01684	290	156	7.662	7506
10 vs. 15	-0.3663	-0.2442	-0.1222	0.0214	105	156	5.708	7506

Within each row, compare columns (simple effects within rows)

Number of fam 6
Number of con 3
Alpha 0.05

Bonferroni's m	Mean Diff.	95.00% CI	Significant	Summary	Adjusted P Value
1					
1% vs. 3%	-0.1581	-0.1928 to	Yes	****	<0.0001
1% vs. 5%	-0.2112	-0.2406 to	Yes	****	<0.0001
3% vs. 5%	-0.05302	-0.08903 to	Yes	**	0.0013
3					
1% vs. 3%	-0.00764	-0.03054 to	No	ns	>0.9999
1% vs. 5%	-0.01833	-0.04157 to	No	ns	0.1769
3% vs. 5%	-0.01069	-0.03207 to	No	ns	0.6938
5					
1% vs. 3%	0.1106	0.08673 to	Yes	****	<0.0001
1% vs. 5%	0.0918	0.0658 to	Yes	****	<0.0001
3% vs. 5%	-0.01877	-0.0439 to	No	ns	0.2213
7					
1% vs. 3%	0.0886	0.05945 to	Yes	****	<0.0001
1% vs. 5%	0.09737	0.06483 to	Yes	****	<0.0001
3% vs. 5%	0.00877	-0.02169 to	No	ns	>0.9999
10					
1% vs. 3%	0.04651	0.01884 to	Yes	***	0.0002
1% vs. 5%	0.07461	0.03115 to	Yes	***	0.0001
3% vs. 5%	0.0281	-0.01681 to	No	ns	0.4022
15					
1% vs. 3%	0.04145	0.01096 to	Yes	**	0.0034
1% vs. 5%	-0.01634	-0.05465 to	No	ns	0.9214
3% vs. 5%	-0.05779	-0.09748 to	Yes	**	0.0015

Test details	Mean 1	Mean 2	Mean Diff.	SE of diff.	N1	N2	t	DF
1								
1% vs. 3%	-0.5818	-0.4236	-0.1581	0.01447	428	202	10.93	7506
1% vs. 5%	-0.5818	-0.3706	-0.2112	0.01229	428	343	17.18	7506
3% vs. 5%	-0.4236	-0.3706	-0.05302	0.01504	202	343	3.526	7506
3								
1% vs. 3%	-0.386	-0.3784	-0.00764	0.009562	543	747	0.799	7506
1% vs. 5%	-0.386	-0.3677	-0.01833	0.009705	543	697	1.889	7506
3% vs. 5%	-0.3784	-0.3677	-0.01069	0.008929	747	697	1.197	7506
5								
1% vs. 3%	-0.2744	-0.385	0.1106	0.009957	538	629	11.1	7506
1% vs. 5%	-0.2744	-0.3662	0.0918	0.01086	538	446	8.455	7506
3% vs. 5%	-0.385	-0.3662	-0.01877	0.0105	629	446	1.788	7506
7								
1% vs. 3%	-0.2758	-0.3644	0.0886	0.01217	336	459	7.278	7506
1% vs. 5%	-0.2758	-0.3732	0.09737	0.01359	336	290	7.165	7506
3% vs. 5%	-0.3644	-0.3732	0.00877	0.01272	459	290	0.6895	7506
10								
1% vs. 3%	-0.2917	-0.3382	0.04651	0.01155	517	369	4.025	7506
1% vs. 5%	-0.2917	-0.3663	0.07461	0.01815	517	105	4.111	7506
3% vs. 5%	-0.3382	-0.3663	0.0281	0.01875	369	105	1.498	7506
15								
1% vs. 3%	-0.2605	-0.302	0.04145	0.01273	401	318	3.256	7506
1% vs. 5%	-0.2605	-0.2442	-0.01634	0.016	401	156	1.021	7506
3% vs. 5%	-0.302	-0.2442	-0.05779	0.01657	318	156	3.487	7506

Table 42 – One-way ANOVA for the effects of time and hydrogel stiffness on Chapter 5 osteogenic data – NUCLEUS STIFFNESS

Table Analyze Data 1

Two-way ANC Ordinary
Alpha 0.05

Source of Var	% of total \	P value	P value sui	Significant?
Interaction	0.6351	<0.0001	****	Yes
Time	7.93	<0.0001	****	Yes
Agarose	0.649	<0.0001	****	Yes

ANOVA table	SS	DF	MS	F (DFn, DF	P value
Interaction	23164	10	2316	F (10, 750	P<0.0001
Time	289220	5	57844	F (5, 7506)	P<0.0001
Agarose	23669	2	11834	F (2, 7506)	P<0.0001
Residual	3311136	7506	441.1		

Number of mi 5922

Within each column, compare rows (simple effects within columns)

Number of fan 3
Number of coi 15
Alpha 0.05

Bonferroni's m	Mean Diff.	95.00% CI	Significant	Summary	Adjusted P Value
1%					
1 vs. 3	-9.216	-13.2 to -5.	Yes	****	<0.0001
1 vs. 5	-12.34	-16.33 to -8	Yes	****	<0.0001
1 vs. 7	-12.01	-16.51 to -7	Yes	****	<0.0001
1 vs. 10	-19.13	-23.16 to -1	Yes	****	<0.0001
1 vs. 15	-19.72	-24 to -15.4	Yes	****	<0.0001
3 vs. 5	-3.122	-6.873 to 0	No	ns	0.2186
3 vs. 7	-2.798	-7.078 to 1	No	ns	0.8253
3 vs. 10	-9.915	-13.7 to -6.	Yes	****	<0.0001
3 vs. 15	-10.5	-14.56 to -6	Yes	****	<0.0001
5 vs. 7	0.3241	-3.964 to 4	No	ns	>0.9999
5 vs. 10	-6.793	-10.59 to -2	Yes	****	<0.0001
5 vs. 15	-7.379	-11.45 to -3	Yes	****	<0.0001
7 vs. 10	-7.118	-11.44 to -2	Yes	****	<0.0001
7 vs. 15	-7.704	-12.26 to -3	Yes	****	<0.0001
10 vs. 15	-0.5859	-4.69 to 3.5	No	ns	>0.9999
3%					
1 vs. 3	-7.638	-12.53 to -2	Yes	****	<0.0001
1 vs. 5	-9.616	-14.6 to -4.	Yes	****	<0.0001
1 vs. 7	-16.81	-22.02 to -1	Yes	****	<0.0001
1 vs. 10	-12.38	-17.77 to -6	Yes	****	<0.0001
1 vs. 15	-22.36	-27.91 to -1	Yes	****	<0.0001
3 vs. 5	-1.977	-5.315 to 1	No	ns	>0.9999
3 vs. 7	-9.171	-12.83 to -5	Yes	****	<0.0001
3 vs. 10	-4.737	-8.661 to -0	Yes	**	0.0059
3 vs. 15	-14.72	-18.85 to -1	Yes	****	<0.0001
5 vs. 7	-7.193	-10.98 to -3	Yes	****	<0.0001
5 vs. 10	-2.76	-6.804 to 1	No	ns	0.6769
5 vs. 15	-12.74	-16.99 to -8	Yes	****	<0.0001
7 vs. 10	4.434	0.1218 to 8	Yes	*	0.0382
7 vs. 15	-5.549	-10.05 to -1	Yes	**	0.0044
10 vs. 15	-9.983	-14.7 to -5.	Yes	****	<0.0001
5%					
1 vs. 3	-2.971	-7.038 to 1	No	ns	0.4804
1 vs. 5	-8.346	-12.77 to -3	Yes	****	<0.0001
1 vs. 7	-16.04	-20.96 to -1	Yes	****	<0.0001
1 vs. 10	-17.49	-24.37 to -1	Yes	****	<0.0001
1 vs. 15	-22.87	-28.83 to -1	Yes	****	<0.0001
3 vs. 5	-5.375	-9.115 to -1	Yes	***	0.0004
3 vs. 7	-13.07	-17.37 to -8	Yes	****	<0.0001
3 vs. 10	-14.52	-20.97 to -8	Yes	****	<0.0001
3 vs. 15	-19.9	-25.36 to -1	Yes	****	<0.0001
5 vs. 7	-7.69	-12.34 to -3	Yes	****	<0.0001
5 vs. 10	-9.142	-15.83 to -2	Yes	***	0.0009
5 vs. 15	-14.52	-20.26 to -8	Yes	****	<0.0001
7 vs. 10	-1.452	-8.476 to 5	No	ns	>0.9999
7 vs. 15	-6.835	-12.96 to -0	Yes	*	0.0158
10 vs. 15	-5.382	-13.17 to 2	No	ns	0.6357

Test details	Mean 1	Mean 2	Mean Diff.	SE of diff.	N1	N2	t	DF
1%								
1 vs. 3	36.1	45.32	-9.216	1.358	428	543	6.788	7506
1 vs. 5	36.1	48.44	-12.34	1.36	428	538	9.069	7506
1 vs. 7	36.1	48.12	-12.01	1.531	428	336	7.848	7506
1 vs. 10	36.1	55.23	-19.13	1.373	428	517	13.94	7506
1 vs. 15	36.1	55.82	-19.72	1.46	428	401	13.51	7506
3 vs. 5	45.32	48.44	-3.122	1.278	543	538	2.443	7506
3 vs. 7	45.32	48.12	-2.798	1.458	543	336	1.919	7506
3 vs. 10	45.32	55.23	-9.915	1.291	543	517	7.683	7506
3 vs. 15	45.32	55.82	-10.5	1.383	543	401	7.593	7506
5 vs. 7	48.44	48.12	0.3241	1.46	538	336	0.2219	7506
5 vs. 10	48.44	55.23	-6.793	1.294	538	517	5.252	7506
5 vs. 15	48.44	55.82	-7.379	1.386	538	401	5.326	7506
7 vs. 10	48.12	55.23	-7.118	1.472	336	517	4.836	7506
7 vs. 15	48.12	55.82	-7.704	1.553	336	401	4.959	7506
10 vs. 15	55.23	55.82	-0.5859	1.398	517	401	0.4192	7506
3%								
1 vs. 3	41.37	49.01	-7.638	1.666	202	747	4.586	7506
1 vs. 5	41.37	50.98	-9.616	1.699	202	629	5.661	7506
1 vs. 7	41.37	58.18	-16.81	1.773	202	459	9.478	7506
1 vs. 10	41.37	53.74	-12.38	1.838	202	369	6.732	7506
1 vs. 15	41.37	63.73	-22.36	1.89	202	318	11.83	7506
3 vs. 5	49.01	50.98	-1.977	1.137	747	629	1.74	7506
3 vs. 7	49.01	58.18	-9.171	1.246	747	459	7.362	7506
3 vs. 10	49.01	53.74	-4.737	1.336	747	369	3.545	7506
3 vs. 15	49.01	63.73	-14.72	1.406	747	318	10.47	7506
5 vs. 7	50.98	58.18	-7.193	1.289	629	459	5.579	7506
5 vs. 10	50.98	53.74	-2.76	1.377	629	369	2.004	7506
5 vs. 15	50.98	63.73	-12.74	1.445	629	318	8.817	7506
7 vs. 10	58.18	53.74	4.434	1.469	459	369	3.019	7506
7 vs. 15	58.18	63.73	-5.549	1.532	459	318	3.621	7506
10 vs. 15	53.74	63.73	-9.983	1.607	369	318	6.212	7506
5%								
1 vs. 3	40.59	43.56	-2.971	1.385	343	697	2.144	7506
1 vs. 5	40.59	48.93	-8.346	1.508	343	446	5.533	7506
1 vs. 7	40.59	56.62	-16.04	1.675	343	290	9.571	7506
1 vs. 10	40.59	58.07	-17.49	2.343	343	105	7.466	7506
1 vs. 15	40.59	63.46	-22.87	2.028	343	156	11.28	7506
3 vs. 5	43.56	48.93	-5.375	1.274	697	446	4.221	7506
3 vs. 7	43.56	56.62	-13.07	1.468	697	290	8.902	7506
3 vs. 10	43.56	58.07	-14.52	2.199	697	105	6.603	7506
3 vs. 15	43.56	63.46	-19.9	1.86	697	156	10.7	7506
5 vs. 7	48.93	56.62	-7.69	1.584	446	290	4.854	7506
5 vs. 10	48.93	58.07	-9.142	2.278	446	105	4.013	7506
5 vs. 15	48.93	63.46	-14.52	1.954	446	156	7.434	7506
7 vs. 10	56.62	58.07	-1.452	2.392	290	105	0.6072	7506
7 vs. 15	56.62	63.46	-6.835	2.085	290	156	3.277	7506
10 vs. 15	58.07	63.46	-5.382	2.651	105	156	2.03	7506

Within each row, compare columns (simple effects within rows)

Number of fam 6
Number of con 3
Alpha 0.05

Bonferroni's m	Mean Diff.	95.00% CI	Significant	Summary	Adjusted P Value
1					
1% vs. 3%	-5.267	-9.56 to -0	Yes	**	0.0099
1% vs. 5%	-4.485	-8.129 to -0	Yes	**	0.0097
3% vs. 5%	0.7826	-3.678 to 5	No	ns	>0.9999
3					
1% vs. 3%	-3.689	-6.526 to -0	Yes	**	0.0055
1% vs. 5%	1.761	-1.118 to 4	No	ns	0.4293
3% vs. 5%	5.45	2.802 to 8.	Yes	****	<0.0001
5					
1% vs. 3%	-2.545	-5.499 to 0	No	ns	0.1173
1% vs. 5%	-0.493	-3.714 to 2	No	ns	>0.9999
3% vs. 5%	2.052	-1.061 to 5	No	ns	0.3435
7					
1% vs. 3%	-10.06	-13.67 to -6	Yes	****	<0.0001
1% vs. 5%	-8.507	-12.54 to -4	Yes	****	<0.0001
3% vs. 5%	1.556	-2.217 to 5	No	ns	0.9703
10					
1% vs. 3%	1.488	-1.939 to 4	No	ns	0.8952
1% vs. 5%	-2.842	-8.225 to 2	No	ns	0.6188
3% vs. 5%	-4.33	-9.893 to 1	No	ns	0.1871
15					
1% vs. 3%	-7.908	-11.68 to -4	Yes	****	<0.0001
1% vs. 5%	-7.638	-12.38 to -2	Yes	***	0.0004
3% vs. 5%	0.2701	-4.646 to 5	No	ns	>0.9999

Test details	Mean 1	Mean 2	Mean Diff.	SE of diff.	N1	N2	t	DF
1								
1% vs. 3%	36.1	41.37	-5.267	1.793	428	202	2.938	7506
1% vs. 5%	36.1	40.59	-4.485	1.522	428	343	2.946	7506
3% vs. 5%	41.37	40.59	0.7826	1.863	202	343	0.4201	7506
3								
1% vs. 3%	45.32	49.01	-3.689	1.184	543	747	3.115	7506
1% vs. 5%	45.32	43.56	1.761	1.202	543	697	1.465	7506
3% vs. 5%	49.01	43.56	5.45	1.106	747	697	4.927	7506
5								
1% vs. 3%	48.44	50.98	-2.545	1.233	538	629	2.064	7506
1% vs. 5%	48.44	48.93	-0.493	1.345	538	446	0.3666	7506
3% vs. 5%	50.98	48.93	2.052	1.3	629	446	1.578	7506
7								
1% vs. 3%	48.12	58.18	-10.06	1.508	336	459	6.673	7506
1% vs. 5%	48.12	56.62	-8.507	1.683	336	290	5.053	7506
3% vs. 5%	58.18	56.62	1.556	1.576	459	290	0.9875	7506
10								
1% vs. 3%	55.23	53.74	1.488	1.431	517	369	1.04	7506
1% vs. 5%	55.23	58.07	-2.842	2.248	517	105	1.264	7506
3% vs. 5%	53.74	58.07	-4.33	2.323	369	105	1.864	7506
15								
1% vs. 3%	55.82	63.73	-7.908	1.577	401	318	5.014	7506
1% vs. 5%	55.82	63.46	-7.638	1.982	401	156	3.854	7506
3% vs. 5%	63.73	63.46	0.2701	2.053	318	156	0.1316	7506

Table 43 – One-way ANOVA for the effects of time and hydrogel stiffness on Chapter 5 adipogenic data – AREA

Table Analyze Data 1

Two-way ANOVA Ordinary
Alpha 0.05

Source of Vari	% of total v	P value	P value su	Significant?
Interaction	2.181	<0.0001	****	Yes
Time	29.91	<0.0001	****	Yes
Agarose	0.474	<0.0001	****	Yes

ANOVA table	SS	DF	MS	F (DFn, DF	P value
Interaction	2.52E+10	10	2.52E+09	F (10, 532	P<0.0001
Time	3.46E+11	5	6.92E+10	F (5, 5329)	P<0.0001
Agarose	5.48E+09	2	2.74E+09	F (2, 5329)	P<0.0001
Residual	7.79E+11	5329	1.46E+08		

Number of mis 4535

Within each column, compare rows (simple effects within columns)

Number of fam 3
Number of cor 15
Alpha 0.05

Bonferroni's m	Mean Diff.	95.00% CI	Significant	Summary	Adjusted P Value
1%					
1 vs. 3	-1468	-4983 to 2(	No	ns	>0.9999
1 vs. 5	-4941	-8552 to -1	Yes	***	0.0009
1 vs. 7	-13312	-16515 to -	Yes	****	<0.0001
1 vs. 10	-16158	-19304 to -	Yes	****	<0.0001
1 vs. 15	-26938	-30326 to -	Yes	****	<0.0001
3 vs. 5	-3474	-6974 to 26	No	ns	0.0537
3 vs. 7	-11844	-14922 to -	Yes	****	<0.0001
3 vs. 10	-14691	-17709 to -	Yes	****	<0.0001
3 vs. 15	-25470	-28741 to -	Yes	****	<0.0001
5 vs. 7	-8371	-11557 to -	Yes	****	<0.0001
5 vs. 10	-11217	-14347 to -	Yes	****	<0.0001
5 vs. 15	-21997	-25370 to -	Yes	****	<0.0001
7 vs. 10	-2846	-5495 to -1	Yes	*	0.0242
7 vs. 15	-13626	-16558 to -	Yes	****	<0.0001
10 vs. 15	-10780	-13650 to -	Yes	****	<0.0001
3%					
1 vs. 3	-3204	-6207 to -2	Yes	*	0.0261
1 vs. 5	-9749	-12606 to -	Yes	****	<0.0001
1 vs. 7	-13192	-16161 to -	Yes	****	<0.0001
1 vs. 10	-13841	-16866 to -	Yes	****	<0.0001
1 vs. 15	-27454	-30648 to -	Yes	****	<0.0001
3 vs. 5	-6545	-8879 to -4	Yes	****	<0.0001
3 vs. 7	-9988	-12458 to -	Yes	****	<0.0001
3 vs. 10	-10637	-13174 to -	Yes	****	<0.0001
3 vs. 15	-24250	-26986 to -	Yes	****	<0.0001
5 vs. 7	-3443	-5733 to -1	Yes	***	0.0002
5 vs. 10	-4092	-6454 to -1	Yes	****	<0.0001
5 vs. 15	-17705	-20280 to -	Yes	****	<0.0001
7 vs. 10	-649	-3145 to 18	No	ns	>0.9999
7 vs. 15	-14262	-16960 to -	Yes	****	<0.0001
10 vs. 15	-13613	-16373 to -	Yes	****	<0.0001
5%					
1 vs. 3	1768	-2121 to 5(	No	ns	>0.9999
1 vs. 5	-15134	-17917 to -	Yes	****	<0.0001
1 vs. 7	-12261	-15105 to -	Yes	****	<0.0001
1 vs. 10	-20573	-24031 to -	Yes	****	<0.0001
1 vs. 15	-22132	-26227 to -	Yes	****	<0.0001
3 vs. 5	-16902	-20525 to -	Yes	****	<0.0001
3 vs. 7	-14029	-17699 to -	Yes	****	<0.0001
3 vs. 10	-22340	-26505 to -	Yes	****	<0.0001
3 vs. 15	-23900	-28607 to -	Yes	****	<0.0001
5 vs. 7	2873	405.2 to 5(	Yes	**	0.0095
5 vs. 10	-5439	-8594 to -2	Yes	****	<0.0001
5 vs. 15	-6998	-10842 to -	Yes	****	<0.0001
7 vs. 10	-8312	-11522 to -	Yes	****	<0.0001
7 vs. 15	-9871	-13759 to -	Yes	****	<0.0001
10 vs. 15	-1560	-5917 to 2(	No	ns	>0.9999

Test details	Mean 1	Mean 2	Mean Diff.	SE of diff.	N1	N2	t	DF
1%								
1 vs. 3	11062	12530	-1468	1197	192	218	1.226	5329
1 vs. 5	11062	16003	-4941	1230	192	195	4.019	5329
1 vs. 7	11062	24374	-13312	1091	192	342	12.21	5329
1 vs. 10	11062	27220	-16158	1071	192	379	15.08	5329
1 vs. 15	11062	38000	-26938	1154	192	257	23.35	5329
3 vs. 5	12530	16003	-3474	1192	218	195	2.914	5329
3 vs. 7	12530	24374	-11844	1048	218	342	11.3	5329
3 vs. 10	12530	27220	-14691	1028	218	379	14.29	5329
3 vs. 15	12530	38000	-25470	1114	218	257	22.87	5329
5 vs. 7	16003	24374	-8371	1085	195	342	7.713	5329
5 vs. 10	16003	27220	-11217	1066	195	379	10.52	5329
5 vs. 15	16003	38000	-21997	1149	195	257	19.15	5329
7 vs. 10	24374	27220	-2846	902	342	379	3.156	5329
7 vs. 15	24374	38000	-13626	998.4	342	257	13.65	5329
10 vs. 15	27220	38000	-10780	977.3	379	257	11.03	5329
3%								
1 vs. 3	12148	15352	-3204	1023	215	400	3.133	5329
1 vs. 5	12148	21897	-9749	973	215	549	10.02	5329
1 vs. 7	12148	25340	-13192	1011	215	428	13.05	5329
1 vs. 10	12148	25989	-13841	1030	215	384	13.44	5329
1 vs. 15	12148	39602	-27454	1088	215	291	25.24	5329
3 vs. 5	15352	21897	-6545	795	400	549	8.232	5329
3 vs. 7	15352	25340	-9988	841.1	400	428	11.87	5329
3 vs. 10	15352	25989	-10637	864	400	384	12.31	5329
3 vs. 15	15352	39602	-24250	931.8	400	291	26.02	5329
5 vs. 7	21897	25340	-3443	779.9	549	428	4.415	5329
5 vs. 10	21897	25989	-4092	804.6	549	384	5.086	5329
5 vs. 15	21897	39602	-17705	877	549	291	20.19	5329
7 vs. 10	25340	25989	-649	850.1	428	384	0.7634	5329
7 vs. 15	25340	39602	-14262	918.9	428	291	15.52	5329
10 vs. 15	25989	39602	-13613	940	384	291	14.48	5329
5%								
1 vs. 3	12807	11040	1768	1324	259	123	1.335	5329
1 vs. 5	12807	27942	-15134	947.6	259	439	15.97	5329
1 vs. 7	12807	25069	-12261	968.4	259	392	12.66	5329
1 vs. 10	12807	33380	-20573	1177	259	178	17.47	5329
1 vs. 15	12807	34940	-22132	1394	259	106	15.87	5329
3 vs. 5	11040	27942	-16902	1234	123	439	13.7	5329
3 vs. 7	11040	25069	-14029	1250	123	392	11.22	5329
3 vs. 10	11040	33380	-22340	1418	123	178	15.75	5329
3 vs. 15	11040	34940	-23900	1603	123	106	14.91	5329
5 vs. 7	27942	25069	2873	840.4	439	392	3.419	5329
5 vs. 10	27942	33380	-5439	1075	439	178	5.061	5329
5 vs. 15	27942	34940	-6998	1309	439	106	5.347	5329
7 vs. 10	25069	33380	-8312	1093	392	178	7.604	5329
7 vs. 15	25069	34940	-9871	1324	392	106	7.456	5329
10 vs. 15	33380	34940	-1560	1484	178	106	1.051	5329

Within each row, compare columns (simple effects within rows)

Number of fam 6
Number of con 3
Alpha 0.05

Bonferroni's m	Mean Diff.	95.00% CI	Significant	Summary	Adjusted P Value
1					
1% vs. 3%	-1086	-3962 to 1(	No	ns	>0.9999
1% vs. 5%	-1746	-4504 to 1(	No	ns	0.389
3% vs. 5%	-659.2	-3331 to 2(	No	ns	>0.9999
3					
1% vs. 3%	-2823	-5261 to -3	Yes	*	0.0167
1% vs. 5%	1490	-1776 to 4(	No	ns	0.8243
3% vs. 5%	4313	1327 to 72	Yes	**	0.0016
5					
1% vs. 3%	-5894	-8308 to -3	Yes	****	<0.0001
1% vs. 5%	-11939	-14431 to -	Yes	****	<0.0001
3% vs. 5%	-6045	-7899 to -4	Yes	****	<0.0001
7					
1% vs. 3%	-966.3	-3067 to 1(	No	ns	0.812
1% vs. 5%	-694.8	-2838 to 1(	No	ns	>0.9999
3% vs. 5%	271.5	-1753 to 2(	No	ns	>0.9999
10					
1% vs. 3%	1231	-866 to 33(	No	ns	0.4795
1% vs. 5%	-6160	-8792 to -3	Yes	****	<0.0001
3% vs. 5%	-7391	-10017 to -	Yes	****	<0.0001
15					
1% vs. 3%	-1602	-4081 to 8(	No	ns	0.3655
1% vs. 5%	3060	-283.1 to 6	No	ns	0.0853
3% vs. 5%	4662	1376 to 79	Yes	**	0.0021

Test details	Mean 1	Mean 2	Mean Diff.	SE of diff.	N1	N2	t	DF
1								
1% vs. 3%	11062	12148	-1086	1201	192	215	0.9047	5329
1% vs. 5%	11062	12807	-1746	1152	192	259	1.516	5329
3% vs. 5%	12148	12807	-659.2	1116	215	259	0.5908	5329
3								
1% vs. 3%	12530	15352	-2823	1018	218	400	2.773	5329
1% vs. 5%	12530	11040	1490	1364	218	123	1.092	5329
3% vs. 5%	15352	11040	4313	1247	400	123	3.459	5329
5								
1% vs. 3%	16003	21897	-5894	1008	195	549	5.846	5329
1% vs. 5%	16003	27942	-11939	1041	195	439	11.47	5329
3% vs. 5%	21897	27942	-6045	774.3	549	439	7.806	5329
7								
1% vs. 3%	24374	25340	-966.3	877.2	342	428	1.102	5329
1% vs. 5%	24374	25069	-694.8	894.9	342	392	0.7765	5329
3% vs. 5%	25340	25069	271.5	845.5	428	392	0.3211	5329
10								
1% vs. 3%	27220	25989	1231	875.7	379	384	1.406	5329
1% vs. 5%	27220	33380	-6160	1099	379	178	5.606	5329
3% vs. 5%	25989	33380	-7391	1097	384	178	6.74	5329
15								
1% vs. 3%	38000	39602	-1602	1035	257	291	1.547	5329
1% vs. 5%	38000	34940	3060	1396	257	106	2.192	5329
3% vs. 5%	39602	34940	4662	1372	291	106	3.398	5329

Table 44 – One-way ANOVA for the effects of time and hydrogel stiffness on Chapter 5 adipogenic data – ASPECT RATIO

Table Anal Data 1

Two-way A Ordinary
Alpha 0.05

Source of \	% of total \	P value	P value sur	Significant?
Interaction	0.9713	<0.0001	****	Yes
Time	4.476	<0.0001	****	Yes
Agarose	5.009	<0.0001	****	Yes

ANOVA tal	SS	DF	MS	F (DFn, DF	P value
Interaction	396.4	10	39.64	F (10, 532	P<0.0001
Time	1827	5	365.3	F (5, 5329)	P<0.0001
Agarose	2044	2	1022	F (2, 5329)	P<0.0001
Residual	36546	5329	6.858		

Number of 4535

Within each column, compare rows (simple effects within columns)

Number of 3
Number of 15
Alpha 0.05

Bonferroni's	Mean Diff.	95.00% CI	Significant?	Summary	Adjusted P Value
1%					
1 vs. 3	0.1502	-0.6109 to	No	ns	>0.9999
1 vs. 5	-1.176	-1.958 to -(	Yes	***	0.0002
1 vs. 7	-2.265	-2.958 to -'	Yes	****	<0.0001
1 vs. 10	-1.632	-2.313 to -(	Yes	****	<0.0001
1 vs. 15	-0.4747	-1.208 to 0	No	ns	0.8621
3 vs. 5	-1.326	-2.084 to -(	Yes	****	<0.0001
3 vs. 7	-2.415	-3.081 to -'	Yes	****	<0.0001
3 vs. 10	-1.782	-2.436 to -'	Yes	****	<0.0001
3 vs. 15	-0.6248	-1.333 to 0	No	ns	0.1438
5 vs. 7	-1.089	-1.779 to -(	Yes	****	<0.0001
5 vs. 10	-0.4562	-1.134 to 0	No	ns	0.7222
5 vs. 15	0.7013	-0.02901 to	No	ns	0.0723
7 vs. 10	0.6324	0.05883 to	Yes	*	0.0182
7 vs. 15	1.79	1.155 to 2.	Yes	****	<0.0001
10 vs. 15	1.157	0.5361 to 1	Yes	****	<0.0001
3%					
1 vs. 3	-0.1902	-0.8405 to	No	ns	>0.9999
1 vs. 5	-0.9666	-1.585 to -(	Yes	****	<0.0001
1 vs. 7	-0.7241	-1.367 to -(	Yes	*	0.0142
1 vs. 10	-0.6703	-1.325 to -(	Yes	*	0.04
1 vs. 15	-0.01264	-0.7042 to	No	ns	>0.9999
3 vs. 5	-0.7764	-1.282 to -(	Yes	****	<0.0001
3 vs. 7	-0.5339	-1.069 to 0	No	ns	0.0508
3 vs. 10	-0.4801	-1.03 to 0.(	No	ns	0.1547
3 vs. 15	0.1775	-0.415 to 0	No	ns	>0.9999
5 vs. 7	0.2425	-0.2534 to	No	ns	>0.9999
5 vs. 10	0.2963	-0.2153 to	No	ns	>0.9999
5 vs. 15	0.9539	0.3963 to 1	Yes	****	<0.0001
7 vs. 10	0.05378	-0.4868 to	No	ns	>0.9999
7 vs. 15	0.7114	0.1271 to 1	Yes	**	0.0053
10 vs. 15	0.6577	0.05997 to	Yes	*	0.0186
5%					
1 vs. 3	0.5985	-0.2436 to	No	ns	0.5538
1 vs. 5	-0.6659	-1.268 to -(	Yes	*	0.0177
1 vs. 7	-1.892	-2.508 to -'	Yes	****	<0.0001
1 vs. 10	-0.6903	-1.439 to 0	No	ns	0.102
1 vs. 15	-0.01688	-0.9036 to	No	ns	>0.9999
3 vs. 5	-1.264	-2.049 to -(	Yes	****	<0.0001
3 vs. 7	-2.491	-3.285 to -'	Yes	****	<0.0001
3 vs. 10	-1.289	-2.191 to -(	Yes	***	0.0004
3 vs. 15	-0.6154	-1.635 to 0	No	ns	>0.9999
5 vs. 7	-1.226	-1.761 to -(	Yes	****	<0.0001
5 vs. 10	-0.0244	-0.7077 to	No	ns	>0.9999
5 vs. 15	0.6491	-0.1832 to	No	ns	0.3307
7 vs. 10	1.202	0.5067 to 1	Yes	****	<0.0001
7 vs. 15	1.875	1.033 to 2.	Yes	****	<0.0001
10 vs. 15	0.6735	-0.27 to 1.(	No	ns	0.5418

Test detail:	Mean 1	Mean 2	Mean Diff.	SE of diff.	N1	N2	t	DF
1%								
1 vs. 3	4.657	4.507	0.1502	0.2592	192	218	0.5794	5329
1 vs. 5	4.657	5.833	-1.176	0.2662	192	195	4.417	5329
1 vs. 7	4.657	6.922	-2.265	0.2362	192	342	9.589	5329
1 vs. 10	4.657	6.289	-1.632	0.232	192	379	7.036	5329
1 vs. 15	4.657	5.132	-0.4747	0.2498	192	257	1.9	5329
3 vs. 5	4.507	5.833	-1.326	0.2581	218	195	5.138	5329
3 vs. 7	4.507	6.922	-2.415	0.227	218	342	10.64	5329
3 vs. 10	4.507	6.289	-1.782	0.2226	218	379	8.007	5329
3 vs. 15	4.507	5.132	-0.6248	0.2411	218	257	2.591	5329
5 vs. 7	5.833	6.922	-1.089	0.235	195	342	4.632	5329
5 vs. 10	5.833	6.289	-0.4562	0.2308	195	379	1.977	5329
5 vs. 15	5.833	5.132	0.7013	0.2487	195	257	2.82	5329
7 vs. 10	6.922	6.289	0.6324	0.1953	342	379	3.238	5329
7 vs. 15	6.922	5.132	1.79	0.2162	342	257	8.279	5329
10 vs. 15	6.289	5.132	1.157	0.2116	379	257	5.47	5329
3%								
1 vs. 3	4.018	4.208	-0.1902	0.2215	215	400	0.8588	5329
1 vs. 5	4.018	4.985	-0.9666	0.2107	215	549	4.588	5329
1 vs. 7	4.018	4.742	-0.7241	0.2189	215	428	3.308	5329
1 vs. 10	4.018	4.688	-0.6703	0.2231	215	384	3.005	5329
1 vs. 15	4.018	4.031	-0.01264	0.2355	215	291	0.05367	5329
3 vs. 5	4.208	4.985	-0.7764	0.1722	400	549	4.51	5329
3 vs. 7	4.208	4.742	-0.5339	0.1821	400	428	2.931	5329
3 vs. 10	4.208	4.688	-0.4801	0.1871	400	384	2.566	5329
3 vs. 15	4.208	4.031	0.1775	0.2018	400	291	0.8799	5329
5 vs. 7	4.985	4.742	0.2425	0.1689	549	428	1.436	5329
5 vs. 10	4.985	4.688	0.2963	0.1742	549	384	1.701	5329
5 vs. 15	4.985	4.031	0.9539	0.1899	549	291	5.024	5329
7 vs. 10	4.742	4.688	0.05378	0.1841	428	384	0.2922	5329
7 vs. 15	4.742	4.031	0.7114	0.199	428	291	3.576	5329
10 vs. 15	4.688	4.031	0.6577	0.2035	384	291	3.231	5329
5%								
1 vs. 3	3.478	2.88	0.5985	0.2868	259	123	2.087	5329
1 vs. 5	3.478	4.144	-0.6659	0.2052	259	439	3.246	5329
1 vs. 7	3.478	5.37	-1.892	0.2097	259	392	9.023	5329
1 vs. 10	3.478	4.168	-0.6903	0.255	259	178	2.708	5329
1 vs. 15	3.478	3.495	-0.01688	0.302	259	106	0.0559	5329
3 vs. 5	2.88	4.144	-1.264	0.2672	123	439	4.733	5329
3 vs. 7	2.88	5.37	-2.491	0.2706	123	392	9.202	5329
3 vs. 10	2.88	4.168	-1.289	0.3071	123	178	4.197	5329
3 vs. 15	2.88	3.495	-0.6154	0.3471	123	106	1.773	5329
5 vs. 7	4.144	5.37	-1.226	0.182	439	392	6.738	5329
5 vs. 10	4.144	4.168	-0.0244	0.2327	439	178	0.1049	5329
5 vs. 15	4.144	3.495	0.6491	0.2834	439	106	2.29	5329
7 vs. 10	5.37	4.168	1.202	0.2367	392	178	5.077	5329
7 vs. 15	5.37	3.495	1.875	0.2867	392	106	6.541	5329
10 vs. 15	4.168	3.495	0.6735	0.3213	178	106	2.096	5329

Within each row, compare columns (simple effects within rows)

Number of 6
Number of 3
Alpha 0.05

Bonferroni's	Mean Diff.	95.00% CI	Significant?	Summary	Adjusted P Value
1					
1% vs. 3%	0.6392	0.0165 to 1	Yes	*	0.042
1% vs. 5%	1.179	0.582 to 1.	Yes	****	<0.0001
3% vs. 5%	0.54	-0.03861 to	No	ns	0.0764
3					
1% vs. 3%	0.2989	-0.2291 to	No	ns	0.5259
1% vs. 5%	1.628	0.9203 to 2	Yes	****	<0.0001
3% vs. 5%	1.329	0.6821 to 1	Yes	****	<0.0001
5					
1% vs. 3%	0.8486	0.3258 to 1	Yes	***	0.0003
1% vs. 5%	1.689	1.15 to 2.2	Yes	****	<0.0001
3% vs. 5%	0.8406	0.4391 to 1	Yes	****	<0.0001
7					
1% vs. 3%	2.18	1.725 to 2.	Yes	****	<0.0001
1% vs. 5%	1.552	1.088 to 2.	Yes	****	<0.0001
3% vs. 5%	-0.628	-1.066 to -(	Yes	**	0.0018
10					
1% vs. 3%	1.601	1.147 to 2.	Yes	****	<0.0001
1% vs. 5%	2.121	1.551 to 2.	Yes	****	<0.0001
3% vs. 5%	0.5199	-0.04871 to	No	ns	0.0858
15					
1% vs. 3%	1.101	0.5644 to 1	Yes	****	<0.0001
1% vs. 5%	1.637	0.9131 to 2	Yes	****	<0.0001
3% vs. 5%	0.5357	-0.1757 to	No	ns	0.2142

Test detail:	Mean 1	Mean 2	Mean Diff.	SE of diff.	N1	N2	t	DF
1								
1% vs. 3%	4.657	4.018	0.6392	0.26	192	215	2.458	5329
1% vs. 5%	4.657	3.478	1.179	0.2494	192	259	4.728	5329
3% vs. 5%	4.018	3.478	0.54	0.2416	215	259	2.235	5329
3								
1% vs. 3%	4.507	4.208	0.2989	0.2205	218	400	1.356	5329
1% vs. 5%	4.507	2.88	1.628	0.2953	218	123	5.511	5329
3% vs. 5%	4.208	2.88	1.329	0.27	400	123	4.921	5329
5								
1% vs. 3%	5.833	4.985	0.8486	0.2183	195	549	3.887	5329
1% vs. 5%	5.833	4.144	1.689	0.2254	195	439	7.495	5329
3% vs. 5%	4.985	4.144	0.8406	0.1677	549	439	5.014	5329
7								
1% vs. 3%	6.922	4.742	2.18	0.1899	342	428	11.48	5329
1% vs. 5%	6.922	5.37	1.552	0.1938	342	392	8.008	5329
3% vs. 5%	4.742	5.37	-0.628	0.1831	428	392	3.43	5329
10								
1% vs. 3%	6.289	4.688	1.601	0.1896	379	384	8.444	5329
1% vs. 5%	6.289	4.168	2.121	0.238	379	178	8.913	5329
3% vs. 5%	4.688	4.168	0.5199	0.2375	384	178	2.19	5329
15								
1% vs. 3%	5.132	4.031	1.101	0.2242	257	291	4.913	5329
1% vs. 5%	5.132	3.495	1.637	0.3023	257	106	5.415	5329
3% vs. 5%	4.031	3.495	0.5357	0.2971	291	106	1.803	5329

Table 45 – One-way ANOVA for the effects of time and hydrogel stiffness on Chapter 5 adipogenic data – F-ACTIN

Table Anal Data 1

Two-way A Ordinary
Alpha 0.05

Source of V	% of total V	P value	P value sur	Significant?
Interaction	1.522	<0.0001	****	Yes
Time	9.436	<0.0001	****	Yes
Agarose	1.831	<0.0001	****	Yes

ANOVA tal	SS	DF	MS	F (DFn, DF	P value
Interaction	8.2E+11	10	8.2E+10	F (10, 532	P<0.0001
Time	5.09E+12	5	1.02E+12	F (5, 5329)	P<0.0001
Agarose	9.87E+11	2	4.94E+11	F (2, 5329)	P<0.0001
Residual	4.7E+13	5329	8.82E+09		

Number of 4535

Within each column, compare rows (simple effects within columns)

Number of 3
Number of 15
Alpha 0.05

Bonferroni's	Mean Diff.	95.00% CI	Significant?	Summary	Adjusted P Value
1%					
1 vs. 3	77344	50046 to 1	Yes	****	<0.0001
1 vs. 5	3818	-24224 to 2	No	ns	>0.9999
1 vs. 7	-22711	-47585 to 2	No	ns	0.1103
1 vs. 10	-31807	-56240 to -	Yes	**	0.002
1 vs. 15	-27216	-53526 to -	Yes	*	0.0359
3 vs. 5	-73527	-100713 to	Yes	****	<0.0001
3 vs. 7	-100056	-123960 to	Yes	****	<0.0001
3 vs. 10	-109152	-132597 to	Yes	****	<0.0001
3 vs. 15	-104560	-129957 to	Yes	****	<0.0001
5 vs. 7	-26529	-51279 to -	Yes	*	0.0248
5 vs. 10	-35625	-59933 to -	Yes	***	0.0003
5 vs. 15	-31034	-57228 to -	Yes	**	0.0076
7 vs. 10	-9096	-29667 to 1	No	ns	>0.9999
7 vs. 15	-4505	-27274 to 1	No	ns	>0.9999
10 vs. 15	4592	-17696 to 2	No	ns	>0.9999
3%					
1 vs. 3	20096	-3228 to 4	No	ns	0.1715
1 vs. 5	-47308	-69498 to -	Yes	****	<0.0001
1 vs. 7	-18583	-41640 to 4	No	ns	0.2697
1 vs. 10	-65419	-88913 to -	Yes	****	<0.0001
1 vs. 15	-91687	-116492 to	Yes	****	<0.0001
3 vs. 5	-67404	-85536 to -	Yes	****	<0.0001
3 vs. 7	-38679	-57861 to -	Yes	****	<0.0001
3 vs. 10	-85515	-105221 to	Yes	****	<0.0001
3 vs. 15	-111783	-133035 to	Yes	****	<0.0001
5 vs. 7	28725	10939 to 4	Yes	****	<0.0001
5 vs. 10	-18111	-36460 to 2	No	ns	0.0565
5 vs. 15	-44379	-64379 to -	Yes	****	<0.0001
7 vs. 10	-46836	-66223 to -	Yes	****	<0.0001
7 vs. 15	-73104	-94060 to -	Yes	****	<0.0001
10 vs. 15	-26268	-47705 to -	Yes	**	0.0048
5%					
1 vs. 3	-9859	-40062 to 2	No	ns	>0.9999
1 vs. 5	-53192	-74803 to -	Yes	****	<0.0001
1 vs. 7	-56218	-78304 to -	Yes	****	<0.0001
1 vs. 10	-83449	-110303 to	Yes	****	<0.0001
1 vs. 15	-92438	-124241 to	Yes	****	<0.0001
3 vs. 5	-43333	-71472 to -	Yes	****	<0.0001
3 vs. 7	-46359	-74865 to -	Yes	****	<0.0001
3 vs. 10	-73590	-105931 to	Yes	****	<0.0001
3 vs. 15	-82579	-119134 to	Yes	****	<0.0001
5 vs. 7	-3025	-22192 to 1	No	ns	>0.9999
5 vs. 10	-30257	-54766 to -	Yes	**	0.0044
5 vs. 15	-39246	-69096 to -	Yes	**	0.0017
7 vs. 10	-27232	-52161 to -	Yes	*	0.0202
7 vs. 15	-36221	-66416 to -	Yes	**	0.0065
10 vs. 15	-8989	-42829 to 2	No	ns	>0.9999

Test detail	Mean 1	Mean 2	Mean Diff.	SE of diff.	N1	N2	t	DF
1%								
1 vs. 3	133250	55905	77344	9296	192	218	8.32	5329
1 vs. 5	133250	129432	3818	9549	192	195	0.3998	5329
1 vs. 7	133250	155961	-22711	8470	192	342	2.681	5329
1 vs. 10	133250	165057	-31807	8320	192	379	3.823	5329
1 vs. 15	133250	160466	-27216	8960	192	257	3.038	5329
3 vs. 5	55905	129432	-73527	9258	218	195	7.942	5329
3 vs. 7	55905	155961	-100056	8140	218	342	12.29	5329
3 vs. 10	55905	165057	-109152	7984	218	379	13.67	5329
3 vs. 15	55905	160466	-104560	8649	218	257	12.09	5329
5 vs. 7	129432	155961	-26529	8428	195	342	3.148	5329
5 vs. 10	129432	165057	-35625	8278	195	379	4.304	5329
5 vs. 15	129432	160466	-31034	8920	195	257	3.479	5329
7 vs. 10	155961	165057	-9096	7005	342	379	1.298	5329
7 vs. 15	155961	160466	-4505	7754	342	257	0.5809	5329
10 vs. 15	165057	160466	4592	7590	379	257	0.605	5329
3%								
1 vs. 3	82974	62878	20096	7943	215	400	2.53	5329
1 vs. 5	82974	130282	-47308	7557	215	549	6.26	5329
1 vs. 7	82974	101557	-18583	7852	215	428	2.367	5329
1 vs. 10	82974	148393	-65419	8001	215	384	8.177	5329
1 vs. 15	82974	174661	-91687	8447	215	291	10.85	5329
3 vs. 5	62878	130282	-67404	6175	400	549	10.92	5329
3 vs. 7	62878	101557	-38679	6532	400	428	5.921	5329
3 vs. 10	62878	148393	-85515	6710	400	384	12.74	5329
3 vs. 15	62878	174661	-111783	7237	400	291	15.45	5329
5 vs. 7	130282	101557	28725	6057	549	428	4.743	5329
5 vs. 10	130282	148393	-18111	6249	549	384	2.898	5329
5 vs. 15	130282	174661	-44379	6811	549	291	6.516	5329
7 vs. 10	101557	148393	-46836	6602	428	384	7.094	5329
7 vs. 15	101557	174661	-73104	7137	428	291	10.24	5329
10 vs. 15	148393	174661	-26268	7300	384	291	3.598	5329
5%								
1 vs. 3	47526	57385	-9859	10285	259	123	0.9585	5329
1 vs. 5	47526	100719	-53192	7359	259	439	7.228	5329
1 vs. 7	47526	103744	-56218	7521	259	392	7.475	5329
1 vs. 10	47526	130976	-83449	9145	259	178	9.125	5329
1 vs. 15	47526	139965	-92438	10830	259	106	8.535	5329
3 vs. 5	57385	100719	-43333	9582	123	439	4.522	5329
3 vs. 7	57385	103744	-46359	9707	123	392	4.776	5329
3 vs. 10	57385	130976	-73590	11013	123	178	6.682	5329
3 vs. 15	57385	139965	-82579	12448	123	106	6.634	5329
5 vs. 7	100719	103744	-3025	6527	439	392	0.4635	5329
5 vs. 10	100719	130976	-30257	8346	439	178	3.625	5329
5 vs. 15	100719	139965	-39246	10165	439	106	3.861	5329
7 vs. 10	103744	130976	-27232	8489	392	178	3.208	5329
7 vs. 15	103744	139965	-36221	10283	392	106	3.522	5329
10 vs. 15	130976	139965	-8989	11524	178	106	0.7801	5329

Within each row, compare columns (simple effects within rows)

Number of 6
Number of 3
Alpha 0.05

Bonferroni's	Mean Diff.	95.00% CI	Significant?	Summary	Adjusted P Value
1					
1% vs. 3%	50276	27941 to 7	Yes	****	<0.0001
1% vs. 5%	85723	64303 to 1	Yes	****	<0.0001
3% vs. 5%	35448	14695 to 5	Yes	***	0.0001
3					
1% vs. 3%	-6972	-25908 to 1	No	ns	>0.9999
1% vs. 5%	-1480	-26846 to 2	No	ns	>0.9999
3% vs. 5%	5492	-17698 to 2	No	ns	>0.9999
5					
1% vs. 3%	-850	-19601 to 1	No	ns	>0.9999
1% vs. 5%	28713	9356 to 48	Yes	**	0.0012
3% vs. 5%	29563	15162 to 4	Yes	****	<0.0001
7					
1% vs. 3%	54404	38090 to 7	Yes	****	<0.0001
1% vs. 5%	52217	35574 to 6	Yes	****	<0.0001
3% vs. 5%	-2187	-17912 to 1	No	ns	>0.9999
10					
1% vs. 3%	16664	377.7 to 3	Yes	*	0.0429
1% vs. 5%	34082	13643 to 5	Yes	***	0.0002
3% vs. 5%	17417	-2978 to 3	No	ns	0.1227
15					
1% vs. 3%	-14195	-33450 to 5	No	ns	0.2326
1% vs. 5%	20501	-5464 to 4	No	ns	0.1761
3% vs. 5%	34696	9178 to 60	Yes	**	0.0034

Test detail	Mean 1	Mean 2	Mean Diff.	SE of diff.	N1	N2	t	DF
1								
1% vs. 3%	133250	82974	50276	9327	192	215	5.391	5329
1% vs. 5%	133250	47526	85723	8945	192	259	9.583	5329
3% vs. 5%	82974	47526	35448	8666	215	259	4.09	5329
3								
1% vs. 3%	55905	62878	-6972	7907	218	400	0.8818	5329
1% vs. 5%	55905	57385	-1480	10592	218	123	0.1397	5329
3% vs. 5%	62878	57385	5492	9684	400	123	0.5672	5329
5								
1% vs. 3%	129432	130282	-850	7830	195	549	0.1086	5329
1% vs. 5%	129432	100719	28713	8083	195	439	3.552	5329
3% vs. 5%	130282	100719	29563	6014	549	439	4.916	5329
7								
1% vs. 3%	155961	101557	54404	6812	342	428	7.986	5329
1% vs. 5%	155961	103744	52217	6950	342	392	7.513	5329
3% vs. 5%	101557	103744	-2187	6566	428	392	0.333	5329
10								
1% vs. 3%	165057	148393	16664	6801	379	384	2.45	5329
1% vs. 5%	165057	130976	34082	8535	379	178	3.993	5329
3% vs. 5%	148393	130976	17417	8517	384	178	2.045	5329
15								
1% vs. 3%	160466	174661	-14195	8040	257	291	1.766	5329
1% vs. 5%	160466	139965	20501	10842	257	106	1.891	5329
3% vs. 5%	174661	139965	34696	10656	291	106	3.256	5329

Table 46 – One-way ANOVA for the effects of time and hydrogel stiffness on Chapter 5 adipogenic data – THICKNESS

Table Anal Data 1

Two-way A Ordinary
Alpha 0.05

Source of \	% of total \	P value	P value sur	Significant?
Interaction	7.548	<0.0001	****	Yes
Time	5.371	<0.0001	****	Yes
Agarose	6.059	<0.0001	****	Yes

ANOVA tal	SS	DF	MS	F (DFn, DF	P value
Interaction	107295	10	10730	F (10, 532	P<0.0001
Time	76350	5	15270	F (5, 5329)	P<0.0001
Agarose	86123	2	43062	F (2, 5329)	P<0.0001
Residual	1151652	5329	216.1		

Number of 4535

Within each column, compare rows (simple effects within columns)

Number of 3
Number of 15
Alpha 0.05

Bonferroni\	Mean Diff.	95.00% CI	Significant?	Summary	Adjusted P Value
1%					
1 vs. 3	30.04	25.77 to 34	Yes	****	<0.0001
1 vs. 5	16.19	11.8 to 20.	Yes	****	<0.0001
1 vs. 7	21.07	17.18 to 24	Yes	****	<0.0001
1 vs. 10	23.09	19.27 to 26	Yes	****	<0.0001
1 vs. 15	29.26	25.14 to 33	Yes	****	<0.0001
3 vs. 5	-13.85	-18.11 to -1	Yes	****	<0.0001
3 vs. 7	-8.971	-12.71 to -5	Yes	****	<0.0001
3 vs. 10	-6.954	-10.62 to -3	Yes	****	<0.0001
3 vs. 15	-0.7876	-4.762 to 3	No	ns	>0.9999
5 vs. 7	4.882	1.009 to 8.	Yes	**	0.0033
5 vs. 10	6.899	3.095 to 10	Yes	****	<0.0001
5 vs. 15	13.07	8.967 to 17	Yes	****	<0.0001
7 vs. 10	2.017	-1.203 to 5	No	ns	0.9882
7 vs. 15	8.184	4.62 to 11.	Yes	****	<0.0001
10 vs. 15	6.167	2.679 to 9.	Yes	****	<0.0001
3%					
1 vs. 3	11.89	8.237 to 15	Yes	****	<0.0001
1 vs. 5	3.887	0.4142 to 7	Yes	*	0.0153
1 vs. 7	12.05	8.445 to 15	Yes	****	<0.0001
1 vs. 10	5.991	2.314 to 9.	Yes	****	<0.0001
1 vs. 15	9.471	5.589 to 13	Yes	****	<0.0001
3 vs. 5	-8.001	-10.84 to -5	Yes	****	<0.0001
3 vs. 7	0.1658	-2.836 to 3	No	ns	>0.9999
3 vs. 10	-5.897	-8.981 to -2	Yes	****	<0.0001
3 vs. 15	-2.417	-5.743 to 0	No	ns	0.4939
5 vs. 7	8.166	5.383 to 10	Yes	****	<0.0001
5 vs. 10	2.103	-0.7685 to	No	ns	0.4732
5 vs. 15	5.584	2.454 to 8.	Yes	****	<0.0001
7 vs. 10	-6.063	-9.097 to -3	Yes	****	<0.0001
7 vs. 15	-2.582	-5.862 to 0	No	ns	0.3123
10 vs. 15	3.481	0.1256 to 6	Yes	*	0.0349
5%					
1 vs. 3	-5.845	-10.57 to -1	Yes	**	0.0043
1 vs. 5	-0.593	-3.975 to 2	No	ns	>0.9999
1 vs. 7	-1.009	-4.466 to 2	No	ns	>0.9999
1 vs. 10	-1.867	-6.069 to 2	No	ns	>0.9999
1 vs. 15	-3.595	-8.573 to 1	No	ns	0.5095
3 vs. 5	5.252	0.8484 to 9	Yes	**	0.007
3 vs. 7	4.836	0.3745 to 9	Yes	*	0.022
3 vs. 10	3.979	-1.083 to 9	No	ns	0.3152
3 vs. 15	2.25	-3.471 to 7	No	ns	>0.9999
5 vs. 7	-0.4164	-3.416 to 2	No	ns	>0.9999
5 vs. 10	-1.274	-5.109 to 2	No	ns	>0.9999
5 vs. 15	-3.002	-7.674 to 1	No	ns	0.8881
7 vs. 10	-0.8571	-4.759 to 3	No	ns	>0.9999
7 vs. 15	-2.586	-7.312 to 2	No	ns	>0.9999
10 vs. 15	-1.729	-7.025 to 3	No	ns	>0.9999

Test detail\	Mean 1	Mean 2	Mean Diff.	SE of diff.	N1	N2	t	DF
1%								
1 vs. 3	50.66	20.62	30.04	1.455	192	218	20.65	5329
1 vs. 5	50.66	34.47	16.19	1.495	192	195	10.83	5329
1 vs. 7	50.66	29.59	21.07	1.326	192	342	15.9	5329
1 vs. 10	50.66	27.57	23.09	1.302	192	379	17.73	5329
1 vs. 15	50.66	21.41	29.26	1.402	192	257	20.86	5329
3 vs. 5	20.62	34.47	-13.85	1.449	218	195	9.561	5329
3 vs. 7	20.62	29.59	-8.971	1.274	218	342	7.042	5329
3 vs. 10	20.62	27.57	-6.954	1.25	218	379	5.565	5329
3 vs. 15	20.62	21.41	-0.7876	1.354	218	257	0.5818	5329
5 vs. 7	34.47	29.59	4.882	1.319	195	342	3.701	5329
5 vs. 10	34.47	27.57	6.899	1.296	195	379	5.325	5329
5 vs. 15	34.47	21.41	13.07	1.396	195	257	9.359	5329
7 vs. 10	29.59	27.57	2.017	1.096	342	379	1.84	5329
7 vs. 15	29.59	21.41	8.184	1.214	342	257	6.744	5329
10 vs. 15	27.57	21.41	6.167	1.188	379	257	5.191	5329
3%								
1 vs. 3	31.85	19.97	11.89	1.243	215	400	9.563	5329
1 vs. 5	31.85	27.97	3.887	1.183	215	549	3.287	5329
1 vs. 7	31.85	19.8	12.05	1.229	215	428	9.809	5329
1 vs. 10	31.85	25.86	5.991	1.252	215	384	4.784	5329
1 vs. 15	31.85	22.38	9.471	1.322	215	291	7.164	5329
3 vs. 5	19.97	27.97	-8.001	0.9664	400	549	8.279	5329
3 vs. 7	19.97	19.8	0.1658	1.022	400	428	0.1622	5329
3 vs. 10	19.97	25.86	-5.897	1.05	400	384	5.615	5329
3 vs. 15	19.97	22.38	-2.417	1.133	400	291	2.134	5329
5 vs. 7	27.97	19.8	8.166	0.9479	549	428	8.615	5329
5 vs. 10	27.97	25.86	2.103	0.978	549	384	2.151	5329
5 vs. 15	27.97	22.38	5.584	1.066	549	291	5.239	5329
7 vs. 10	19.8	25.86	-6.063	1.033	428	384	5.868	5329
7 vs. 15	19.8	22.38	-2.582	1.117	428	291	2.312	5329
10 vs. 15	25.86	22.38	3.481	1.143	384	291	3.046	5329
5%								
1 vs. 3	17.76	23.61	-5.845	1.61	259	123	3.631	5329
1 vs. 5	17.76	18.35	-0.593	1.152	259	439	0.5148	5329
1 vs. 7	17.76	18.77	-1.009	1.177	259	392	0.8575	5329
1 vs. 10	17.76	19.63	-1.867	1.431	259	178	1.304	5329
1 vs. 15	17.76	21.36	-3.595	1.695	259	106	2.121	5329
3 vs. 5	23.61	18.35	5.252	1.5	123	439	3.502	5329
3 vs. 7	23.61	18.77	4.836	1.519	123	392	3.183	5329
3 vs. 10	23.61	19.63	3.979	1.724	123	178	2.308	5329
3 vs. 15	23.61	21.36	2.25	1.948	123	106	1.155	5329
5 vs. 7	18.35	18.77	-0.4164	1.022	439	392	0.4077	5329
5 vs. 10	18.35	19.63	-1.274	1.306	439	178	0.9749	5329
5 vs. 15	18.35	21.36	-3.002	1.591	439	106	1.887	5329
7 vs. 10	18.77	19.63	-0.8571	1.329	392	178	0.6451	5329
7 vs. 15	18.77	21.36	-2.586	1.609	392	106	1.607	5329
10 vs. 15	19.63	21.36	-1.729	1.804	178	106	0.9585	5329

Within each row, compare columns (simple effects within rows)

Number of 6
Number of 3
Alpha 0.05

Bonferroni\	Mean Diff.	95.00% CI	Significant?	Summary	Adjusted P Value
1					
1% vs. 3%	18.81	15.31 to 22	Yes	****	<0.0001
1% vs. 5%	32.9	29.55 to 36	Yes	****	<0.0001
3% vs. 5%	14.09	10.84 to 17	Yes	****	<0.0001
3					
1% vs. 3%	0.6509	-2.313 to 3	No	ns	>0.9999
1% vs. 5%	-2.99	-6.96 to 0.9	No	ns	0.2141
3% vs. 5%	-3.641	-7.27 to -0.	Yes	*	0.049
5					
1% vs. 3%	6.504	3.569 to 9.	Yes	****	<0.0001
1% vs. 5%	16.12	13.09 to 19	Yes	****	<0.0001
3% vs. 5%	9.613	7.359 to 11	Yes	****	<0.0001
7					
1% vs. 3%	9.788	7.235 to 12	Yes	****	<0.0001
1% vs. 5%	10.82	8.213 to 13	Yes	****	<0.0001
3% vs. 5%	1.03	-1.432 to 3	No	ns	0.9494
10					
1% vs. 3%	1.708	-0.841 to 4	No	ns	0.3259
1% vs. 5%	7.944	4.745 to 11	Yes	****	<0.0001
3% vs. 5%	6.236	3.043 to 9.	Yes	****	<0.0001
15					
1% vs. 3%	-0.9781	-3.992 to 2	No	ns	>0.9999
1% vs. 5%	0.04809	-4.016 to 4	No	ns	>0.9999
3% vs. 5%	1.026	-2.968 to 5	No	ns	>0.9999

Test detail\	Mean 1	Mean 2	Mean Diff.	SE of diff.	N1	N2	t	DF
1								
1% vs. 3%	50.66	31.85	18.81	1.46	192	215	12.88	5329
1% vs. 5%	50.66	17.76	32.9	1.4	192	259	23.5	5329
3% vs. 5%	31.85	17.76	14.09	1.356	215	259	10.39	5329
3								
1% vs. 3%	20.62	19.97	0.6509	1.238	218	400	0.5259	5329
1% vs. 5%	20.62	23.61	-2.99	1.658	218	123	1.803	5329
3% vs. 5%	19.97	23.61	-3.641	1.516	400	123	2.402	5329
5								
1% vs. 3%	34.47	27.97	6.504	1.226	195	549	5.307	5329
1% vs. 5%	34.47	18.35	16.12	1.265	195	439	12.74	5329
3% vs. 5%	27.97	18.35	9.613	0.9412	549	439	10.21	5329
7								
1% vs. 3%	29.59	19.8	9.788	1.066	342	428	9.18	5329
1% vs. 5%	29.59	18.77	10.82	1.088	342	392	9.945	5329
3% vs. 5%	19.8	18.77	1.03	1.028	428	392	1.002	5329
10								
1% vs. 3%	27.57	25.86	1.708	1.064	379	384	1.605	5329
1% vs. 5%	27.57	19.63	7.944	1.336	379	178	5.947	5329
3% vs. 5%	25.86	19.63	6.236	1.333	384	178	4.678	5329
15								
1% vs. 3%	21.41	22.38	-0.9781	1.258	257	291	0.7773	5329
1% vs. 5%	21.41	21.36	0.04809	1.697	257	106	0.02834	5329
3% vs. 5%	22.38	21.36	1.026	1.668	291	106	0.6153	5329

Table 47 – One-way ANOVA for the effects of time and hydrogel stiffness on Chapter 5 adipogenic data – ALIGNMENT

Table Anal Data 1

Two-way A Ordinary
Alpha 0.05

Source of \	% of total \	P value	P value sur	Significant?
Interaction	1.267	<0.0001	****	Yes
Time	7.628	<0.0001	****	Yes
Agarose	6.036	<0.0001	****	Yes

ANOVA tal	SS	DF	MS	F (DFn, DF	P value
Interaction	0.281	10	0.0281	F (10, 532	P<0.0001
Time	1.692	5	0.3383	F (5, 5329)	P<0.0001
Agarose	1.339	2	0.6693	F (2, 5329)	P<0.0001
Residual	18.86	5329	0.00354		

Number of 4535

Within each column, compare rows (simple effects within columns)

Number of 3
Number of 15
Alpha 0.05

Bonferroni's	Mean Diff.	95.00% CI	Significant?	Summary	Adjusted P Value
1%					
1 vs. 3	-0.01071	-0.028 to 0	No	ns	>0.9999
1 vs. 5	-0.00614	-0.0239 to	No	ns	>0.9999
1 vs. 7	-0.0149	-0.03065 to	No	ns	0.0827
1 vs. 10	-0.03357	-0.04904 to	Yes	****	<0.0001
1 vs. 15	-0.06319	-0.07986 to	Yes	****	<0.0001
3 vs. 5	0.004565	-0.01266 to	No	ns	>0.9999
3 vs. 7	-0.00419	-0.01933 to	No	ns	>0.9999
3 vs. 10	-0.02286	-0.03771 to	Yes	****	<0.0001
3 vs. 15	-0.05249	-0.06858 to	Yes	****	<0.0001
5 vs. 7	-0.00876	-0.02443 to	No	ns	>0.9999
5 vs. 10	-0.02743	-0.04282 to	Yes	****	<0.0001
5 vs. 15	-0.05705	-0.07365 to	Yes	****	<0.0001
7 vs. 10	-0.01867	-0.0317 to	Yes	***	0.0004
7 vs. 15	-0.0483	-0.06272 to	Yes	****	<0.0001
10 vs. 15	-0.02963	-0.04375 to	Yes	****	<0.0001
3%					
1 vs. 3	-0.02304	-0.03781 to	Yes	****	<0.0001
1 vs. 5	-0.03518	-0.04924 to	Yes	****	<0.0001
1 vs. 7	-0.05101	-0.06562 to	Yes	****	<0.0001
1 vs. 10	-0.05141	-0.06629 to	Yes	****	<0.0001
1 vs. 15	-0.07849	-0.0942 to	Yes	****	<0.0001
3 vs. 5	-0.01215	-0.02363 to	Yes	*	0.0286
3 vs. 7	-0.02798	-0.04013 to	Yes	****	<0.0001
3 vs. 10	-0.02837	-0.04085 to	Yes	****	<0.0001
3 vs. 15	-0.05545	-0.06891 to	Yes	****	<0.0001
5 vs. 7	-0.01583	-0.0271 to	Yes	***	0.0006
5 vs. 10	-0.01622	-0.02785 to	Yes	***	0.0006
5 vs. 15	-0.0433	-0.05597 to	Yes	****	<0.0001
7 vs. 10	-0.00039	-0.01267 to	No	ns	>0.9999
7 vs. 15	-0.02747	-0.04075 to	Yes	****	<0.0001
10 vs. 15	-0.02708	-0.04066 to	Yes	****	<0.0001
5%					
1 vs. 3	-0.02594	-0.04507 to	Yes	**	0.001
1 vs. 5	-0.02581	-0.0395 to	Yes	****	<0.0001
1 vs. 7	-0.01266	-0.02665 to	No	ns	0.1184
1 vs. 10	-0.04786	-0.06487 to	Yes	****	<0.0001
1 vs. 15	-0.04467	-0.06481 to	Yes	****	<0.0001
3 vs. 5	0.000127	-0.0177 to	No	ns	>0.9999
3 vs. 7	0.01328	-0.004782 to	No	ns	0.4636
3 vs. 10	-0.02192	-0.04241 to	Yes	*	0.0253
3 vs. 15	-0.01873	-0.04188 to	No	ns	0.2636
5 vs. 7	0.01315	0.001007 to	Yes	*	0.0222
5 vs. 10	-0.02205	-0.03757 to	Yes	***	0.0005
5 vs. 15	-0.01886	-0.03776 to	No	ns	0.0513
7 vs. 10	-0.03519	-0.05099 to	Yes	****	<0.0001
7 vs. 15	-0.032	-0.05113 to	Yes	****	<0.0001
10 vs. 15	0.00319	-0.01825 to	No	ns	>0.9999

Test detail	Mean 1	Mean 2	Mean Diff.	SE of diff.	N1	N2	t	DF
1%								
1 vs. 3	0.08648	0.09719	-0.01071	0.005889	192	218	1.818	5329
1 vs. 5	0.08648	0.09262	-0.00614	0.006049	192	195	1.015	5329
1 vs. 7	0.08648	0.1014	-0.0149	0.005366	192	342	2.776	5329
1 vs. 10	0.08648	0.12	-0.03357	0.00527	192	379	6.369	5329
1 vs. 15	0.08648	0.1497	-0.06319	0.005676	192	257	11.13	5329
3 vs. 5	0.09719	0.09262	0.004565	0.005865	218	195	0.7784	5329
3 vs. 7	0.09719	0.1014	-0.00419	0.005157	218	342	0.8128	5329
3 vs. 10	0.09719	0.12	-0.02286	0.005058	218	379	4.52	5329
3 vs. 15	0.09719	0.1497	-0.05249	0.005478	218	257	9.581	5329
5 vs. 7	0.09262	0.1014	-0.00876	0.005339	195	342	1.64	5329
5 vs. 10	0.09262	0.12	-0.02743	0.005244	195	379	5.23	5329
5 vs. 15	0.09262	0.1497	-0.05705	0.005651	195	257	10.1	5329
7 vs. 10	0.1014	0.12	-0.01867	0.004438	342	379	4.207	5329
7 vs. 15	0.1014	0.1497	-0.0483	0.004912	342	257	9.833	5329
10 vs. 15	0.12	0.1497	-0.02963	0.004808	379	257	6.162	5329
3%								
1 vs. 3	0.09315	0.1162	-0.02304	0.005031	215	400	4.578	5329
1 vs. 5	0.09315	0.1283	-0.03518	0.004787	215	549	7.35	5329
1 vs. 7	0.09315	0.1442	-0.05101	0.004974	215	428	10.26	5329
1 vs. 10	0.09315	0.1446	-0.05141	0.005068	215	384	10.14	5329
1 vs. 15	0.09315	0.1716	-0.07849	0.005351	215	291	14.67	5329
3 vs. 5	0.1162	0.1283	-0.01215	0.003911	400	549	3.106	5329
3 vs. 7	0.1162	0.1442	-0.02798	0.004138	400	428	6.761	5329
3 vs. 10	0.1162	0.1446	-0.02837	0.004251	400	384	6.674	5329
3 vs. 15	0.1162	0.1716	-0.05545	0.004584	400	291	12.1	5329
5 vs. 7	0.1283	0.1442	-0.01583	0.003837	549	428	4.126	5329
5 vs. 10	0.1283	0.1446	-0.01622	0.003958	549	384	4.098	5329
5 vs. 15	0.1283	0.1716	-0.0433	0.004314	549	291	10.04	5329
7 vs. 10	0.1442	0.1446	-0.00039	0.004182	428	384	0.09373	5329
7 vs. 15	0.1442	0.1716	-0.02747	0.004521	428	291	6.077	5329
10 vs. 15	0.1446	0.1716	-0.02708	0.004624	384	291	5.856	5329
5%								
1 vs. 3	0.1242	0.1502	-0.02594	0.006515	259	123	3.981	5329
1 vs. 5	0.1242	0.15	-0.02581	0.004662	259	439	5.537	5329
1 vs. 7	0.1242	0.1369	-0.01266	0.004764	259	392	2.658	5329
1 vs. 10	0.1242	0.1721	-0.04786	0.005793	259	178	8.261	5329
1 vs. 15	0.1242	0.1689	-0.04467	0.00686	259	106	6.511	5329
3 vs. 5	0.1502	0.15	0.000127	0.00607	123	439	0.02092	5329
3 vs. 7	0.1502	0.1369	0.01328	0.006149	123	392	2.159	5329
3 vs. 10	0.1502	0.1721	-0.02192	0.006976	123	178	3.142	5329
3 vs. 15	0.1502	0.1689	-0.01873	0.007885	123	106	2.375	5329
5 vs. 7	0.15	0.1369	0.01315	0.004135	439	392	3.18	5329
5 vs. 10	0.15	0.1721	-0.02205	0.005287	439	178	4.17	5329
5 vs. 15	0.15	0.1689	-0.01886	0.006439	439	106	2.928	5329
7 vs. 10	0.1369	0.1721	-0.03519	0.005378	392	178	6.545	5329
7 vs. 15	0.1369	0.1689	-0.032	0.006514	392	106	4.913	5329
10 vs. 15	0.1721	0.1689	0.00319	0.0073	178	106	0.437	5329

Within each row, compare columns (simple effects within rows)

Number of 6
Number of 3
Alpha 0.05

Bonferroni's	Mean Diff.	95.00% CI	Significant?	Summary	Adjusted P Value
1					
1% vs. 3%	-0.00666	-0.02081 to	No	ns	0.7781
1% vs. 5%	-0.03774	-0.05131 to	Yes	****	<0.0001
3% vs. 5%	-0.03108	-0.04422 to	Yes	****	<0.0001
3					
1% vs. 3%	-0.01899	-0.03099 to	Yes	***	0.0005
1% vs. 5%	-0.05297	-0.06904 to	Yes	****	<0.0001
3% vs. 5%	-0.03398	-0.04867 to	Yes	****	<0.0001
5					
1% vs. 3%	-0.03571	-0.04758 to	Yes	****	<0.0001
1% vs. 5%	-0.05741	-0.06967 to	Yes	****	<0.0001
3% vs. 5%	-0.02171	-0.03083 to	Yes	****	<0.0001
7					
1% vs. 3%	-0.04278	-0.05311 to	Yes	****	<0.0001
1% vs. 5%	-0.03551	-0.04605 to	Yes	****	<0.0001
3% vs. 5%	0.007272	-0.002689	No	ns	0.2414
10					
1% vs. 3%	-0.0245	-0.03482 to	Yes	****	<0.0001
1% vs. 5%	-0.05203	-0.06498 to	Yes	****	<0.0001
3% vs. 5%	-0.02753	-0.04045 to	Yes	****	<0.0001
15					
1% vs. 3%	-0.02196	-0.03415 to	Yes	****	<0.0001
1% vs. 5%	-0.01922	-0.03566 to	Yes	*	0.0155
3% vs. 5%	0.002742	-0.01342 to	No	ns	>0.9999

Test detail	Mean 1	Mean 2	Mean Diff.	SE of diff.	N1	N2	t	DF
1								
1% vs. 3%	0.08648	0.09315	-0.00666	0.005908	192	215	1.128	5329
1% vs. 5%	0.08648	0.1242	-0.03774	0.005666	192	259	6.661	5329
3% vs. 5%	0.09315	0.1242	-0.03108	0.005489	215	259	5.662	5329
3								
1% vs. 3%	0.09719	0.1162	-0.01899	0.005009	218	400	3.792	5329
1% vs. 5%	0.09719	0.1502	-0.05297	0.00671	218	123	7.895	5329
3% vs. 5%	0.1162	0.1502	-0.03398	0.006134	400	123	5.539	5329
5								
1% vs. 3%	0.09262	0.1283	-0.03571	0.00496	195	549	7.199	5329
1% vs. 5%	0.09262	0.15	-0.05741	0.00512	195	439	11.21	5329
3% vs. 5%	0.1283	0.15	-0.02171	0.003809	549	439	5.698	5329
7								
1% vs. 3%	0.1014	0.1442	-0.04278	0.004315	342	428	9.913	5329
1% vs. 5%	0.1014	0.1369	-0.03551	0.004402	342	392	8.065	5329
3% vs. 5%	0.1442	0.1369	0.007272	0.00416	428	392	1.748	5329
10								
1% vs. 3%	0.12	0.1446	-0.0245	0.004308	379	384	5.687	5329
1% vs. 5%	0.12	0.1721	-0.05203	0.005406	379	178	9.624	5329
3% vs. 5%	0.1446	0.1721	-0.02753	0.005395	384	178	5.103	5329
15								
1% vs. 3%	0.1497	0.1716	-0.02196	0.005093	257	291	4.311	5329
1% vs. 5%	0.1497	0.1689	-0.01922	0.006868	257	106	2.798	5329
3% vs. 5%	0.1716	0.1689	0.002742	0.00675	291	106	0.4062	5329

Table 48 – One-way ANOVA for the effects of time and hydrogel stiffness on Chapter 5 adipogenic data – CURVATURE

Table Anal Data 1

Two-way A Ordinary
Alpha 0.05

Source of \	% of total \	P value	P value sur	Significant?
Interaction	1.072	<0.0001	****	Yes
Time	6.856	<0.0001	****	Yes
Agarose	4.132	<0.0001	****	Yes

ANOVA tal	SS	DF	MS	F (DFn, DF	P value
Interaction	0.5613	10	0.05613	F (10, 532	P<0.0001
Time	3.59	5	0.7181	F (5, 5329)	P<0.0001
Agarose	2.164	2	1.082	F (2, 5329)	P<0.0001
Residual	46.05	5329	0.008642		

Number of 4535

Within each column, compare rows (simple effects within columns)

Number of 3
Number of 15
Alpha 0.05

Bonferroni's	Mean Diff.	95.00% CI	Significant?	Summary	Adjusted P Value
1%					
1 vs. 3	0.02755	0.0005275	Yes	*	0.0415
1 vs. 5	0.01817	-0.009585	No	ns	0.8191
1 vs. 7	0.04223	0.01761	Yes	****	<0.0001
1 vs. 10	0.06569	0.04151	Yes	****	<0.0001
1 vs. 15	0.1049	0.07888	Yes	****	<0.0001
3 vs. 5	-0.00938	-0.03628	No	ns	>0.9999
3 vs. 7	0.01468	-0.008977	No	ns	>0.9999
3 vs. 10	0.03814	0.01494	Yes	****	<0.0001
3 vs. 15	0.07737	0.05223	Yes	****	<0.0001
5 vs. 7	0.02406	-0.0004386	No	ns	0.0591
5 vs. 10	0.04752	0.02346	Yes	****	<0.0001
5 vs. 15	0.08675	0.06082	Yes	****	<0.0001
7 vs. 10	0.02346	0.003101	Yes	*	0.0108
7 vs. 15	0.06269	0.04015	Yes	****	<0.0001
10 vs. 15	0.03923	0.01717	Yes	****	<0.0001
3%					
1 vs. 3	0.04746	0.02437	Yes	****	<0.0001
1 vs. 5	0.06581	0.04385	Yes	****	<0.0001
1 vs. 7	0.07686	0.05404	Yes	****	<0.0001
1 vs. 10	0.08401	0.06076	Yes	****	<0.0001
1 vs. 15	0.1139	0.08936	Yes	****	<0.0001
3 vs. 5	0.01835	0.0004941	Yes	*	0.0403
3 vs. 7	0.0294	0.01041	Yes	****	<0.0001
3 vs. 10	0.03655	0.01705	Yes	****	<0.0001
3 vs. 15	0.06645	0.04542	Yes	****	<0.0001
5 vs. 7	0.01105	-0.006556	No	ns	0.9811
5 vs. 10	0.0182	3.908e-005	Yes	*	0.049
5 vs. 15	0.0481	0.02831	Yes	****	<0.0001
7 vs. 10	0.007153	-0.01204	No	ns	>0.9999
7 vs. 15	0.03706	0.01632	Yes	****	<0.0001
10 vs. 15	0.0299	0.008687	Yes	***	0.0005
5%					
1 vs. 3	0.01751	-0.01238	No	ns	>0.9999
1 vs. 5	0.03788	0.01649	Yes	****	<0.0001
1 vs. 7	0.01142	-0.01044	No	ns	>0.9999
1 vs. 10	0.04602	0.01944	Yes	****	<0.0001
1 vs. 15	0.0581	0.02662	Yes	****	<0.0001
3 vs. 5	0.02037	-0.00748	No	ns	0.4766
3 vs. 7	-0.00609	-0.0343	No	ns	>0.9999
3 vs. 10	0.0285	-0.003506	No	ns	0.1343
3 vs. 15	0.04058	0.004404	Yes	*	0.0149
5 vs. 7	-0.02646	-0.04543	Yes	***	0.0006
5 vs. 10	0.008133	-0.01612	No	ns	>0.9999
5 vs. 15	0.02021	-0.009331	No	ns	0.6686
7 vs. 10	0.03459	0.009919	Yes	***	0.0006
7 vs. 15	0.04667	0.01679	Yes	****	<0.0001
10 vs. 15	0.01208	-0.02141	No	ns	>0.9999

Test detail	Mean 1	Mean 2	Mean Diff.	SE of diff.	N1	N2	t	DF
1%								
1 vs. 3	0.2797	0.2522	0.02755	0.009201	192	218	2.994	5329
1 vs. 5	0.2797	0.2615	0.01817	0.009452	192	195	1.922	5329
1 vs. 7	0.2797	0.2375	0.04223	0.008383	192	342	5.037	5329
1 vs. 10	0.2797	0.214	0.06569	0.008235	192	379	7.977	5329
1 vs. 15	0.2797	0.1748	0.1049	0.008868	192	257	11.83	5329
3 vs. 5	0.2522	0.2615	-0.00938	0.009163	218	195	1.023	5329
3 vs. 7	0.2522	0.2375	0.01468	0.008057	218	342	1.822	5329
3 vs. 10	0.2522	0.214	0.03814	0.007902	218	379	4.827	5329
3 vs. 15	0.2522	0.1748	0.07737	0.00856	218	257	9.039	5329
5 vs. 7	0.2615	0.2375	0.02406	0.008342	195	342	2.884	5329
5 vs. 10	0.2615	0.214	0.04752	0.008193	195	379	5.8	5329
5 vs. 15	0.2615	0.1748	0.08675	0.008829	195	257	9.825	5329
7 vs. 10	0.2375	0.214	0.02346	0.006933	342	379	3.384	5329
7 vs. 15	0.2375	0.1748	0.06269	0.007674	342	257	8.168	5329
10 vs. 15	0.214	0.1748	0.03923	0.007512	379	257	5.222	5329
3%								
1 vs. 3	0.2732	0.2257	0.04746	0.007861	215	400	6.037	5329
1 vs. 5	0.2732	0.2073	0.06581	0.007479	215	549	8.799	5329
1 vs. 7	0.2732	0.1963	0.07686	0.007771	215	428	9.89	5329
1 vs. 10	0.2732	0.1891	0.08401	0.007919	215	384	10.61	5329
1 vs. 15	0.2732	0.1592	0.1139	0.00836	215	291	13.63	5329
3 vs. 5	0.2257	0.2073	0.01835	0.006111	400	549	3.003	5329
3 vs. 7	0.2257	0.1963	0.0294	0.006465	400	428	4.547	5329
3 vs. 10	0.2257	0.1891	0.03655	0.006642	400	384	5.503	5329
3 vs. 15	0.2257	0.1592	0.06645	0.007163	400	291	9.278	5329
5 vs. 7	0.2073	0.1963	0.01105	0.005995	549	428	1.843	5329
5 vs. 10	0.2073	0.1891	0.0182	0.006184	549	384	2.943	5329
5 vs. 15	0.2073	0.1592	0.0481	0.006741	549	291	7.136	5329
7 vs. 10	0.1963	0.1891	0.007153	0.006534	428	384	1.095	5329
7 vs. 15	0.1963	0.1592	0.03706	0.007063	428	291	5.246	5329
10 vs. 15	0.1891	0.1592	0.0299	0.007225	384	291	4.139	5329
5%								
1 vs. 3	0.2108	0.1933	0.01751	0.01018	259	123	1.72	5329
1 vs. 5	0.2108	0.1729	0.03788	0.007284	259	439	5.201	5329
1 vs. 7	0.2108	0.1994	0.01142	0.007444	259	392	1.535	5329
1 vs. 10	0.2108	0.1648	0.04602	0.009051	259	178	5.084	5329
1 vs. 15	0.2108	0.1527	0.0581	0.01072	259	106	5.42	5329
3 vs. 5	0.1933	0.1729	0.02037	0.009484	123	439	2.148	5329
3 vs. 7	0.1933	0.1994	-0.00609	0.009608	123	392	0.6339	5329
3 vs. 10	0.1933	0.1648	0.0285	0.0109	123	178	2.615	5329
3 vs. 15	0.1933	0.1527	0.04058	0.01232	123	106	3.294	5329
5 vs. 7	0.1729	0.1994	-0.02646	0.00646	439	392	4.096	5329
5 vs. 10	0.1729	0.1648	0.008133	0.008261	439	178	0.9845	5329
5 vs. 15	0.1729	0.1527	0.02021	0.01006	439	106	2.009	5329
7 vs. 10	0.1994	0.1648	0.03459	0.008402	392	178	4.117	5329
7 vs. 15	0.1994	0.1527	0.04667	0.01018	392	106	4.586	5329
10 vs. 15	0.1648	0.1527	0.01208	0.01141	178	106	1.059	5329

Within each row, compare columns (simple effects within rows)

Number of 6
Number of 3
Alpha 0.05

Bonferroni's	Mean Diff.	95.00% CI	Significant?	Summary	Adjusted P Value
1					
1% vs. 3%	0.00656	-0.01555	to 0.0	No	ns	>0.9999
1% vs. 5%	0.0689	0.0477	to 0.0	Yes	****	<0.0001
3% vs. 5%	0.06234	0.0418	to 0.0	Yes	****	<0.0001
3						
1% vs. 3%	0.02647	0.007731	to 0.0	Yes	**	0.0022
1% vs. 5%	0.05887	0.03376	to 0.0	Yes	****	<0.0001
3% vs. 5%	0.03239	0.009439	to 0.0	Yes	**	0.0022
5						
1% vs. 3%	0.0542	0.03564	to 0.0	Yes	****	<0.0001
1% vs. 5%	0.08861	0.06945	to 0.0	Yes	****	<0.0001
3% vs. 5%	0.03441	0.02016	to 0.0	Yes	****	<0.0001
7						
1% vs. 3%	0.04119	0.02504	to 0.0	Yes	****	<0.0001
1% vs. 5%	0.03809	0.02162	to 0.0	Yes	****	<0.0001
3% vs. 5%	-0.0031	-0.01866	to 0.0	No	ns	>0.9999
10						
1% vs. 3%	0.02488	0.008761	to 0.0	Yes	***	0.0007
1% vs. 5%	0.04923	0.029	to 0.	Yes	****	<0.0001
3% vs. 5%	0.02435	0.004158	to 0.0	Yes	*	0.0117
15						
1% vs. 3%	0.01556	-0.0035	to 0.0	No	ns	0.1519
1% vs. 5%	0.02208	-0.00362	to 0.0	No	ns	0.1191
3% vs. 5%	0.006521	-0.01874	to 0.0	No	ns	>0.9999

Test detail	Mean 1	Mean 2	Mean Diff.	SE of diff.	N1	N2	t	DF
1								
1% vs. 3%	0.2797	0.2732	0.00656	0.009231	192	215	0.7107	5329
1% vs. 5%	0.2797	0.2108	0.0689	0.008853	192	259	7.782	5329
3% vs. 5%	0.2732	0.2108	0.06234	0.008577	215	259	7.268	5329
3								
1% vs. 3%	0.2522	0.2257	0.02647	0.007826	218	400	3.383	5329
1% vs. 5%	0.2522	0.1933	0.05887	0.01048	218	123	5.615	5329
3% vs. 5%	0.2257	0.1933	0.03239	0.009585	400	123	3.38	5329
5								
1% vs. 3%	0.2615	0.2073	0.0542	0.00775	195	549	6.993	5329
1% vs. 5%	0.2615	0.1729	0.08861	0.008	195	439	11.08	5329
3% vs. 5%	0.2073	0.1729	0.03441	0.005952	549	439	5.781	5329
7								
1% vs. 3%	0.2375	0.1963	0.04119	0.006743	342	428	6.109	5329
1% vs. 5%	0.2375	0.1994	0.03809	0.006879	342	392	5.538	5329
3% vs. 5%	0.1963	0.1994	-0.0031	0.006499	428	392	0.4762	5329
10								
1% vs. 3%	0.214	0.1891	0.02488	0.006731	379	384	3.696	5329
1% vs. 5%	0.214	0.1648	0.04923	0.008447	379	178	5.827	5329
3% vs. 5%	0.1891	0.1648	0.02435	0.00843	384	178	2.888	5329
15								
1% vs. 3%	0.1748	0.1592	0.01556	0.007958	257	291	1.955	5329
1% vs. 5%	0.1748	0.1527	0.02208	0.01073	257	106	2.057	5329
3% vs. 5%	0.1592	0.1527	0.006521	0.01055	291	106	0.6183	5329

Table 49 – One-way ANOVA for the effects of time and hydrogel stiffness on Chapter 5 adipogenic data – STELLATE FACTOR

Table Anal Data 1

Two-way A Ordinary
Alpha 0.05

Source of \	% of total \	P value	P value sur	Significant?
Interaction	1.043	<0.0001	****	Yes
Time	22.69	<0.0001	****	Yes
Agarose	0.1395	0.0076	**	Yes

ANOVA tal	SS	DF	MS	F (DFn, DF	P value
Interaction	2.749	10	0.2749	F (10, 532	P<0.0001
Time	59.77	5	11.95	F (5, 5329)	P<0.0001
Agarose	0.3675	2	0.1838	F (2, 5329)	P=0.0076
Residual	200.6	5329	0.03764		

Number of 4535

Within each column, compare rows (simple effects within columns)

Number of 3
Number of 15
Alpha 0.05

Bonferroni's	Mean Diff.	95.00% CI	Significant?	Summary	Adjusted P Value
1%					
1 vs. 3	-0.0364	-0.09279 to	No	ns	0.8708
1 vs. 5	-0.1593	-0.2172 to	Yes	****	<0.0001
1 vs. 7	-0.3234	-0.3748 to	Yes	****	<0.0001
1 vs. 10	-0.3344	-0.3849 to	Yes	****	<0.0001
1 vs. 15	-0.3259	-0.3803 to	Yes	****	<0.0001
3 vs. 5	-0.1229	-0.179 to -(	Yes	****	<0.0001
3 vs. 7	-0.287	-0.3364 to	Yes	****	<0.0001
3 vs. 10	-0.298	-0.3465 to	Yes	****	<0.0001
3 vs. 15	-0.2895	-0.342 to -(	Yes	****	<0.0001
5 vs. 7	-0.1641	-0.2153 to	Yes	****	<0.0001
5 vs. 10	-0.1752	-0.2254 to	Yes	****	<0.0001
5 vs. 15	-0.1667	-0.2208 to	Yes	****	<0.0001
7 vs. 10	-0.01102	-0.05351 to	No	ns	>0.9999
7 vs. 15	-0.00253	-0.04956 to	No	ns	>0.9999
10 vs. 15	0.008497	-0.03754 to	No	ns	>0.9999
3%					
1 vs. 3	-0.1028	-0.151 to -(	Yes	****	<0.0001
1 vs. 5	-0.2249	-0.2707 to	Yes	****	<0.0001
1 vs. 7	-0.2668	-0.3145 to	Yes	****	<0.0001
1 vs. 10	-0.2905	-0.3391 to	Yes	****	<0.0001
1 vs. 15	-0.3005	-0.3517 to	Yes	****	<0.0001
3 vs. 5	-0.122	-0.1595 to	Yes	****	<0.0001
3 vs. 7	-0.164	-0.2036 to	Yes	****	<0.0001
3 vs. 10	-0.1877	-0.2284 to	Yes	****	<0.0001
3 vs. 15	-0.1976	-0.2415 to	Yes	****	<0.0001
5 vs. 7	-0.04196	-0.07869 to	Yes	*	0.0121
5 vs. 10	-0.06566	-0.1036 to	Yes	****	<0.0001
5 vs. 15	-0.0756	-0.1169 to	Yes	****	<0.0001
7 vs. 10	-0.0237	-0.06375 to	No	ns	>0.9999
7 vs. 15	-0.03365	-0.07694 to	No	ns	0.3375
10 vs. 15	-0.00994	-0.05422 to	No	ns	>0.9999
5%					
1 vs. 3	-0.03159	-0.09398 to	No	ns	>0.9999
1 vs. 5	-0.1855	-0.2301 to	Yes	****	<0.0001
1 vs. 7	-0.259	-0.3046 to	Yes	****	<0.0001
1 vs. 10	-0.2571	-0.3126 to	Yes	****	<0.0001
1 vs. 15	-0.2181	-0.2838 to	Yes	****	<0.0001
3 vs. 5	-0.1539	-0.212 to -(	Yes	****	<0.0001
3 vs. 7	-0.2274	-0.2863 to	Yes	****	<0.0001
3 vs. 10	-0.2255	-0.2923 to	Yes	****	<0.0001
3 vs. 15	-0.1865	-0.262 to -(	Yes	****	<0.0001
5 vs. 7	-0.07354	-0.1131 to	Yes	****	<0.0001
5 vs. 10	-0.07163	-0.1223 to	Yes	***	0.0005
5 vs. 15	-0.03263	-0.09429 to	No	ns	>0.9999
7 vs. 10	0.001908	-0.04959 to	No	ns	>0.9999
7 vs. 15	0.04091	-0.02146 to	No	ns	0.8123
10 vs. 15	0.039	-0.0309 to	No	ns	>0.9999

Test detail	Mean 1	Mean 2	Mean Diff.	SE of diff.	N1	N2	t	DF
1%								
1 vs. 3	0.2976	0.334	-0.0364	0.0192	192	218	1.896	5329
1 vs. 5	0.2976	0.4569	-0.1593	0.01973	192	195	8.074	5329
1 vs. 7	0.2976	0.6211	-0.3234	0.0175	192	342	18.48	5329
1 vs. 10	0.2976	0.6321	-0.3344	0.01719	192	379	19.46	5329
1 vs. 15	0.2976	0.6236	-0.3259	0.01851	192	257	17.61	5329
3 vs. 5	0.334	0.4569	-0.1229	0.01912	218	195	6.424	5329
3 vs. 7	0.334	0.6211	-0.287	0.01681	218	342	17.07	5329
3 vs. 10	0.334	0.6321	-0.298	0.01649	218	379	18.07	5329
3 vs. 15	0.334	0.6236	-0.2895	0.01786	218	257	16.21	5329
5 vs. 7	0.4569	0.6211	-0.1641	0.01741	195	342	9.428	5329
5 vs. 10	0.4569	0.6321	-0.1752	0.0171	195	379	10.24	5329
5 vs. 15	0.4569	0.6236	-0.1667	0.01843	195	257	9.046	5329
7 vs. 10	0.6211	0.6321	-0.01102	0.01447	342	379	0.7617	5329
7 vs. 15	0.6211	0.6236	-0.00253	0.01602	342	257	0.1576	5329
10 vs. 15	0.6321	0.6236	0.008497	0.01568	379	257	0.542	5329
3%								
1 vs. 3	0.2784	0.3813	-0.1028	0.01641	215	400	6.269	5329
1 vs. 5	0.2784	0.5033	-0.2249	0.01561	215	549	14.41	5329
1 vs. 7	0.2784	0.5453	-0.2668	0.01622	215	428	16.45	5329
1 vs. 10	0.2784	0.569	-0.2905	0.01653	215	384	17.58	5329
1 vs. 15	0.2784	0.5789	-0.3005	0.01745	215	291	17.22	5329
3 vs. 5	0.3813	0.5033	-0.122	0.01275	400	549	9.569	5329
3 vs. 7	0.3813	0.5453	-0.164	0.01349	400	428	12.15	5329
3 vs. 10	0.3813	0.569	-0.1877	0.01386	400	384	13.54	5329
3 vs. 15	0.3813	0.5789	-0.1976	0.01495	400	291	13.22	5329
5 vs. 7	0.5033	0.5453	-0.04196	0.01251	549	428	3.354	5329
5 vs. 10	0.5033	0.569	-0.06566	0.01291	549	384	5.087	5329
5 vs. 15	0.5033	0.5789	-0.0756	0.01407	549	291	5.374	5329
7 vs. 10	0.5453	0.569	-0.0237	0.01364	428	384	1.738	5329
7 vs. 15	0.5453	0.5789	-0.03365	0.01474	428	291	2.282	5329
10 vs. 15	0.569	0.5789	-0.00994	0.01508	384	291	0.6593	5329
5%								
1 vs. 3	0.3153	0.3469	-0.03159	0.02125	259	123	1.487	5329
1 vs. 5	0.3153	0.5008	-0.1855	0.0152	259	439	12.2	5329
1 vs. 7	0.3153	0.5743	-0.259	0.01554	259	392	16.67	5329
1 vs. 10	0.3153	0.5724	-0.2571	0.01889	259	178	13.61	5329
1 vs. 15	0.3153	0.5334	-0.2181	0.02237	259	106	9.75	5329
3 vs. 5	0.3469	0.5008	-0.1539	0.01979	123	439	7.775	5329
3 vs. 7	0.3469	0.5743	-0.2274	0.02005	123	392	11.34	5329
3 vs. 10	0.3469	0.5724	-0.2255	0.02275	123	178	9.914	5329
3 vs. 15	0.3469	0.5334	-0.1865	0.02571	123	106	7.254	5329
5 vs. 7	0.5008	0.5743	-0.07354	0.01348	439	392	5.454	5329
5 vs. 10	0.5008	0.5724	-0.07163	0.01724	439	178	4.155	5329
5 vs. 15	0.5008	0.5334	-0.03263	0.021	439	106	1.554	5329
7 vs. 10	0.5743	0.5724	0.001908	0.01754	392	178	0.1088	5329
7 vs. 15	0.5743	0.5334	0.04091	0.02124	392	106	1.926	5329
10 vs. 15	0.5724	0.5334	0.039	0.0238	178	106	1.639	5329

Within each row, compare columns (simple effects within rows)

Number of 6
Number of 3
Alpha 0.05

Bonferroni's	Mean Diff.	95.00% CI	Significant?	Summary	Adjusted P Value
1					
1% vs. 3%	0.01922	-0.02691 to	No	ns	0.9555
1% vs. 5%	-0.01763	-0.06187 to	No	ns	>0.9999
3% vs. 5%	-0.03685	-0.07971 to	No	ns	0.1188
3					
1% vs. 3%	-0.04723	-0.08634 to	Yes	*	0.0116
1% vs. 5%	-0.01282	-0.06521 to	No	ns	>0.9999
3% vs. 5%	0.03441	-0.01349 to	No	ns	0.2564
5					
1% vs. 3%	-0.04641	-0.08514 to	Yes	*	0.0124
1% vs. 5%	-0.04386	-0.08384 to	Yes	*	0.026
3% vs. 5%	0.002555	-0.02719 to	No	ns	>0.9999
7					
1% vs. 3%	0.07578	0.04208 to	Yes	****	<0.0001
1% vs. 5%	0.04676	0.01238 to	Yes	**	0.0034
3% vs. 5%	-0.02903	-0.06151 to	No	ns	0.0972
10					
1% vs. 3%	0.0631	0.02946 to	Yes	****	<0.0001
1% vs. 5%	0.05969	0.01747 to	Yes	**	0.0021
3% vs. 5%	-0.00342	-0.04555 to	No	ns	>0.9999
15					
1% vs. 3%	0.04466	0.00489 to	Yes	*	0.0216
1% vs. 5%	0.09019	0.03656 to	Yes	***	0.0002
3% vs. 5%	0.04553	-0.007181	No	ns	0.1159

Test detail	Mean 1	Mean 2	Mean Diff.	SE of diff.	N1	N2	t	DF
1								
1% vs. 3%	0.2976	0.2784	0.01922	0.01927	192	215	0.9977	5329
1% vs. 5%	0.2976	0.3153	-0.01763	0.01848	192	259	0.954	5329
3% vs. 5%	0.2784	0.3153	-0.03685	0.0179	215	259	2.058	5329
3								
1% vs. 3%	0.334	0.3813	-0.04723	0.01633	218	400	2.891	5329
1% vs. 5%	0.334	0.3469	-0.01282	0.02188	218	123	0.5858	5329
3% vs. 5%	0.3813	0.3469	0.03441	0.02	400	123	1.72	5329
5								
1% vs. 3%	0.4569	0.5033	-0.04641	0.01617	195	549	2.869	5329
1% vs. 5%	0.4569	0.5008	-0.04386	0.0167	195	439	2.627	5329
3% vs. 5%	0.5033	0.5008	0.002555	0.01242	549	439	0.2057	5329
7								
1% vs. 3%	0.6211	0.5453	0.07578	0.01407	342	428	5.385	5329
1% vs. 5%	0.6211	0.5743	0.04676	0.01436	342	392	3.257	5329
3% vs. 5%	0.5453	0.5743	-0.02903	0.01356	428	392	2.14	5329
10								
1% vs. 3%	0.6321	0.569	0.0631	0.01405	379	384	4.492	5329
1% vs. 5%	0.6321	0.5724	0.05969	0.01763	379	178	3.386	5329
3% vs. 5%	0.569	0.5724	-0.00342	0.01759	384	178	0.1941	5329
15								
1% vs. 3%	0.6236	0.5789	0.04466	0.01661	257	291	2.689	5329
1% vs. 5%	0.6236	0.5334	0.09019	0.0224	257	106	4.027	5329
3% vs. 5%	0.5789	0.5334	0.04553	0.02201	291	106	2.068	5329

Table 50 – One-way ANOVA for the effects of time and hydrogel stiffness on Chapter 5 adipogenic data – LENGTH

Table Anal Data 1

Two-way A Ordinary
Alpha 0.05

Source of \	% of total \	P value	P value sur	Significant?
Interaction	0.4814	0.0029	**	Yes
Time	2.026	<0.0001	****	Yes
Agarose	1.584	<0.0001	****	Yes

ANOVA tal	SS	DF	MS	F (DFn, DF	P value
Interaction	230028	10	23003	F (10, 532	P=0.0029
Time	968216	5	193643	F (5, 5329)	P<0.0001
Agarose	756795	2	378397	F (2, 5329)	P<0.0001
Residual	45832398	5329	8601		

Number of 4535

Within each column, compare rows (simple effects within columns)

Number of 3
Number of 15
Alpha 0.05

Bonferroni\	Mean Diff.	95.00% CI	Significant?	Summary	Adjusted P Value
1%					
1 vs. 3	9.104	-17.85 to 3	No	ns	>0.9999
1 vs. 5	-15.37	-43.06 to 1	No	ns	>0.9999
1 vs. 7	-37.36	-61.92 to -1	Yes	***	0.0001
1 vs. 10	-52.92	-77.04 to -2	Yes	****	<0.0001
1 vs. 15	-4.632	-30.61 to 2	No	ns	>0.9999
3 vs. 5	-24.47	-51.31 to 2	No	ns	0.1117
3 vs. 7	-46.46	-70.07 to -2	Yes	****	<0.0001
3 vs. 10	-62.02	-85.17 to -3	Yes	****	<0.0001
3 vs. 15	-13.74	-38.81 to 1	No	ns	>0.9999
5 vs. 7	-21.99	-46.43 to 2	No	ns	0.1237
5 vs. 10	-37.55	-61.55 to -1	Yes	****	<0.0001
5 vs. 15	10.74	-15.13 to 3	No	ns	>0.9999
7 vs. 10	-15.56	-35.87 to 4	No	ns	0.3678
7 vs. 15	32.73	10.25 to 55	Yes	***	0.0003
10 vs. 15	48.29	26.28 to 70	Yes	****	<0.0001
3%					
1 vs. 3	14.19	-8.84 to 37	No	ns	>0.9999
1 vs. 5	-3.662	-25.57 to 1	No	ns	>0.9999
1 vs. 7	-2.181	-24.95 to 2	No	ns	>0.9999
1 vs. 10	-17.4	-40.6 to 5.3	No	ns	0.4143
1 vs. 15	0.5435	-23.95 to 2	No	ns	>0.9999
3 vs. 5	-17.85	-35.75 to 0	No	ns	0.0514
3 vs. 7	-16.37	-35.31 to 2	No	ns	0.1675
3 vs. 10	-31.59	-51.05 to -1	Yes	****	<0.0001
3 vs. 15	-13.65	-34.63 to 7	No	ns	0.8433
5 vs. 7	1.481	-16.08 to 1	No	ns	>0.9999
5 vs. 10	-13.74	-31.86 to 4	No	ns	0.3894
5 vs. 15	4.205	-15.54 to 2	No	ns	>0.9999
7 vs. 10	-15.22	-34.37 to 3	No	ns	0.2934
7 vs. 15	2.725	-17.97 to 2	No	ns	>0.9999
10 vs. 15	17.95	-3.218 to 3	No	ns	0.192
5%					
1 vs. 3	16.94	-12.88 to 4	No	ns	>0.9999
1 vs. 5	-5.373	-26.71 to 1	No	ns	>0.9999
1 vs. 7	-34.28	-56.09 to -1	Yes	****	<0.0001
1 vs. 10	-20.13	-46.64 to 6	No	ns	0.3877
1 vs. 15	-2.675	-34.08 to 2	No	ns	>0.9999
3 vs. 5	-22.32	-50.1 to 5.	No	ns	0.2756
3 vs. 7	-51.22	-79.37 to -2	Yes	****	<0.0001
3 vs. 10	-37.07	-69 to -5.1	Yes	**	0.0098
3 vs. 15	-19.62	-55.71 to 1	No	ns	>0.9999
5 vs. 7	-28.91	-47.83 to -9	Yes	***	0.0001
5 vs. 10	-14.75	-38.95 to 9	No	ns	>0.9999
5 vs. 15	2.697	-26.77 to 3	No	ns	>0.9999
7 vs. 10	14.15	-10.46 to 3	No	ns	>0.9999
7 vs. 15	31.6	1.79 to 61.	Yes	*	0.0279
10 vs. 15	17.45	-15.96 to 5	No	ns	>0.9999

Test detail\	Mean 1	Mean 2	Mean Diff.	SE of diff.	N1	N2	t	DF
1%								
1 vs. 3	90.44	81.34	9.104	9.179	192	218	0.9919	5329
1 vs. 5	90.44	105.8	-15.37	9.429	192	195	1.63	5329
1 vs. 7	90.44	127.8	-37.36	8.363	192	342	4.467	5329
1 vs. 10	90.44	143.4	-52.92	8.215	192	379	6.442	5329
1 vs. 15	90.44	95.07	-4.632	8.846	192	257	0.5236	5329
3 vs. 5	81.34	105.8	-24.47	9.141	218	195	2.677	5329
3 vs. 7	81.34	127.8	-46.46	8.037	218	342	5.781	5329
3 vs. 10	81.34	143.4	-62.02	7.883	218	379	7.868	5329
3 vs. 15	81.34	95.07	-13.74	8.539	218	257	1.609	5329
5 vs. 7	105.8	127.8	-21.99	8.322	195	342	2.643	5329
5 vs. 10	105.8	143.4	-37.55	8.173	195	379	4.595	5329
5 vs. 15	105.8	95.07	10.74	8.807	195	257	1.219	5329
7 vs. 10	127.8	143.4	-15.56	6.917	342	379	2.25	5329
7 vs. 15	127.8	95.07	32.73	7.656	342	257	4.275	5329
10 vs. 15	143.4	95.07	48.29	7.494	379	257	6.444	5329
3%								
1 vs. 3	88	73.81	14.19	7.842	215	400	1.809	5329
1 vs. 5	88	91.66	-3.662	7.461	215	549	0.4908	5329
1 vs. 7	88	90.18	-2.181	7.752	215	428	0.2814	5329
1 vs. 10	88	105.4	-17.4	7.899	215	384	2.203	5329
1 vs. 15	88	87.46	0.5435	8.34	215	291	0.06517	5329
3 vs. 5	73.81	91.66	-17.85	6.096	400	549	2.928	5329
3 vs. 7	73.81	90.18	-16.37	6.45	400	428	2.538	5329
3 vs. 10	73.81	105.4	-31.59	6.626	400	384	4.768	5329
3 vs. 15	73.81	87.46	-13.65	7.145	400	291	1.91	5329
5 vs. 7	91.66	90.18	1.481	5.98	549	428	0.2476	5329
5 vs. 10	91.66	105.4	-13.74	6.17	549	384	2.227	5329
5 vs. 15	91.66	87.46	4.205	6.725	549	291	0.6253	5329
7 vs. 10	90.18	105.4	-15.22	6.519	428	384	2.335	5329
7 vs. 15	90.18	87.46	2.725	7.046	428	291	0.3867	5329
10 vs. 15	105.4	87.46	17.95	7.208	384	291	2.49	5329
5%								
1 vs. 3	67.67	50.73	16.94	10.16	259	123	1.668	5329
1 vs. 5	67.67	73.05	-5.373	7.266	259	439	0.7394	5329
1 vs. 7	67.67	102	-34.28	7.426	259	392	4.616	5329
1 vs. 10	67.67	87.8	-20.13	9.029	259	178	2.229	5329
1 vs. 15	67.67	70.35	-2.675	10.69	259	106	0.2502	5329
3 vs. 5	50.73	73.05	-22.32	9.461	123	439	2.359	5329
3 vs. 7	50.73	102	-51.22	9.585	123	392	5.344	5329
3 vs. 10	50.73	87.8	-37.07	10.87	123	178	3.409	5329
3 vs. 15	50.73	70.35	-19.62	12.29	123	106	1.596	5329
5 vs. 7	73.05	102	-28.91	6.444	439	392	4.485	5329
5 vs. 10	73.05	87.8	-14.75	8.241	439	178	1.79	5329
5 vs. 15	73.05	70.35	2.697	10.04	439	106	0.2687	5329
7 vs. 10	102	87.8	14.15	8.382	392	178	1.688	5329
7 vs. 15	102	70.35	31.6	10.15	392	106	3.113	5329
10 vs. 15	87.8	70.35	17.45	11.38	178	106	1.534	5329

Within each row, compare columns (simple effects within rows)

Number of 6
Number of 3
Alpha 0.05

Bonferroni\	Mean Diff.	95.00% CI	Significant?	Summary	Adjusted P Value
1					
1% vs. 3%	2.441	-19.61 to 2	No	ns	>0.9999
1% vs. 5%	22.77	1.617 to 4	Yes	*	0.0299
3% vs. 5%	20.33	-0.1649 to	No	ns	0.0527
3					
1% vs. 3%	7.527	-11.17 to 2	No	ns	>0.9999
1% vs. 5%	30.61	5.561 to 5	Yes	*	0.0103
3% vs. 5%	23.08	0.1817 to 4	Yes	*	0.0475
5					
1% vs. 3%	14.15	-4.366 to 3	No	ns	0.2019
1% vs. 5%	32.76	13.65 to 5	Yes	***	0.0001
3% vs. 5%	18.61	4.395 to 3	Yes	**	0.0052
7					
1% vs. 3%	37.62	21.51 to 5	Yes	****	<0.0001
1% vs. 5%	25.85	9.415 to 4	Yes	***	0.0005
3% vs. 5%	-11.77	-27.3 to 3.	No	ns	0.2084
10					
1% vs. 3%	37.96	21.88 to 5	Yes	****	<0.0001
1% vs. 5%	55.56	35.38 to 7	Yes	****	<0.0001
3% vs. 5%	17.6	-2.536 to 3	No	ns	0.1091
15					
1% vs. 3%	7.617	-11.39 to 2	No	ns	>0.9999
1% vs. 5%	24.72	-0.9128 to	No	ns	0.0629
3% vs. 5%	17.11	-8.089 to 4	No	ns	0.3121

Test detail\	Mean 1	Mean 2	Mean Diff.	SE of diff.	N1	N2	t	DF
1								
1% vs. 3%	90.44	88	2.441	9.209	192	215	0.2651	5329
1% vs. 5%	90.44	67.67	22.77	8.832	192	259	2.578	5329
3% vs. 5%	88	67.67	20.33	8.556	215	259	2.375	5329
3								
1% vs. 3%	81.34	73.81	7.527	7.807	218	400	0.9641	5329
1% vs. 5%	81.34	50.73	30.61	10.46	218	123	2.927	5329
3% vs. 5%	73.81	50.73	23.08	9.562	400	123	2.414	5329
5								
1% vs. 3%	105.8	91.66	14.15	7.731	195	549	1.83	5329
1% vs. 5%	105.8	73.05	32.76	7.981	195	439	4.105	5329
3% vs. 5%	91.66	73.05	18.61	5.938	549	439	3.135	5329
7								
1% vs. 3%	127.8	90.18	37.62	6.726	342	428	5.593	5329
1% vs. 5%	127.8	102	25.85	6.862	342	392	3.767	5329
3% vs. 5%	90.18	102	-11.77	6.483	428	392	1.816	5329
10								
1% vs. 3%	143.4	105.4	37.96	6.715	379	384	5.653	5329
1% vs. 5%	143.4	87.8	55.56	8.427	379	178	6.593	5329
3% vs. 5%	105.4	87.8	17.6	8.409	384	178	2.093	5329
15								
1% vs. 3%	95.07	87.46	7.617	7.939	257	291	0.9595	5329
1% vs. 5%	95.07	70.35	24.72	10.71	257	106	2.309	5329
3% vs. 5%	87.46	70.35	17.11	10.52	291	106	1.626	5329

Table 51 – One-way ANOVA for the effects of time and hydrogel stiffness on Chapter 5 adipogenic data – CHROMATIN CONDENSATION

Table Anal Data 1

Two-way A Ordinary
Alpha 0.05

Source of \	% of total \	P value	P value sur	Significant?
Interaction	1.486	<0.0001	****	Yes
Time	2.661	<0.0001	****	Yes
Agarose	0.08957	0.0828	ns	No

ANOVA tal	SS	DF	MS	F (DFn, DF	P value
Interaction	0.003395	10	0.00034	F (10, 532	P<0.0001
Time	0.00608	5	0.001216	F (5, 5329)	P<0.0001
Agarose	0.000205	2	0.000102	F (2, 5329)	P=0.0828
Residual	0.2188	5329	4.11E-05		

Number of 4535

Within each column, compare rows (simple effects within columns)

Number of 3
Number of 15
Alpha 0.05

Bonferroni's	Mean Diff.	95.00% CI	Significant?	Summary	Adjusted P Value
1%					
1 vs. 3	0.002154	0.0002915	Yes	*	0.0103
1 vs. 5	0.002428	0.0005148	Yes	**	0.0029
1 vs. 7	0.002614	0.000917	Yes	****	<0.0001
1 vs. 10	0.003546	0.001879	Yes	****	<0.0001
1 vs. 15	0.002201	0.0004059	Yes	**	0.0048
3 vs. 5	0.000274	-0.001581	No	ns	>0.9999
3 vs. 7	0.00046	-0.001171	No	ns	>0.9999
3 vs. 10	0.001392	-0.0002076	No	ns	0.1595
3 vs. 15	0.000047	-0.001686	No	ns	>0.9999
5 vs. 7	0.000186	-0.001503	No	ns	>0.9999
5 vs. 10	0.001118	-0.0005404	No	ns	0.717
5 vs. 15	-0.00023	-0.002014	No	ns	>0.9999
7 vs. 10	0.000932	-0.0004715	No	ns	0.7684
7 vs. 15	-0.00041	-0.001966	No	ns	>0.9999
10 vs. 15	-0.00135	-0.002866	No	ns	0.1413
3%					
1 vs. 3	0.001139	-0.0004523	No	ns	0.5343
1 vs. 5	0.002254	0.00074	Yes	***	0.0002
1 vs. 7	0.001819	0.000246	Yes	*	0.0103
1 vs. 10	0.00123	-0.0003726	No	ns	0.3641
1 vs. 15	0.002486	0.0007937	Yes	***	0.0002
3 vs. 5	0.001115	-0.0001221	No	ns	0.1223
3 vs. 7	0.00068	-0.0006287	No	ns	>0.9999
3 vs. 10	0.000091	-0.001253	No	ns	>0.9999
3 vs. 15	0.001347	-0.0001025	No	ns	0.0959
5 vs. 7	-0.00044	-0.001648	No	ns	>0.9999
5 vs. 10	-0.00102	-0.002276	No	ns	0.2451
5 vs. 15	0.000232	-0.001133	No	ns	>0.9999
7 vs. 10	-0.00059	-0.001912	No	ns	>0.9999
7 vs. 15	0.000667	-0.0007628	No	ns	>0.9999
10 vs. 15	0.001256	-0.0002066	No	ns	0.1756
5%					
1 vs. 3	-7.6E-05	-0.002137	No	ns	>0.9999
1 vs. 5	0.003567	0.002093	Yes	****	<0.0001
1 vs. 7	0.000682	-0.0008245	No	ns	>0.9999
1 vs. 10	0.005232	0.0034	Yes	****	<0.0001
1 vs. 15	0.004307	0.002137	Yes	****	<0.0001
3 vs. 5	0.003643	0.001723	Yes	****	<0.0001
3 vs. 7	0.000758	-0.001187	No	ns	>0.9999
3 vs. 10	0.005308	0.003102	Yes	****	<0.0001
3 vs. 15	0.004383	0.001889	Yes	****	<0.0001
5 vs. 7	-0.00289	-0.004193	Yes	****	<0.0001
5 vs. 10	0.001665	-7.153e-00	No	ns	0.0521
5 vs. 15	0.00074	-0.001297	No	ns	>0.9999
7 vs. 10	0.00455	0.002849	Yes	****	<0.0001
7 vs. 15	0.003625	0.001565	Yes	****	<0.0001
10 vs. 15	-0.00093	-0.003234	No	ns	>0.9999

Test details	Mean 1	Mean 2	Mean Diff.	SE of diff.	N1	N2	t	DF
1%								
1 vs. 3	0.02294	0.02078	0.002154	0.000634	192	218	3.396	5329
1 vs. 5	0.02294	0.02051	0.002428	0.000652	192	195	3.727	5329
1 vs. 7	0.02294	0.02032	0.002614	0.000578	192	342	4.523	5329
1 vs. 10	0.02294	0.01939	0.003546	0.000568	192	379	6.247	5329
1 vs. 15	0.02294	0.02073	0.002201	0.000611	192	257	3.601	5329
3 vs. 5	0.02078	0.02051	0.000274	0.000632	218	195	0.4338	5329
3 vs. 7	0.02078	0.02032	0.00046	0.000555	218	342	0.8283	5329
3 vs. 10	0.02078	0.01939	0.001392	0.000545	218	379	2.555	5329
3 vs. 15	0.02078	0.02073	0.000047	0.00059	218	257	0.07965	5329
5 vs. 7	0.02051	0.02032	0.000186	0.000575	195	342	0.3235	5329
5 vs. 10	0.02051	0.01939	0.001118	0.000565	195	379	1.98	5329
5 vs. 15	0.02051	0.02073	-0.00023	0.000609	195	257	0.373	5329
7 vs. 10	0.02032	0.01939	0.000932	0.000478	342	379	1.95	5329
7 vs. 15	0.02032	0.02073	-0.00041	0.000529	342	257	0.7807	5329
10 vs. 15	0.01939	0.02073	-0.00135	0.000518	379	257	2.597	5329
3%								
1 vs. 3	0.022	0.02086	0.001139	0.000542	215	400	2.102	5329
1 vs. 5	0.022	0.01975	0.002254	0.000516	215	549	4.372	5329
1 vs. 7	0.022	0.02018	0.001819	0.000536	215	428	3.396	5329
1 vs. 10	0.022	0.02077	0.00123	0.000546	215	384	2.253	5329
1 vs. 15	0.022	0.01952	0.002486	0.000576	215	291	4.314	5329
3 vs. 5	0.02086	0.01975	0.001115	0.000421	400	549	2.647	5329
3 vs. 7	0.02086	0.02018	0.00068	0.000446	400	428	1.526	5329
3 vs. 10	0.02086	0.02077	0.000091	0.000458	400	384	0.1988	5329
3 vs. 15	0.02086	0.01952	0.001347	0.000494	400	291	2.728	5329
5 vs. 7	0.01975	0.02018	-0.00044	0.000413	549	428	1.053	5329
5 vs. 10	0.01975	0.02077	-0.00102	0.000426	549	384	2.402	5329
5 vs. 15	0.01975	0.01952	0.000232	0.000465	549	291	0.4993	5329
7 vs. 10	0.02018	0.02077	-0.00059	0.00045	428	384	1.308	5329
7 vs. 15	0.02018	0.01952	0.000667	0.000487	428	291	1.37	5329
10 vs. 15	0.02077	0.01952	0.001256	0.000498	384	291	2.522	5329
5%								
1 vs. 3	0.02254	0.02261	-7.6E-05	0.000702	259	123	0.1083	5329
1 vs. 5	0.02254	0.01897	0.003567	0.000502	259	439	7.104	5329
1 vs. 7	0.02254	0.02185	0.000682	0.000513	259	392	1.329	5329
1 vs. 10	0.02254	0.0173	0.005232	0.000624	259	178	8.386	5329
1 vs. 15	0.02254	0.01823	0.004307	0.000739	259	106	5.829	5329
3 vs. 5	0.02261	0.01897	0.003643	0.000654	123	439	5.572	5329
3 vs. 7	0.02261	0.02185	0.000758	0.000662	123	392	1.145	5329
3 vs. 10	0.02261	0.0173	0.005308	0.000751	123	178	7.064	5329
3 vs. 15	0.02261	0.01823	0.004383	0.000849	123	106	5.161	5329
5 vs. 7	0.01897	0.02185	-0.00289	0.000445	439	392	6.479	5329
5 vs. 10	0.01897	0.0173	0.001665	0.000569	439	178	2.924	5329
5 vs. 15	0.01897	0.01823	0.00074	0.000694	439	106	1.067	5329
7 vs. 10	0.02185	0.0173	0.00455	0.000579	392	178	7.856	5329
7 vs. 15	0.02185	0.01823	0.003625	0.000702	392	106	5.167	5329
10 vs. 15	0.0173	0.01823	-0.00093	0.000786	178	106	1.177	5329

Within each row, compare columns (simple effects within rows)

Number of 6
Number of 3
Alpha 0.05

Bonferroni's	Mean Diff.	95.00% CI	Significant?	Summary	Adjusted P Value
1					
1% vs. 3%	0.000932	-0.0005918	No	ns	0.4292
1% vs. 5%	0.0004	-0.001061	No	ns	>0.9999
3% vs. 5%	-0.00053	-0.001948	No	ns	>0.9999
3					
1% vs. 3%	-8.3E-05	-0.001375	No	ns	>0.9999
1% vs. 5%	-0.00183	-0.003561	Yes	*	0.0341
3% vs. 5%	-0.00175	-0.003329	Yes	*	0.0246
5					
1% vs. 3%	0.000758	-0.0005211	No	ns	0.468
1% vs. 5%	0.001539	0.0002183	Yes	*	0.0158
3% vs. 5%	0.000781	-0.0002016	No	ns	0.1711
7					
1% vs. 3%	0.000137	-0.000976	No	ns	>0.9999
1% vs. 5%	-0.00153	-0.002668	Yes	**	0.0037
3% vs. 5%	-0.00167	-0.002742	Yes	***	0.0006
10					
1% vs. 3%	-0.00138	-0.002495	Yes	**	0.0086
1% vs. 5%	0.002086	0.0006916	Yes	**	0.001
3% vs. 5%	0.00347	0.002078	Yes	****	<0.0001
15					
1% vs. 3%	0.001217	-9.664e-00	No	ns	0.0797
1% vs. 5%	0.002506	0.0007345	Yes	**	0.0021
3% vs. 5%	0.001289	-0.000452	No	ns	0.2288

Test details	Mean 1	Mean 2	Mean Diff.	SE of diff.	N1	N2	t	DF
1								
1% vs. 3%	0.02294	0.022	0.000932	0.000636	192	215	1.465	5329
1% vs. 5%	0.02294	0.02254	0.0004	0.00061	192	259	0.6554	5329
3% vs. 5%	0.022	0.02254	-0.00053	0.000591	215	259	0.8998	5329
3								
1% vs. 3%	0.02078	0.02086	-8.3E-05	0.00054	218	400	0.1539	5329
1% vs. 5%	0.02078	0.02261	-0.00183	0.000723	218	123	2.532	5329
3% vs. 5%	0.02086	0.02261	-0.00175	0.000661	400	123	2.644	5329
5								
1% vs. 3%	0.02051	0.01975	0.000758	0.000534	195	549	1.419	5329
1% vs. 5%	0.02051	0.01897	0.001539	0.000552	195	439	2.791	5329
3% vs. 5%	0.01975	0.01897	0.000781	0.00041	549	439	1.903	5329
7								
1% vs. 3%	0.02032	0.02018	0.000137	0.000465	342	428	0.2948	5329
1% vs. 5%	0.02032	0.02185	-0.00153	0.000474	342	392	3.231	5329
3% vs. 5%	0.02018	0.02185	-0.00167	0.000448	428	392	3.725	5329
10								
1% vs. 3%	0.01939	0.02077	-0.00138	0.000464	379	384	2.983	5329
1% vs. 5%	0.01939	0.0173	0.002086	0.000582	379	178	3.582	5329
3% vs. 5%	0.02077	0.0173	0.00347	0.000581	384	178	5.972	5329
15								
1% vs. 3%	0.02073	0.01952	0.001217	0.000549	257	291	2.219	5329
1% vs. 5%	0.02073	0.01823	0.002506	0.00074	257	106	3.388	5329
3% vs. 5%	0.01952	0.01823	0.001289	0.000727	291	106	1.773	5329

Table 52 – One-way ANOVA for the effects of time and hydrogel stiffness on Chapter 5 adipogenic data – NUCLEUS VOLUME

Table Anal Data 1

Two-way A Ordinary
Alpha 0.05

Source of \	% of total \	P value	P value sur	Significant?
Interaction	0.5054	0.0017	**	Yes
Time	3.328	<0.0001	****	Yes
Agarose	0.623	<0.0001	****	Yes

ANOVA tal	SS	DF	MS	F (DFn, DF	P value
Interaction	1.552	10	0.1552	F (10, 532	P=0.0017
Time	10.22	5	2.045	F (5, 5329)	P<0.0001
Agarose	1.914	2	0.9568	F (2, 5329)	P<0.0001
Residual	293.5	5329	0.05507		

Number of 4535

Within each column, compare rows (simple effects within columns)

Number of 3
Number of 15
Alpha 0.05

Bonferroni's	Mean Diff.	95.00% CI	Significant?	Summary	Adjusted P Value
1%					
1 vs. 3	-0.09748	-0.1657 to	Yes	***	0.0004
1 vs. 5	-0.1059	-0.176 to -(	Yes	***	0.0001
1 vs. 7	-0.1267	-0.1889 to	Yes	****	<0.0001
1 vs. 10	-0.01131	-0.07236 to	No	ns	>0.9999
1 vs. 15	-0.149	-0.2148 to	Yes	****	<0.0001
3 vs. 5	-0.00846	-0.07639 to	No	ns	>0.9999
3 vs. 7	-0.02923	-0.08896 to	No	ns	>0.9999
3 vs. 10	0.08616	0.02759 to	Yes	***	0.0002
3 vs. 15	-0.05157	-0.115 to 0	No	ns	0.2556
5 vs. 7	-0.02077	-0.08261 to	No	ns	>0.9999
5 vs. 10	0.09463	0.03389 to	Yes	****	<0.0001
5 vs. 15	-0.04311	-0.1086 to	No	ns	0.7972
7 vs. 10	0.1154	0.064 to 0.	Yes	****	<0.0001
7 vs. 15	-0.02234	-0.07922 to	No	ns	>0.9999
10 vs. 15	-0.1377	-0.1934 to	Yes	****	<0.0001
3%					
1 vs. 3	-0.01119	-0.06947 to	No	ns	>0.9999
1 vs. 5	-0.07245	-0.1279 to	Yes	**	0.0019
1 vs. 7	-0.09335	-0.151 to -(	Yes	****	<0.0001
1 vs. 10	0.01659	-0.04211 to	No	ns	>0.9999
1 vs. 15	-0.1257	-0.1877 to	Yes	****	<0.0001
3 vs. 5	-0.06126	-0.1066 to	Yes	**	0.0011
3 vs. 7	-0.08216	-0.1301 to	Yes	****	<0.0001
3 vs. 10	0.02778	-0.02145 to	No	ns	>0.9999
3 vs. 15	-0.1145	-0.1676 to	Yes	****	<0.0001
5 vs. 7	-0.0209	-0.06534 to	No	ns	>0.9999
5 vs. 10	0.08904	0.04319 to	Yes	****	<0.0001
5 vs. 15	-0.05328	-0.1032 to	Yes	*	0.0263
7 vs. 10	0.1099	0.0615 to 0	Yes	****	<0.0001
7 vs. 15	-0.03238	-0.08474 to	No	ns	>0.9999
10 vs. 15	-0.1423	-0.1959 to	Yes	****	<0.0001
5%					
1 vs. 3	-0.1036	-0.1791 to	Yes	***	0.0008
1 vs. 5	-0.07097	-0.125 to -(	Yes	**	0.0017
1 vs. 7	-0.07127	-0.1264 to	Yes	**	0.0023
1 vs. 10	0.02245	-0.04464 to	No	ns	>0.9999
1 vs. 15	-0.08304	-0.1625 to	Yes	*	0.0324
3 vs. 5	0.03262	-0.03768 to	No	ns	>0.9999
3 vs. 7	0.03233	-0.03889 to	No	ns	>0.9999
3 vs. 10	0.126	0.04524 to	Yes	****	<0.0001
3 vs. 15	0.02056	-0.07077 to	No	ns	>0.9999
5 vs. 7	-0.00029	-0.04818 to	No	ns	>0.9999
5 vs. 10	0.09342	0.03219 to	Yes	***	0.0001
5 vs. 15	-0.01206	-0.08664 to	No	ns	>0.9999
7 vs. 10	0.09372	0.03143 to	Yes	***	0.0002
7 vs. 15	-0.01177	-0.08721 to	No	ns	>0.9999
10 vs. 15	-0.1055	-0.19 to -0.	Yes	**	0.0038

Test detail	Mean 1	Mean 2	Mean Diff.	SE of diff.	N1	N2	t	DF
1%								
1 vs. 3	1.006	1.104	-0.09748	0.02323	192	218	4.197	5329
1 vs. 5	1.006	1.112	-0.1059	0.02386	192	195	4.44	5329
1 vs. 7	1.006	1.133	-0.1267	0.02116	192	342	5.987	5329
1 vs. 10	1.006	1.017	-0.01131	0.02079	192	379	0.5443	5329
1 vs. 15	1.006	1.155	-0.149	0.02239	192	257	6.658	5329
3 vs. 5	1.104	1.112	-0.00846	0.02313	218	195	0.3658	5329
3 vs. 7	1.104	1.133	-0.02923	0.02034	218	342	1.437	5329
3 vs. 10	1.104	1.017	0.08616	0.01995	218	379	4.319	5329
3 vs. 15	1.104	1.155	-0.05157	0.02161	218	257	2.387	5329
5 vs. 7	1.112	1.133	-0.02077	0.02106	195	342	0.9864	5329
5 vs. 10	1.112	1.017	0.09463	0.02068	195	379	4.575	5329
5 vs. 15	1.112	1.155	-0.04311	0.02229	195	257	1.934	5329
7 vs. 10	1.133	1.017	0.1154	0.0175	342	379	6.593	5329
7 vs. 15	1.133	1.155	-0.02234	0.01937	342	257	1.153	5329
10 vs. 15	1.017	1.155	-0.1377	0.01896	379	257	7.263	5329
3%								
1 vs. 3	1.085	1.097	-0.01119	0.01984	215	400	0.564	5329
1 vs. 5	1.085	1.158	-0.07245	0.01888	215	549	3.837	5329
1 vs. 7	1.085	1.179	-0.09335	0.01962	215	428	4.759	5329
1 vs. 10	1.085	1.069	0.01659	0.01999	215	384	0.83	5329
1 vs. 15	1.085	1.211	-0.1257	0.0211	215	291	5.957	5329
3 vs. 5	1.097	1.158	-0.06126	0.01543	400	549	3.971	5329
3 vs. 7	1.097	1.179	-0.08216	0.01632	400	428	5.034	5329
3 vs. 10	1.097	1.069	0.02778	0.01677	400	384	1.657	5329
3 vs. 15	1.097	1.211	-0.1145	0.01808	400	291	6.335	5329
5 vs. 7	1.158	1.179	-0.0209	0.01513	549	428	1.381	5329
5 vs. 10	1.158	1.069	0.08904	0.01561	549	384	5.703	5329
5 vs. 15	1.158	1.211	-0.05328	0.01702	549	291	3.131	5329
7 vs. 10	1.179	1.069	0.1099	0.0165	428	384	6.665	5329
7 vs. 15	1.179	1.211	-0.03238	0.01783	428	291	1.816	5329
10 vs. 15	1.069	1.211	-0.1423	0.01824	384	291	7.803	5329
5%								
1 vs. 3	1.039	1.143	-0.1036	0.0257	259	123	4.031	5329
1 vs. 5	1.039	1.11	-0.07097	0.01839	259	439	3.86	5329
1 vs. 7	1.039	1.11	-0.07127	0.01879	259	392	3.793	5329
1 vs. 10	1.039	1.017	0.02245	0.02285	259	178	0.9825	5329
1 vs. 15	1.039	1.122	-0.08304	0.02706	259	106	3.069	5329
3 vs. 5	1.143	1.11	0.03262	0.02394	123	439	1.362	5329
3 vs. 7	1.143	1.11	0.03233	0.02425	123	392	1.333	5329
3 vs. 10	1.143	1.017	0.126	0.02752	123	178	4.581	5329
3 vs. 15	1.143	1.122	0.02056	0.0311	123	106	0.661	5329
5 vs. 7	1.11	1.11	-0.00029	0.01631	439	392	0.01797	5329
5 vs. 10	1.11	1.017	0.09342	0.02085	439	178	4.48	5329
5 vs. 15	1.11	1.122	-0.01206	0.0254	439	106	0.4749	5329
7 vs. 10	1.11	1.017	0.09372	0.02121	392	178	4.418	5329
7 vs. 15	1.11	1.122	-0.01177	0.02569	392	106	0.4581	5329
10 vs. 15	1.017	1.122	-0.1055	0.02879	178	106	3.664	5329

Within each row, compare columns (simple effects within rows)

Number of 6
Number of 3
Alpha 0.05

Bonferroni's	Mean Diff.	95.00% CI	Significant?	Summary	Adjusted P Value
1					
1% vs. 3%	-0.07942	-0.1352 to	Yes	**	0.002
1% vs. 5%	-0.03303	-0.08654 to	No	ns	0.4186
3% vs. 5%	0.04639	-0.005459	No	ns	0.0966
3					
1% vs. 3%	0.00687	-0.04044 to	No	ns	>0.9999
1% vs. 5%	-0.03914	-0.1025 to	No	ns	0.4176
3% vs. 5%	-0.04601	-0.104 to 0	No	ns	0.1718
5					
1% vs. 3%	-0.04592	-0.09277 to	No	ns	0.0568
1% vs. 5%	0.00194	-0.04642 to	No	ns	>0.9999
3% vs. 5%	0.04786	0.01188 to	Yes	**	0.0044
7					
1% vs. 3%	-0.04605	-0.08681 to	Yes	*	0.0205
1% vs. 5%	0.02242	-0.01916 to	No	ns	0.5902
3% vs. 5%	0.06847	0.02918 to	Yes	****	<0.0001
10					
1% vs. 3%	-0.05151	-0.0922 to	Yes	**	0.0073
1% vs. 5%	0.000737	-0.05033 to	No	ns	>0.9999
3% vs. 5%	0.05225	0.00129 to	Yes	*	0.0423
15					
1% vs. 3%	-0.0561	-0.1042 to	Yes	*	0.0157
1% vs. 5%	0.03298	-0.03189 to	No	ns	0.6703
3% vs. 5%	0.08908	0.02533 to	Yes	**	0.0025

Test detail	Mean 1	Mean 2	Mean Diff.	SE of diff.	N1	N2	t	DF
1								
1% vs. 3%	1.006	1.085	-0.07942	0.0233	192	215	3.408	5329
1% vs. 5%	1.006	1.039	-0.03303	0.02235	192	259	1.478	5329
3% vs. 5%	1.085	1.039	0.04639	0.02165	215	259	2.143	5329
3								
1% vs. 3%	1.104	1.097	0.00687	0.01976	218	400	0.3477	5329
1% vs. 5%	1.104	1.143	-0.03914	0.02646	218	123	1.479	5329
3% vs. 5%	1.097	1.143	-0.04601	0.0242	400	123	1.902	5329
5								
1% vs. 3%	1.112	1.158	-0.04592	0.01956	195	549	2.347	5329
1% vs. 5%	1.112	1.11	0.00194	0.0202	195	439	0.09606	5329
3% vs. 5%	1.158	1.11	0.04786	0.01503	549	439	3.186	5329
7								
1% vs. 3%	1.133	1.179	-0.04605	0.01702	342	428	2.706	5329
1% vs. 5%	1.133	1.11	0.02242	0.01736	342	392	1.291	5329
3% vs. 5%	1.179	1.11	0.06847	0.01641	428	392	4.174	5329
10								
1% vs. 3%	1.017	1.069	-0.05151	0.01699	379	384	3.032	5329
1% vs. 5%	1.017	1.017	0.000737	0.02132	379	178	0.03456	5329
3% vs. 5%	1.069	1.017	0.05225	0.02128	384	178	2.455	5329
15								
1% vs. 3%	1.155	1.211	-0.0561	0.02009	257	291	2.793	5329
1% vs. 5%	1.155	1.122	0.03298	0.02709	257	106	1.218	5329
3% vs. 5%	1.211	1.122	0.08908	0.02662	291	106	3.346	5329

Table 53 – One-way ANOVA for the effects of time and hydrogel stiffness on Chapter 5 adipogenic data – POISSON'S RATIO

Table Anal Data 1

Two-way A Ordinary
Alpha 0.05

Source of \	% of total \	P value	P value sur	Significant?
Interaction	3.029	<0.0001	****	Yes
Time	9.259	<0.0001	****	Yes
Agarose	1.813	<0.0001	****	Yes

ANOVA tal	SS	DF	MS	F (DFn, DF	P value
Interaction	4.034	10	0.4034	F (10, 532	P<0.0001
Time	12.33	5	2.466	F (5, 5329)	P<0.0001
Agarose	2.414	2	1.207	F (2, 5329)	P<0.0001
Residual	114.4	5329	0.02146		

Number of 4535

Within each column, compare rows (simple effects within columns)

Number of 3
Number of 15
Alpha 0.05

Bonferroni\	Mean Diff.	95.00% CI	Significant?	Summary	Adjusted P Value
1%					
1 vs. 3	0.05031	0.007731 t	Yes	**	0.0079
1 vs. 5	0.05669	0.01295 to	Yes	**	0.0021
1 vs. 7	0.1161	0.07731 to	Yes	****	<0.0001
1 vs. 10	-0.03078	-0.06889 to	No	ns	0.2661
1 vs. 15	0.02573	-0.01531 to	No	ns	0.9848
3 vs. 5	0.00638	-0.03602 to	No	ns	>0.9999
3 vs. 7	0.0658	0.02852 to	Yes	****	<0.0001
3 vs. 10	-0.08109	-0.1177 to	Yes	****	<0.0001
3 vs. 15	-0.02458	-0.06419 to	No	ns	>0.9999
5 vs. 7	0.05942	0.02082 to	Yes	****	<0.0001
5 vs. 10	-0.08747	-0.1254 to	Yes	****	<0.0001
5 vs. 15	-0.03096	-0.07182 to	No	ns	0.3916
7 vs. 10	-0.1469	-0.179 to -	Yes	****	<0.0001
7 vs. 15	-0.09038	-0.1259 to	Yes	****	<0.0001
10 vs. 15	0.05651	0.02175 to	Yes	****	<0.0001
3%					
1 vs. 3	0.03762	0.00124 to	Yes	*	0.0361
1 vs. 5	0.01551	-0.0191 to	No	ns	>0.9999
1 vs. 7	-0.01325	-0.04921 to	No	ns	>0.9999
1 vs. 10	-0.1175	-0.1541 to	Yes	****	<0.0001
1 vs. 15	-0.09235	-0.131 to -	Yes	****	<0.0001
3 vs. 5	-0.02211	-0.05039 to	No	ns	0.3259
3 vs. 7	-0.05087	-0.08079 to	Yes	****	<0.0001
3 vs. 10	-0.1551	-0.1858 to	Yes	****	<0.0001
3 vs. 15	-0.13	-0.1631 to	Yes	****	<0.0001
5 vs. 7	-0.02876	-0.0565 to	Yes	*	0.0351
5 vs. 10	-0.133	-0.1616 to	Yes	****	<0.0001
5 vs. 15	-0.1079	-0.1391 to	Yes	****	<0.0001
7 vs. 10	-0.1042	-0.1344 to	Yes	****	<0.0001
7 vs. 15	-0.0791	-0.1118 to	Yes	****	<0.0001
10 vs. 15	0.0251	-0.008336 t	No	ns	0.4131
5%					
1 vs. 3	0.07824	0.03113 to	Yes	****	<0.0001
1 vs. 5	-0.04817	-0.08188 to	Yes	***	0.0004
1 vs. 7	-0.02759	-0.06204 to	No	ns	0.2808
1 vs. 10	-0.1579	-0.1998 to	Yes	****	<0.0001
1 vs. 15	-0.1112	-0.1608 to	Yes	****	<0.0001
3 vs. 5	-0.1264	-0.1703 to	Yes	****	<0.0001
3 vs. 7	-0.1058	-0.1503 to	Yes	****	<0.0001
3 vs. 10	-0.2361	-0.2866 to	Yes	****	<0.0001
3 vs. 15	-0.1894	-0.2464 to	Yes	****	<0.0001
5 vs. 7	0.02058	-0.009315 t	No	ns	0.6492
5 vs. 10	-0.1097	-0.1479 to	Yes	****	<0.0001
5 vs. 15	-0.06302	-0.1096 to	Yes	**	0.0011
7 vs. 10	-0.1303	-0.1692 to	Yes	****	<0.0001
7 vs. 15	-0.0836	-0.1307 to	Yes	****	<0.0001
10 vs. 15	0.04669	-0.006091 t	No	ns	0.1412

Test detail\	Mean 1	Mean 2	Mean Diff.	SE of diff.	N1	N2	t	DF
1%								
1 vs. 3	-0.3371	-0.3874	0.05031	0.0145	192	218	3.47	5329
1 vs. 5	-0.3371	-0.3938	0.05669	0.01489	192	195	3.806	5329
1 vs. 7	-0.3371	-0.4532	0.1161	0.01321	192	342	8.789	5329
1 vs. 10	-0.3371	-0.3063	-0.03078	0.01298	192	379	2.372	5329
1 vs. 15	-0.3371	-0.3628	0.02573	0.01397	192	257	1.841	5329
3 vs. 5	-0.3874	-0.3938	0.00638	0.01444	218	195	0.4418	5329
3 vs. 7	-0.3874	-0.4532	0.0658	0.0127	218	342	5.182	5329
3 vs. 10	-0.3874	-0.3063	-0.08109	0.01245	218	379	6.512	5329
3 vs. 15	-0.3874	-0.3628	-0.02458	0.01349	218	257	1.822	5329
5 vs. 7	-0.3938	-0.4532	0.05942	0.01315	195	342	4.52	5329
5 vs. 10	-0.3938	-0.3063	-0.08747	0.01291	195	379	6.775	5329
5 vs. 15	-0.3938	-0.3628	-0.03096	0.01391	195	257	2.225	5329
7 vs. 10	-0.4532	-0.3063	-0.1469	0.01093	342	379	13.44	5329
7 vs. 15	-0.4532	-0.3628	-0.09038	0.01209	342	257	7.473	5329
10 vs. 15	-0.3063	-0.3628	0.05651	0.01184	379	257	4.774	5329
3%								
1 vs. 3	-0.4572	-0.4948	0.03762	0.01239	215	400	3.037	5329
1 vs. 5	-0.4572	-0.4727	0.01551	0.01179	215	549	1.316	5329
1 vs. 7	-0.4572	-0.4439	-0.01325	0.01225	215	428	1.082	5329
1 vs. 10	-0.4572	-0.3397	-0.1175	0.01248	215	384	9.412	5329
1 vs. 15	-0.4572	-0.3648	-0.09235	0.01318	215	291	7.009	5329
3 vs. 5	-0.4948	-0.4727	-0.02211	0.009631	400	549	2.296	5329
3 vs. 7	-0.4948	-0.4439	-0.05087	0.01019	400	428	4.993	5329
3 vs. 10	-0.4948	-0.3397	-0.1551	0.01047	400	384	14.82	5329
3 vs. 15	-0.4948	-0.3648	-0.13	0.01129	400	291	11.51	5329
5 vs. 7	-0.4727	-0.4439	-0.02876	0.009447	549	428	3.044	5329
5 vs. 10	-0.4727	-0.3397	-0.133	0.009746	549	384	13.64	5329
5 vs. 15	-0.4727	-0.3648	-0.1079	0.01062	549	291	10.15	5329
7 vs. 10	-0.4439	-0.3397	-0.1042	0.0103	428	384	10.12	5329
7 vs. 15	-0.4439	-0.3648	-0.0791	0.01113	428	291	7.106	5329
10 vs. 15	-0.3397	-0.3648	0.0251	0.01139	384	291	2.204	5329
5%								
1 vs. 3	-0.4329	-0.5111	0.07824	0.01604	259	123	4.877	5329
1 vs. 5	-0.4329	-0.3847	-0.04817	0.01148	259	439	4.196	5329
1 vs. 7	-0.4329	-0.4053	-0.02759	0.01173	259	392	2.352	5329
1 vs. 10	-0.4329	-0.275	-0.1579	0.01426	259	178	11.07	5329
1 vs. 15	-0.4329	-0.3217	-0.1112	0.01689	259	106	6.582	5329
3 vs. 5	-0.5111	-0.3847	-0.1264	0.01495	123	439	8.458	5329
3 vs. 7	-0.5111	-0.4053	-0.1058	0.01514	123	392	6.99	5329
3 vs. 10	-0.5111	-0.275	-0.2361	0.01718	123	178	13.75	5329
3 vs. 15	-0.5111	-0.3217	-0.1894	0.01942	123	106	9.756	5329
5 vs. 7	-0.3847	-0.4053	0.02058	0.01018	439	392	2.022	5329
5 vs. 10	-0.3847	-0.275	-0.1097	0.01302	439	178	8.428	5329
5 vs. 15	-0.3847	-0.3217	-0.06302	0.01585	439	106	3.975	5329
7 vs. 10	-0.4053	-0.275	-0.1303	0.01324	392	178	9.84	5329
7 vs. 15	-0.4053	-0.3217	-0.0836	0.01604	392	106	5.212	5329
10 vs. 15	-0.275	-0.3217	0.04669	0.01797	178	106	2.598	5329

Within each row, compare columns (simple effects within rows)

Number of 6
Number of 3
Alpha 0.05

Bonferroni\	Mean Diff.	95.00% CI	Significant?	Summary	Adjusted P Value
1					
1% vs. 3%	0.1201	0.08527 to	Yes	****	<0.0001
1% vs. 5%	0.09578	0.06237 to	Yes	****	<0.0001
3% vs. 5%	-0.02433	-0.0567 to	No	ns	0.2157
3					
1% vs. 3%	0.1074	0.07788 to	Yes	****	<0.0001
1% vs. 5%	0.1237	0.08415 to	Yes	****	<0.0001
3% vs. 5%	0.01629	-0.01988 t	No	ns	0.8426
5					
1% vs. 3%	0.07893	0.04968 to	Yes	****	<0.0001
1% vs. 5%	-0.00908	-0.03927 t	No	ns	>0.9999
3% vs. 5%	-0.08801	-0.1105 to	Yes	****	<0.0001
7					
1% vs. 3%	-0.00925	-0.0347 to	No	ns	>0.9999
1% vs. 5%	-0.04792	-0.07388 t	Yes	****	<0.0001
3% vs. 5%	-0.03867	-0.0632 to	Yes	***	0.0005
10					
1% vs. 3%	0.03344	0.008037 t	Yes	**	0.0049
1% vs. 5%	-0.03132	-0.0632 to	No	ns	0.056
3% vs. 5%	-0.06476	-0.09657 t	Yes	****	<0.0001
15					
1% vs. 3%	0.00203	-0.028 to 0	No	ns	>0.9999
1% vs. 5%	-0.04114	-0.08164 t	Yes	*	0.0451
3% vs. 5%	-0.04317	-0.08297 t	Yes	*	0.0283

Test detail\	Mean 1	Mean 2	Mean Diff.	SE of diff.	N1	N2	t	DF
1								
1% vs. 3%	-0.3371	-0.4572	0.1201	0.01455	192	215	8.257	5329
1% vs. 5%	-0.3371	-0.4329	0.09578	0.01395	192	259	6.865	5329
3% vs. 5%	-0.4572	-0.4329	-0.02433	0.01352	215	259	1.8	5329
3								
1% vs. 3%	-0.3874	-0.4948	0.1074	0.01233	218	400	8.71	5329
1% vs. 5%	-0.3874	-0.5111	0.1237	0.01652	218	123	7.488	5329
3% vs. 5%	-0.4948	-0.5111	0.01629	0.0151	400	123	1.078	5329
5								
1% vs. 3%	-0.3938	-0.4727	0.07893	0.01221	195	549	6.463	5329
1% vs. 5%	-0.3938	-0.3847	-0.00908	0.01261	195	439	0.7202	5329
3% vs. 5%	-0.4727	-0.3847	-0.08801	0.00938	549	439	9.383	5329
7								
1% vs. 3%	-0.4532	-0.4439	-0.00925	0.01063	342	428	0.8705	5329
1% vs. 5%	-0.4532	-0.4053	-0.04792	0.01084	342	392	4.421	5329
3% vs. 5%	-0.4439	-0.4053	-0.03867	0.01024	428	392	3.776	5329
10								
1% vs. 3%	-0.3063	-0.3397	0.03344	0.01061	379	384	3.152	5329
1% vs. 5%	-0.3063	-0.275	-0.03132	0.01331	379	178	2.353	5329
3% vs. 5%	-0.3397	-0.275	-0.06476	0.01328	384	178	4.875	5329
15								
1% vs. 3%	-0.3628	-0.3648	0.00203	0.01254	257	291	0.1619	5329
1% vs. 5%	-0.3628	-0.3217	-0.04114	0.01691	257	106	2.433	5329
3% vs. 5%	-0.3648	-0.3217	-0.04317	0.01662	291	106	2.597	5329

Table 54 – One-way ANOVA for the effects of time and hydrogel stiffness on Chapter 5 adipogenic data – NUCLEUS STIFFNESS

Table Anal Data 1

Two-way A Ordinary
Alpha 0.05

Source of \	% of total \	P value	P value sur	Significant?
Interaction	3.123	<0.0001	****	Yes
Time	24.93	<0.0001	****	Yes
Agarose	0.3197	<0.0001	****	Yes

ANOVA tal	SS	DF	MS	F (DFn, DF	P value
Interaction	100756	10	10076	F (10, 532	P<0.0001
Time	804125	5	160825	F (5, 5329)	P<0.0001
Agarose	10314	2	5157	F (2, 5329)	P<0.0001
Residual	2310627	5329	433.6		

Number of 4535

Within each column, compare rows (simple effects within columns)

Number of 3
Number of 15
Alpha 0.05

Bonferroni\	Mean Diff.	95.00% CI	Significant?	Summary	Adjusted P Value
1%					
1 vs. 3	-2.69	-8.742 to 3	No	ns	>0.9999
1 vs. 5	-10.77	-16.99 to -4	Yes	****	<0.0001
1 vs. 7	-31.3	-36.82 to -2	Yes	****	<0.0001
1 vs. 10	-31.01	-36.43 to -2	Yes	****	<0.0001
1 vs. 15	-46.4	-52.23 to -4	Yes	****	<0.0001
3 vs. 5	-8.081	-14.11 to -2	Yes	**	0.0013
3 vs. 7	-28.61	-33.91 to -2	Yes	****	<0.0001
3 vs. 10	-28.32	-33.52 to -2	Yes	****	<0.0001
3 vs. 15	-43.71	-49.34 to -3	Yes	****	<0.0001
5 vs. 7	-20.53	-26.02 to -1	Yes	****	<0.0001
5 vs. 10	-20.24	-25.63 to -1	Yes	****	<0.0001
5 vs. 15	-35.63	-41.44 to -2	Yes	****	<0.0001
7 vs. 10	0.2923	-4.268 to 4	No	ns	>0.9999
7 vs. 15	-15.1	-20.15 to -1	Yes	****	<0.0001
10 vs. 15	-15.39	-20.33 to -1	Yes	****	<0.0001
3%					
1 vs. 3	-8.487	-13.66 to -3	Yes	****	<0.0001
1 vs. 5	-19.09	-24.01 to -1	Yes	****	<0.0001
1 vs. 7	-21.09	-26.21 to -1	Yes	****	<0.0001
1 vs. 10	-20.64	-25.84 to -1	Yes	****	<0.0001
1 vs. 15	-36.92	-42.42 to -3	Yes	****	<0.0001
3 vs. 5	-10.6	-14.62 to -6	Yes	****	<0.0001
3 vs. 7	-12.61	-16.86 to -8	Yes	****	<0.0001
3 vs. 10	-12.15	-16.52 to -7	Yes	****	<0.0001
3 vs. 15	-28.43	-33.14 to -2	Yes	****	<0.0001
5 vs. 7	-2.005	-5.947 to 1	No	ns	>0.9999
5 vs. 10	-1.546	-5.614 to 2	No	ns	>0.9999
5 vs. 15	-17.83	-22.26 to -1	Yes	****	<0.0001
7 vs. 10	0.4588	-3.839 to 4	No	ns	>0.9999
7 vs. 15	-15.82	-20.47 to -1	Yes	****	<0.0001
10 vs. 15	-16.28	-21.03 to -1	Yes	****	<0.0001
5%					
1 vs. 3	4.324	-2.372 to 1	No	ns	0.8697
1 vs. 5	-24.95	-29.74 to -2	Yes	****	<0.0001
1 vs. 7	-20.36	-25.26 to -1	Yes	****	<0.0001
1 vs. 10	-30.2	-36.15 to -2	Yes	****	<0.0001
1 vs. 15	-30.71	-37.77 to -2	Yes	****	<0.0001
3 vs. 5	-29.27	-35.51 to -2	Yes	****	<0.0001
3 vs. 7	-24.69	-31.01 to -1	Yes	****	<0.0001
3 vs. 10	-34.52	-41.69 to -2	Yes	****	<0.0001
3 vs. 15	-35.04	-43.14 to -2	Yes	****	<0.0001
5 vs. 7	4.585	0.3359 to 8	Yes	*	0.0231
5 vs. 10	-5.247	-10.68 to 0	No	ns	0.0689
5 vs. 15	-5.767	-12.38 to 0	No	ns	0.1579
7 vs. 10	-9.832	-15.36 to -4	Yes	****	<0.0001
7 vs. 15	-10.35	-17.05 to -3	Yes	****	<0.0001
10 vs. 15	-0.5198	-8.022 to 6	No	ns	>0.9999

Test detail\	Mean 1	Mean 2	Mean Diff.	SE of diff.	N1	N2	t	DF
1%								
1 vs. 3	24.01	26.7	-2.69	2.061	192	218	1.305	5329
1 vs. 5	24.01	34.78	-10.77	2.117	192	195	5.088	5329
1 vs. 7	24.01	55.31	-31.3	1.878	192	342	16.67	5329
1 vs. 10	24.01	55.02	-31.01	1.845	192	379	16.81	5329
1 vs. 15	24.01	70.41	-46.4	1.986	192	257	23.36	5329
3 vs. 5	26.7	34.78	-8.081	2.052	218	195	3.937	5329
3 vs. 7	26.7	55.31	-28.61	1.805	218	342	15.85	5329
3 vs. 10	26.7	55.02	-28.32	1.77	218	379	16	5329
3 vs. 15	26.7	70.41	-43.71	1.917	218	257	22.8	5329
5 vs. 7	34.78	55.31	-20.53	1.869	195	342	10.99	5329
5 vs. 10	34.78	55.02	-20.24	1.835	195	379	11.03	5329
5 vs. 15	34.78	70.41	-35.63	1.978	195	257	18.02	5329
7 vs. 10	55.31	55.02	0.2923	1.553	342	379	0.1882	5329
7 vs. 15	55.31	70.41	-15.1	1.719	342	257	8.783	5329
10 vs. 15	55.02	70.41	-15.39	1.683	379	257	9.147	5329
3%								
1 vs. 3	29.59	38.07	-8.487	1.761	215	400	4.82	5329
1 vs. 5	29.59	48.68	-19.09	1.675	215	549	11.39	5329
1 vs. 7	29.59	50.68	-21.09	1.741	215	428	12.12	5329
1 vs. 10	29.59	50.22	-20.64	1.774	215	384	11.63	5329
1 vs. 15	29.59	66.5	-36.92	1.873	215	291	19.71	5329
3 vs. 5	38.07	48.68	-10.6	1.369	400	549	7.746	5329
3 vs. 7	38.07	50.68	-12.61	1.448	400	428	8.706	5329
3 vs. 10	38.07	50.22	-12.15	1.488	400	384	8.166	5329
3 vs. 15	38.07	66.5	-28.43	1.604	400	291	17.72	5329
5 vs. 7	48.68	50.68	-2.005	1.343	549	428	1.493	5329
5 vs. 10	48.68	50.22	-1.546	1.385	549	384	1.116	5329
5 vs. 15	48.68	66.5	-17.83	1.51	549	291	11.81	5329
7 vs. 10	50.68	50.22	0.4588	1.464	428	384	0.3135	5329
7 vs. 15	50.68	66.5	-15.82	1.582	428	291	10	5329
10 vs. 15	50.22	66.5	-16.28	1.618	384	291	10.06	5329
5%								
1 vs. 3	30.89	26.57	4.324	2.28	259	123	1.896	5329
1 vs. 5	30.89	55.84	-24.95	1.632	259	439	15.29	5329
1 vs. 7	30.89	51.25	-20.36	1.667	259	392	12.21	5329
1 vs. 10	30.89	61.09	-30.2	2.027	259	178	14.89	5329
1 vs. 15	30.89	61.61	-30.71	2.401	259	106	12.79	5329
3 vs. 5	26.57	55.84	-29.27	2.124	123	439	13.78	5329
3 vs. 7	26.57	51.25	-24.69	2.152	123	392	11.47	5329
3 vs. 10	26.57	61.09	-34.52	2.442	123	178	14.14	5329
3 vs. 15	26.57	61.61	-35.04	2.76	123	106	12.7	5329
5 vs. 7	55.84	51.25	4.585	1.447	439	392	3.169	5329
5 vs. 10	55.84	61.09	-5.247	1.85	439	178	2.836	5329
5 vs. 15	55.84	61.61	-5.767	2.253	439	106	2.559	5329
7 vs. 10	51.25	61.09	-9.832	1.882	392	178	5.224	5329
7 vs. 15	51.25	61.61	-10.35	2.28	392	106	4.541	5329
10 vs. 15	61.09	61.61	-0.5198	2.555	178	106	0.2035	5329

Within each row, compare columns (simple effects within rows)

Number of 6
Number of 3
Alpha 0.05

Bonferroni\	Mean Diff.	95.00% CI	Significant?	Summary	Adjusted P Value
1					
1% vs. 3%	-5.575	-10.53 to -1	Yes	*	0.0211
1% vs. 5%	-6.879	-11.63 to -2	Yes	**	0.0016
3% vs. 5%	-1.304	-5.905 to 3	No	ns	>0.9999
3					
1% vs. 3%	-11.37	-15.57 to -7	Yes	****	<0.0001
1% vs. 5%	0.1351	-5.488 to 5	No	ns	>0.9999
3% vs. 5%	11.51	6.365 to 16	Yes	****	<0.0001
5					
1% vs. 3%	-13.89	-18.05 to -9	Yes	****	<0.0001
1% vs. 5%	-21.06	-25.35 to -1	Yes	****	<0.0001
3% vs. 5%	-7.163	-10.36 to -3	Yes	****	<0.0001
7					
1% vs. 3%	4.634	1.017 to 8.	Yes	**	0.0065
1% vs. 5%	4.06	0.3707 to 7	Yes	*	0.0253
3% vs. 5%	-0.5737	-4.06 to 2.9	No	ns	>0.9999
10					
1% vs. 3%	4.801	1.19 to 8.4	Yes	**	0.0044
1% vs. 5%	-6.064	-10.59 to -1	Yes	**	0.0041
3% vs. 5%	-10.86	-15.39 to -6	Yes	****	<0.0001
15					
1% vs. 3%	3.91	-0.3589 to 8	No	ns	0.085
1% vs. 5%	8.807	3.051 to 14	Yes	***	0.0008
3% vs. 5%	4.898	-0.7596 to 1	No	ns	0.1146

Test detail\	Mean 1	Mean 2	Mean Diff.	SE of diff.	N1	N2	t	DF
1								
1% vs. 3%	24.01	29.59	-5.575	2.068	192	215	2.696	5329
1% vs. 5%	24.01	30.89	-6.879	1.983	192	259	3.469	5329
3% vs. 5%	29.59	30.89	-1.304	1.921	215	259	0.6789	5329
3								
1% vs. 3%	26.7	38.07	-11.37	1.753	218	400	6.487	5329
1% vs. 5%	26.7	26.57	0.1351	2.348	218	123	0.05751	5329
3% vs. 5%	38.07	26.57	11.51	2.147	400	123	5.359	5329
5								
1% vs. 3%	34.78	48.68	-13.89	1.736	195	549	8.003	5329
1% vs. 5%	34.78	55.84	-21.06	1.792	195	439	11.75	5329
3% vs. 5%	48.68	55.84	-7.163	1.333	549	439	5.373	5329
7								
1% vs. 3%	55.31	50.68	4.634	1.51	342	428	3.068	5329
1% vs. 5%	55.31	51.25	4.06	1.541	342	392	2.635	5329
3% vs. 5%	50.68	51.25	-0.5737	1.456	428	392	0.3941	5329
10								
1% vs. 3%	55.02	50.22	4.801	1.508	379	384	3.184	5329
1% vs. 5%	55.02	61.09	-6.064	1.892	379	178	3.205	5329
3% vs. 5%	50.22	61.09	-10.86	1.888	384	178	5.754	5329
15								
1% vs. 3%	70.41	66.5	3.91	1.782	257	291	2.193	5329
1% vs. 5%	70.41	61.61	8.807	2.404	257	106	3.664	5329
3% vs. 5%	66.5	61.61	4.898	2.362	291	106	2.073	5329

Appendix D – Supplementary data for Chapter 7

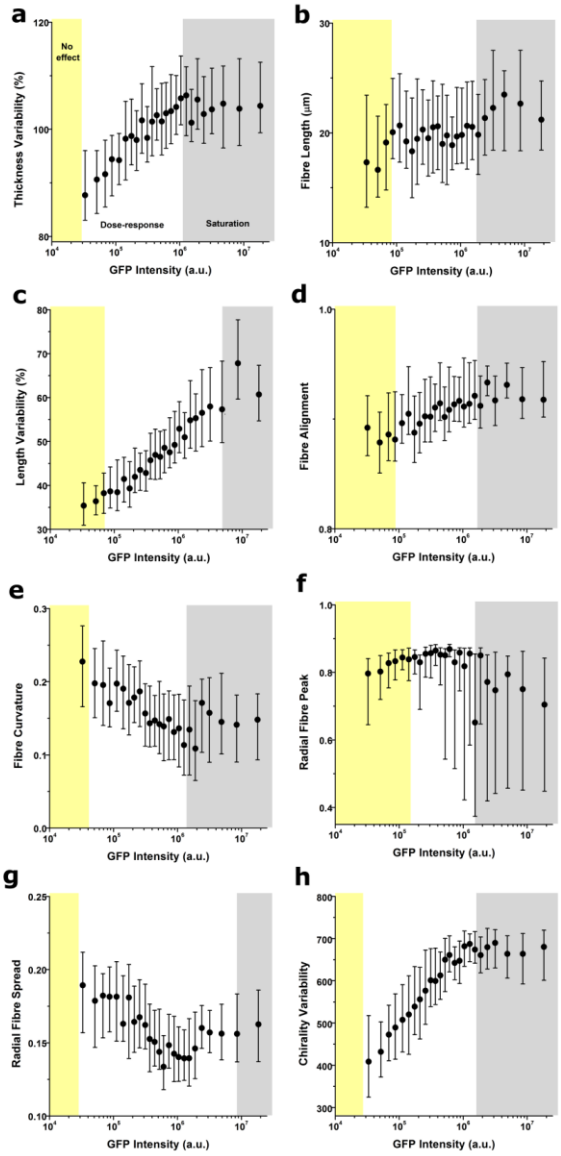

Figure 11-1 –Lifeact expression affects cellular morphology and cytoskeletal organization in a dose-response manner. Dose-response curves quantifying the effect of Lifeact expression in whole cell aspect ratio (a), fibre thickness variability (b), fibre alignment (c) and curvature (d), peak fibre location (e) and spread (f), fibre length (g) and associated variability (h), and variability of chirality of fibres (i). Values for >100 cells were pooled together to compute each individual data point. Data is presented as mean, error bars indicate interquartile range (Q1–Q3). Background colours indicate the regimes where cells display no Lifeact-induced effect (yellow background), a dose-response trend (white background) and a saturation plateau (gray background), as identified from analyses of peak changes in variability in the neighbourhood of each point for each parameter plotted.

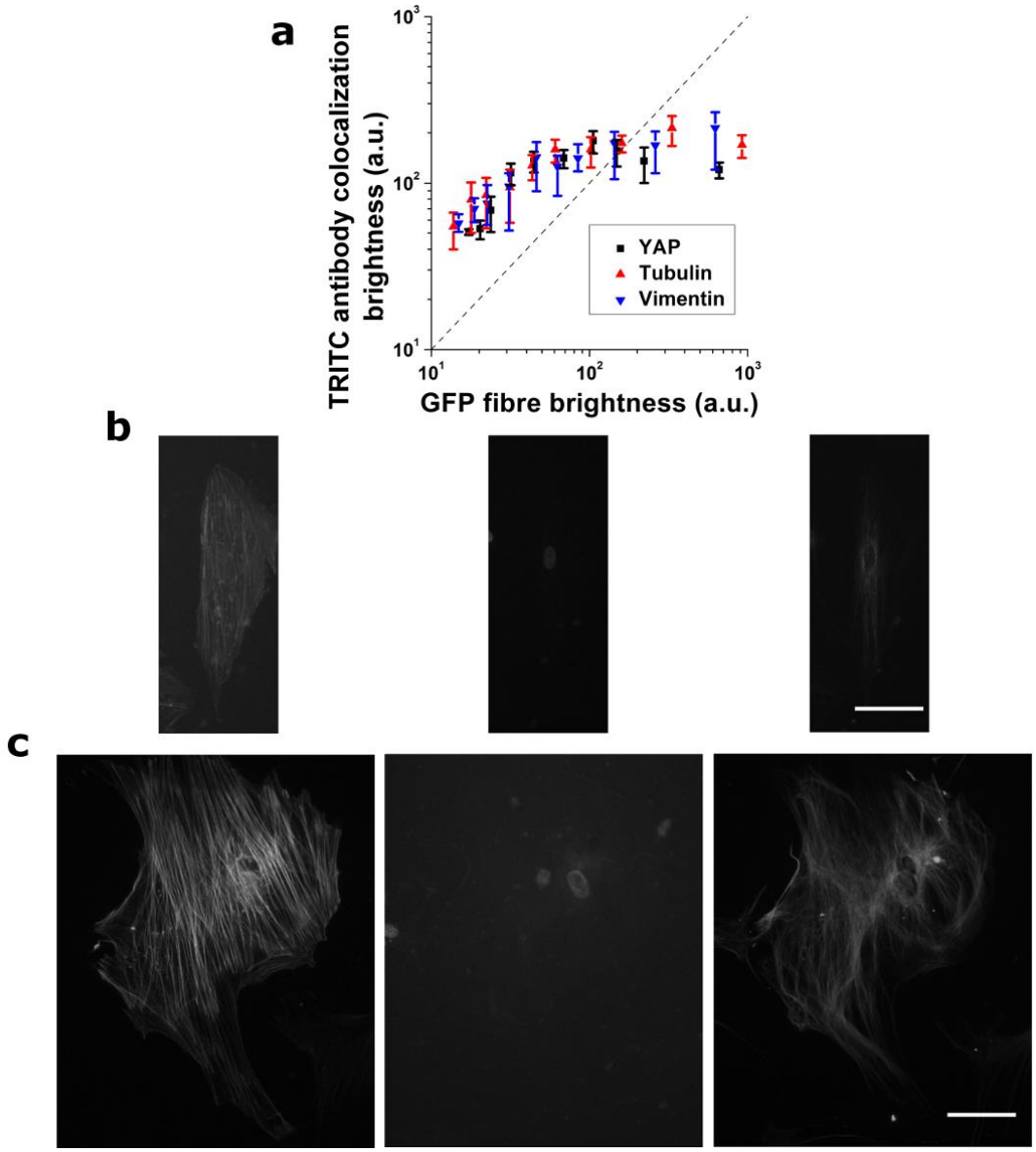

Figure 11-2 – Verification of lack of bleed-through between the GFP and TRITC secondary fluorescence channels. (a) Relationship between GFP fibre intensity and colocalized intensities measured on the TRITC channel. All proteins plotted were imaged using the same secondary antibody (goat anti-mouse IgG-TRITC, sc-3796). Note the dashed identity line would correspond to bleed-through behaviour (α=1). Instead, when data was fitted using the function $I_{TRITC} = aI_{GFP}^{\alpha}$, the measured slope α was significantly smaller than 1. YAP, α = 0.156 (-0.041 – 0.354); Tubulin, α = 0.199 (0.078 – 0.320); Vimentin, α = 0.275 (0.188 – 0.362); values in parenthesis correspond to 95% lower and upper confidence levels). (b) Example of a cell displaying no localization of tubulin staining to Lifeact-containing stress fibres, the cell has been transduced with Lifeact (left) subsequently stained with DAPI (middle) and against YAP (right). Scale bar is 20 μm. (c) Example of a cell displaying no localization of vimentin staining to Lifeact-containing stress fibres, the cell has been transduced with Lifeact (left) subsequently stained with DAPI (middle) and against vimentin (right). Scale bar is 20 μm.

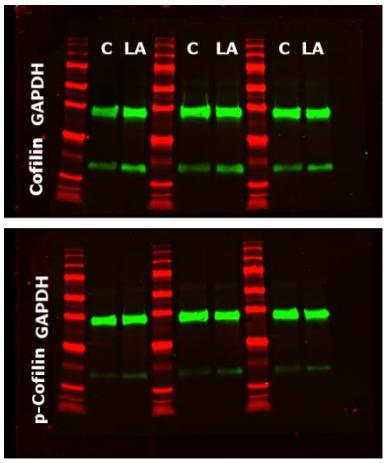

Figure 11-3 – Western blots used to quantify cofilin (top gel) and p-cofilin (bottom gel) expression levels relative to GADPH for cell populations treated with control of Lifeact. The pictures has been edited to include labels for blots.

Bibliography

[1] H. R. Hapsara, “World Health Organization (WHO): Global Health Situation,” in *Wiley Encyclopedia of Clinical Trials*, John Wiley & Sons, Inc., 2008.

[2] X. Wei, X. Yang, Z. Han, F. Qu, L. Shao, and Y. Shi, “Mesenchymal stem cells: a new trend for cell therapy,” *Acta Pharmacol. Sin.*, vol. 34, no. 6, pp. 747–754, 2013.

[3] M. P. Duffy and C. R. Jacobs, “Seeing the Unseen: Cell Strain and Mechanosensing,” *Biophys. J.*, vol. 108, no. 7, pp. 1583–1584, 2015.

[4] J. M. Seong, B.-C. Kim, J.-H. Park, I. K. Kwon, A. Mantalaris, and Y.-S. Hwang, “Stem cells in bone tissue engineering,” *Biomed. Mater.*, vol. 5, no. 6, p. 62001, 2010.

[5] C. E. Murry and G. Keller, “Differentiation of Embryonic Stem Cells to Clinically Relevant Populations: Lessons from Embryonic Development,” *Cell*, vol. 132, no. 4, pp. 661–680, 2008.

[6] R. Langer and J. Vacanti, “Tissue engineering,” *Science (80-.).*, vol. 260, no. 5110, pp. 920–926, 1993.

[7] H. E. Blum, “Advances in individualized and regenerative medicine,” *Adv. Med. Sci.*, vol. 59, no. 1, pp. 7–12, 2014.

[8] J. Vacanti, “Tissue engineering and regenerative medicine: from first principles to state of the art,” *J. Pediatr. Surg.*, vol. 45, no. 2, pp. 291–294, 2010.

[9] N. Baker, L. B. Boyette, and R. S. Tuan, “Characterization of bone marrow-derived mesenchymal stem cells in aging,” *Bone*, vol. 70, pp. 37–47, 2015.

[10] Y. Jiang *et al.*, “Pluripotency of mesenchymal stem cells derived from adult marrow,” *Nature*, vol. 418, no. 6893, pp. 41–49, 2002.

[11] A. J. Engler, S. Sen, H. L. Sweeney, and D. E. Discher, “Matrix Elasticity Directs Stem Cell Lineage Specification,” *Cell*, vol. 126, no. 4, pp. 677–689, 2006.

[12] R. K. Das and O. F. Zouani, “A review of the effects of the cell environment physicochemical nanoarchitecture on stem cell commitment,” *Biomaterials*, vol. 35, no. 20, pp. 5278–5293, 2014.

[13] A. Augello, T. B. Kurth, and C. De Bari, “Mesenchymal stem cells: a perspective from in vitro cultures to in vivo migration and niches,” *Eur. Cells Mater.*, vol. 20, pp. 121–133, 2010.

[14] J. J. Bara, R. G. Richards, M. Alini, and M. J. Stoddart, “Concise Review: Bone Marrow-Derived Mesenchymal Stem Cells Change Phenotype Following In Vitro Culture: Implications for Basic Research and the Clinic,” *Stem Cells*, vol. 32, no. 7, pp. 1713–1723, 2014.

[15] K. Takahashi and S. Yamanaka, “Induction of Pluripotent Stem Cells from Mouse Embryonic and Adult Fibroblast Cultures by Defined Factors,” *Cell*, vol. 126, no. 4, pp. 663–676, 2006.

[16] A. J. Friedenstein, “Precursor Cells of Mechanocytes,” *International Review of Cytology*. Elsevier, pp. 327–359, 1976.

[17] M. F. Pittenger, “Multilineage Potential of Adult Human Mesenchymal Stem Cells,” *Science (80-.).*, vol. 284, no. 5411, pp. 143–147, 1999.

[18] J. P. Beier *et al.*, “Myogenic differentiation of mesenchymal stem cells co-cultured with primary myoblasts,” *Cell Biol. Int.*, vol. 35, no. 4, pp. 397–406, 2011.

[19] P. Tropel *et al.*, “Functional Neuronal Differentiation of Bone Marrow-Derived Mesenchymal Stem Cells,” *Stem Cells*, vol. 24, no. 12, pp. 2868–2876, 2006.

[20] Y. Wang, Z. Han, Y. Song, and Z. C. Han, “Safety of Mesenchymal Stem Cells for Clinical Application,” *Stem Cells Int.*, vol. 2012, pp. 1–4, 2012.

[21] M. B. Murphy, K. Moncivais, and A. I. Caplan, “Mesenchymal stem cells: environmentally responsive therapeutics for regenerative medicine,” *Exp. Mol. Med.*, vol. 45, no. 11, pp. e54–e54, 2013.

[22] A. Uccelli, L. Moretta, and V. Pistoia, “Mesenchymal stem cells in health and disease,” *Nature Reviews Immunology*, vol. 8, no. 9. pp. 726–736, 2008.

[23] E. M. Horwitz *et al.*, “Clarification of the nomenclature for MSC: The International Society for Cellular Therapy position statement,” *Cytotherapy*, vol. 7, no. 5, pp. 393–395, 2005.

[24] M. Dominici *et al.*, “Minimal criteria for defining multipotent mesenchymal stromal cells. The International Society for Cellular Therapy position statement,” *Cytotherapy*, vol. 8, no. 4, pp. 315–317, 2006.

[25] K. C. Russell, D. G. Phinney, M. R. Lacey, B. L. Barrilleaux, K. E. Meyertholen, and K. C. O’Connor, “In Vitro High-Capacity Assay to Quantify the Clonal Heterogeneity in Trilineage Potential of Mesenchymal Stem Cells Reveals a Complex Hierarchy of Lineage Commitment,” *Stem Cells*, vol. 28, no. 4, pp. 788–798, 2010.

[26] W. C. Lee *et al.*, “Multivariate biophysical markers predictive of mesenchymal stromal cell multipotency,” *Proc. Natl. Acad. Sci.*, vol. 111, no. 42, pp. E4409–E4418, 2014.

[27] A. I. Caplan, “Mesenchymal stem cells,” *J. Orthop. Res.*, vol. 9, no. 5, pp. 641–650, 1991.

[28] D. Loncaric *et al.*, “The majority of cells in so-called ‘mesenchymal stem cell’ population are neither stem cells nor progenitors,” *Transfusion Clinique et Biologique*, 2018.

[29] A. Blocki *et al.*, “Not All MSCs Can Act as Pericytes: Functional In Vitro Assays to Distinguish Pericytes from Other Mesenchymal Stem Cells in Angiogenesis,” *Stem Cells Dev.*, vol. 22, no. 17, pp. 2347–2355, 2013.

[30] S. Fickert *et al.*, “Human mesenchymal stem cell proliferation and osteogenic differentiation during long-term ex vivo cultivation is not age dependent,” *J. Bone Miner. Metab.*, vol. 29, no. 2, pp. 224–235, 2010.

[31] C. Yang, M. W. Tibbitt, L. Basta, and K. S. Anseth, “Mechanical memory and dosing influence stem cell fate,” *Nat. Mater.*, vol. 13, no. 6, pp. 645–652, 2014.

[32] M. Rodrigues, L. G. Griffith, and A. Wells, “Growth factor regulation of proliferation and survival of multipotential stromal cells,” *Stem Cell Res. Ther.*, vol. 1, no. 4, p. 32, 2010.

[33] L. A. Solchaga, K. J. Penick, and J. F. Welter, “Chondrogenic Differentiation of Bone Marrow-Derived Mesenchymal Stem Cells: Tips and Tricks,” *Mesenchymal Stem Cell Assays and Applications*. Humana Press, pp. 253–278, 2011.

[34] T. Heino and T. Hentunen, “Differentiation of Osteoblasts and Osteocytes from Mesenchymal Stem Cells,” *Curr. Stem Cell Res. Ther.*, vol. 3, no. 2, pp. 131–145, 2008.

[35] H. Orimo, “The Mechanism of Mineralization and the Role of Alkaline Phosphatase in Health and Disease,” *J. Nippon Med. Sch.*, vol. 77, no. 1, pp. 4–12, 2010.

[36] R. Marom, I. Shur, R. Solomon, and D. Benayahu, “Characterization of adhesion and differentiation markers of osteogenic marrow stromal cells,” *J. Cell. Physiol.*, vol. 202, no. 1, pp. 41–48, 2004.

[37] R. L. Mauck, X. Yuan, and R. S. Tuan, “Chondrogenic differentiation and functional maturation of bovine mesenchymal stem cells in long-term agarose culture,” *Osteoarthr. Cartil.*, vol. 14, no. 2, pp. 179–189, 2006.

[38] R. McBeath, D. M. Pirone, C. M. Nelson, K. Bhadriraju, and C. S. Chen, “Cell Shape, Cytoskeletal Tension, and RhoA Regulate Stem Cell Lineage Commitment,” *Dev. Cell*, vol. 6, no. 4, pp. 483–495, 2004.

[39] A. W. James, “Review of Signaling Pathways Governing MSC Osteogenic and Adipogenic Differentiation,” *Scientifica (Cairo).*, vol. 2013, pp. 1–17, 2013.

[40] G. Yourek, M. A. Hussain, and J. J. Mao, “Cytoskeletal Changes of Mesenchymal Stem Cells During Differentiation,” *ASAIO J.*, vol. 53, no. 2, pp. 219–228, 2007.

[41] M. Fakhry, “Molecular mechanisms of mesenchymal stem cell differentiation towards osteoblasts,” *World J. Stem Cells*, vol. 5, no. 4, p. 136, 2013.

[42] P. Singh and J. E. Schwarzbauer, “Fibronectin and stem cell differentiation - lessons from chondrogenesis,” *J. Cell Sci.*, vol. 125, no. 16, pp. 3703–3712, 2012.

[43] H. V Desai, I. S. Voruganti, C. Jayasuriya, Q. Chen, and E. M. Darling, “Live-Cell, Temporal Gene Expression Analysis of Osteogenic Differentiation in Adipose-Derived Stem Cells,” *Tissue Eng. Part A*, vol. 20, no. 5–6, pp. 899–907, 2014.

[44] J. Cao *et al.*, “The Characterisation of Pluripotent and Multipotent Stem Cells Using Fourier Transform Infrared Microspectroscopy,” *Int. J. Mol. Sci.*, vol. 14, no. 9, pp. 17453–17476, 2013.

[45] F. Matsuoka *et al.*, “Morphology-Based Prediction of Osteogenic Differentiation Potential of Human Mesenchymal Stem Cells,” *PLoS One*, vol. 8, no. 2, p. e55082, 2013.

[46] T. Bongiorno *et al.*, “Mechanical stiffness as an improved single-cell indicator of osteoblastic human mesenchymal stem cell differentiation,” *J. Biomech.*, vol. 47, no. 9, pp. 2197–2204, 2014.

[47] J. Levsky, “Gene expression and the myth of the average cell,” *Trends Cell Biol.*, vol. 13, no. 1, pp. 4–6, 2003.

[48] N. D. Evans and E. Gentleman, “The role of material structure and mechanical properties in cell–matrix interactions,” *J. Mater. Chem. B*, vol. 2, no. 17, p. 2345, 2014.

[49] T. Iskratsch, H. Wolfenson, and M. P. Sheetz, “Appreciating force and shape — the rise of mechanotransduction in cell biology,” *Nat. Rev. Mol. Cell Biol.*, vol. 15, no. 12, pp. 825–833, 2014.

[50] E. Moeendarbary and A. R. Harris, “Cell mechanics: principles, practices, and prospects,” *Wiley Interdiscip. Rev. Syst. Biol. Med.*, vol. 6, no. 5, pp. 371–388, 2014.

[51] M. I. Z. Ridzwan, S. Shuib, A. Y. Hassan, A. A. Shokri, and M. N. Mohammad Ibrahim, “Problem of stress shielding and improvement to the hip implant designs: A review,” *Journal of Medical Sciences*, vol. 7, no. 3. pp. 460–467, 2007.

[52] E. van Haaften, C. Bouten, and N. Kurniawan, “Vascular Mechanobiology: Towards Control of In Situ Regeneration,” *Cells*, vol. 6, no. 3, p. 19, 2017.

[53] R. M. Pedrigi *et al.*, “Disturbed Cyclical Stretch of Endothelial Cells Promotes Nuclear Expression of the Pro-Atherogenic Transcription Factor NF-κB,” *Ann. Biomed. Eng.*, vol. 45, no. 4, pp. 898–909, 2017.

[54] K. R. Levental *et al.*, “Matrix Crosslinking Forces Tumor Progression by Enhancing Integrin Signaling,” *Cell*, vol. 139, no. 5, pp. 891–906, 2009.

[55] D. E. Discher, “Tissue Cells Feel and Respond to the Stiffness of Their Substrate,” *Science (80-.).*, vol. 310, no. 5751, pp. 1139–1143, 2005.

[56] M. Darnell *et al.*, “Substrate Stress-Relaxation Regulates Scaffold Remodeling and Bone Formation In Vivo,” *Adv. Healthc. Mater.*, 2017.

[57] M. Darnell and D. J. Mooney, “Leveraging advances in biology to design biomaterials,” *Nat. Mater.*, vol. 16, no. 12, pp. 1178–1185, Dec. 2017.

[58] A. Chramiec and G. Vunjak-Novakovic, “Tissue engineered models of healthy and malignant

human bone marrow," *Adv. Drug Deliv. Rev.*, Apr. 2019.

[59] R. J. McMurray, M. J. Dalby, and P. M. Tsimbouri, "Using biomaterials to study stem cell mechanotransduction, growth and differentiation," *J. Tissue Eng. Regen. Med.*, vol. 9, no. 5, pp. 528–539, 2014.

[60] T. D. Ross *et al.*, "Integrins in mechanotransduction," *Curr. Opin. Cell Biol.*, vol. 25, no. 5, pp. 613–618, 2013.

[61] B. D. Hoffman, C. Grashoff, and M. A. Schwartz, "Dynamic molecular processes mediate cellular mechanotransduction," *Nature*, vol. 475, no. 7356, pp. 316–323, 2011.

[62] L. MacQueen, Y. Sun, and C. A. Simmons, "Mesenchymal stem cell mechanobiology and emerging experimental platforms," *J. R. Soc. Interface*, vol. 10, no. 84, p. 20130179, 2013.

[63] M. L. Gardel, I. C. Schneider, Y. Aratyn-Schaus, and C. M. Waterman, "Mechanical Integration of Actin and Adhesion Dynamics in Cell Migration," *Annu. Rev. Cell Dev. Biol.*, vol. 26, no. 1, pp. 315–333, Nov. 2010.

[64] M. L. G. W. O. Designed Research; P, "Lamellipodium is a myosin-independent mechanosensor."

[65] B. Klapholz and N. H. Brown, "Talin - the master of integrin adhesions.," *J. Cell Sci.*, vol. 130, no. 15, pp. 2435–2446, Aug. 2017.

[66] A. Carisey and C. Ballestrem, "Vinculin, an adapter protein in control of cell adhesion signalling," *Eur. J. Cell Biol.*, vol. 90, no. 2–3, pp. 157–163, Feb. 2011.

[67] H. B. Schiller, C. C. Friedel, C. Boulegue, and R. Fässler, "Quantitative proteomics of the integrin adhesome show a myosin II-dependent recruitment of LIM domain proteins.," *EMBO Rep.*, vol. 12, no. 3, pp. 259–66, Mar. 2011.

[68] J. E. Frith, R. J. Mills, J. E. Hudson, and J. J. Cooper-White, "Tailored Integrin–Extracellular Matrix Interactions to Direct Human Mesenchymal Stem Cell Differentiation," *Stem Cells Dev.*, vol. 21, no. 13, pp. 2442–2456, 2012.

[69] E. Ruoslahti, "RGD AND OTHER RECOGNITION SEQUENCES FOR INTEGRINS," *Annu. Rev. Cell Dev. Biol.*, vol. 12, no. 1, pp. 697–715, 1996.

[70] S. L. Bellis, "Advantages of RGD peptides for directing cell association with biomaterials," *Biomaterials*, vol. 32, no. 18, pp. 4205–4210, 2011.

[71] M. A. Schwartz and D. W. DeSimone, "Cell adhesion receptors in mechanotransduction," *Current Opinion in Cell Biology*, vol. 20, no. 5. pp. 551–556, 2008.

[72] C. Ciobanasu, B. Faivre, and C. Le Clainche, "Actin Dynamics Associated with Focal Adhesions," *Int. J. Cell Biol.*, vol. 2012, pp. 1–9, 2012.

[73] J. Seong, N. Wang, and Y. Wang, "Mechanotransduction at focal adhesions: from physiology to cancer development," *J. Cell. Mol. Med.*, vol. 17, no. 5, pp. 597–604, 2013.

[74] B. Li, C. Moshfegh, Z. Lin, J. Albuschies, and V. Vogel, "Mesenchymal stem cells exploit extracellular matrix as mechanotransducer," *Sci. Rep.*, vol. 3, 2013.

[75] S. Huveneers and J. de Rooij, "Mechanosensitive systems at the cadherin-F-actin interface," *J. Cell Sci.*, vol. 126, no. 2, pp. 403–413, 2013.

[76] K. Xu, H. P. Babcock, and X. Zhuang, "Dual-objective STORM reveals three-dimensional filament organization in the actin cytoskeleton," *Nat. Methods*, vol. 9, no. 2, pp. 185–188, 2012.

[77] J. Käs *et al.*, "F-actin, a model polymer for semiflexible chains in dilute, semidilute, and liquid crystalline solutions.," *Biophys. J.*, vol. 70, no. 2, pp. 609–25, Feb. 1996.

[78] S. Rhee, H. Jiang, C.-H. Ho, and F. Grinnell, "Microtubule function in fibroblast spreading is modulated according to the tension state of cell-matrix interactions.," *Proc. Natl. Acad. Sci. U.*

S. A., vol. 104, no. 13, pp. 5425–30, Mar. 2007.

[79] S. R. K. Meka, L. A. Chacko, A. Ravi, K. Chatterjee, and V. Ananthanarayanan, “Role of Microtubules in Osteogenic Differentiation of Mesenchymal Stem Cells on 3D Nanofibrous Scaffolds,” *ACS Biomater. Sci. Eng.*, vol. 3, no. 4, pp. 551–559, Apr. 2017.

[80] K. A. Jansen, D. M. Donato, H. E. Balcioglu, T. Schmidt, E. H. J. Danen, and G. H. Koenderink, “A guide to mechanobiology: Where biology and physics meet,” *Biochim. Biophys. Acta - Mol. Cell Res.*, vol. 1853, no. 11, pp. 3043–3052, Nov. 2015.

[81] S. D. Thorpe and D. A. Lee, “Dynamic regulation of nuclear architecture and mechanics—a rheostatic role for the nucleus in tailoring cellular mechanosensitivity,” *Nucleus*, vol. 8, no. 3. pp. 287–300, 2017.

[82] J. Irianto, I. L. Ivanovska, J. Swift, and D. E. Discher, “The Nuclear Lamina: From Mechanosensing in Differentiation to Cancer Cell Migration,” in *Molecular and Cellular Mechanobiology*, 2016, pp. 175–195.

[83] J. Swift *et al.*, “Nuclear lamin-A scales with tissue stiffness and enhances matrix-directed differentiation,” *Science (80-.).*, vol. 341, no. 6149, 2013.

[84] E. S. Chhabra and H. N. Higgs, “The many faces of actin: matching assembly factors with cellular structures,” *Nat. Cell Biol.*, vol. 9, no. 10, pp. 1110–1121, 2007.

[85] L. Blanchoin, R. Boujemaa-Paterski, C. Sykes, and J. Plastino, “Actin Dynamics, Architecture, and Mechanics in Cell Motility,” *Physiol. Rev.*, vol. 94, no. 1, pp. 235–263, 2014.

[86] S. Tojkander, G. Gateva, and P. Lappalainen, “Actin stress fibers - assembly, dynamics and biological roles,” *J. Cell Sci.*, vol. 125, no. 8, pp. 1855–1864, 2012.

[87] MBInfo, “How are actin filaments distributed in cells and tissues?” [Online]. Available: https://www.mechanobio.info/cytoskeleton-dynamics/what-is-the-cytoskeleton/what-are-actin-filaments/how-are-actin-filaments-distributed-in-cells-and-tissues/. [Accessed: 12-Feb-2018].

[88] I. Titushkin and M. Cho, “Modulation of Cellular Mechanics during Osteogenic Differentiation of Human Mesenchymal Stem Cells,” *Biophys. J.*, vol. 93, no. 10, pp. 3693–3702, 2007.

[89] E. Puklin-Faucher, M. Gao, K. Schulten, and V. Vogel, “How the headpiece hinge angle is opened: New insights into the dynamics of integrin activation,” *J. Cell Biol.*, vol. 175, no. 2, pp. 349–360, 2006.

[90] A. R. Gingras *et al.*, “Structural and dynamic characterization of a vinculin binding site in the talin rod,” *Biochemistry*, vol. 45, no. 6, pp. 1805–1817, 2006.

[91] N. Wang, J. D. Tytell, and D. E. Ingber, “Mechanotransduction at a distance: mechanically coupling the extracellular matrix with the nucleus,” *Nat. Rev. Mol. Cell Biol.*, vol. 10, no. 1, pp. 75–82, 2009.

[92] S. Piccolo, S. Dupont, and M. Cordenonsi, “The Biology of YAP/TAZ: Hippo Signaling and Beyond,” *Physiol. Rev.*, vol. 94, no. 4, pp. 1287–1312, 2014.

[93] S. Dupont *et al.*, “Role of YAP/TAZ in mechanotransduction,” *Nature*, vol. 474, no. 7350, pp. 179–183, 2011.

[94] S. Dupont, “Role of YAP/TAZ in cell-matrix adhesion-mediated signalling and mechanotransduction,” *Exp. Cell Res.*, vol. 343, no. 1, pp. 42–53, Apr. 2016.

[95] D. Li, J. Zhou, F. Chowdhury, J. Cheng, N. Wang, and F. Wang, “Role of mechanical factors in fate decisions of stem cells,” *Regen. Med.*, vol. 6, no. 2, pp. 229–240, 2011.

[96] A. Elosegui-Artola *et al.*, “Force Triggers YAP Nuclear Entry by Regulating Transport across Nuclear Pores,” *Cell*, vol. 171, no. 6, p. 1397–1410.e14, 2017.

[97] M. Ahearne, “Introduction to cell-hydrogel mechanosensing,” *Interface Focus*, vol. 4, no. 2, p.

20130038, 2014.

[98] M. L. Oyen, “Mechanical characterisation of hydrogel materials,” *Int. Mater. Rev.*, vol. 59, no. 1, pp. 44–59, 2013.

[99] W. Megone, N. Roohpour, and J. E. Gautrot, “Impact of surface adhesion and sample heterogeneity on the multiscale mechanical characterisation of soft biomaterials,” *Sci. Rep.*, vol. 8, no. 1, 2018.

[100] J. H. Wen *et al.*, “Interplay of matrix stiffness and protein tethering in stem cell differentiation,” *Nat. Mater.*, vol. 13, no. 10, pp. 979–987, 2014.

[101] J. Fu *et al.*, “Mechanical regulation of cell function with geometrically modulated elastomeric substrates,” *Nat. Methods*, vol. 7, no. 9, pp. 733–736, 2010.

[102] M. Guvendiren and J. A. Burdick, “Stiffening hydrogels to probe short- and long-term cellular responses to dynamic mechanics,” *Nat. Commun.*, vol. 3, no. 1, 2012.

[103] J. Lee, A. A. Abdeen, and K. A. Kilian, “Rewiring mesenchymal stem cell lineage specification by switching the biophysical microenvironment,” *Sci. Rep.*, vol. 4, no. 1, 2014.

[104] O. F. Zouani, J. Kalisky, E. Ibarboure, and M.-C. Durrieu, “Effect of BMP-2 from matrices of different stiffnesses for the modulation of stem cell fate,” *Biomaterials*, vol. 34, no. 9, pp. 2157–2166, 2013.

[105] B. Trappmann *et al.*, “Extracellular-matrix tethering regulates stem-cell fate,” *Nat. Mater.*, vol. 11, no. 7, pp. 642–649, 2012.

[106] O. Chaudhuri and D. J. Mooney, “Anchoring cell-fate cues,” *Nat. Mater.*, vol. 11, p. 568, 2012.

[107] A. S. Rowlands, P. A. George, and J. J. Cooper-White, “Directing osteogenic and myogenic differentiation of MSCs: interplay of stiffness and adhesive ligand presentation,” *Am. J. Physiol. Physiol.*, vol. 295, no. 4, pp. C1037–C1044, 2008.

[108] E. A. Cavalcanti-Adam, T. Volberg, A. Micoulet, H. Kessler, B. Geiger, and J. P. Spatz, “Cell spreading and focal adhesion dynamics are regulated by spacing of integrin ligands.,” *Biophys. J.*, vol. 92, no. 8, pp. 2964–74, Apr. 2007.

[109] M. Schvartzman *et al.*, “Nanolithographic Control of the Spatial Organization of Cellular Adhesion Receptors at the Single-Molecule Level,” *Nano Lett.*, vol. 11, no. 3, pp. 1306–1312, Mar. 2011.

[110] X. Wang, C. Yan, K. Ye, Y. He, Z. Li, and J. Ding, “Effect of RGD nanospacing on differentiation of stem cells,” *Biomaterials*, vol. 34, no. 12, pp. 2865–2874, 2013.

[111] J. E. Frith, R. J. Mills, and J. J. Cooper-White, “Lateral spacing of adhesion peptides influences human mesenchymal stem cell behaviour,” *J. Cell Sci.*, vol. 125, no. 2, pp. 317–327, 2012.

[112] B. M. Baker *et al.*, “Cell-mediated fibre recruitment drives extracellular matrix mechanosensing in engineered fibrillar microenvironments,” *Nat. Mater.*, vol. 14, no. 12, pp. 1262–1268, 2015.

[113] J. Xie, M. Bao, S. M. C. Bruekers, and W. T. S. Huck, “Collagen Gels with Different Fibrillar Microarchitectures Elicit Different Cellular Responses,” *ACS Appl. Mater. Interfaces*, vol. 9, no. 23, pp. 19630–19637, 2017.

[114] K. A. Kilian, B. Bugarija, B. T. Lahn, and M. Mrksich, “Geometric cues for directing the differentiation of mesenchymal stem cells,” *Proc. Natl. Acad. Sci.*, vol. 107, no. 11, pp. 4872–4877, 2010.

[115] R. Peng, X. Yao, and J. Ding, “Effect of cell anisotropy on differentiation of stem cells on micropatterned surfaces through the controlled single cell adhesion,” *Biomaterials*, vol. 32, no. 32, pp. 8048–8057, 2011.

[116] X. Yao, R. Peng, and J. Ding, “Effects of aspect ratios of stem cells on lineage commitments

with and without induction media," *Biomaterials*, vol. 34, no. 4, pp. 930–939, 2013.

[117] M. J. Dalby *et al.*, "The control of human mesenchymal cell differentiation using nanoscale symmetry and disorder," *Nat. Mater.*, vol. 6, no. 12, pp. 997–1003, 2007.

[118] G. Abagnale *et al.*, "Surface topography enhances differentiation of mesenchymal stem cells towards osteogenic and adipogenic lineages," *Biomaterials*, vol. 61, pp. 316–326, 2015.

[119] H. Lu *et al.*, "Effect of cell density on adipogenic differentiation of mesenchymal stem cells," *Biochem. Biophys. Res. Commun.*, vol. 381, no. 3, pp. 322–327, 2009.

[120] R. Peng, X. Yao, B. Cao, J. Tang, and J. Ding, "The effect of culture conditions on the adipogenic and osteogenic inductions of mesenchymal stem cells on micropatterned surfaces," *Biomaterials*, vol. 33, no. 26, pp. 6008–6019, 2012.

[121] B. D. Cosgrove *et al.*, "N-cadherin adhesive interactions modulate matrix mechanosensing and fate commitment of mesenchymal stem cells," *Nat. Mater.*, 2016.

[122] Y. Sun, C. S. Chen, and J. Fu, "Forcing Stem Cells to Behave: A Biophysical Perspective of the Cellular Microenvironment," *Annu. Rev. Biophys.*, vol. 41, no. 1, pp. 519–542, 2012.

[123] J. S. Park, J. S. F. Chu, C. Cheng, F. Chen, D. Chen, and S. Li, "Differential effects of equiaxial and uniaxial strain on mesenchymal stem cells," *Biotechnol. Bioeng.*, vol. 88, no. 3, pp. 359–368, 2004.

[124] Y.-K. Wang and C. S. Chen, "Cell adhesion and mechanical stimulation in the regulation of mesenchymal stem cell differentiation," *J. Cell. Mol. Med.*, vol. 17, no. 7, pp. 823–832, 2013.

[125] D. R. Wagner *et al.*, "Hydrostatic Pressure Enhances Chondrogenic Differentiation of Human Bone Marrow Stromal Cells in Osteochondrogenic Medium," *Ann. Biomed. Eng.*, vol. 36, no. 5, pp. 813–820, 2008.

[126] A. J. Steward, S. D. Thorpe, T. Vinardell, C. T. Buckley, D. R. Wagner, and D. J. Kelly, "Cell–matrix interactions regulate mesenchymal stem cell response to hydrostatic pressure," *Acta Biomater.*, vol. 8, no. 6, pp. 2153–2159, 2012.

[127] D. Pelaez, C.-Y. Charles Huang, and H. S. Cheung, "Cyclic Compression Maintains Viability and Induces Chondrogenesis of Human Mesenchymal Stem Cells in Fibrin Gel Scaffolds," *Stem Cells Dev.*, vol. 18, no. 1, pp. 93–102, 2009.

[128] J. Liu *et al.*, "Hydrostatic pressures promote initial osteodifferentiation with ERK1/2 not p38 MAPK signaling involved," *J. Cell. Biochem.*, vol. 107, no. 2, pp. 224–232, 2009.

[129] E. Michalopoulos, R. L. Knight, S. Korossis, J. N. Kearney, J. Fisher, and E. Ingham, "Development of Methods for Studying the Differentiation of Human Mesenchymal Stem Cells Under Cyclic Compressive Strain," *Tissue Eng. Part C Methods*, vol. 18, no. 4, pp. 252–262, 2012.

[130] A. Sittichokechaiwut, J. H. Edwards, A. M. Scutt, and G. C. Reilly, "Short bouts of mechanical loading are as effective as dexamethasone at inducing matrix production by human bone marrow mesenchymal stem cells," *Eur. Cells Mater.*, vol. 20, pp. 45–57, 2010.

[131] Y. Huang *et al.*, "Effect of Cyclic Strain on Cardiomyogenic Differentiation of Rat Bone Marrow Derived Mesenchymal Stem Cells," *PLoS One*, vol. 7, no. 4, p. e34960, 2012.

[132] T. M. Maul, D. W. Chew, A. Nieponice, and D. A. Vorp, "Mechanical stimuli differentially control stem cell behavior: morphology, proliferation, and differentiation," *Biomech. Model. Mechanobiol.*, vol. 10, no. 6, pp. 939–953, 2011.

[133] Y.-J. Chen, C.-H. Huang, I.-C. Lee, Y.-T. Lee, M.-H. Chen, and T.-H. Young, "Effects of Cyclic Mechanical Stretching on the mRNA Expression of Tendon/Ligament-Related and Osteoblast-Specific Genes in Human Mesenchymal Stem Cells," *Connect. Tissue Res.*, vol. 49, no. 1, pp.

7–14, 2008.

[134] C.-H. Huang, M.-H. Chen, T.-H. Young, J.-H. Jeng, and Y.-J. Chen, “Interactive effects of mechanical stretching and extracellular matrix proteins on initiating osteogenic differentiation of human mesenchymal stem cells,” *J. Cell. Biochem.*, vol. 108, no. 6, pp. 1263–1273, 2009.

[135] M. Ngiam *et al.*, “Effects of mechanical stimulation in osteogenic differentiation of bone marrow-derived mesenchymal stem cells on aligned nanofibrous scaffolds,” *J. Bioact. Compat. Polym.*, vol. 26, no. 1, pp. 56–70, 2010.

[136] J. S. Lee, L. Ha, J.-H. Park, and J. Y. Lim, “Mechanical stretch suppresses BMP4 induction of stem cell adipogenesis via upregulating ERK but not through downregulating Smad or p38,” *Biochem. Biophys. Res. Commun.*, vol. 418, no. 2, pp. 278–283, 2012.

[137] L. F. Bonewald, “The amazing osteocyte,” *J. Bone Miner. Res.*, vol. 26, no. 2, pp. 229–238, 2011.

[138] R. M. Delaine-Smith and G. C. Reilly, “Mesenchymal stem cell responses to mechanical stimuli.,” *Muscles. Ligaments Tendons J.*, vol. 2, no. 3, pp. 169–80, 2012.

[139] P. Flood, H. Page, and E. G. Reynaud, “Using hydrogels in microscopy: A tutorial,” *Micron*, vol. 84, pp. 7–16, 2016.

[140] S. I. Fraley *et al.*, “A distinctive role for focal adhesion proteins in three-dimensional cell motility,” *Nat. Cell Biol.*, vol. 12, no. 6, pp. 598–604, 2010.

[141] M.-P. Pebworth, S. A. Cismas, and P. Asuri, “A Novel 2.5D Culture Platform to Investigate the Role of Stiffness Gradients on Adhesion-Independent Cell Migration,” *PLoS One*, vol. 9, no. 10, p. e110453, 2014.

[142] F. Rehfeldt *et al.*, “Hyaluronic acid matrices show matrix stiffness in 2D and 3D dictates cytoskeletal order and myosin-II phosphorylation within stem cells,” *Integr. Biol.*, vol. 4, no. 4, p. 422, 2012.

[143] N. Huebsch *et al.*, “Harnessing traction-mediated manipulation of the cell/matrix interface to control stem-cell fate,” *Nat. Mater.*, vol. 9, no. 6, pp. 518–526, 2010.

[144] M. Bao, J. Xie, A. Piruska, and W. T. S. Huck, “3D microniches reveal the importance of cell size and shape,” *Nat. Commun.*, vol. 8, no. 1, 2017.

[145] P. Viswanathan *et al.*, “3D surface topology guides stem cell adhesion and differentiation,” *Biomaterials*, vol. 52, pp. 140–147, 2015.

[146] S. Tripathy and E. J. Berger, “Measuring Viscoelasticity of Soft Samples Using Atomic Force Microscopy,” *J. Biomech. Eng.*, vol. 131, no. 9, p. 94507, 2009.

[147] L. Li, J. Eyckmans, and C. S. Chen, “Designer biomaterials for mechanobiology,” *Nature Materials*, vol. 16, no. 12. pp. 1164–1168, 2017.

[148] S. Misra, K. T. Ramesh, and A. M. Okamura, “Modeling of tool-tissue interactions for computer-based surgical simulation: A literature review,” *Presence Teleoperators Virtual Environ.*, vol. 17, no. 5, pp. 463–491, 2008.

[149] A. R. Cameron, J. E. Frith, and J. J. Cooper-White, “The influence of substrate creep on mesenchymal stem cell behaviour and phenotype,” *Biomaterials*, vol. 32, no. 26, pp. 5979–5993, 2011.

[150] O. Chaudhuri *et al.*, “Substrate stress relaxation regulates cell spreading,” *Nat. Commun.*, 2015.

[151] O. Chaudhuri *et al.*, “Hydrogels with tunable stress relaxation regulate stem cell fate and activity,” *Nat. Mater.*, 2016.

[152] C. Storm, J. J. Pastore, F. C. MacKintosh, T. C. Lubensky, and P. A. Janmey, “Nonlinear

elasticity in biological gels," *Nature*, vol. 435, no. 7039, pp. 191–194, 2005.

[153] J. P. Winer, S. Oake, and P. A. Janmey, "Non-linear elasticity of extracellular matrices enables contractile cells to communicate local position and orientation," *PLoS One*, vol. 4, no. 7, 2009.

[154] R. K. Das, V. Gocheva, R. Hammink, O. F. Zouani, and A. E. Rowan, "Stress-stiffening-mediated stem-cell commitment switch in soft responsive hydrogels," *Nat. Mater.*, vol. 15, no. 3, pp. 318–325, 2016.

[155] S. Khetan, M. Guvendiren, W. R. Legant, D. M. Cohen, C. S. Chen, and J. A. Burdick, "Degradation-mediated cellular traction directs stem cell fate in covalently crosslinked three-dimensional hydrogels," *Nat. Mater.*, vol. 12, no. 5, pp. 458–465, 2013.

[156] S. R. Caliari, S. L. Vega, M. Kwon, E. M. Soulas, and J. A. Burdick, "Dimensionality and spreading influence MSC YAP/TAZ signaling in hydrogel environments," *Biomaterials*, 2016.

[157] Y. Peng, Q. J. Liu, T. He, K. Ye, X. Yao, and J. Ding, "Degradation rate affords a dynamic cue to regulate stem cells beyond varied matrix stiffness," *Biomaterials*, vol. 178, pp. 467–480, 2018.

[158] S. Nam, J. Lee, D. G. Brownfield, and O. Chaudhuri, "Viscoplasticity Enables Mechanical Remodeling of Matrix by Cells," *Biophys. J.*, vol. 111, no. 10, pp. 2296–2308, 2016.

[159] S. Nam, K. H. Hu, M. J. Butte, and O. Chaudhuri, "Strain-enhanced stress relaxation impacts nonlinear elasticity in collagen gels," *Proc. Natl. Acad. Sci.*, vol. 113, no. 20, pp. 5492–5497, 2016.

[160] J. Kim *et al.*, "Stress-induced plasticity of dynamic collagen networks," *Nat. Commun.*, vol. 8, no. 1, p. 842, 2017.

[161] A. K. Shalek and M. Benson, "Single-cell analyses to tailor treatments," *Sci. Transl. Med.*, vol. 9, no. 408, 2017.

[162] K. W. Eliceiri *et al.*, "Biological imaging software tools," *Nat. Methods*, vol. 9, no. 7, pp. 697–710, 2012.

[163] S. M. C. Bruekers, M. Bao, J. M. A. Hendriks, K. W. Mulder, and W. T. S. Huck, "Adaptation trajectories during adhesion and spreading affect future cell states," *Sci. Rep.*, vol. 7, no. 1, 2017.

[164] B. Eltzner, C. Wollnik, C. Gottschlich, S. Huckemann, and F. Rehfeldt, "The filament sensor for near real-time detection of cytoskeletal fiber structures," *PLoS One*, vol. 10, no. 5, 2015.

[165] M. C. Keeling, L. R. Flores, A. H. Dodhy, E. R. Murray, and N. Gavara, "Actomyosin and vimentin cytoskeletal networks regulate nuclear shape, mechanics and chromatin organization," *Sci. Rep.*, vol. 7, no. 1, pp. 1–14, 2017.

[166] S. J. Heo *et al.*, "Differentiation alters stem cell nuclear architecture, mechanics, and mechano-sensitivity," *Elife*, vol. 5, no. NOVEMBER2016, 2016.

[167] M. Gupta *et al.*, "Adaptive rheology and ordering of cell cytoskeleton govern matrix rigidity sensing," *Nat. Commun.*, vol. 6, 2015.

[168] N. Gavara and R. S. Chadwick, "Relationship between cell stiffness and stress fiber amount, assessed by simultaneous atomic force microscopy and live-cell fluorescence imaging," *Biomech. Model. Mechanobiol.*, vol. 15, no. 3, pp. 511–523, 2015.

[169] A. H. Dodhy, "Population based evaluation of actin cytoskeletal morphometric descriptors as characterisation of stem cell differentiation," QMUL, 2018.

[170] A. Zemel, F. Rehfeldt, A. E. X. Brown, D. E. Discher, and S. A. Safran, "Optimal matrix rigidity for stress-fibre polarization in stem cells," *Nat. Phys.*, vol. 6, no. 6, pp. 468–473, 2010.

[171] J. M. Phillip *et al.*, "Biophysical and biomolecular determination of cellular age in humans," *Nat.*

Biomed. Eng., vol. 1, no. 7, 2017.

[172] M. D. Treiser *et al.*, “Cytoskeleton-based forecasting of stem cell lineage fates,” *Proc. Natl. Acad. Sci.*, vol. 107, no. 2, pp. 610–615, 2009.

[173] S. L. Vega *et al.*, “High-content imaging-based screening of microenvironment-induced changes to stem cells,” *J. Biomol. Screen.*, vol. 17, no. 9, pp. 1151–1162, 2012.

[174] H. Sasaki *et al.*, “Label-free morphology-based prediction of multiple differentiation potentials of human mesenchymal stem cells for early evaluation of intact cells,” *PLoS One*, vol. 9, no. 4, 2014.

[175] C. Sommer and D. W. Gerlich, “Machine learning in cell biology – teaching computers to recognize phenotypes,” *J. Cell Sci.*, vol. 126, no. 24, pp. 5529–5539, 2013.

[176] A. L. Tarca, V. J. Carey, X. Chen, R. Romero, and S. Drăghici, “Machine Learning and Its Applications to Biology,” *PLoS Comput. Biol.*, vol. 3, no. 6, p. e116, 2007.

[177] C. A. Herring, B. Chen, E. T. McKinley, and K. S. Lau, “Single-Cell Computational Strategies for Lineage Reconstruction in Tissue Systems,” *CMGH*, vol. 5, no. 4. pp. 539–548, 2018.

[178] S. C. Bendall *et al.*, “Single-cell trajectory detection uncovers progression and regulatory coordination in human b cell development,” *Cell*, vol. 157, no. 3, pp. 714–725, 2014.

[179] E. Lummertz Da Rocha *et al.*, “Reconstruction of complex single-cell trajectories using CellRouter,” *Nat. Commun.*, vol. 9, no. 1, 2018.

[180] C. Trapnell *et al.*, “The dynamics and regulators of cell fate decisions are revealed by pseudotemporal ordering of single cells,” *Nat. Biotechnol.*, vol. 32, no. 4, pp. 381–386, 2014.

[181] D. Georgios, “Support Vector Machine vs Logistic Regression.” [Online]. Available: https://towardsdatascience.com/support-vector-machine-vs-logistic-regression-94cc2975433f. [Accessed: 12-Feb-2018].

[182] M. Melak, M. Plessner, and R. Grosse, “Correction: Actin visualization at a glance,” *J. Cell Sci.*, vol. 130, no. 9, pp. 1688–1688, 2017.

[183] J. Wehland, M. Osborn, and K. Weber, “Phalloidin-induced actin polymerization in the cytoplasm of cultured cells interferes with cell locomotion and growth,” *Proc. Natl. Acad. Sci.*, vol. 74, no. 12, pp. 5613–5617, 1977.

[184] J. Riedl *et al.*, “Lifeact: a versatile marker to visualize F-actin.,” *Nat. Methods*, vol. 5, no. 7, pp. 605–607, 2008.

[185] N. Courtemanche, T. D. Pollard, and Q. Chen, “Avoiding artefacts when counting polymerized actin in live cells with LifeAct fused to fluorescent proteins,” *Nat. Cell Biol.*, vol. 18, no. 6, pp. 676–683, 2016.

[186] A. J. Spracklen, T. N. Fagan, K. E. Lovander, and T. L. Tootle, “The pros and cons of common actin labeling tools for visualizing actin dynamics during Drosophila oogenesis,” *Dev. Biol.*, vol. 393, no. 2, pp. 209–226, 2014.

[187] P. Zarrintaj *et al.*, “Agarose-based biomaterials for tissue engineering,” *Carbohydrate Polymers*, vol. 187. pp. 66–84, 2018.

[188] Z. Cao, R. J. Gilbert, and W. He, “Simple Agarose−Chitosan Gel Composite System for Enhanced Neuronal Growth in Three Dimensions,” *Biomacromolecules*, vol. 10, no. 10, pp. 2954–2959, 2009.

[189] Y. Suzawa, N. Kubo, S. Iwai, Y. Yura, H. Ohgushi, and M. Akashi, “Biomineral/agarose composite gels enhance proliferation of mesenchymal stem cells with osteogenic capability,” *Int. J. Mol. Sci.*, vol. 16, no. 6, pp. 14245–14258, 2015.

[190] M. Köpf, D. F. D. Campos, A. Blaeser, K. S. Sen, and H. Fischer, “A tailored three-

dimensionally printable agarose-collagen blend allows encapsulation, spreading, and attachment of human umbilical artery smooth muscle cells," *Biofabrication*, vol. 8, no. 2, p. 25011, 2016.

[191] A. D. Cigan *et al.*, "High seeding density of human chondrocytes in agarose produces tissue-engineered cartilage approaching native mechanical and biochemical properties," *J. Biomech.*, vol. 49, no. 9, pp. 1909–1917, 2016.

[192] M. A. Soltz, "Functional Tissue Engineering of Articular Cartilage Through Dynamic Loading of Chondrocyte-Seeded Agarose Gels," *J. Biomech. Eng.*, vol. 122, no. 3, p. 252, 2000.

[193] B. Pingguan-Murphy, D. A. Lee, D. L. Bader, and M. M. Knight, "Activation of chondrocytes calcium signalling by dynamic compression is independent of number of cycles," *Arch. Biochem. Biophys.*, vol. 444, no. 1, pp. 45–51, 2005.

[194] M. C. Dodla and R. V. Bellamkonda, "Anisotropic scaffolds facilitate enhanced neurite extension in vitro," in *Journal of Biomedical Materials Research - Part A*, 2006, vol. 78, no. 2, pp. 213–221.

[195] C. Somaiah *et al.*, "Collagen promotes higher adhesion, survival and proliferation of mesenchymal stem cells," *PLoS One*, vol. 10, no. 12, 2015.

[196] K. M. Hennessy *et al.*, "The effect of collagen I mimetic peptides on mesenchymal stem cell adhesion and differentiation, and on bone formation at hydroxyapatite surfaces," *Biomaterials*, vol. 30, no. 10, pp. 1898–1909, 2009.

[197] J. Irianto, "Nuclear Related Responses to Osmotic Challenge in Chondrocytes," QMUL, 2013.

[198] R. M. Delaine-Smith and G. C. Reilly, "The Effects of Mechanical Loading on Mesenchymal Stem Cell Differentiation and Matrix Production," *Vitamins & Hormones*. Elsevier, pp. 417–480, 2011.

[199] Q. Tseng *et al.*, "Spatial organization of the extracellular matrix regulates cell-cell junction positioning," *Proc. Natl. Acad. Sci.*, vol. 109, no. 5, pp. 1506–1511, 2012.

[200] W. M. Jackson, M. J. Jaasma, R. Y. Tang, and T. M. Keaveny, "Mechanical loading by fluid shear is sufficient to alter the cytoskeletal composition of osteoblastic cells," *AJP Cell Physiol.*, vol. 295, no. 4, pp. C1007–C1015, 2008.

[201] M. Koike, H. Shimokawa, Z. Kanno, K. Ohya, and K. Soma, "Effects of mechanical strain on proliferation and differentiation of bone marrow stromal cell line ST2," *J. Bone Miner. Metab.*, vol. 23, no. 3, pp. 219–225, 2005.

[202] J. T. Connelly, A. J. García, and M. E. Levenston, "Interactions between integrin ligand density and cytoskeletal integrity regulate BMSC chondrogenesis," *J. Cell. Physiol.*, vol. 217, no. 1, pp. 145–154, 2008.

[203] J. T. Connelly, T. A. Petrie, A. J. García, and M. E. Levenston, "Fibronectin- and collagen-mimetic ligands regulate bone marrow stromal cell chondrogenesis in three-dimensional hydrogels," *Eur. Cells Mater.*, vol. 22, pp. 168–177, 2011.

[204] T. A. Ulrich, A. Jain, K. Tanner, J. L. MacKay, and S. Kumar, "Probing cellular mechanobiology in three-dimensional culture with collagen-agarose matrices," *Biomaterials*, vol. 31, no. 7, pp. 1875–1884, 2010.

[205] D. A. Young, Y. S. Choi, A. J. Engler, and K. L. Christman, "Stimulation of adipogenesis of adult adipose-derived stem cells using substrates that mimic the stiffness of adipose tissue," *Biomaterials*, vol. 34, no. 34, pp. 8581–8588, 2013.

[206] C. G. Tusan *et al.*, "Collective Cell Behavior in Mechanosensing of Substrate Thickness," *Biophys. J.*, vol. 114, no. 11, pp. 2743–2755, 2018.

[207] C. Gaudet *et al.*, “Influence of Type I Collagen Surface Density on Fibroblast Spreading, Motility, and Contractility,” *Biophys. J.*, vol. 85, no. 5, pp. 3329–3335, 2003.

[208] S. Syed, A. Karadaghy, and S. Zustiak, “Simple Polyacrylamide-based Multiwell Stiffness Assay for the Study of Stiffness-dependent Cell Responses,” *J. Vis. Exp.*, no. 97, 2015.

[209] R. S. Fischer, K. A. Myers, M. L. Gardel, and C. M. Waterman, “Stiffness-controlled three-dimensional extracellular matrices for high-resolution imaging of cell behavior,” *Nat. Protoc.*, vol. 7, no. 11, pp. 2056–2066, 2012.

[210] T. Chaudhuri, F. Rehfeldt, H. L. Sweeney, and D. E. Discher, “Preparation of collagen-coated gels that maximize in vitro myogenesis of stem cells by matching the lateral elasticity of in vivo muscle.,” *Methods Mol. Biol.*, vol. 621, pp. 185–202, 2010.

[211] B. Li, J. Chen, and J. H.-C. Wang, “RGD peptide-conjugated poly(dimethylsiloxane) promotes adhesion, proliferation, and collagen secretion of human fibroblasts,” *J. Biomed. Mater. Res. Part A*, vol. 79A, no. 4, pp. 989–998, 2006.

[212] J. R. Tse and A. J. Engler, “Preparation of hydrogel substrates with tunable mechanical properties,” *Current Protocols in Cell Biology*, no. SUPPL. 47. 2010.

[213] H. J. Kwon, “Chondrogenesis on sulfonate-coated hydrogels is regulated by their mechanical properties,” *J. Mech. Behav. Biomed. Mater.*, vol. 17, pp. 337–346, 2012.

[214] A. Farrukh *et al.*, “Hydrogels BioconjugatingThiols to Poly(acrylamide)Gels forCell Culture Using Methylsulfonyl Co-monomers.”

[215] T. Razafiarison *et al.*, “Biomaterial surface energy-driven ligand assembly strongly regulates stem cell mechanosensitivity and fate on very soft substrates.,” *Proc. Natl. Acad. Sci. U. S. A.*, vol. 115, no. 18, pp. 4631–4636, May 2018.

[216] S. Fusco, V. Panzetta, V. Embrione, and P. A. Netti, “Crosstalk between focal adhesions and material mechanical properties governs cell mechanics and functions,” *Acta Biomater.*, vol. 23, pp. 63–71, Sep. 2015.

[217] E. Schuh, S. Hofmann, K. Stok, H. Notbohm, R. Müller, and N. Rotter, “Chondrocyte redifferentiation in 3D: The effect of adhesion site density and substrate elasticity,” *J. Biomed. Mater. Res. Part A*, vol. 100A, no. 1, pp. 38–47, Jan. 2012.

[218] Y. Yang, X. Liu, W. Yu, H. Zhou, X. Li, and X. Ma, “Homogeneous synthesis of GRGDY grafted chitosan on hydroxyl groups by photochemical reaction for improved cell adhesion,” *Carbohydr. Polym.*, vol. 80, no. 3, pp. 733–739, May 2010.

[219] N. Rahman, K. A. Purpura, R. G. Wylie, P. W. Zandstra, and M. S. Shoichet, “The use of vascular endothelial growth factor functionalized agarose to guide pluripotent stem cell aggregates toward blood progenitor cells,” *Biomaterials*, vol. 31, no. 32, pp. 8262–8270, 2010.

[220] Y. Luo and M. S. Shoichet, “A photolabile hydrogel for guided three-dimensional cell growth and migration,” *Nat. Mater.*, vol. 3, no. 4, pp. 249–253, 2004.

[221] C. T. Buckley, S. D. Thorpe, F. J. O’Brien, A. J. Robinson, and D. J. Kelly, “The effect of concentration, thermal history and cell seeding density on the initial mechanical properties of agarose hydrogels,” *J. Mech. Behav. Biomed. Mater.*, vol. 2, no. 5, pp. 512–521, 2009.

[222] G. G. Bilodeau, “Regular Pyramid Punch Problem,” *J. Appl. Mech.*, vol. 59, no. 3, p. 519, 1992.

[223] N. Gavara, “Combined strategies for optimal detection of the contact point in AFM force-indentation curves obtained on thin samples and adherent cells,” *Sci. Rep.*, vol. 6, 2016.

[224] X. Zhao, N. Huebsch, D. J. Mooney, and Z. Suo, “Stress-relaxation behavior in gels with ionic and covalent crosslinks,” in *Journal of Applied Physics*, 2010, vol. 107, no. 6.

[225] E. Ban *et al.*, “Mechanisms of Plastic Deformation in Collagen Networks Induced by Cellular

Forces," *Biophys. J.*, vol. 114, no. 2, pp. 450–461, 2018.

[226] S. Sen, A. J. Engler, and D. E. Discher, "Matrix strains induced by cells: Computing how far cells can feel," *Cell. Mol. Bioeng.*, vol. 2, no. 1, pp. 39–48, 2009.

[227] H. Mohammadi, P. D. Arora, C. A. Simmons, P. A. Janmey, and C. A. McCulloch, "Inelastic behaviour of collagen networks in cell-matrix interactions and mechanosensation," *J. R. Soc. Interface*, vol. 12, no. 102, 2015.

[228] Q. Wen and P. A. Janmey, "Effects of non-linearity on cell-ECM interactions," *Experimental Cell Research*, vol. 319, no. 16. pp. 2481–2489, 2013.

[229] A. Prasad and E. Alizadeh, "Cell Form and Function: Interpreting and Controlling the Shape of Adherent Cells," *Trends in Biotechnology*, 2018.

[230] O. Chaudhuri, "Viscoelastic hydrogels for 3D cell culture," *Biomaterials Science*, vol. 5, no. 8. pp. 1480–1490, 2017.

[231] G. Vertelov, E. Gutierrez, S.-A. Lee, E. Ronan, A. Groisman, and E. Tkachenko, "Rigidity of silicone substrates controls cell spreading and stem cell differentiation," *Sci. Rep.*, vol. 6, no. 1, p. 33411, Dec. 2016.

[232] A. M. Rosales, S. L. Vega, F. W. DelRio, J. A. Burdick, and K. S. Anseth, "Hydrogels with Reversible Mechanics to Probe Dynamic Cell Microenvironments," *Angew. Chemie - Int. Ed.*, vol. 56, no. 40, pp. 12132–12136, 2017.

[233] S. R. Caliari, M. Perepelyuk, E. M. Soulas, G. Y. Lee, R. G. Wells, and J. A. Burdick, "Gradually softening hydrogels for modeling hepatic stellate cell behavior during fibrosis regression," *Integr. Biol. (United Kingdom)*, vol. 8, no. 6, pp. 720–728, 2016.

[234] M. Versaevel, T. Grevesse, and S. Gabriele, "Spatial coordination between cell and nuclear shape within micropatterned endothelial cells," *Nat. Commun.*, vol. 3, 2012.

[235] W. J. Hadden *et al.*, "Stem cell migration and mechanotransduction on linear stiffness gradient hydrogels," *Proc. Natl. Acad. Sci.*, vol. 114, no. 22, pp. 5647–5652, 2017.

[236] Z. Gong *et al.*, "Matching material and cellular timescales maximizes cell spreading on viscoelastic substrates," *Proc. Natl. Acad. Sci.*, p. 201716620, 2018.

[237] N. Pernodet, M. Maaloum, and B. Tinland, "Pore size of agarose gels by atomic force microscopy," *Electrophoresis*, vol. 18, no. 1, pp. 55–58, 1997.

[238] J. Narayanan, J. Y. Xiong, and X. Y. Liu, "Determination of agarose gel pore size: Absorbance measurements vis a vis other techniques," *J. Phys. Conf. Ser.*, vol. 28, no. 1, pp. 83–86, 2006.

[239] L. Bittnerová, A. Jiroutová, E. Rudolf, M. Řezáčová, and J. Kanta, "EFFECT OF COLLAGEN I GEL ON APOPTOSIS OF RAT HEPATIC STELLATE CELLS," 2013.

[240] J. Jokinen *et al.*, "Integrin-mediated Cell Adhesion to Type I Collagen Fibrils," *J. Biol. Chem.*, vol. 279, no. 30, pp. 31956–31963, Jul. 2004.

[241] M. Y. Ali, C.-Y. Chuang, and M. T. A. Saif, "Reprogramming cellular phenotype by soft collagen gels.," *Soft Matter*, vol. 10, no. 44, pp. 8829–37, Nov. 2014.

[242] S. Syed, A. Karadaghy, and S. Zustiak, "Simple polyacrylamide-based multiwell stiffness assay for the study of stiffness-dependent cell responses.," *J. Vis. Exp.*, no. 97, Mar. 2015.

[243] R. J. Pelham and Y. l Wang, "Cell locomotion and focal adhesions are regulated by substrate flexibility.," *Proc. Natl. Acad. Sci. U. S. A.*, vol. 94, no. 25, pp. 13661–5, Dec. 1997.

[244] E. E. Antoine, P. P. Vlachos, and M. N. Rylander, "Review of collagen I hydrogels for bioengineered tissue microenvironments: characterization of mechanics, structure, and transport.," *Tissue Eng. Part B. Rev.*, vol. 20, no. 6, pp. 683–96, Dec. 2014.

[245] J. T. Elliott, J. T. Woodward, K. J. Langenbach, A. Tona, P. L. Jones, and A. L. Plant,

"Vascular smooth muscle cell response on thin films of collagen," *Matrix Biol.*, vol. 24, no. 7, pp. 489–502, Oct. 2005.

[246] A. L. Plant, K. Bhadriraju, T. A. Spurlin, and J. T. Elliott, "Cell response to matrix mechanics: Focus on collagen," *Biochim. Biophys. Acta - Mol. Cell Res.*, vol. 1793, no. 5, pp. 893–902, May 2009.

[247] J. T. Elliott, M. Halter, A. L. Plant, J. T. Woodward, K. J. Langenbach, and A. Tona, "Evaluating the performance of fibrillar collagen films formed at polystyrene surfaces as cell culture substrates," 2008.

[248] W. S. Leong *et al.*, "Thickness sensing of hMSCs on collagen gel directs stem cell fate," *Biochem. Biophys. Res. Commun.*, vol. 401, no. 2, pp. 287–292, Oct. 2010.

[249] D. Kong, W. Megone, K. D. Q. Nguyen, S. Di Cio, M. Ramstedt, and J. E. Gautrot, "Protein Nanosheet Mechanics Controls Cell Adhesion and Expansion on Low-Viscosity Liquids," *Nano Lett.*, vol. 18, no. 3, pp. 1946–1951, Mar. 2018.

[250] T. R. J. Heathman *et al.*, "Characterization of human mesenchymal stem cells from multiple donors and the implications for large scale bioprocess development," *Biochem. Eng. J.*, vol. 108, pp. 14–23, 2016.

[251] S. Mohamed-Ahmed *et al.*, "Adipose-derived and bone marrow mesenchymal stem cells: A donor-matched comparison," *Stem Cell Res. Ther.*, vol. 9, no. 1, 2018.

[252] S. L. Dallas and L. F. Bonewald, "Dynamics of the transition from osteoblast to osteocyte," in *Annals of the New York Academy of Sciences*, 2010, vol. 1192, pp. 437–443.

[253] C. A. Mullen, T. J. Vaughan, M. C. Voisin, M. A. Brennan, P. Layrolle, and L. M. McNamara, "Cell morphology and focal adhesion location alters internal cell stress," *J. R. Soc. Interface*, vol. 11, no. 101, 2014.

[254] C. A. Mullen, M. G. Haugh, M. B. Schaffler, R. J. Majeska, and L. M. McNamara, "Osteocyte differentiation is regulated by extracellular matrix stiffness and intercellular separation," *J. Mech. Behav. Biomed. Mater.*, vol. 28, pp. 183–194, 2013.

[255] S. J. Heo, S. D. Thorpe, T. P. Driscoll, R. L. Duncan, D. A. Lee, and R. L. Mauck, "Biophysical regulation of chromatin architecture instills a mechanical memory in mesenchymal stem cells," *Sci. Rep.*, vol. 5, 2015.

[256] L. Lv, Y. Tang, P. Zhang, Y. Liu, X. Bai, and Y. Zhou, "Biomaterial Cues Regulate Epigenetic State and Cell Functions—A Systematic Review," *Tissue Eng. Part B Rev.*, p. ten.teb.2017.0287, 2017.

[257] Q. Xu, C. Li, Y. Kang, and Y. Zhang, "Long term effects of substrate stiffness on the development of hMSC mechanical properties," *RSC Adv.*, vol. 5, no. 128, pp. 105651–105660, 2015.

[258] P. Kumar, Y. Tan, and P. Cahan, "Understanding development and stem cells using single cell-based analyses of gene expression," *Development*, vol. 144, no. 1, pp. 17–32, 2017.

[259] L. R. Flores, M. C. Keeling, X. Zhang, K. Sliogeryte, and N. Gavara, "Lifeact-GFP alters F-actin organization, cellular morphology and biophysical behaviour," *Sci. Rep.*, vol. 9, no. 1, p. 3241, Dec. 2019.

[260] L. N. Munsie, N. Caron, C. R. Desmond, and R. Truant, "Lifeact cannot visualize some forms of stress-induced twisted f-actin," *Nature Methods*, vol. 6, no. 5. p. 317, 2009.

[261] M. G. Lemieux, D. Janzen, R. Hwang, J. Roldan, I. Jarchum, and D. A. Knecht, "Visualization of the actin cytoskeleton: Different F-actin-binding probes tell different stories," *Cytoskeleton*, vol. 71, no. 3, pp. 157–169, 2014.

[262] B. J. Belin, B. A. Cimini, E. H. Blackburn, and R. D. Mullins, “Visualization of actin filaments and monomers in somatic cell nuclei,” *Mol. Biol. Cell*, vol. 24, no. 7, pp. 982–994, 2013.

[263] S. Patel *et al.*, “Functional characterisation of filamentous actin probe expression in neuronal cells,” *PLoS One*, vol. 12, no. 11, 2017.

[264] J. Dyachok, J. A. Sparks, F. Liao, Y. S. Wang, and E. B. Blancaflor, “Fluorescent protein-based reporters of the actin cytoskeleton in living plant cells: Fluorophore variant, actin binding domain, and promoter considerations,” *Cytoskeleton*, vol. 71, no. 5, pp. 311–327, 2014.

[265] L. M. Rebelo, J. S. De Sousa, J. Mendes Filho, and M. Radmacher, “Comparison of the viscoelastic properties of cells from different kidney cancer phenotypes measured with atomic force microscopy,” *Nanotechnology*, vol. 24, no. 5, 2013.

[266] S. Charrier *et al.*, “Quantification of lentiviral vector copy numbers in individual hematopoietic colony-forming cells shows vector dose-dependent effects on the frequency and level of transduction,” *Gene Ther.*, vol. 18, no. 5, pp. 479–487, 2011.

[267] S. C. Materna and W. Marwan, “Estimating the number of plasmids taken up by a eukaryotic cell during transfection and evidence that antisense RNA abolishes gene expression in Physarum polycephalum,” *FEMS Microbiol. Lett.*, vol. 243, no. 1, pp. 29–35, 2005.

[268] M. Harterink *et al.*, “DeActs: Genetically encoded tools for perturbing the actin cytoskeleton in single cells,” *Nat. Methods*, vol. 14, no. 5, pp. 479–482, 2017.

[269] K. L. Weirich, S. Banerjee, K. Dasbiswas, T. A. Witten, S. Vaikuntanathan, and M. L. Gardel, “Liquid behavior of cross-linked actin bundles,” *Proc. Natl. Acad. Sci.*, vol. 114, no. 9, pp. 2131–2136, 2017.

[270] T. P. Driscoll, B. D. Cosgrove, S. J. Heo, Z. E. Shurden, and R. L. Mauck, “Cytoskeletal to Nuclear Strain Transfer Regulates YAP Signaling in Mesenchymal Stem Cells,” *Biophys. J.*, vol. 108, no. 12, pp. 2783–2793, 2015.

[271] G. Nardone *et al.*, “YAP regulates cell mechanics by controlling focal adhesion assembly,” *Nat. Commun.*, vol. 8, 2017.

[272] P. Hotulainen, “Actin-depolymerizing Factor and Cofilin-1 Play Overlapping Roles in Promoting Rapid F-Actin Depolymerization in Mammalian Nonmuscle Cells,” *Mol. Biol. Cell*, vol. 16, no. 2, pp. 649–664, 2004.

[273] K. Mizuno, “Signaling mechanisms and functional roles of cofilin phosphorylation and dephosphorylation.,” *Cell Sinalling*, vol. 25, no. 2, pp. 457–69, 2013.

[274] K. Hayakawa, H. Tatsumi, and M. Sokabe, “Actin filaments function as a tension sensor by tension-dependent binding of cofilin to the filament,” *J. Cell Biol.*, vol. 195, no. 5, pp. 721–727, 2011.

[275] H. Wioland *et al.*, “ADF/Cofilin Accelerates Actin Dynamics by Severing Filaments and Promoting Their Depolymerization at Both Ends,” *Curr. Biol.*, vol. 27, no. 13, p. 1956–1967.e7, 2017.

[276] K. Sliogeryte, S. D. Thorpe, Z. Wang, C. L. Thompson, N. Gavara, and M. M. Knight, “Differential effects of LifeAct-GFP and actin-GFP on cell mechanics assessed using micropipette aspiration,” *J. Biomech.*, vol. 49, no. 2, pp. 310–317, 2016.